PB-251 328

AIR POLLUTION: PROCEEDINGS OF THE INTERNATIONAL TECHNICAL MEETING ON AIR POLLUTION MODELING AND ITS APPLICATION (6TH) HELD AT FRANKFURT AM MAIN (WEST GERMANY) ON 24 - 26 SEPTEMBER 1975

NATO Committee on the Challenges of
Modern Society

Prepared for:

Environmental Protection Agency

1975

DISTRIBUTED BY:

NTIS
National Technical Information Service
U. S. DEPARTMENT OF COMMERCE

100006

PB 251 328

COMMITTEE ON THE CHALLENGES OF MODERN SOCIETY

NATO CDSM
OTAN CCMS

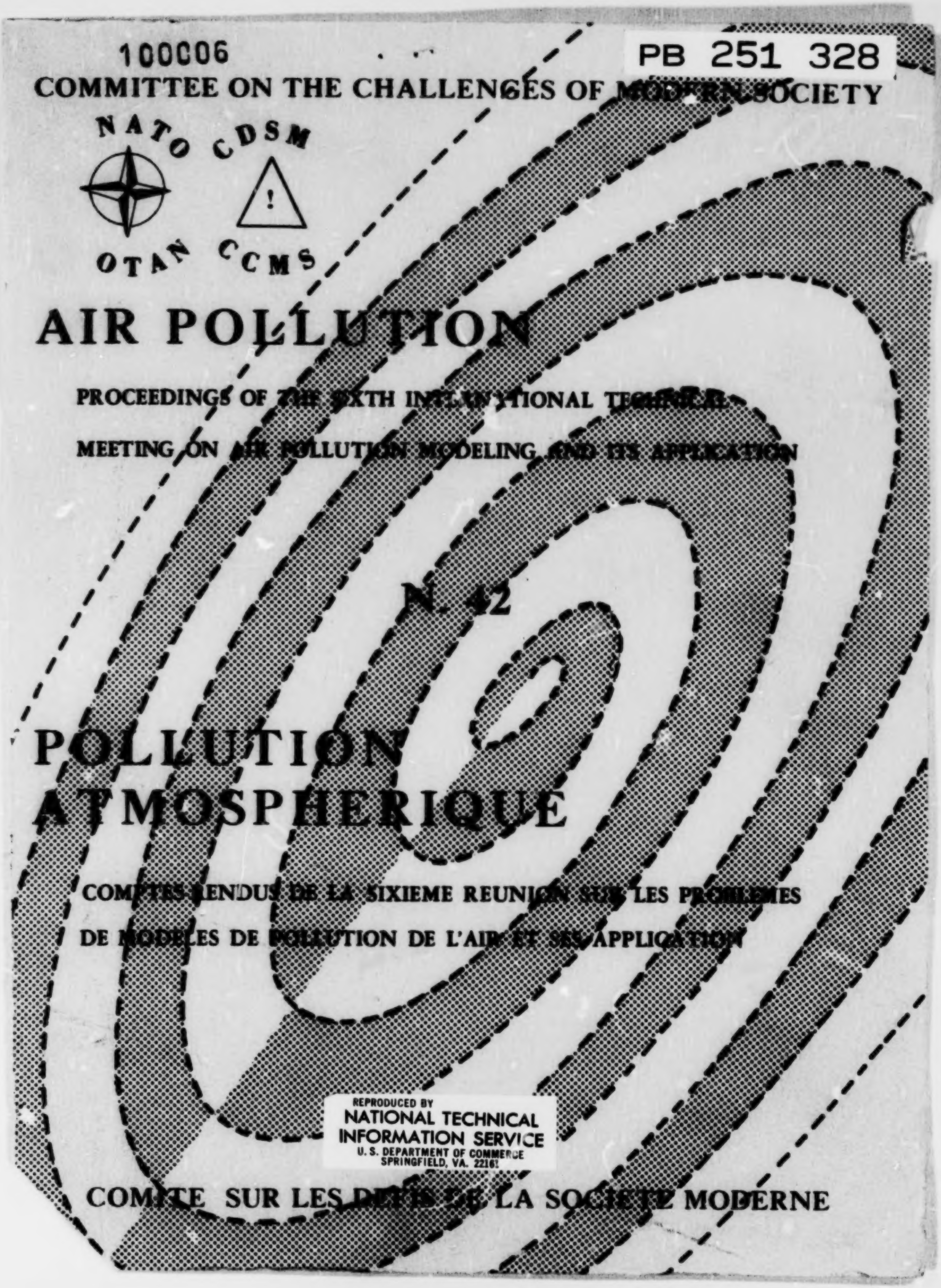

AIR POLLUTION

PROCEEDINGS OF THE SIXTH INTERNATIONAL TECHNICAL
MEETING ON AIR POLLUTION MODELING AND ITS APPLICATION

N. 42

POLLUTION ATMOSPHERIQUE

COMPTES RENDUS DE LA SIXIEME REUNION SUR LES PROBLEMES
DE MODELES DE POLLUTION DE L'AIR ET SES APPLICATION

REPRODUCED BY
NATIONAL TECHNICAL
INFORMATION SERVICE
U. S. DEPARTMENT OF COMMERCE
SPRINGFIELD, VA. 22161

COMITE SUR LES DEFIS DE LA SOCIETE MODERNE

BIBLIOGRAPHIC DATA SHEET	1. Report No. 42	2.	3. Recipient's Accession No. PB251328

4. Title and Subtitle
Air Pollution
Proceedings of the Sixth International Technical Meeting on Air Pollution Modeling and Its Application

5. Report Date
1975

6.

7. Author(s)

8. Performing Organization Rept. No.

9. Performing Organization Name and Address
Battelle - Institute e. V.
Frankfurt a/M
Federal Republic of Germany

10. Project/Task/Work Unit No.

11. Contract/Grant No.

12. Sponsoring Organization Name and Address

13. Type of Report & Period Covered

14.

15. Supplementary Notes

16. Abstracts

The five main areas discussed at this meeting and reported on are: 1) Current and Future Application of Air Pollution Modeling and Accuracy Requirements; 2) Requirements of Standardization of Air Quality Simulation Models and Requirements of a Common Data Base for Air Quality Simulation Models; 3) Validation of Air Quality Simulation Models; 4) Regional and Interregional Dispersion Models; 5) New Modeling Techniques

17. Key Words and Document Analysis. 17a. Descriptors

air pollution modeling
ambient air quality
sulfur dioxide concentrations
air quality measurement
meteorological data

17b. Identifiers/Open-Ended Terms

17c. COSATI Field/Group

PRICES SUBJECT TO CHANGE

18. Availability Statement unlimitec	19. Security Class (This Report) UNCLASSIFIED	21. No. of Pages 757
	20. Security Class (This Page UNCLASSIFIED	22. Price 12.75

FORM NTIS-35 (REV. 10-73) ENDORSED BY ANSI AND UNESCO. THIS FORM MAY BE REPRODUCED USCOMM-DC 8265-P74

PROCEEDINGS OF THE SIXTH INTERNATIONAL TECHNICAL MEETING ON AIR POLLUTION MODELING AND ITS APPLICATION

24 - 26 September 1975

BATTELLE - INSTITUT e. V.
Frankfurt a/M
Federal Republic of Germany

A Report of the Air Pollution Pilot Study,

NATO Committee on the Challenges to Modern Society
1975

OTHER NATO/CCMS AIR POLLUTION PUBLICATIONS

Technical Report on the Conference on Low Pollution Power Systems Development, N.4

Proceedings of the Second Meeting of the Expert Panel on Air Pollution Modeling, N.5

Guidelines to Assessment of Air Quality (Revised) SO_x, TSP, CO, HC, NO_x and Oxidants, N.6*

Air Quality Criteria for Sulfur Oxides, N.7*

Air Quality Criteria for Particulate Matter, N.8*

Air Quality Criteria for Carbon Monoxide, N.10*

Control Techniques for Sulfur Oxide Air Pollutants, N.12*

Control Techniques for Particulate Air Pollutants, N.13*

Proceedings of the Third Meeting of the Expert Panel on Air Pollution Modeling, N.14

Air Quality Criteria for Nitrogen Oxides, N.15*

Control Techniques for Carbon Monoxide Emissions from Stationary Sources, N.18*

Control Techniques for Hydrocarbons and Organic Solvent Emissions from Stationary Sources, N.19*

Control Techniques for Nitrogen Oxide Emissions from Stationary Sources, N.20*

Air Quality Criteria for Photochemical Oxidants and Related Hydrocarbons, N.29*

Proceedings of the Fourth Meeting of the Expert Panel on Air Pollution Modeling, N.30

Symposium on Low Pollution Power Systems Development, N.32

Proceedings of the Fifth Meeting of the Expert Panel on Air Pollution Modeling, N.35

Symposium on Low Pollution Power Systems Development, N.39

First Follow-up Report - Air Pollution Pilot Study, N.41

*Also available in French

These documents may be obtained from the NATO Committee on the Challenges of Modern Society, 1110 Bruxelles, Brussels, Belgium; from the Air Pollution Technical Information Center, Office of Air and Waste Management, U.S. Environmental Protection Agency, Research Triangle Park, North Carolina 27711, U.S.A.; and from the National Technical Information Service, 5285 Port Royal Road, Springfield, Virginia 22161, U.S.A. (English only)

PREFACE

The Federal Republic of Germany as pilot nation for the new NATO/CCMS Air Pollution Pilot Study " Assessment Methodology and Modeling " invited the designers of air quality models and the users or decision makers in the air quality management process for another International Technical Meeting on Air Pollution Modeling in keeping with a five-year-tradition.
Five topics relating to air quality modeling have been discussed: the current and future applications of air pollution modeling and accuracy requirements, the requirements of standardization of Air Quality Simulation Models and requirements of a common data base for AQSM's, the validation of AQSM's, the regional and interregional dispersion models and new modeling techniques.

71 international experts attended the meeting representing 14 countries: Belgium (4), Canada (1), Denmark (1), France (3), Federal Republic of Germany (29), Italy (11), Japan (1), Netherlands (5), Norway (2), Spain (1), Sweden (3), Switzerland (2), USA (6), United Kingdom (3).

Special thanks are due to the Battelle - Institute, to Mr. Strott and his staff in their capacity as hosts for the meeting and for making available all technical support required.

This document contains the papers that were submitted together with the reports of the several rapporteurs to the different sessions of the meeting, summarizing the discussions which followed each presentation. Due to the limited time available it was not possible to provide time for an oral presentation of all papers.

The secretariat of the NATO/CCMS Air Pollution Pilot Study takes this opportunity to thank all authors and rapporteurs for having submitted their presentation and reports so promptly.

Christa Morawa
Secretariat for the NATO/CCMS Air Pollution
Pilot Study

UMWELTBUNDESAMT

1 Berlin 33
Bismarckplatz 1

CONTENTS

Agenda .... Page 1

Participants 9

Opening (and Closing) Remarks 21

CHAPTER I

Current and Future Application of Air Pollution Modeling and Accuracy Requirements 27

1. Introduction: Present and Future Problems and Feasible Applications of Air Pollution Modeling (H. Fortak) 29

2. The Use of Atmospheric Dispersion Models for Control and Enforcement by the Environmental Protection Agency (H.H. Slater) 33

3. On the Calculation of Optimal Long-Term Air Pollution Abatement Strategies for Multiple Source Areas (S.-A. Gustafson, K.O. Kortanek) 43

4. Rapporteur's Report on Session I: K.E.Grønskei 58

5. Using Line Sources for the Simulation of Area Sources (K. Herrmann) 61

6. Results of the Revised ATDL - Model Compared to the Results of the AQDM - and CDM - Models (A. Craig) 75

Preceding page blank

7. Preliminary Report about a Diffusion Model for Milano (Italy) Urban Area: Gifford - Hanna Model (C.E. Cantoni, R. Gualdi, L. Santomauro) 93

8. Rapporteur's Report on Session II: J. Strott 123

9. Application of an Air Pollution Model to the Problem of Feasible Industrialization of a Planned Deep-Sea Harbour (H. Fortak) 125

10. Further Investigations of the Ambient Air Quality Situation in the Unter-Main Region Making Use of Fortak's Dispersion Model (B. Gutsche) 149

11. The State of Air Pollution Modeling and Model Applications in Sweden (B. Bringfelt) 171

12. Rapporteur's Report on Session III: R.F. Lee 182

12a. A Gaussian-Plume Algorithm for Point, Area, and Line Sources (D.B. Turner, W.B. Petersen) 185

13. Statistical Properties of Sulfur Dioxide Concentrations at Continuous Monitoring Stations in Japan (R. Inouye) 229

14. Methodology for an Integrated System of Air Pollution Control Project MASC-AP (L.F. Escudero, R. del Llano) 251

15. Rapporteur's Report on Session IV: S. - A. Gustafson 267

CHAPTER II

Requirements of Standardization of Air Quality Simulation Models and Requirements of a Common Data Base for Air Quality Simulation Models 269

16. Dispersion Characteristics via Tracer Techniques (K. - H. Müller) 271

17. Some Features of Turbulent Diffusion Process Resulting from Experimental Field Tests (A. Saab, M. Ribon, P. Méry).................. 283

18. Determination of Actual Vertical Windspeed Profiles in the Friction Layer Based on Beforeknown Mean Profiles (L.M. Malet) 297

19. Rapporteur's Report on Session V: C.A. Velds... 309

20. Models of Temperature Profiles under Convective and Inversion Condition, Connected to Air Pollution (P. Bacci, A. Longhetto, D. Anfossi) 313

21. Air Quality Measurements in Turin 1971 - 1974 (P.P. Gaddo, F. Corazzari, L. Giaconelli).... 331

22. A Standardized Model for the Projection of Ground Level Concentrations and its Application in the Approval Process for Air Polluting Industrial Facilities (S. Külske) 421

23. A Standardized Dispersion Model for Judging the Permissibility of Air Polluting Industrial Facilities (U.A. Schmitt) 433

24. Rapporteur's Report on Session VI: D. Jost 440

CHAPTER III

Validation of Air Quality Simulation Models 441

25. Using Sensitivity Analysis to Determine Dispersion Modeling Input Requirements (C.C. Masser, J.R. Hammerle) 443

25a. Validation of a Single Source Dispersion Model (R.F. Lee, M.T. Mills, R.W. Stern) 463

26. Applicability of Meteorological Data to Distant Locations and their Influence on the Calculation of Pollutant Concentrations (H. Bresser, Ch. Heger) 513

27. Rapporteur's Report on Session VII: B. Turner 527

28. Sensitivity Analysis of Parameters Effecting the Results of Gaussian Models (J. Strott, W. Christ) 529

29. Urban Air Modeling Support (K.H. Müller) 545

30. Rapporteur's Report on Session VIII: F.B. Smith 547

CHAPTER IV

Regional and Interregional Dispersion Models 549

31. Feasibility Demonstration of an Air-Budget Model for the Assessment of Transfrontier Air Pollution (W.B. Johnson, D.E. Wolf, R.L. Manusco) 551

32. Validation of a Multiple Source Diffusion Model Based on the Gaussian Plume Model (F.T.M. Nieuwstadt, H. van Dop).............. 601

33. Rapporteur's Report on Session IX: C.F. Barrett 630

CHAPTER V

New Modeling Techniques 633

34. Simulation of SO_2 - Dispersion in the Venetian Area (E. Runca, P. Melli, P. Zanetti) 635

35. A Gaussian Model in Complex Topographical Surroundings (A. Scholberg) 663

36. The Role of Wind - Tunnel Modelling in Predicting Dispersion (C.F. Barrett)........... 685

37. Provisional Model of Gaseous Pollutant Distribution for Optimal Control of Emitting Sources (G.L. Marziano, A. Butera, L. Gianolio, M. Ciprian) 693

38. Rapporteur's Report on Session X: W.B. Johnson 757

39. Invitation for the 7th International Technical Meeting on Air Pollution Modeling and its Application 1976 759

Reproduced from best available copy.

6th NATO/CCMS
International Technical Meeting
on Air Pollution Modeling

AGENDA

BATTELLE-INSTITUT E. V. FRANKFURT AM MAIN

Federal Republic of Germany

Tuesday 23 September, 1975

20.00	Social Hour at the Battelle Cafeteria
	Preparatory Meeting of the Chairmen

Wednesday, 24 September

9.00 - 10.00 Registration of Participants

10.00 Opening Remarks, RD E. Weber

Topic I, Chairman Prof. Dr. H. Fortak.
"Current and Future Application of Air Pollution Modeling and Accuracy Requirements"

Rapporteur: K. E. Grønskei

a) EPA's Use of Dispersion Models for Control and Enforcement

H. H. Slater

EPA

b) On the Calculation of Optimal Long-Term Air Pollution Abatement Strategies for Multiple Source Areas

S.-A. Gustafson, K. O. Kortanek

Royal Institute of Technology

11.05 - 11.30 Coffee break

11.30 Topic I (continued)

Rapporteur: J. Strott

c) Air Quality Simulation Model Based on the ATDL-Model by Hanna and Gifford

K. Herrmann

TH Darmstadt

d) Results of the Revised ATDL-Model Compared to the Results of the AQDM- and CDM-Models

A. Braig

Battelle-Institut

e) About a Diffusion Model for a Weak Atmospheric Circulation Urban Area: Gifford-Hanna Model

C. Ermini Cantoni, R. Gualdi
L. Santomauro
Osservatore Meteorologico di Brera

13.00 - 14.30 Lunch

14.30 Topic I (continued), Chairman H. H. Slater

Rapporteur: R. F. Lee

f) Application of an Air Pollution Model to the Problem of Possible Industrialization of a Planned Deep-Sea Harbor

H. Fortak

Deutsche Forschungs- und Versuchsanstalt für Luft- und Raumfahrt e.V.

g) Further Investigations of the Ambient Air Quality Situation in the Untermain-Region making use of Fortak's Dispersion Model

B. Gutsche

Freie Universität Berlin

h) The State of Air Pollution Modeling and Model Applications in Sweden

B. Bringfelt

The Swedish Meteorological and Hydrological Institute

15.50 - 16.20 Coffee break

16.20 Topic I (continued),

Rapporteur: S.-A. Gustafson

i) A Gaussian-Plume Algorithm for Point, Area, and Line Sources

[illegible] Turner, [illegible] Petersen

j) Statistical Properties of Sulfur Oxides Concentrations at Continuous Monitoring Stations in Japan

[illegible] Inouye

Hokkaido University

Thursday, 25 September

9.30 Topic II, Chairman Dr. K. L. Calder
"Requirements of Standardization of AQSM's and Requirements of a Common Data Base for AQSM's"

Rapporteur: C. A. Velds

a) Dispersion Charakteristics via Tracer Techniques

K. H. Müller

Euratom

b) Some Features of Turbulent Diffusion Process Resulting from Experimental Field Tests

A. Saab, M. Ribon, P.Méry
Electricité de France

c) Determination of Actual Vertical Wind Speed Profiles in the Friction Layer based on Beforeknown Mean Profiles

L. M. Malet

Institut Royal Météorologique

10.50 - 11.20 Coffee break

11.20 Topic II (continued)

d) Models of Temperature Profiles under Convective and Inversion Conditions Connected to Air Pollution

D. Anfossi, P. Bacci, A. Longhetto

Osservatore Meteorologico di Brera

Rapporteur: D. Jost

e) Air Quality, Measurements in Turin 1971 - 1974

P. P. Gaddo, F. Corazzari , L. Giacomelli

Fiat Central Research, Laboratories,

Orbassano

f) A Standarized Dispersion Model for Judging Permissibility of Air Polluting Facilities

S. Külske, D. A. Schmitt

Landesanstalt für Immissions- und Bodennutzungsschutz, Ministerium für Arbeit, Gesundheit und Soziales des Landes Nordrhein-Westfalen.

13.00 - 14.30 Lunch

14.30 Topic III, Chairman W. B. Johnson
"Validation of AQSM's"

Rapporteur: D. Turner

a) Using Sensitivity Analysis to Determine Dispersion Modeling Input Requirements

C. C. Masser, J. R. Hammerle
EPA

b) Validation of a Single Source Dispersion Model

R. F. Lee, M. T. Mills

EPA

c) Application of Meteorological Evaluations to other Locations and its Influence on Immission Calculations

Ch. Heger, H. Bresser

TÜV Rheinland

16.00 - 16.30 Coffee break

16.30 Topic III (continued)

Rapporteur: F. B. Smith

d) Sensitivity Analysis of Paramenters Influencing the Results of Gaussian Models (tentatively)

J. Strott

Battelle-Institut

e) Urban Air Modeling Support
K. H. Müller
Euratom /Ispra.

19.00 Frankfurt Dinner

9.30 Topic IV, Chairman Dr. M. Kwizak
"Regional and Interregional Dispersion Models"

Rapporteur: C. F. Barrett

a) An efficient Gaussian-Plume Multiple-Source Air Quality Algorithm
J. M. Hrenko, D. B. Turner

b) Feasibility Demonstration of an Air-Budget Model for the Assessment of Transfrontier Air Pollution

W. B. Johnson, D. E. Wolf, R. L. Mancuso

Stanford Research Institute

c) Validation of a Multiple Source Diffusion Model, Based on the Gaussian Plume

H. van Dop, F. T. M. Nieuwstadt

Koninklijk Nederlands Meteorologisch Instituut

11.00 - 11.30 Coffee break

11.30 Topic V, Chairman B. Bringfelt
"New Modeling Techniques"

Rapporteur: W. B. Johnson

a) Simulation of SO_2-Dispersion in the Venetian Area

E. Runca, P. Zanetti, P. Melli

b) Validation of a Model in Complex Topographical Surroundings

A. Scholberg

SEDE SA

c) The Role of Wind-Tunnel Modeling in Predicting Dispersion

C. F. Barrett

Spring Laboratory

13.00 Closing Remarks: E. Weber, J. R. Hammerle

13.10 Lunch

Participants in the 6th International Technical Meeting on Air Pollution Modeling and its Application

BATTELLE Institut e.V., Frankfurt/M.

Federal Republic of Germany

September 24 - 26, 1975

BELGIUM

Institut Royal
Meteorologique de Belgique

Dr. A. Joukoff
Dr. L. M. Malet

Koninklijk Meteorologisch
Instituut

L. van der Auwera

German Delegation to Nato

Dr. F. Schneller

Université Catholique de
Louvain - Institut Astronomie -
Geophysique

Dr. A. L. Berger

CANADA

Atmospheric Environment Service

Dr. M. Kwizak

DENMARK

Meteorological Institute
Air Pollution Section

L. P. Prahm

ENGLAND

Meteorological Office Met.O.14

Dr. F. B. Smith

Warren Spring Laboratory

C. F. Barrett
F. M. Williams

FRANCE

Ecole Centrale de Lyon
Laboratoire de Méchanique
des Fluides

J.-P. Schoen

Electricité de France
Direction des Etudes et
Recherches

Dr. P. Mery
M. Ribon

GERMANY,

Federal Republic of

Battelle Institut

Dr. A. Braig
G. Strott

Bundesministerium des Innern
- U III 2 -

MR. E. Weber

Deutsche Forschungs- und
Versuchsanstalt für Luft- und
Raumfahrt e. V.
Institut für Physik der
Atmosphaere

Prof. H. Fortak

Deutscher Wetterdienst
Zentralamt

DRR H. Bartels
Dr. W. Ott
V. Pancer

Freie Universität Berlin
Institut für Theoretische
Meteorologie

Dr. Gutsche
H. Stern

Hessische Landesanstalt
für Umwelt

Dr. M. Büchen

Kernforschungsanlage Jülich
Zentralabteilung Strahlenschutz

Dr. K. J. Vogt

I A B G / S Z A

Dr. M. Schorling

Landesanstalt für Immissions-
und Bodennutzungsschutz
des Landes NRW

S. Kuelske

Landesanstalt für Umweltschutz
Karlsruhe

D. Ahrens

Ministerium für Arbeit
Gesundheit und Soziales
des Landes NRW

M. R. Schmitt

Regionale Planungsgemeinschaft
Untermain

Frau G. N. Harp

Senator für Gesundheit
und Umweltschutz Berlin

Dr. Lenschow

Technischer Überwachungsverein
Rheinland e. V.

Dr. Bresser
Gerold
Dr. Heger

TH Darmstadt

B. Dietzer
K. Herrmann

TÜV - Norddeutschland

Dr. Heinrich

Umweltbundesamt

Dr. K. E. Joerss
Dr. D. Jost
R. S. Kaller
Fr. Ch. Morawa
Dr. J. Pankrath

VDI-Kommission
Reinhaltung der Luft

J. V. Chamier-Gliesen

ITALY

Euratom - Ispra
Division Physik

Dr. K.-H. Müller

I B M Italia Spa
Centro di ricerca

E. Runca

Laboratori Centrali Fiat

Dr. F. Corazzari

Laboratorio Cosmogeofisica
del C N R

D. Anfossi

Laboratorio Ricerca Ambientale
- E N E L -

P. Bacci
A. Longhetto

Osservatorio
Meteorologico di Brera

R. Gualdi
Prof. L. Santomauro

Philips - Ecologica
Igiene Industriale Sezione Pit

Dr. G. A. Laneve

Tecneco S. P. A.

Dr. I. Giovannini
Dr. A. Levy

JAPAN

Hokkaido University

Prof. K. Inouye

NETHERLANDS

Centraal Technisch Instituut
TNO

Dr. G. A. Boschloo

DOW Chemical Netherlands

R. M. Dauwe

N. V. KEMA

IR. A. J. Elshout

Koninklijk Nederlands
Meteorologisch Instituut

Dr. H. van Dop
Dr. C. A. Velds

NORWAY

Norwegian Institute for Air
Research

K. E. Gronskei
Dr. B. Sivertsen

SPAIN

Centro de Investigacion IBM

R. Del Llano

SWEDEN

Royal Institute of Technology
Department for Computer
Sciences

S. A. Gustafson

S M H I

N.-A. Andersson
B. Bringfelt

SWITZERLAND

Institut Suisse de Meteorologie
Section de la Protection
de L'Air

P. Jeannet

Société D'Etude de
L'Environnement SA Sede SA

A. Scholberg

U. S. A.

Environmental Protection Agency

J. R. Hammerle

Environmental Protection Agency
Environmental Sciences Research
Lab. Meteorology and Assessment
Div., ESRL

K. L. Calder
D. B. Turner

Environmental Protection Agency
Office of Air Quality
Planning and Standards

R. F. Lee
H. H. Slater

Stanford Research Institute
Atmospheric Sciences Laboratory

Dr. W. B. Johnson

D. Ahrens
Landesanstalt für Umweltschutz

D - Karlsruhe

Griesbachstr. 3
W. GERMANY

N. A. Andersson
SMHI
Fack

S - 601 Norrköping

SWEDEN

D. Anfossi
Laboratorio Cosmogeofisica
DEL CNR

Corso Fiume 4

I - Torino

ITALY

L. Van der Auwera
Koninklijk Meteorologisch
Instituut

Ringlaan, 3

B - 1180 Brüssel

BELGIUM

P. Bacci
Laboratorio Ricerca Ambientale
- ENEL -

Str. Stat. 31 bis

I - Torino VC.

ITALY

C. F. Barrett
Warren Spring Laboratory

Po. Box 20, Gunnels Wood Road

GB - Stevenage Herfordshire SG 1
2 B X

ENGLAND

ORR. H. Bartels
Deutscher Wetterdienst
Zentralamt

D - 6050 Offenbach /Main

Frankfurter Str. 135

W. - GERMANY

Dr. A. L. Berger
Université Catholique
de Louvain - Institut
Astronomie - Geophysique

2, Chemin du Cyclotron

B - 1348 Louvain-La-Neuve

BELGIUM

Dr. G. A. Boschloo
Centraal Technisch Instituut
TNO

NL - Apeldoorn

Postbox 342

NETHERLANDS

Dr. A. Craig
Batelle Institut

D - 6000 Frankfurt /Main 10

Am Römerhof 35

W. - GERMANY

Dr. Bresser
Technischer Überwachungs-Verein
Rheinland e. V.

D - 5000 Köln 1

Postfach 10 1750

W. - GERMANY

U. Bringfelt
SMHI

S - 60101 Norköping

SWEDEN

Dr. M. Büchen
Hessische Landesanstalt
für Umwelt

D - 6200 Wiesbaden

Kranzplatz 5/6

W. - GERMANY

Dr. K. L. Calder
Environmental Protection Agency
Environmental Sciences Research
Lab.

Research Triangle Park

USA - Carolina 27711

J. V. Chamier - Gliesen

VDI-Kommission Reinhaltung
der Luft - Geschäftsstelle

D - 4000 Düsseldorf

Graf-Recke-Str. 84 Postf.1139

W. - GERMANY

Dr. F. Corazzari
Laboratori Centrali Fiat

Strada Torino 50

I - 10043 Orbassano (Torino)

ITALY

R. M. Dauwe
Dow Chemical Netherlands

NL - Terneuzen

H. H. Dowweg

NETHERLANDS

B. Dietzer
TH Darmstadt
Sektion Meteorologie

D - 6100 Darmstadt

Hochschulstr. 1

W. - Germany

Dr. H. Van Dop
Koninklijk Nederlands
Meteorologisch Instituut

Utrechtseweg 297 -

De Bilt

NETHERLANDS

IR. A. J. Elshout
N. V. KEMA

Utrechtseweg 310

NL - Arnhem

NETHERLANDS

Prof. H. Fortak
Deutsche Forschungs- und
Versuchsanstalt für Luft- und
Raumfahrt e. V.
Institut für Physik
der Atmosphäre

D - 8031 Oberpfaffenhofen

Post Wessling /Obb.

W.-GERMANY

Gerold
Technischer Überwachungs-Verein
Rheinland e. V.

D - 5000 Köln 1

Postfach 10 1750

W. - GERMANY

Dr. I. Giovannini
Tecnesco S. P. A.

Pian di Rose

I - S. Ippolito (PS)

ITALY

K. E. Gronskei
Norwegian Institute
For Air Research

P. B. 115

N - 2007 Kjeller

NORWAY

R. Gualdi
Osservatorio Meteorologico
di Brera

Via Brera, 28

I - 20121 Milano

ITALY

S.-A. Gustafson
Royal Institute of Technology
Department for Computer
Sciences

S - 100 44 Stockholm 70

SWEDEN

Dr. Gutsche
Freie Universität Berlin
Institut für Theoretische
Meteorologie

D - 1000 Berlin

W. - GERMANY

Dr. J. R. Hammerle
Environmental Protection Agency

Research Triangle Park

USA - North Carolina 27711

U. S. A.

Frau G. N. Harp
Regionale Planungsgemeinschaft
Untermain

D - 6000 Frankfurt (Main)

Zeil 127

W. - GERMANY

Dr. Heger
Technischer Überwachungs-Verein
Rheinland e. V.

D - 5000 Köln 1

Postfach 10 1750

W. - GERMANY

Dr. Heinrich
TÜV - Norddeutschland

D 2000 Hamburg 54

Große Bahnstr. 31

W.-GERMANY

K. Herrmann
TH Darmstadt
Sektion Meteorologie

D - 6100 Darmstadt

Hochschulstr. 1

W. - GERMANY

Prof. R. Inouye
Hokkaido University

Kita - 13 Jo Nishi-Chome

J - Sapporo 060

JAPAN

P. Jeannet
Institut Suisse de Meteorologie
Section de la Protection de L'Air

Les Invuardes

CH - 1530 Payerne

SWITZERLAND

Dr. K. E. Joerss
Umweltbundesamt

D - 1000 Berlin 33

Bismarckplatz 1

W. - GERMANY

Dr. W. B. Johnson
Stanford Research Institute
Atmospheric Sciences Laboratory

333 Ravenswood Ave.

USA - Menlo Park, California 94025

U. S. A.

Dr. D. Jost
Umweltbundesamt

D - 1000 Berlin 33
Bismarckplatz 1

W.-GERMANY

Dr. A. Joukoff
Institut Royal Meteorologique
de Belgique

Avenue Circulaire, 3

B - 1180 Bruxelles

BELGIUM

R. S. Kaller
Pilotstation des
Umweltbundesamtes

D - 6000 Frankfurt (Main)

Feldbergstr. 45

W. - GERMANY

S. Külske
Landesanstalt für Immissions-
und Bodennutzungsschutz
des Landes NRW

D - 4300 Essen-Bredeney

Wallneyer Str. 6

W. - GERMANY

Dr. M. Kuizak
Atmospheric Environment Service

4905 Dufferin Street

Downsview, Ontario M 3 H 5 T 4

CANADA

Dr. G. A. Laneve
Philips - Ecologieca
Igiene Industriale Sezione Pit

I - 20052 Monza

V. Le Elvezia, 2

ITALY

R. F. Lee
Environmental Protection Agency
Office of Air Quality
Planning and Standards

Research Triangle Park

USA - Nort Carolina 27 711

U. S. A.

Dr. Lenschow
Senator für Gesundheit
und Umweltschutz

D - 1000 Berlin 30

An der Urania 14
W. - GERMANY

Dr. A. Levy
Tecneco S. P. A.

Pian di Rose

I - S. Ippolito (PS)

ITALY

R. Del Llano
Centro de Investigacion IBM

Paseo de la Castellana, 4

E - Madrid - 1

Spain

A. Longhetto
Laboratorio Ricerca Ambientale
- ENEL -

Str. Stat. 31 Bis

I - Torino VC.

ITALY

Dr. L. M. Malet
Institut Royal Meteorologique
de Belgique

Avenue Circulaire, 3

B - 1180 Bruxelles

BELGIUM

Pr. M. Mery
Electricité de France, Direction
des Etudes et Recherches

6, Quai Watier

F - 78400 Chatou

FRANCE

Frau
Ch. Morawa
Umweltbundesamt

D - 1000 Berlin 33

Bismarckplatz 1

W. - GERMANY

Dr. K.-H. Müller
Euratom - Ispra
Division Physik

I - 21020 Centro Euratom
di Ispra (Varese)

ITALY

Dr. W. Ott
Deutscher Wetterdienst

D - 6050 Offenbach (Main)

Frankfurter Str. 135

W. - GERMANY

V. Pander
Deutscher Wetterdienst

D - 6060 Offenbach (Main)

Frankfurter Str. 135

W. - GERMANY

Dr. J. Pankrath
Umweltbundesamt

D - 1000 Berlin 33

Bismarckplatz 1

W. - GERMANY

L. P. Prahm
Meteorological Institute
Air Pollution Section

Lyngny 100

DK - 2100 Koebenhaven

DENMARK

M. Ribon
Electricité de France Direction
des Etudes et Recherches

6, Quai Watier

F - 78400 Chatou

FRANCE

E. Runca
I B M Italia SPA
Centro di Ricerca

S. Polo 1364

I - 30125 Venezia

ITALY

Prof. L. Santomauro
Osservatorio Meteorologico
di Brera

Via Brera, 28

I - 20121 Milano

ITALY

M. R. Schmitt
Ministerium für Arbeit, Gesundheit
und Soziales des Landes
Nordrhein-Westfalen

D - 4000 Düsseldorf

Postfach

W. - GERMANY

Dr. M. Schneller
German Delegation to Nato

Bd. Leopold III

B - 1110 Bruxelles

BELGIUM

J.-P. Schon
Ecole Centrale de Lyon
Laboratoire de Mecanique
des Fluides

36, Route de Dardilly

F - 69130 Ecully

France

A. Scholberg
Société d'Etude de
l'environnement SA Sede Sa
Rue du Midi 33
CH - 1800 Vevey
SWITZERLAND

Dr. M. Schorling
IABG/SZA
D - 8012 Ottobrunn
W. - GERMANY

Dr. B. Sivertsen
Norwegian Institute
for Air Research
P.B. 115
N - 2000 Kjeller
NORWAY

H. H. Slater
Environmental Protection Agency
Office of Air Quality
Planning and Standards
Research Triangle Park
USA - North Carolina 27711
U. S. A.

Dr. F. B. Smith
Meteorological Office, Met.O.14
London Road
GB - Bracknell Berkshire RG 122SZ
ENGLAND

R. Stern
Freie Universität Berlin
Institut für Theor.
Meteorologie
D - 1000 Berlin
W.- GERMANY

J. Strott
Batelle Institut
D - 6000 Frankfurt (Main) 10
Am Römerhof 35
W. - GERMANY

D. B. Turner
Environmental Proteciton Agency
Meteorology and Assessment
Div. ESRL
Research Triangle Park, N.C.27711
Mail Drop 80
U. S. A.

Dr. C. A. Velds
Koninklijk Nederlands
Meteorologisch Instituut
Utrechtseweg 297
NL - De Bilt
NETHERLANDS

Dr. K. J. Vogt
Kernforschungsanlage Jülich
Zentralabteilung Strahlenschutz
D - 5170 Jülich
W. - GERMANY

RD. E. Weber
Bundesministerium des Innern
- U III 2 -
D - 5300 Bonn
Rheindorfer Str. 198
W. - GERMANY

Dr. F. P. Williams
Warren Spring Laboratory
P.O. Box 20, Gunnels Wood Road
GB - Stevenage Hertfordshire SG1 2BX
ENGLAND

6th NATO /CCMS
International Technical Meeting on Air Pollution Modeling

OPENING (AND CLOSING) REMARKS

by

Erich Weber

Bundesministerium des Innern
- Abteilung Umwelt -

Battelle-Institut e. V. Frankfurt /M
Germany, FR

24 - 26 September, 1975

Preceding page blank

On behalf of the Government of the Federal Republic of Germany and as chairman of the Pilot Study on Air Pollution Assessment Methodology and Modeling I am very pleased to welcome you here in Frankfurt. This is the third time that the international Symposium on Modeling is held in this city. The first meeting in October 1970 was attended by about 10 or 12 experts from the various NATO member countries. At that time the main subject had been modeling in the cities of Ankara, Frankfurt and St. Louis in conformity with the task set by CCMS. In 1973 we met again at Oberursel, near Frankfurt, about 40 or 50 experts attended. The chairman was Mr. Ken Calder whom I have to welcome in particular, since for several years he chaired the NATO/CCMS Expert Panels on Modeling and he has been very successful in calling together more or less all major experts in this field from all over the Western World to cooperate in this work. We should like to continue this tradition today. I see quite a number of new faces among the audience, and I am particularly pleased that I can welcome some of the familiar co-workers again. I remember very well the day when the Panel on Modeling was set up in 1970. Then Mr. McCormick and Mr. Ken Calder from the US EPA, Professor Heinz Fortak from Berlin and myself met in Paris on a very beautiful day. We sat in a sidewalk café, discussed the tasks of the new working group and wrote a report to NATO /CCMS and to the Governments, dealing with the necessity of establishing the Panel on Modeling. Successful work can even be done in a coffee-house as is evidenced in this case as much as five years later.

Last year the expert meeting on Modeling was held at Risø in Denmark, where we had to thank Mr. Niels Busch for the organization of the meeting as well as the Danish Atomic Energy Commission for their support. The meeting at Risø was at the same time the last meeting within the framework of the NATO /CCMS Pilot Study on Air Pollution which was conducted from 1970 to 1974 under the chairmanship of the United States. As a result of this first Pilot Study, the Governments of the NATO member countries adopted 15 recommendations of the Committee on the

Challenges of Modern Society. Recommendation XIV says that the member countries agree to continue the modeling activites and that the experts will continue to meet for an exchange of information. With these considerations and the objectives of other recommendations in mind, the Federal Republic of Germany proposed to NATO /CCMS in March 1974 to initiate another Pilot Study. This proposal being generally accepted, a working group for the Pilot Study on Air Pollution Assessment Methodology and Modeling was set up in Cologne this march, under the umbrella of which we are about to continue the former meetings of the Expert Panel on Modeling under the new title: "International Technical Meetings on Air Pollution Modeling and its Application". The results of this meeting are intended to be published as the first NATO document of the new Pilot Study.

The programme of the 6th meeting is very extensive and we have 3 busy days ahead. For this reason we put particular emphasis on accurate scheduling of our programme and I have instructed the chairmen to take care that the time schedules are adhered to. I appreciate that the organisation of this meeting has been running very smooth so far. The papers have almost all been registered in time, and we have even been able to supply you with summaries comprising the majority of the lectures to be held and I should like to express my thanks to the various speakers for their cooperation. At the same time I should like to ask all experts intending to present a paper here to submit a complete clean copy of their presentation to the secretariate, so as to enable us to publish the NATO document on this meeting.

I do not wish to close without expressing my particular thanks to the Battelle Institute for the excellent organisation and hospitality. We are, of course, particularly obliged to the members of the Battelle Institute who made the preparations and are responsible for the organisational part of the meeting during the three days ahead.

The work they have done under the supervision of Mr. Strott, to whom I am particularly grateful, has been very efficient. Later on Mr. Strott will give you a few details on the technical organization of the meeting, transport problems, the evening program and so on.

But first I would like to introduce Dr. Dieter Jost from the Umweltbundesamt in Berlin (Federal Environmental Agency) who will act as the chairman for this meeting. Turning the floor to him I thank you for attending this meeting and I hope that our work will be successful.

Conclusive Remarks

Ladies and Gentlemen,

we are now at the end of our conference and I do not want to bore you with another official statement. Just allow me to give you some statistical figures for the record first: 27 papers have been presented, more than 70 experts from 10 NATO and 4 non-NATO countries have been attending. On the behalf of our secretariat I would kindly ask all authors of papers once more who could not yet give us a master copy of their presentation to send them as soon as possible to Miss Morawa at the Umweltbundesamt.

Secondly I would like to thank all of you for your active participation in this meeting, to thank the chairmen, the authors of the papers, the discussion partners and the rapporteurs as well and allow me to express my particular thanks to the secretariat who prepared and organized this meeting together with the BATTELLE-Institute. I am especially grateful to the BATTELLE Institute for its great hospitality.

The last speaker of this conference will be Jim Hammerle from the United States EPA who will give some conclusive remarks and a preview for the next International Technical Meeting on Air Pollution Modeling and its Application in fall 1976 in the United States. Giving the floor to him I would like to draw your attention to an information sheet concerning this meeting which we distributed this morning and which shall give you an outline of the topics to be discussed next year.

6th NATO/CCMS
International Technical Meeting
on Air Pollution Modeling

TOPIC I

CURRENT AND FUTURE APPLICATIONS OF AIR POLLUTION MODELING AND ACCURACY REQUIREMENTS

Battelle - Institut e.V. Frankfurt / M
Germany, FR

24 - 26 September, 1975

Preceding page blank

INTRODUCTION

by

H. Fortak

PRESENT AND FUTURE PROBLEMS AND FEASIBLE APPLICATIONS OF AIR POLLUTION MODELING

The general structure of problems in modeling air pollution has not changed much during the last decade. The main goal of air pollution modeling is, as it is generally in meteorology, to predict the state of the atmosphere (here the chemical composition of the atmosphere) in terms of real-time short-term prediction and in terms of prediction of climatic changes within the atmosphere (here of climatic changes of air pollution).

In my opinion, the prediction of man-made climatic changes of air pollution for a given region was in some sense the first success in climate forecast of one important parameter of the atmosphere. This is especially true for air pollution models which predict frequency distributions of concentrations for as many grid points in an urban area or a region as necessary. This is true according to the definitions of climatology, because not only mean values but also the distribution of a meteorological parameter is predicted in case that man-made changes of the normal atmospheric input, i.e. the sources, are predicted. We are now in a position to predict the long-term changes of air pollution sources fairly well. This may be an increase of sources, a planned decrease, a change of source arrangement, a change to other types of fuel, for example. It is surprising enough that simple Gaussian plume-type models seem to be able to predict climatic changes of air pollution sufficiently well, and now can be used for planning purposes

Preceding page blank

in many regions in the world. This fact was known and validated almost ten years ago and the method is now used in numerous countries by a large number of research groups. This type of forecast is a purely statistical one, not only because an empirical statistical distribution (the Gaussian plume model) is used. In addition, the statistics of meteorological conditions of transport and diffusion during a normal meteorological year is utilized, that is also based on statistics of at least five years of meteorological data. Further statistics of ground level concentration fields, that constitute the concentration inventory of the region, are utilized to calculate a detailed air pollution climatology for many locations within the area of a city or a region.

There are, however, a certain number of problems left unsolved. First, the problem of air pollution transport and diffusion above irregular terrain. Secondly is the problem of finding a suitable model for treating light wind conditions, that are associated with temperature inversions occuring above the ground.

The effects of irregular terrain are rather poorly understood theoretically, although considerable empirical field studies and studies in the laboratory have been performed for many years. In the case of irregular terrain the vertical and horizontal wind - shear structure is distorting the actual plume in such a way that neither a Gaussian plume model nor the common types of puff models will be applicable. It seems to me that from a practical point of view only numerical models using the K - theory together with a dynamical model for air flow over such terrain could be able to guarantee some progress in that field.

In case of light wind conditions with inversions, observations from aircraft and even laboratory and numerical investigations by Deardorff indicate that especially under conditions of convective instability below inversions these layers are layers of extremely high concentrations. If the inversion layers are broken up by thermal convection, we always find strong downward turbulent diffusion and concentration peaks for shorter periods of time at the ground.

To me it seems to be extremely important to develop a time-dependent comprehensive model, which describes the transition from normal conditions, for which the Gaussian plume theory can be applied, to windless conditions (with built up inversions) and vice versa. In this respect I have the impression that a time-dependent K-theory, which does not use entirely numerical methods of solution, could be used, especially in order to avoid numerical diffusion effects.

Much have been said about other complications in modeling. For example about the validity of the Gaussian plume model at large distances from the sources, and about departures from passive diffusion. I won't repeat this here. However, if for a given area the appropriate type of model for prediction of air pollution climatologies has been developed, an almost unlimited number of useful applications in the field of environmental planning can be handled.

Examples are the analysis of environmental impact caused by changes in the source arrangement, by changes of the types of sources or of the types of fuel. Another example is the planning of land use and, therefore, the possibility of deciding where new industrial installations can be built or not be built.

Up to now, an almost unsolved problem is the problem of predicting air pollution in a given region on a real-time basis. This real-time prediction of air pollution requires a real-time prediction of the behavior of complicated properties, which are responsible for transport and diffusion within the planetary boundary layer. Up to now, we don't have satisfactory numerical models for these scales involved. Most investigations on predictability of atmospheric processes indicate that deterministic forecasts for regions of 100 x 100 km in size are possible only for short periods of time, say less than 6 hours in advance. Most urban areas and regions are smaller than this, and therefore we have in principle a limit of predictability, even though we might have a good nesting model within a steering large-scale model that would describe the physics of the planetary boundary layer sufficiently well. However, there is some indication that modern dynamic-stochastic forecasting models will be able to predict the state of the atmosphere in a statistical sense much further. In the scale, that we are considering here, a prediction perhaps almost one day in advance seems to be feasible. Even if this problem of forecasting of time series of properties of the planetary boundary layer could be solved, there remains the solution of an additional equation for transport and diffusion that obtains its input time-step by time-step from the forecasting model. In my opinion, only Eulerian models for transport and diffusion of pollutants can be used, and these are essentially models belonging to the group of time-dependent K-type theories. Although various attempts to solve this problem come to mine, I have not seen much progress in the direction I described previously. However, solutions to these problems are urgently needed, not only to forecast high-level air pollution episodes and, therefore, to build up a warning and control system, but also for testing many assumptions made in statistical models for the prediction of air pollution climatologies.

6th NATO/CCMS
International Technical Meeting
on Air Pollution Modeling

The Use of Atmospheric Dispersion Models for Control and Enforcement by the Environmental Protection Agency

by

Herschel H. Slater
Monitoring and Data Analysis Division
Environmental Protection Agency

BATTELLE - INSTITUT E.V., Frankfurt/Main

Germany, FR

24 - 26 September, 1975

The Use of Atmospheric Dispersion Models for Control and Enforcement by the Environmental Protection Agency

Dispersion models have been used extensively by the Environmental Protection Agency (EPA) during the past year to assist in developing air pollution control policies and to support several specific enforcement actions. At the fifth meeting of this panel in Denmark last year, the range of modeling applications for the development of control procedures and policies and enforcement of regulations was described.(1) The year that has elapsed since that meeting has seen a continued demand for analyses which allow air pollution control agencies to estimate the impact of policies and regulations on air quality before they are promulgated.

The energy problem experienced by all NATO countries has created in the United States major additional needs for air quality modeling. It may be instructive to describe the energy legislation which was passed by the Congress in an attempt to lessen the Nation's dependence on other countries for energy supply and at the same time to keep at a minimum adverse impacts on the environment. The administration of the law requires decisions founded on sound technical bases. Since the decisions involve estimates of future conditions, the technical bases have to be developed from modeling analyses.

The Energy Supply and Environmental Coordination Act of 1974 (ESECA) was passed in June of last year. The Act requires the Federal Energy Administration (FEA) to prohibit power plants from burning natural gas or oil, as a primary energy source, to conserve supplies of these scarce fuels. It also allows the prohibition of the use of gas or oil in other fuel-burning facilities. The Act permits the Environmental Protection Agency to relax temporarily the environmental constraints for sources affected by FEA orders where certain legal and environmental criteria are satisfied. The criteria in brief are:

a. A regional limitation provision. The source must be located in an Air Quality Control Region where the national primary ambient air quality standard is being met for the pollutant under consideration.

b. A primary standard provision. The relaxed emission regulation must be sufficiently stringent so that the primary (health-related) ambient air quality standard is not exceeded.

c. A significant risk provision. The relaxed emission regulation must not result in a significant risk to public health by an unregulated pollutant.

The regional limitation provision prevents a power plant from converting to coal if it is located in an air quality control region where the primary air quality standards are exceeded. At present, the requirements of the regional limitation provision are determined by air quality measurements. No estimates of air quality by analytical techniques are necessary. However, Congress has been considering changing this feature of the law to allow a plant to convert if it does not affect those portions of the air quality control regions where the air quality standards are exceeded. If such a provision is passed, considerable modeling will be required to determine whether the facility should be allowed to increase emissions of pollutants. It will be necessary to determine rather precisely where, as well as how much, the facility degrades the air quality.

The primary standard condition applies when it is determined that the emission regulations which currently pertain to the fuel-burning facility are more stringent than required to meet the primary air quality standard. It is an emission limitation which must be met when a source converts from gas or oil to coal as a fuel.

A primary standard condition may be specified by:

(1) An emission limitation (in units such as grams per second or grams per million BTU's).

(2) Requirements on the coal characteristics (percent sulfur and ash content and heat content).

(3) Authorizing a supplementary control system (reducing emissions during periods when meteorological conditions are conducive to high ground-level concentrations of pollutants).

Of the approximately 270 large oil-fired power plants in the United States, 79 have been identified as being potentially capable of using coal. These plants have a total capacity of about 24,500 MW. If all were converted, about 525,000 barrels of oil could be saved daily. By the end of June, 32 of the 79 had been issued orders to convert by the Federal Energy Administration. It is now the responsibility of the Environmental Protection Agency to ascertain whether the regional limitations are met and to specify the primary standard conditions.

The determination of the primary standard conditions will require an analysis of the impact of each plant. The modeling of these facilities can become quite complicated. Many of the plants proposed for conversion are 15-20 years old, consist of several individual units (boilers and stacks) and were originally designed to use coal. Because of changing market conditions in the late 40's and 50's and the environmental movement during the 60's and early 70's, they had been converted to oil or gas. Some plants have one or more boilers that cannot be re-converted because the fly ash control devices have been removed or are in such a poor state of repair that it is uneconomical to bring them to the required level of efficiency. Therefore, the modeling needs to take into consideration the individual impact of converting each of several units or combinations of units.

Several of the facilities are located within a few kilometers of each other. Where this situation prevails, additional analyses are required to determine whether two or more facilities contribute simultaneously to a threat to the primary air quality standards. The older plants are often located on sites which were selected with little concern for the impact of their effluents on the surroundings. Some are near prominent terrain features or in areas where high buildings have been constructed close by. Nearby terrain features introduce elements of complexity which modeling analyses can rarely adequately resolve without a detailed case-by-case investigation of each facility. Eventually, questions of this nature will be resolved by physical modeling - that is, modeling in a wind or water tunnel. There is a proposal to use the new EPA wind tunnel to investigate the impact of one of the plants now under an order to convert. EPA has the capability; whether sufficient time is available is not known.

When the analyses are complete, the decision is made as to the emission limitation -- the primary standard condition -- which will apply to the power plant. If, as is likely, only a portion of the power plant will be converted, primary standard conditions may have to be determined separately for each of the several units of the power generating facility.

The significant risk provision of ESECA directs the Administrator of EPA to suspend an order requiring conversion of an oil or gas burning facility if the conversion may cause a significant risk to public health from any unregulated pollutant. Although there are many possible pollutants that may create a risk to public health, the health effects of most are so ill-defined at this time that EPA is considering only the control of sulfates under the significant risk provision. Studies by EPA, the Science Advisory Board (SAB) and the National Academy of Sciences (NAS) all support the conclusion that extensive research is needed before a sulfate standard can be set and that the current objectives should be to limit increases of emissions of sulfate precursors near polluted urban areas.[2,3]

The Science Advisory Board believed that measurements of water-soluble sulfates were not a good indicator of toxic substances present in the "sulfur oxides/particulate complex." The SAB report states that for the present "increases in exposure to sulfur oxides or particulates in localities where sulfur dioxide and/or total suspended particulates exceed primary standards should be viewed with grave concern." EPA's proposed policy is designed to be consistent with the judgments of the Science Advisory Board and the National Academy of Sciences.

In the United States, sulfate levels tend to be highest in the 24 states that make up the northeastern part of the United States. The proposed significant risk procedures would be applicable primarily to this critical 24-state area and would require the State Implementation Plan emission requirements for SO_2 to be met where air quality standards for total suspended particulates (TSP) are exceeded. Similarly, the State Implementation Plan emission requirements for TSP would be required to be met in areas where SO_2 primary standards are exceeded in the vicinity of plants selected for conversion. The definition of "vicinity" was generally proposed as 20 kilometers for a large power plant. This distance was chosen following a review of the results of modeling the impact on air quality of the Nation's 670 large fossil-fueled power plants.

EPA's modeling has not been confined to power plants and sulfur dioxide and suspended particulate matter. A great deal of work has been performed to support the development of new source performance standards. Models have been applied to estimate the degree of improvement in ambient air quality that would result from applying stringent emission limitations to a variety of industrial activities. These include: sulfuric acid plants, gray iron foundaries, refuse combustion and waste oil combustion in steam generators, kraft paper mills, phosphate rock processing plants, carbon black plants, asphalt roofing plants and others.

Last fall, it came to light that a rare form of liver cancer occurred among those who worked in or lived near vinyl chloride manufacturing plants. Over 250 individual analyses have been performed to estimate the areas (and population) exposed to a variety of ambient concentrations and to assess the effect of changing manufacturing procedures, the effect of altering the degree of control on various portions of the manufacturing operations, and the effect of different climatological regimes.

Analyses continue to be made to estimate the impact of automobiles on the air environment. In fact, EPA, in cooperation with other governmental agencies is presently completing an analysis of the effect of the automobile on the environment through the year 2000.

Major enforcement actions have dealt with air pollution caused by smelters, power plants, iron and steel mills. Most actions have required use of models to make estimates of the impact of one or more facilities.

The point of these remarks is that models play a vital role in determining required levels of control. In the United States, their use has brought greater understanding of how they may be applied most appropriately. And their credibility is improved as air quality data becomes available with which to more rigorously evaluate their performance. Other papers presented at this meeting will describe evaluation studies that are underway.

In EPA, pressing requirements exist now for analytical techniques to assess the distribution of ozone and oxides of nitrogen. Numerical models to handle these pollutants which react rapidly in the ambient atmosphere will not be generally accepted - cannot be reliable - until the photochemical processes are much better understood. There are also pressing requirements for models which can better represent the distribution of pollutants in complex or rough terrain areas. The Air Resources Laboratory, National Oceanic and Atmospheric Administration has recently issued reports of investigations of dispersion in rough terrain, which will prove helpful.[4,5] Physical modeling - the simulation of dispersion in air and water tunnels - is finding greater use. EPA researchers will soon report on work to determine the appropriate minimum stack height near terrain features. Broadly, the results confirm the usefulness of the 2-1/2 times rule to avoid local pollution problems caused by aerodynamic downwash.

In conclusion, at last year's meetings in Denmark, Mr. Corlin of Copenhagen and Mr. Simmons of California, two highly respected and experienced air pollution control officials, made strong appeals for clear descriptions as to how each model may be applied and for unequivocal statements of the confidence that can be placed in model results.[6,7] Progress has been made to respond to them in a meaningful manner. But it is clear that much must be done before completely responsible answers to their challenges can be made. The proposed work of the NATO/CCMS will produce data on the efficacy of models that will go far in responding to their needs.

REFERENCES

1. Slater, H. H., Applications of Air Quality Models by E.P.A., Procedures of the Fifth Meeting of the Expert Panel on Air Pollution Modeling, NATO/CCMS, N. 35, Aug. 1974, p. 8-1.

2. Scientific and Technical Issues Relating to Sulfates. Ad Hoc Panel of the Science Advisory Board, EPA, Washington, D. C., March 13, 1975.

3. National Academy of Sciences, Air Quality and Stationary Source Emission Control. A Report for the Committee on Public Works, United States Senate, Serial No. 94-4, March 3, 1975. Superintendent of Documents, U. S. Government Printing Office, Washington, D. C. 20402.

4. Start, G. E., D. R. Dickson, L. L. Wendell, Diffusion in a Canyon within Rough Mountainous Terrain, NOAA Tech Memo ERL ARL-38, Air Resources Lab., Idaho Falls, Idaho, Aug. 1973.

5. Start, G. E., N. R. Ricks, C. R. Dickson, Effluent Dilutions Over Mountainous Terrain, NOAA Tech Memo ERL ARL-51, Air Resources Lab., Idaho Falls, Idaho, Dec. 1974.

6. Corlin, A., The Users Need for Precise Description and Verification of a Model, Procedures of Fifth Meeting of Expert Panel on Air Pollution Modeling, NATO/CCMS N. 35, Aug. 1974, p. 15-1.

7. Simmons, W., Comments on Modeler-User Conference, Procedures of Fifth Meeting of Expert Panel on Air Pollution Modeling, NATO/CCMS N. 35, Aug. 1974, p. 40-1.

6th NATO/CCMS
International Technical Meeting
on Air Pollution Modeling

ON THE CALCULATION OF OPTIMAL LONGTERM AIR POLLUTION ABATEMENT STRATEGIES FOR MULTIPLE SOURCE AREAS

by

S.-A. Gustafson, Royal Institute of Technology,
Stockholm, Sweden
and
K.O. Kortanek, Carnegie-Mellon University,
Pittsburgh, USA

BATTELLE - INSTITUT E.V., Frankfurt/Main
Germany, FR
24 - 26 September, 1975

TRITA-NA-7514
Inst för informationsbehandling
KTH
100 44 STOCKHOLM 70

Dept of Information Processing
The Royal Institute of Technology
S-100 44 STOCKHOLM 70, Sweden

ON THE CALCULATION OF OPTIMAL LONGTERM AIR POLLUTION ABATEMENT STRATEGIES FOR MULTIPLE SOURCE AREAS

by

S.-Å. Gustafson

and

K.O. Kortanek *)

---

*) Carnegie-Mellon University,
Pittsburgh, USA

ABSTRACT

In this paper a mathematical model is given which permits the calculation of an optimal long-term air pollution abatement policy. It is assumed that the pollution to be controlled emanates from several sources or groups of sources which may be regulated independently. In our computational scheme we require that the constraints on the choice of abatement policy may be represented as linear inequalities, in general infinitely many. Then an optimal policy may be computed using semi-infinite programming, provided that the preference function is linear or convex. We treat in detail the problem when a maximum pollutant concentration and a maximal permitted deposition rate (annual mean in both cases) are prescribed and one seeks a policy which meets these two standards simultaneously while minimizing total control costs. The scheme is applicable to regulate emissions of sulfur compounds, e.g. SO_2.

1. GOALS FOR LONG-TERM POLLUTION ABATEMENT

Human activity is associated by the release of noxious substances into the environment. It is well-known, that air quality in industrialized areas has detoriated due to increasing concentrations of various pollutants. Therefore, many countries have established standards which define maximum permissible levels for the concentration in the air of certain species like sulfur dioxide, hydrocarbons and so on. See Yanagisawa, 1973. These standards give bounds on the mean concentration for a longer period (a month or a year). They also prescribe that the concentration may temporarily rise beyond given levels during a stated fraction of the time, at most. One could say that the standards on the mean concentration protect against damages due to "attrition" caused by a permanently low air quality while the supplementary rules aim to prevent that the concentration under unfavourable conditions reaches dangerously high levels, which of course is conceivable, even if the mean value is satisfactory. It is clear that temporary drastic measures like shutting down factories and restricting traffic may be taken in order to meet a sudden crisis but that more permanent devices must be relied upon in order to meet the standards on mean concentrations. The air quality at a receptor point cannot be defined by a single number. Instead one must for each point determine a frequency distribution which indicates how often the concentration surpasses certain values. When the mean value is decreased due to control measures the whole frequency curve moves to the left and the frequency of dangerous levels is decreased also. However, we shall not include this effect in our analysis but content ourselves with treating control strategies destined to meet the standard on the mean value. One reason for this is the wellknown fact, that it is often difficult to estimate the tails of a frequency curve with good accuracy. Compare e.g. Fortak, 1974. Therefore, an optimal abatement policy calculated by means of the methods to be described in the sequel must be tested in order to ascertain that the conditions on the frequencies of high concentrations are met. Otherwise the permanent controls must be supplemented with temporary measures. Another possibility would be to lower the permitted mean concentration further than prescribed by the standard in order to decrease the frequencies of high concentrations that way.

It has been observed that pollutants travel long distances with the wind and then are deposited on the ground or in lakes damaging the soil and making the water less favourable for fish-life. See Air pollution ..., 197 and Begränsning av svavelutsläpp, 1974. Mathematical models describing this transportation process have been proposed (Bolin-Persson, 1974). For example the sulfur deposited on the ground in a country may to a certain extent emanate from foreign sources which cannot be regulated domestically. Hence international cooperation is called for in order to reach least-cost solutions. If one knows the proportion of the sulfur released into the air in a certain country that is deposited in each of the other countries, the simple mathematical model in Gustafson-Kortanek, 1975 may be used to calculate reductions policies which meet deposition targets (in the form of maximal deposited amounts for each country) while minimizing combined control costs. In this paper we shall assume that foreign sources cannot be regulated but are represented as a fixed back-ground source. We shall introduce a deposition standard which requires that the deposition per square unit each year is not allowed to surpass a given value. The latter need not be constant over the pollution control area. The goal is to determine an abatement policy which meets simultaneously the standards on concentration in the air and annual deposition on the ground. Optimization problems in the area of air pollution control which are treated by means of linear or semi-infinite programming are described in the referenced papers by Carbone et alias, Gorr, Gustafson, Kohn, Kortanek and Sweigart. The matter is also discussed in Fortak, 1974.

2. MATHEMATICAL FORMULATION OF THE OPTIMIZATION PROBLEM

We consider a fixed area S, henceforth called the control area. S is large and may comprise a whole country. An air quality standard, specified by a function φ is given. We observe that the permitted annual mean concentration may be different in different parts of S.

At a point x in S it is hence $\varphi(x)$. We have also a standard φ_D for the maximum allowed deposition per square unit and year. Thus at x in S the deposition per year must not exceed $\varphi_D(x)$. The pollution appearing in S originates from sources which may be in the control area or outside its boundaries. We split the sources into group $G_0, G_1, \ldots, G_n$ where G_0 is the outside sources and G_r is a group of sources which must be regulated in the same way. Group G_0 cannot be regulated at all, however. If Group G_r releases the amount Q_r of a pollutant into the atmosphere, its contribution to the concentration in the air at x is $Q_r \cdot u_r(x)$, and to the deposition at the same point $Q_r \cdot v_r(x)$. The functions u_r and v_r are called transfer functions. They relate source strength to the contribution of the group to concentration in the air and to deposition rate respectively. The total concentration $\chi(x)$ and deposition rate $\Delta(x)$ at x before regulation are given by

$$\chi(x) = \sum_{r=0}^{n} u_r(x)$$

$$\Delta(x) = \sum_{r=0}^{n} v_r(x)$$

The division of the sources into groups can be based on different principles. The groups may represent different industries (activities) or different categories of owners. Thus one could conceive an example where G_0 is foreign sources, G_1 transportation activities G_2 housing, locally heated, G_3 district heating plants, G_4 steel plants and G_5 remaining industry. Thus the sources within a group may be geographically widely separated. We shall also introduce a standard on the total amount of the pollutant released into the atmosphere within S. It must not exceed Q per annum. Hence no control measures need to be taken if the following conditions are met simultaneously

$$\sum_{r=1}^{n} Q_r < Q$$

$$\chi(x) = \sum_{r=0}^{n} u_r(x) \leq \varphi(x), \ x \in S$$

$$\Delta(x) = \sum_{r=0}^{n} v_r(x) \leq \varphi_D(x),\ x \in S$$

In case of violation we require that the sources in Group G_r cut back their emissions with the fraction E_r, where

$$0 \leq E_r \leq e_r \leq 1,\ r = 1,2,\ldots,n$$

Here e_r is a technical limit on the maximum possible cut back without forcing the shut down of the activities in Group G_r. There is a cost associated with the vector E. We shall denote the combined control cost G(E) and our goal is to render G(E) a minimum while meeting the constraints on combined emissions, air quality, deposition rates and technical constraints on possible cut-backs. We observe that an optimal solution vector E^* in general has components of a different magnitude. The equity problems which might be caused hereby are discussed in Carbone-Sweigart, 1974 and Carbone et al 1975. Other principles of selecting a reductions policy have been proposed in order to avoid this equity issue (See e.g. Gustafson, 1974). If one of these other principles is accepted, then a loss in efficiency occurs. Therefore it must be of interest to compare the control costs of such a more "fair" policy with those of an optimal solution. We remark also, that control measures which change u_r and v_r are not encompassed by our treatment. Hence we do not consider change of stack heights, relocation of sources or redistribution of emissions within the sources of a group.

After reductions as specified by E we get total emissions Q_E, concentration χ_E and deposition rate Δ_E where

$$Q_E = \sum_{r=1}^{n} (1-E_r)Q_r\ ,$$

$$\chi_E = u_0 + \sum_{r=1}^{n} (1-E_r)u_r\ ,$$

$$\Delta_E = v_0 + \sum_{r=1}^{n} (1-E_r)\ v_r\ .$$

The optimal reductions vector E^* is hence an optimal solution of

Program I

Compute inf $G(E)$

subject to

emission condition: $\sum_{r=1}^{n} Q_r(1-E_r) \leq Q$

concentration condition $u_0(x) + \sum_{r=1}^{n} u_r(x)(1-E_r) \leq \varphi(x),\ x \in S$

deposition rate
condition: $v_0(x) + \sum_{r=1}^{r} v_r(x)\ (1-E_r) \leq \varphi_D(x),\ x \in S$

technical
conditions $0 \leq E_r \leq e_r,\ r = 1,2,\ldots,n.$

Program I is said to be consistent, if there exists a vector E meeting all constraints. This occurs if and only if the following conditions are met:

$$\sum_{r=1}^{n} Q_r(1-e_r) \leq Q$$

$$u_0(x) + \sum_{r=1}^{n} u_r(x)(1-e_r) \leq \varphi(x),\ x \in S\ ,$$

$$v_0(x) + \sum_{r=1}^{n} v_r(x)(1-e_r) \leq \varphi_D(x),\ x \in S.$$

If Program I is inconsistent, the standards cannot be met by any permissible control strategy. If Program I is consistent, S is closed and bounded and the functions G, u_0, $u_1,\ldots,u_n$, $v_0, v_1,\ldots,v_n$, φ and φ_D all are continuous over their domains of definition, then optimal solution vectors exist and the infimum value is assumed. These regularity assumptions can always be placed on air pollution control models. In particular, u_r are derived from diffusion models (See e.g. Fortak, 1974 and Hanna, 1971) which only deliver a table of values at a discrete point-set. Therefore it is natural to assume that the corresponding functions are continuous and differentiable. See also Gustafson-Kortanek, 1972.

3. CHARACTERIZATION OF OPTIMAL SOLUTIONS BY MEANS OF THE THEORY OF SEMI-INFINITE PROGRAMMING

In this Section we shall assume that G is linear,

$$G(E) = \sum_{r=1}^{n} E_r \mu_r$$

where μ_r are fixed constants. Our theory may well be extended to the case when G is a general convex and continuously differentiable function. We shall also require that $u_0, u_1, \ldots, u_n$, $v_0, v_1, \ldots, v_n$, φ and φ_D have continuous partial derivatives of the second order. Rewriting the conditions of Program I we arrive at

Program D

Compute min $\sum_{r=1}^{n} E_r \mu_r$

for all E subject to

$$(1) \qquad \sum_{r=1}^{n} E_r Q_r \geq \Psi_Q,$$

$$(2) \qquad \sum_{r=1}^{n} E_r u_r(x) \geq \Psi(x),\ x \in S$$

$$(3) \qquad \sum_{r=1}^{n} E_r v_r(x) \geq \Psi_D(x),\ x \in S$$

$$(4) \qquad E_r \geq 0,\ r = 1,2,\ldots,n$$

$$(5) \qquad -E_r \geq -e_r,\ r = 1,2,\ldots,n$$

where

$$\Psi_Q = \sum_{r=1}^{n} Q_r - Q$$

$$\Psi(x) = \sum_{r=0}^{n} u_r(x) - \varphi(x)$$

$$\Psi_D(x) = \sum_{r=0}^{n} v_r(x) - \varphi_D(x).$$

Remark The conditions of Program D are equivalent to those of Program I. $\Psi_Q, \Psi(x), \Psi_D(x)$ may be interpreted as the excess above the given standards when no reduction is done. Hence the conditions express the fact that the decrease in total emissions, concentration and deposition rate must not be less than the excess.

Program D is a semi-infinite program of the type treated in Gustafson-Kortanek, 1973 and Gustafson 1973. Arguing analogously with Glashoff-Gustafson 1974 we conclude that Program I, if consistent, has the same optimal value as the task:

Program P

Compute max $\gamma\Psi_Q + \sum_{i=1}^{n_c} m_i \Psi(x^i) + \sum_{j=1}^{n_d} \rho_j \Psi_D(t^j) - \sum_{r=1}^{n} \frac{|\beta_r| - \beta_r}{2} e_r$

over all integers n_c, n_d, *all nonnegative numbers* γ, m_i *and* ρ_j, *all real numbers* $\beta_1, \beta_2, \ldots, \beta_n$ *and all points* $x^i \in S$ *and* $t^j \in S$ *subject to the constraints:*

$$\text{sign}(\gamma) + n_c + n_d + \sum_{r=1}^{n} \text{sign}\,(|m_r|) \le n,$$

$$\gamma Q_r + \sum_{i=1}^{n_c} m_i u_r(x^i) + \sum_{j=1}^{n_d} \rho_j v_r(t^j) + \beta_r = \mu_r, \quad r = 1,2,\ldots,n$$

Here the function sign is defined by $\text{sign}(z) = 1$, if $z > 0$ $\text{sign}(z) = -1$, if $z < 0$ and $\text{sign}(z) = 0$, if $z = 0$.

Using the results on complementary slackness we also find that the optimal solutions of Programs P and D satisfy the relations:

$$\gamma\left\{\sum_{r=1}^{n} E_r Q_r - \Psi_Q\right\} = 0 \tag{6}$$

$$m_i\left\{\sum_{r=1}^{n} E_r u_r(x^i) - \Psi(x^i)\right\} = 0, \quad i = 1,2,\ldots,n_c, \tag{7}$$

$$(8) \qquad \rho_j \left\{ \sum_{r=1}^{n} E_r v_r(t^j) - \Psi_D(t^j) \right\} = 0, \; j = 1,2,\ldots,n_d,$$

$$(9) \qquad \frac{|\beta_r|+\beta_r}{2} E_r = 0, \; r = 1,2,\ldots,n.$$

$$(10) \qquad \frac{|\beta_r|-\beta_r}{2} (e_r-E_r) = 0, \; r = 1,2,\ldots,n.$$

These relations admit a physical interpretation. Thus if $\beta_r > 0$, then (9) entails $E_r = 0$, that is Group G_r shall not reduce its emission. But if $\beta_r < 0$ maximum possible cut-back, namely e_r is called for according to (10). $\beta_r = 0$ means that the reduction fraction E_r satisfies $0 < E_r < e_r$. If $\gamma = 0$, then the optimal solution passes the requirement on total emissions with a margin, but $\gamma > 0$ implies that this constraint is active. $m_i > 0$ implies that

$$\sum_{r=1}^{n} E_r u_r(x^i) = \Psi(x^i)$$

or

$$\sum_{r=1}^{n} (1-E_r)u_r(x^i) = \varphi(x^i).$$

That means that after reduction the standard on concentration is exactly met at x^i. (7) implies that there are at least n_c such points. In the same way we conclude that the deposition rate exactly meets the standard at the n_d points t^j. We now make the observation: the function

$$(11) \qquad u_0 + \sum_{r=1}^{n} (1-E_r)u_r - \varphi$$

must be nonpositive everywhere and it assumes the value 0 at x^i. Thus we conclude

(12) The function (11) has a local maximum at x^i, $i = 1,2,\ldots,n_c$.

In the same way we find

(13) The function $v_0 + \sum_{r=1}^{n} (1-E_r)v_r - \varphi_D$ has a local maximum at t^j, $j = 1,2,\ldots,n_d$.

From (12) and (13) we get conditions involving derivatives, e.g. if x^i and t^j lie in the interior of S. If we combine (6) through (10) with relations generated by (12) and (13), we get a nonlinear system from whose solutions an optimal abatement strategy can be determined. One easily verifies that the number of equations and unknowns agree, e.g. if x^i and t^j all are in the interior of S. We remark also that the point-sets $\{x^i\}$ and $\{t^j\}$ may or may not be disjoint.

4. COMPUTATIONAL DETERMINATION OF OPTIMAL ABATEMENT POLICIES

A direct attack on the Equations (6) through (10) combined with (11) and (12) is generally not feasible since neither the integers n_c and n_d are known nor the equations generated by (11) and (12). Instead, the computational treatment is carried out in two phases: A and B. In Phase A n_c and n_d are determined together with approximations to the optimal solutions of Programs P and D. In Phase B these approximations are improved by solving the nonlinear system generated by (5) through (13) with a numerical procedure, e.g. Newton-Raphson's method. See Gustafson-Kortanek, 1973. Often the approximation obtained in Phase A is sufficiently accurate for practical purposes.

In Phase A we discretize Program D, that is we replace (2) and (3) by finite sets of inequalities. Then we get

Program $\tilde{D}$

Compute min $\sum_{r=1}^{n} E_r\mu_r$

for all E *subject to*

$$(1)' \quad \sum_{r=1}^{n} E_rQ_r \geq \Psi_Q$$

$$(2)' \quad \sum_{r=1}^{n} E_ru_r(\xi^\ell) \geq \Psi(\xi^\ell),\ \ell = 1,2,\ldots,N_c$$

$$(3)' \quad \sum_{r=1}^{n} E_rv_r(\tau^p) \geq \Psi_D(\tau^p),\ p = 1,2,\ldots,N_d$$

(4)' $E_r \geq 0$, $r = 1,2,\ldots,n$

(5)' $-E_r \geq -e_r$, $r = 1,2,\ldots,n$

where Ψ_Q, Ψ *and* Ψ_D *are defined as in Program* D, N_c *and* N_d *are fixed integers, and* $\{\xi^\ell\}$, $\{\tau^p\}$ *are point-sets in S.*

Program $\tilde{D}$ may be solved using a linear programming code. It is important to realize that all vectors E meeting the constraints of Program D a fortiori meet the constraints of Program $\tilde{D}$. Therefore the optimal value of the latter Program is not larger than that of the former. But a reductions vector E meeting Conditions (2)' and (3)' might violate the standards at points not belonging to the sets $\{\xi^\ell\}$ and $\{\tau^p\}$. This fact is the basis of an analysis of the error committed when replacing Program D with Program $\tilde{D}$. Compare Gustafson-Kortanek, 1973 and Fahlander-Gustafson-Olsson, 1974. We discuss a particular case: Let $\{\xi^\ell\}$ and $\{\tau^p\}$ be rectangular grids and assume that $u_1,u_2,\ldots,u_n,v_1,v_2,\ldots v_n$, Ψ and Ψ_D are linear within each subrectangle. Then we verify directly that Conditions (2), (2)' and (3), (3)' are equivalent. Thus, if we interpolate $u_1,u_2,\ldots,u_n,v_1,v_2,\ldots,v_r$, Ψ and Ψ_D linearly and neglect the interpolation errors, then Programs D and $\tilde{D}$ are equivalent. Hence we have, by coincidence found a connection between linear interpolation and linear programming.

Computational experiments with semi-infinite programming applied to environmental problems are reported by Carbone et al 1975, Fahlander-Gustafson-Olsson 1974, Gustafson-Kortanek 1973 and Sweigart 1974. Worked examples illustrating the use of semi-infinite programming for optimal control problem governed by partial differential equations are given in Glashoff-Gustafson, 1974. Fahlander, 1973 gives several solved examples on semi-infinite programming, including one with a nonlinear convex preference function.

4. CONCLUSION

Optimization problems in environmental protection may be formulated and successfully solved thus providing a rational basis for the choice of abatement policy. Computer codes, now in existence, can be applied to handle problems governed by linear diffusion models.

ACKNOWLEDGEMENT

This research was financially supported by The National Science Foundation, USA under Grant Gk-31833 and by The Environmental Protection Agency, USA.

REFERENCES

Air pollution across national boundaries. Sweden's case study for the UN conference on the human environment. P.A. Norstedt och Söner, Stockholm, 1971

Begränsning av svavelutsläpp - en studie av styrmedel, SOU 1974:101, Allmänna Förlaget, Stockholm, 1974 (Summary in English).

Bolin B. and C. Persson, Regional dispersion and deposition of atmospheric pollutants with particular application to sulfur pollution over Western Europe, Rep AC-28, International Meteorological Institute in Stockholm, 1974. To appear in Tellus.

Carbone, R. and J.R. Sweigart, Equity and selective pollution abatement procedures, Series in numerical optimization and pollution abatement, No 17, School of Urban and Public Affairs, Carnegie-Mellon University, Pittsburgh, Penn 15213, 1974

Carbone, R., W.L. Gorr, S.-Å. Gustafson, K.O. Kortanek and J.R. Sweigart, Environmental-energy-equity models for resource management in an airshed, Series in numerical optimization and pollution abatement, School of Urban and Public Affairs, Carnegie-Mellon University, Pittsburgh, Penn 15213, 1975

Fahlander, K., Computer programs for semi-infinite optimization, TRITA-NA-7312, Department of Information Processing, Royal Institute of Technology, 100 44 Stockholm 70, Sweden, 1973

Fahlander, K., S.-Å. Gustafson and L.E. Olsson, Computing optimal air pollution abatement strategies - some numerical experiments on field data, Proceedings of the 5th meeting of the NATA/CCMS expert panel on air pollution modeling, chap 27, 1974

Fortak, H., Potential applications of mathematical-meteorological diffusion models to the solution of problems of air quality maintenance, Proceedings of the 5th meeting of the NATO/CCMS expert panel on air pollution modeling, chap 7, 1974

Glashoff, K. and S.-Å. Gustafson, Numerical treatment of a parabolic boundary-value control problem, TRITA-NA-7409, Department of Information Processing, Royal Institute of Technology, 100 44 Stockholm 70, Sweden, 1974, to appear in JOTA

Gorr, W., S.-Å. Gustafson and K.O. Kortanek, Optimal control for air quality standards and regulatory policy, Environment and Planning 4 (1974), 183-192

Gustafson, S.-Å., Nonlinear systems in semi-infinite programming, in (C.B. Byrnes and C.A. Hall, Eds), Numerical solution of systems of nonlinear algebraic equations, Academic Press, 1973, 63-99.

Gustafson, S.-Å., Optimization problems in air quality control, Methods of Operations Research, to appear, (1974)

Gustafson, S.-Å. And K.O. Kortanek, Analytical properties of some multiple-source urban diffusion models, Environment and Planning 4 (1972), 31-41

Gustafson, S.-Å. and K.O. Kortanek, Numerical treatment of a class of semi-infinite programming problems, NRLQ 20(1973), 477-504

Gustafson, S.-Å. and K.O. Kortanek, Mathematical models for air pollution control: Numerical determination of optimizing policies, in (R.A. Deininger, Ed), Models for Environmental Pollution Control, Ann Arbor Science Publishers, 1973, 251-265

Gustafson, S.-Å., and K.O. Kortanek, On the calculation of optimal long-term air pollution abatement strategies for multiple source areas, International Conference on Mathematical Models for Environmental Problems, University of Southampton, UK, Sept 1975

Hanna, S.R., A simple method of calculating dispersion from urban area sources, JAPCA 21 (1971), 774-777

Kohn, R.E., Optimal air quality standards, Econometrica 39 (1971), 983-995

Sweigart, J.R., Practicable tools for initial studies in air pollution abatement, Series in numerical optimization and pollution abatement, No 15, School of Urban and Public Affairs, Carnegie-Mellon University, Pittsburgh, Penn 15213, 1973

Yanagisawa, S., Air quality standards, national and international, JAPCA 23 (1973), 945-948.

Rapporteur's Report, Topic I, September 24, 1975
by K. E. Grønskei

H. H. Slater: EPA's Use of Dispersion Models for Control and Enforcement.

Discussion:

W. B. Johnson asked whether the degree of sulphate pollution to be considered in relation to the significant deterioration aspect was quantified by measurements.
Slater confirmed this and pointed out that consistently high suplphate concentrations were obeserved in 24 states in the northeastern part of U. S. A. No sulphate standards have been promulgated, but evidence of the health risk from this component has been documented. On this basis steps have been taken not to allow unnecessary SO_2-emissions, as these are sulphate precursors.

It was further pointed out on a question from D. Jost that model calculations carried out by different groups in the U.S.A., are a part of the information on which the decisions on air pollution control actions are made.

At the end of the discussion it was pointed out on a question from K. E. Grønskei (Norway) that in the U.S.A. no guidelines have been yet adopted as to how stack height should be used as an air pollution control method. EPA requires that "reasonable efforts" is made to reduce the amount of emission before stack height requirements are considered. Reasonable efforts are implicit in the new source performance standards for various types of industrial sources. For existing sources, "reasonable efforts" are assessed for each individual case.

S. A. Gustavson: On the Calculation of optimal Long-Term Air Pollution Abatement Strategies for Multiple Source Areas

Discussion:

H. Fortak asked how deposition velocities were calculated. Gustavson answered that work by professor Bolin would be used as a part of the basis for this development, but that the details on this have not yet been worked out.

6th NATO/CCMS
International Technical Meeting
on Air Pollution Modeling

Using Line Sources for the Simulation of Area Sources

by

Klaus Herrmann
Technische Hochschule
Darmstadt
Institut für Meteorologie

Battelle-Institut e.V.,Frankfurt/Main
Germany,F.R.
24-26 September,1975

Preceding page blank

Abstract

The Gifford-Hanna-model allows the simulation of area sources in a simple way,because the area sources are treated as ground level sources.This method is not applicable in some cases,in which an area source represents a greater number of small,elevated point sources (as for example the heating emission for SO_2-simulations) and an area weighted source height has to be attached to the source grid.
The paper shows,that the influence of this source height can be neglected only for great grid distances.For all cases,in which small grid distances are given by the emmission inventory, (as for example in Germany,F.R.) the height of the area source becomes an important parameter.For those cases another method is introduced,based on Gifford's concept of simulating area sources by crosswind line sources,but now including the source height parameter

Using Line Sources for the Simulation of Area Sources

by Klaus Herrmann

1.) Introduction

One of the many problems connected with urban air pollution modeling is the simulation of area sources.A number of successful but rather complicated and computer-time-consuming methods have been introduced during the last years,as for example the method of an upwind the area source located single point source by Martin and Tikvart,or the Fortak-method of building up an area source by equally distributed point sources.
In contrast the Gifford-model gave a very simple solution by using the 'Narrow Plume' concept and the line source formula ((3) and (4)).The applications of this simple model in the USA were rather successful,but a test in Germany (7) showed, that the assumption of the model (all area sources are ground level sources) is not valid for small grid distances if the area source represents a number of elevated point sources,like the heating emissions, with a real source height.
Limitations of the assumptions of the Gifford-model are introduced in chapter 3.
Starting with the 'Narrow Plume' concept and using small grid

distances,a new method is introduced,that includes the source height parameter.The model requires more computational effort than the Gifford-model,but in comparison with other methods it gives a simple solution for the area sources.The application for long time averaged concentration values using a wind direction distribution is very simple and allows the direct use of a 36-part wind direction scale.

A test of the new model in Germany (7) gave good results,comparable to those of the more complicated models,but reducing computer time considerably.

2.) Gifford's line source method

The details of a concentration field simulated by a multiple source diffusion model are determined to a large degree by the details in the emission inventory.Since the smaller sources within one quadrant are not treated individually but collectively,the details depend on the grid size.The same is true for the concentration field where the concentration in the center of a quadrant is representative for the concentration within it.This gives rise to the 'Narrow Plume' concept, where the changes in concentration in crosswind direction are neglected.The 'Narrow Plume' concept allows the simulation of an area source by crosswind line sources (1).The two-dimensional plume of one of these line sources is given by the Gauß-formula:

①
$$C_L = \frac{Q_L}{u\sqrt{2\pi}} \cdot F(x,z,H,s)$$

(1a)
$$F(x,z,H,s) = \left[\exp\left\{-\frac{(z-H)^2}{2\sigma^2}\right\} + \exp\left\{-\frac{(z+H)^2}{2\sigma^2}\right\}\right] / \sigma$$

$$\sigma = \sigma_z = a_s \cdot x^{b_s}$$

with index s showing the dependence of σ on atmospheric stability,given as stability classes (5).

To come to an area source model one has to consider a row of area sources upwind the receptor (see figure 1),the concentration at which is given by

$$C_A = C_o + C_1 + C_2 + \ldots + C_k + \ldots + C_N$$

A single concentration contribution of grid k is given by the sum of the concentrations of the line sources within the grid:

$$② \quad C_K = \int_{xu(k)}^{xo(k)} C_L \, dx = \frac{Q_A(K)}{u\sqrt{2\pi}} \cdot \int_{xu(k)}^{xo(k)} F(x,z,H,s)\, dx = \frac{Q_A(K)}{u\sqrt{2\pi}} \cdot \mathcal{J}_K(z,H,s)$$

with integration limits

$xo(k) = (2k+1)\cdot DX/2$ $\qquad$ $xu(k) = (2k-1)\cdot DX/2 \quad k=1,2,3,\ldots$

$xu(0) = 0$

The concentration at the receptor can be written as:

$$C_A = u/\sqrt{2\pi} \cdot (Q_o I_o + Q_1 I_1 + Q_2 I_2 + \ldots + Q_k I_k + \ldots + Q_N I_N)$$

Figure 1: The row of area sources upwind of the receptor. The index k starts with 0 from the receptor grid.

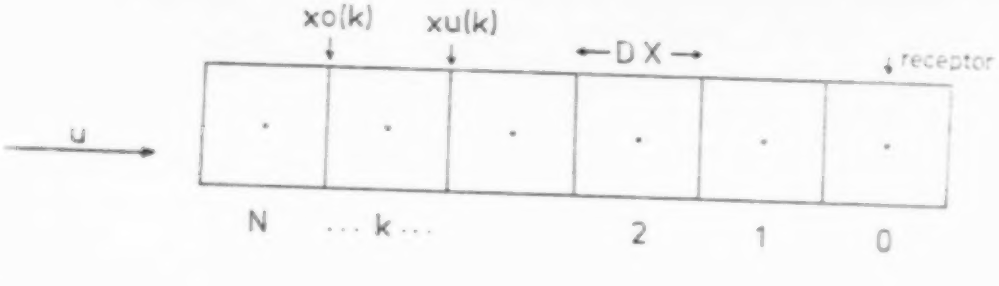

3.) Assumptions of the Gifford-model

To find simple solutions of the integrals I_k, more assumptions are necessary, which can best be explained by looking upon the function F, given for various source heights and stability classes in figure 2. The influence of the source height disappears a few kilometers downwind from the source depending on source height and then F(H) approaches F(H=0). The assumption H=0, z=0 for all area sources allows a direct solution of the integrals and gives the Gifford-model.

Looking upon figure 2 one can recognize,that the smaller the grid distance must be chosen the greater is the difference between $I_k(H)$ and $I_k(0)$;the relative integration error can be identified as the area between the two curves $F(H)$ and $F(0)$ related to the area below $F(H)$.The greater the interval of integration (that is the grid distance),the less important is the error.

The assumption $H=0,z=0$ for all area sources results in an overestimation of the concentration.This overestimation increases with source height and stability and decreases with grid spacing.

4.) The influence of the source height

The integrals $I_k(H)$ can be solved as exact as required by numerical methods (Romberg-method or others).For the receptor grid with the index $k=0$ a $\sigma(x=0)=c=\text{constant}$ must be used, because F is not defined for $x=0$.The integral values do scarcely depend on the constant c (for $0.1 \le c \le 5$) as long as $|z-H| \ge 1\text{m}$,a condition that can easily be met.

An impression of the influence of the source height depending on grid distance is given by Table 1.For various stability classes (Smith-Singer-classes as used by Gifford) the index of that grid (compare fig.1) is tabled,where first the condition $|I_k(H)-I_k(0)|/I_k(0)<1\%$ is met,meaning that the Gifford-model gives the same solution.

Table 1: Index k of that grid (compare fig.1),where first the condition $|I_k(H)-I_k(0)|/I_k(0)<1\%$ is met.The first number asigns a grid length of DX=10km,the second DX=5km,and the third DX=1km.

H	very unst.			unstable			neutral			slightly st.			stable		
10m	1	1	1	1	1	1	1	1	2	1	1	4	3	5	22
20m	1	1	1	1	1	2	1	1	4	2	2	10	6	12	55
30m	1	1	2	1	1	2	1	1	6	2	4	16	10	21	99

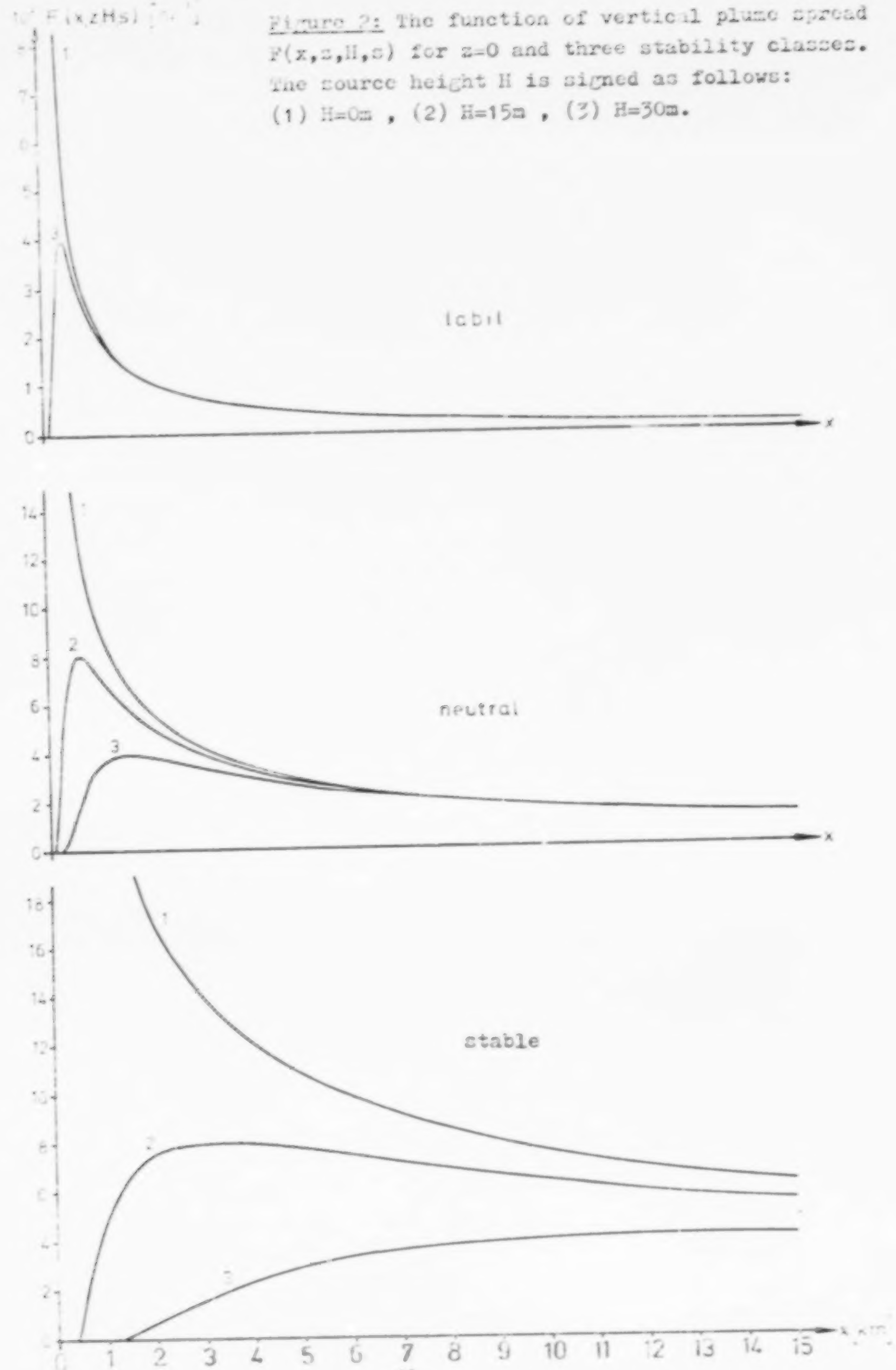

Figure 2: The function of vertical plume spread $F(x,z,H,s)$ for $z=0$ and three stability classes. The source height H is signed as follows: (1) $H=0m$, (2) $H=15m$, (3) $H=30m$.

For great grid distances (DX=5km or DX=10km) best agreement is reached very near the receptor except in the stable class. Against that for the small grids of DX=1km or less as were used in Germany,F.R. this agreement is reached only at greater distances from the receptor,saying that in this cases the source height has become an important parameter.

Figure 3 gives the values of the relative difference of the integrals as a function of the source height H and grid distance DX for the stable classes,where the effect is mostly pronounced.

5.) A simple model for small grids

To consider the source-height in the model,the integrals I_k must be solved in a simple way.Using the fact of small grids, F can be treated as linear in the interval [xo(k),xu(k)] for $k > 0$ and the integrals are then given by the approximation

$$\int_{xu(k)}^{xo(k)} F(x,z,H,s)\,dx = F(xm_k,z,H,s) \cdot DX$$

where $xm_k = (xu(k) + xo(k))/2$.

This approximation is the better the smaller the grid distances are and the greater the stability is.

The integrals of the receptor grid must be solved numerically as it was mentioned in chapter 4.These calculations have to be done once to get a table of 75-80 $I_0(H)$-values for some source heights and the five or six stability classes.The table can be used in every further application for the estimation of $I_0(H)$,as it is shown in formula 3a.

For the calculation of annual or seasonal averaged concentration values all the surrounding sources have to be considered and the integral-estimation allows a very simple method (see fig.4).The concentration contribution of a source with index i to the receptor is then given by $I_i = F(R) \cdot DX$

Denote the synoptic meteorological data set windspeed,winddirection and stability class with ff,dd,kk and the frequency with which they appear with Hfkt(ff,dd,kk),the calculations will proceed as follows:

Figure 3: Relativ difference between the integral values $I_k(H)$ (numerical solution) and the $I_k(0)$ (Gifford-model) as a function of source height H for the first (k=1) and the second (k=2) grid. (1) DX=1km , (2) DX=5km , (3) DX=10km.

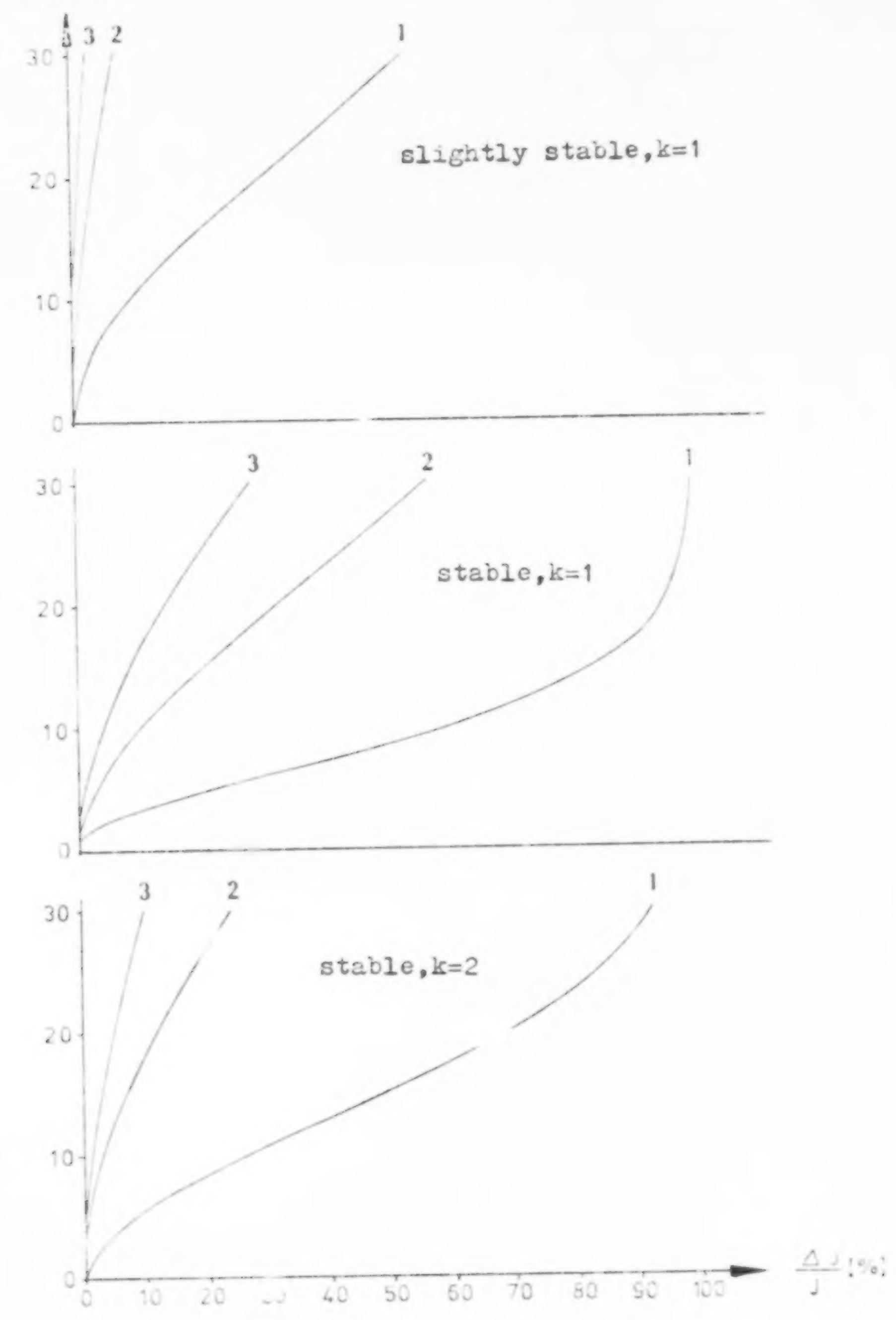

③ $$\bar{C}_A = C_o + \sum_i C_i$$

③a $$C_o = \frac{Q_o}{\sqrt{2\pi}} \cdot \sum \cdot J_o(H,kk) \cdot \sum_{dd} \sum_{ff} \frac{Hfkt(ff,dd,kk)}{u(ff)}$$

$$J_o(H,kk) = Tab(IH,kk)$$

③b $$C_i = \frac{Q_i}{\sqrt{2\pi}} \cdot \sum_{kk} \sum_{ff} \frac{J_i(H,kk)}{u(ff)} \cdot Hfkt(ff,dd,kk)$$

$$J_i(H,kk) = F(R,H,kk) \cdot DX$$

$$dd = \arcsin(Y_i/R) = \arccos(X_i/R)$$

Figure 4: Calculation of direction and distance of surrounding grids if a wind direction distribution is used.

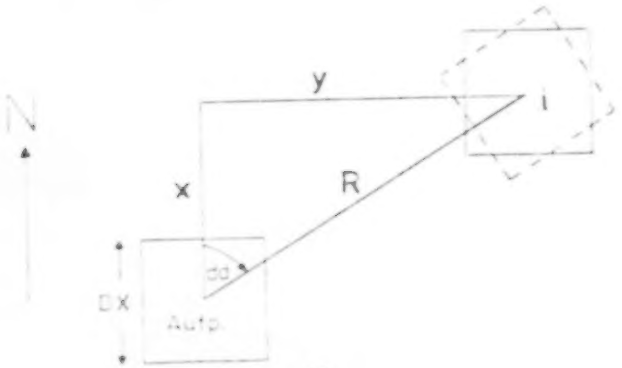

6.) Comparison with the Fortak-model

The Fortak-method (3) of simulating an area source by equally distributed point sources is equivalent to the numerical solution (if the point source density per grid is high enough), so that a comparison with this model can show,how the assumptions 'Narrow Plume' and 'Integral Estimation' change the pattern for small grid lengths.

The concentration distribution of a single area source shows even for small grids of 0.5km,that very small concentrations are computed at receptor points located not directly downwind of the source grid.These concentrations are only a few percent of the center line values,so that the 'Narrow Plume'-concept is also valid for small grid spaces.

To demonstrate the influence of the simple integral estimation and the effect of 'Narrow Plume',statistics of the differences between the two models were made as follows:For a constant wind direction and a source distribution of 20x15 grids the concentration patterns have been calculated for ten various source strength and source height distributions in each stability class.The relative difference between the two models for each case and each grid have been summarized to a statistical error distribution for each stability class,shown in figure 5.For stable and neutral stability the differerces are too small to be plotted.

Using now various wind direction distributions and going the same procedure,a curve like that signed with 1 has been found for grid lengths DX=1km and DX=0.5km.

The differences between the two models (that is the error caused by the integral estimation and the 'Narrow Plume') are not very important and they appear only in those stability classes in which small ground level concentrations can be found.

These results give rise to the hope for a successful application of the simple model for German urban air pollution modeling with smaller grid sizes.As it has been shown in (7), the model gave rather successful results for the test-region Frankfurt,comparable to the results of more complicated models with much more computer effort.

Figure 5: Cumulative frequency of the differences between the simple model and the Fortak-method (the point source density for an area source is chosen so high, that this method corresponds to the numerical solution) for various stability classes and the grid distances DX=1km and DX=0.5km.

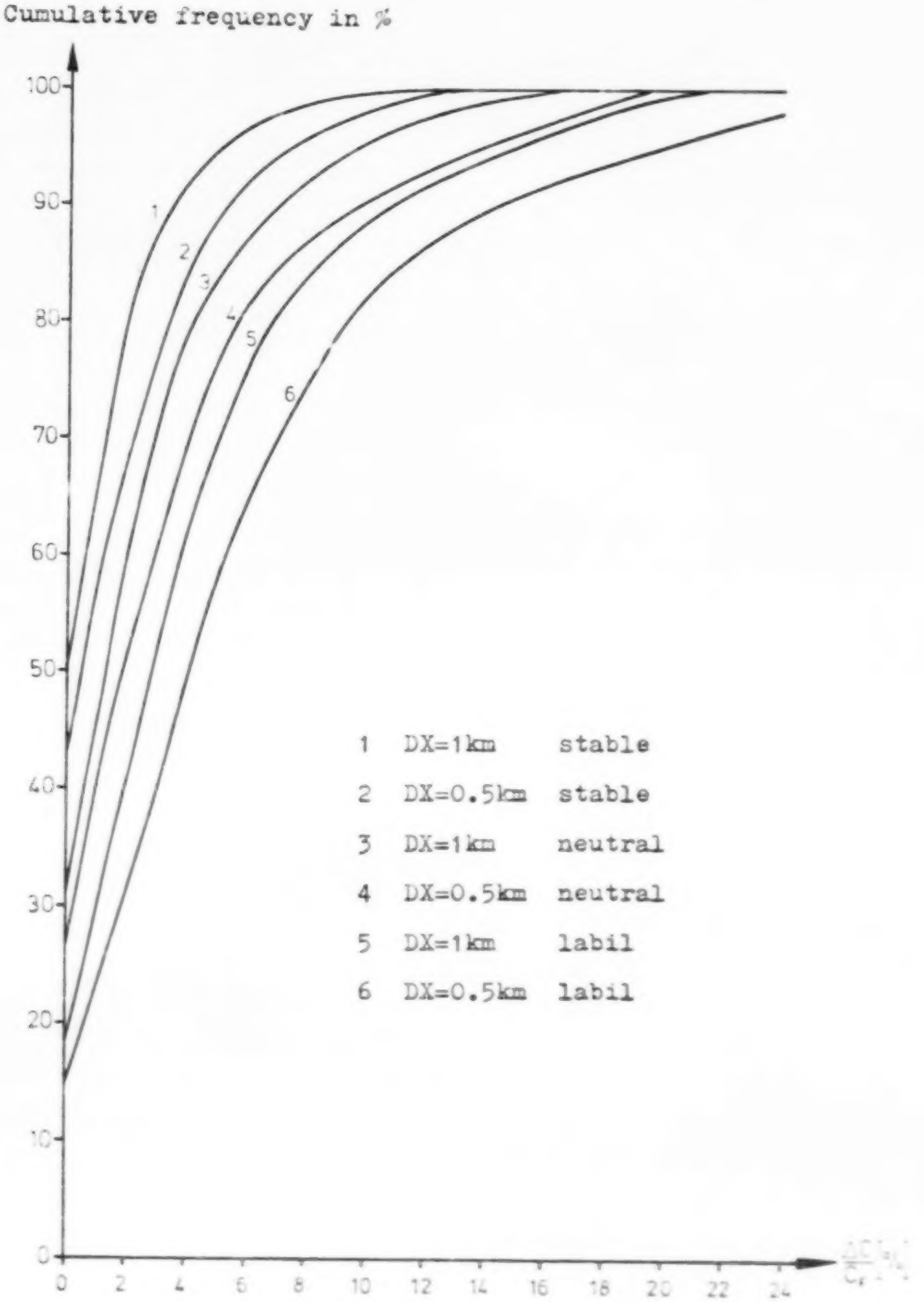

References

(1) K.L. Calder
A Climatological Model For Multiple Source Urban Air Pollution
in: Air Pollution, Proceedings of the 2nd meeting of the expert panel on air pollution modeling

(2) H. Fortak
Anwendungsmöglichkeiten von mathematisch-meteorologischen Diffusionsmodellen zur Lösung von Fragen der Luftreinhaltung (herausgegeben vom Minister für Arbeit, Gesundheit und Soziales des Landes Nordrhein-Westfalen, Düsseldorf, 1972)

(3) F.A. Gifford
1. Applications Of A Simple Urban Pollution Model
   in: Proceedings of the conference on urban environment and second conference on Biometeorology, Philadelphia, Pa., 1972
2. The Simple ATDL Urban Air Pollution Model
   in: Proceedings of the 4th meeting of NATO/CCM panel on modeling, 1973
3. Atmospheric Diffusion In An Urban Area
   in: Proceedings of the 2nd IRPA conference Brighton, England, 1970
4. Urban Air Pollution Modeling
   in: paper presented at 1970 International Air Pollution Conference of the International Union of Air Pollution Prevention Associations

(4) S.R. Hanna
1. Description Of ATDL Computer Model For Dispersion From Multiple Sources
   in: Proceedings of the 2nd annual Industrial Air Pollution Control Conference, University of Tennessee, Knoxville, 1972

(4) S.R. Hanna

2. Application Of A Simple Dispersion Model To A Rural Industrial Region
in: Proceedings of the 3rd annual Industrial Air Pollution Control Conference,University of Tennessee, Knoxville,1973

3. An Air Quality Model For Knox County, Tennessee
in: Paper of Air Resources Atmospheric Turbulence and Diffusion Laboratory, National Oceanic and Atmospheric Administration,Oak Ridge,Tenn.

4. Air Pollution Meteorology Of The Rockwood-Harriman,Tennessee,Valley
in: see 3.

(5) W. Klug

Ein Verfahren zur Bestimmung der Aus=breitungsbedingungen aus synoptischen Beobachtungen
in: Staub,Reinhaltung der Luft 29 (1969) Nr.4 (April)

(6) K. Herrmann

Vergleich von Ausbreitungsmodellen für Flächenquellen
Diplomarbeit (unveröffentlicht) an der Technischen Hochschule Darmstadt,April 1974

(7) J. Strott
K. Michelmann
A. Braig

Vergleich von Rechenmodellen zur Aus=breitungsrechnung
in: Battelle-Bericht (herausgegeben vom Battelle-Institut e.V.,Frankfurt/Main),4 Bände von 1974-1975

list of parameters

x, y, z	Cartesian coordinates (m)
H	source height (m)
Q_A	area source strength (g/m^2sec)
Q_L	line source strength (g/msec)
u	averaged wind speed (m/sec)
s	index for stability class
$F(x,z,H,s)$	vertical dispersion function of the Gauß-formula (m^{-1})
σ	standard deviation of the vertical dispersion (m)
k	index for signing an area source relativ to the receptor
DX	grid length (m)
xu(k)	lower grid limit of an area source (m)
xo(k)	upper grid limit of an area source (m)
N	number of the upwind area sources
xm(k)	distance of the center of an area source from the receptor (m)
R	the same as xm,but used for cases with a wind direction distribution (m)
ff	wind speed (kn)
dd	wind direction (degr.)
kk	index for stability class
Hfkt(ff,dd,kk)	frequency of meteorological condition ff,dd,kk
i	index for area sources around the receptor

6th NATO /CCMS
International Technical Meeting
on Air Pollution Modeling

Results of the Revised ATDL-Model Compared with the Results of the AQDM- and CDM-Models

by

A. Braig
Battelle-Institut e. V. Frankfurt /M

Battelle-Institut e. V. Frankfurt /M
Germany, FR
24 - 26, September 1975

Introductory remarks

For two years a team of mathematicians and physicists have been developing diffusion models in collaboration with the Institut für Meteorologie, Darmstadt. The first goal was to test and evaluate diffusion models for European conditions and to check the difference between the so called "sophisticated" and "simple" models. Variations of the AQDM /1,2/ and the ATDL /3/ model were tested and applied to the Frankfurt area. The AQDM gives a good estimate of the ground level concentration, whereas the results of the ATDL-model were unreliable. However since the computation time for the ATDL-model was by a factor of 20 less than the computation time for the AQDM, the ATDL model should be modified. For a critical examination of the performance of the AQDM and ATDL-model the CDM /4/ was tested too. In the following the different approaches of the three models are described and the results of the application to Frankfurt are analyzed statistically.

Some different aspects of the three models

All three models are based on the Gaussian plume formula. The common assumption is that the meteorological conditions can be regarded as steady-state and that these conditions may be adequately approximated with a unique horizontal mean wind direction and uniform wind speed for the entire urban area. For calculating the concentration resulting from point sources, all three models use the same formula. In the ATDL model, however is a restriction for the location of the point sources: they are located in the centre of an area source.

In the original version of the AQDM Holland's plume rise formula is used. However, we replaced the old plume rise formula with the more recent ones suggested by Briggs. In the CDM- and ATDL-model also the Briggs-formula is used.

Contrary to point sources the modeling of area sources is different for the three models.

The AQDM-model handles area sources by converting them to equivalent or "virtual" point sources.

In the CDM-model area sources are calculated using the narrow plume hypothesis applied for winds within a sector which involves an upwind integration over the area sources within a sector.

To obtain the concentration contribution at the receptor being originated by the area sources distribution it is necessary to perform a double integration with respect to the circular arc ϑ and radial distance ϱ . The narrow plume hypothesis is also underlying the ATDL model. But in this model a double integration has not been performed. The variation in the cross-wind direction of the source-strength pattern is ignored and therefore merely an integration in the upwind direction of a cross-wind infinite line-source diffusion formula is necessary. The application of the original version of the ATDL-model gave an overestimation of the concentration. However the computation time for the ATDL model was by a factor of 20 smaller than the computation time for the AQDM. Therefore, a modification of the ATDL-model was made /6/ taking into account the following points:

- three dimensional frequency distribution of meteorological parameters

- variable height of the area sources

- simplified calculation of concentration resulting from area sources outside the domain of the receptor-point /7/

- integration of the line source diffusion formula in those cases in which a receptor point is located in the center of an area source.

Model input data and parameters

All three models are based on the assumption that the meteorological conditions can be regarded as steady and uniform over the entire urban area and can be described by a joint frequency function of wind direction, wind speed and stability category. In our case the frequency function was derived from the statistics of the Rhein-Main-Airport. The values of the standard deviation function σ_z used in the application of the AQDM and ATDL model are those of Pasquill ($\sigma_z = ax^b$). In the CDM those of Pasquill and Gifford are chosen (s. Table 1). However to incorporate the thermal and mechanical influences of the urban area two types of correction of σ_z are used in the CDM. It has to be mentioned that in the urban air pollution model of the CDM an initial value of 30 meters for σ_z is assumed for low level-area sources. On the contrary in the AQDM the effect of the initial σ_0 is implemented by using a virtual source regarding the σ_0-values as the result of diffusion from an imaginary source located upwind of the real source.

Only in the AQDM and CDM the mixing depth is a model parameter.

It is not usual to apply any correction for plume rise to area sources. But because the ATDL-model has overestimated the contribution of the central area a detailed analyses was performed. The result of this analysis was one should estimate the plume rise for area sources as a function of the stability category.

Application of the models and discussion of the results

The models were applied to the calculation of annual mean SO_2-concentration in an area of 10 km x 19 km which includes the City of Frankfurt. The emission inventory and immission data were compiled by the RPU /5/. In the area-source emission inventory each square is 500 m x 500 m and therefore for the ATDL-model a special conversion on a grid of 1 km x 1 km was necessary. To save computer time, all emission from point sources emitting less than 5 kg SO_2/h where added to area sources. Only 46 point sources with emissions of more than 5 kg SO_2/h were considered individually (altogether 350 point sources are recorded in the emission inventory).

The results of the calculations of the different models are given in Figures 1-3 as isopleths of average pollution concentrations ($\mu g/m^3$). Figure 4 illustrates a comparison of observed and calculated annual mean concentrations.

To evaluate the three different models, 12 different statistics /4/ were used. The results of the comparison of model estimates with measurements are given in Table 2.

Figure 5 shows the regression lines of observed versus calculated average SO_2 concentrations.

In Table 3 the actually 95 % value for the concentration frequency distribution to those calculated for three stations are compared. The AQDM and the ATDL-model overestimate the 95 %-values in all stations, the CDM underestimate the 95 %-values.

It is worth mentioning, that all results were obtained without calibration of the models.

The calculations of average air quality were made usimg a Burroughs B6700 computer and the ratio of running times was 2:1 for CDM vs. AQDM and 4:1 for AQDM and ATDL-model (s. Table 4).

Conclusions

There is no model that is superior in all statistics. The AQDM gives a good estimate for the mean concentrations and there is no significant difference between the standard deviation of the AQDM and the measured values. The CDM-model underestimates the mean concentration but the standard deviation is the same as that of the measured values and therefore a calibration of the CDM would give a positive correction of the results. The ATDL-model overestimates both the mean concentration and the maximum SO_2 concentration. The mean absolute error is somewhat larger than those of the other two models.

Considering the running times of the models and the obtained results the modification of the ATDL-model has increased the performance of this model.

As to the future the AQDM and the other are currently subject of an input-output sensitivity analysis /8/, which will lead to an improvement of the performance of all three models.

Reference

/1/ TRW Systems Group
Air Quality Display Model (1969),
Contract No PH 22-68-60 USDHEW
Public Health Service, NAPCA, Washington, D.C.

/2/ J.A. Tikvart, D.O. Martin
A general atmospheric diffusion model for
estimating the effects of one or more sources
on air quality
Annual meeting of the Air Pollution Control
Association, June 1968

/3/ F.A. Gifford, St.R. Hanna
Urban Air Pollution Modeling
Proc. 2nd Int. Clean Air Congress
H.M. England and W.T. Bury, Eds. 1146-1151

/4/ A.D. Busse, J.R. Zimmermann
User's guide for the Climatological Dispersion Model
EPA-R4-73-024, Dez. 1973

/5/ Lufthygienisch-meteorologische Modelluntersuchung
in der Region Untermain
5. Arbeitsbericht
Regionale Planungsgemeinschaft Untermain, Frankfurt (Main)

/6/ Battelle-Bericht
Vergleich von Rechenmodellen zur Ausbreitungsrechnung,
Teil 4
Bericht für das Bundesministerium des Innern, Juni 1975

/7/ K. Herrmann
Air Quality Simulation Model based on the
ATDL-Model by Hanna and Gifford
(in this proceedings)

/8/ J. Strott
Sensitivity Analysis of Parameter Influencing
the Results of Gaussian Models
(in this proceedings)

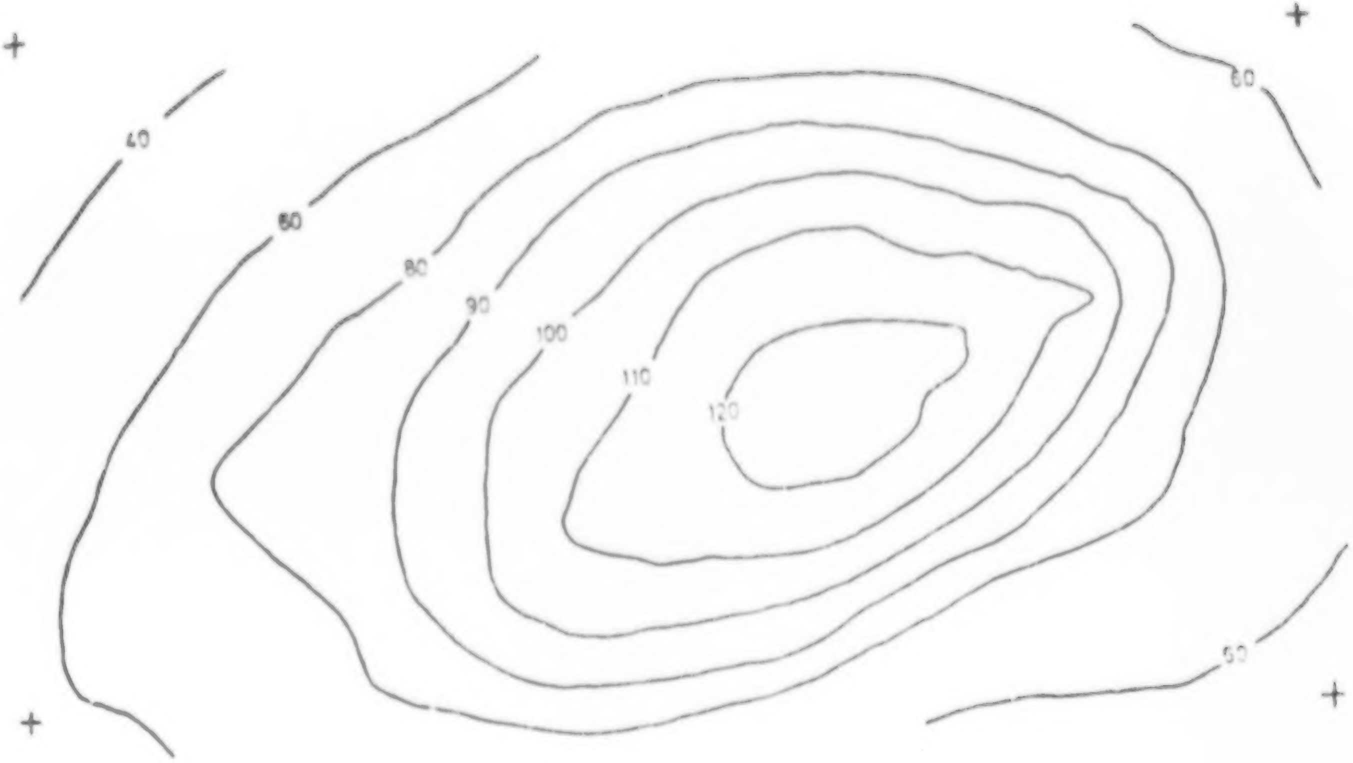

Fig. 1: Isopleths of annual mean concentration of SO_2 ($\mu g/m^3$) calculated with AQDM

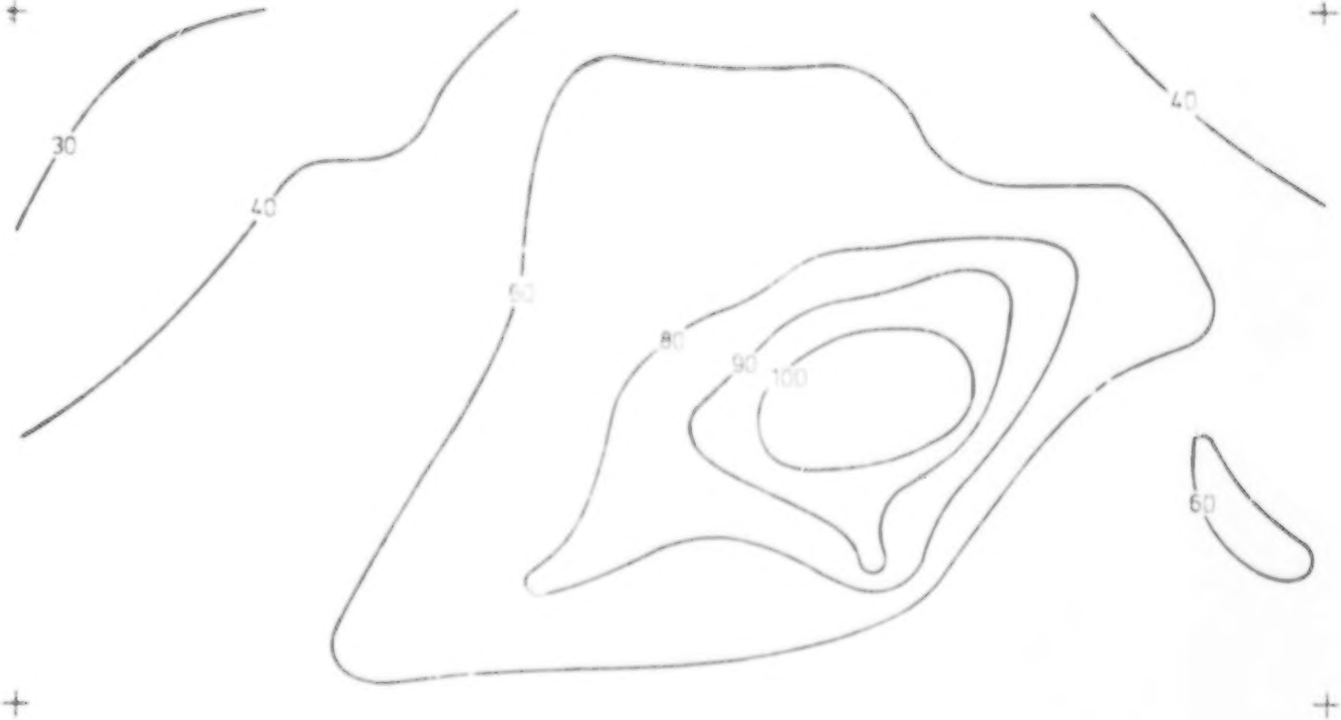

Fig. 2: Isopleths of annual mean concentration of SO_2 ($\mu g/m^3$) calculated with CDM

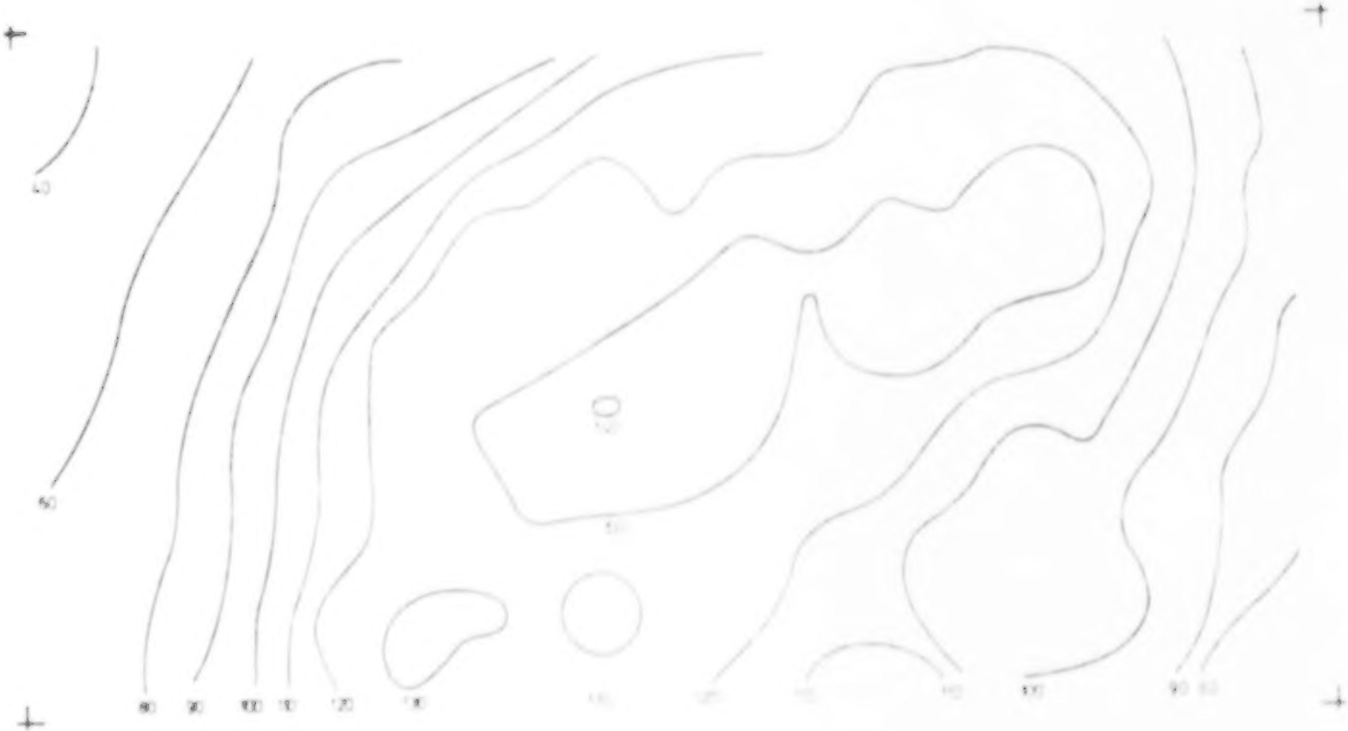

Fig. 1 Isopleths of annual mean concentration of SO_2 (µg/m^3) calculated with revised ATDL model

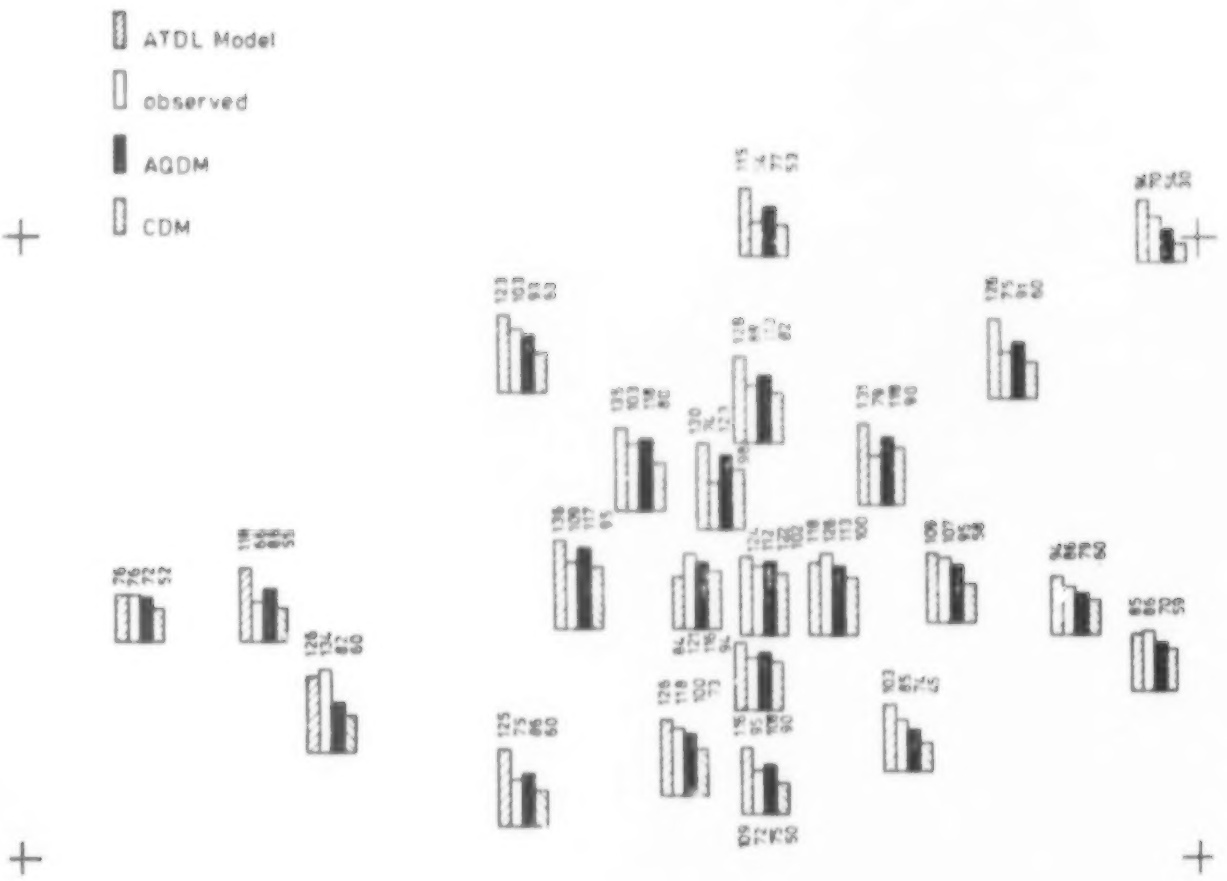

Fig. 4: Comparison of observed and calculated annual mean concentrations ($\mu g/m^3$). Measurements made by Institut für Wasser-, Boden- und Lufthygiene, Berlin

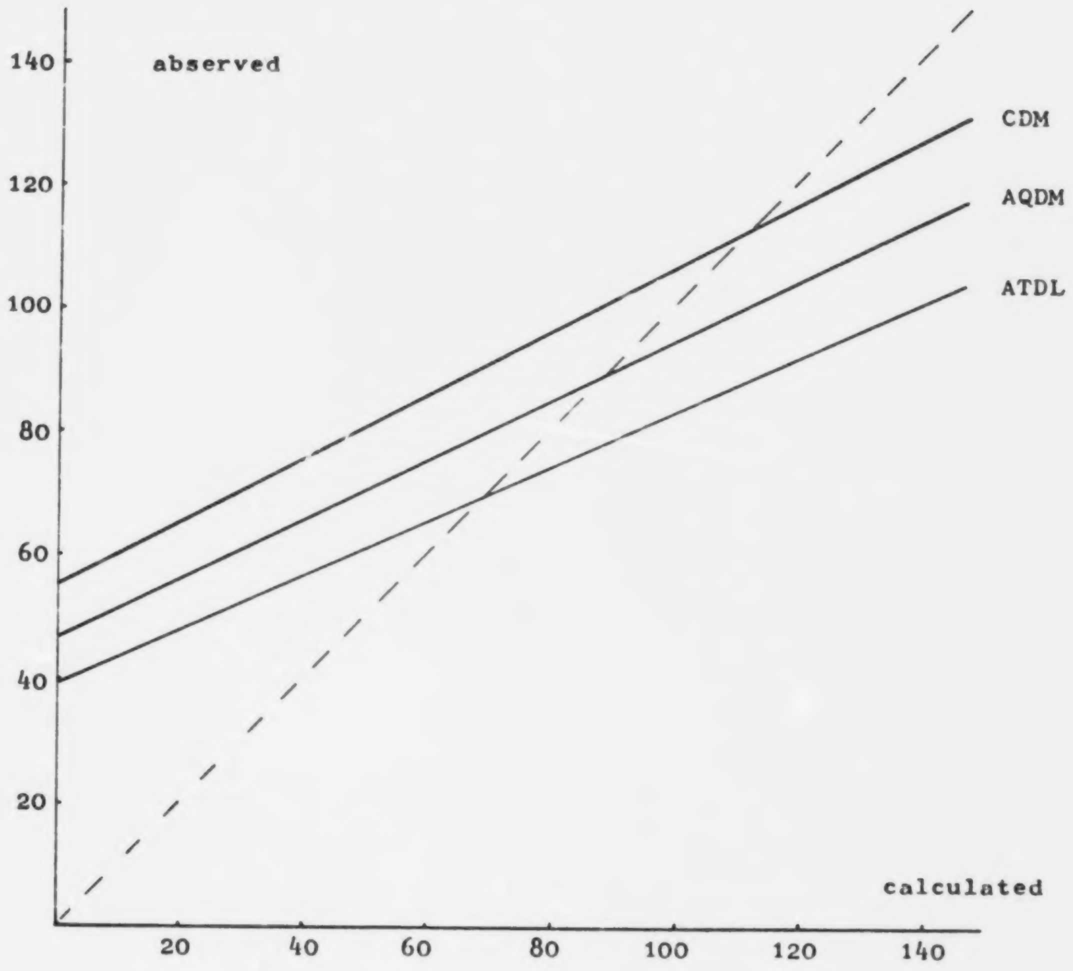

Fig. 5: Regression lines of observed versus calculated annual mean concentrations of SO_2 ($\mu g/m^3$)

AQDM, ATDL model: PASQUILL

Stability category (KLUG)	$\sigma_z = a\ x^b$	
	a	b
I	0.11727	0.67
II	0.14856	0.73
III_1	0.19943	0.76
III_2	0.22294	0.80
IV	0.22547	0.85
(V)	0.27934	0.90

CDM: PASQUILL and GIFFORD

Stab. cl.	Distance (m)					
	100 to 500		500 to 5000		5000 to 50 000	
	a	b	a	b	a	b
1	0.0383	1.2812	0.2539×10^{-3}	2.0886	-	-
2	0.1393	0.9467	0.4936×10^{-1}	1.1137	-	-
3	0.1120	0.9100	0.1014	0.9260	0.1154	0.9109
4	0.0856	0.8650	0.2591	0.6869	0.7368	0.5642
5	0.0818	0.8155	0.2529	0.6341	1.2969	0.4421
6	0.0545	0.8124	0.2017	0.6020	1.5763	0.3606

Table 1: Dispersion parameter cofficients and exponents

	observed SO_2-imm.	AQDM	CDM	ATDL
Mean concentration for all stations	92	95	70	116
Standard deviation	20.8	19.6	20.5	16.0
mean absolute error	-	17.2	25.0	26.0
largest mg. error	-	52	74	8
largest pos. error	-	49	24	61
range of error	-	101	98	69
lin. correlation coeff.	-	0.45	0.49	0.39
Variance of corr.	-	0.21	0.25	0.12
Slope of regression line	-	0.48	0.52	0.45
Intercept	-	46.1	55.2	39.5
error at location with highest measurement conc.	-	-52	-74	8
max. estimate conc. at any of the meas. locations	(126)	123	102	136

Table 2: Statistics of the AQDM, CDM and ATDL model

	Observed	AQDM	CDM	ATDL
Zentralstation	295	420.4	247.7	460
Ackermannschule	300	344.7	175.2	530
Posthochhaus	236	347.4	125.1	380

Table 3: Observed and calculated 95% values for the cumulation frequency distribution

	Emission-inventory	Frequency-distribution	CPU-Time/rec.-point	Ratio of CPU-Time
CDM	SAME	36 x 6 x 6	80 sec.	ca. 2
AQDM		16 x 6 x 6	47 sec.	ca. 4
ATDL		16 x 6 x 6	12 sec.	

Table 4: Ratios of running times for the CDM, AQDM and ATDL model

6th NATO/CCMS
International Technical Meeting
on Air Pollution Modeling

PRELIMINARY REPORT ABOUT A DIFFUSION MODEL FOR MILANO (ITALY) URBAN AREA: GIFFORD-HANNA MODEL

by

C. Ermini Cantoni (°)-R. Gualdi (°°)-L. Santomauro (°)
(°)-Osservatorio Meteorologico di Brera-Milano (Italy)
(°°)-Laboratorio Provinciale di Igiene e Profilassi:
Reparto Chimico - Milano (Italy)

BATTELLE - INSTITUT E. V., Frankfurt / Main
Germany, FR

24 - 26 September, 1975

Preceding page blank

PRELIMINARY REPORT ABOUT A DIFFUSION MODEL FOR MILANO (ITALY) URBAN AREA: GIFFORD-HANNA MODEL

C. Ermini Cantoni (°)-R. Gualdi (°°)-L. Santomauro (°)

1 - SUMMARY

The Milan (Italy) meteorological view is characterized, under the anemologic profile, by the frequent calm periods; also the wind speed results weakly intense; the air mixing caused by horizontal motion is therefore low, while the one due to vertical motion is often inhibited chiefly in the winter months, by persistent inversions.

By aim of arranging a control system and forecast the air pollution episodes, we have used the Gifford-Hanna model. The research is developped according to the data given by an urban network formed by 13 SO_2 monitors, 5 meteorological sites to recording temperature, wind speed and direction and one station to measure thermic lapse rate.

The urban area is divided into a square grid pattern, with grid distance of 2000 m; the Gifford-Hanna model has been experimented with the follow semidaily meteorological parameters: (a) C, D and E Pasquill stability classes, (b) wind direction frequency distribution and (c) ground wind speed.

(°)-Osservatorio Meteorologico di Brera- Milano (Italy)
(°°)-Laboratorio Provinciale di Igiene e Profilassi: Reparto Chimico - Milano (Italy)

The range of correlation coefficients obtained for observed-computed values is from 0.704 to 0.900; the angular coefficient of regression line for all considered cases is about 45°.

The research is developped just for the winter months (December 1974 and January 1975); later on it will extend to whole year.

The elaboration has been obtained by I.B.M. 370/135 of "Amministrazione Provinciale" of Milan; the input data are given to the model by punched card supply.

2 - METEOROLOGICAL VIEW OF URBAN AREA OF MILAN

The urban area of Milan is subject especially during the cold months to considerably high overall levels of air pollution due, as is the case in all intensely urbanized and industrialized zones, to household, motor vehicles and industrial sources. But in the area of Milan the industrial pollution sources are not entirely located in the outskirts part of the city. Furthermore, the urban area of Milan has other peculiar characteristics in its atmospheric environment which contribute remarkably to increasing and maintaining high levels of pollution; the include scarce ventilation nearly throughout the year.

In fact the correlation of the data gathered by five urban observation sites showed that the incoming air masses enter the urban area of Milan mostly from south-south-east and that at least the winds in the velocity range from 0.7 to 7.0 km hr^{-1} do not follow a very uniform direction of motion but weers as a rigid cyclonic system around the central area of the city at a very slow radial velocity, probably on account of the precence of the urban heat island (SANTOMAURO L. , 1971; MUNN R.E., 1973).

In the literature the ventilation time is said to vary usually over a range of 2 to 12 hours in big cities with light winds. Still in Milan, where the wind has a minimum speed of 0.7 km hr^{-1} when the air masses moves in the direction of the resulting wind (coming about from 160°) the ventilation time appears to be more than 31 hours. This suggests that the air mass entering from a peripheral south-south-east compass point becomes remarkably polluted when it reaches the north-north-west area of city.

Another peculiarity, consequence of weak atmospheric circulation is also the persistence of stable conditions in the lower atmospheric layers not only in the urban area but also at a fairly large radius from the city, especially in eastern and southern sectors of Po Valley. The consequence of this on air pollution is very slow mixing of the air layers which at times is almost nil; owing to the peculiar flat orography of the region this phenomenon extends well beyond the urban and metropolitan area of Milan (SANTOMAURO L. , 1972).

Hence, the need for developing a prediction model for air pollution.

3 - CHEMICAL AND METEOROLOGICAL NETWORK

The chemical and meteorological network in whole Milan district is composed by (fig. 1):

(i) urban network
(ii) metropolitan network
(iii) district network.

The station list, meteorological and chemical equipement are enumered in table 1. Beside the above mentionned stations, belong the network also: 1 tower (with heigth 110 meter above the ground) for the continuous measure of lapse rate and wind profile; 1 reference chemical and meteorological sampling site (SO_2 and dust) in Cannobio. SO_2 monitors seattle are model Philips PW 9700; dust monitors are model Philips PW 9790 for automatic sampling and A.I.S.I. 500L/H for semiautomatic ones; meteorological detectors are SIAP-VT5502 for wind speed, VT5512 for wind direction, TM5020 for temperature, UM5515 for relative humidity.

All measured values detected by chemical and meteorological monitors are converted first, to an electric current between zero and 20 milliamps, then converted to a proportional frequency from 5 to 25 Hz. This frequency modulates a multi tone transmitter connected by a leased thelephone line to a Philips P855 mini computer.

The automatic data management is performed by process control programs which check the signal validity, call the measuring equipement calibrations, twice daily at two levels, and compute the exact range; store the data and print, according to internal clock, the average every 1, 6, 12, 24 hours.

TABLE 1 - CHEMICAL AND METEOROLOGICAL NETWORK AT MILANO (Italy) DISTRICT AREA
(at 1st Sept. 1975)

Code	Station	Urban	Metropolitan	District	SO_2	Particulate	Wind	Temp.	Rel.Hum.
1	Sesto S.Giovanni (Asilo)		X		X				
2	Sesto S.Giovanni (Piscina)		X		X				
3	Sesto S.Giovanni (Comune)		X		X		X	X	
4	Legnano			X	X		X	X	X
5	Pancrazio	X			X				
6	Marche	X			X	X			
7	Lattanzio	X			X				
8	Vetra	X			X	X			
9	Washington	X			X				
10	Juvara	X			X	X	X	X	X
13	Zavattari	X			X	X*	X	X	X
14	Niguarda	X			X	X*	X	X	X
15	Liguria	X			X	X	X	X	X
16	Brera	X			X	X*	X	X	X
17	Monza		X		X	X*			
18	Bertonico			X	X		X	X	X
19	Turano			X	X				
20	Terranova			X	X				
21	Cassina de'Pecchi			X	X				
22	Pioltello			X	X				
23	Magenta			X	X				
24	Cassano d'Adda			X	X				
25	Tavazzano			X	X				
26	S.Rocco al Porto			X	X				
27	Villasanta			X	X				
28	Rho		X		X*	X*			
29	Lodi			X	X*	X*			
30	Cologno			X	X*	X*			
31	Abbiategrasso			X			X	X	X
32	Carate Brianza			X			X	X	X
33	Trezzo d'Adda			X			X	X	X

X* = Semiautomatic monitor

General purpose peripheral connected to the computer include a logging typewriter for real-time presentation of data, a dialog typewriter to print calibration values and error, a paper tape punch, a high-speed paper tape reader, and a topographic display of detector sites to allow real-time surveillance of the region. For special purpose monitoring an analog recorder is available.

The so structured network has allowed to analize in a continuous way the meteorological influence on SO_2 and suspended particulate matter course, and also to establish a correlation between these ones and total sulfur quantity emitted through the combustion. Next configuration of P855 computer has been designed with magnetic equipement to load a complete data-base of all pollution values. So will be possible a statistical analysis with off-line computer tecniques.

4 - URBAN AREA MODEL SELECTION CRITERIA

As you know, the aims of an atmospheric pollution model for an urban area, in relation to one or more pollutants, are: 1) to simulate the pollution conditions on the whole area, or its part by the different emission conditions and if possible meteorological conditions, so as to forecast the evolution for the air quality determination; 2) to employ the results of the model to program the future installations in the examinated territory.

Equally is know the availability offered to researchers from the several kinds of atmospheric pollution models, like those based themselves on the gaussian diffusion, on the diffusion differential equation, on the statistical and climatologic analysis.

It goes without saying the choice of the algorithm and its relative practical integration depends on the forecast objects (simulation, foresigth, programming), on the model convenience and applicability being in mind the different environmental characteristics of the area to investigate.

Owing to prevailing meteorological conditions on urban and metropolitan area of Milan, especially in winter and summer season, generally speaking, the model that goes nearer to the reality of facts just in account of its flexibility, is which based itself on the diffusion equation; this because it offers a quite realistic picture of the pollution dynamics, whether for the total course on a generalized area (metropolitan area) or for an analysis to local level. Obviously this kind of model requires the continuous bringing update of differents parameters, enclosed therein those resultant from the sources inventory. This one, at the moment, is going to be studied for Milan urban area. However, as we need a model to be utilized in real-time, to get a better understanding of pollutant behaviour and of boundary conditions weight on the pollution dynamic itself, and for a later enlargement of monitoring network we decided to use "ATMOSPHERIC TURBULENCE AND DIFFUSION LABORATORY ATDL" (GIFFORD F.A. jr, HANNA S.R. , 1971).

The GIFFORD-HANNA model describes, with good agreement, the behaviour of a certain pollutant amount emitted by a source group, either spreaded, either pointed enclosed in a given area, called a source area; moreover such model is not presenting great development and employement difficulties and allow concentrating the energies on area analysis by employing an algorithm structured by two weight methods (gaussian plume and integral of diffusion equation).

Therefore it gives the following advantages:

a) readyness in computer applications
b) low elaboration time (in our case about 30", running on IBM 370/135 computer)
c) semplicity and clearness in input data
d) flexibility in changing parameters, obtained by simple and fast methods
e) separated management of source area and point ones.

As the model employement for metropolitan and urban area has its own importance for foreseeing eventual episodes of strong pollution, GIFFORD-HANNA model, also because its high elaboration speed, is easily employed for a real time control. Before describing computational executed procedures (sect. 5), we think it is better to pay attention to the fact that Milan urban area, beside the environmental characteristics already described (sect. 2) is surrounded by a belt inclosing higly populating suburb and provided with considerable industrial installations, almost uninterrupted. It is obvious that in a modelling we cannot forget the aid of emissions coming from the outer belt for a correct simulation and a forecast of the pollution behaviour in urban area, properly called.

On this purpose we must clear that the ATDL model also showing some limitation in the low wind speed, allow to value the source and point weight inclosed in Milan belt.

5 - COMPUTATIONAL PROCEDURE

Before explaining the computational procedure used for application of A.T.D.L. model, we sum up, for clearness, the essential point (HANNA S.R., 1971):

a) The urban area is divided in a square grid pattern; in the center of every square is placed the ideal receptor point.

b) The source points are analized separately, while the small sources contributions are grouped in a variable X_a, concentration of a source area.

c) The ground concentration of a pollutant χ, coming from a source area (supposed relatively smooth), is function of pollutant emitted quantity, of speed and wind direction and of stability class of low atmospheric layer.

d) The source area strength (in amount m^{-2} sec^{-1}) varies by less than a factor of ten over a distance of a few kilometres.

e) The trend of pollutant vertical distribution has a low meaning on the result.

f) The standard deviation σ_z is function of atmospheric low layer stability.

g) The surface concentration χ in grid number center, if the frequency distribution of 16 wind directions is known, according GIFFORD and HANNA formula is:

$$\chi = \sqrt{\frac{2}{\pi}}\ \frac{(\Delta x/2)^{1-b}}{u\ a(1-b)} \left[Q_A(0,0) + \sum_{i=-4}^{4} \sum_{j=-4}^{4} Q_A(i,j)\ f(i,j) \left[(2r+1)^{1-b} - (2r-1)^{1-b} \right] \right]$$

In this first research we have not used a telescopic grid as we really should have done considering the urban topography (SANTOMAURO L. , 1972) because at the moment we just dispose of a orientative source emission inventory. Later on, when we shall be able to dispose a detailed inventory of all urban and metropolitan sources, managed by a computer and always updated, it will be possible to specialize much more the source area strength, reducing the square size. For the same reason in first research, we did not consider the point source (really very rare in urban area, but many in metropolitan area) considering the present difficulty in taking inventory and qualify them entirely. In this research stage we have not also considered the sources temporal variation: this fact must not be considered too approximative because, as we have already calculated, the concentration in a 12 hours period these variations do not weight in a sensitive way.

This research has been carried out considerating, by a good topographic agreement, Milan urban area interested by a 36 square grid, each 2000m side. For every grid square we have calculated a potential emission in $\mu g\ m^{-2}\ sec^{-1}$(fig.9)

On the ground of these structure informations we have calculated every 12 hours the SO_2 concentrations average (in $\mu g\ m^{-3}$) for december 1974 and january 1975. To get these averages, the model has been provided with the necessary status informations, so as wind speed and direction and atmospheric stability classes, as we have obtained by the meteorological detectors network.

To calculate σ_z, corresponding to classes C and D (according to Pasquill cathegories) has been used the coefficients suggested by SMITH M. E. (1968):

	class C	class D
a	0.22	0.15
b	0.80	0.75

for class E, a first study has advised with good agreement, the choice for Milan of the empirical following values:

$a = 0.13$

$b = 0.74$

instead of 0.06 and 0.71 respectively. This change has been necessary because, applying the original Smith values of the stability conditions, we obtained very high concentrations point, which were, also statistically, different from real thing. We should think that such anomalia are due to the orographyc and topographyc feature of Milan urban area (flat area) and the considerable widespread sources number (domestic central heating) in uniform heights and to particular anemologic trend (fig. 3). Very likely this situation could determinate homogeneousness of pollutant in the upper urban area layer.

The model has been programmed in FORTRAN IV language and is similar to the one included in a S.R. HANNA issue (1972); this program presents a considerable flexibility because it is possible conveniently changing the general type informations relating to the grid size and the power area source.

The elaboration has been obtained by I.B.M. 370/135 of "Amministrazione Provinciale" of Milan; the input data are given to the model by punched card supply.

6 - DISCUSSION

To test the reliability of GIFFORD-HANNA model, we have realized, for the two months analized (dec. 74 and jan. 75) and for the five stations LATTANZIO (7), JUVARA (10), ZAVATTARI (13), NIGUARDA (14), LIGURIA (15), (fig. 3,4,5,6,7), the dispersion diagrams in function of observed SO_2 concentration (ordinates) and computated ones (abscisses).

It was not possible to compare the computated and observed values in BRERA central station, because, for the time considered, the monitor was upkept.

The calculation of linear correlation coefficients for each point set, shows well correlated values series; in effect for these coefficients we obtain a value range between 0.704 and 0.900. The linear correlation coefficient was calculated with know formula:

$$r = \frac{\sum xy}{\sqrt{(\sum x^2)(\sum y^2)}}$$

where $x = X - \bar{x}$; $y = Y - \bar{y}$; $\bar{x}$, $\bar{y}$ average values; X calculated concentration values; Y observed concentration values.

By aim to estimate furthermore the agreement of set of observed values with set of computed ones, we have developed the regression line equations with least square method for x and y:

$$y = \frac{\sum yx}{\sum x^2} \ x.$$

The line slope (fig. 3 ÷ 7) keeps itself near to 45° (the angular coefficient is, seven times on ten, equal to 0.9; the lowest value is 0.7, the highest one is 1.32).

The standard error (tab.3), that gives a dispersion measure around regression line for x on y, is

$$s_e = \sqrt{\frac{\sum (Y - Y_s)^2}{N}}$$

where N is the points number, Y_s represents the Y value for given X, valued with regression line equation; it shows values contained in the range from 114 to 185 ($\mu g \ m^{-3}$).

The GIFFORD-HANNA model application has well reacted in meteorological conditions varying, especially respect wind bias direction. Some strong differences (O-C) (tab. 2) found, are due to limited accuracy of source inventory, as already mentioned in the fourth paragraph. Because of these inexactness we can remark, in computing values, same variation respect to real concentrations: the different wind bias direction can, in same grid share, influence the SO_2 amount spilled on the upwind square.

It is interesting to note how the model ATDL reacts positively to the variation of anemological conditions prevailing on the urban area during the analyzed periods.

The SO_2 isoconcentration simulations calculated for the same period of two different days are reported in the figures 8 and 9. The first (fig. 8) is referred to the afternoon situation (1 - 12 / Z) of 24th december 1974, in which the winds from E (0.8) and SE (0.2) with average speed 2.1 m sec^{-1} are prevailed, and the second (fig. 9) on 30th december 1974, in which the wind from N (1.0) has been prevailing with average speed 8 m sec^{-1}. While in the first case the wind speed of 2.1 m sec^{-1} causes a maximum nucleus of 700 $\mu g\ m^{-3}$, in the second case the speed of 8 m sec^{-1} determines a maximum nucleus of 210 $\mu g\ m^{-3}$, in the same way the maximum nucleus dislocation is function of the direction and wind force.

At last it is possible to point out that the secondary maximum, referred to 24th december 1974 (600 $\mu g\ m^{-3}$), corresponds with the historical center of the urban area, more intensely populated.

TABLE 2 - CORRELATION ANALYSIS (x and y = $\mu g\ m^{-3}$)

code	station	1974, december				1975, january			
		$\bar{x}_c$	$\bar{y}_o$	o-c	r	$\bar{x}_c$	$\bar{y}_o$	o-c	r
7	LATTANZIO	738	666	-72	0.853	614	557	-57	0.859
10	JUVARA	745	737	- 8	0.893	623	650	+27	0.900
13	ZAVATTARI	486	587	+101	0.814	408	540	+132	0.821
14	NIGUARDA	669	667	- 2	0.774	543	708	+163	0.736
15	LIGURIA	481	486	+ 5	0.723	379	425	+46	0.704

TABLE 3 - REGRESSION LINE COEFFICIENTS (°)

code	station	1974, december				1975, january			
		X	Y	C	s_e	X	Y	C	s_e
7	LATTANZIO	0.960	1	-42.5	±150	0.905	1	+ 1.3	±153
10	JUVARA	1.207	1	-162.2	157	0.982	1	+38.2	128
13	ZAVATTARI	1.318	1	-53.5	185	0.972	1	+143.4	114
14	NIGUARDA	0.932	1	+43.5	177	0.932	1	+202.0	85
18	LIGURIA	0.903	1	+51.7	139	0.766	1	+134.7	131

(°) $y = \frac{\sum xy}{\sum x^2}\ x \ ; \qquad x = X - \bar{x}_c \ ; \qquad y = Y - \bar{y}_o$

7 - FUTURE RESEARCH PROGRAM

The future research development is a more wide and detailed application of GIFFORD-HANNA model; at the same time a model based on a concentration diffusion equation will be realized by degree and tested step by step. to obtain this, it is necessary to complete the source emission inventory beside a more careful use of meteorological parameters and data processing improvement.

Since, in air pollution modelling applications, an available source inventory is of main importance, chiefly in real-time purpose, we will develop numerical and logical tecniques for inventory management with computer programs. Source inventory will include the environment of urban area; for this aim will be assembled all gainable resources and informations necessary for an automatic data management which allow loading and computing each new condition, so we supply to the model the structure input always updated. By means of so structured data management, we'll obtain more possible exact source area values and their change whether in daily or seasonal arc. Obviously grid distance could be reduced from 2000 m to 500 m.

In this research we have used the meteorological values detected by instruments settled by "Osservatorio Meteorologico di Brera" which is placed in middle-town; in future development we'll also use the values drawn in other four urban meteorological stations; so it will be possible to take into account the urban heat island analitically; finally we shall increase the research to determine the coefficients a and b.

For that is concerning data processing management, the last aim is to realize an automatic and integrated data flow so to obtain the SO_2 isoconcentration patterns; to store calculated data on magnetic equipements, to compare them with observed values, so it will be possible carrying out a feedback system to keep the model self-reguled.

ACKNOWLEDGEMENTS

The Authors acknowledge Dr. A. Cavallaro and Dr. G. Rebuzzini respectively Director and Deputy Director of Chemical Department of Laboratorio di Igiene e Profilassi dell'Amministrazione Provinciale di Milano; the Rag. G. Rogiani, E.D.P. Manager and Dr. G. Tebaldi, meteorologist.

LIST OF FIGURES

Fig. 1 - Chemical and meteorological network of Milano district area.

Fig. 2 - Grid pattern, source emission inventory and SO_2 monitors location in Milan urban area.

Fig. 3 - Comparison of observed vs. computed SO_2 semidaily values, december 1974 and january 1975 for Lattanzio (7) station.

Fig. 4 - idem Juvara (10) station.

Fig. 5 - idem Zavattari (13) station.

Fig. 6 - idem Niguarda (14) station.

Fig. 7 - idem Liguria (15) station.

Fig. 8 - Simulation of SO_2 isoconcentration december 24, 1974.

Fig. 9 - Simulation of SO_2 isoconcentration december 30, 1974.

BIBLIOGRAPHY

1 - GIFFORD F.A. Jr, 1970 - Atmospheric Diffusion in an Urban Area; paper presented 2nd IRPA Conference, Brighton, Engl., May 5, pp 5 + 1 fig.

2 - GIFFORD F.A. Jr
HANNA R.S., 1970 - Urban Air Pollution Modelling; Paper ME-32C, 2nd International Clean Air Congress, Washington, Dec. 11, 1970, 17 pp + 7 figs (in Proceedings of the 2nd Int. Clean Air Congress Academic Press, N.Y., 1971, p. 1145-1151 + 5 figs.

3 - HANNA R.S. 1971 - A Simple Method of Calculating Dispersion from Urban Area Sources Jour. of APCA - vol. 21, N. 12, p. 774 + 5 figs.

4 - HANNA R.S. 1972 - Description of ATDL Computer Model for Dispersion from Multiple Sources; 2nd Industrial Air Pollution Control Conference, University of Tennessee-ATDL Contribution File N. 56.

5 - MUNN R.E. 1973 - Urban Meteorology: some Selected Topics, Bull. Am; Met. Soc., vol. 54 p. 90-93.

6 - SANTOMAURO L. 1971 - Analysis of Wind Trend in an Urban Area situated on Flat Land; Osserva= torio Astr. Milano-Merate; Suppl.

Meteorologici N. 21.

7 - SANTOMAURO L. 1972 - Proposal for a Mathematical Model of Air Pollution Survey in Milan; Proceedings of the 3d Meeting of the Expert Panel on Air Pollution Modeling- NATO / CCMS, N. 14, Paris, France, Oct. 2-4; Chapt. V.

8 - SMITH M.E. 1968 - Recommended Guide for the Predictions of the Dispersion of Airborne Effluents ASME, IX and 85 pp.

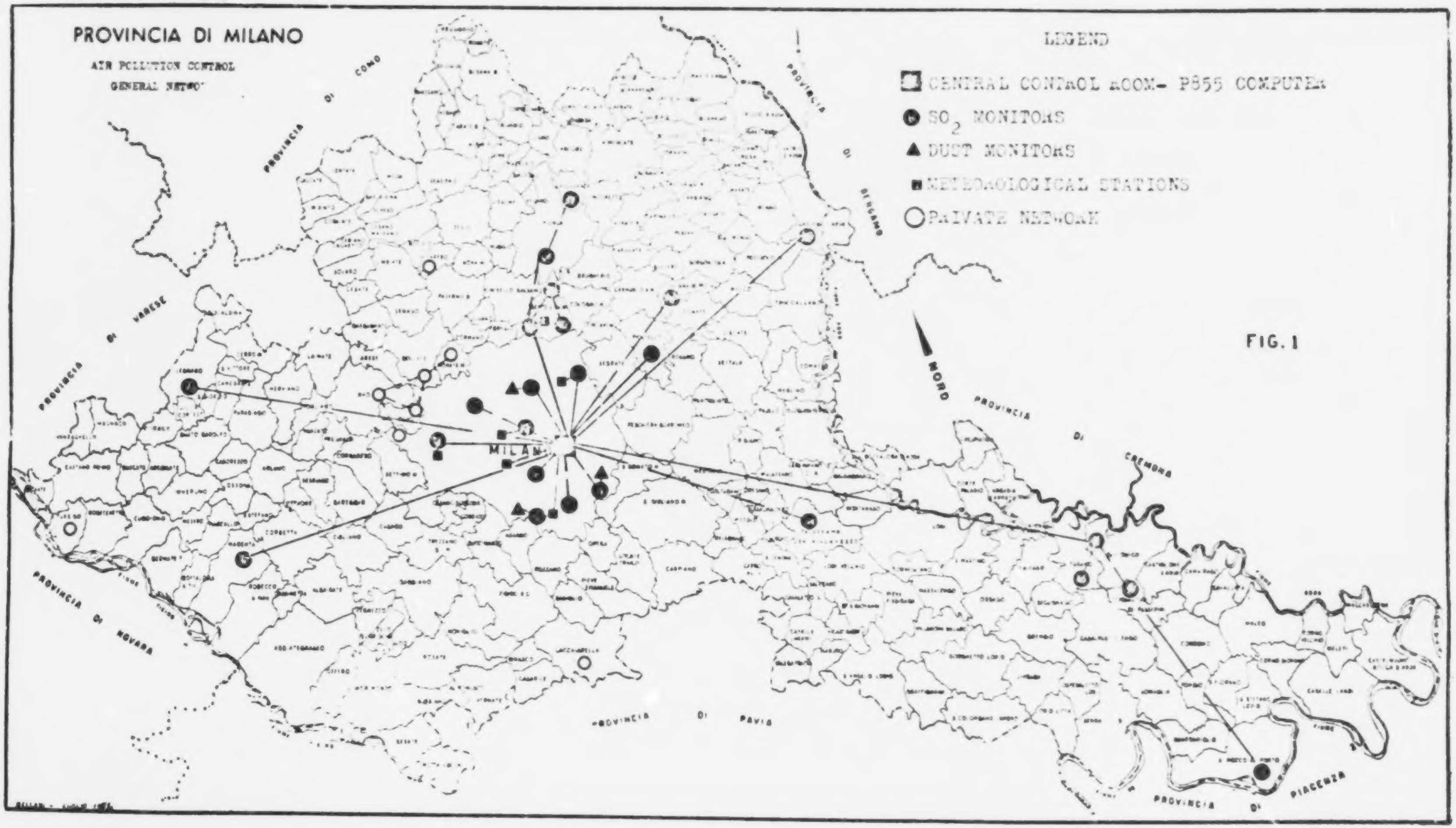
PROVINCIA DI MILANO
AIR POLLUTION CONTROL
GENERAL NETWO'
LEGEND
CENTRAL CONTROL ROOM- P855 COMPUTER
SO_2 MONITORS
DUST MONITORS
METEOROLOGICAL STATIONS
PRIVATE NETWORK
NORD
MILANO
PROVINCIA DI COMO
PROVINCIA DI BERGAMO
PROVINCIA DI CREMONA
PROVINCIA DI PIACENZA
PROVINCIA DI PAVIA
PROVINCIA DI NOVARA
PROVINCIA DI VARESE

FIG. 1

MILAN URBAN AREA

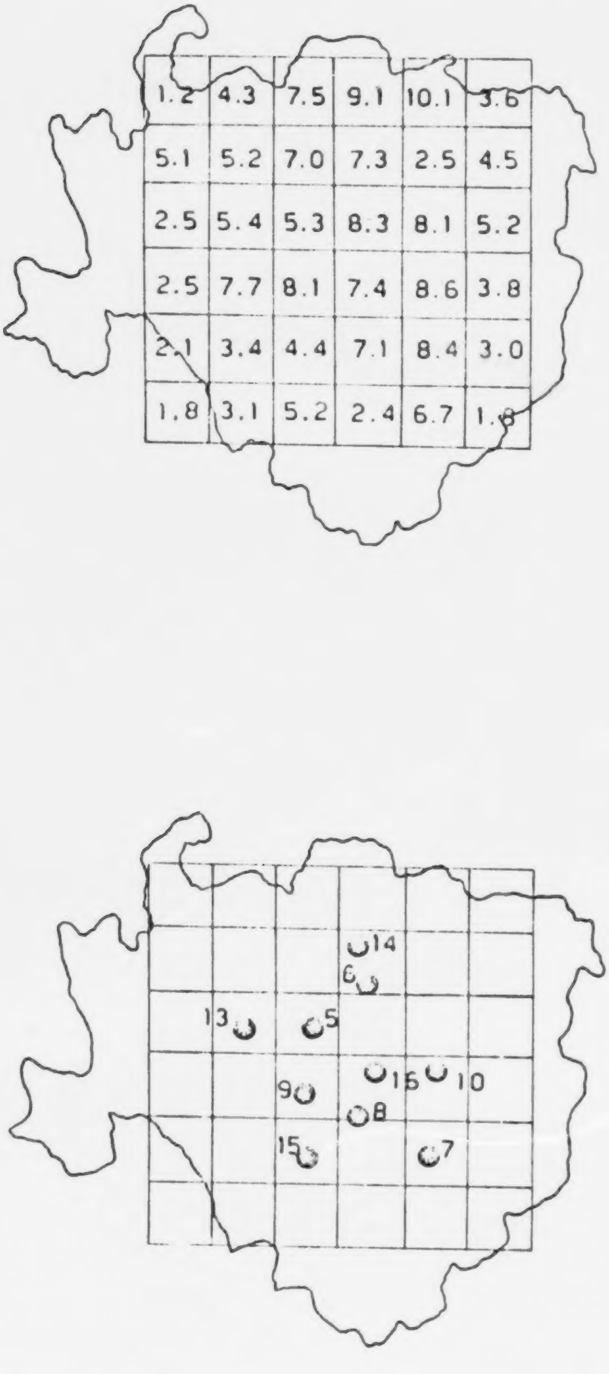

1.2	4.3	7.5	9.1	10.1	3.6
5.1	5.2	7.0	7.3	2.5	4.5
2.5	5.4	5.3	8.3	8.1	5.2
2.5	7.7	8.1	7.4	8.6	3.8
2.1	3.4	4.4	7.1	8.4	3.0
1.8	3.1	5.2	2.4	6.7	1.8

Area source strength

$Q = \mu g/m^2\ sec$

Grid distance = 2000 m

SO_2 monitors

14	NIGUARDA
16	MARCHE
13	ZAVATTARI
5	PANCRAZI
9	WASHINGTON
16	BRERA
10	IUVARA
8	VETRA
15	LIGURIA
7	LATTANZIO

FIG. 2

LATTANZIO

(7)

fig. n° 3

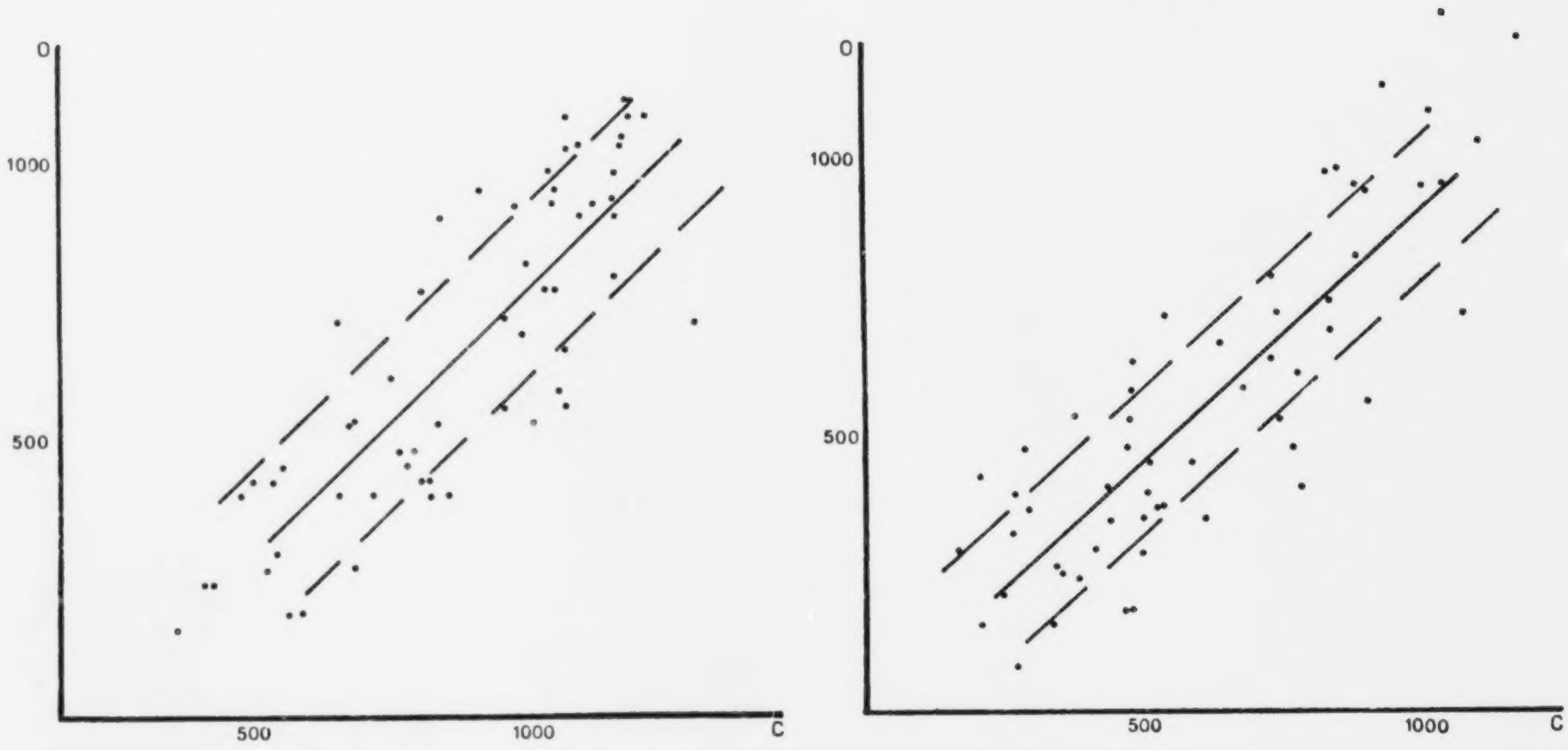

DICEMBRE 1974
r : 0,853
s_e : 150

GENNAIO 1975
r : 0,859
s_e : 153

JUVARA
(10)

fig. n°4

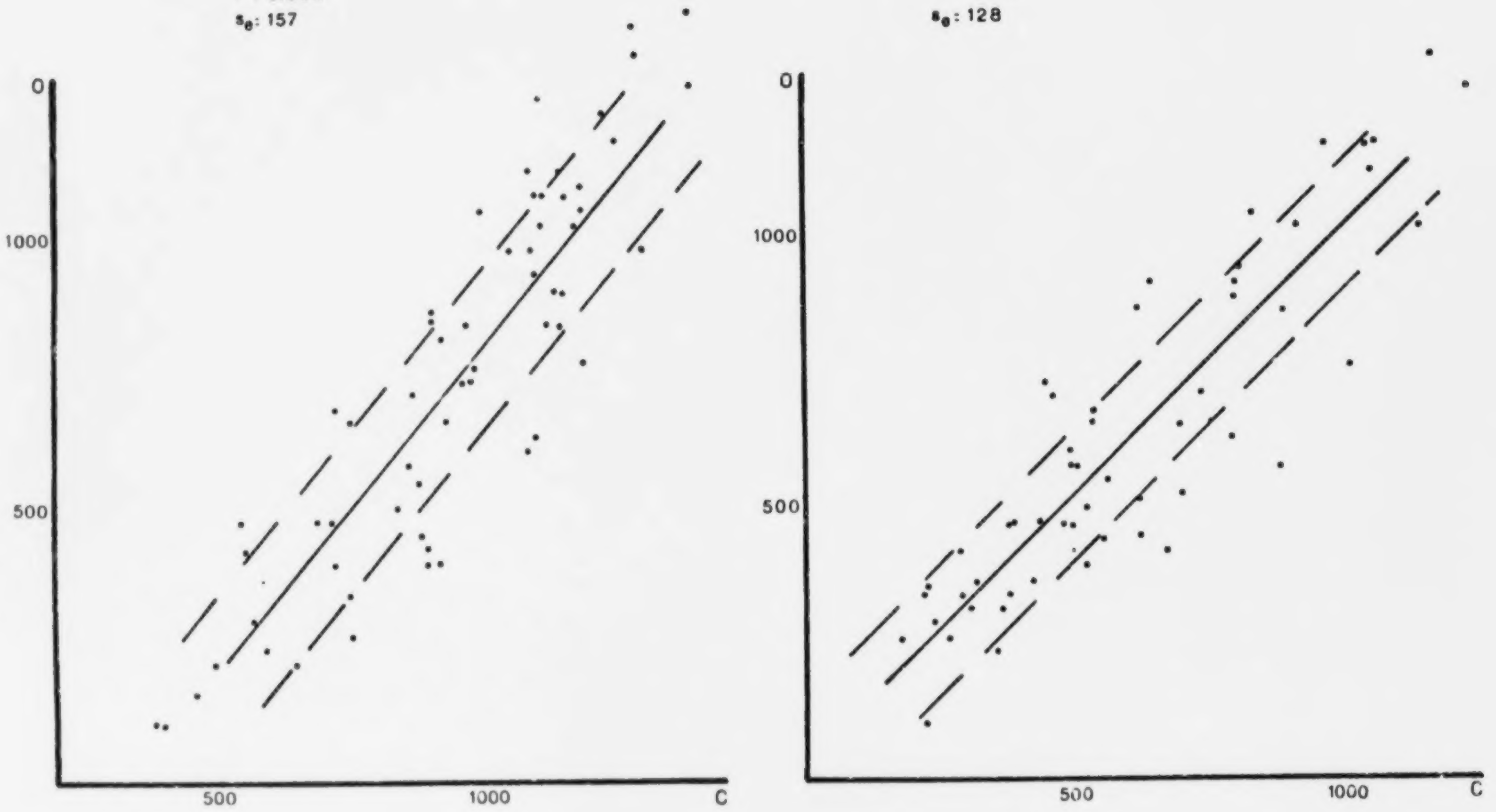

DICEMBRE 1974
r : 0.893
s_e: 157

GENNAIO 1975
r : 0,900
s_e: 128

ZAVATTARI
(13)

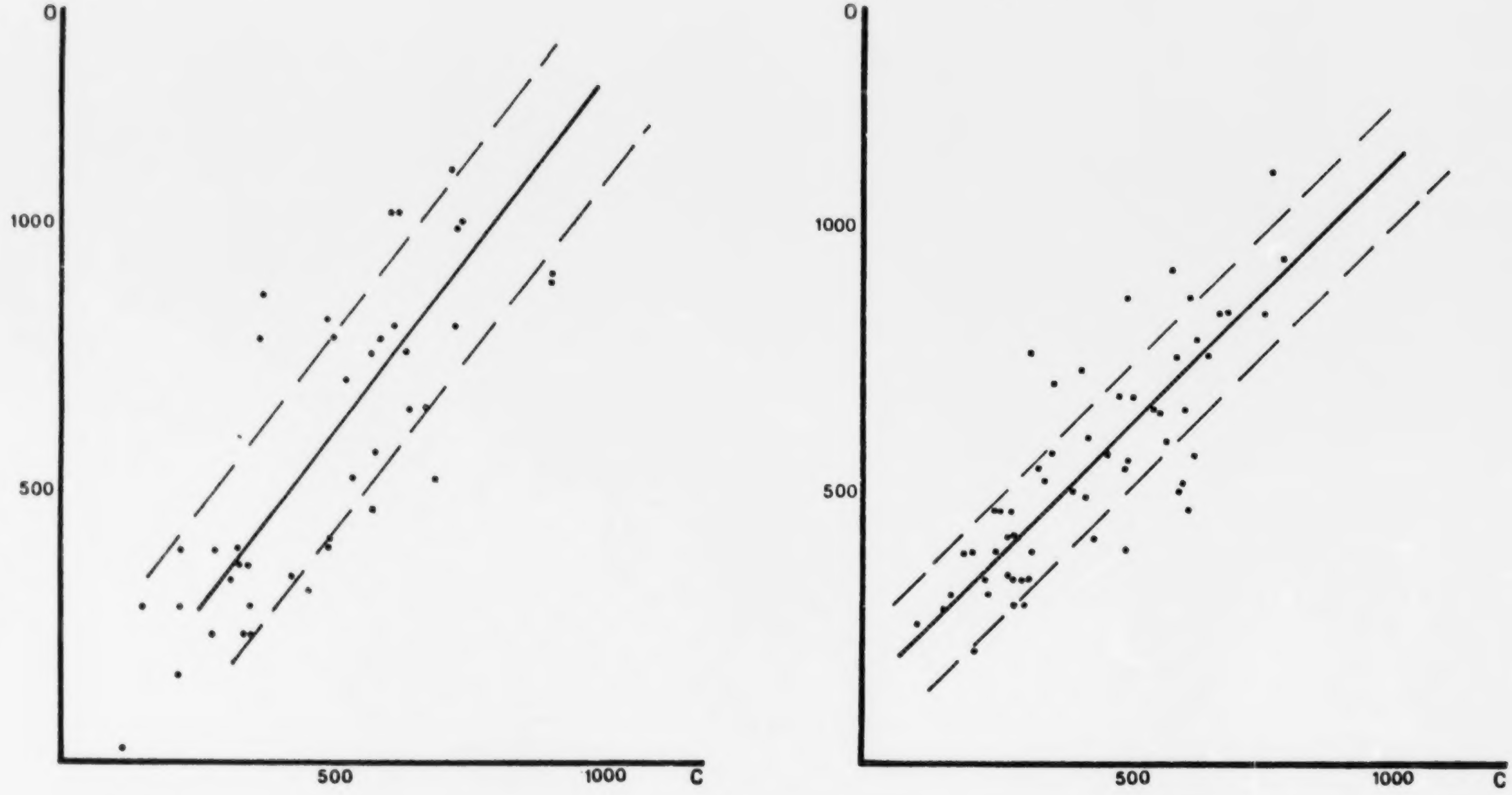

DICEMBRE 1974

r : 0,814
s_e: 185

GENNAIO 1975

r : 0,821
s_e: 114

fig. n°5

NIGUARDA

(14)

fig. n°6

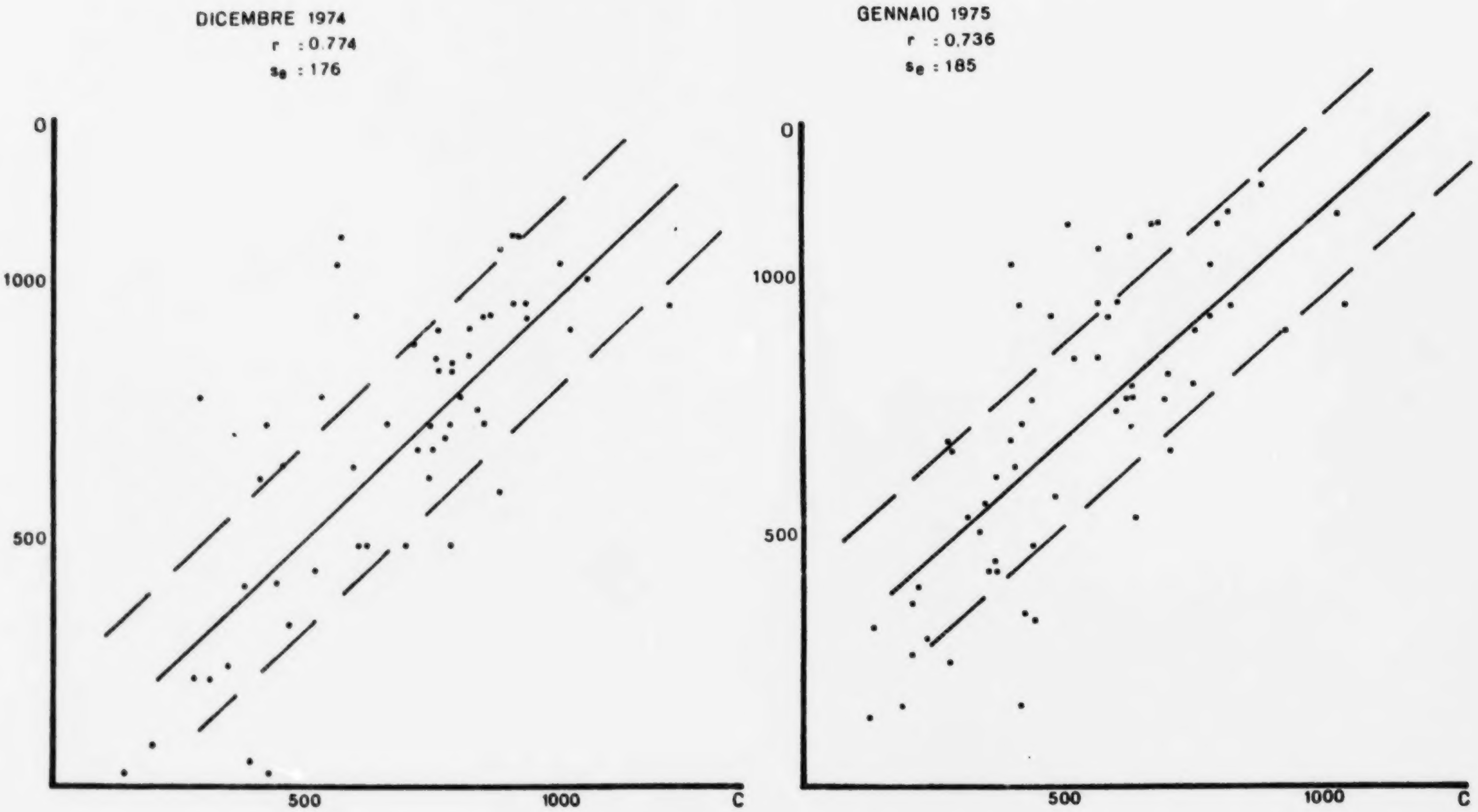

DICEMBRE 1974
r : 0.774
s_e : 176

GENNAIO 1975
r : 0.736
s_e : 185

LIGURIA

(15)

fig. n° 7

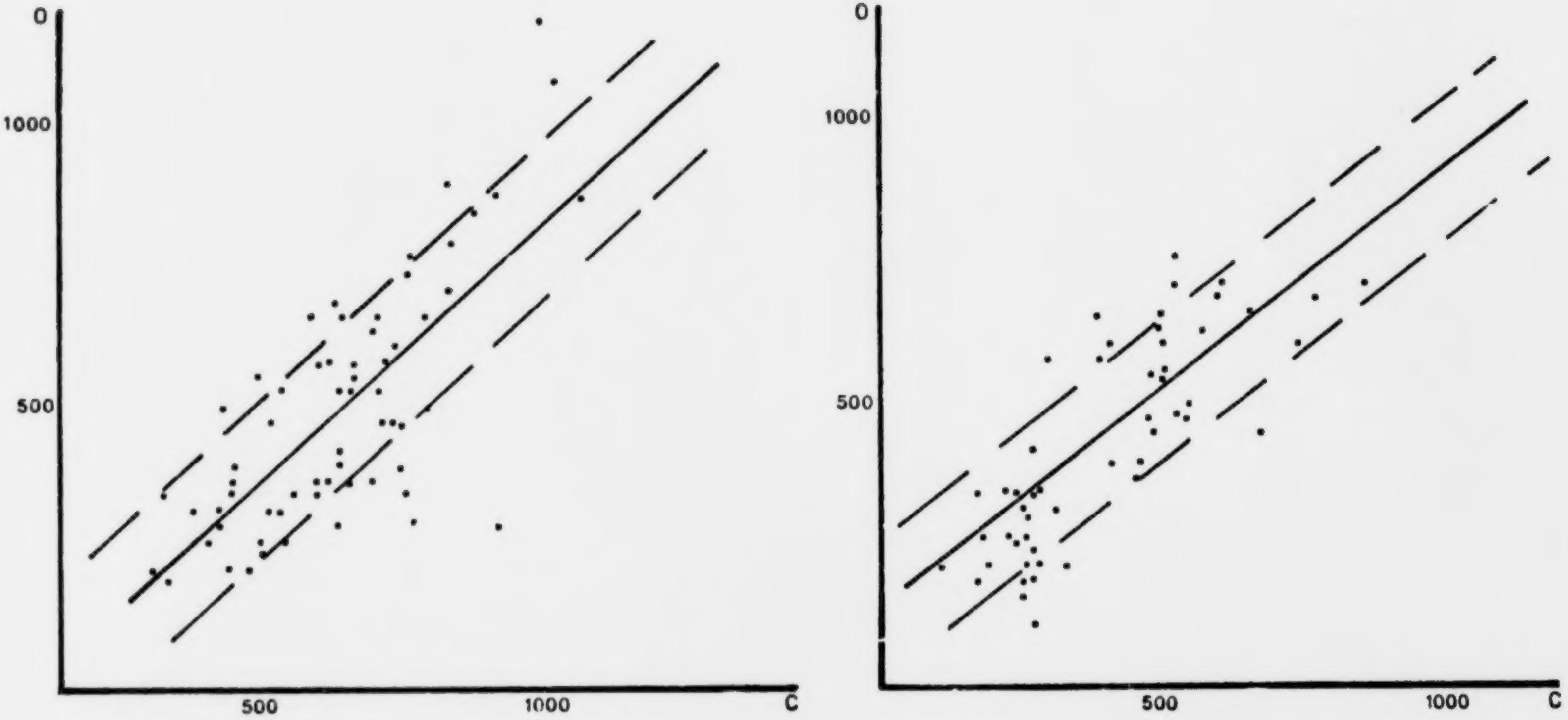

DICEMBRE 1974
r : 0.723
s_e : 139

GENNAIO 1975
r : 0.704
s_e: 131

Milan urban area

SIMULATION OF SO_2 ISOCONCENTRATION ($\mu g\ m^{-3}$)

DEC. 24 1974
11Z - 12 Z PM

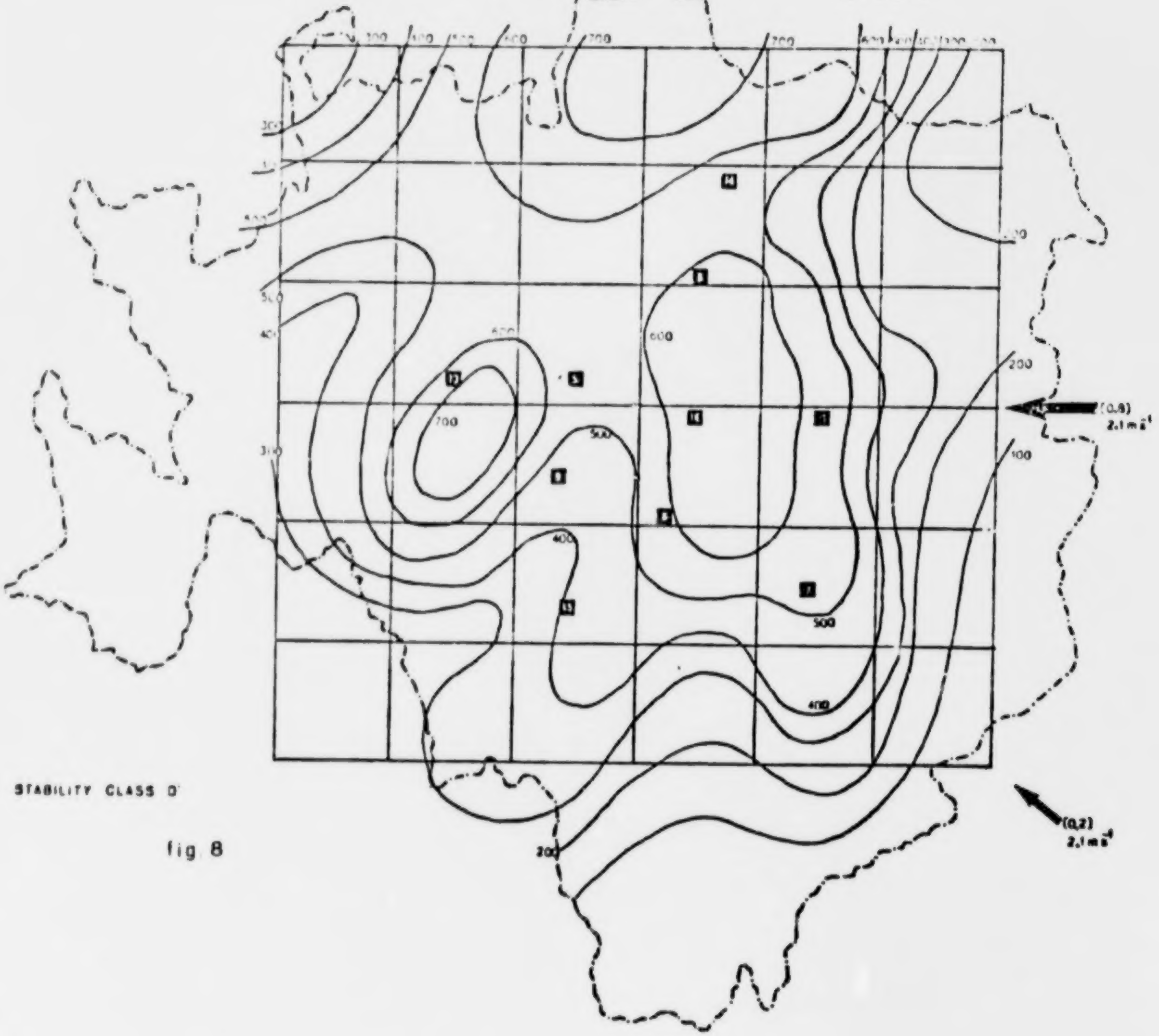

STABILITY CLASS D

fig. 8

Milan urban area

SIMULATION OF SO_2 ISOCONCENTRATION ($\mu g\ m^{-3}$) DEC. 30.1974
1/2 - 12/2 PM

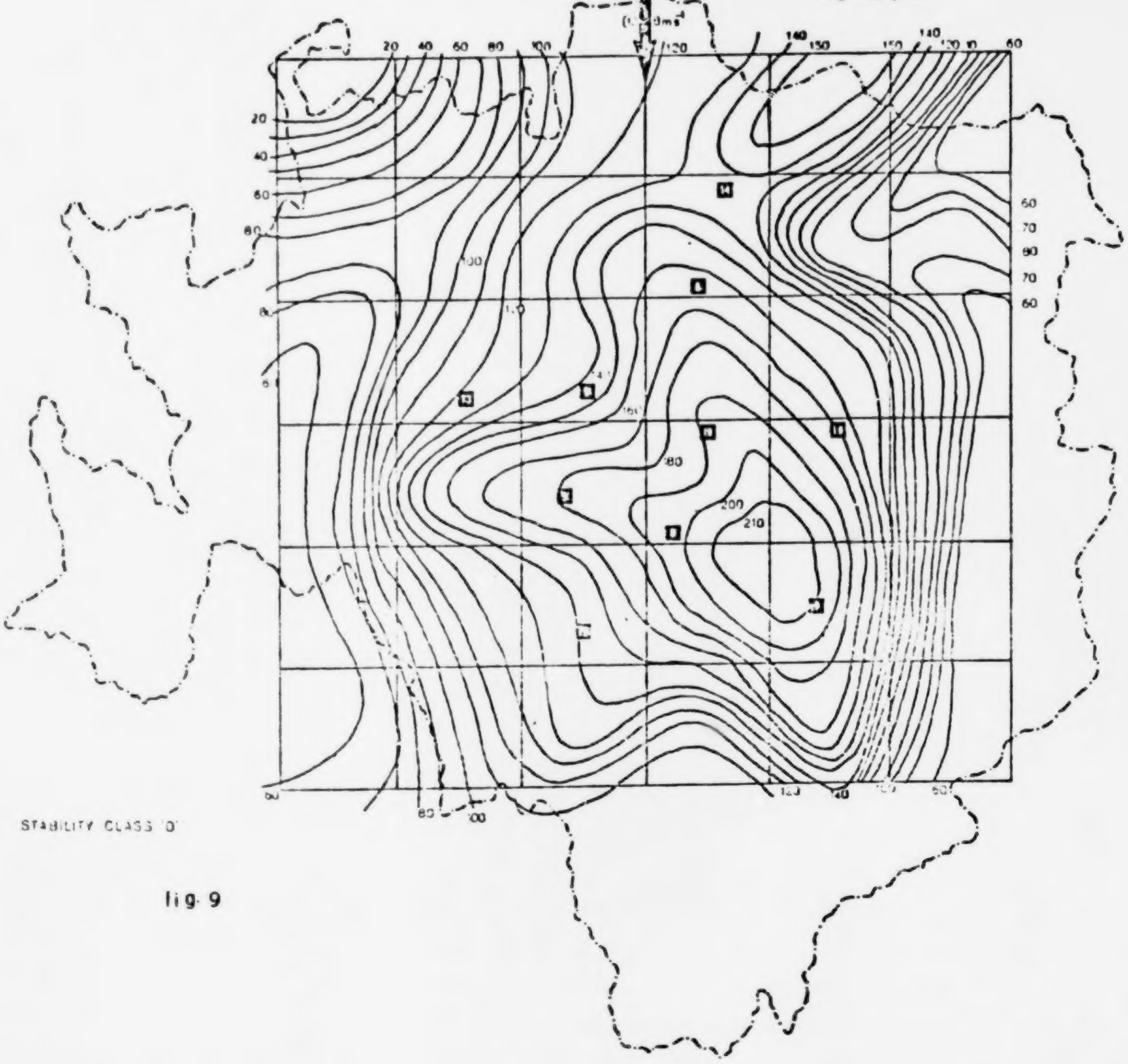

STABILITY CLASS 'D'

lig. 9

Rapporteur's Report, Topic I (continued), September 24, 1975

by J. K. Strott

Chairman: H. Fortak

K. Herrmann:	Using Line Sources for Simulation of Area Sources
A. Braig:	Results of the Revised ATDL Model Compared to the Results of the AQDM and CDM Models.
R. Gualdi:	Preliminary Report about a Diffusion Model for Milano, Italy, Urban Area: Gifford-Hanna Model.

Discussion:

The three papers had the same basis: the ATDL model by Hanna and Gifford. While the first two papers described variations and extensions, the third one presented by R. Gualdi showed an application of the original version.

F. B. Smith asked K. Herrmann if the model allows an introduction of a mixing height. This is not the case, the mixing height is only considered by using appropriate σ_z functions. W. B. Johnson stated that the selection of the appropriate stability classification scheme is the critical point, because the diffusion and, therefore, the concentration varies by orders of magnitude depending upon the exact stability classifications. The Chairman, H. Fortak, confirmed this by mentioning statistical experiments with dispersion parameters. He found by experiments that it is necessary to use finer classifications than four or five categories in order to avoid concentration gaps and inhomogeneous concentration fields in and between different stability categories.

K. H. Vogt wanted to know if the differently calculated concentrations of the two models could be caused by using different $_z$ functions. The question was answered by J. K. Strott as the models were applied to the City of Frankfurt by the Battelle-Institute e. V. It was pointed out that both versions of the ATDL Model were computed with the same stability classifications and σ_z functions, so that the differences are due to the different modeling techniques.

K. E. Grønskei mentioned that he applied the Hanna/Gifford Model with satisfying results. He suggested to smooth the emissions and keep the original grid size. He received the answer that this would not work as the concentration field would be a mirror of the emission field; the problem can only be solved by introducing a source height.

B. Turner pointed out that the underestimation of ground level concentrations as reported by A. Braig might be due to emission sources outside the range of the model, which had a radius of about 15 km. W. B. Johnson added that he thinks the reason for the slope being approximately the half of what would be desirable is not only the underestimation of background concentration but also that SO_2 is no inert gas. This has to be taken into account at least for large distance transports.

As there was no discussion of the third paper the last remarks to this group of papers were made by H. H. Slater, who explained that EPA, similarly to Battelle, uses the Briggs plume rise formula for the AQDM. EPA prefers the AQDM for control actions as this model identifies source categories, i. e. the contribution of individual sources is shown, which is rather an attractive feature.

6 th NATO/CCMS
International Technical Meeting
on Air Pollution Modeling

APPLICATION OF AN AIR POLLUTION MODEL TO THE PROBLEM OF FEASIBLE INDUSTRIALIZATION OF A PLANNED DEEP-SEA HARBOR

by

H. Fortak

Deutsche Forschungs- und Versuchsanstalt
für Luft- und Raumfahrt e.V.
Institut für Physik der Atmosphäre

BATTELLE-INSTITUT E.V., Frankfurt/Main
Germany, FR

24 - 26 September, 1975

ABSTRACT

On the basis of model simulation air pollution climatologies for the surrounding area of the planned deep-sea harbor are predicted, corresponding to different spatial distributions of emission sources. Assuming a total emission rate of pollutants of 10 to/h, an optimal solution of the planning problem of the deep-sea harbor area with respect to environmental protection is obtained when five stacks, each 300 m in height, are lined up at 1 km intervals in SW to NE direction. Compared with other source distributions this configuration gives minimum concentration levels with mean values of less than 5 $\mu g/m^3$, and 97,5 th percentiles of less than 50 $\mu g/m^3$ for the whole area.

INTRODUCTION

Until now, in the field of air pollution abatement the problem of climatological air pollution forecast arose when either new emission sources with known data were planned or when improvements of already existing sources were attempted. Today, both problems can be solved by means of mathematical-meteorological simulation models [1].

The problem becomes far more complicated if certain limits for air pollution climatology of a region are prescribed and if one is asking for feasible installation of industrial complexes according to total source emission and source configuration without exceeding the given concentration values. This question arose for the first time during the planning phase of the deep-sea harbor Neuwerk/Scharhörn.

Basis of the solution of problems of air quality management planning are not individual concentration values at a few locations within the considered area produced by the emission sources. Because of the high variability of meteorological conditions for transport and diffusion a broad spectrum of concentrations is produced at each location. Therefore, it is necessary to derive frequency distributions of air pollution concentrations that result from observations over a sufficiently long period of time. The frequency distributions are characterized by a set of statistical parameters which form the basis of what was called "air pollution climatology" [1]. These parameters are for instance the mean value of concentrations for a given period of time, and the so-called percentiles, i.e. the percentage of observations that showed concentration values exceeding a certain limit.

In case of solving environmental planning problems obviously observations of concentration values do not yet exist. Therefore, the time development of concentrations has to be simulated by means of air pollution models in order to derive the air pollution climatology. For this, a certain "normal development" of meteorological conditions for transport and diffusion is derived from long-term meteorological observations in the considered region. Then, it is divided into classes of actual weather situations, and for each a concentration field is calculated. The knowledge of frequency distributions of these weather situations (conditions for transport and diffusion) allows to derive frequency distributions of concentrations for any location within the area. This method of simulating an air pollution climatology has first been applied to the city of Bremen [2], [3], and shall be applied to the present case too, for until today it is the only reasonable method when dealing with air pollution climatology forecasts.

In detail, the following has to be done: First the statistics of meteorological conditions for transport and diffusion for the flats and coastal area are made available. Since synoptic observations at Scharhörn are missing, wind observations at Scharhörn are related to synoptic observations at Nordholz. Then, a total source strength is assumed for the deep-sea harbor area and is uniformly distributed on different source configurations. With regard to the frequency distribution of the meteorological conditions for transport and diffusion the characteristic air pollution climatology parameters are simulated for any source configuration and especially for a wind direction of 300° (that is the direction from the deep-sea harbor via Neuwerk to Sahlenburg-Duhnen) which is the most interesting one with respect to its effects. The field representation of the parameters for the whole region will complete this investigation.

BASIC CHARACTERISTICS OF THE APPLIED SIMULATION MODEL

Because of the large number of cases to be calculated it was only possible to adopt the most simple but yet most approved model [3], [4], [5]. Here, the spatial distribution of concentrations produced by a single source of strength Q [mg/sec] is given by

$$(1) \quad S(x,y,z) = \frac{Q}{\bar{U}_1} \frac{\exp[-y^2/2\sigma_y^2]}{\sqrt{2\pi}\,\sigma_y} \left\{ \frac{\exp[-(H_{eff}-z)^2/2\sigma_z^2]}{\sqrt{2\pi}\,\sigma_z} + \frac{\exp[-(H_{eff}+z)^2/2\sigma_z^2]}{\sqrt{2\pi}\,\sigma_z} \right\}$$

assuming unlimited vertical dispersion ($S \to 0$ if $z \to \infty$), and reflexion of the pollutant at the earth's surface ($\partial S/\partial z = 0$ if $z = 0$), i.e. a non-absorbing ground.

Removal of the assumption of unlimited vertical dispersion by introducing a lid caused by a temperature inversion layer was possible [3], [6] but was omitted since these weather situations scarcely occur in the considered region. Inclusion of partial absorption of pollutants at water surfaces was performed and was estimated by a series of experimental calculations. The boundary condition at the earth's surface is then replaced by

$$K_z \frac{\partial S}{\partial z} = \beta S \quad : \ z = 0$$

expressing the fact that a fraction of the turbulent vertical transport $K_z \partial S/\partial z$ of pollutants is absorbed proportional to the ground level concentration S. This part of investigation is feasible only by means of a very complex numerical method [7], and is not worthwhile considering the incomplete knowledge of the absorption parameter β. Therefore, it was only possible to estimate the effect of absorption at water surfaces up to the limit of total absorption. This can simply be formulated by equation (1) where the sign between the two terms in parantheses becomes negative. Denoting (1) by $S_{Refl.}$ in case of the assumption of non-absorbing ground, and denoting the solution in case of total absorption by $S_{Abs.}$, then the difference between both limiting cases is

$$\Delta S = S_{Refl.} - S_{Abs.} = 2\,\frac{Q}{\bar{U}_1}\;\frac{\exp[-y^2/2\sigma_y^2]}{\sqrt{2\pi}\,\sigma_y}\;\frac{\exp[-(H_{eff}+z)^2/2\sigma_z^2]}{\sqrt{2\pi}\,\sigma_z} \tag{2}$$

$S_{Abs.} = 0$ at the earth's surface in case of total absorption, i.e. $\Delta S = S_{Refl.}$ if $z = 0$. For all layers $z > 0$ a finite value of $S_{Abs.}$ is obtained and can be compared with $S_{Refl.}$. Upon introduction of

$$\sigma_y = F\,x^f \quad ; \quad \sigma_z = G\,x^g \tag{3}$$

for the standard deviations, the maximum downwind values ($y = 0$) of ΔS are to be found in a distance

$$x_{max}(\Delta S) = \left[\frac{H_{eff}+z}{G\sqrt{2r}}\right]^{1/g} \qquad \text{where} \quad 2r = \frac{f+g}{g} \tag{4}$$

from the emission source, and are given by

$$(\Delta S)_{max} = 2\,\frac{Q}{\bar{U}_1}\;\frac{1}{\sqrt{2\pi}\,\sigma_y(x_{max})}\;\frac{\exp[-r]}{\sqrt{2\pi}\,\sigma_z(x_{max})} \tag{5}$$

Realizing that (4) with $z = 0$ and (5) together with (4) represent exactly the maximum distance $x_{max}(S_{Refl.})$ and the maximum ground level concentration $(S_{Refl.})_{max}$, the effect of absorption turns out to be highest in the neighborhood of maximum ground level concentration values. This is especially true when the concentration layer z is low compared to the effective stack height H_{eff}.

Deriving the expression for the turbulent downward flux of pollutants at the earth's surface in the case of total absorption, $K_z \partial S_{Abs.}/\partial z$ for $z = 0$, and integrating this over the entire domain in crosswind direction $(-\infty < y < \infty)$ and from the emission source $(x = 0)$ to a certain distance x respectively, then the total amount of pollutants being absorbed up to the distance x is given by

$$(6) \qquad A(x) = \int_0^x dx \int_{-\infty}^{\infty} K_z \, \partial S_{Abs.}/\partial z \; dy = Q \; erfc\left[\frac{H_{eff}}{\sqrt{2}\,\sigma_z(x)}\right]$$

where $\mathrm{erfc}\,X = 1 - \mathrm{erf}\,X$, and $\mathrm{erf}\,X = \frac{2}{\sqrt{\pi}} \int_0^X \exp[-t^2]\,dt$ is the well known error integral.

Analysis of (6) has shown that for all meteorological conditions in case of total absorption at water surfaces a considerable amount of pollutants is filtered out from the atmosphere along the distance between the deep-sea harbor and the coast. Partial absorption is to be found in between this extreme and the case of absolutely missing absorption. It cannot be examined, though, without comprehensive knowledge of the absorption coefficient β.

With respect to planning problems it therefore seems to be more feasible to assume non-absorbing water surfaces. For this case the ground level concentration is obtained from equation (1):

(7) $$S(x,y,0) = 2\,\frac{Q}{\overline{U}_1}\,\frac{\exp[-y^2/2\sigma_y^2]}{\sqrt{2\pi}\,\sigma_y}\,\frac{\exp[-H_{eff}^2/2\sigma_z^2]}{\sqrt{2\pi}\,\sigma_z}$$

where the mean transport velocity $\overline{U}_1$ and the effective stack height H_{eff} need to be explained.

In the theory of turbulent diffusion it is taken into account that the wind velocity increases with increasing height. The exponential law

(8) $$U(z) = U(z_A)\left(\frac{z}{z_A}\right)^m$$

allows to estimate the vertical velocity distribution from the measured wind velocity $U(z_A)$ at anemometer level z_A. The representative transport velocity of pollutants then may be defined by taking the mean value of (8) over the polluted layer

(9) $$\overline{U}_1 = \frac{1}{2H_{eff}}\int_0^{2H_{eff}} U(z)\,dz$$

where the effective stack height H_{eff} is the sum of emission height h and plume rise Δh according to

(10) $$H_{eff} = h + \Delta h$$

At the time being, the problem of specifying the plume rise is not sufficiently well solved. The present investigation applies an approved representation [8] in the following form

(11) $$\Delta h = 135\left(\frac{E^*}{\overline{U}_2^3}\right)^{0,4}$$

where E^* is a technical emission value and $\overline{U}_2$ the mean value of $U(z)$

taken over the range of plume rise:

(12)
$$\bar{U}_2 = \frac{1}{\Delta h} \int_{h}^{H_{eff}} U(z)\, dz$$

By this the basic characteristics of the applied model are fully described. Only the standard deviation parameters are still to be determined. They depend on the stability classes being obtained from synoptic observations. For the purposes of this investigation the problem has been considered anew and a more suitable classification of the parameters was found by which certain discrepancies regarding the statistical results are avoided. Very comprehensive numerical investigations resulted in the following modified version of BROOKHAVEN diffusion parameters for effective stack heights $H_{eff} \geq 100$ m ([9], [10]):

Stability class		Diffusion parameters			Wind profile
TURNER	BROOKHAVEN	f = g	F	G	m
1	B_2	0,91	0,40	0,41	0,111
2	B_1	0,86	0,36	0,33	0,208
3		0,81	0,34	0,27	0,250
4	C	0,78	0,32	0,22	0,288
5		0,76	0,315	0,18	0,325
6		0,74	0,31	0,13	0,355
7	D	0,71	0,31	0,06	0,400

Table 1

STATISTICS OF METEOROLOGICAL CONDITIONS FOR TRANSPORT AND DIFFUSION

According to Turner's method [11] for the determination of stability classes not only wind velocity but also a number of synoptic observations are to be used. These data are needed at a representative location within the area of diffusion. At Scharhörn only excellent observations of wind velocity and wind direction were available [12]. Therefore, a station close to the coast (Nordholz) was chosen. Its wind statistic, however, was entirely different from that on the island of Scharhörn. There is good reason to assume that all other synoptic data which are connected with the large-scale weather situation are identical on the island of Scharhörn and at Nordholz. The horizontal distance between both locations is approximately 20 km. The only problem is to relate the wind observations at the station Nordholz to those on the island of Scharhörn for all observation dates. A very complicated procedure led to this relationship such that the statistics of modified Nordholz wind data became identical with that obtained by observations at Scharhörn. A typical example for the region of the Deutsche Bucht is given by figure 1 which shows that the most frequent weather situation is characterized during July by a wind direction of 300° (directed from the planned deep-sea harbor towards the beaches near Cuxhaven). The corresponding wind velocity is around 10 m/sec. In the same manner the complete statistics of meteorological conditions for transport and diffusion became available. The period of observations which forms the basis of these statistics was 17.4.1963 - 31.12.1967. As a summary of these statistics it follows that especially during the summer months the region between the island of Scharhörn and the beaches near Cuxhaven are very frequently loaded with air pollution. However, this takes place in most cases with high wind velocities.

PROBLEMS OF SOURCE CONFIGURATION

It is difficult to assume source configurations without knowing the planned structure of industrialization in the area of the deep-sea harbor. It is logical to use stack heights as a first varying parameter. As classification

$$h = 50,\ 100,\ 150,\ 200,\ 250,\ 300 \text{ m}$$

was chosen. Stack height 50 m was only used for comparison. Since weather situations with fog and low level inversions are quite frequent [12] a tendency towards high stacks is definitely required. In that case emissions take place above all low level inversions and therefore no ground level concentration is produced anywhere.

This motivation for high stacks excludes other favorable solutions assuming a great number of low level sources. With regard to the geometrical arrangement of more than one source it is logical to arrange them such that they are parallel to the receptors which must be protected most. Otherwise, the superposition of sources would lead to a considerable increase of ground level concentrations. A number of numerical experiments demonstrated this superposition impressively. Finally, only five geometrical configurations were utilized:

1. a single source
2. two sources 4 km apart
3. five sources on a line each 1 km apart
4. two groups of nine sources with a grid distance of 600 m
5. a uniform distribution of 36 sources over an area of 3 × 3 km with a grid distance of 600 m.

For each geometrical source configuration the whole set of stack heights was used to produce air pollution climatologies in that region. In total 30 air pollution climatologies actually were calculated. The total source strength of the industrialized area was assumed to be 10 to/h of any type of air pollutants (SO_2 or NO_x . . .). This amount was distributed equally on the sources of each configuration. Difficulties arose when it was attempted to calculate plume rise. The technical emission value depends on the type of the installation, i. e. the stack height and the source strength. Without knowledge of the actual data only statistical relationships could be used. Utilizing the source inventories of the cities of Bremen, Düsseldorf and Frankfurt the relationships

$$h = A\sqrt{Q} \; ; \quad E^{*} = BQ \; ; \quad E^{*} = C\,h^{2}$$

were obtained. The factors A, B, C were obtained by regression analysis. In case of a single source $E^{*} = 150Q = 1\,500\,[m^4/sec^3]$ was used, for all other source configurations $E^{*} = 200Q$ gave the best results.

RESULTS OF THE NUMERICAL EXPERIMENTS

The program was composed of two main parts : calculation of the parameters for air pollution climatology only for the wind direction 300^{o} which was considered to be the critical one. For that wind direction the frequency distributions of wind velocity and stability classes were used. In that case very detailed information were obtained. The second main part was concerned with calculations of two - dimensional fields of the parameters of the air pollution climatologies. The considered area is seen on the subsequent figures.

The first pre - investigation was concerned with maximum ground level concentrations along the wind direction 300^{o}. All combinations of source configuration, wind velocity and stability class were varied. Figure 2 shows the result. As an example the experiment h = 150 m and five sources may be considered : as a result of the different combinations of wind velocity and stability class two regions are produced where absolute maxima are caused by a certain stability class (2 and 3). Up to a distance of 16 km those stability classes are responsible for the highest maxima. Further downwind the maxima are less than 200 µg/m^3 and are produced by stability class 4 which is a very frequent one. Looking at Figure 2 it is reasonable to choose first of all a source configuration which produces maximum ground level concentrations which are as small as possible. According to this statement Figure 2 recommends as the best solution an arrangement of five sources each 300 m high. In that case maximum ground level concentrations rarely exceed 100 µg/m^3. More detailed information can be obtained from Figures 3, 4 and 5. Here, the stability class is not indicated but the possible maximum ground level concentrations are drawn for all assumed stack heights and all source distances up to 24 km. In the figures it should be realized that the scale of the ordinate is logarithmic. It is easily seen that from this point of view the configuration with five sources certainly is most favorable. This is especially true for the region around 4 km where the island of Neuwerk is located.

Parameters of the complete air pollution climatology are represented as two - dimensional fields in the subsequent figures. Firstly, the fields of mean values are compared with each other. In case of only one source the mean values of concentration for a time period of a normal year are given by Figures 6 and 7. The difference between Figure 6 (stack height 100 m) and Figure 7 (stack height 300 m) is considerable. The latter case is the favorable one because the island of Neuwerk is fairly well protected, what is also true for the beaches west of Cuxhaven. The former case is most unfavorable because of the very high mean values found exactly near the island of Neuwerk. Compared with this result the arrangement of five sources seems to be not too different from the former case. Stack heights of 100 m give almost the same mean values in a slightly changed geometrical form. Stack heights of 300 m change the pattern of the mean values only slightly. Comparing these two cases (one stack and five stacks) one should keep in mind that Figures 2 and 3 showed that the five stack arrangement is favorable with regard to maximum ground level concentrations even if the fields of mean values differ so less from each other. The final decision will be found by comparing the 97,5 th percentiles (see later). The last field of mean values given in that paper shows the case in which an arrangement of 36 sources (each stack 100 m high) was considered. Compared with Figure 6 and Figure 8 this Figure 10 shows very unfavorable results.

In deciding what the best solution with regard to a maximum protection of the environment is, the former discussed properties of the statistics of concentration fields are not sufficient. A comparison of the 97,5 th percentiles (Figures 11, 12, 13, 14, 15) will give the final answer. Considering Figure 11 (one source, 100 m high), Figure 13 (five sources, 100 m high), and Figure 15 (36 sources, 100 m high) it can be seen that the five source arrangement gives the lowest 97,5 th percentiles not only at the beaches, but also protects the island of Neuwerk sufficiently. This situation becomes even better if Figure 12 (one source, 300 m high) and Figure 14 (five sources, 300 m high) are compared with each other. In the case of one source, at the beaches values between 60 and 70 $\mu g/m^3$ are found whereas in the case of five sources values of slightly higher than 40 $\mu g/m^3$ are produced. The difference at Neuwerk between both cases is even greater. A typical 97,5 th percentile value of 60 $\mu g/m^3$ for the one source case stands against a value of 25 $\mu g/m^3$ for the case of five sources.

The selection of experiments shown in this paper indicates that the five source arrangement with stack heights of 300 m can be considered the optimum solution of the stated problem. This solution is not a trivial one, because the many non-linear relationships together with the complicated statistical relationships are working together in a very complex manner and might have given quite different source arrangements as optimal solutions as those we found in this paper. The found optimal solution gives very low mean values and 97,5 th percentiles in the whole area in case of a total emission strength of 10 to/h. It can be estimated that approximately twice as much could be emitted in that area without violating air pollution control standards.

The cooperation with my collegues Prof. W. Fett and Dipl. Ing. A. Tamer who did the programming, and with Dipl. Met. B. Dußler who helped in scientific and technical respects is gratefully acknowledged.

REFERENCES

[1] FORTAK, H. Anwendungsmöglichkeiten von mathematisch - meteorologischen Diffusionsmodellen zur Lösung von Fragen der Luftreinhaltung. Herausgegeben vom Minister für Arbeit, Gesundheit und Soziales des Landes Nordrhein - Westfalen. Düsseldorf 1972.

[2] FORTAK, H. Rechnerische Ermittlung der SO_2 - Grundbelastung aus Emissionsdaten. Inst. f. Theor. Met. der FU Berlin, 1966.

[3] FORTAK, H. Numerical Simulation of the Temporal and Spatial Distribution of Urban Air Pollution Concentration. Proc. Symp. Multiple - Source Urban Diffusion Models, RTP, North Carolina, Nov. 1970.

[4] PASQUILL, F. Atmospheric Diffusion. London 1962.

[5] FETT, W. Simulation der Ausbreitung von Luftverunreinigungen mittels einer Tischrechenanlage. Schr. Reihe Ver. Wasser - Boden - Lufthyg., Berlin - Dahlem, Heft 41, Stuttgart 1974.

[6] FORTAK, H. Ausbreitung von Staub und Gasen um eine kontinuierliche Punktquelle in einer bezüglich Windgeschwindigkeit und Austausch geschichteten Atmosphäre. VDI - Forsch. H. 483, 1961.

[7] FORTAK, H. Einbeziehung der Sinkgeschwindigkeit und partiellen Absorption am Erdboden in die Ausbreitungsrechnung, speziell im Falle nicht-Fick'scher Diffusion. Inst. f. Theor. Met. der FU Berlin, 1964.

[8] FORTAK, H. Vergleich von berechneten und gemessenen maximalen Bodenimmissionen und deren Entfernungen von der Quelle für den Fall von Großemittenten. Staub 29, 1969, 493 - 498.

[9] SINGER, I. A. and M. E. SMITH: Atmospheric Dispersion at Brookhaven National Laboratory. Int. J. Air and Water Poll. 10, 1966, 125 - 135.

[10] FORTAK, H. Diagramme zur Beurteilung des Einflusses verschiedener Parametersätze für die Streuungen auf die maximale Bodenkonzentration und die zugehörige Quellentfernung.
Absolute Immissionsmaxima im Lee einer Punktquelle. Eingereicht zur Veröff. in Staub.

[11] TURNER, D. B. A Diffusion Model for an Urban Area. J. Appl. Meteor. 3 (1), 1964.

[12] ANTFANG, H. Die Wind- und Nebelverhältnisse im Elbmündungsgebiet. Hamburger Küstenforschung, Nr. 9, Juni 1969.

CAPTION OF FIGURES

Figure 1 : Relative frequency distribution of wind direction and classified wind velocities for one selected month (July).

Figure 2 : Maximum SO_2 concentrations at the ground as a function of source distance and stability class, calculated for a variety of source configurations.

Maximum ground level concentration as a function of source distance and stack height :

Figure 3 : 1 source   Figure 4 : 5 sources   Figure 5 : 36 sources

Two - dimensional field of annual mean value of ground level concentrations:

Figure 6 : 1 stack, 100 m high   Figure 7 : 1 stack, 300 m high
Figure 8 : 5 stacks, 100 m high   Figure 9 : 5 stacks, 300 m high
Figure 10 : 36 stacks, 100 m high

97,5 th percentile of the annual frequency distribution of ground level concentrations :

Figure 11 : 1 stack, 100 m high   Figure 12 : 1 stack, 300 m high
Figure 13 : 5 stacks, 100 m high   Figure 14 : 5 stacks, 300 m high
Figure 15 : 36 stacks, 100 m high

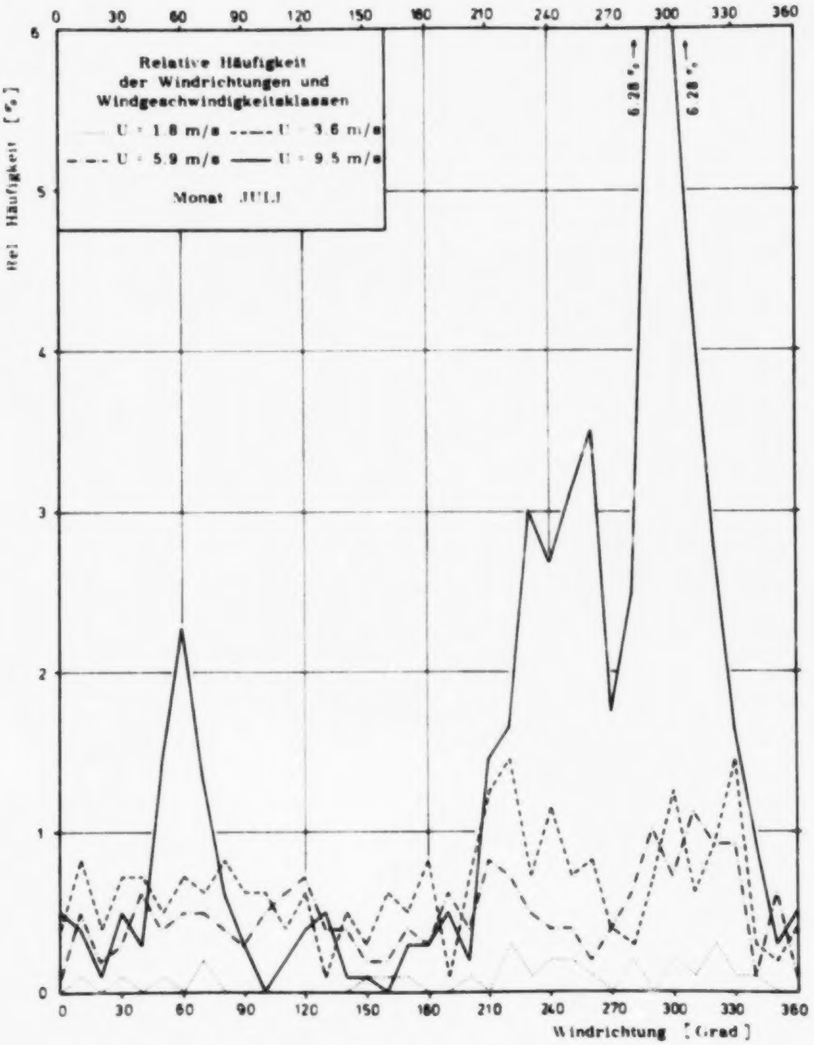
Relative Häufigkeit
der Windrichtungen und
Windgeschwindigkeitsklassen
U = 1.8 m/s
U = 3.6 m/s
U = 5.9 m/s
U = 9.5 m/s
Monat JULI
6.28 %
6.28 %
Rel. Häufigkeit [%]
Windrichtung [Grad]
0
30
60
90
120
150
180
210
240
270
300
330
360
0
1
2
3
4
5
6

FIGURE 1

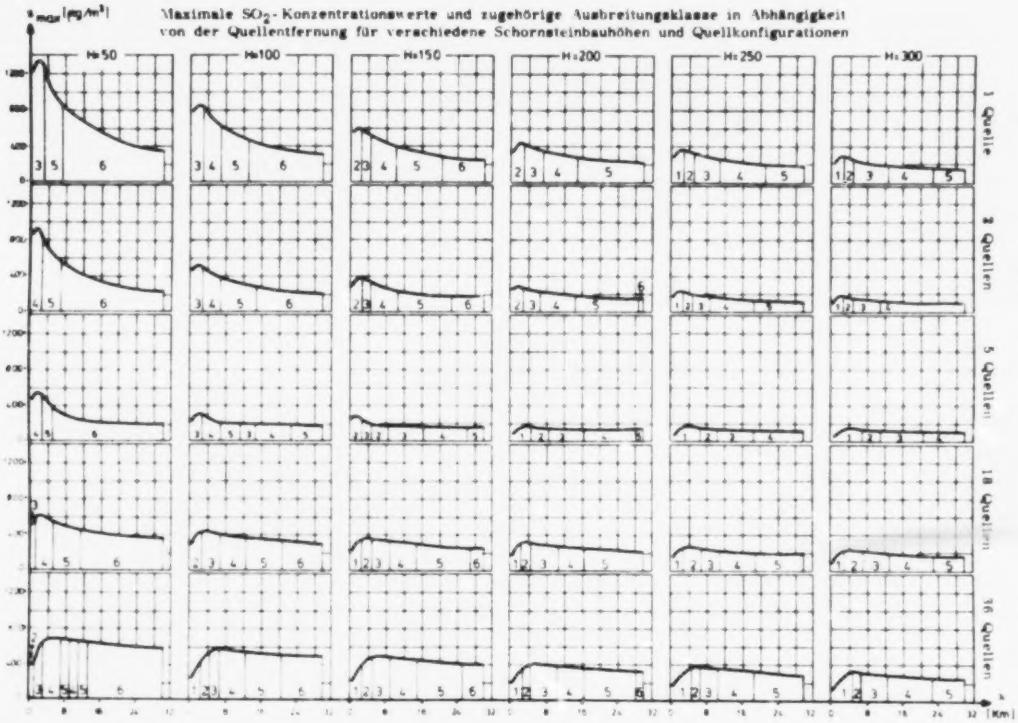

FIGURE 2

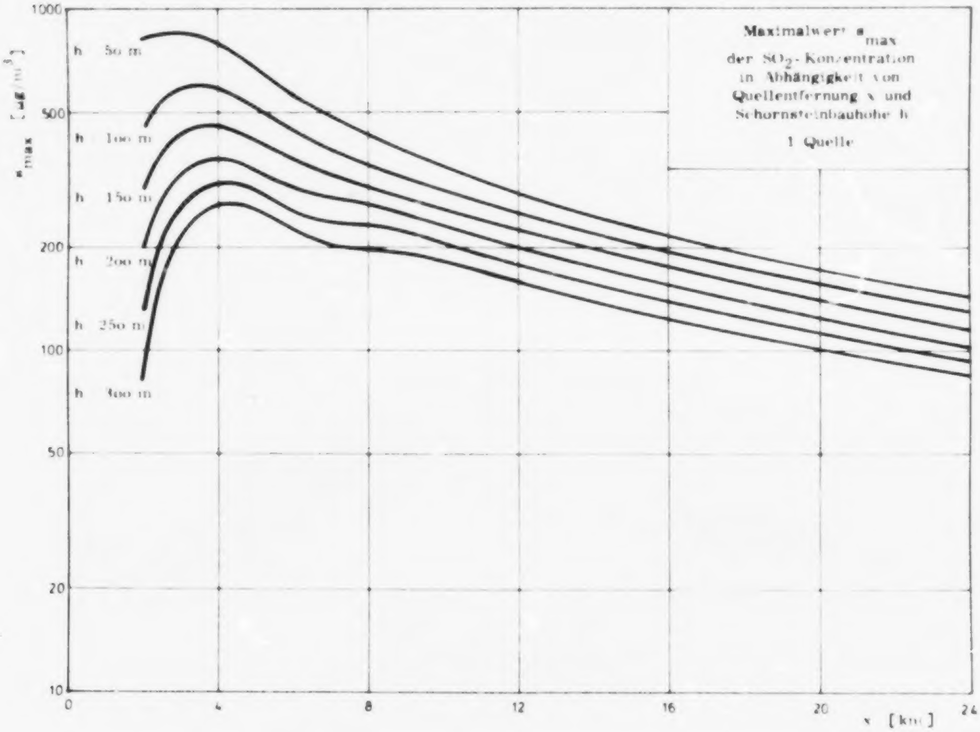

FIGURE 3

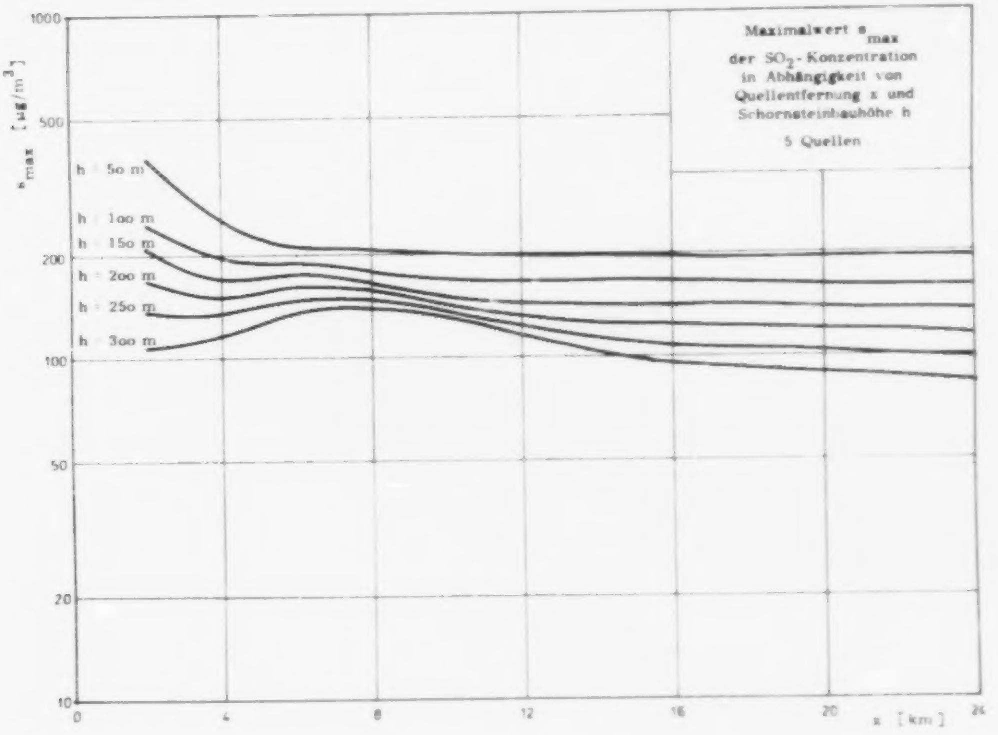

FIGURE 4

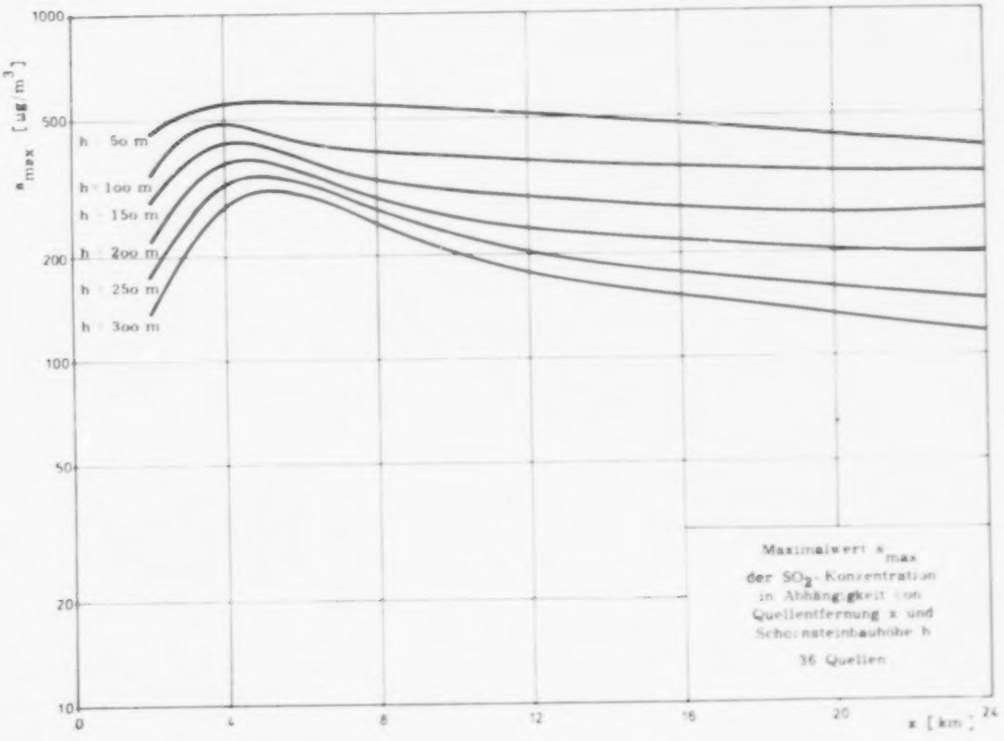

FIGURE 5

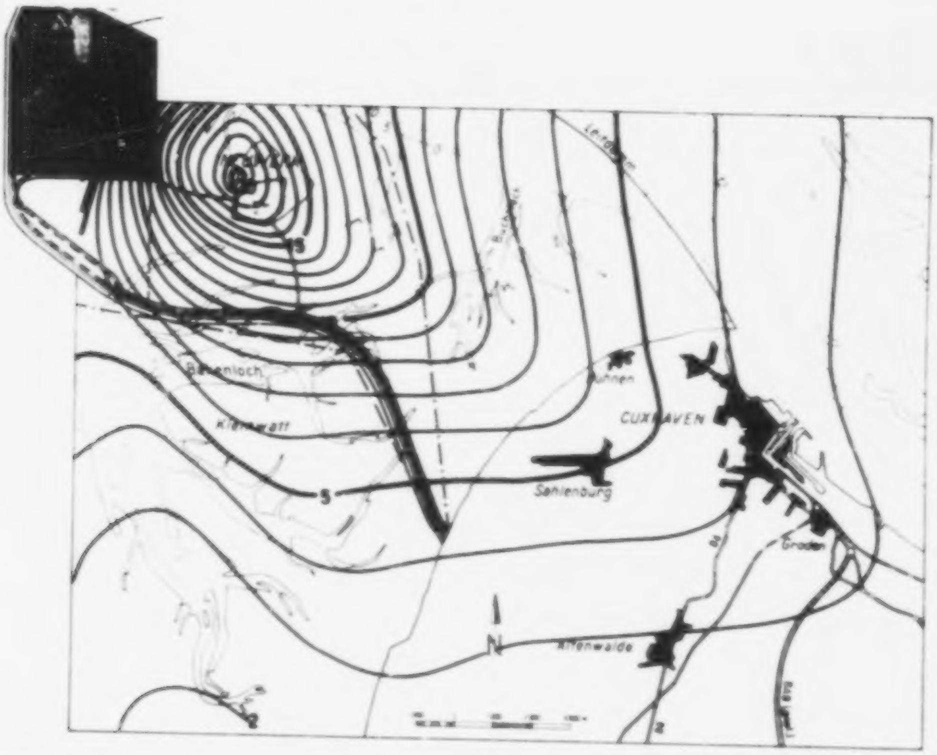

FIGURE 6

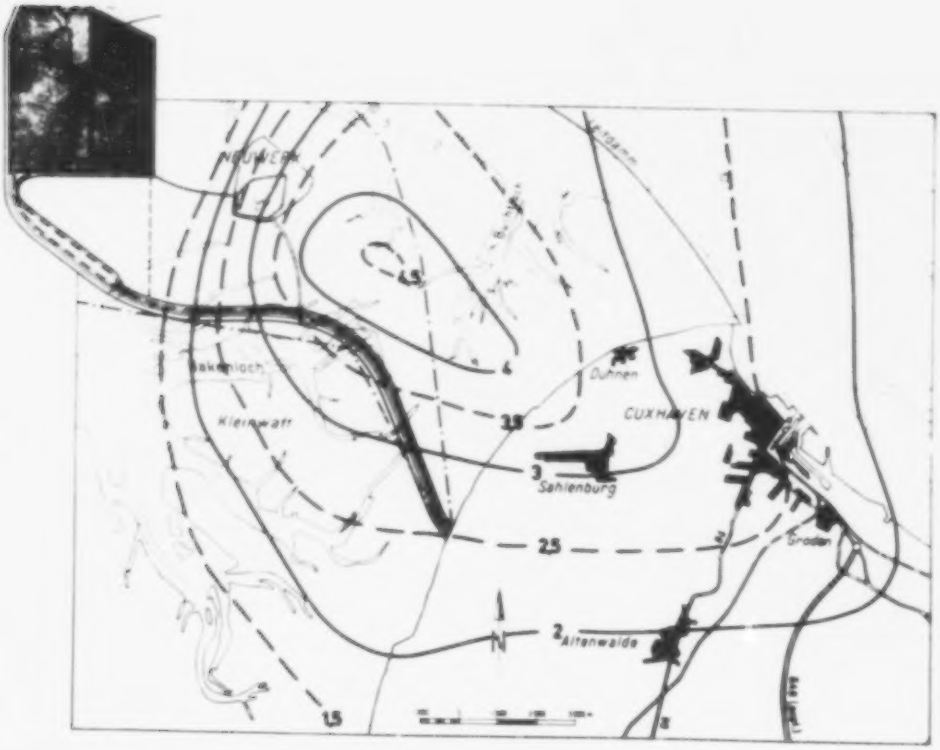

FIGURE 7

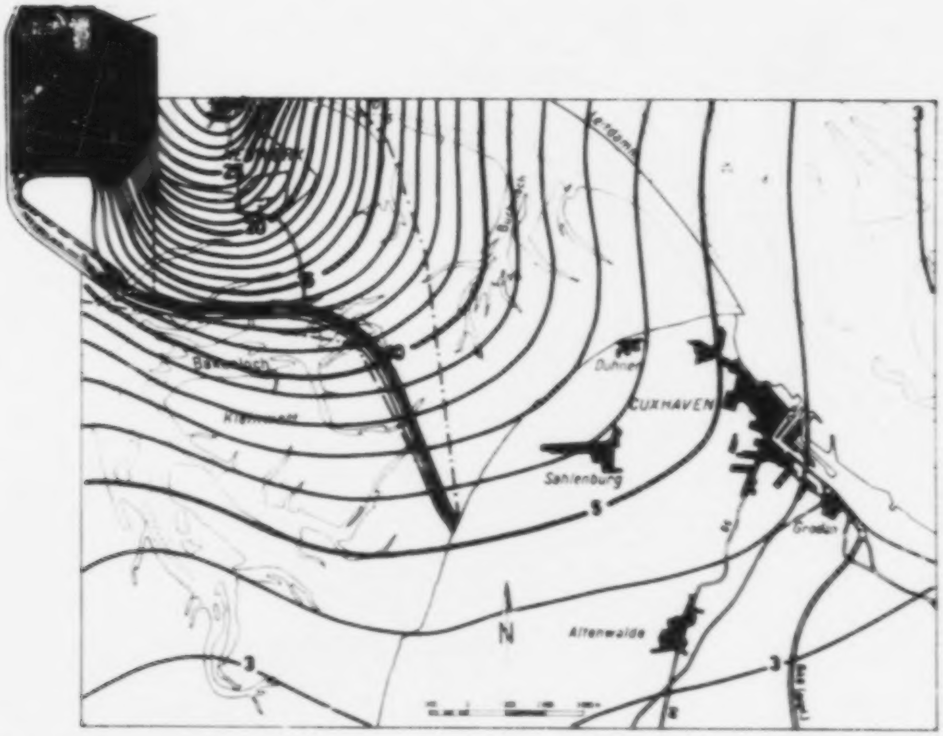

FIGURE 8

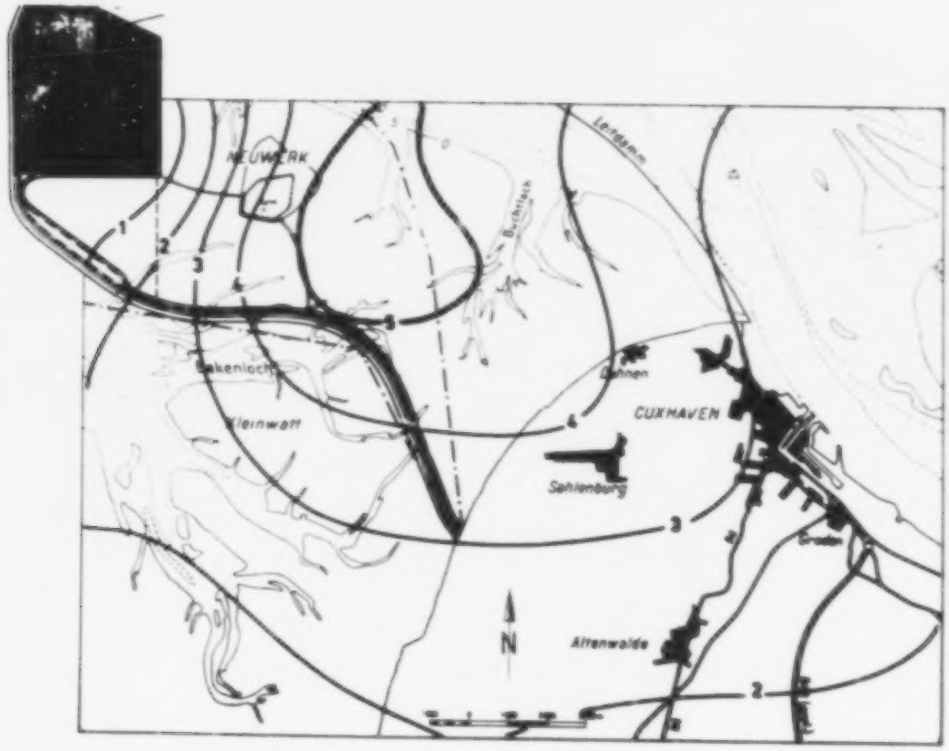

FIGURE 9

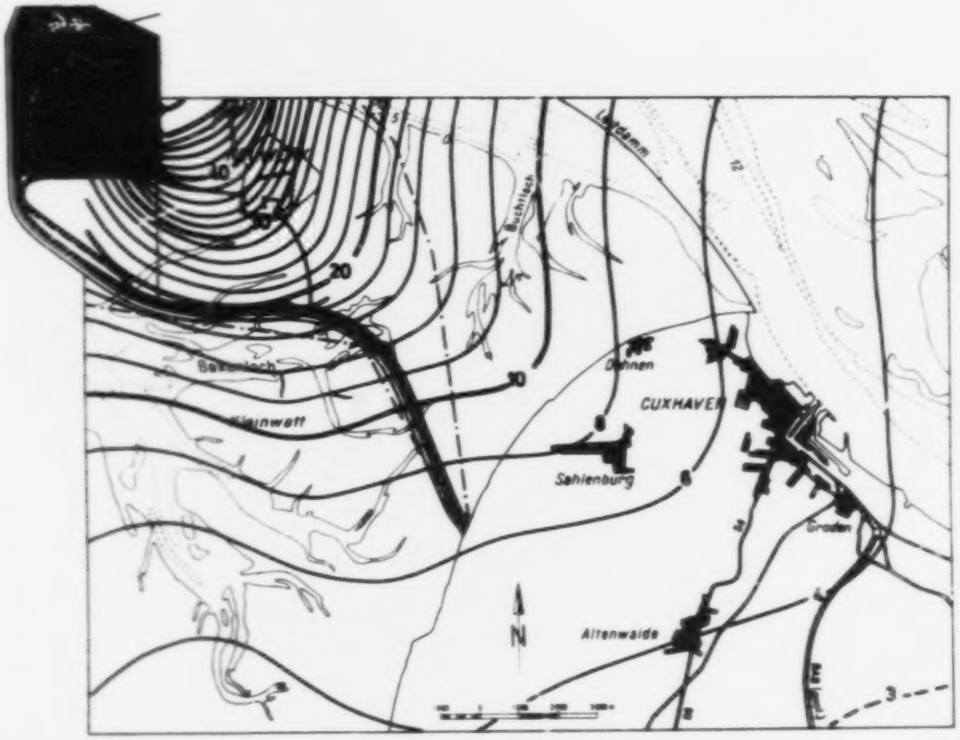

FIGURE 10

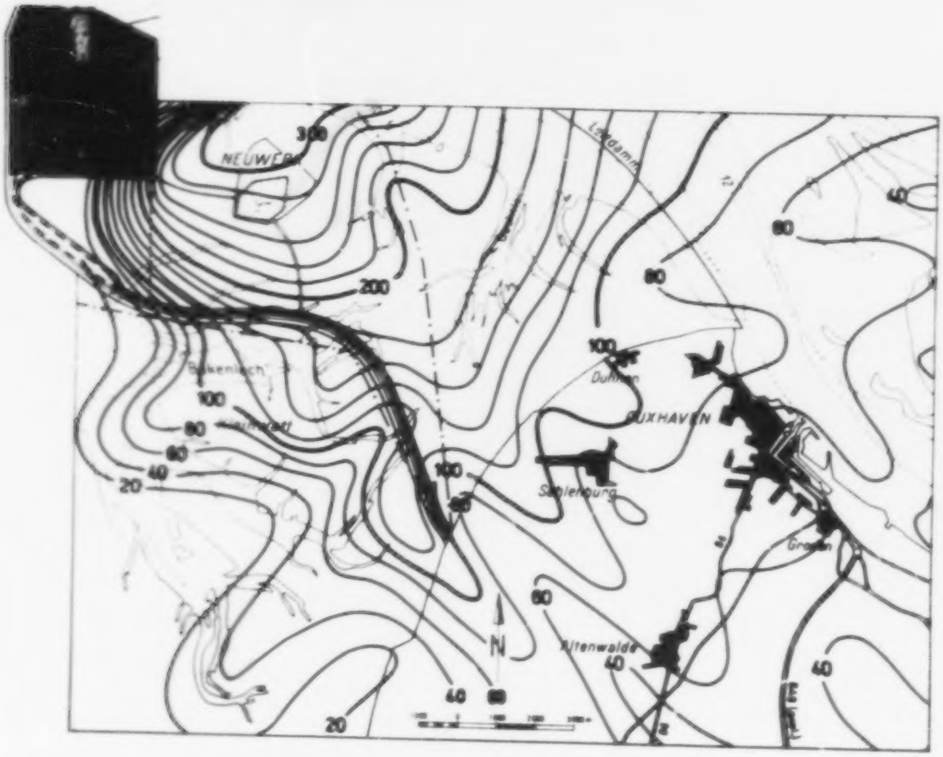

FIGURE 11

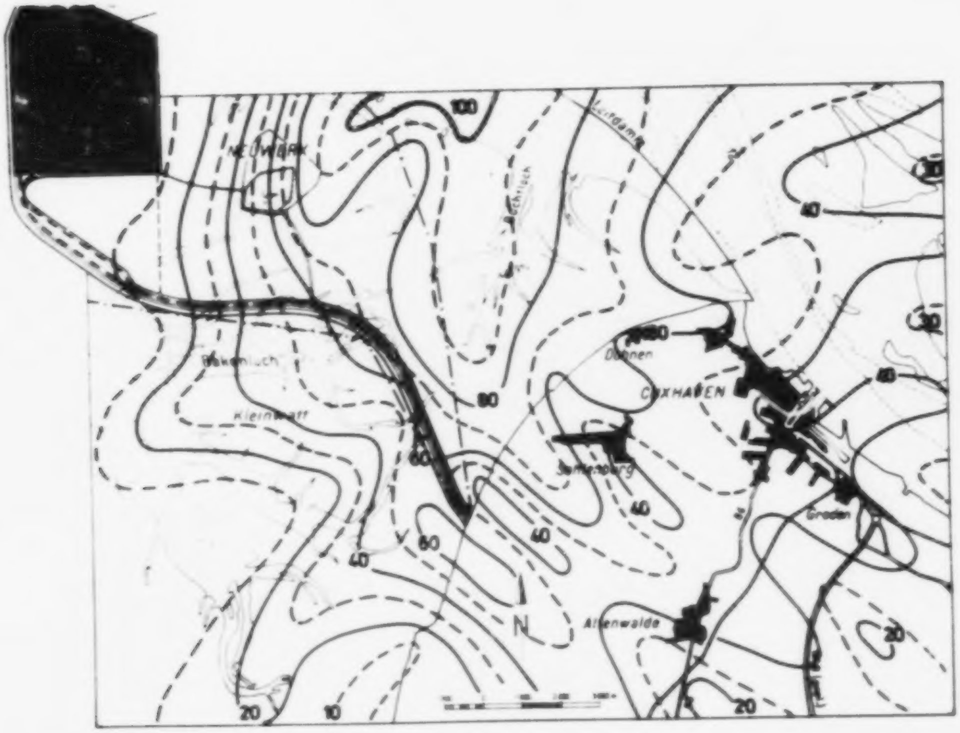

FIGURE 12

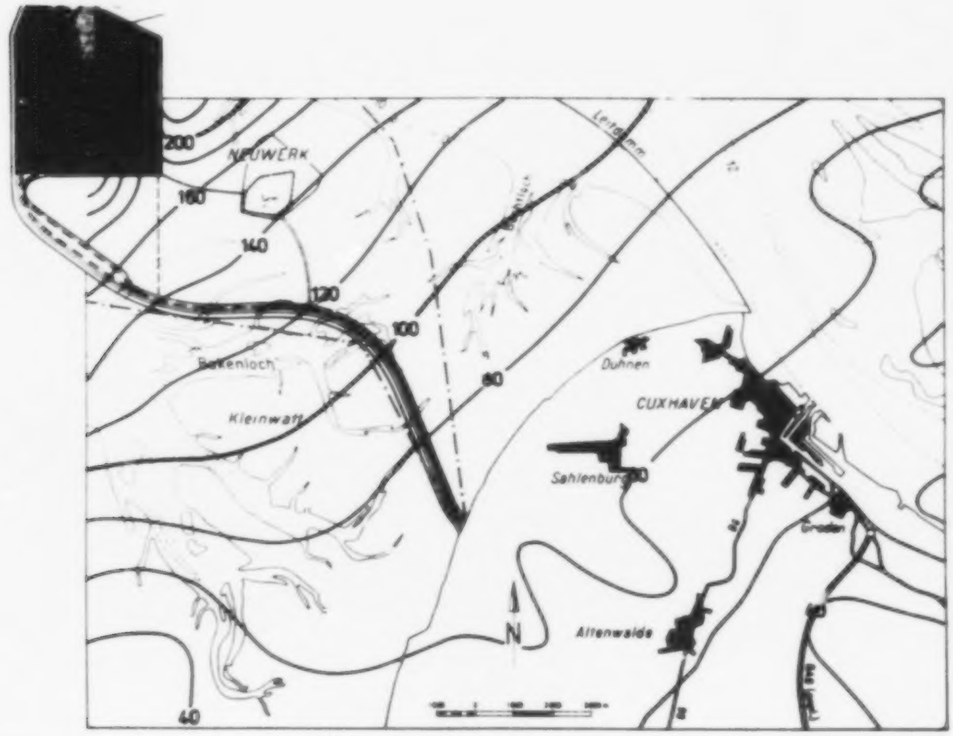

FIGURE 13

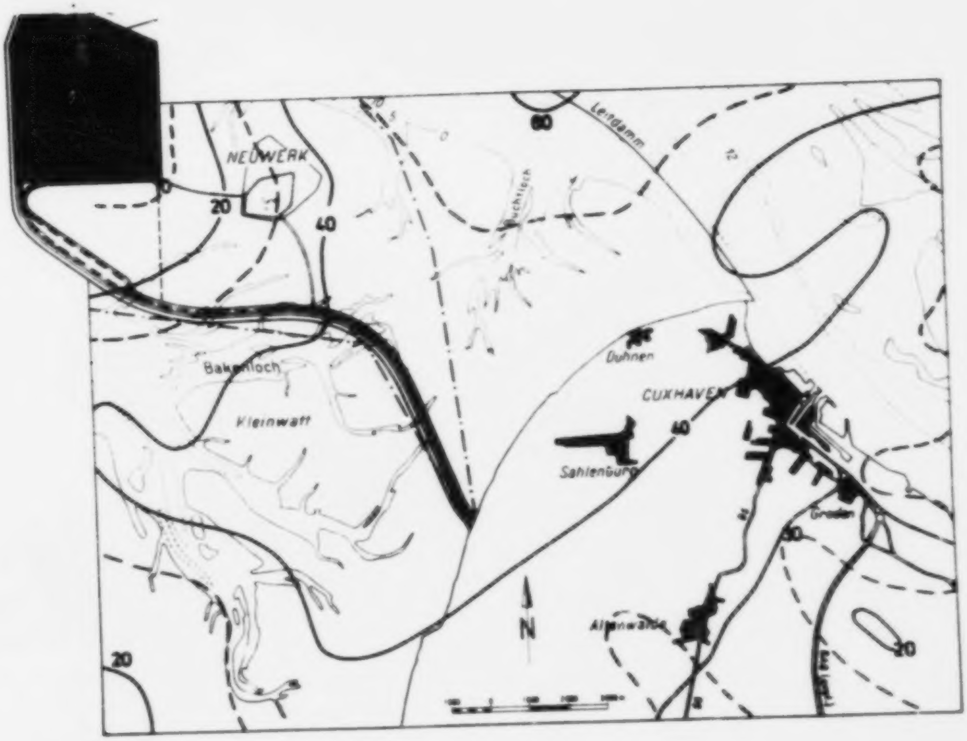

FIGURE 14

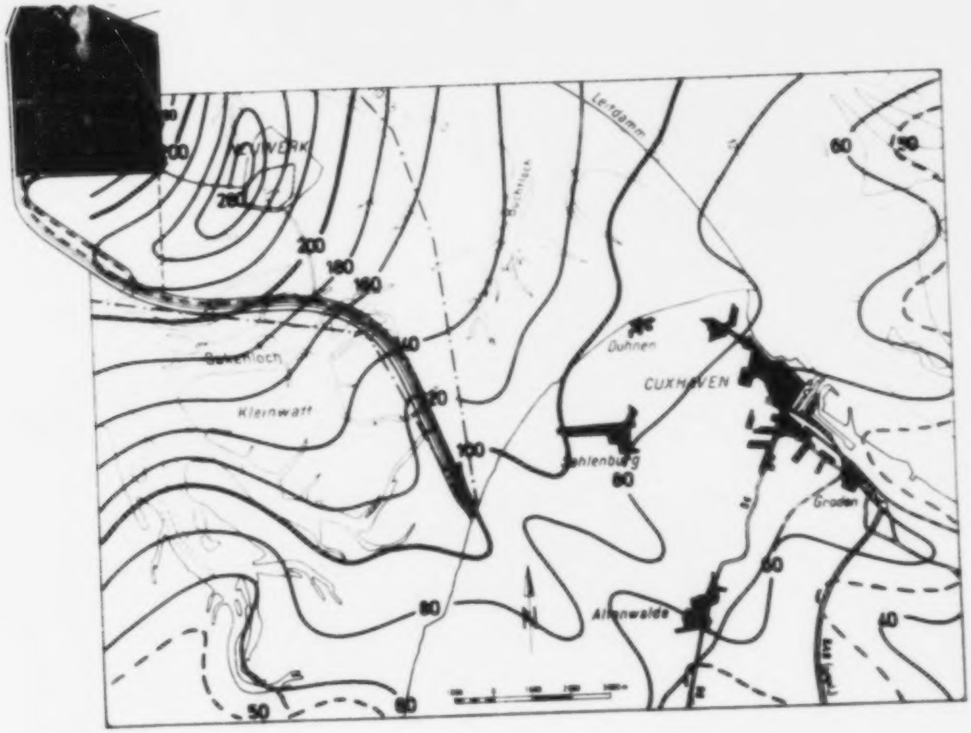

FIGURE 15

6th NATO /CCMS
International Technical Meeting
on Air Pollution Modeling

H. Fortak; B. Gutsche *; R. Stern

FURTHER INVESTIGATIONS OF THE AMBIENT AIR QUALITY SITUATION IN THE UNTER-MAIN REGION MAKING USE OF FORTAK'S DISPERSION MODEL

*present address: Umweltbundesamt (Federal Environmental
Agency); D-1000 Berlin 33; Bismarckplatz 1

Battelle-Institut e. V. Frankfurt/M
Germany, FR
24 - 26 September, 1975

ABSTRACT

The former model investigations of the ambient air quality in the Region Undermain (FORTAK, 5th Progress Report of the Regional Planning Community Undermain) have been continued improving the model program and extending the underlying meteorological data material.

By comparison with data from continuously working SO_2-monitoring stations and from random tests a model validation was performed for single meteorological situation as well as for long-term statistical values. As a result we found a concentration gradient between city-center and suburbs being less pronounced in the measurements than in the model results with correct values in the city-center and too low values outside the city.
Annual mean values show good agreement between measured and calculated concentrations, but there are considerable discrepancies in the structure of the cumulative frequency distributions. Thus, these cumulative frequency distributions seem to be a more appropriate instrument for model verification then the rather insensitive annual mean values.
The calculation of the effect of a planned power station upon the ambient air quality of Frankfurt allows a comparison with the corresponding results of the Battelle-Institute where the AQDM-model had been applied to the same emittents. Differences in the structure of these results emphasize the need for model standardization.

1. Introduction

There are two arguments supporting the retention and the further development of GAUSSian plume models:

(1) because of the difficulty of more complicated models to supply long-term concentration values they cannot be used for several planning activities;

(2) at the current state of development, GAUSSian plume models appear to be the only ones in widespread operational use in many countries for which a model-standardization is possible and realizable.

In view of these points we want to report on the application of FORTAK's GAUSSian plume model to the Untermain region, although we are developing model-systems at our Institute that apply to more complicated meteorological and topographic conditions than can be treated by GAUSSian plume models.

2. Brief description of FORTAK's dispersion model
Main model assumptions (1), (2)

FORTAK's dispersion model is based on the GAUSSian plume equation for steady and horizontally homogeneious meteorological conditions and for flat terrain.

Boundary conditions are those of total reflection at the ground-surface and in the inversion height.

Chemical and photochemical transformation processes, that can formally be taken into account by use of a SO_2-half-life, are neglected within this study,

Thus, the working equations are
for total reflection at the ground-surface

$$\bar{S}(x,y,z) = \frac{Q}{2\pi\bar{u}\sigma_y\sigma_z}\exp\left(-\frac{y^2}{2\sigma_y^2}\right)\left\{\exp\left(-\frac{(z-H)^2}{2\sigma_z^2}\right)+\exp\left(-\frac{(z+H)^2}{2\sigma_z^2}\right)\right\}$$

and for total reflection at the ground-surface and in the inversion heigth

$$\bar{S}(x,y,z) = \frac{Q}{2\pi\bar{u}\sigma_y\sigma_z}\exp\left(-\frac{y^2}{2\sigma_y^2}\right)\sum_{n=-\infty}^{+\infty}\left\{\exp\left(-\frac{(z-H+2nH_I)^2}{2\sigma_z^2}\right)+\exp\left(-\frac{(z+H+2n}{2\sigma_z^2}\right.\right.$$

in conventional notation.

Besides steadiness and horizontal homogeneity, the neglect of turbulent diffusion in the transportation direction compared with the advective transport of pollutants in this direction, which is inherent in the GAUSSian plume equation, seems to be the most serious model assumption, because it limits the applicability of this model to meteorological conditions with mean wind speeds of more than about three knots and, thus, excludes the treatment of calms and weak-wind situations.

Fig. 1 shows the frequency distribution of wind speed in the Region Untermain, demonstrating the relatively high occurence probability of weak-wind situations for this region. Due to the assumption of a relatively uniform class distribution the following wind speed classification can be derived for Frankfurt/Germany

class	u(kn)	$\bar{u}$(m/sec)
1	≤2	0.9
2	3, 4	1.7
3	5, 6	2.4
4	7, 8, 9	3.6
5	10, 11, 12, 13	5.2
6	≥14	7.1

Class 1 (weak-wind situations) have to be excluded with respect to the main model assumptions.

3. Emission Data

The model's emission data used to apply FORTAK's dispersion model to the Untermain region were derived from the detailed emission inventory, partly published in the 5th Progress report of the Regional Planning Community Untermain, Frankfurt.

235 single emittents with an emission of more than 1 kg SO_2/h are treated as individual point sources. As corresponding plume rise equation for these singular emittents STÜMKE's 1963-formula had been chosen.

Space heating and 476 minor single emittents with an emission of less than 1 kg SO_2/h are interpreted as area sources. Total emissions by the minor emission sources amounted to only 1.4% (168 kg SO_2/h) of those by the major sources (11682 kg SO_2/h), and, thus, play only a minor role in the total emission picture. For comparison, the contribution of space heating to the SO_2-emission amounted to 8190 kg/h at $-12^{\circ}C$.

Each area source, which is identical with a grid square of mesh-size 500 by 500 meters, is simulated by 100 point sources distributed uniformly over the grid square. Source strength and emission heights of these point sources correspond to the average conditions within the grid square. For practical reasons these emission heights were grouped in 6 height classes.

The influence of the daily mean temperature on the domestic fuel xxxxxx consumption has been ascertained in such a way, that the daily emission variations depending upon the daily mean temperature are prescribed using the results of the emission inventory study in Cologne.

4. Results

4.1 Statistics of meteorological dispersion characteristics

Fig. 2 and 3 demonstrate the important effect of the specific topographic situation of the Region Untermain on the statistics of meteorological dispersion characteristics(3).

The orientation of the Taunus ridge from WSW to ENE produces a frequency distribution of wind direction with pronounced maxima in the SW- and NE-sectors.

This phenomenon is independent of the wind speed class (Fig. 2) and of the stability of the atmosphreic stratification (Fig. 3). We always recognize the same orientation of the maxima in the wind rose.

The following can be said in conclusion:

The meteorological conditions in the Untermain region are characterized by a number of weak-wind situations and by the specific topographic conditions, thus, questioning the basic assumptions of the GAUSSian plume model.

But, as BARTELS, CASPAR, and SCHARRER(4) have pointed out in the 5th Progress Report of the Planning Community Undermain, there still remains a sufficient number of meteorological situations to which FORTAK's dispersion model may be applied.

Fig. 4 shows the relative frequency of unstable, neutral, and stable situations for the period 1967 to 1972, divided into heating period and unheated period.

4.2 Calculated SO_2-concentrations for selected meteorological situations

To illustrate the concentration fields calculated by the dispersion model we selected situations which clearly fulfill the main model assumptions: steadiness, horizontal homogeneity, and wind speeds greater than 1.5 m/sec.

For this demonstration purpose we chose SW- and NE-wind-situations since outside these prevailing wind directions frequencies become very low.

Fig. 5 shows the calculated ground-level SO_2-concentration field for the 12th Dec. 1968, 7 to 9 p.m..
The corresponding meteorological situation is charaterized by NNE-winds (20°), a wind speed of 5 knots and a stable atmosphreic stratification (TURNER class 5). For this situation and two other ones(3) average measured SO_2-concentration values from 3 continuously working SO_2-monitoring stations are compared with the concentrations calculated by the model. The agreement is reasonable.

It must be mentioned that for the simulation of these actual concentration fields the actual wind speed had been used and not the corresponding class mean as it has proved useful for the calculation of long-term statistical concentration values.

1.) 7. Feb. 1969

$\varphi = 220^{\circ}$
$\bar{u} = 5$ kn
AK = 5 (TURNER class)
$T = -4.9^{\circ}C$

time	SO_2 - concentrations ($\mu g/m^3$)		
	Central-station	Posthochhaus	Ackermann-Schule
1 a.m.	286	249	175
2 a.m.	269	289	154
3 a.m.	252	223	149
averaged	269	254	160
calculated	310	220	160

2.) 12. Dec. 1968

$\varphi = 20^{\circ}$
$\bar{u} = 5$ kn
AK = 5
$T = -5.8^{\circ}C$

time	SO_2 - concentrations ($\mu g/m^3$)		
	Central-station	Posthochhaus	Ackermann-Schule
7 p.m.	383	326	474
8 p.m.	449	297	574
9 p.m.	497	354	637
averaged	443	326	562
calculated	440	360	570

3.) 13. Dec. 1968

$\varphi = 20^{\circ}$
$\bar{u} = 4$ kn
AK = 4
$T = -4.6^{\circ}C$

time	SO_2 - concentrations ($\mu g/m^3$)		
	Central-station	Posthochhaus	Ackermann-Schule
2 p.m.	291	269	341
3 p.m.	291	291	322
averaged	291	280	332
calculated	310	280	390

Table: Comparison between measured and calculated ground-level SO_2-concentrations for selected meteorological situations

4.3 Calculated long-term ground-level SO_2-concentrations compared with measured values

On the basis of a receptor-oriented version of FORTAK's dispersion model and the meteorological dispersion climatology for the time period 1967 to 1972 long-term ground-level SO_2-concentration values have been simulated for the location of several measuring sites.

In the following table calculated annual mean values of ground-level SO_2-values are compared with measured values from three continuously working SO_2-monitoring stations(from LINK and KALLER (5)).

measuring site	model calculations (1967 - 1972)	measured values (1.7.67 - 30.4.71)	
		total data set	selected data
Central-station	115	123	114
Post-Hochhaus	90	100	94
Ackermannschule	97	108	94

Table: Calculated and measured annual-mean values of ground-level SO_2-concentrations ($\mu g/m^3$)

The relatively good agreement between calculated values and the total set of measured data can even be improved by selecting only those meteorological situations to which a GAUSSian plume model may be applied with some confidence.

But it must be mentioned in this connection that these three measuring sites are typical city-center stations, and it is a characteristic feature of several diffusion models that they show a concentration gradient between city-center and suburbs that is too large compared with corresponding measurements. This effect can be reduced by an extension and improvement of the emission inventory, especially that of residential combustion (2).

For a better test of the calculated field structure other stations have to be used. Unfortunately there exist only random tests so that only annual mean values may be compared.

Fig. 6 shows the results of these random tests for two years compared with model calculations using the meteorological statistics for the years 1967 to 1972 and for 1972 alone. Since the respective data sets are not directly comparable the spread of the mean values is greater. But the structure of the field of annual mean values is reproduced correctly by the model, although the large city-center to suburb gradient can be recognized in these results, too.

The calculated contributions of different emission sources (space heating and single emittents, respectively) to the ambient air quality situation in Frankfurt can be found in (6).

The conformity between calculated and measured annual mean concentration values gives the impression of a satisfying model verification.

But this result has to be differentiated if instead of the annual mean value the cumulative frequency distribution of ground-level SO_2-concentrations at various places are examined.

Figs.7 and 8 show the calculated and measured cumulative frequency distributions of ground-level SO_2-concentrations for the Centralstation in Frankfurt and for the station in Offenbach.

These diagrams demonstrate that in spite of a good agreement between the annual mean values there ara discrepancies in the corresponding cumulative frequency distributions. The intersection of the measured and the calculated cumulative frequency distributions results in an overestimation of low concentration values as well as of high concentration values. It has not yet been possible fully to determine all reasons for these overestimations.

But a general conclusion can be drawn from these results: these cumulative frequency distributions seem to be a more appropriate instrument for model verification than the rather insensitive annual mean concentrations. Perhaps, just as a result of this conclusion only very few cumulative frequency distributions have been published in the literature.

Furthermore, from these figures as well as from other results (3), the conclusion can be drawn that meteorological data or ground-level concentrations taken from one year alone are insufficient for a correct description of the dispersion climatology or the ambient air quality of the region under consideration. Thus, the statement of the new German 'Technical Instructions for Ensuring Clean Air', that, if in the course of an approval procedure concentration measurements are required, the duration of these measurements shall not exceed one year, can be improved significantly by including meteorological information going beyond this year and by taking into account long-term model calculations.

4.4 Effect of a planned power station upon the long-term ambient air quality situation in Frankfurt

Planning activities and air pollution legislation require a correct and incontroversible prediction of the ambient air quality situation to be expected. We wanted to test the ability of GAUSSian plume models to solve this problem. Therefore, we repeated an experiment which had already been performed by the BATELLE-Institute. They applied the MARTIN-TIKVART model to the Untermain region and examined the influence of a planned power station on the long-term ambient air quality of Frankfurt. MARTIN and TIKVART's model is quite similar to FORTAK's dispersion model. There are some differences in the internal structure of the models, and they use different area source representations and plume rise formulas. Furthermore, the classification of meteorological parameters differs: particularly, MARTIN and TIKVART use a wind rose in 16 parts with 22.5 degree sectors and not in 36 parts with 10 degree sectors. For stability classification the BATELLE-Institute used KLUG's scheme instead of the TURNER-scheme used in FORTAK's model.

BATELLE's results partly differ from those presented here. Especially, there is much less structure in the annual mean SO_2-concentration field calculated by BATELLE than in those predicted by FORTAK's model.

Because the new German 'Technical Instructions for Ensuring Clean Air' recommend the application of dispersion models in approval procedures for major emittents, a comparison between the results of these models is an absolute necessity for a case in which these models are applied to the same power station.

The data of the planned power station Fechenheim used in both models are as follows:
4 single stacks with am emission of 1000 kg SO_2/h each;
physical stack height: 200 m;
inside stack diameter: 5 m;
stack gas velocity : 15 m/sec;
stack gas temperature: 140 °C.

Fig. 9 shows the calculated annual mean values for selected receptor sites. These results can be summarized as follows:

The BATELLE calculation yields an increase in annual mean SO_2-concentration due to the power station of about 1 to 3 $\mu g/m^3$ in the city-center and in distances of 10 km south-west and north-east of Fechenheim; the respective contributions calculated by FORTAK's model are about 6 $\mu g/m^3$, i.e. two to three times the BATELLE values.

In 3 to 5 km distance, which is an important distance for the measuring regulations of the 'Technical Instructions for Ensuring Clean Air', the BATELLE calculations predict no increase in annual mean SO_2-concentrations, while FORTAK's model predicts an increase of 7 to 10 $\mu g/m^3$.

These differences, most of which can be explained in a quite simple way, emphasize the need for a thorough sensitivity analysis of GAUSSian plume models and for increased efforts in model standardization.

Literature:

(1) FORTAK,H.: Numerical simulation of temporal and spatial distributions of urban air pollution concentration Proc. Symp. Multiple-Source Urban Diffusion Models; Air Poll. Control Office Publication No. AP-86 (1970)

(2) GUTSCHE,B.; LENSCHOW,P.: Untersuchung zur Luftverunreinigungssituation Berlins unter besonderer Berücksichtigung der politischen Lage der Gesamtstadt. Publ. Inst. Theor. Meteorology; Free University Berlin 1973

(3) FORTAK,H.; GUTSCHE,B.; STERN,R.: Immissionsklimatologische Untersuchungen der Luftverunreinigungssituation der Region Untermain unter Verwendung des FORTAKschen Ausbreitungsmodells. To be published in the 6th Progress Report of the Regional Planning Community Undermain, Frankfurt 1975.

(4) BARTELS,H.; CASPAR,J.W.; SCHARRER,H.: Meteorologische Messungen. 5th Progress Report of the Regional Planning Community Undermain, Frankfurt 1974.

(5) LINK,A.;KALLER, R.S.: Vergleich der Windrichtungs-, Windgeschwindigkeits- und SO_2-Immissionskonzentrationsverteilungen für einen mehrjährigen Zeitraum und für ausgewählte Termine zur Anwendung eines Ausbreitungsmodells im Frankfurter Raum. 4th Progress Report of the Regional Planning Community Undermain,Frankfurt 1972.

(6) STERN,R.; LUDWIG,Ch.; GUTSCHE,B.: Contributions of various emission sources of SO_2 to the ambient air quality situation in Frankfurt/Germany. Contribution to the OECD-Ad hoc meeting of experts to examine methodologies for estimating the contribution to ground level concentrations of various emission sources of sulphur oxides, Paris 15.-17. Oct. 1975

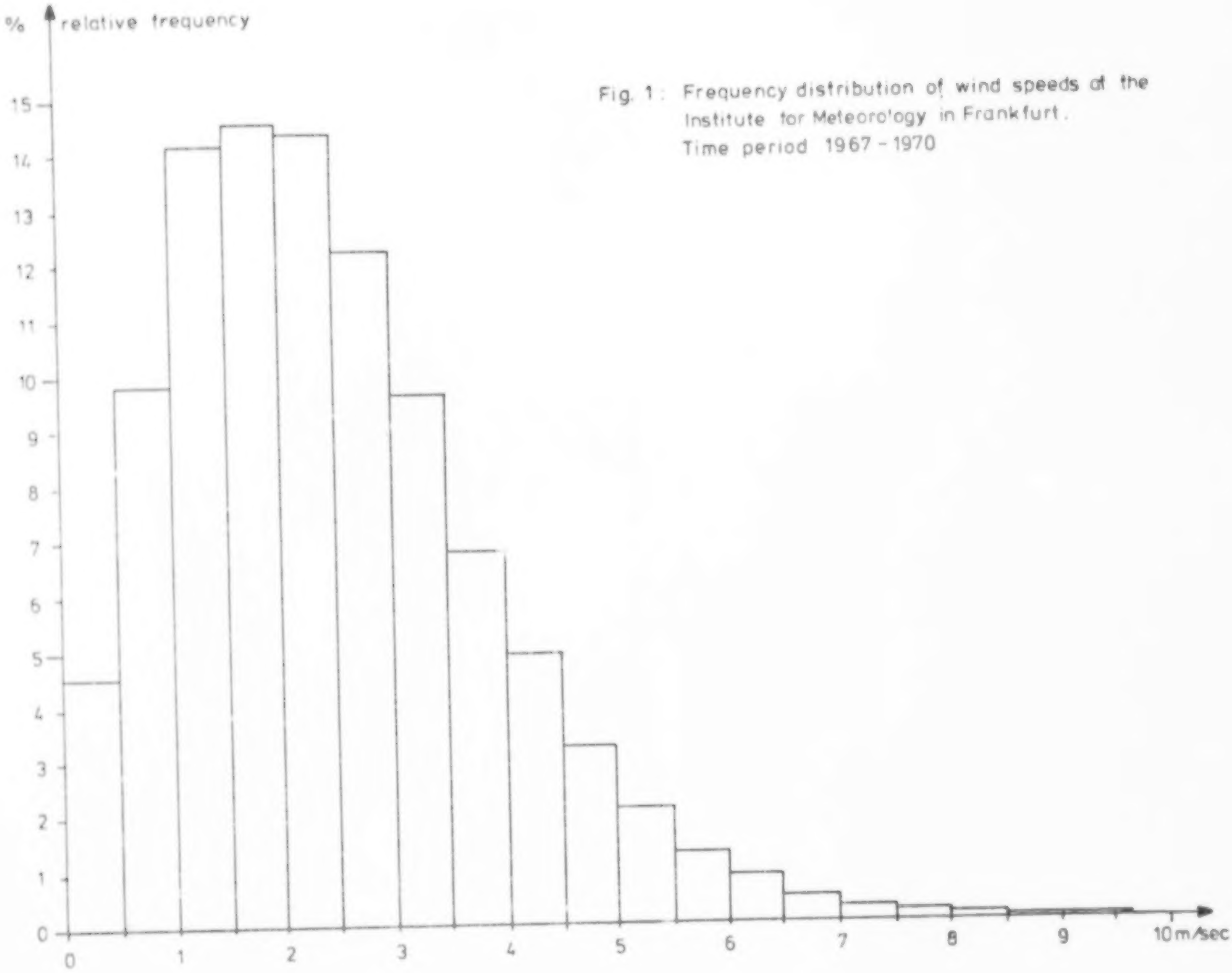

Fig. 1: Frequency distribution of wind speeds at the Institute for Meteorology in Frankfurt. Time period 1967 - 1970

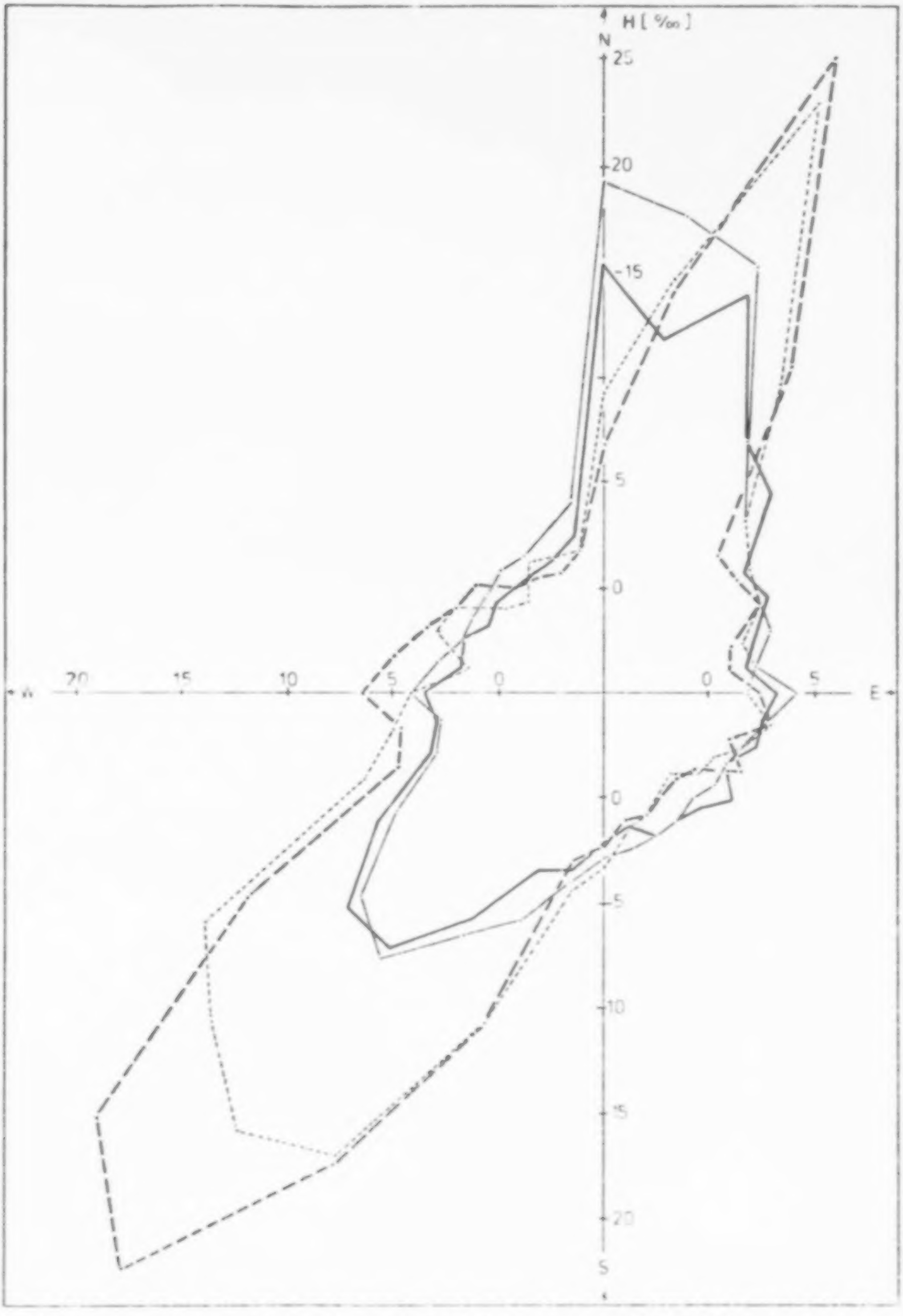

Fig.2/[illegible] Frequency distribution of wind direction for two classes of wind velocity
time period 1967–1972

— — unheated period 2nd wind speed class ū=1.7 m/sec
— — ″ ″ 4th ″ ″ ″ ū=3.6 ″
—— heating period 2nd ″ ″ ″ ū=1.7 ″
– – – ″ ″ 4th ″ ″ ″ ū=3.6 ″

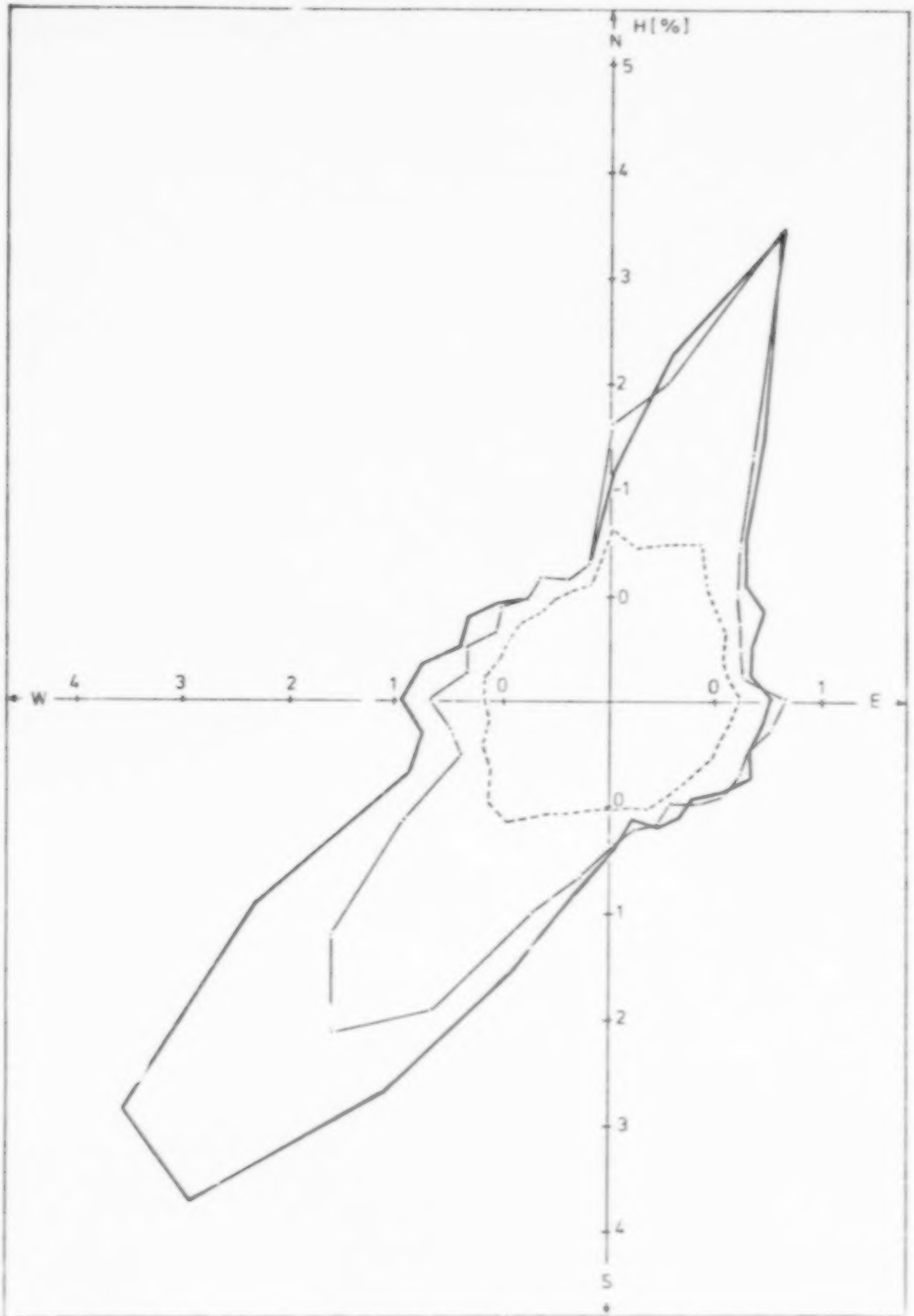

Fig 3 Frequency distribution of wind direction for different atmospheric stabilities
heiting period 1957–1972

—— neutral situations (TURNER class 4)
stable " (" " 5)
unstable " (" classes 2 and 3)

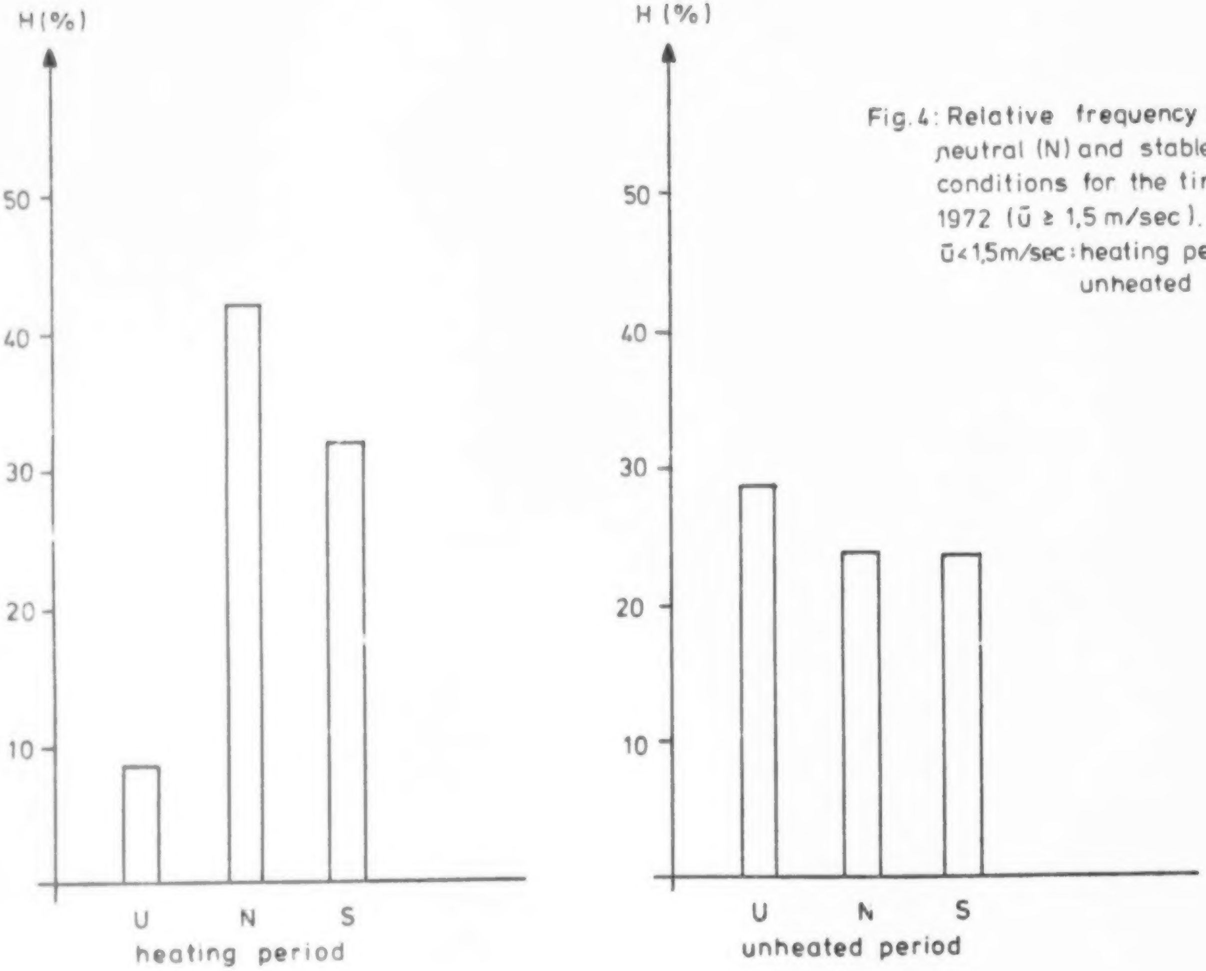

Fig. 4: Relative frequency of unstable (U), neutral (N) and stable (S) meteorological conditions for the time period 1967-1972 ($\bar{u} \geq 1,5$ m/sec).
$\bar{u} < 1,5$ m/sec: heating period 21,2 %
unheated " 24,5 %

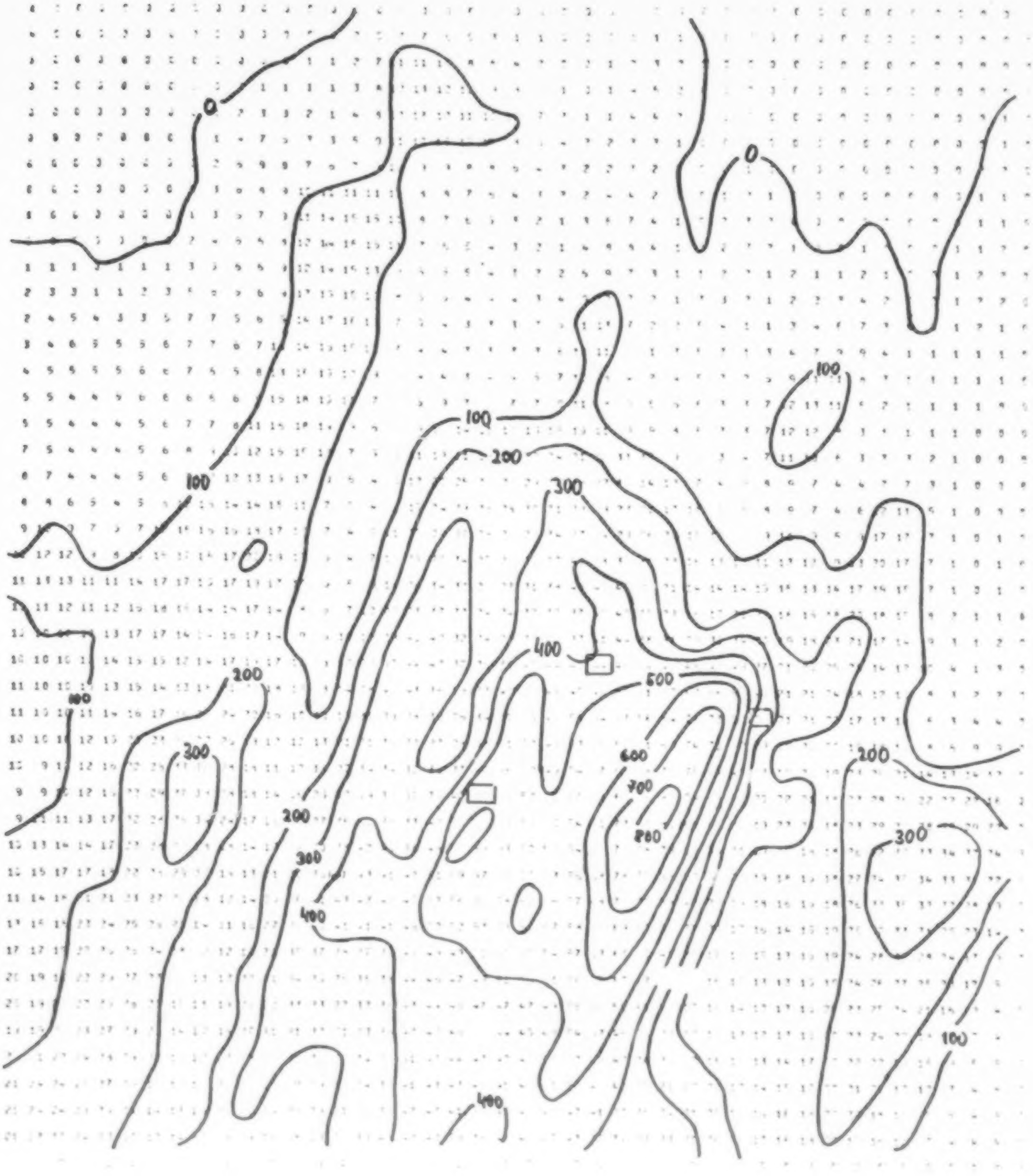

Fig.5: Calculated ground-level concentration field for
12. 12. 1968, 7 to 9 p. m.
wind direction 20 °, wind speed 5 kn, [illegible]class 5,
daily mean temperature − 5.8 °
printed figures in 10 $\mu g/m^3$, isolines in $\mu g/m^3$
coordinates of the upper left corner [illegible] in
the [illegible]-system.

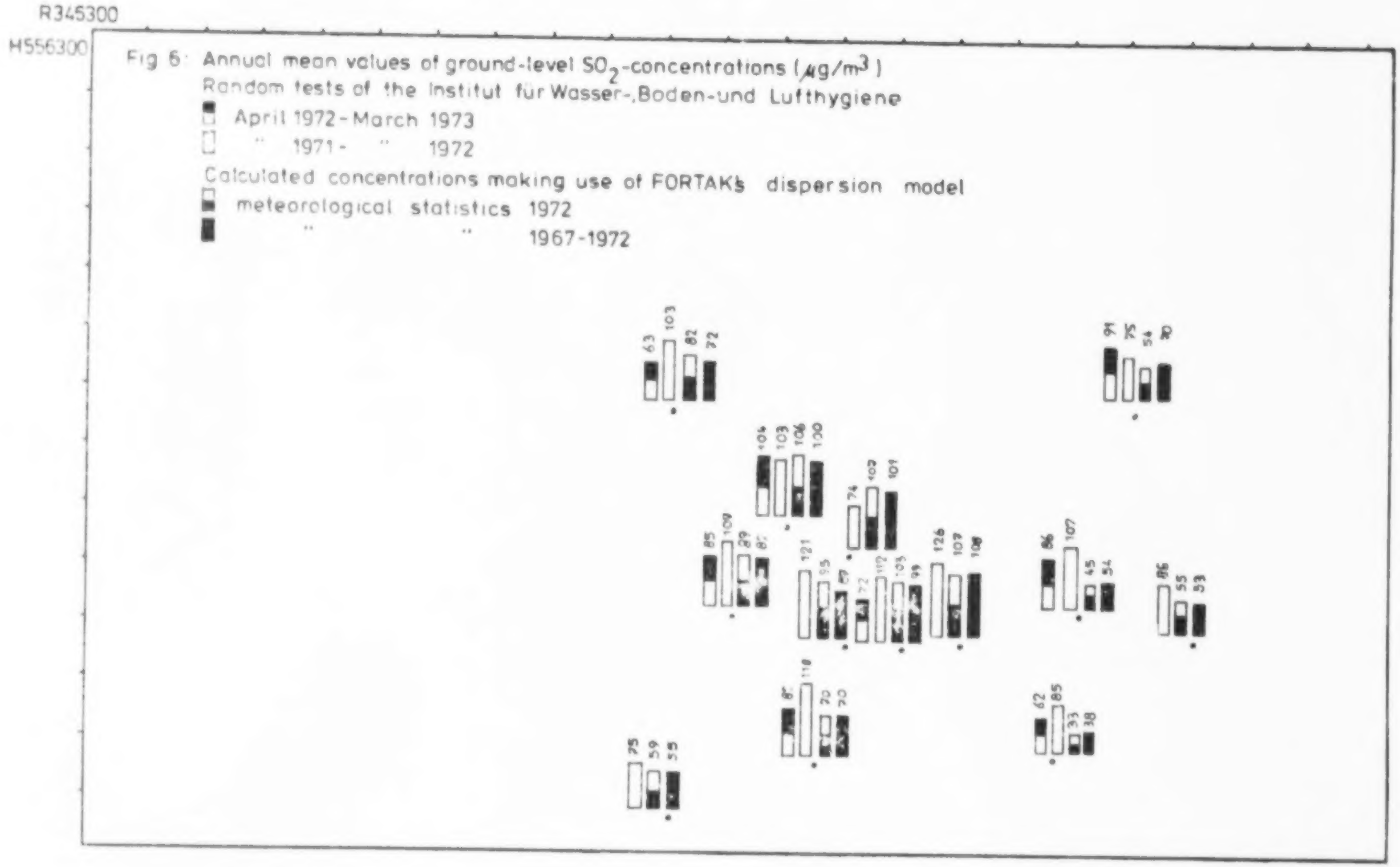

Fig 6: Annual mean values of ground-level SO_2-concentrations ($\mu g/m^3$)

Random tests of the Institut für Wasser-,Boden-und Lufthygiene

◧ April 1972 - March 1973

☐ " 1971 - " 1972

Calculated concentrations making use of FORTAK's dispersion model

◧ meteorological statistics 1972

■ " " 1967-1972

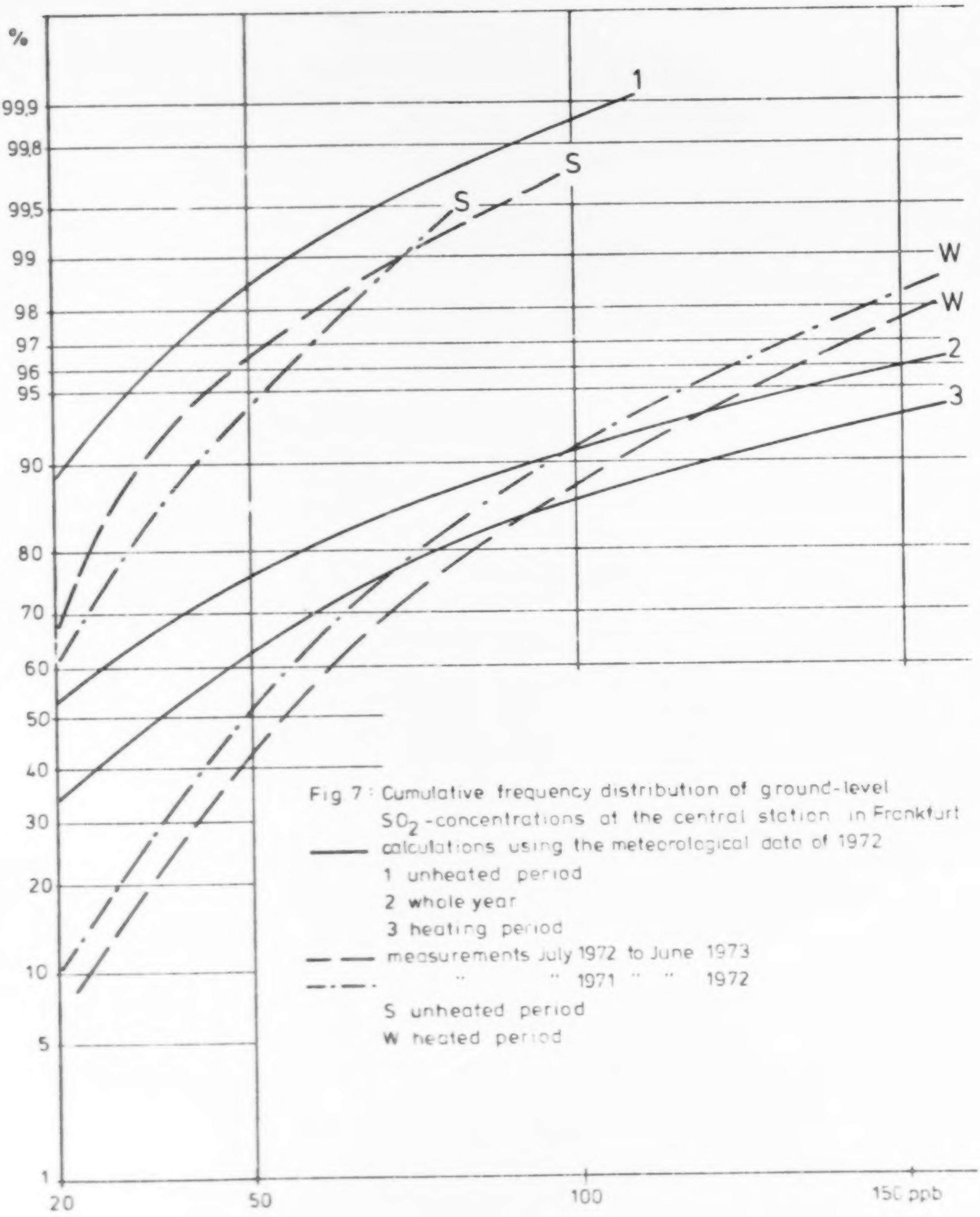

Fig 7: Cumulative frequency distribution of ground-level SO_2-concentrations at the central station in Frankfurt

—— calculations using the meteorological data of 1972

1 unheated period

2 whole year

3 heating period

— — measurements July 1972 to June 1973

—·—· " " 1971 " " 1972

S unheated period

W heated period

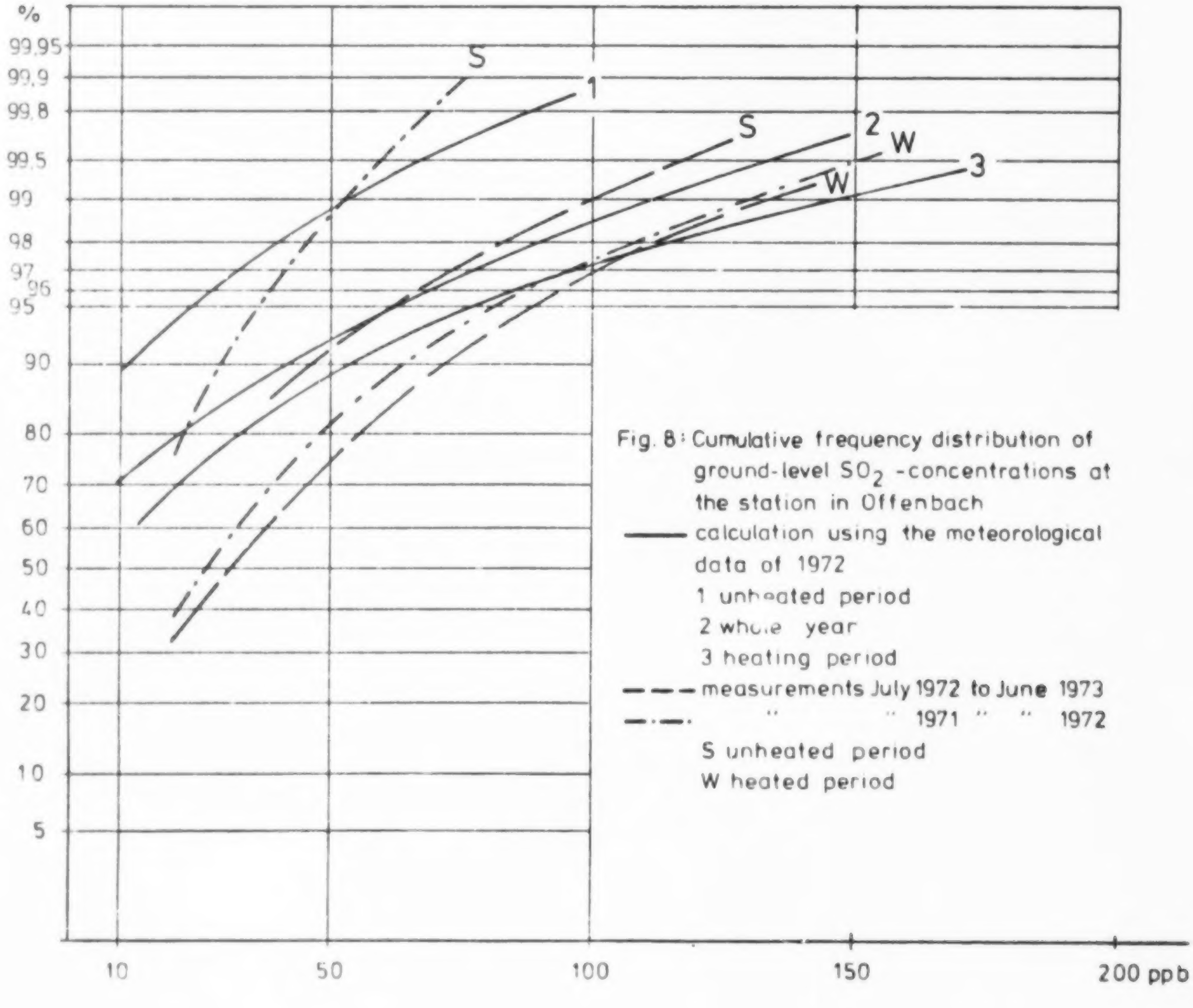

Fig. 8: Cumulative frequency distribution of ground-level SO_2 -concentrations at the station in Offenbach

—— calculation using the meteorological data of 1972
1 unheated period
2 whole year
3 heating period
– – – measurements July 1972 to June 1973
–·–· " " 1971 " " 1972
S unheated period
W heated period

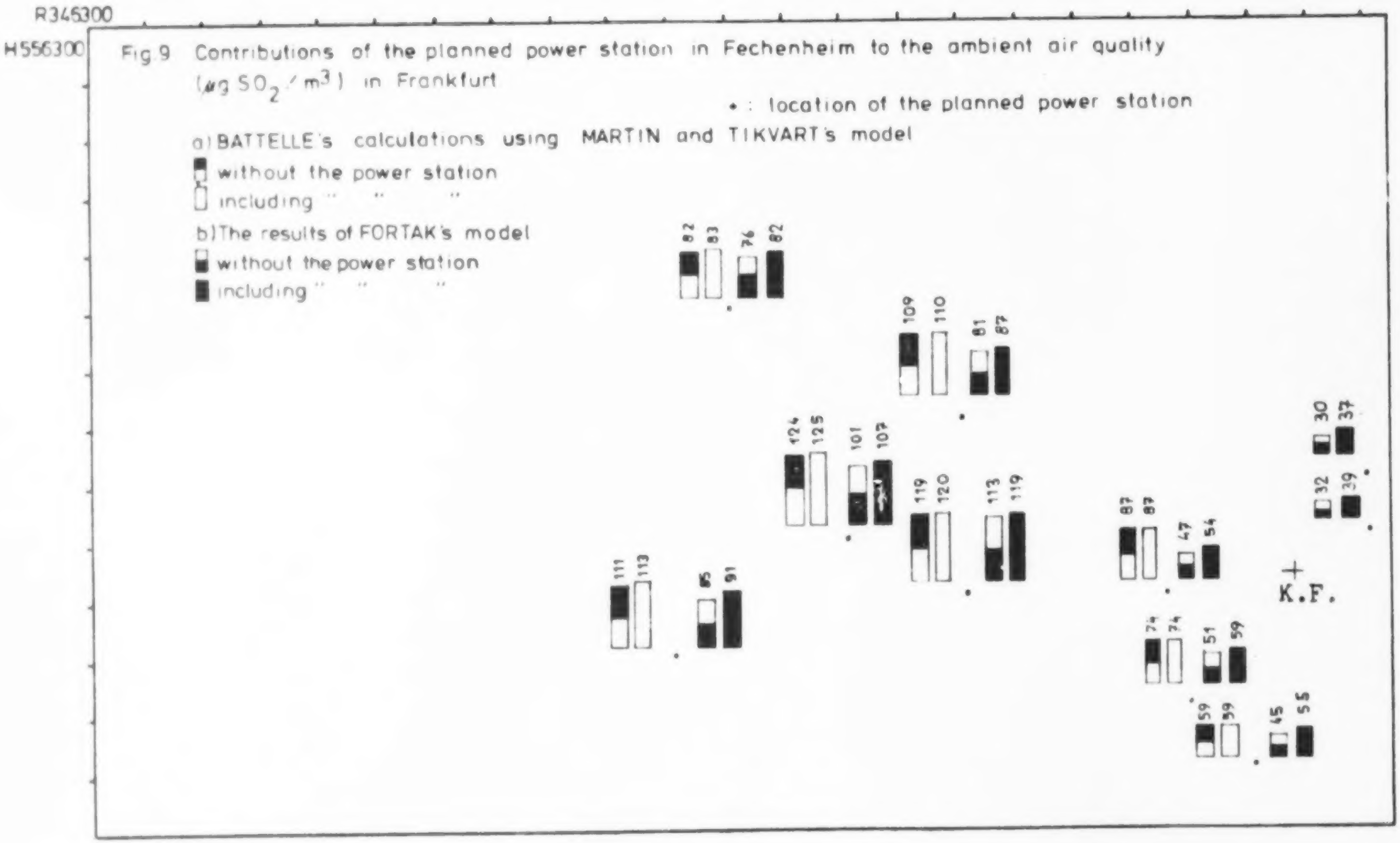

Fig.9 Contributions of the planned power station in Fechenheim to the ambient air quality ($\mu g\ SO_2/m^3$) in Frankfurt

6th NATO /CCMS
International Technical Meeting
on Air Pollution Modeling

THE STATE OF AIR POLLUTION MODELING AND MODEL APPLICATIONS IN SWEDEN

Björn Bringfelt
The Swedish Meteorological and Hydrological Institute
Norrköping, Sweden

Battelle-Institut e. V. Frankfurt/M
Germany, FR
24 - 26 September, 1975

Preceding page blank

URBAN MODELS IN CURRENT USE IN SWEDEN

Description, verification

During 1973 dispersion models for SO_2 have been completed for the Swedish cities of Malmö, Lund, Landskrona, Göteborg and Helsingborg.

The same model technique originally presented by Fortak has been used in all these cities. In Sweden the model was first developed for Stockholm, Bringfelt et al (1968). Some data about the cities and the respective models are given in table 1.

Some results will now be presented from the verification of the model for Göteborg.

Figure 1 gives the locations of the SO_2-stations. Table 2 summarizes the model verification for Göteborg. The table shows that the monthly means are simulated successfully. It can also be seen that the correlation coefficients between the individual calculated and measured daily values are high.

They are of the same order of magnitude as obtained when correlating daily SO_2-values from two measuring stations situated near each other.

The model can also successfully simulate the high daily values in a period as shown in table 3.

In Fig 2 a map shows the median of calculated daily SO_2-values during February 1970. The corresponding measured data are given at the positions of the SO_2-stations.

The verification results for the remaining cities are nearly as good as for Göteborg. For Helsingborg the agreement is moderately good due probably to the more complex topography.

Applications of existing models

In 1973 the Stockholm model was used to study the consequences for air quality of various systems of district heating. Three degrees of centralizing the heat distribution system were treated:

(1) heating by local units only
(2) all heating supplied by 30 MW hot water units
(3) an alternative with a small number of very large 300 MW units.

For two communities near Stockholm model studies have been performed in order to study the consequences for air quality of various phases in building out the district heating system.

At present a model study is made in connection with the planning of the heat and energy supply of the whole metropolitan region of Stockholm.

In Göteborg the model has been used to simulate expected SO_2 levels due to various degrees of sulphur reduction.

Studies of the consequences of district heating expansion alternatives have also been made with the Göteborg model.

The model for Landskrona is used in a tentative study of the contribution to SO_2-pollution from present and planned chemical industries.

An air conservancy plan will be elaborated in the near future for the densely populated and developing southwestern part of Skåne in the very south of Sweden. That is an area of about 30 x 30 km containing the cities of Malmö and Lund. The air conservancy plan will include an extended version of the urban model for Malmö-Lund.

CURRENT AND PLANNED WORK

Model for the dispersion and deposition of dust

In the city of Luleå in northern Sweden a large extension of the steel industry is planned.Serious dust problems exist already around the present units and since the new industry will be several times larger it is obvious that effective measures have to be taken to prevent much larger problems in the future.

To be able to predict the air pollution situation in various alternatives for the planning of the new steel industry and its associated activities a model which can treat the deposition of dust has been proposed and ordered from the SMHI by the steel company after discussions with Swedish Environmental Protection Board.

The model mechanism is planned to work after the lines used by [illegible] ([illegible]).

That model is a simple Gaussian model with inclusion of a weakening of the plume due to dust deposition. This simple approach implies that the weakening of the plume is immediately spread over its cross-section as the dust falls out or impacts on the ground. Since the ground is rough with industry and city blocks this may be a good simplification. As a result concentration and deposition rate of particles in a specified size interval can be calculated at an arbitrary location. The advantage of this approach is that the dust deposition calculation can be attached to the city model computer program already in operation in Sweden.

A preliminary test of this simple model against existing dust concentration and deposition measuring data at 8 stations in an area of radius about two km will be performed. A dust emission inventory for 4 intervals of particle diameter (preliminary intervals: 0-5 µ, 5-10 µ, 10-20 µ and > 20 µ) is being performed for emissions in the existing industry. The terrain is flat and meteorological data will be taken from the airport of Luleå.

In 1976-77 an extensive net of several measuring stations covering an area of many km in diameter will be operating. Using about one year of data from this net the model will be validated more thoroughly.

One of the difficulties which will be met in the development of this model is the determination of deposition velocity for impaction of particles on erecting structures such as houses and trees. This velocity must depend on the height and degree of density of forest and built-up areas. Possibly a comparison of the measured data on impaction between stations at various distances from the source can give information about the deposition velocity.

For particles larger than about 10 μ the calculation will be easier since these are deposited mostly by sedimentation and therefore the deposition velocity is due to gravitation falling. However, at least for the planned foundry it has been stated that the majority of particles will be smaller than 5 μ.

Model for dispersion of traffic exhaust gases

Earlier work in Sweden in order to reduce air pollution from traffic has mainly concentrated on reducing the emission from the single motorcar. Now it is realized that such measures are not sufficient due partly to difficulties in keeping the emission from each car sufficiently low and partly to the increasing number of cars. Therefore it is considered necessary to attack the problems by a combination of traffic planning activities and technical measures.

In order to make a meaningful planning as regards auto exhaust gases a forecast method is needed. To develop such a method we can consider the following requirements:

- Inventory of emission patterns from various kinds of motor roads
- Development of a model for dispersion of the traffic emissions
- Verification of the model by making measurements of air pollution.

It has been considered suitable to start building a model for a part of Stockholm and concentrate the work on carbon monoxide. This gas is relatively stable in the city atmosphere.

A project group will soon be formed with representatives from the National Environment Protection Board, the SMHI and authorities of the city of Stockholm.

The model will be partly based on the version of the Stanford model which has been developed for Copenhagen.

Much of the necessary meteorological information for the model is already included in the model for SO_2 developed for Stockholm.

References

Bringfelt B, Hjorth T, and Ring S (1974)
A numerical air pollution dispersion model for central Stockholm
Atmospheric Environment, Vol 8, No 2, pp 131-148

Narai K (1977)
Computermodell der turbulenten diffusion von teilchen
Időjárás, 4

Table 1. Swedish urban models for dispersion of SO_2.

City	[illegible]	[illegible]	[illegible]	Landskrona	Helsingborg
Dimensions of model area km x km	[illegible]	[illegible]	[illegible] x [illegible]	[illegible] x [illegible]	5,5 x 6,5
Inhabitants in model area	[illegible]	[illegible]	[illegible]	[illegible]	100 000
Terrain, location	Flat. [illegible] and water surfaces.	Rather flat [illegible] [illegible] [illegible] [illegible] on the [illegible] coast of Sweden.	Very flat. [illegible] [illegible] to the [illegible].	Very flat. [illegible] to the [illegible].	Terrain to the west. A N-S plateau, 20-30 m high divides the city.
VALIDATION PERIOD: Length months	[illegible]	[illegible]	[illegible]	1	1
Number of SO_2-stations with daily values	[illegible]	[illegible]	[illegible]	[illegible]	9
1/2-hourly values	[illegible]	[illegible]	[illegible]	[illegible]	2
POINT SOURCES					
Number of	[illegible]	[illegible]	[illegible]	[illegible]	[illegible]
Total emission [illegible] (average of winter months)	[illegible]	[illegible]	[illegible]	[illegible]	[illegible]
AREA SOURCES					
Number of	[illegible]	[illegible]	[illegible]	[illegible]	[illegible]
Total emission [illegible] (average of winter months)	[illegible]	[illegible]	[illegible]	[illegible]	[illegible]
Grid size km	[illegible]	[illegible]	[illegible]	[illegible]	[illegible]

Table 2. Summary of model verification in Göteborg

$\overline{M}$ = arithmetic mean of measured SO_2 [pphm]

DLM = standard deviation of $\left\{ {}^{10}\log (X_M) \right\}$

$\overline{B}$ = arithmetic mean of calculated SO_2 [pphm]

DLB = standard deviation of $\left\{ {}^{10}\log (X_B) \right\}$

X_M and X_B = daily measured and calculated SO_2-value.

RMB = correlation between $[\log X_M]$ and $[\log X_B]$

		November 1969						December 1969						Januari 1970					
Stn	Per	$\overline{M}$	DLM	$\overline{B}$	DLB	RMSQ	RMB	$\overline{M}$	DLM	$\overline{B}$	DLB	RMSQ	RMB	$\overline{M}$	DLM	$\overline{B}$	DLB	RMSQ	RMB
G 1	24	0,5	0,328	0,7	0,550	0,8	0,523	1,5	0,294	1,4	0,580	1,4	0,520	1,5	0,354	2,0	0,630	2,1	0,251
G 2	"	1,6	0,261	1,8	0,227	1,1	0,362	2,8	0,426	3,1	0,281	2,4	0,429	3,0	0,389	4,1	0,292	2,3	0,752
G 3	"	1,6	0,329	1,8	0,227	1,1	0,400	3,0	0,435	3,1	0,291	2,7	0,352	3,1	0,384	4,1	0,292	2,2	0,768
G 4	"	-	-	-	-	-	-	-	-	-	-	-	-	3,3	0,263	2,8	0,317	2,3	0,370
G 5	"	0,9	0,488	1,2	0,427	1,2	0,848	2,8	0,438	2,2	0,507	1,8	0,443	2,3	0,223	3,3	0,404	2,4	0,359
G 6	"	-	-	-	-	-	-	-	-	-	-	-	-	4,2	0,289	3,6	0,322	2,1	0,743
G 7	"	0,6	0,439	0,7	0,334	0,8	0,532	2,5	0,474	1,3	0,505	1,8	0,339	1,8	0,369	1,9	0,536	1,2	0,371
G 8	"	-	-	-	-	-	-	-	-	-	-	-	-	-	-	-	-	-	-
G 9	"	1,6	0,550	1,4	0,420	1,5	0,641	2,5	0,381	3,0	0,377	2,6	0,438	2,9	0,410	3,8	0,245	3,0	0,355
G 10	"	-	-	-	-	-	-	-	-	-	-	-	-	-	-	-	-	-	-

		Februari 1970						Mars 1970					
Stn	Per	$\overline{M}$	DLM	$\overline{B}$	DLB	RMSQ	RMB	$\overline{M}$	DLM	$\overline{B}$	DLB	RMSQ	RMB
G 1	24	2,3	0,286	1,3	0,529	2,2	0,340	0,9	-0,162	0,8	-0,314	0,8	0,619
G 2	"	4,8	0,224	4,9	0,290	1,9	0,735	2,2	0,177	3,0	0,210	1,5	0,390
G 3	"	5,4	0,273	4,9	0,290	4,3	0,537	2,8	0,208	3,0	0,216	2,3	0,062
G 4	"	4,7	0,193	4,3	0,411	8,2	-0,100	2,9	0,209	2,3	0,326	1,9	0,348
G 5	"	3,4	0,331	2,6	0,301	2,5	0,363	1,4	0,200	1,7	0,426	1,2	0,807
G 6	"	5,0	0,233	3,7	0,312	2,4	0,709	2,4	0,218	2,6	0,245	1,3	0,497
G 7	"	3,1	0,395	1,2	0,502	2,9	0,219	1,2	0,262	1,0	0,532	0,6	0,506
G 8	"	4,1	0,234	4,1	0,255	2,2	0,568	2,6	0,321	2,6	0,370	1,9	0,311
G 9	"	5,4	0,242	3,6	0,258	3,8	0,284	1,7	0,343	2,2	0,345	1,7	0,463
G 10	"	3,3	0,370	4,7	0,483	3,1	0,766	1,6	0,206	1,5	0,496	1,3	0,214

Table 3. Göteborg 1969-70. Measured (M) and calculated (B) second largest daily values of SO_2 ($\mu g/m^3$) for each station and month.

	nov		dec		jan		feb		mars	
	B	M	B	M	B	M	B	M	B	M
G1	60	26	137	86	106	116	151	75	74	60
G2	100	108	245	251	306	260	287	266	175	149
G3	100	109	245	264	306	260	287	286	175	234
G4		-		-	267	211	537	229	193	146
G5	104	54	175	174	245	111	132	243	142	93
G6		-		-	224	229	232	294	177	143
G7	117	77	145	149	303	220	212	180	150	86
G8		-		-		-	172	263	120	180
G9	113	160	218	257	242	346	205	357	168	126
G10		-		-		-	336	237	87	83

[illegible]

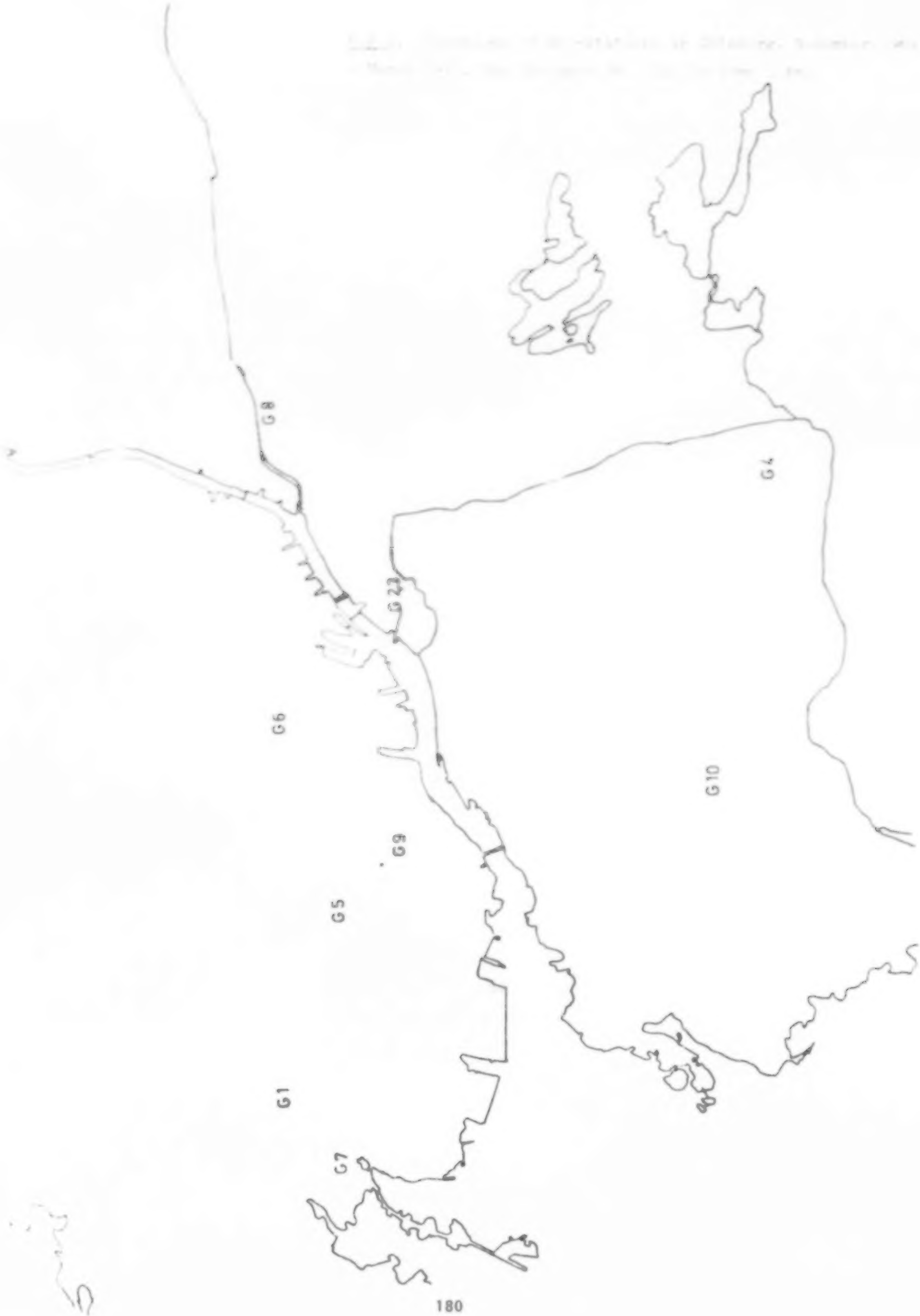
G8
G4
G2
G6
G10
G9
G5
G1
G7

[illegible]

GEOGRAFISK FÖRDELNING AV SIMULERADE SO_2-NIVÅER

[illegible]

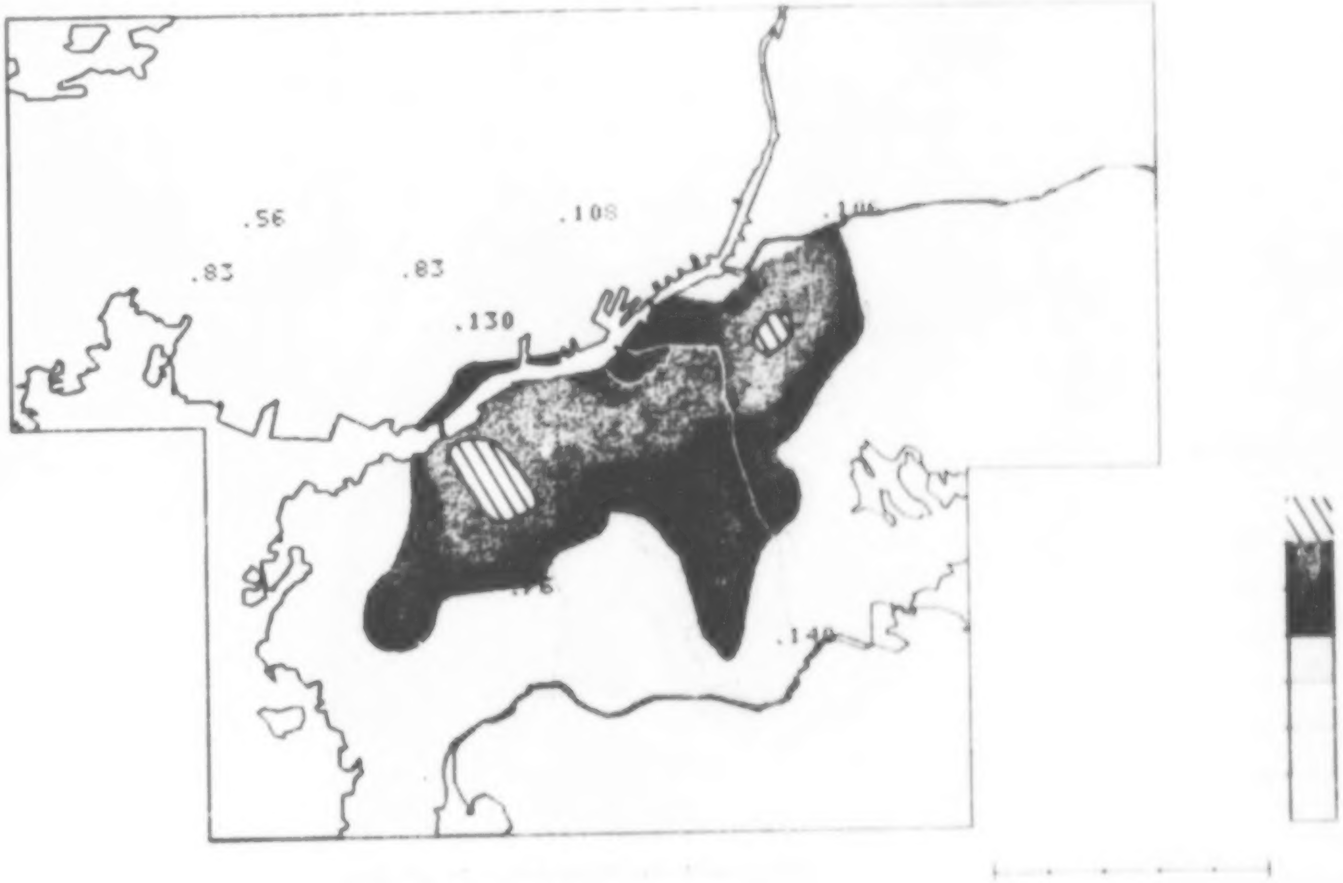

Rapporteur's Report, Topic I (continued), September 24, 1975
by R. F. Lee.

Chairman: H. M. Slater

H. Fortak: Application of an Air Pollution Model to the Problem of feasable Industrialization of a planned Deep-Sea Harbour.

Discussion:

Mr. Johnson noted that a single plume height was used regardless of the temperature profile.

Mr. Fortak responded that since only long-term averages were being considered, this procedure was considered satisfactory.

M. Schorling asked whether an analysis had been made of the impact of the proposed part on Denmark.

H. Fortak responded that such an analysis had not been made, but that he did not expect a significant effect since Denmark is some 40 km away, and the modeling shows little effect beyond about 10 km. Also a "worst case" situation was assumed.

D. Jost also commented that much of the SO_2 would probably be absorbed in the water before reaching Denmark. The modeling did not account for any absorption.

J. Gutsche: Further Investigations of the Ambient Air Quality Situation in the Unter-Main Region making use of Fortak's Dispersion Model

Discussion:

Some questions were raised regarding the reasons for the differences between the results of the Fortak and the Battelle Models.

J. Strott commented that the differences are probably to

1) the use of 16 wind direction categories in one model and 36 in the other, and

2) the use of the Stümke plume rise formula in the Fortak Model, and the Briggs formula in the Battelle Model.

H. Slater asked for the height the wind observations were taken.

J. Gutsche responded that the transport speed was an integrated speed profile based on measured values at about 10 miles.

B. Bringfelt: The State of Air Pollution Modeling and Model Applications in Sweden.

Discussion:

D. Jost inquired as to the averaging times considered in the modeling.

B. Bringfelt responded that hourly, daily, and monthly averaging times were included.

It was noted that areas of high concentrations showed high correlations between predicted and observed, while areas of low concentrations showed low correlations. The question was raised as to whether similar results were obtained when the model was applied to other cities. Mr. Bringfelt responded in the affirmative.

6th NATO/CCMS

International Technical Meeting APM 6 / 1

on Air Pollution Modeling

A GAUSSIAN-PLUME ALGORITHM FOR POINT, AREA, AND LINE SOURCES

by

D. Bruce Turner and William B. Petersen
Meteorology and Assessment Division
Environmental Protection Agency
Research Triangle Park, NC 27711

At BATTELLE - INSTITUT E.V., Frankfurt/Main
Germany, FR

24 - 26 September, 1975

Preceding page blank

A GAUSSIAN-PLUME ALGORITHM FOR POINT, AREA, AND LINE SOURCES

by

D. Bruce Turner* and William B. Petersen

Meteorology Laboratory, EPA, Research Triangle Park, NC 27711

ABSTRACT

The information presented in this paper is directed to the users of air quality simulation models.

PAL is an acronym for this point, area, and line source algorithm. PAL is a method of estimating short-term dispersion using Gaussian-plume steady-state assumptions. The algorithm can be used for estimating concentrations of non-reactive pollutants at 30 receptors for averaging times of from one to twenty-four hours, and for a limited number of point, area, and line sources (30 of each type).

Calcualtions are performed for each hour. The hourly meteorological data required are wind direction, wind speed, stability class, and mixing height. Single values of each of these four parameters are assumed representative for the area modeled.

This algorithm is not intended for application to entire urban areas but, rather, to assess the impact on air quality, on scales of tens to hundreds of meters, of portions of urban areas such as shopping centers, large parking areas, and airports. Level terrain is assumed.

The Gaussian point source equation estimates concentrations from point sources after determining the effective height of emission as well as the upwind and crosswind distance of the source from the receptor.

Numerical integration of the Gaussian point source equation is used to determine concentrations from line sources. Subroutines are included that estimate concentrations for special cases such as slant-line source (line sources with end points at different heights above ground) and curved-path sources. Numerical integration of the point source equation is also used for these special cases.

Integration over the area source includes edge effects from the source region. This is done by considering finite line sources perpendicular to the wind at intervals upwind from the receptor. The crosswind integration is done analytically. Integration upwind is done numerically by successive approximations.

---

*On Assignment from National Oceanic and Atmospheric Administration, U.S. Department of Commerce

A GAUSSIAN-PLUME ALGORITHM FOR POINT, AREA, AND LINE SOURCES

by D. Bruce Turner and William B. Petersen

INTRODUCTION

The PAL algorithm is intended for making air pollutant concentration estimates for a small portion of an urban area. The sources considered are point, area, and line sources. The principal use of the algorithm is to estimate the increase in pollutant concentrations caused by a new facility such as a shopping area, a sports stadium with included parking lot, or a facility as large as an airport and its associated emissions.

PAL is not intended to estimate concentrations for an entire urban area. Because of the details which the algorithm considers, such as edge effects from area sources, the application to an entire urban area would, in general, be prohibited by computer costs. Also, since meteorological data are entered hour by hour, a normal run for this algorithm would be to simulate a period of from 1 to 24 hours. Calculations for more than several 24-hour periods would also be costly.

The intended users of the PAL algorithm are the air pollution meteorologist and the air pollution control engineer who are attempting to estimate air quality on a scale of tens to hundreds of meters in the vicinity of the sources considered. The PAL algorithm offers a considerable amount of flexibility to the user. Any or all of the six source subroutines may be utilized. The user also has the option of employing a diurnal variation to emission rates, and allowing the wind speed to change with height.

This algorithm is useful for estimating short-term dispersion of stable pollutants using Gaussian plume, steady-state assumptions. The Gaussian point source equation is the heart of the algorithm. Numerical integration of the point source equation is used for both line and area sources. Meteorological data used by the algorithm are for hourly periods. Averages of concentrations for up to 24 hours can be obtained directly by averaging hourly estimates.

TYPES OF SOURCES CONSIDERED AND INPUTS REQUIRED

The PAL algorithm can consider six types of sources. In any single execution, any combination of these six source types can be used. However, the maximum number of input sources for any given type cannot exceed thirty. All input data are read in by the main program. The input parameters for the six source types will be discussed in this section.

POINT SOURCES

The treatment of point source in PAL is similar to that in many other air quality simulation models. In order to calculate plume rise, the stack gas temperature in combination with stack gas volume flow, or stack inside diameter and stack gas velocity are required. Point source information consists of the following for each source:

- Point source strength, g sec^{-1}
- Physical stack height, m
- Stack gas temperature, °K
- Stack gas velocity, m sec^{-1}
- Stack inside top diameter, m
- Stack gas volume flow, m^3 sec^{-1}
- East coordinate of stack, km
- North coordinate of stack, km
- Initial σ_y, m
- Initial σ_z, m

AREA SOURCES

In PAL the shape of area sources may be squares or rectangles. Boundaries must be oriented north-south and east-west. There are no special restrictions about source size. A unique feature of PAL is that negative area source strengths can be considered in order to account for smaller areas with no emission within larger area sources. For example, an area occupied by buildings within a large parking lot can be given an area source strength equal to that of the parking lot but negative in sign. (See "Specific Example" section.) Area source information consists of the following for each source:

- Area source strength, g $sec^{-1}m^{-2}$
- Area source height, m (Assumed to be effective height.)
- East coordinate of south-west corner, km
- North coordinate of south-west corner, km

- East-west length of area source, km
- North-south length of area source, km

HORIZONTAL LINE SOURCES

Line sources of finite horizontal extent can be considered by PAL. Single-line sources or multiple-line sources such as parallel lanes of traffic, hereinafter referred to as multi-lane sources, can be input into the model. The end points of the line source are points A and B. Provision for some initial size of the source, such as turbulent mixing of effluent in the wake of vehicles or aircraft engines, is through initial σ_y's and σ_z's. Line source information consists of the following for each source:

- Line source strength, g $\sec^{-1} m^{-1}$
- Line source height, m
- Number of lanes if multilane, dimensionless
- East coordinate of point A, km
- North coordinate of point A, km
- East coordinate of point B, km
- North coordinate of point B, km
- Initial σ_y, m
- Initial σ_z, m

Line source strength as a 1-hour average for mobile sources can be calculated in the manner shown on p 3 of Zimmerman and Thompson (1975) by multiplying appropriate vehicle emission factors in either g mi^{-1} vehicle^{-1}

or g km^{-1} $vehicle^{-1}$ by the vehicle flow rate (vehicles hr^{-1}) and appropriate conversion factors. The vehicle emission factor can be found from publications such as EPA's AP-42 (second edition). These vehicle emission factors should be corrected for average vehicle speed along the specific segment, as most pollutant emissions vary with vehicle speed. For multi-lane sources, additional information is needed. An emission rate is given for each lane. Lanes are ordered from left to right when looking from point A to point B. The additional information below is expected by the program if the number of lanes given above is greater than one. Only an even number of lanes can be considered. For multi-lane sources, the points A and B are expected midway between the outermost lanes, that is, in the middle of the median for a roadway.

. Total width of line source, m
. Width of median of line source, m
. Line source strength for each lane, g $sec^{-1}m^{-1}$

HORIZONTAL CURVED SOURCES

In addition to line sources, curved sources can also be included in PAL. The curved sources are assumed to be of constant radius. Like the line sources, they can be single or multi-lane sources. In order to describe the curved segment, the coordinates of the end points as well as the coordinates of one point in between are needed. This point need not be in the middle of the curve. Emissions are handled the same as for horizontal line sources. As with line sources, multi-lane curved sources have to have an even number of lanes in order to be handled as one source. Points A and C are the end points of the curved source. Point B is a point on the curve between A and C. Curved source information consists of the following for each source:

- East coordinate of point A, km
- North coordinate of point A, km
- East coordinate of point B, km
- North coordinate of point B, km
- East coordinate of point C, km
- North coordinate of point C, km
- Curved source height, m
- Number of lanes, dimensionless
- Width of curved source, m
- Width of median, m
- Initial σ_y, m
- Initial σ_z, m
- Curved source strength for each lane, g $\sec^{-1} m^{-1}$

SPECIALIZED LINE SOURCES

The inclusion of specialized line sources in PAL is to account for additional variations in two variables. The first is to account for a changing effective height of the line source from one end of the source to the other. The effective height is the height above the surrounding terrain. The second is to account for variations of the emission rate from one end of the source to the other.

For specialized line sources the emission in the usual line source units, g $sec^{-1}m^{-1}$, is calculated within the computer program for each point evaluated by dividing the input emission rate by the average velocity of vehicles past that point. The input emission rate, g sec^{-2}, can be determined by multiplying the average vehicle emission rate, g min^{-1} $vehicle^{-1}$, [for example, see pp 59-61 of Kunselman et al. (1974)] by the vehicle flow rate, vehicles hr^{-1}, for this segment and appropriate conversion factors. Neither the specialized line nor curved source will accept multi-lane input as a single source. The input parameters for the specialized line source follow:

. Emission rate, g sec^{-2}

. Height of point A, m

. Height of point B, m

. East coordinate of point A, km

. North coordinate of point A, km

. East coordinate of point B, km

. North coordinate of point B, km

. Initial speed of vehicles, m sec^{-1} (at point A)

. Final speed of vehicles, m sec^{-1} (at point B)

. Initial σ_y, m

. Initial σ_z, m

SPECIALIZED CURVED SOURCES

The specialized curved source algorithm is very similar to the specialized line source routine except it incorporates the added feature of allowing the source to be a curve with a constant radius. Input for the curved sources is identical to the specialized line source except for the addition of the coordinates of a third point along the curved source to define the curved path. As with the horizontal curved sources, points A and C are the ends of the curved segment, and point B is a point on the curve between A and C. The initial speed is at point A; the final speed is at point C. This speed can be increasing or decreasing from point A to C. The input parameters for the specialized curved sources follow:

- Curved-source emission rate, g sec^{-2}
- Height of point A, m
- Height of point B, m
- East coordinate point A, km
- North coordinate of point A, km
- East coordinate of point B, km
- North coordinate of point B, km
- East coordinate of point C, km
- North coordinate of point C, km
- Initial speed of vehicles, m sec^{-1} (at point A)
- Final speed of vehicles, m sec^{-1} (at point C)
- Initial σ_y, m
- Initial σ_z, m

RECEPTORS

Receptors may be located at any position relative to the air pollutant sources. However, common sense should be used so that receptors are not positioned in the center of lanes of traffic, etc. The data required for each receptor consist of the east and north coordinates of the receptor and the height of the receptor above ground level. PAL is designed to make estimates over relatively level terrain. The receptor height should not be used in an attempt to simulate topographic differences. The height of a receptor is the distance of that receptor above the local ground level, not the height of the ground above some reference plane. The three receptor parameters are:

- East coordinate of receptor, km
- North coordinate of receptor, km
- Height of receptor above ground, m

METEOROLOGICAL DATA

The input of meteorological data for each simulated hour, up to 24 hours, follows all required source and receptor data. Care should be taken to ensure that the meteorological data are representative of the source-receptor locality. Availability airport data may not be representative of an urban or suburban site. Wind speed and direction are especially sensitive to the local environment especially in the vicinity of buildings. Depending upon the nature of the problem being considered, special instrumentation may be established in the field in order to gather representative meteorological data —— of wind, in particular. At the present state of development of this algorithm, the dispersion parameter values incorporated in PAL are those given in EPA's Workbook of Atmospheric Dispersion Estimates (Turner, 1974). These are most representative for open countryside, that is, rural areas. Therefore if the source-receptor locality is in an essentially rural area, the Pasquill stability class can be determined in the usual way, as in the Workbook. However, if the area of concern is in a more built-up area, the stability may need to be modified toward more unstable conditions in order to perform the calculations with the increased dispersion caused by the thermal and roughness characteristics of the locality.

Mixing height will frequently be of little importance if source-receptor distances are small. Mixing height is the top of the unstable or neutral layer near the ground. Therefore, mixing height is not used if the lowest atmospheric layer is stable. Mixing height is usually more nearly the same over larger areas than wind speed or wind direction. However, urban influences may cause the existance of a neutral layer at the surface and a mixing height at night compared to stable conditions for this period in the rural area.

The ambient air temperature is used only for the calculation of plume rise for the point sources. If there are no point sources, the air temperature is not required.

Since a meteorological data card is read for each simulated hour, some additional optional data related to diurnal emission rates are included with the meteorological data. If the option is employed to vary the emission rates of the sources, a dimensionless factor for each source type is read in for each hour. The computations for each source are then multiplied by this factor using the individual emissions previously read. For example, if information indicates that for this hour the emissions from all point sources are about half the emission rates previously read in, the factor would be 0.5. Or, if the emissions are thought to be about 30 per cent higher for this hour, the factor would be 1.30.

The meteorological and diurnal factor input parameters follow:

- Wind direction, deg
- Wind speed, m sec^{-1}
- Pasquill stability class, dimensionless
- Mixing height, m
- Ambient air temperature, °K

- -

- Diurnal variation for point sources, dimensionless
- Diurnal variation for area sources, dimensionless
- Diurnal variation for horizontal line sources, dimensionless
- Diurnal variation for curved sources, dimensionless
- Diurnal variation for specialized line sources, dimensionless
- Diurnal variation for specialized curved sources, dimensionless

GENERAL FRAMEWORK OF ALGORITHM

The algorithm consists of a main program which reads in the information and also prints the output and subroutines which are called to perform the bulk of the calculations. Control information is initially read into the program to determine what source types are going to be used. Controls for the two optional features are also included. The wind speed can be assumed constant for all heights for each simulated hour, or the option employed to include an increase in wind speed with height above 10 meters, assuming the wind is constant below 10 meters. An exponential increase with height is assumed with the exponent of the profile dependent upon the stability class. Emission rates can be assumed constant with the values as read in, or the option may be employed to multiply calculations by a factor for each source type for each simulated hour.

After reading the control data, the emission information - that which is expected depending upon the indicated controls - is read for each parameter within each source type. Any number or combination of the six source types may be used. All input to the program is printed as output after being read so that a complete listing is available.

Receptor coordinates and heights are read following all emission information. Meteorological data for each hour are then included for up to 24 hours.

After reading all required input for sources, receptors, and meteorology, the subroutines that are needed are called to perform the calculations for each source type.

The concentration output is arranged in a table with one line for each receptor. The receptors are numbered sequentially as read. This receptor number and the receptor coordinates are given on this printed line. In addition to total concentration from all sources, the partial concentrations due to each source type (not each individual source) are also included. For details, see "Specific Example" section.

BASIS FOR CALCULATIONS

The following assumptions are made: 1) Dispersion from points, and area and line elements result in Gaussian distributions in both the horizontal and vertical directions through the dispersing plume from that point or element, and therefore steady-state Gaussian plume equations can be used for point sources and the integration of these equations for line and area sources. 2) Concentration estimates may be made for each hourly period using the mean meteorological conditions appropriate for each hour. 3) The total concentration at a receptor is the sum of the concentrations estimated from all point and area sources, that is, concentrations are additive.

POINT SOURCES

The basis for the point source calculations is the point source form of the Gaussian diffusion equation. A computation is made for each source-receptor pair. The upwind distance of a source from an individual receptor is first calculated. If this distance is negative, indicating that the source is downwind of the receptor, no calculation for this source-receptor pair is needed. For positive upwind distances, the crosswind distance of the source from the receptor is also determined. Plume rise for each source is calculated once for each hourly simulation period. The plume rise is added to the physical stack height to give effective height of emission. The dispersion equation is then evaluated. The standard deviations of plume spreading are determined as functions of the Pasquill stability class and of the source-receptor distance. As each concentration from a point source at a receptor is calculated, it is added to the accumulated concentrations from point sources for that particular hour.

AREA SOURCES

The calculation of concentrations from area sources is simulated by a number of finite crosswind line sources. If all four corners of the area source have positive upwind distances from the receptor, an integration will be performed starting from the corner of minimum distance to the corner of maximum distance. If some but not all of the corners have a negative upwind distance, then the integration will be performed from an upwind distance of zero to the greatest distance. If all four corners have negative distances from the receptor, this indicates the entire area source is downwind of the receptor position. A number of crosswind (that is, perpendicular to the upwind direction) line sources at various distances from the minimum to the maximum distance are considered. Concentrations for each of these distances are calculated using the infinite line source form of the Gaussian equation. This concentration from an infinite line source is corrected for the finite extent of each individual line by considering the distance in units of σ_y of each end of the line from the upwind azimuth line through the receptor. The fraction of the area under a Gaussian curve between these limits determines the correction. An integration is performed using the concentration contribution from a number of lines and considering the distance between lines. This integration is the first estimate of the concentration from the area source. A second estimate is made by using the first estimate with additional calculations made for lines lying half-way between all the previously calculated lines. This second estimate is compared with the first and if the second falls within a set criteria the second estimate is taken as the final concentration. If the second estimate is not within the criteria, additional calculations are made, each time choosing additional lines lying half-way between lines of the previous total set.

LINE SOURCES

The calculation of concentrations from line sources is done by an integration of the point source equation in the same manner as in Zimmerman and Thompson (1975). Distances to the end points of the lines are determined in terms of upwind and crosswind distances. The line source is limited to those parts of the line which contribute concentrations to the receptor. Calculations are made for a number of points on the line, and, assuming linear change in concentration between these points, an estimate of the concentration from the line is determined. This first estimate is then compared to a second estimate, made by taking additional points between the existing ones and then assuming linear changes of concentrations between each of the adjacent points. The second estimate is compared to the first, and if it falls within a set criteria, the second estimate is taken as the concentration. If the second estimate is not within the criteria, third and subsequent estimates may be required by taking additional points. Estimates for curved sources are determined similarly by evaluating for locations on the curve and integrating. For the specialized line and curved sources, provisions are included to determine the height and emission rate for each location evaluated.

SPECIFIC EXAMPLE

In order to help clarify some of the terms and procedures mentioned previously, an example run of the PAL model is shown. The source inputs into PAL are one point source, two area sources, two line sources, and one curved source, shown in Figure 1.

Consider this example as a simple model of a shopping center, where the hatched region is occupied by buildings and walkways and the rest of the regions within the rectangular boundary represent the parking lot. Notice that the area source strength for the shopping area is the same as that for the parking lot but negative in sign (see Table 1). The effect of the negative area source strength is to make the concentration from the shopping area equal to zero. Also within the area source is a point source whose point source strength and other input variables are shown in Table 1.

The highway around the area source consists of two four-lane line sources and one four-lane curved source. The length of the two line sources is one kilometer. The line source strengths for each lane of the two line sources and the curved source are given in Table 1. For this example run no specialized line or specialized curved sources were used.

Table 1 is a copy of the computer output from PAL. The output begins with a listing of all input parameters and options used. PINA ana PINL are the area and line source integration accuracies. Under the column titled "Source Included," the "yes's" refer to the different subroutines that are used in the model. In the second column headed "Wind Increase With Height," the "no's" mean that the option of having the wind increase with height is not used. Notice also that no average concentration is calculated, since only one hour's data are input, nor is the diurnal variation in emission option used. First, the sources are listed in the input section of the print-out. Following the source input information, the coordinates of the receptors are printed out. Meteorological information follows next and concludes the listing of the input. Included in the meteorological input is the value of the diurnal variation fraction for each source type. In this case the diurnal variation in emissions is not used, and the fractions are set to 1.0 by the program. The final output for this particular run is the "CONCENTRATIONS AT RECEPTORS." Concentrations are given in g m^{-3} for each source type and a total for all types. At the conclusion of this print-out, three options are available besides termination of the job. These depend upon the value punched on a control card. The options are:

1. To start a new problem giving all the input information.
2. To leave all sources the same but input new information on receptors and meteorology.
3. To input new information on meteorology.

SUMMARY

The PAL algorithm is intended to evaluate the contribution of sources within a limited area. This can be the impact of a new facility in a relatively rural environment or the additional impact of a number of sources added to a portion of an urban area. Gaussian plume dispersion equations are used with straight- and curved- lines, sloping-lines, area, and point sources. Briggs plume rise is used. Receptors may be at elevated heights above ground level. Level terrain is assumed. Concentration estimates are for short time periods between one hour and 24 hours. The algorithm is not intended for calculations for entire urban areas or for a long period of time. Although this algorithm may be best run in a batch mode. it is anticipated that a conversational version will also be made available for UNAMAP (Users Network for Applied Modeling of Air Pollution).

REFERENCES

Compilation of Air Pollutant Emission Factors, 2nd Ed. U.S. Environmental Protection Agency. Research Triangle Park, North Carolina. Publication No. AP-42. April 1973.

Kunselman, Paul; McAdams, H.T.; Domke, Charles J.; and Williams, Marcia. Automobile Exhaust Emission Modal Analysis Model. U. S. Environmental Protection Agency. Ann Arbor, Michigan. Publication No. EPA-460/3-74-005. January 1974. 179 pages.

Turner, D.B. Workbook of Atmospheric Dispersion Estimates. U.S. Environmental Protection Agency. Research Triangle Park, North Carolina. Publication No. AP-26. 1970. 84 p.

Zimmerman, John R.; and Thompson, Roger S. User's Guide For HIWAY, A Highway Air Pollution Model. U. S. Environmental Protection Agency. Research Triangle Park, North Carolina. Publication No. EPA-650/4-74-008. February 1975. 58 pages.

ACKNOWLEDGEMENT

The authors wish to thank Lea Prince for her invaluable assistance.

APPENDIX - DISPERSION AND ANALYTIC GEOMETRY EQUATIONS USED IN PAL

EXPRESSIONS

These expressions are used in the discussions that follow:

$$g_1 = \exp\left(-0.5\ y^2/\sigma_y^2\right)$$

$$g_2 = \exp\left[-0.5(z-H)^2/\sigma_z^2\right] + \exp\left[-0.5(z+H)^2/\sigma_z^2\right]$$

$$g_3 = \sum_{N=-\infty}^{\infty} \left\{ \exp\left[-0.5(z-H+2NL)^2/\sigma_z^2\right] + \exp\left[-0.5(z+H+2NL)^2/\sigma_z^2\right] \right\}$$

(This infinite series converges rapidly, and evaluation with the integer, N, varying from -4 to +4 is usually sufficient.)

where: H = effective height of emission, meters

L = mixing height, the top of the unstable layer, meters

y = crosswind distance, meters

z = receptor height above ground, meters

σ_y = standard deviation of plume concentration distribution in the vertical, meters

σ_z = standard deviation of plume concentration distribution in the vertical, meters

POINT SOURCE COMPUTATIONS

The upwind distance, x, and the crosswind distance, y, of a point source from a receptor (see Figure 2) are given by:

$$x = (S_p - S_r)\cos\theta + (R_p - R_r)\sin\theta \qquad \text{(A1)}$$

$$y = (S_p - S_r)\sin\theta - (R_p - R_r)\cos\theta \qquad \text{(A2)}$$

where R_p, S_p are the coordinates of the point source; R_r, S_r are the coordinates of the receptor, and θ is the wind direction (the direction from which the wind blows). The units of x and y will be the same as those of the coordinate system R, S. Frequently a conversion is required in order to express x and y in meters or kilometers.

The contribution to the concentration, χ_p, from a single point source to a receptor is given by one of the three following equations where χ_p is in g m^{-3}, Q is point source emission rate in g sec^{-1}, u is wind speed in m sec^{-1}, and σ_y and σ_z are evaluated for the upwind distance x, and the stability class.

For stable conditions or unlimited mixing:

$$\chi_p = Q\, g_1\, g_2/(2\pi\sigma_y\sigma_z u) \tag{A3}$$

In unstable or neutral conditions and if σ_z is greater than 1.6 times the mixing height, L, the distribution below the mixing height is uniform with height provided that both the effective height, H, and the receptor height, z, are below the mixing height:

$$\chi_p = Q\, g_1/[\sigma_y L u (2\pi)^{1/2}] \tag{A4}$$

(If H or z is above the mixing height, $\chi_p = 0$.)

In all other unstable or neutral conditions, that is, if σ_z is less than 1.6 times the mixing height:

$$\chi_p = Q\ g_1\ g_3/(2\pi\sigma_y\sigma_z u) \tag{A5}$$

AREA SOURCE COMPUTATIONS

Equation (A1) is used to determine the upwind distance, x, of a corner of the area source with coordinates R_p, S_p from a receptor with coordinates R_r, S_r.

By evaluating x for the four corners of the area source, the maximum and minimum upwind distances of the area source from the receptor are determined (see Figure 3). (If the x's are negative for all four corners, indicating the entire area source is downwind, no calculation is performed. If the minimum x is negative, the minimum considered is zero, as no computations need to be performed for that portion of the area source downwind of the receptor.)

For a given upwind distance, x, from a receptor at point R_r, S_r, the north coordinate, S_L, of the intersection of a crosswind line with a north-south boundary given by $R = R_b$ is:

$$S_L = \frac{x - (R_b - R_r)\sin\theta}{\cos\theta} + S_r \tag{A6}$$

The coordinates of this intersection are then R_b, S_L.

Similarly, for a given upwind distance, x, from a receptor at R_r, S_r, the east coordinate, R_L, of the intersection of a crosswind line with an east-west boundary given by $S = S_b$ is:

$$R_L = \frac{x - (S_b - S_r) \cos \theta}{\sin \theta} + R_r \qquad \text{(A7)}$$

The coordinates of this intersection are then R_L, S_b.

Using the above relationships and special tests for $\sin \theta = 0$ and $\cos \theta = 0$, along with the equations for the four boundaries of the area source, the two intersections (A and B) of the crosswind line and the boundaries of the area source can be found.

The two crosswind distances, y_A and y_B, of these points from the receptor can be found using equation (A2).

Assuming that the distances y_A and y_B are in km, the number of standard deviations in the Gaussian distribution of these points from the upwind azimuth through the receptor are given by:

$$s_A = (1000\ y_A) / \sigma_y \qquad \text{(A8)}$$

$$s_B = (1000\ y_B) / \sigma_y \qquad \text{(A9)}$$

where σ_y is in meters and is determined for the distance x and the atmospheric stability. s_A and s_B can be used to determine the fractional portion of the area under a Gaussian curve between these limits. In PAL this is accomplished by interpolating between values in a table. The values in the table are from -3.8 s to 3.8 s at intervals of 0.1 s.

To account for the finite length of the line source, the fraction determined above is used to correct the calculation for a crosswind line source, infinite in extent.

The first estimate, C_1, for the concentration, χ_A, from an area source is given by:

$$C_1 = \frac{q_A}{u} \left[\frac{f_c(x_{min})}{2} + \frac{f_c(x_{max})}{2} + \sum_{i=1}^{9} f_c\,(x_{min} + i\,\Delta\,x) \right] \Delta x \qquad \text{(A10)}$$

where q_A is area emission rate

u is mean wind speed

f_c is defined below

and $\Delta x = (x_{max} + x_{min})\ /10$

The second estimate, C_2, for the concentration, χ_A, from an area source is given by:

$$C_2 = \frac{C_1}{2} + \frac{q_A \Delta x}{2u} \sum_{j=1}^{10} f_c\,(x_{min} - \Delta x/2 + j\,\Delta x) \qquad \text{(A11)}$$

The second estimate is compared with the first estimate and if the ratio of the two are within a set criteria, $\chi_A = C_2$. If not, a third estimate is made, by evaluating f_c for additional lines, then comparing with the second estimate. The notation f_c means each f as defined below is corrected for the finite length of each line. The following defines the function, f, which is related to the concentration contribution from an infinite crosswind line source.

For stable conditions or unlimited mixing:

$$f = g_2 / [\sigma_z (2\pi)^{\frac{1}{2}}] \quad \text{(A12)}$$

where g_2 was defined at the beginning of this appendix.

In unstable or neutral conditions and if σ_z is greater than 1.6 times the mixing height, L, the distribution below the mixing height is uniform with height provided that both the effective height, H, and the receptor height, z, are below the mixing height:

$$f = 1/L \quad \text{(A13)}$$

(If H or z is above the mixing height, f = 0.)

In all other unstable or neutral conditions, that is, if σ_z is less than 1.6 times the mixing height:

$$f = g_3 / [\sigma_z (2\pi)^{\frac{1}{2}}] \quad \text{(A14)}$$

LINE SOURCE COMPUTATIONS

The line source and receptor relationships are shown in Figure 4. Points A and B are the beginning and ending points of the line. x and y are the upwind and crosswind distances from a receptor to a point on the line source. x and y are given by equations (A1) and (A2).

R_p and S_p are the coordinates of any point on the line and are functions of length, ℓ, along the line and total length of the line, D:

$$R_p = \frac{\ell}{D} (R_B - R_A) + R_A \tag{A15}$$

$$S_p = \frac{\ell}{D} (S_B - S_A) + S_A \tag{A16}$$

Since R_p and S_p are functions of ℓ (see Figure 2), x and y are also functions of ℓ.

The upwind distances, x, of the receptor to points A and B are calculated. If both of these x's are negative, then the line source is downwind of the receptor and the concentration at the receptor due to the line source is zero. If either or both x's are positive, it is determined if there is a point on the line source directly upwind of the receptor. The equation for the line source is:

$$(R - R_A) / (S - S_A) = (R_B - R_A) / (S_B - S_A) \tag{A17}$$

The equation of the line through the receptor in the upwind direction is:

$$R - R_r = (S - S_r) \tan \theta \tag{A18}$$

Solving these two equations simultaneously for R and S by letting:

$$m = (R_B - R_A) / (S_B - S_A).$$

$$S = \frac{m S_A - S_r \tan \theta + R_r - R_A}{m - \tan \theta} \tag{A19}$$

and $$R = (S - S_r) \tan \theta + R_r \qquad \text{(A20)}$$

This resulting intersection R, S (see point I, Figure 4) must be tested to see if it is upwind of the receptor by testing for positive x using equation (A1), and if it lies on the line source between points A and B. If both of these conditions are met, the line source is considered to be made up of two segments: The first segment from point A to the intersection point, and the second segment from the intersection point to point B. The point directly upwind has a significant contribution to the concentration at the receptor. The line is broken into two segments so that this point will be considered in the integration estimate that follows. If there are two segments to the line source, the total concentration is given by the sum of the two concentrations from the segments.

The concentration from a line source is then given by the following equation.

$$\chi = \frac{q_\ell}{u} \int_0^D f_p \, d\ell \qquad \text{(A21)}$$

where:

q_ℓ = line source emission rate, g sec^{-1}m^{-1}

u = wind speed, m sec^{-1}

D = line source length, meters

and f_p = point source dispersion function

The point source dispersion function is given by one of the three following equations where σ_y and σ_z are evaluated for the upwind distance, x, and the stability class.

For stable conditions, or unlimited mixing:

$$f_p = \frac{g_1 g_2}{2\pi \sigma_y \sigma_z} \tag{A22}$$

where g_1 and g_2 have been previously defined.

In unstable or neutral conditions, if σ_z is greater than 1.6 times the mixing height, L (meters), the distribution below the mixing height is uniform with height regardless of source or receptor height, provided both are less than the mixing height.

$$f_p = \frac{g_1}{\sigma_y L (2\pi)^{\frac{1}{2}}} \tag{A23}$$

In all other unstable or neutral conditions:

$$f_p = \frac{g_1 g_3}{2\pi \sigma_y \sigma_z} \tag{A24}$$

It should be noted that in PAL, initial σ_y's and σ_z's, such as to account for initial dispersion in the turbulent wake behind vehicles, are input values. The virtual distance for the given stability class is calculated within the algorithm. These virtual distances are added to the physical distances prior to determining σ_y and σ_z for each concentration computation.

The integral, A21, is evaluated using the trapezoidal rule by making a first estimate, C_1, given by:

$$C_1 = \frac{q_\ell \Delta\ell}{u} \left\{ \frac{1}{2} \left[f_p(o) + f_p(10\Delta\ell) \right] + \sum_{i=1}^{9} f_p(i\Delta\ell) \right\} \qquad \text{(A25)}$$

where $\Delta\ell = D/10$, and f_p is defined above. For each of the 11 evaluations of f_p, the upwind distance, x, of the point on the line from the receptor is determined as a function of $\Delta\ell$, and x is used to determine σ_x and σ_y in the function f_p. Portions of the line where f_p equals zero are eliminated and the line is redefined. Then equation (A25) is again evaluated.

A second estimate, C_2, is determined from:

$$C_2 = \frac{C_1}{2} + \frac{q_\ell \Delta\ell}{2u} \left[\sum_{j=1}^{10} f_p(-\Delta\ell/2 + j\Delta\ell) \right] \qquad \text{(A26)}$$

A calculation is made of $(C_2 - C_1)/C_2$. If this value is within a set criteria, $\chi = C_2$. If not within the criteria, a third estimate is made by evaluating f_p for additional points midway between those points previously calculated and assuming linear concentration change between adjacent points (trapezoidal rule). This is continued until the approximation to the integral converges, that is, until two successive estimates are within the criteria. The last estimate is the concentration, χ, from this line source.

For line sources with an intersection point upwind from the receptor, the contribution from the second segment must also be determined. If the point directly upwind was not used to break the line into two segments, and the entire line source is considered as one segment, it is possible for the entire portion of the line that contributes significantly to the concentration to be between two of the eleven points, and thus an erroneous concentration of zero would result.

For line sources with multiple lanes, the integral would be evaluated for each lane and the concentration summed to represent the total concentration at that receptor from the line source.

CURVED SOURCE COMPUTATIONS

Figure 5 shows the curved source and receptor relationships. Points A and C are the end points of the curved path. Point B is an arbitrary point on the curve between A and C. The curve is assumed to be of constant radius.

The radius of the circle, of which the curve is a part, is determined in the following way: The coordinates of point D midway between A and B on a chord are found by averaging the R and S coordinates of A and B. Similarly the coordinates of point E midway between B and C on a chord are found. The perpendicular bisector of a chord of a circle will pass through the center of a circle. Also the slope of the perpendicular bisector is the negative reciprocal of the slope of the chord. The slope of chord AB is:

$$(R_B - R_A) / (S_B - S_A)$$

and the slope of chord BC is:

$$(R_c - R_B) / (S_c - S_B)$$

The slope of the bisector through D, call this m_1, is:

$$- (S_B - S_A) / (R_B - R_A) = m_1$$

The slope of the bisector through E, call this m_2, is:

$$- (S_C - S_B) /(R_C - R_B) = m_2$$

The resulting equation of the bisector through D is:

$$R_o - R_D = m_1 (S_o - S_D) \tag{A27}$$

and the equation of the bisector through E is:

$$R_o - R_E = m_2 (S_o - S_E) \tag{A28}$$

R_o and S_o can be determined from these two equations, for example:

$$S_o = (m_1 S_D - m_2 S_E - R_D + R_E) / (m_1 - m_2) \tag{A29}$$

$$\text{and} \quad R_o = m_1 (S_o - S_D) + R_D \tag{A30}$$

The radius of the circle can then be determined from the coordinates of the center (R_o, S_o) and any one of the three points on the curve, for example:

$$\rho = \sqrt{(S_A - S_o)^2 + (R_A - R_o)^2} \qquad \text{(A31)}$$

In order to provide a proper estimate of the concentrations from the curved source at a receptor, it is desirable to determine if a line in the upwind direction from the receptor intersects the curve. The equation of the line through the receptor in the direction of the upwind azimuth is:

$$R - R_r = (S - S_r) \tan \theta \qquad \text{(A32)}$$

The equation of the circle of which the curve is a part is:

$$\rho^2 = (S - S_o)^2 + (R - R_o)^2 \qquad \text{(A33)}$$

The two possible intersections of the line and the circle are found by solving a quadratic equation for one of the two variables, for example, of the form:

$$a R^2 + b R + c = 0 \qquad \text{(A34)}$$

where $a = 1 + \cot^2\theta$ (A35)

$$b = -2 R_r \cot^2\theta + 2 S_r \cot\theta - 2 S_o \cot\theta - 2 R_o \qquad \text{(A36)}$$

$$\text{and } c = R_r^2 \cot^2\theta - 2 R_r S_r \cot\theta - 2 R_r S_o \cot\theta - 2 S_o S_r$$

$$+ S_r^2 + S_o^2 + R_o^2 - \rho^2 \qquad \text{(A37)}$$

Two possible values of R are found from:

$$R = \frac{-b \pm \sqrt{b^2-4ac}}{2a} \tag{A38}$$

If b^2-4ac is negative, R has imaginary roots and there is no intersection of the circle and the line. If b^2-4ac is zero, the line is tangent to the circle and there is one intersection. If b^2-4ac is positive there are two intersections and both roots of the equation are found. If one or two values of R are found, then one or two values of S are found from:

$$S = (R-R_r) \cot\theta + S_r \tag{A39}$$

If one or more intersections were found for the line and circle, the upwind distance of this (these) point(s) from the receptor can be determined using equation (A1). If this value is negative, indicating the point is downwind from the receptor, it need not be considered further. However, for a point with a positive x, it must be determined if this intersection on the circle is also on the curve, that is, between points A and C.

The direction from the center of the circle (R_o, S_o) to a point (R_p, S_p) on the circle is:

$$\phi = \tan^{-1} [\ (R_p-R_o) \ / \ (S_p - S_o)\ ] \tag{A40}$$

The directed azimuth from the circle's center to any intersection and to points A, B, and C can then be found. With some logic to consider the crossover point (from 360° to 0°), it can be determined if the ϕ for the intersection is within the range of ϕ swept out by the curve.

After determining if any intersections are on the curve, the curve is considered in three pieces if there are two intersections, two if there is one intersection, and as a single curve if there are no intersections. The computation is done very similarly to that for line sources. Whereas the length along the line is used to make calculations at intervals for the line source, the variation of the azimuth from the center of the circle, ϕ, is used for the curved source. The coordinates of a point on the curve for which the concentration contribution is being evaluated are found from:

$$R_p = R_o + \rho \sin \phi \tag{A41}$$

$$S_p = S_o + \rho \sin \phi \tag{A42}$$

The upwind and crosswind distances, x and y, of a given point on the curve with coordinates (R_p, S_p) from the receptor (R_r, S_r) are calculated as previously using equations (A1) and (A2). The same point source dispersion function, f_p, as given in the "Line Source Computations" section is used.

Portions of the curve that contribute no concentration to the receptor are eliminated, and the curve is redefined. An initial estimate of the concentration from the remaining curve is made using eleven equally spaced points along the curve. These and the ten points in between are then used for a second estimate. Comparison is made of the two estimates and, as with the area and line source estimates, if these two are within the given criteria, the concentration is that of the second estimate. If additional estimates are made, concentration contributions for additional points, midway between these points already considered, are determined assuming the concentration varies linearly between adjacent points, that is, trapezodial integration.

If the curve was broken into pieces because of intersections, the contribution from the additional pieces must be determined as above.

TABLE 1

```
EXAMPLE PROBLEM OF PAL 'A GAUSSIAN-PLUME ALGORITHM FOR POINT,AREA,LINE SOURCES'

PINA =    .02000 PINL =    .02000

              SOURCE     WIND INCREASE
             INCLUDED    WITH  HEIGHT

   POINT        YES             NO

   AREA         YES             NO

HORIZONTAL
LINE SOURCE     YES             NO

    CURVE
PATH SOURCE     YES             NO

   SPECIAL
LINE SOURCE      NO             NO

   SPECIAL
PATH SOURCE      NO             NO                       AVERAGE      NO   DIURNAL    NO


* * * P O I N T   S O U R C E S * * *
     NO.     POINT     PHYSICAL     STACK       STACK      STACK      VOLUME       COORDINATES        INITIAL SIGMAS
            SOURCE      HEIGHT      TEMP         GAS      DIAMETER     FLOW      EAST      NORTH        Y         Z
           STRENGTH   (METERS)   (DEG-K)   VELOCITY   (METERS)  (CU M/SEC)   (KM)      (KM)        (M)       (M)
            (G/SEC)                          (M/SEC)

     1        5.00       10.0       320.0        .00        .00      12.00      .240      .185        1.0       1.0


 * * A R E A   S O U R C E S * * *
     NO.      AREA        AREA          COORDINATES         AREA SIZE
             SOURCE      SOURCE          SW-CORNER
            STRENGTH     HEIGHT       EAST      NORTH   EAST-WEST NORTH-SOUTH
         (G/SEC-M**2)  (METERS)      (KM)       (KM)      (KM)       (KM)

     1    -.00020000        .0        .240      .150      .070       .030
     2     .00020000        .0        .120      .070      .200       .120


 * * H O R I Z O N T A L   L I N E   S O U R C E S * * *
     NO.     LINE        LINE                      COORDINATES
            SOURCE      SOURCE           POINT A               POINT B           INITIAL SIGMAS                 NO.      TOTAL     MEDIAN
           STRENGTH     HEIGHT       EAST      NORTH       EAST      NORTH        Y         Z                   OF       WIDTH      WIDTH
          (G/SEC-M)   (METERS)      (KM)       (KM)       (KM)       (KM)       (M)       (M)                 LANES   (METERS)  (METERS)
                                                                                                                 4.       20.0        .0
     1     .00200000        .0        .160      .037      1.160       .037      3.00      1.50
     2     .00180000        .0        .160      .032      1.160       .032      3.00      1.50
     3     .00190000        .0        .160      .028      1.150       .028      3.00      1.50
     4     .00200000        .0        .160      .023      1.160       .023      3.00      1.50
                                                                                                                 4.       20.0        .0
```

TABLE 1 (CONTINUED)

```
    5    .00050000       .0      .063      .110      .063    1.110      3.00      1.50
    6    .00080000       .0      .068      .110      .068    1.110      3.00      1.50
    7    .000F0000       .0     -.072      .110      .072    1.110      3.00      1.50
    8    .00100000       .0      .077      .110      .077    1.110      3.00      1.50

 * *C U R V E D   H O R I Z O N A L   P A T H   S O U R C E S * * *
NO.     LINE        LINE                    COORDINATES
       SOURCE      SOURCE       POINT A                POINT M             POINT B          INITIAL SIGMAS       NO.     TOTAL      MEDIAN
       STRENGTH    HEIGHT    EAST      NORTH       EAST      NORTH      EAST      NORTH       Y          Z         OF      WIDTH      WIDTH
      (G/SEC-M)   (METERS)   (KM)      (KM)        (KM)      (KM)       (KM)      (KM)       (M)        (M)       LANES  (METERS)   (METERS)
  1   .00200000     .000     .160      .030        .110      .042       .070      .110      3.00       1.50        4      20.00       .00
  2   .00030000     .000     .160      .030        .110      .042       .070      .110      3.00       1.50        4      20.00       .00
  3   .00150003     .000     .160      .030        .110      .042       .070      .110      3.00       1.50        4      20.00       .00
  4   .00190000     .000     .160      .030        .110      .042       .070      .110      3.00       1.50        4      20.00       .00

 * * R E C E P T O R S * * *
    NO.    RREC(KM)   SREC(KM)     Z (M)

     1       .170       .120        .0
     2       .120       .070        .0
     3       .098       .040        .0
     4       .060       .013        .0
     5       .240       .030        .0
     6       .240       .070        .0
     7       .240       .050        .0
     8       .240       .010        .0

 * * M E T E O R O L O G Y * * *
    NO.  THETA(DEG)     U (M/SEC)  KST      HL (M)   T (DEG-K)    P (MB)  DIURNAL VARIATIONS (FRACTIONS OF GIVEN Q)
                                                                                                 HORIZONAL   CURVED    SPECIAL   SPECIAL
                                                                           POINT      AREA       LINE       PATH      LINE       PATH
     1.       45.         3.0         4     1000.       293.        960.  1.0000     1.0000     1.0000     1.0000    1.0000     1.0000

 * * C O N C E N T R A T I O N S   A T   R E C E P T O R S * * *
   CONCENTRATIONS IN GRAMS PER CUBIC METER                      FROM        FROM       FROM        FROM
HOUR RECEPTOR      RECEPTOR COORDINATES      FROM       FROM     HORIZONAL   CURVED     SPECIAL     SPECIAL
       NO.       EAST     NORTH    HEIGHT    POINTS      AREAS      LINES       PATHS      LINES       PATHS       TOTAL


  1     1        .170     .120      .00     2.315-08   3.677-03   0.000      0.000      0.000       0.000       3.677-03
  1     2        .120     .070      .00     1.360-05   4.572-03   0.000      0.000      0.000       0.000       4.586-03
  1     3        .098     .040      .00     5.622-05   1.683-03   1.032-17   7.698-04   0.000       0.000       2.509-03
  1     4        .060     .013      .00     1.112-04   1.210-03   9.338-12   4.317-04   0.000       0.000       1.753-03
  1     5        .240     .030      .00     0.000      3.854-03   0.000      0.000      0.000       0.000       3.854-03
  1     6        .240     .070      .00     0.000      4.087-03   0.000      0.000      0.000       0.000       4.087-03
  1     7        .240     .050      .00     0.000      1.473-03   4.311-12   0.000      0.000       0.000       1.473-03
  1     8        .240     .010      .00     0.000      3.312-04   1.021-03   0.000      0.000       0.000       1.352-03
```

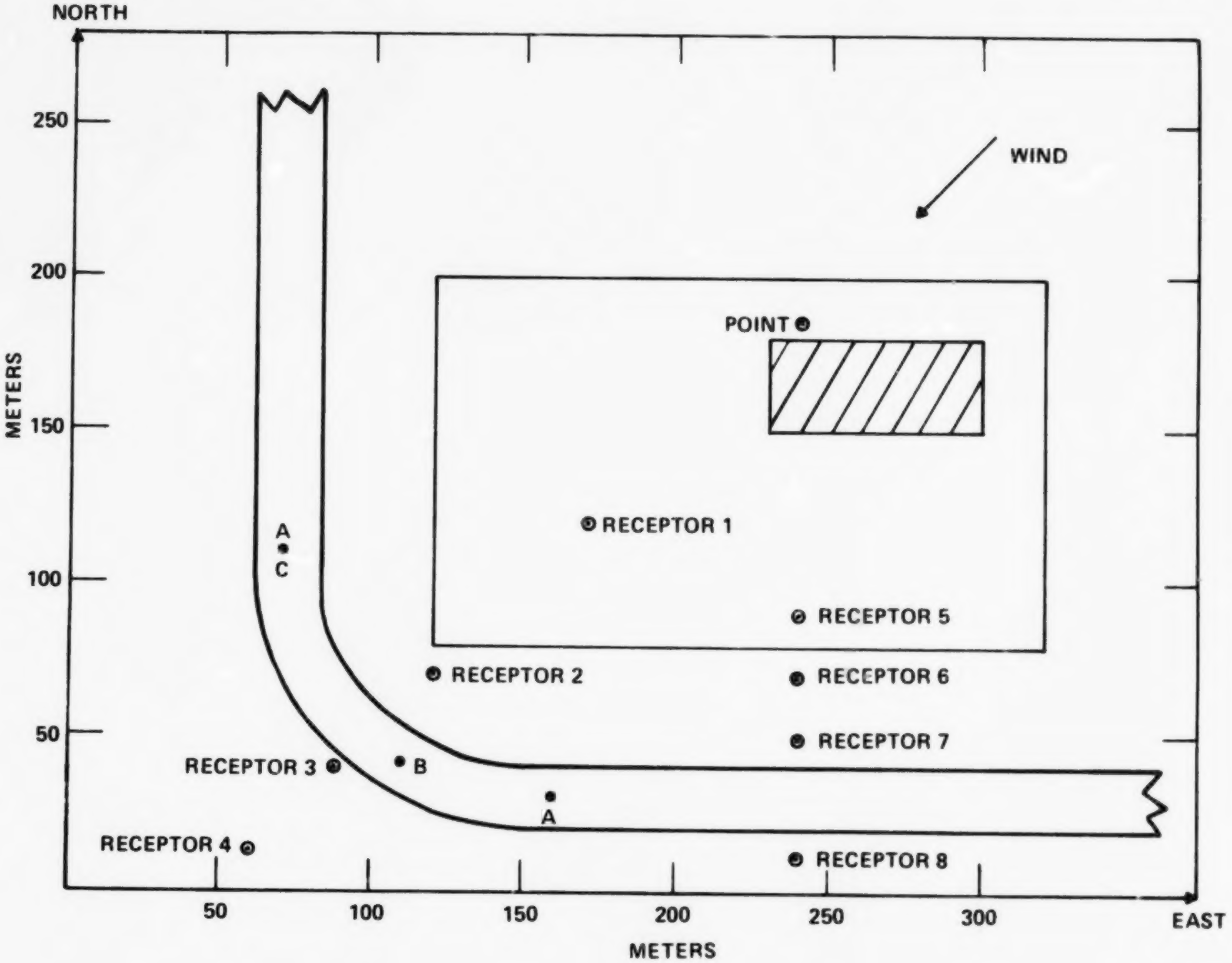
NORTH
METERS
250
200
150
100
50
WIND
POINT
RECEPTOR 1
A
C
RECEPTOR 5
RECEPTOR 2
RECEPTOR 6
RECEPTOR 7
RECEPTOR 3
B
A
RECEPTOR 4
RECEPTOR 8
50
100
150
200
250
300
EAST
METERS

Figure 1.

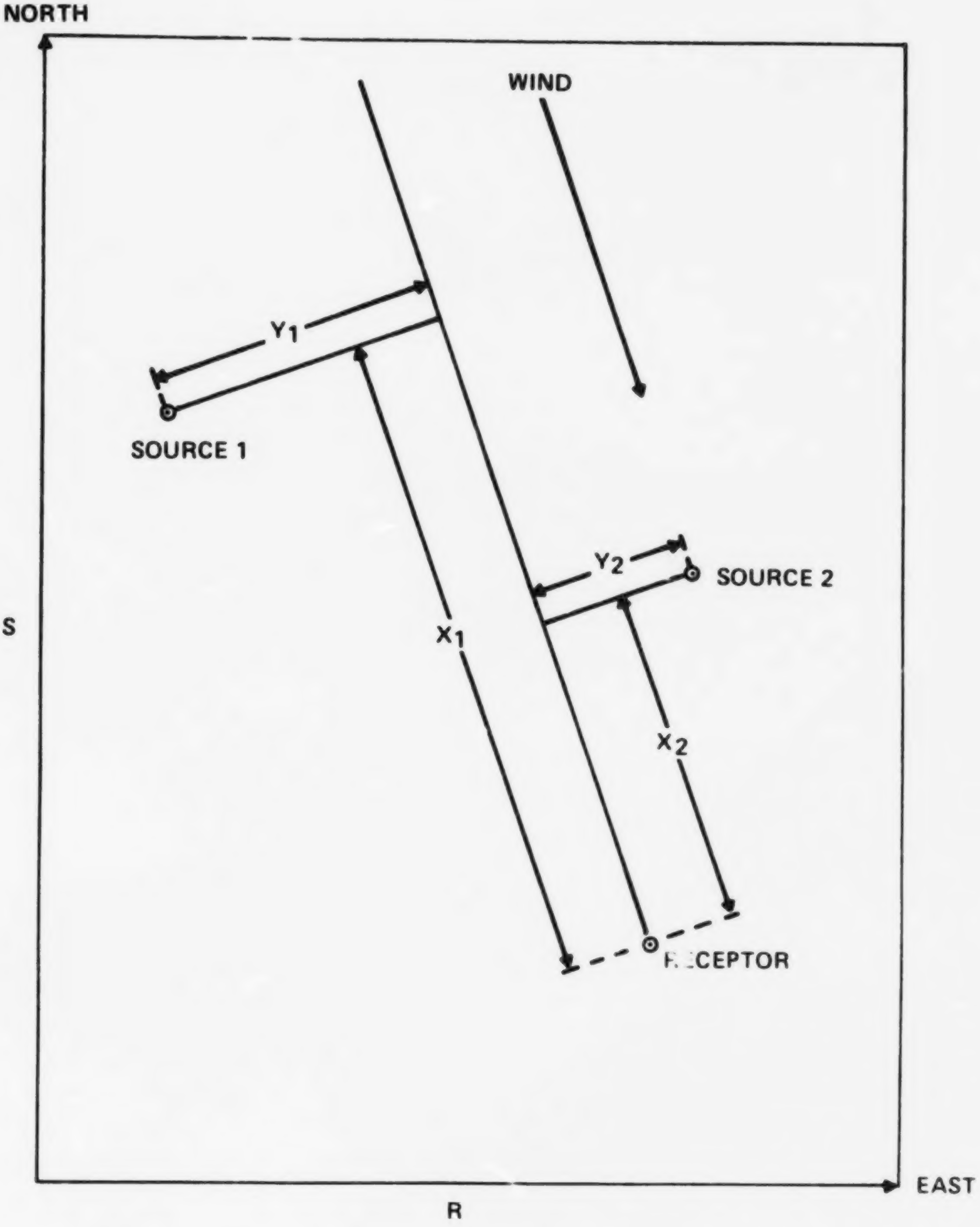

Figure 2. Upwind and crosswind distances of point sources from a receptor.

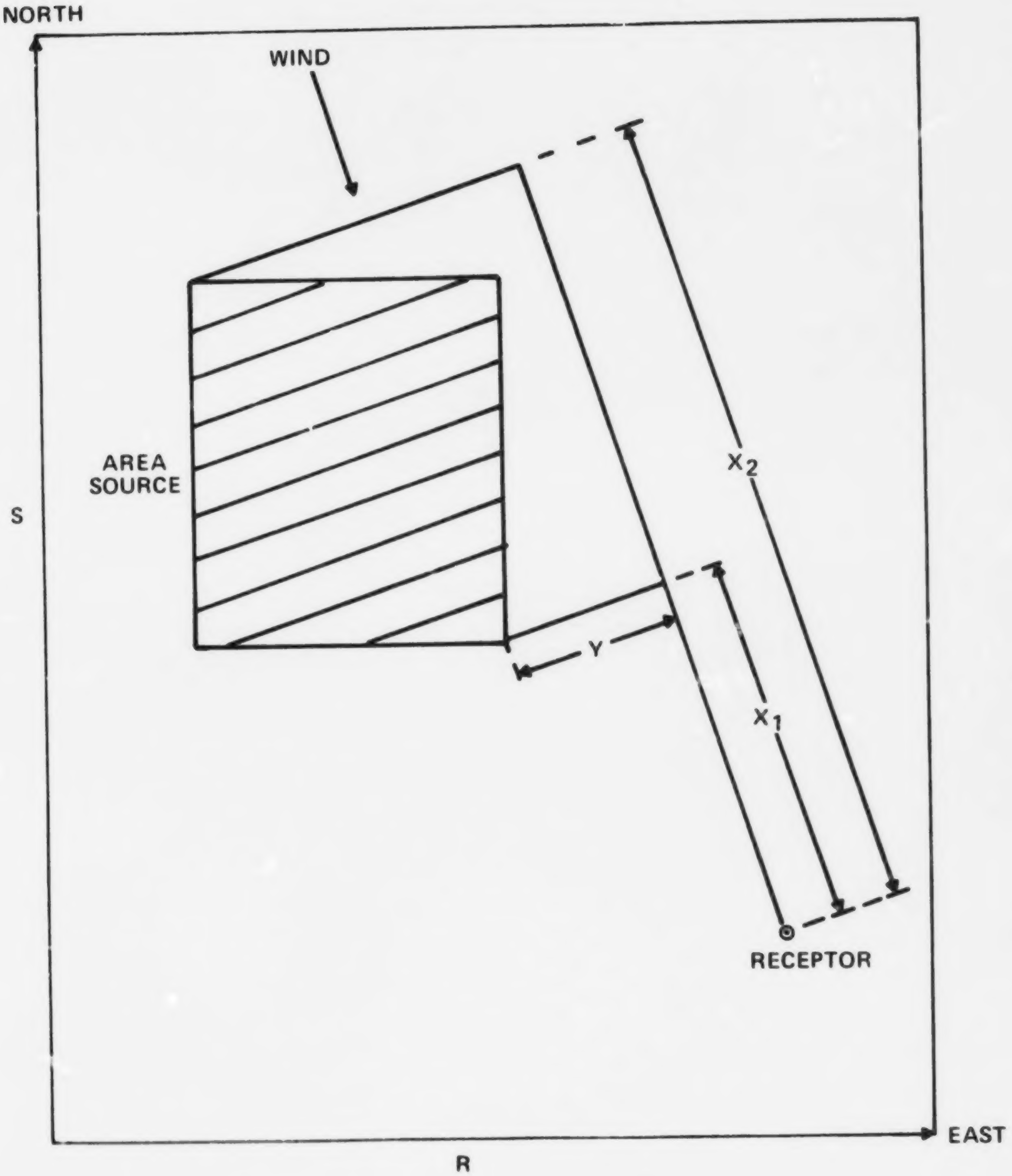

Figure 3. Minimum, X_1, and maximum, X_2, upwind distances of an area source from a receptor and crosswind line sources.

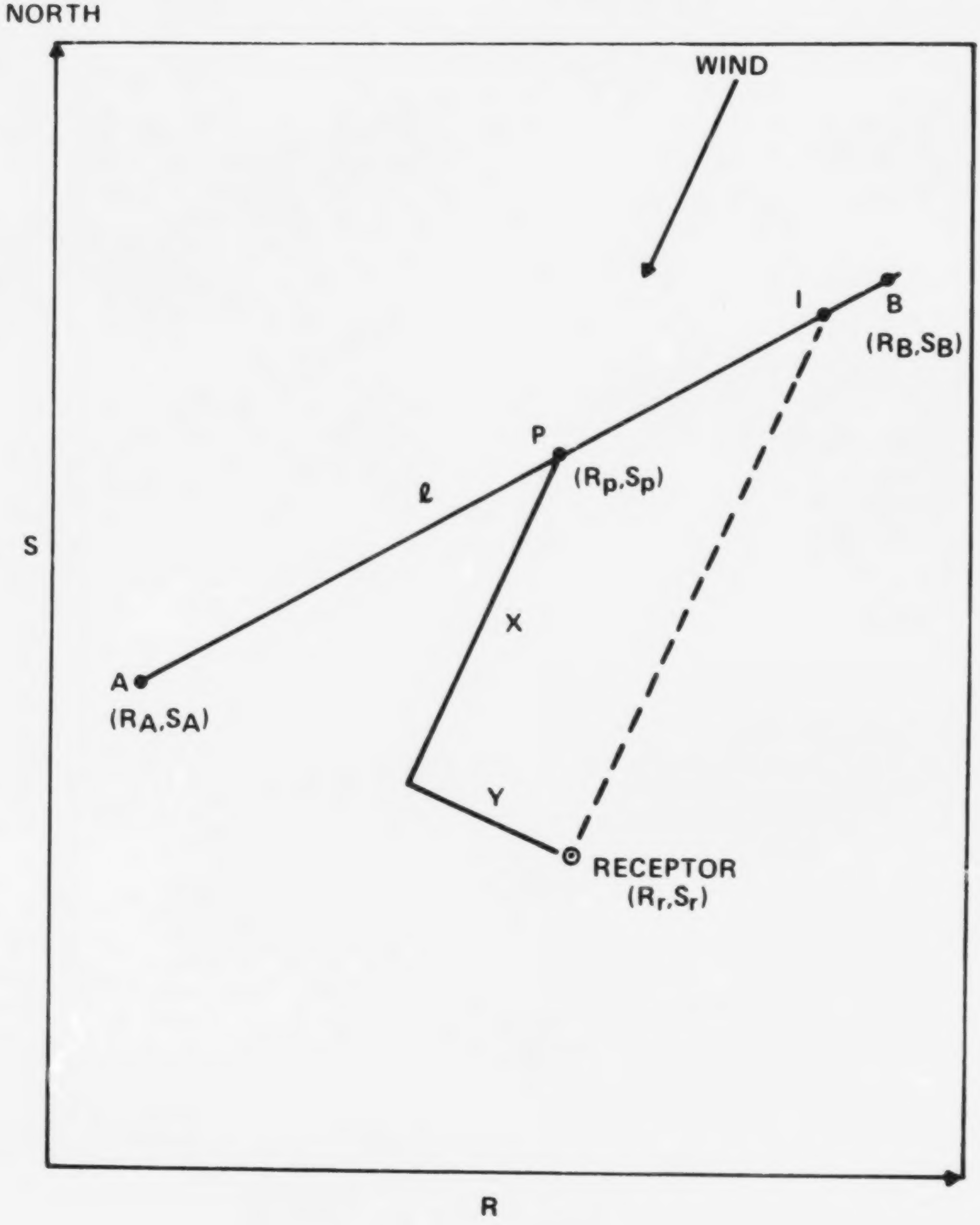

Figure 4. Line source and receptor relationships.

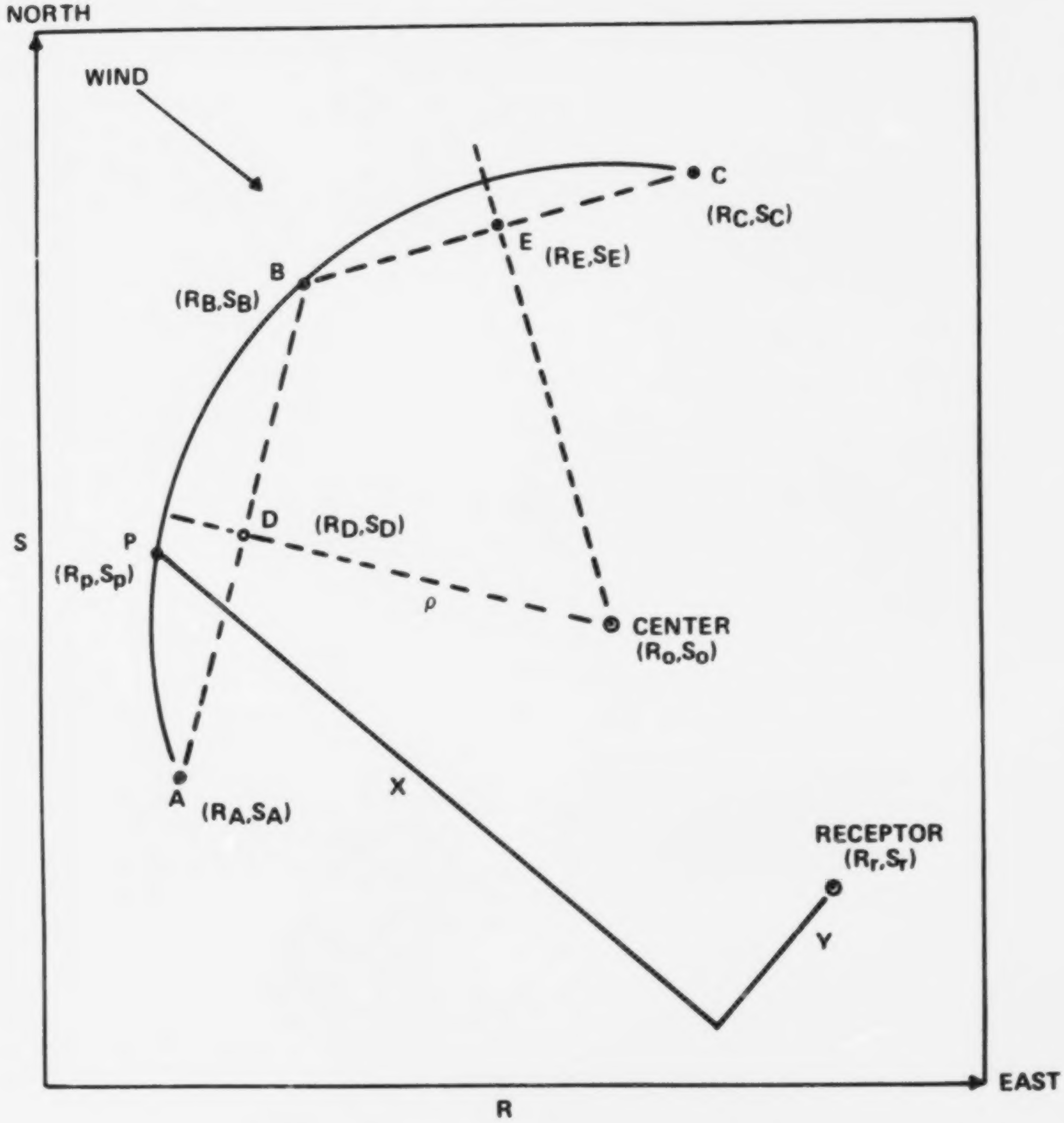

Figure 5. Curved source and receptor relationships.

6th NATO/CCMS
International Technical Meeting
on Air Pollution Modeling

STATISTICAL PROPERTIES OF SULFUR DIOXIDE CONCENTRATIONS AT CONTINUOUS MONITORING STATIONS IN JAPAN

by

RIKITA INOUYE

Faculty of Engineering, Hokkaido University

Sapporo, Japan

BATTELLE-INSTITUT E.V., Frankfurt/Main

Germany, FR

24-26 September,1975

NOMENCLATURE

$\bar{C}$	Annual mean concentration (ppm)
C_{99}	99th percentile value for one hour average
C_{max}	Annual maximum value for one hour average
C_{dm}	Annual maximum value for one day average
$C_{max,s}$	Annual maximum value for s hours average
$\bar{C}_g$	Annual geometric mean for one hour average
$\bar{C}_{gd}$	Annual geometric mean for one day average
$\bar{C}_{gs}$	Annual geometric mean for s hours average
$\bar{C}_{gm}$	Virtual geometric mean corresponds to C_{max}
$\bar{C}_g'$	Virtual geometric mean correspond to 99.84 percentile value for one hour average
$\bar{C}_{gd}'$	Annual geometric mean for one day average derived by calculation from the model (Eq. 10 in the text)
S_g	Logarithmic value of geometric standard deviation for one hour average
S_{gd}	Logarithmic value of geometric standard deviation for one day average
S_{gs}	Logarithmic value of geometric standars deviation for s hours average
S_{gm}	Logarithmic value of geometric standard deviation for one hour average corresponds to C_{gm}

NOMENCLATURE (Continued)

T	Sampling time; 8760 hours in this text
s	Averaging time
a, a_d, a_m, a', a'_d b, b_d, b_m, b', b'_d	Slopes and intercepts in the regression lines;
$\Delta\bar{C}_g, \Delta\bar{C}_{gm}, \Delta\bar{C}_{gd}$	The standard deviation from a regression line of $\bar{C}_g$ to $\bar{C}$, etc.
$\Delta C_{99}, \Delta C_{max}, \Delta C_{dm}$	The probable error in Eq. (8) in the text.

1. Statistical properties of sulfur dioxide concentrations

In an effort to improve air quality governments at national and local levels in Japan have been involved in monitoring pollutants in the air on a continuous basis by setting up monitoring stations; their number has rapidly increased in recent years. Table 1 shows the breakdown of the total number of such stations at the end of 1973.

Table 1

Pollutants subject to monitoring	No. of monitoring stations
SO_2	1,017
NO_x	329
O_x	349
HC	93
CO	100
Suspended particulates	865

As to data obtained at these stations, however, sufficient analyses have not been carried out about what statistical properties the pollutants have. Accordingly, this author began with SO_2 concentrations in investigating statistical properties of the readings, on the basis of which he has formulated a mathematical model related to the Arrowhead Chart.

The readings of concentration at each monitoring point are compiled statistically for a period of one fiscal year starting on April 1 in the preceding year and ending on March 31 and reported to the Environment

Agency of the Japanese Government, which consolidates the nation-wide reports for publication.

The published data serve each municipality concerned for its evaluation as to whether or not it meets the environmental standard specified by the national government. Statistical categories in this publication are derived from hourly mean readings for a one-year period. They include: annual arithmetic mean; 99th percentile value of one-hour readings (the reading of concentration, under which 99% of the total readings are included); frequencies not exceeding 0.1 ppm and 0.2 ppm in one-hour readings; frequency not exceeding 0.05 ppm in daily mean; maxima of one-hour readings and daily mean readings throughout the year specified.

Using these data, the author attemted to clarify statistical properties of readings of SO_2 concentrations.

The frequency distribution of readings of air pollutants is believed to show a variety of patterns, depending on the kinds of pollutants, conditions under which they are emitted, location of a monitoring point in relation to sources of pollutants, topography, and meteorological conditions, However, as shown by a result of studies done by Larsen(1) and others, it can be represented approximately by log-normal distribution.

Then, a linear relation(2), as shown in Fig. 1, was obtained as regards a relation between $\overline{C}_g$, the geometric mean (50th percentile value), and $\overline{C}$, the annual mean in a specific year by using the following two equations, which are valid for lognormal distribution, whereby $\overline{C}_g$ and S_g, the logarithmic value of geometric standard deviation, were calculated from C_{99}, the 99th percentile value mentioned above, and $\bar{C}$:

$$\bar{C} = \bar{C}g \exp(0.5\, Sg^2) \qquad (1)$$

$$C_{99} = \bar{C}g \exp(2.33\, Sg) \qquad (2)$$

Now, on the assumption that $\bar{C}_g = a\bar{C} + b$, a and b were obtained by a yearly regression line, as shown in Table 2-I.

A number of features are brought to attention by this table. First, the sign of values of b is negative in all the years. This means that, the smaller is the value $\bar{C}$, the larger is S_g, the logarithmic value of geometric standard deviation, which is given by Eq. (3):

$$Sg = \left\{ \ln\left(\frac{\bar{C}}{a\bar{C}+b}\right)^2 \right\}^{0.5} \qquad (3)$$

In other words, the trend is that the lower is the annual mean, the larger is $\exp(S_g)$, the geometric standard deviation. However, the absolute value of b shows a yearly decrease, as shown by the table, which signifies that the geometric standard deviation has tended to have a definite value regardless of the annual mean.

Moreover, the standard deviation $\Delta\bar{C}_g$, which stands for how much calculated values deviate from a regression line, shows a yearly decrease, which means that the prediction accuracy of C_{99} derived from the annual mean $\bar{C}$ has increased from year to year.

Calculation can be made likewise by Eqs. (4) and (5) by means of C_{max} , the annual maximum of one-hour readings, and $\bar{C}$, the annual mean. Should the frequency distribution of concentration show a complete lognormal distribution, $\bar{C}_{gm}$, the geometric mean, and S_{gm}, the logarithmic value of geometric standard deviation, are to coincide with $\overline{C}_g$ and S_g, respectively.

Shown in Table 2-II are yearly values of a_m and b_m in the equation for the regression line, $\overline{C}_{gm} = a_m\overline{C} + b_m$, which are derived on the basis of S_{gm} and $\overline{C}_{gm}$ calculated from Eqs. (4) and (5):

$$\overline{C} = \overline{C}_{gm} \exp(0.5\, S_{gm}^2) \qquad (4)$$

$$C_{max} = \overline{C}_{gm} \exp(3.81\, S_{gm}) \qquad (5)$$

According to this result, the sign of values of b_m is always negative, and both their absolute values and $\Delta\overline{C}_{gm}$ show yearly decreases, having similar qualitative properties to b and $\Delta\overline{C}_g$, while values of $\overline{C}_g$ and $\overline{C}_{gm}$ do not coincide with one another, and $\overline{C}_{gm} > \overline{C}_g$ in the range of the annual mean readings.

Namely, the foregoing shows that in many cases the accumulation line of concentrations bends toward the side of lower concentrations in the range above the 99th percentile value in a logarithmic probability graph. However, from year to year a difference between $\overline{C}_{gm}$ and $\overline{C}_g$ has lessened, and the distribution of concentrations approached a lognormal pattern.

From the foregoing results there will be no serious error, should an accumulation line of one-hour readings be represented by a broken line with the 99th percentile value as a point of bending.

An analysis was made likewise as to daily mean values. Namely, a calculation similar to the above was made by the following Eqs. (6) and (7) by using C_{dm}, the annual maximum of daily mean, and $\overline{C}$, the annual mean, whereby $\overline{C}_{gd}$, the geometric mean of daily mean, and S_{gd}, the logarithmic values of geometric standard deviation, were obtained, from which yearly values of a_d and b_d in the regression line represented by $\overline{C}_{gd}$ and $\overline{C}$ are expressed by $\overline{C}_{gd} = a_d\overline{C} + b_d$; Table 2-III shows yearly values of a_d and b_d

$$\bar{C} = \bar{C}_{gd} \exp(0.5\, S_{gd}^2) \qquad (6)$$

$$C_{dm} = \bar{C}_{gd} \exp(2.94\, S_{gd}) \qquad (7)$$

As noted in Table 2, a qualitative trend is shown for b_d and $\Delta\overline{C}_{gd}$ similarly to b and $\Delta\overline{C}_g$.

The next attempt is to see if C_{99} , C_{max} , C_{dm} , etc., can be estimated only from the annual mean value $\overline{C}$ by using the results obtained thus far. For instance, as for C_{99} , the only process needed is to substitute $\overline{C}_g = a\overline{C} + b$ for the term $\overline{C}_g$ in Eqs. (1) and (2), in which case, the probable error of the estimated value is obtained from:

$$\Delta C_{99} = \left(1 - \frac{2.33}{Sg}\right) \exp(2.33\, Sg)\Delta\bar{C}_g \qquad (8)$$

Table 3 and Fig. 2 show the value estimated from the annual mean by this method and its probable error concerning each concentration on the basis of the statistical data for from April 1, 1971 to March 31 1972.

As regards deviations of calculated values around the regression line, they show features somewhat characteristic of regions. For instance, Fig.3 shows relations between C_{99} and $\overline{C}$ both in the Pacific seacoast region and the Inland Sea region in which the real line stands for the regression line based on the foregoing calculation. It is shown from the above that higher concentrations take place in the latter region even with the same annual mean value. Also derived from the above are significant suggestions as to what kind of factors should be added to this method of estimation which depends only on the annual mean value $\bar{C}$ in order that prediction accuracy can be raised.

2. Representation of Arrowhead Chart; its mathematical models

Described in the following are how to represent the so-called Arrowhead Chart and its mathematical models.

To begin with, the author's opinion is offered about a way in which the Arrowhead Chart is prepared.

First, as for the adoption of sampling time, the author holds a one-year period appropriate, considering life cycle of living things and cycles of meteorological changes. Possible as it may be to take a period longer than one year, it would be problematical to use a fairly long period of time for such air pollution as has a time series with conspicuous trends.

Next, there is a question about how to handle time averaging concerning the readings of concentration. As for Larsen(1), he uses non-overlapping time for averaging. However, according to his method, for instance, when one month is used as averaging time, the number of data obtained for a one-year period is limited to as small as 12. Should not only this but also the need for comparison between data and the effects of pollutions be considered, the taking of a moving average is a convincing one.

However, when effects on human beings and other living things are discussed, due attention should be paid to the fact that they make normally a period of one day as a fundamental life cycle; from this viewpoint, in case an averaging time taken is longer than one day, it will be advisable to use a moving average on the basis of the one- day average as basic data.

However, should a moving average be taken for a limited time series, the number of data will decrease when averaging time is extended longer, which presents a problem.

Hence, in this case, as the average time is extended, the value of a plotting position of the annual maximum will decrease. Likewise, when a limited time series is treated by a simple moving average, the daily mean value, which serve as the basis for this average, are not used in the equal number of times in the entire process; so, there is a question about whether a perfect evaluation of concentrations of a specific year can be made; besides, there is no agreement between the average of the entire moving average and the annual average, which presents another problem.

Accordingly, the author processed the data on the assumption that a one-year time series for concentrations forms a sample in an infinite time series in which the one-year time series continues permanently, repeating itself every year. Hence, in this case, there are, for instance, 365 data both for the number of moving average over a shifting interval of 30 days and for the number of one-day data; also the annual average value remains unchanged.

The maximum in the 365 data has a plotting position of 99.84th percentile value in terms of non-exceeding frequency in a logarithmic probability graph.

Now, as regards the averaging time over a period shorter than one day, it suffices that the concentration of 99.84 percentile value in terms of non-exceeding frequency is obtained from the distribution of accumulation frequency of the data derived from non-overlapping averaging and then this concentration is caused to correspond to the maximum of values based on averaging time for a period of more than one day.

In this case, for instance, as for one-hour values, 14 data are to exceed this concentration.

However, for instance, even as regards how to express the stipulation of an environmental standard, in the light of the instability seen in the annual maxmum of one-hour readings or from a viewpoint of the need for emergency control, etc., the author believes it appropriate that in the case of the averaging time for a period shorter than one day, such a stipulation should accompany an appropriate non-exceeding frequency and in the case of the averaging time for a period longer than one day, it should be expressed by the maximum .

Then, in order that a mathematical model is made in accordance with the Arrowhead Chart, it will be adequate to formulate a model for the accumulation line in each averaging time.

As mentioned earlier, the author handled an accumulation line in such a way that it can be represented by a broken line with tne 99 percentile value as the point of bending in a logarithmic probability graph.

This case calls forth three factors for the decision of an accumulation line. As a way to express an accumulation line of one-hour values only by the annual mean the author has proposed that such three factors are $\overline{C}$, the annual mean; $\overline{C}_g$, the annual geometric mean; and $\overline{C}_{gm}$, the virtual geometric mean which correspond to the annual maxmum of one-hour values; and from the results of the nation-wide statistical data $\overline{C}_g$ and $\overline{C}_{gm}$ are related to C for this process.

Moreover, as a simple approximation, it is supposed that a one-hour mean has $\overline{C}$, the arithmetic mean, and that an accumlation line is expressed by a line which passes a point of 99,84 percentile value in the foregoing expression of a broken line; namely, it is expressed by a lognormal distribution.

Should $\overline{C}_g'$ be taken as a geometric mean in this case, then $\overline{C}_g'$ can be calculated from $\overline{C}_g$ and $\overline{C}_{gm}$. When a regression line of $\overline{C}_g'$ thus calculated against $\overline{C}$ is made $\overline{C}_g' = a'\overline{C} + b'$, values of a' and b' are as shown in Table 2-IV.

Besides, if such a hypothesis is valid for all the averaging times, as for the Arrowhead Chart, it suffices that $\overline{C}_{gs}$, the geometric mean for the averaging time s, can be expressed by a function of $\overline{C}$ and s, in which case it is natural that the following should hold:

$$[\bar{C}gs]_{s=1} = \bar{C}g' \;; \qquad [\bar{C}gs]_{s=T} = \bar{C}.$$

From the results of case studies on the hypothesis that the functional form of $\overline{C}_{gs}$ take a form shown by the following Eq. (9), the author found that the value r=2 represents the functional form of $\overline{C}_{gs}$ in the best way (Fig. 4) :

$$\frac{\bar{C} - \bar{C}gs}{\bar{C} - \bar{C}g'} = \left\{ \frac{\ln(\frac{T}{s})}{\ln(T)} \right\}^r \qquad (9)$$

If the relations r=2 and $\overline{C'_g} = a'\overline{C} + b'$ are substituted in Eq. (9) then Eq. (10) is derived:

$$\bar{C}_{gs} = \left[1-(1-a')\left\{\frac{\ln(\frac{T}{s})}{\ln(T)}\right\}^2\right]\bar{C} + b'\left\{\frac{\ln(\frac{T}{s})}{\ln(T)}\right\}^2 \qquad (10)$$

Next, this model is compared with the nation-wide statistical data. In Table 2-V, the values a'_d and b'_d, which are derived by calculation from Eq. (10) as to one-day mean value, correspond respectively to the values a_d and b_d, Which are obtained from the statistics. When a conparison is made between $\overline{C'_{gd}}$ derived from these values and $\overline{C}gd$ calculated from a_d and b_d, the largest error is 0.64 ppb for a period from April 1, 1970 to March 31, 1971 under the annual mean $\overline{C}$ = 0.06 ppm. This value is less than one half of the standard error, that is, 1.4 ppb, around the regression line.

As to the validity of this mathematical model for an averaging time longer than one day, no direct comparison is possible because there are no statistical data avalable concerning the maxmum based on a moving average for such an averaging time. However, since the monthly mean values are given for a non-overlapping basis, a comparison between the maxmum among them and the annual mean value is made, as shown in Fig.5. The real line in this figure shows a relation between the monthly maxima calculated from the model based on Eq. (10) and the annual mean.

Appendix

A number of forms have been presented concerning this kind of modeling.

For instance, Larsen(1) presumed that the 50th percentile value increases in an exponential proportion to the averaging time; namely, the following equation should hold:

$$\bar{C}_{gs} = Rs^{q} \quad (1)$$

According to him, noted at the same time as the above is a relation in which the maximum decrease in an inverse exponential proportion to the averaging time; that is, he gives the following eqation:

$$C_{max,s} = Ks^{-p} \quad (2)$$

In the meantime, presuming that the standard geometric deviation decreases in an inverse exponential proportion to the averaging time, Saltzman(3) gives the following equation:

$$SGD = \exp(S_{gs}) = As^{-B} \quad (3)$$

Since these equations are derived under conditions in which the way of taking sampling time , the way of taking averaging time, etc.,are not necessarily identical with those taken by the author, it is not possible to make a simple comparison among their equations and the author's. If it is assumed that these equations hold for the author's and also for all the ranges of averaging time, the following equations are derived: Namely , from Eq. (1):

$$\frac{\ln\left(\frac{\bar{C}_{gs}}{\bar{C}}\right)}{\ln\left(\frac{\bar{C}_{g}}{\bar{C}}\right)} = \frac{\ln\left(\frac{T}{s}\right)}{\ln(T)} \quad (4)$$

From Eq. (2);

$$\frac{\ln\left(\frac{\bar{C}gs}{\bar{C}}\right)\left\{4.16-\left(\ln\left(\frac{\bar{C}}{\bar{C}gs}\right)\right)^{0.5}\right\}}{\ln\left(\frac{\bar{C}g}{\bar{C}}\right)\left\{4.16-\left(\ln\left(\frac{\bar{C}}{\bar{C}g}\right)\right)^{0.5}\right\}}=\left\{\frac{\ln\left(\frac{T}{s}\right)}{\ln(T)}\right\}^{2} \qquad (5)$$

And from Eq. (3);

$$\frac{\ln\left(\frac{\bar{C}gs}{\bar{C}}\right)}{\ln\left(\frac{\bar{C}g}{\bar{C}}\right)}=\left\{\frac{\ln\left(\frac{T}{s}\right)}{\ln(T)}\right\}^{2} \qquad (6)$$

Since $\overline{C}_{gs}$ and $\overline{C}_{g}$ take values close to $\overline{C}$ the left side of this equation can be approximated by:

$$\frac{\ln(\bar{C}gs/\bar{C})}{\ln(\bar{C}g/\bar{C})}=\frac{\bar{C}-\bar{C}gs}{\bar{C}-\bar{C}g} \qquad (7)$$

In such a case of approximation, one of the author's equations, that is, Eq. (9) in the text, agrees with the Saltzman's result, also it agrees approximately with the result of Eq. (5), but does not with Eq. (4).

REFERENCES

1. Larsen, R.I., (1969) " A New Mathematical Model of Air Pollutant Concentration, Averaging Time and Frequency," J. Air Poll. Contr. Assoc., 19; 20-30

   Larsen, R.I., (1973) " Air Quality Frequency Distributions and Meteorology," Proc. 4th Meeting of the Expert Panel of Air Pollution Modelling.

2. Inouye,R., and Watanabe, Y.,(1973) "Statistical Properties of Sulfur Oxides Concentrations at Continuous Monitoring Stations in Japan (1)," ---in Japanese--- JOurnal of Japan Society of Air Pollution vol8 No. 4 pp28-35

3 Saltzman, P.E., (1970) "Significance of Sampling Time in Air Monitoring," J. Air Poll. Contr. Assoc., 10; 660-665

Table 2 Slopes and intercepts in the regression lines of the geometric mean to the arithmetic mean concentrations, number of data used in the statistics, the probable errors of the calculated values from the regression lines and the correlation coefficients.

		Apr. 1969 - Mar. 1970	Apr. 1970 - Mar. 1971	Apr. 1971- Mar. 1972	Apr. 1972 - Mar. 1973
I	a(slope)	0.856	0.856	0.874	0.846
	b(intercept)	-0.0042	-0.0030	-0.0023	-0.00068
	n(No. of data used)	177	211	379	583
	$\Delta\bar{c}_g$(RMSE)	0.0027	0.0024	0.0022	0.0018
	r(correlation)	0.981	0.982	0.975	0.972
II	a_m	0.896	0.891	0.901	0.897
	b_m	-0.0030	-0.0024	-0.0021	-0.0012
	n	190	253	408	612
	$\Delta\bar{c}_{gm}$	0.0019	0.0019	0.0016	0.0013
	r	0.992	0.986	0.986	0.984
III	ad	0.935	0.935	0.953	0.942
	b_d	-0.0013	-0.0010	-0.0009	-0.0004
	n	170	256	409	612
	$\Delta\bar{c}_{gd}$	0.0016	0.0014	0.0012	0.0011
	r	0.993	0.993	0.992	0.989
IV	a'	0.879	0.876	0.903	0.882
	b'	-0.0035	-0.0026	-0.0025	-0.0010
V	a'_d	0.949	0.947	0.959	0.950
	b'_d	-0.0015	-0.0011	-0.0011	-0.0004

Table 3 Estimated values of C_{99}, C_{max}, and C_{d_m} from the annual mean values $\overline{C}$ and the probable error of the estimated values. (ppm)

ANNUAL MEAN CONC. $\overline{C}$	ESTIMATED VALUES AND PROBABLE ERRORS					
	C_{99}	ΔC_{99}	C_{max}	ΔC_{max}	C_{dm}	ΔC_{dm}
0.01	0.041	0.021	0.117	0.086	0.033	0.022
0.02	0.073	0.021	0.163	0.068	0.059	0.022
0.03	0.106	0.021	0.214	0.063	0.086	0.022
0.04	0.138	0.021	0.265	0.061	0.112	0.022
0.05	0.171	0.021	0.318	0.060	0.138	0.022
0.06	0.203	0.021	0.370	0.059	0.164	0.022

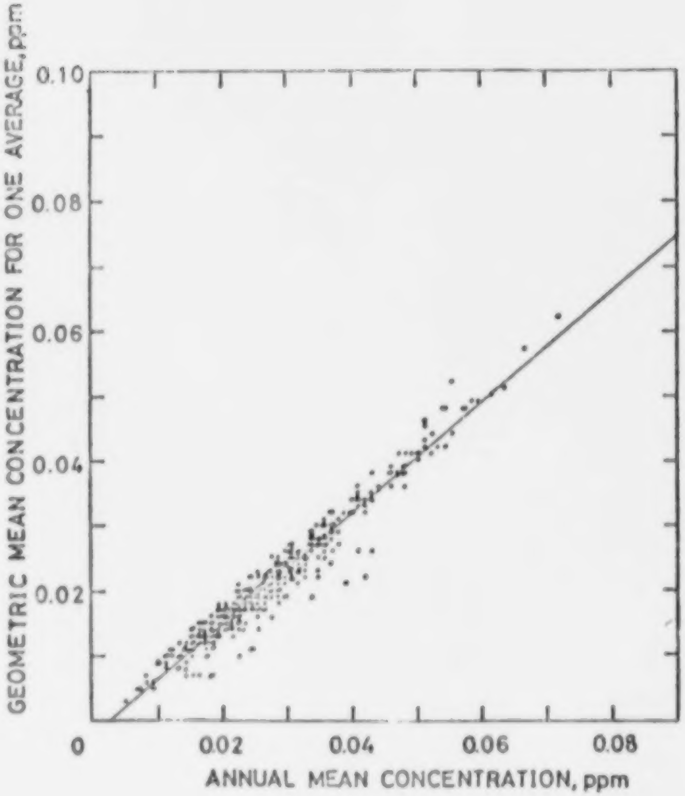

Figure 1. Plot of observed annual mean against predicted geometric mean concentrations of sulfur dioxide when averaging time is one hour, Apr., 1971 to Mar., 1972.

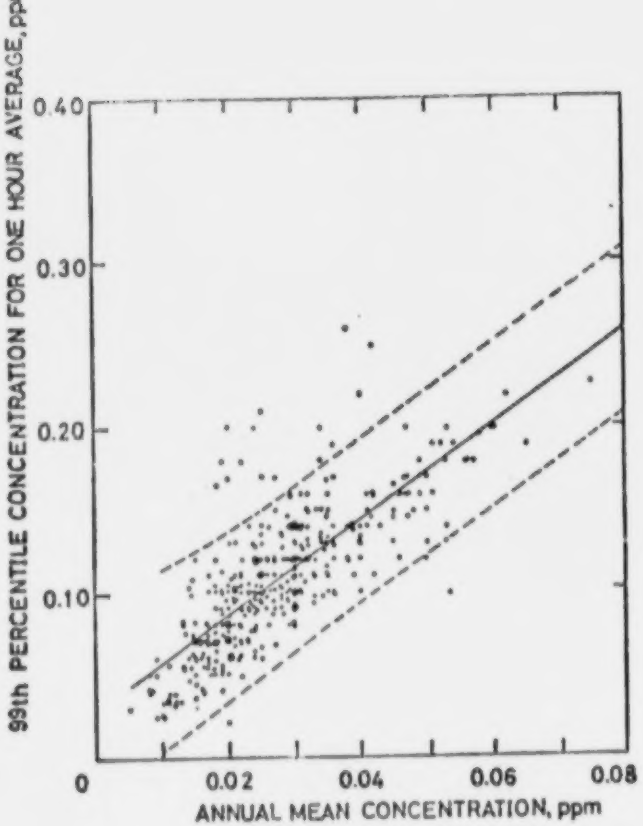

Figure 2. Relation between hourly 99th percentile and annual mean concentrations of sulfur dioxide at selected 408 stations in Japan. Solid line is derived from the regression eq. related $\bar{C}$ and $\bar{C}_g$. Apr., 1971 to Mar., 1972.

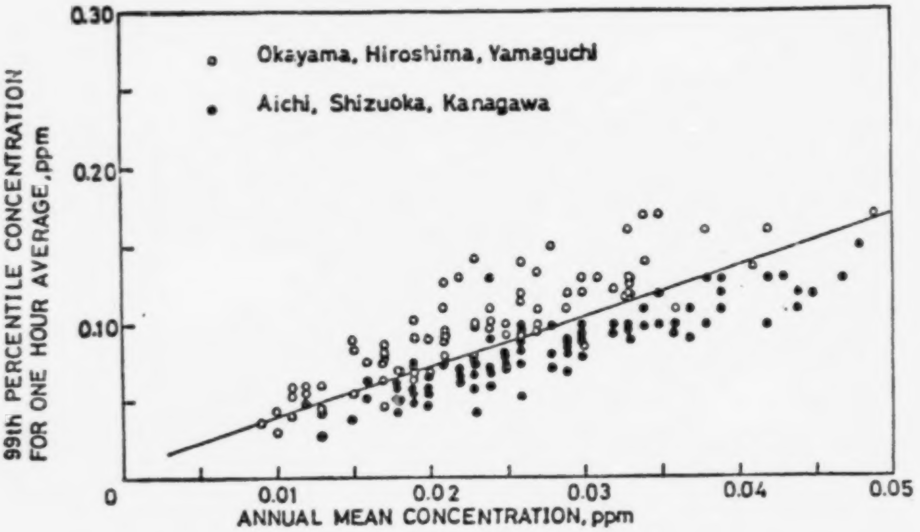

Figure 3. Relations between annual mean and 99th percentile concentrations at stations in the Coastal district of the Inland Sea of Seto(○) and the Coastal districts of the Pacific Ocean in Central Honshu (●), Apr., 1972 to Mar., 1973.
Solid line in the figure is derived from the regression Eq. related $\bar{C}$ and $\bar{C}_g$ at the stations of all Japan.

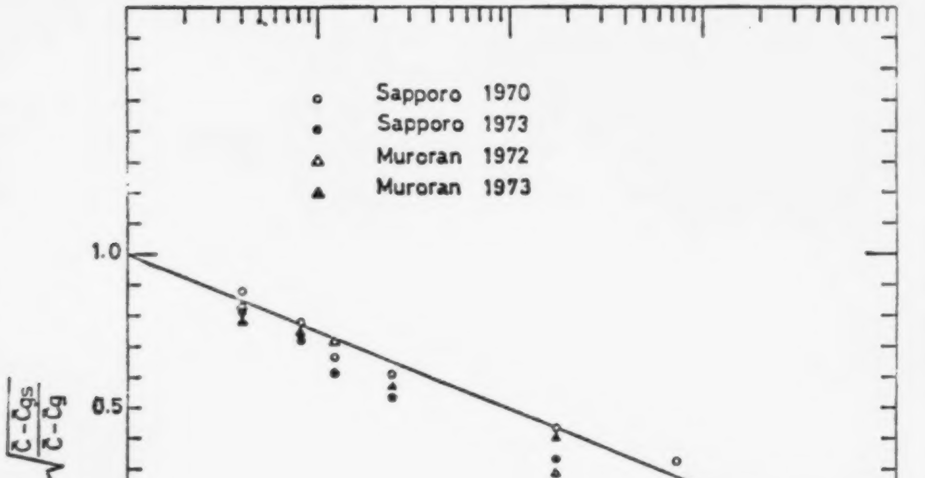

Figure 4. Relation between $\sqrt{\frac{\bar{C}-\bar{C}_{gs}}{\bar{C}-\bar{C}_g}}$ and averaging time s.

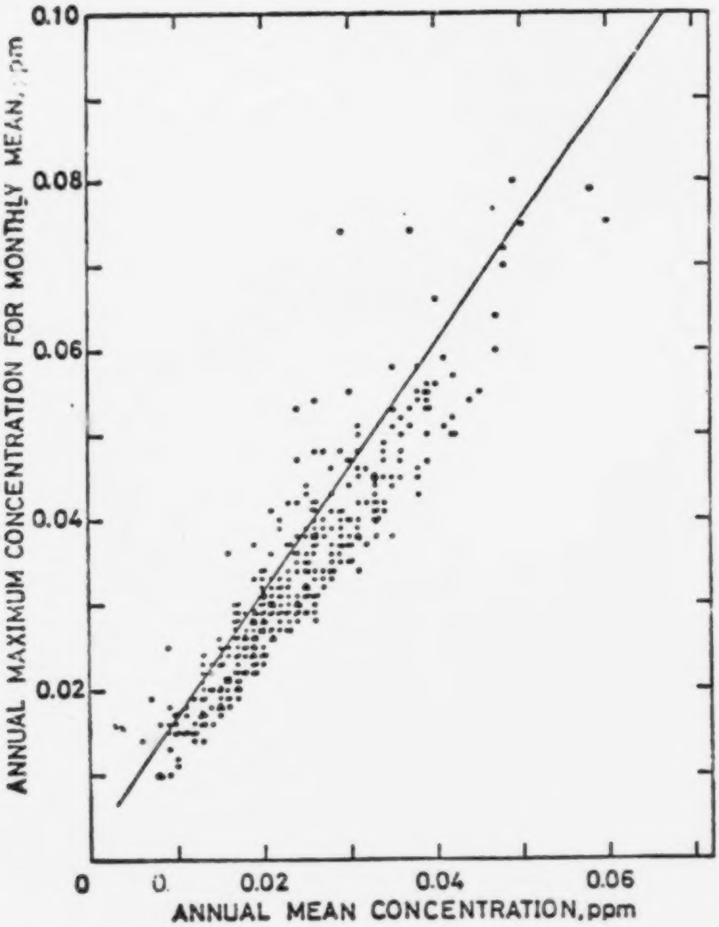

Figure 5. Relation between annual maximum for one month average (non-overlapping basis) and annual mean concentrations of sulfur dioxide at selected stations in Japan. Solid line in the figure is derived from the Eq.(10), Apr.,1973 to Mar.,1974.

6th NATO/CCMS
International Technical Meeting
on Air Pollution Modeling

METHODOLOGY FOR AN INTEGRATED SYSTEM OF AIR POLLUTION CONTROL PROJECT MASC-AP

by

L.F. Escudero and
R. del Llano

The Environmental Sciences Group of the
UAM-IBM Scientific Center, Madrid (SPAIN)

BATTELLE - INSTITUT E.V., Frankfurt/Main
Germany, FR

24 - 26 September, 1975.

Preceding page blank

ABSTRACT

The UAM-IBM Scientific Center, in collaboration with the Management Corporation of Gran Bilbao (North of Spain), has developed a project for the control, prediction and planning of the reduction of air pollution in the Gran Bilbao area. The general methodology of this project, which consisted in the integration of different studies, is presented in this paper. The different individual studies are described in greater detail separetely in other papers.

1. INTRODUCTION

The emission of gases produced as a consequence of different types of human activity are by their nature dispersed into the atmosphere. The dynamic of this medium of transportation is basically defined by meteorological factors and topographical features. The laws which govern this dynamic and the nature of the polluting agents produce different effects at the different sites at which they are deposited, the natural areas of the biosphere (fauna, flora, etc.) and the artificial elements added by man (artistic monuments, etc).

Thus, we are dealing with what may be considered a system having particular inputs (emissions and meteorological factors) which produces the corresponding outputs (a definite quality of air and the subsequent effects it has on the systems which interact with it). The description of this system phenomenon form the point of view of its evolution leads us to speak of generator areas (different types of sources), agents (SO_2, NO_x, etc.), a medium of transportation of these agents (the air) whose dynamic conditions their diffusion, and finally of deposit areas for these agents where they cause different effects.

The extraordinary complexity of the air pollution problem which has the interdisciplinary character proper to the so-called environment sciences makes it necessary to divide research into the following areas which are coordinated by close collaboration of all the elements involved. The bibliography gives references to other papers which deal extensively with each of the subjects treated here.

2. THE AREA STUDIED

The area studied covers approximately 150 Km^2 and has almost one million inhabitants. It is primarily an industrial area with a continuous succession of pollution sources and urban centers. The three most important zones in the region studied are the following: the valley of the Asua River, the valley of the Nervion River and the mouth of the latter. The features of these three zones are described below.

The Asua River Valley

The axis of this valley runs in an ESE-WNW direction and covers an area of approximately 30 Km^2 at altitudes of less than 100 meters. The foot of the valley has an altitude of approximately 300 meters. It is bordered on the north by a mountain range with altitudes between 100 and 300 meters. The south it is bordered by a mountain range which separates it from the Nervion River valley with altitudes between 200 and 400 meters.

The Nervión River Valley

The axis of this valley runs in a SE-NW direction and covers an area of approximately 26 Km^2 at altitues of less than 100 meters. The foot of the valley has an altitude of approximately 300 meters. It is bordered on the north by the mountain range which separates it from the Asua River valley. Its greatest elevations up to 100 meters are found to the south. It includes the city of Bilbao and is joined to the Asua River valley at Arriagas.

The mouth of the Nervión River

This zone has a SE-NW direction and covers an area of approximately 65 Km^2 at altitudes of less than 100 meters. It is bordered on the north by a mountain range with altitudes of some 200 meters. It is bordered on the south by a mountain range with heights of 400 to 500 meters. It includes the towns of Santurces, Sestao, Baracaldo and Portugalete.

3. AN AUTOMATIC NETWORK OF METEOROLOGICAL AND AIR QUALITY SENSORS.

One of the basic phases, together with the inventory of point and area sources contributing to pollution [1], in the study of the control, and planning of the reduction of SO_2 pollutant emissions in the Gran Bilbao area, is the placement and the type of meteorological and air quality sensors which make up the minimum automatic network. This network is connected in real time with a central system which obtains and processes the information which is supplied continuously.

Determining the number of sensors needed, their correct location, and the most suitable instrument is a very complex problem, especially when the area to be monitored is very large, such as a city, an entire region, or even an entire country. In these circumstances, the topographical features of each area and the location and intensity of the emissions may vary so much from one place to another that it is not possible to establish a systematically valid methodology for all of the areas. There are however, some general criteria for the design of such networks in the case of a city, which we list below. For more details, see reference [2].

The following questions arise in the planning of an automatic network for the study of air pollution: How many meteorological sensors and how many concentration monitors must be set up, what kind, and where?.

These question are inevitably tied to the economic aspect of the problem. Obviously the answers should be given from a scientific point of view so that both the meteorological and pollutant concentration monitors form an adequate network for the study of air pollution in the area under consideration in spite of the fact that the economic factor must be kept in mind. Any later expansion of this minimum network will increase the research potential and effectiveness of the system.

The placement of the meteorological sensors should be fixed after a prior meteorological analysis [3] of the area (carried out with manual sensors) and a detailled study of the topography of the area. This involves wind and temperature-humidity sensors which make possible an estimate of the horizontal and vertical spatial distribution of the wind and of the atmospheric stability in the most contrasting areas in the region. Sensors for the measurement of other variables should also be included, such as pressure, solar radiation and precipitation, as well as instruments needed to judge the atmospheric stability and the energy contained in various intervals of frequencies of the turbulence spectrum.

The placement of the air quality monitors may be decided according to the following procedure: the application of an approximate mathematical model of atmospheric diffusion, and an objective analysis of the results obtained with this model. This makes it possible to decide upon the minimum number of monitors to be installed in the area and upon the distance between them so that the data they furnish makes it possible to calculate the map of isopleths of concentration.

Given the special features of the Gran Bilbao area, the general methodology for the design of a network of air quality sensors could not be used. It was necessary to develop a special methodology based on the technique of objective analysis of scalar fields which involves the following phases:

1. The calculation of a series of influential sources in the area applying a mathematical model of atmospheric diffusion.

2. Assuming the concentrations calculated to be real, the correlation coefficient between the values for each pair of receptor points is estimated.

3. The curve of the variation of the correlation coefficient is plotted in function with the distance between the receptor points. Given a certain value for the correlation coefficient, a distance correspond to it according to the curve plotted. This distance will be the maximum separation allowed between the air quality monitors whose data will make it possible to plot the isopleths of concentration with a precision relative to the correlation coefficient taken as significant.

4. METEOROLOGICAL FACTORIAL ANALYSIS

It is important, keeping in mind both the design of the information network and the analysis of the factors which influence the pollutant concentration, to estimate for the entire area studied first which meteorological variables or combination of these variables really influence the propagation of the pollutants. Usually, the models simulating the pollution phenomena consider the meteorological elements which influence the concentration of the pollutant to be, among others, the following [7]: the direction and velocity of the wind, the intensity of rain, the temperature, pressure, relative humidity, cloudiness, the number of low-hanging clouds, the visibility, solar radiation, the thickness of the mixing layer, type of stability, etc.

Now, it is possible that these meteorological elements (which undoubtedly do have a marked influence on the pollutant concentration) may not be independent of each other and may be correlated in such a way that they have certain relations of dependency with one or more meteorological factors common to all or a part of them. The study of this type of relation is called Factorial Analysis. Its objective is to obtain and weigh the sources of variation in certain observed variables (the meteorological elements mentioned above). These sources which are not measured directly are the underlying causes (meteorological factors) common to different variables. In general, and this is what makes them most useful, the meteorological factors will be much fewer in number than the elements.

Once the meteorological elements have been expressed in function with the common factors which represent the greatest contribution to their variability, it is easy to obtain the inverse relation: the factors in function with the variables or meteorological elements indicated above.

If any of the factors estimated is closely correlated (linearly or non-linearly) with some meteorological element that is physical, it is said that this factor is a "real" factor. If not, it is said to be a "theoretical" factor. In the first case, the meteorological element can be replaced by the estimated factor. Using this analysis, the models simulating the pollutant concentration work with the factors only whether real or theoretical.

5. TYPIFICATION OF METEOROLOGICAL SITUATIONS

To facilitate the forecasting of the most influential meteorological factors in the phase of the transportation of the pollutants, estimated in the manner described above, which in principle may be the direction and velocity of the wind and the stability, it is necessary to establish the relations existing between the synoptic, situation, which can be known at any time and even predicted short term, and the observed weather in the Gran Bilbao area. Certain statistical techniques can be applied to determine these relations which are the basis for the local forecasting methods.

To achieve this objective, first a subjective classification is made of the weather observed in the Gran Bilbao area into "types of weather" for each of the four season of the years included in the historical file. The classification is made on the basis of using meteorological variables averaged in groups of six hours which have been observed to be most influential in the pollutant concentration.

A definitive classification is made on the basis of this initial classification using statistical techniques of the clustering type which will finally yield a classification into types of probabilistically certain weather with a certain percentage of risk given.

Once this classification has been obtained, using the surface data, it is necessary, as we have said, to interrelate it with the altitude situation or synoptic situation (the set of analysis and synoptic maps which describes the state of the atmosphere at a regional level), that is, to find the parameters of the synoptic situation which defines the types of weather so that the classes established remain probabilistically correct. The objective of this study, which is carried out using pattern recognition techniques, is the design of an adequate meteorological classifier that minimizes the number of cases assigned incorrectly to one of the types of weather established.

Parallel to this line of procedure, another is followed in the sense of classifying the synoptic situations directly with clustering techniques using certain parameters taken as discriminating (wind direction, intensity and curvature of flow, difluence, etc.).

Both procedures tend to the same end, the estimation of the most probable value of the meteorological variables mentioned within margins of error which will be wider the greater the variance of these variables in the classes obtained.

6. DAILY METEOROLOGICAL FORECASTING

Once the daytime sinoptic maps have been typified for each climatological season, an analysis is made for each geographically homogeneous area and for the day corresponding to each map of the hourly values of each of the meteorological factors representative of the mateorological elements which influence the pollutant concentration: direction and velocity of the wind, and the stability registered in the meteorological file of the area under study.

In this study it is assumed that there has been obtained previously for each meteorological factor the number of strates, the amplitude and the limits of each that cause the most homogeneous pollutant concentration in each receptor grid square for the values of the factor considered to belong to the same strate, and the most heterogeneous for values typified in other strates. In the description of the analysis described in this section only the numeration of the strate for each factor is considered in which the hourly value is included. Both in the meteorological forecast and in its later use in models simulating the pollutant concentration, only the types (median of the interval) which have been assumed to be influential in each factor are considered.

As a result of the analysis of the meteorological file, the hourly frequency of each of the meteorological strates of wind direction and velocity and stability is obtained in each geographically homogeneous area. These frequencies are the basis for the estimation of the meteorological probabilistic matrix to be used in the stochastic diffusion model [6].

In the same circumstances as before, the hourly persistance tables are obtained for each of the strates of each meteorological factor. These tables show the probability that a strate be maintained 2, 3, 4, ... hours.

Also, considering the hours (7-8) to (20-21) of each of the days included in the historical file, the most probable meteorological strate is obtained in each homogeneous area, climatological season, meteorological situation and meteorological factor for each of the next six hours for each possible binomial of strates in the hours -1 and 0. It is considered that the first daily binomial of hours is (7-8) and (8-9) and that the last hour for which the forecasting analysis is made is (20-21).

Both in the estimation of the meteorological probabilistic matrix and in the determination of the most frequent meteorological strate, those strates or the binomial of metorological strates are eliminated whose frequency in the historical file is not significant. For each meteorological situation there will be many meteorological strates with null frequency.

The hourly forecast of the meteorological condition: wind direction, wind velocity, and stability for each of the next six hours is made for each climatological season and geographically homogeneous area in the following form:

1. Forecast of the daily meteorological synoptic map.

2. Application of the meteorological map to the discriminant classifier created using the typological analysis carried out by the procedure described in section 5. The result is the daytime meteorological situation forecast.

3. Collection in each geographically homogeneous area and for the hours -1 and 0 of the information from the meteorological sensors for wind direction and velocity and stability. Typification of these values into the corresponding meteorological strates.

4. Analysis of the table of meteorological strates and estimation of the most frequent strates for each of the next six hours. This analysis is of the historical file of strates which corresponds to the daytime meteorological situation forecast in step (3).

7. AIR POLLUTION SIMULATION MODELS

The phenomenon of the air pollution may be looked at from several perspectives. When the phenomenon is understood as a complex system with its inputs (meteorological conditions and spatial distribution of the intensity of pollutant emission) and its outputs (pollutant concentration), the idea of using a model arises, considering the model to be any procedure which makes possible the reproduction of the system with identical inputs and outputs.

In general lines, the simulation models in this field may be classified from two points of view. One, from the point of view of use, might be: climatological, meteorological (short term) and episodic. Another, from the point of view of the techniques used in the simulation, might be to classify the models as diffusion or probabilistic models.

Below some brief comments are made on these types of models. However, reference [6] has a detailled description of the diffusion models, and reference [4] describes the probabilistic models in greater detail.

A. ACCORDING TO FIELD OF APPLICATION

A.1. Climatological Models

The purpose of these models is to estimate the average spatial distribution of the pollution over a long period of time. The input data are the average or climatological values of the meteorological variables for this period of time. The final result of these models might be a distribution of the frequencies of the concentrations or their average value, depending on the later use to which the results are put. Basically, all the models of this type use the gaussion hyposthesis with regard to the distribution of the pollutant. The principal differences between them are in the treatment of the plane sources (integration or equivalent point source) and the form of the dispersion functions. The probabilistic models have a greater field of application in this case.

The results obtained with the application of one or another of these models are in general comparable, and the choice a priori of any of them will be based on the characteristics of the area. In the case of Gran Bilbao, in which the pollution comes from industry, and in which there is a great number of important point sources, the differences obtained in the results from using one or another of the models are minimal since the important sources must be treated separately in accord with the classic gaussian plume formula in all the climatological models.

A.2 Meteorological Models

The purpose of these models is the estimation of the spatial distribution of the pollution over short periods of time, on the order of one or two hours. The input data is made up of the average hourly values of the meteorological values which affect the distribution.

In this type of application, the probabilistic models or the diffusion models should always be preceded by a suitable meteorological forecast of the input variables. The previous sections have described the methodology to be applied in the Gran Bilbao area for the meteorological forecast which with a model of this type will give a forecast of pollution for a short period (six hours).

A.3. Episodic Models.

The purpose of this type of model is to forecast pollution due to meteorological situations which are maintained over long periods of time and cause levels of pollution which may be dangerous. The development of these models is special for each area and therefore must be constructed on the basis of results obtained from the network during an operation time in which this type of situation occurs. It is also possible to attack the problem using a statistical analysis of the temporal series produced by the meteorological model an the clamatology of the area.

B. ACCORDING TO METHOD OF SIMULATION

B.1. Diffusion Models.

These models are based on the solution of the general equation of atmospheric diffusion:

$$\frac{\partial \chi}{\partial t} + \underset{\sim}{v} \cdot \underset{\sim}{\nabla} \chi = \frac{\partial}{\partial x} \left(K_x \frac{\partial \chi}{\partial x}\right) + \frac{\partial}{\partial y} \left(K_y \frac{\partial \chi}{\partial y}\right) + \frac{\partial \chi}{\partial z} \left(K_z \frac{\partial \chi}{\partial z}\right)$$

in which the coefficients of diffusion K are not constant, which makes impossible an analytic solution of the equation. The numerical integration, with the appropriate boundary condtions, is a long and complex operation even for computers with great capacity. This is the reason why drastically approximate simplification are used such as the gaussian solution and other similar solutions instead of complete integration.

B.2. Probabilistic Models

These models are based on collecting a great quantity of data and using statistical techniques on them which give inferred results with a certain probability as to what the pollutant concentration is going to be in the future.

8. ESTIMATING THE POLLUTED AREAS

One of the basic objectives of the MASC-AP project (see papers [8] and [9]) is to estimate for the Gran Bilbao area which areas are polluted and therefore where the pollution must be reduced. In this paper we have limited ourselves to the study of SO_2, although the procedure for studying any other pollutant would be similar.

For the purpose of this study the Gran Bilbao area has been divided into sixteen homogeneous areas to study their pollution. A sensor has been installed in each area which measures the real concentration ($\mu g/m^3$) of SO_2 [3]. The placement of these sensors is such that the deviations between squares which belong to the same geographically homogeneous area do not have an SO_2 sensor.

Another basis is the meteorological sensors of wind direction and velocity and stability installed in each geographically homogeneous area, and the estimation of the frequency of the type of meteorological situation [5] for the period being analyzed.

On the basis of the seasonal typology of meteorological situations (sections 5 and 6), an estimate is made of the frequency of each meteorological situation in the given period. Also, the probability is obtained statistically for each situation of each of the types of wind direction and stability considered, and also therefore the probability that each meteorological condition occurs in the seasonal period considered. This probability will be corrected by the deviations registered in the forecast corresponding to the previous period. Another initial datum is the point and area source emissions foreseen for each contributing grid square area in the period being studied.

The objective of this study consists in estimating the probability distribution of the pollutant concentration in each receptor grid square area for each meteorological condition corresponding to the geographically homogeneous area to which the grid square belongs, and for the seasonal domain which includes the probabilistic matrix obtained in accord with the procedure indicated in this section.

The results of the diffusion model employed [8] are used to obtain the probabilistic distribution of the concentration. It is assumed that for each meteorological condition only those points and area source emission influence each receptor grid square area which have been detected to be significant for the model just referred to. The procedure used to obtain this probabilistic distribution is to estimate the fitting of the pollutant diffusion coefficients of each source which influences the polluted grid square area, using techniques of linear and non-linear regression, employing the theoretical forecast of the diffusion model and the real concentration measured by the sensors installed in each grid square area.

On the basis of the probability distribution of the concentration, the probability is obtained for the set of foreseen emissions that the receptor grid square will have a foreseeable concentration greater than the absolute limit established. A polluted grid square area is considered to be one in which this probability exceeds the relative limit or maximum frequency.

In this phase of the MASC-AP project an estimate is also made of the problem area under study, and a weighting is given to each point and area source contributing to the pollution of the problem area. A problem is defined as the set of contributing areas and polluted grid square areas which have at least one square area in common. A contributing area is defined as the set of emission grid square areas which influence a particular polluted grid square area. The procedure in the application is described in detail in reference [9].

9. ESTIMATION OF THE REDUCTION OF EMISSIONS OF AN AIR POLLUTANT

In accord with the procedure described in the previous section, a polluted grid square area is considered to be one in which the probability estimated using the stochastic diffusion model that the real concentration is greater than a specific limit is in turn, in the seasonal period considered, greater than an allowed maximum frequency.

The objective of a reduction model is the evaluation of the alternatives for the reduction of emission in point and area sources that will make the polluted area studied no longer a polluted area. Polluted area has been defined in the previous section.

The objective of this algorithm is the estimation of the reduction required in the emissions of the contributing sources (both point and area sources) so that in a given seasonal period the grid squares which make up the polluted area will no longer do so. The principal condition for the new set of emissions is that the probability that in each polluted grid square area the maximum limit of concentration be exceeded not be greater than the maximum frequency allowed.

The function to be minimized is the level of reduction of the emissions such that the maximum levels of reduction set by socio-economic criteria be respected, and that those emissions which the model estimate as contributing most to the pollutant concentration be penalized.

The alternatives for reduction are estimated on the basis of the criteria that the emission reduction to be imposed on each contributing source be both the minimum possible and proportional to its effect on the polluted area.

The information required by the reduction model described in reference [9] is the following:

a) The contribution of the emitter sources (both point and area sources) of each grid square area to the concentration in the polluted area.

b) The emission from each source during the seasonal period studied.

c) The theoretical influence per unit of emission (both point and area) of each source in each polluted grid square area, defined by the corresponding stochastic diffusion model.

d) The maximum reduction of the emissions foreseen set according to socio-economic considerations in the emitter grid square area.

e) The theoretical concentration of the pollutant in each polluted grid square area for each meteorological condition studied, and for the set of emissions foreseen for the seasonal period. These concentrations have been estimated by models described in sections 7 and 8.

f) The absolute limit of the concentration (e.g., 400 g/^{3}).

g) The relative limit (e.g., 20%): the maximum probability allowed that the real concentration exceed the absolute limit.

h) The probabilistic meteorological matrices estimated for the seasonal period and problem areas considered.

The algorithm which optimizes the reduction model is based on techniques of mixed integer programming [10].

REFERENCES

This section lists an extensive bibliography of the works referred to which treat the subjects of each of the previous sections.

[1] F. Gómez-Pallete, 1973, "Air Pollution (survey on Emission Inventory, Bases and Techniques)". IBM - Madrid Scientific Center, PCI-07.73.

[2] J. Mantero, 1974, "Design of an Air Monitoring Network for the Control of Air Pollution in Bilbao". IBM - Madrid Scientific Center, PCI-01.74.

[3] J. Mantero and B. Orfila, 1973, "Meteorological Study of the Bilbao Area", IBM - Madrid Scientific Center, PCI-05.73.

[4] L.F. Escudero, 1973, "The Mathematical Formulation of a Probabilistic Model for the Estimation and Reduction of Atmospheric Pollutants", IBM - Madrid Scientific Center, PCI-10.73.

[5] J. López Navalón and B. Orfila, 1975, "Tipología y asignación de situaciones meteorológicas", I Congreso Iberoamericano del Medio Ambiente, Madrid.

[6] R. del Llano, J. Mantero and E. Thomas, 1975, "Modelos de difusión: Teoría, descripción y parametros", I Congreso Iberoamericano del Medio Ambiente, Madrid.

[7] R. del Llano, 1974, "Sobre ciertos fenómenos de mesoescala en una atmósfera urbana", Centro de Investigación UAM-IBM, PCI-04.75.

[8] J. Jimenez and L.F. Escudero, 1975, "Explotación estadística de un modelo de contaminación", I Congreso Iberoamericano del Medio Ambiente, Madrid.

[9] L.F. Escudero and J. Jimenez, 1975, "Estimación de zonas contaminadas", I Congreso Iberoamericano del Medio Ambiente, Madrid.

[10] L.F. Escudero and A. Vazquez Muñiz, 1975, "Algoritmo para la estimación de reducción de emisiones de un contaminante atmosférico", I Congreso Iberoamericano del Medio Ambiente, Madrid.

[11] R. del Llano et al., 1973 "Research Methodology for Air Pollution Control Systems" IBM - Madrid Scientific Center, PCI-04.73.

Rapporteur's Report, Topic I, (continued) September 24, 1975
by S.-A. Gustafson

Chairman: H. H. Slater

B. Turner: A Gaussian-Plume Algorithm for Point, Area and Line Sources

Discussion:

M. Schorling: Is it possible to simulate the dispersion in street canyons with your model?

B. Turner: Building influence is difficult to model. The model created by Stanford Research Institute is recommended for simulating dispersion in street canyons. However, if the distance between source and receptor exceeds about 300 m, then our algorithm might be satisfactory.

W. B. Johnson: Will your algorithm be included in UNAMAP?

B. Turner: We plan to include it (UNAMAP is a series put out by the EPA).

R. Inouye: Statistical Properties of Sulfur Oxides Concentrations at Continuous Monitoring Stations in Japan.

Diskussion:

H. H. Slater: Upper percentiles of observed frequency distributions of SO_2 concentrations do not fit the log-normal distribution very well. What are your results in this respect?

R. Inouye: Up to the 99 % percentile log-normality holds with satisfactory precision.

6th NATO/CCMS
International Technical Meeting
on Air Pollution Modeling

TOPIC II

REQUIREMENTS OF STANDARDIZATION OF AIR QUALITY SIMULATION MODELS AND REQUIREMENTS OF A COMMON DATA BASE FOR AIR QUALITY SIMULATION MODELS

Battelle - Institut e.V. Frankfurt / M
Germany, FR

24 - 26 September 1975

Preceding page blank

6th NATO/CCMS
International Technical Meeting
on Air Pollution Modeling

DISPERSION CHARACTERISTICS VIA TRACER TECHNIQUES

by

Karl-Heinz Müller
EURATOM
Ispra/Italy

BATTELLE - INSTITUT E.V., Frankfurt/Main
Germany, FR
24 - 26 September, 1975

Preceding page blank

Introduction

Dispersion models need input parameters characterizing the dispersion behaviour of an area. These parameters can be determined either indirectly by combining meteorological information, or directly via dispersion experiments. Tracer techniques are the most suitable in this case. Evidently, one has to perform these experiments in a way having regard to the structure of the model to be used. The parameters found by an in-situ tracer-study cover, in an integral way, both the micro-meteorology and the topography of the region under study. Since each datum about meteorology and air quality, can be obtained only at discrete space-time points, it is obviously sensible to represent the area of a city and its surroundings as a multicompartment system, where the air monitoring stations are separated from one another by transmission regions, each with its own homogeneous dispersion characteristics.

Such a representation can be done in two different ways, firstly by a model, i.e. a mathematical formalism including the parameter set mentioned above, secondly by the space-time dependent tracer density G generated by point-burst experiments. If this path is chosen the dispersion parameters and the model structure do not appear explicitly at all. G acts as a transfer function or Green's function.

Empirical distributions

This idea requires that, for a given weather situation, one covers the whole region simultaneously by two or more tracers to discover any dependence of G on the source position.

The dispersion calculation itself consists here only of a simple superposition of the type

$$\chi(\vec{r},t)=\iint G(\vec{\varrho},\tau\,|\,\vec{r}-\vec{\varrho},t-\tau)\,S(\vec{\varrho},\tau)\,d\varrho\,d\tau \tag{1}$$

where S denotes the source strength and χ the tracer concentrations.

In practice, such an empirical Green's function can throughout be used for continuous source distributions, where one works with a constant mean emission height. Obviously, such a tracering needs - at least during the phase of orientation - a certain number of points of release and many sampling stations. We, therefore, developed and constructed some simple and inexpensive sequential air sampling automats.

In the case of single industrial emitters, of course, one will apply a mathematical model instead of an empirical characterization-function.

Gaussian formula and modifications

A first step consists in replacing the empirical dispersion function G by an analytic expression with free parameters which have to be fixed by a fitting to the measured tracer concentrations. This expression must have the structure of a transfer function. PASQUILL used the so-called Gaussian formula as a transfer function for a homogeneous wind field and flat grassland. The application of this transfer function to tracer experiments over a wood-covered, built-up or hilly terrain, however, will lead to parameters which deviate more or less from **PASQUILL**'s. Those discrepancies bring out, in an integral way, both the different surface structure and the rather complex three-dimensional airflow over an urban area for instance.

Here, indeed, the question rises, of to what extent it is reasonable to apply a dispersion formula constructed for idealized conditions as a transfer function for more complex situations. Before one proceeds to construct different transfer functions one will try to discover - by a correlation analysis of the measured tracer concentrations - subregions, within which the application of the simple structured transfer function is justified. The above-mentioned subdivision and the data set of a simultaneous multi-tracering will be a valuable help here.

We suppose the dispersion formula

$$G = \frac{Q}{t^{3/2}} \exp\left[- \frac{(x-ut)^2}{4K_1 t} - \frac{y^2}{4K_2 t} - \frac{(z-h)^2}{4K_3 t} \right] \tag{2}$$

is used, (u, K_1, K_2, K_3, Q) being free parameters which we try to fix via tracer concentrations μ_i recorded at $(\vec{r}_i t_i)$. We take the logarithm of (2) and manipulate it into the linear form $\vec{\mu} = \Psi \vec{a}$. The vector containing all the parameters sought will be calculated from $(\Psi^T\vec{\mu} - \Psi^T\Psi\vec{a})^2$ = minimum. If one removes different subsets $\vec{\nu}^j$ consisting of stochastically chosen measurements from the set $\vec{\mu}$ of all air samples taken, and if one inserts them into $(\Psi^T\vec{\nu}^j - \Psi^T\Psi\vec{a})^2$ = minimum, one gets a statistical distribution for $\vec{a}$. Now, a constant set of parameters - the mean value $\vec{a}_m$ - can be attributed to the space-time domain covered by the $\vec{\mu}$, as a dispersion characteristic. The spread $\delta\vec{a}$ is suitable as a "measure of homogeneity" useful in discovering "homogeneous" sub-domains or, finally, to subdivide suitably the entire space-time region under study.

A corresponding method can also be applied when the K_i show the structure $K_i = C_i t^{\alpha_i}$. Sometimes authors /1/ use a three-zone structure for the (C_i, α_i)'s.

If, however, the spread $\delta\vec{a}$ cannot be diminuished to a desired level despite a refined sub-division of the region, the reason must be the structure of the transfer function used. One has to choose another one better suited to the circumstances. In such a case, a study of the dispersion mechanism is inevitable.

The Gaussian formula is a basic solution of the convective diffusion equation which has a weak point; it presumes an infinite diffusion velocity. From this, misleading interpretations of density measurements near to the boundaries of the tracer cloud might result. To avoid such difficulties, one could replace the parabolic equation by a telegraphers equation /2/. This substitution can be justified physically. We illustrate the consequences in the following discussion.

The equation

$$\frac{1}{c^2}\frac{\partial^2 G}{\partial t^2} + \frac{1}{a}\frac{\partial G}{\partial t} - \Delta G = 4\pi S\,\delta(\vec{r})\,\delta(t) \tag{3}$$

has for $\xi = \sqrt{1 - r^2/c^2t^2} < 1$ the solution

$$G = \frac{Sc}{2at\xi}\, I_1(c^2 t\xi/2a)\cdot \exp(-c^2 t/2a) \tag{4}$$

For an increasing argument: $I_1(\eta) \to \frac{e^\eta}{\sqrt{2\pi\eta}}$ holds and in consequence

(5) $$G \rightarrow G^{as} = \frac{S}{\sqrt{4\pi a}} (\xi t)^{-3/2} \exp\left[-(1-\xi)c^2 t/2a\right]$$

The Gaussian formula follows from (5) for $\xi \rightarrow 1$ and $(1-\xi) \rightarrow r^2/2c^2t^2$.

A graphical comparison of G and G^{as} illustrates the type of approximation best. (MONIN /2/ proposed: $c \sim 10$ cm/sec, $a \sim 10^3 - 10^4$ cm^2/sec).

Only after a certain "relaxation time" after passing of the concentration maximum at the sampling station is the diffusion solution able to give relevant information. This is a substantial handicap for the evaluation of tracer experiments.

Other difficulties arise from the boundary conditions. Since the tracer is neither ideally absorbed, nor completely reflected at solid and liquid interfaces, one has, even for $t \gg \tau$, to satisfy $\beta \frac{\partial G}{\partial n} + \gamma G = 0$ with β as reflexion-coefficient or γ- as absorption coefficient. This represents a fresh complication.

A practical way out is to dispense, at least partially, with the conventional meaning of the parameters $\vec{u}$ and K_i, and to interpret them as free parameters. One considers, for instance, $\vec{u}$ to be (in view of the tracer dispersion) an "effective" velocity and K_i to be an "effective" eddy diffusion coefficients, the numerical values of which have to be determined by tracer dispersion experiments only. In this way the surface effects can easily be taken into account.

Another phenomenon influencing the dispersion is the stochastic fluctuation of the wind vector around a mean velocity. It acts, for a finite sampling time, like an intensified eddy diffusion. The Gaussian formula has to be modified:

(6) $$G = \frac{Q}{t^{3/2}} \exp\left[-\frac{(\vec{r}-\vec{s})^2}{4Kt}\right] \; ; \qquad \vec{s} = \vec{u}_m t + \vec{w}\int_0^t R(\tau)d\tau$$

Mean value $\vec{u}_m$ and amplitude $\vec{w}$ can be taken, as "effective" parameters, from the tracer concentrations, whereas anemometer readings reveal the time function R.

To get an idea about the structure of the so-called "eddy diffusivity" K, one has to enter the theory of irreversible processes. The tracer transport is governed mainly by three phenomena: the convection by the airflow, the macroscopic diffusion of air parcels and the molecular diffusion. The theory of the Brownian motion offers a suitable mathematical tool to deal with the dominant stochastic processes. Our starting point may be the LIOUVILLE equation:

(7) $$\frac{\partial f}{\partial t} + \vec{v}\cdot\frac{\partial f}{\partial \vec{r}} + \vec{a}\cdot\frac{\partial f}{\partial \vec{v}} = 0$$

f denotes the distribution function of the more or less stable eddies, $\vec{v}$ the particle velocity and $\vec{a}$ their acceleration. In the particular case of liquid friction in a parallel airflow $\vec{u}$ = constant, the acceleration is given by $\vec{a} = -\xi(\vec{v}-\vec{u})$, where ξ is the "friction coefficient" and $\tau = 1/\xi$ the "relaxation time".

For a point-burst in an infinite medium the tracer concentration $G = \int f dv^3$ derived from equation (7) satisfies the convective diffusion equation /3/

(8) $$\frac{\partial G}{\partial t} + \vec{u}\cdot\nabla G = K_0\left(1-e^{-2t/\tau}\right)\Delta G$$

Only for $t \gg \tau$ the diffusivity $K \rightarrow K_0$ = constant (for $t \rightarrow 0$ it goes to $K \rightarrow 0$).

For the evaluation of air samples near to the sources and, more generally, of small-scale tracer experiments, a complex K-structure creates some difficulties. The simplest way to overcome them is to omit the relaxation time; but this sometimes weakens the tracer concentrations to an unacceptable extent.

Galerkin technique

If, however, despite including all these ingredients, the simple transfer function cannot be adapted, one has to abandon the Gaussian structure and try to construct a solution of type $G = \vec{a}(t) \cdot \vec{\varphi}(\vec{r})$ for a given class $\vec{\varphi}$ of space-dependent functions. The Galerkin technique applied to a parabolic operator L gives the differential equation $\frac{d\vec{a}}{dt} + A\vec{a} = \vec{b}$ governing the unknown coefficient vector $\vec{a}$. We obtain for the Roberts' operator

$$L = \frac{\partial}{\partial t} + u\frac{\partial}{\partial r} - K_1\frac{\partial^2}{\partial x^2} - K_2\frac{\partial^2}{\partial y^2} - K_3\frac{\partial^2}{\partial z^2}$$

and the class

$$\varphi_k(\vec{r}) \sim exp\{-[(x-ut_k)^2/K_1 + y^2/K_2 + z^2/K_3]/4t_k\}$$

the matrix

$$A = \{\varphi_{ik}\}^{-1}\{[(5t_k-\tau)/4t_k^2 + \gamma(1-\gamma)\,u^2/K_1]\varphi_{ik}\}$$

where

$$\varphi_{ik} = (\tau/2)^{3/2} exp(-\tau\gamma^2 u^2/K_1) \;;\; \gamma = \frac{t_i - t_k}{4\sqrt{t_i t_k}} \;;\; \tau = \frac{4t_i t_k}{t_i - t_k}$$

When we replace the parameter combination u^2/K_1 in A according to /4/, using the relation $K_1 \sim u^2 \cdot \Delta t$, the coefficient $\vec{a}(t)$ fortunately becomes parameter-independent.

We explicitly must point out here the fact, that both the operator L and the transfer function G contain the dispersion parameters sought as free coefficients, which have to be fixed by fitting G to the measured tracer concentrations. The fitting procedure is rather complicated due to non-linearities.

Separation

It is a wellknown fact, that the vertical component of the eddy diffusion is much more sensitive to fluctuations of micro-meteorology than the horizontal components. For this reason, it seems reasonable to use tracer concentrations registered along the ground only for determining the horizontal parameters, and special vertical measurements for the vertical parameters.

We start from the parabolic equation LG = 0 and restrict our study to coefficients of the type

$$(9)\quad u = \begin{pmatrix} u_1(xyt) \\ u_2(xyt) \\ u_3(zt) \end{pmatrix} \qquad \text{and} \qquad K = \begin{pmatrix} K_1(xyt) & 0 & 0 \\ 0 & K_2(xyt) & 0 \\ 0 & 0 & K_3(zt) \end{pmatrix}$$

The diffusion equation now can be separated. The two factors of the ansatz $G = \phi(xyt)\cdot\psi(zt)$ are solutions of the parabolic equations $L_1\phi = 0$ and $L_2\psi = 0$. The ratio $\frac{G(z\neq 0)}{G(z=0)}$ is independent of the (xy)-position. The question of how far such a solution is physically realistic has still to be discussed; the Gaussian formula, in any case, possesses this attribute.

The ground level concentration $G_o = \phi\cdot\psi_o$ satisfies the extended parabolic equation

(10) $$(L_1 + g)\,G_0 = 0 \qquad \text{with} \qquad g = \frac{1}{\Psi_0}\frac{d\Psi_0}{dt}$$

Again one has two different possibilities to determine the dispersion characteristics:

- the adaptation of an analytic solution of (10) to the measured concentrations, as explained above, with regard to the time dependence of g,

- the direct use of the tracer measurements to calculate the derivatives $C_{klm} = \frac{\partial^{k+l+m} G_0}{\partial x^k \partial y^l \partial t^m}$ approximately and to insert them into (10), which becomes, then, an algebraic equation

(11) $$\left[2C_{200}K_1 + 2C_{020}K_2 + C_{000}\,g - C_{100}w_1 - C_{010}w_2\right]^{ij} = \left[C_{001}\right]^{ij}$$

connecting the unknown K_1, g and $\vec{w} = \vec{u} - \nabla K$. Equation (11) holds for one air sample taken at (x_i, y_i, t_j), where i = 1,2,...I and j = 1,2,...J.

The corresponding algebraic system possesses a useful solution, if the density of the (i,j) grid allows the representation of the function-shape of the L_1-coefficients to a reasonable approximation by less than ((4I+1)J) measured tracer concentrations.

In such a case we get for the horizontal parameters a mean value $\vec{a}_m$, useful as a "horizontal" dispersion characteristic, and a spread $\delta\vec{a}$, suitable as a measure of the "horizontal homogeneity".

The vertical parameters have to be calculated separately, from vertical tracer measurements. There are again two different possibilities.

- The analytic way uses the formula

(12) $$\int_0^{t_j} \exp\left\{-\int_\tau^{t_j} g(\xi)\,d\xi\right\} F(z, t_j - \tau)\,d\tau = \left(G/G_0\right)^{ij}$$

coupling two measurements of different z but of the same (i,j)-position. F denotes the Green's function of the operator L_2 for a dipole source at $(z = 0, t = 0)$. Measurements at different space-time points lead again to mean value and spread.

- The algebraic way calculates the derivatives $b_{kl} = \frac{\partial^{k+l} G}{\partial z^k \partial t^l}$ directly from the tracer concentrations and finally solves the algebraic system corresponding to the operator L_2.

Conclusions

The ground-level immission of a tracer provides an empirical Green function from which the pollutant dispersion function can be derived. This dispersion function is suited for the calculation the dispersion of pollutant from continuous source distributions.

The sub-division of the space-time domain into "homogeneous" compartments together with the concept of "effective parameters", allows - in many practical cases - a simple characterization of the dispersion behaviour of an urban region by tracer experiments and a Gaussian formula.

The algebraic approach based upon the separation of the convective diffusion equation seems to be by far more universal and easier to handle than the other methods discussed; moreover, it is able to supply the required input for the numerical integration of the dispersion equations.

Literature

/1/ Turner, D.B. in "Proc. 3rd NATO/CCMS Panel on Air Pollution Modeling", Paris 1972

/2/ Monin, A.S. in "Advances in Geophysics", Vol. 6, ed. F.N. Frankiel, New York 1959

/3/ Green, H.S in "Pollution Engineering and Scientific Solutions", ed. E.S. Barrekette, New York 1973

/4/ Sheih, C.M. and Moroz, W.J. in "Proc. 3rd Int. Clean Air Congress", Dusseldorf 1973

6th NATO/CCMS

International Technical Meeting
on Air Pollution Modeling

SOME FEATURES OF TURBULENT DIFFUSION PROCESS RESULTING FROM EXPERIMENTAL FIELD TESTS

SAAB A., RIBON M., MERY P.

ELECTRICITE DE FRANCE

Direction des Etudes et Recherches

BATTELLE - INSTITUT E.V. - Frankfurt/Main
GERMANY F.R.

24 - 26 September 1975

ÉLECTRICITÉ DE FRANCE
DIRECTION DES ÉTUDES ET RECHERCHES

Service Générateurs et Échangeurs de chaleur
Thermiques et Nucléaires
Département Echanges Atmosphériques
et Pollutions

September 1975

DIVISION "METEOROLOGIE ET
POLLUTION ATMOSPHERIQUE"

6, quai Watier 78 400 CHATOU

Tél. 977-02-44 Poste 464

SAAB A., RIBON M., MERY P.

SOME FEATURES OF TURBULENT DIFFUSION PROCESS RESULTING FROM EXPERIMENTAL FIELD TESTS

Rapport E 42/75 N° 11

Résumé

Paper presented to the 6th NATO/CCMS International Technical Meeting on Air Pollution Modeling and its Application 24 - 26 September 1975 FRANKFURT.

INTRODUCTION

At the present time, our knowledge of evaluating atmospheric diffusion in the turbulent boundary layer is far from being complete. The need for a comprehensive understanding of Lagrangian characteristics necessitates continuing experimental studies in the field.

For this end a special field studies program on turbulent diffusion process is developed by Electricité de FRANCE, Direction des Etudes et Recherches. The research aims toward the description of Lagrangian caracteristics of turbulence resulting from tracer releases experiments and their correlation with parameters of Eulerian turbulence measured on a 100-meter meteorological tower.

Besides, the results of this investigation allowed us to point out certain informations about the applications and limitations of the statistical theory of turbulent diffusion. Although this theory is highly successful in describing the ideal situation of isotropic and homogeneous turbulence, its application to atmospheric boundary layer presents some problems.

The Experimental System and Procedure.

An investigation of the lateral diffusion of a light tracer-SF_6 or Freon-emanating from a source located on the meteorological tower was carried out by determining the concentrations distribution near the ground by means of a collectors system previously placed according to meteorological conditions.

Fourteen tracer releases experiments were conducted on the "JUMEAUVILLE" site on September 1974, in various types of meteorological conditions. During each experiment, tracers were released simultaneously from two different levels (40, 72 and 100 m), and 100 to 120 collectors were placed along four or five arcs centred on the presumed plume axis and distant of 300 to 10 000 m in terms of wind speed and direction, thermal stratification and height of emission. The concentrations were obtained for sampling time intervals of 1 hour and 1/4 hour.

A quantitative analysis of the collected tracers was made, using gaseous chromatography techniques. This process allows a very good sensitivity - 10 - 11 $\mu g/m^3$ and limits the rate of emission to 8 - 10 g/s.

The data concerning the conditions of the experiments are summarized in Table 1.

Thus a statistical model of dispersion was taken as a basis of the investigation. According to that model the distribution of concentrations was assumed Gaussian and the coefficient of lateral turbulent diffusion was deduced from measurement results of the averaged lateral variance. Yet some of these results indicated the non-validity of the assumption of a Gaussian distribution caused by the turning of the wind with height and by the non-stationary character of the air flow.

The use of the results of this investigation made it possible to check the variance calculated through the observation of the fluctuating wind vector using the HAY - PASQUILL method - equivalent Lagrangian averaging - [1]

The turbulence characteristics were measured by means of GILL UVW tridimensional anemometers, set at three levels - 18, 36 and 72 m -. In addition, tower instrumentation is designed to provide temperature, wind speed and direction and their fluctuations at eight levels selected on a logarithmic spacing - 3, 6, 12, 24, 48, 72, 96 and 100 m.

To obtain these meteorological data most efficiently, an automated collection and processing data is designed. A routine preprocessing of raw data allows the arithmetic operations required to reduce the volume of stored data. Thus, magnetic tape recording on a continuous base is done for computed means and statistical parameters.

In addition, the data-logger provide capability for selecting different averaging times [1 sec to 60 sec] and sampling durations [10 min to 60 min] and a special mode permits acquisition of UVW instantaneous values for the covariance calculations and correlation functions.

Practical adaptations of the statistical theory of turbulence.

Presently, the use of the Taylor treatment is still the most adequate and convenient to give simple working formulae for diffusion modeling. [2]

In the simplest case of a uniform and isotropic turbulent velocity field, TAYLOR proved the well-known expression for the rate of dispersion of particles in terms of the Lagrangian correlation coefficient - $R_L(\tau)$ -

$$\left[\begin{aligned} \sigma^2(t) &= 2\,\overline{v'^2}\int_0^t\int_0^\tau R_L(\xi)\,d\xi\,d\tau \\ &= 2\,\overline{v'^2}\int_0^t (t-\tau)\,R_L(\tau)\,d\tau \end{aligned}\right.$$

Thus a statistical model of dispersion was taken as a basis of the investigation. According to that model the distribution of concentrations was assumed Gaussian and the coefficient of lateral turbulent diffusion was deduced from measurement results of the averaged lateral variance. Yet some of these results indicated the non-validity of the assumption of a Gaussian distribution caused by the turning of the wind with height and by the non-stationary character of the air flow.

The use of the results of this investigation made it possible to check the variance calculated through the observation of the fluctuating wind vector using the HAY - PASQUILL method - equivalent Lagrangian averaging - [1]

The turbulence characteristics were measured by means of GILL UVW tridimensional anemometers, set at three levels - 18, 36 and 72 m -. In addition, tower instrumentation is designed to provide temperature, wind speed and direction and their fluctuations at eight levels selected on a logarithmic spacing - 3, 6, 12, 24, 48, 72, 96 and 100 m.

To obtain these meteorological data most efficiently, an automated collection and processing data is designed. A routine preprocessing of raw data allows the arithmetic operations required to reduce the volume of stored data. Thus, magnetic tape recording on a continuous base is done for computed means and statistical parameters.

In addition, the data-logger provide capability for selecting different averaging times [1 sec to 60 sec] and sampling durations [10 min to 60 min] and a special mode permits acquisition of UVW instantaneous values for the covariance calculations and correlation functions.

Practical adaptations of the statistical theory of turbulence.

Presently, the use of the Taylor treatment is still the most adequate and convenient to give simple working formulae for diffusion modeling. [2]

In the simplest case of a uniform and isotropic turbulent velocity field, TAYLOR proved the well-known expression for the rate of dispersion of particles in terms of the Lagrangian correlation coefficient - $R_L(\tau)$ -

$$\left[\begin{aligned} \sigma^2(t) &= 2\,\overline{v^2}\int_0^t\int_0^\tau R_L(\xi)\,d\xi\,d\tau \\ &= 2\,\overline{v^2}\int_0^t (t-\tau)\,R_L(\tau)\,d\tau \end{aligned}\right.$$

Assuming that the form of the distribution of diffusing particles is normal or Gaussian, by using this variance one can carry out the necessary calculations to estimate the mean field of concentration C (x, y, z, t). Despite the fact that isotropic homogeneous flow assumes :

$$\sigma_x^2 = \sigma_y^2 = \sigma_z^2$$

this expression can be extended to the case of anisotropic turbulence for which :

$$\sigma_x^2, \sigma_y^2 \text{ and } \sigma_z^2$$

are expressed via the tridimensional characteristics.

The use of this model presupposes the knowledge of the Lagrangian correlation function and its dependance on stratification and other meteorological parameters. Commonly, empirical methods are used to define the dispersion coefficients : The most widely used is based on PASQUILL'S equivalent Lagrangian method ; alternatives have been proposed by other investigators using power law approximations [3] :

$$\left[\begin{array}{lll} \sigma = a\ x^{b} & \left.\right] & \text{Power law} \\ \quad = ax\ (1 + bx)^{\alpha} & \left.\right] & \text{approximations} \\ \sigma^2 = \bar{v}^2_{t/\beta}\ t^2 & & \text{PASQUILL} \end{array}\right.$$

β ratio of the Lagrangian - Eulerian time scales.

In our approach, we intend to make use of the data obtained in tracer release experiments to carry out the expression of the Lagrangian correlation coefficient which yields to the best adjustment with the TAYLOR'S expression for variance and to point out the significance of the intensity and the time scale of turbulence as two basic flow parameters.

Assuming, in a first step, an exponential decay function for the Lagrangian correlation coefficient $R(\tau) = e^{-\tau/t_L}$ - $t_L = \int_0^{\infty} R(\tau)\, d\tau$ is the Lagrangian time scale -, the variance of the dispersion is then well represented by the relation :

$$\left[\ \sigma^2 = 2\ \bar{v}^2\ t_L^2 \left[\frac{t}{t_L} - (1 - e^{-t/t_L})\right]\right.$$

Thus, the knowledge of the intensity and time scale of turbulence appears sufficient to describe the magnitude of the particle spread. The influence of stratification and dynamic structure is not yet well defined and needs more investigations. But we think that this approach is worth being developed when meteorological tower data are available.

Refering to our field tests, we deduced the couple of values - lateral intensity and time scale - which yield to the best adjustment with experimental results for three types of weather data [see fig. 1] :

- neutral near stable $v = 0,58$ m/s $t_L = 550$ s
- neutral strong winds $v = 0,81$ m/s $t_L = 350$ s
- neutral lightly instable $v = 0,95$ m/s $t_L = 300$ s

The results of the comparison of σ values determined by this method and those resulting from PASQUILL'S method are shown in Fig. 2.

The Eulerian approach needs a correction to take into account the variation of lateral intensity of turbulence with height - v must be determined at the height of emission -, and a Eulerian Lagrangian time scale ratio substantially larger [equal to 10 - 12 instead of 4 for neutral stability]. This high value of β might be attributed to the meandering effect in the atmosphere which is added to the spreading effect in our diffusion data. Finally, we hope that further tests will allow us to improve, on one hand, the forme of the correlation coefficient using polynomial functions and the corresponding dispersion parameter and, on the other hand, the influence of stratification and dynamic structure on the intensity and the time scale of turbulence.

Validity of the Gaussian distribution hypothesis.

Despite the fact that Taylor's approach was derived for an ideal situation of isotropic and homogeneous turbulence, it seemed to us appropriate and useful to describe the major part of our experiments covering some situations of inhomogeneous and anisotropic turbulence, but respecting stationnarity.

However some serious difficulties appeared [illegible] vertical wind shear or a turning of wind with height occurred [

In the case of a strong vertical wind shear, we noticed a disparity in the evolution of lateral dispersion with time. This yields to assume that two approximation laws are suitable, the first for short dispersion time and the second for long dispersion time. The Gaussian distribution is not valid at intermediate distances [Fig. 3].

The non-validity of the Gaussian distribution is found also when the wind rotation with height exceeds 8 - 10° between the top and the bottom of the meteorological tower. The concentration profile is then characterized by two peaks. In the proximity of emission, the highest peak was centered on the wind direction near the ground ; further away this peak decreased whereas the peak centered on the wind direction in altitude was prevailing [Fig. 4].

Unfortunately, we have not yet adequate supply of experiments to give theoretical arguments to estimate the dispersion in these complicated structures, but we expect some progress from further experiments.

Relations between sampling time and concentrations.

As we indicated previously, the concentrations were collected in the axis of the plume for sampling durations of 1 hour and 15 minutes. This allowed us firstly to test the stationarity of the flow during all the period of emission and secondly to deduce the corresponding ratio between the maximum concentrations averaged over 1hour and 15 minutes.

The effect of sampling time on concentrations could be obtained as we indicated in a prevous work [5] by operating on the horizontal and vertical wind fluctuations. We shall compare here the results measured and those computed from fluctuations of wind vector averaged over 10 minutes and 1 hour.

	$\frac{(C_{max})\ 15\ min.}{(C_{max})\ 1\ hour}$ measured	$\frac{(C_{max})\ 10\ min.}{(C_{max})\ 1\ hour}$ computed
- neutral, near stable	0.61	0.66
- neutral, strong wind	0.78	0.84
- neutral, lightly instable	0.52	0.55

The agreement is excellent, but it is important to note that fluctuations are computed at the height of emission, and this is not always possible.

The effect of source height.

As a practical result of experimental field tests, the effect of source height on maximum concentration location was analyzed : The range of the distance from the source to the point of maximum concentration can be expressed as 15 to 30 times the height of emission for neutral stability. However the main remark is that the upper limit of this range (25-30) is obtained for strong winds. We think that it is caused by the strong decrease of lateral intensity with height.

The Gaussian plume formula may be corrected in order to take into account the vertical variability of the term ($U\ \sigma_y\ \sigma_z$).

CONCLUSION.

The results obtained in the present study are based on a limited range of experimental field tests ; some conclusions can be drawn but further investigations are necessary.

That is why, a complementary field study was developed lately, on June 1975. All the results are not yet analyzed, but we are expecting some progress.

In addition, special tests on very short duration releases were realized. The difficulty of measuring the dispersion from instantaneous source - blowing up a balloon-lead us to use this emission.

Let us note, finally, that considering E D F intends to equip all subsequent power plant sites with 80 m meteorological tower, our ideal is to develop diffusion modeling which allows the maximum use of thermal and dynamic structure data continously measured on tower.

REFERENCES

[1]	HAY - PASQUILL	1959	Diffusion from a continuous source in relation to the spectrunn and scale of turbulences. Adv. in Geophysics, 6, Academic Press, 35.
[2]	FORTIER	1968	Considérations théoriques sur l'emploi de la diffusivité turbulente. Société Hydrotechnique de France. Journées "diffusion turbulente dans les fluides" 21-22 nov.
[3]	SLADE	1968	Meteorology and Atomic Energy. USAEC.
[4]	PASQUILL	1969	The influence of the turning of wind with height on crosswind diffusion. Phil. Trans. ROY. Soc. London A. 265, 173.
[5]	GRANIER, MERY, SAAB.	1974	A quantitative approach of climatological site study 5th Meeting NATO/CCMS - ROSKILDE - DENMARK June 4-6.

TABLE 1 : TRACER RELEASE EXPERIMENTS.

Operation Day - Hour	Nature of emission Height of emission	Wind data (72 m) Direction - Speed	Stability
1 17 - 9 15h	Continuous 72 - 100	Stationary 180° - 3.6 m/s	neutral
2 18 - 9 15h	Continuous 72 - 100	Direction shear 30 – 7 m/s	neutral
3 18 - 9 17h	Continuous 72 - 100	Vertical wind shear 32.5 7.8 m/s	neutral
4 19 - 9 15h	Continuous 72 - 100	Stationary 355 5.6 m/s	lightly instable
5 20 - 9 7h	Instantaneous 72 Continuous 100	Turning with height 305 4.8 m/s	stable
6 20 - 9 14h	Continuous 72 - 100	Direction shear 315-325 4 m/s	lightly instable
7 21 - 9 10h	Continuous ground	Stationary 230 5 m/s	neutral
8 23 - 9 15h	Stopped	Strong direction shear	
9 24 - 9 14h	Continuous 72 - 100	Stationary 295 10.3 m/s	neutral
10 25 - 9 11h	Continuous 40 - 72	Direction shear 245-265 10.1 m/s	neutral
11 25 - 9 17h	Continuous 40 - 72	Stationary 270 12 m/s	neutral
12 26 - 9 12h	Instantaneous 72 Continuous 100	Direction shear 285-295 8.5m/s	neutral
13 26 - 9 18h	Continuous 72 - 100	Vertical wind shear 230 7.5 m/s	lightly stable
14 27 - 9 10h	Continuous 40 - 72	Stationary 205 12 m/s	neutral

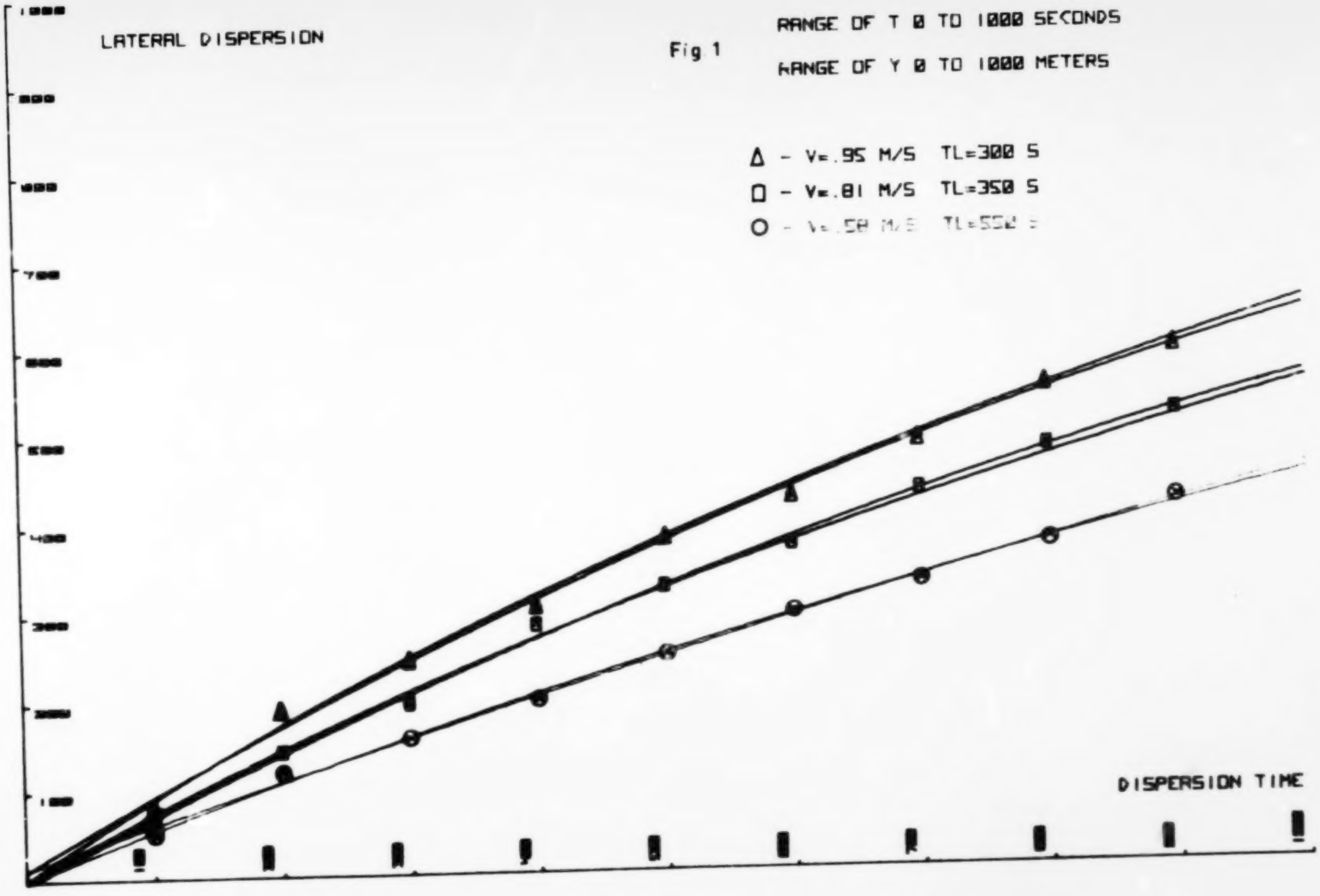
LATERAL DISPERSION
RANGE OF T 0 TO 1000 SECONDS
RANGE OF Y 0 TO 1000 METERS
Δ - V=.95 M/S TL=300 S
□ - V=.81 M/S TL=350 S
○ - V=.58 M/S TL=550 S
DISPERSION TIME
1000
900
800
700
600
500
400
300
200
100

Fig 1

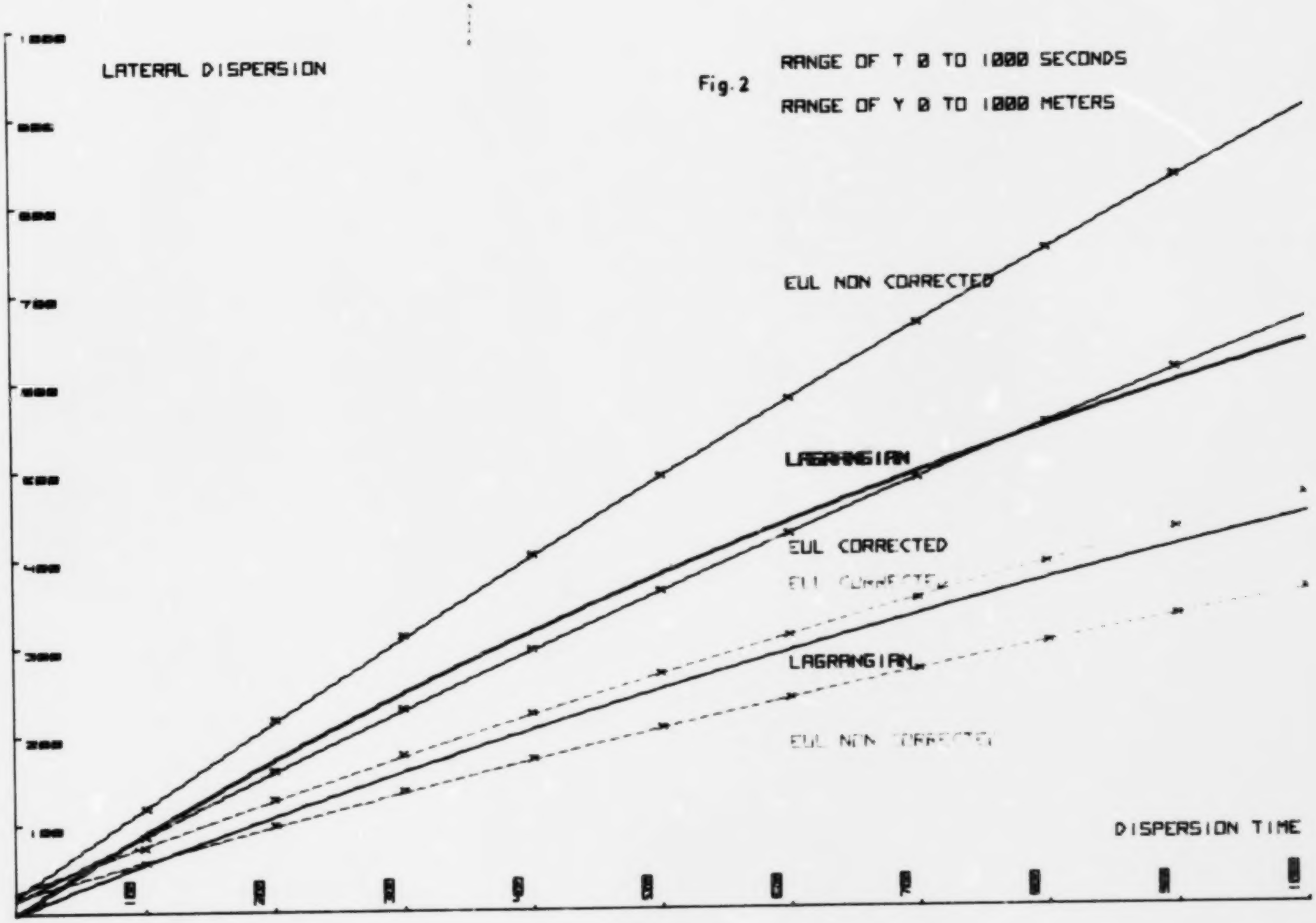
LATERAL DISPERSION
RANGE OF T 0 TO 1000 SECONDS
RANGE OF Y 0 TO 1000 METERS
EUL NON CORRECTED
LAGRANGIAN
EUL CORRECTED
EUL CORRECTED
LAGRANGIAN
EUL NON CORRECTED
DISPERSION TIME
1000
700
500
400
300
200
100

Fig. 2

Fig.3 VERTICAL WIND SHEAR.

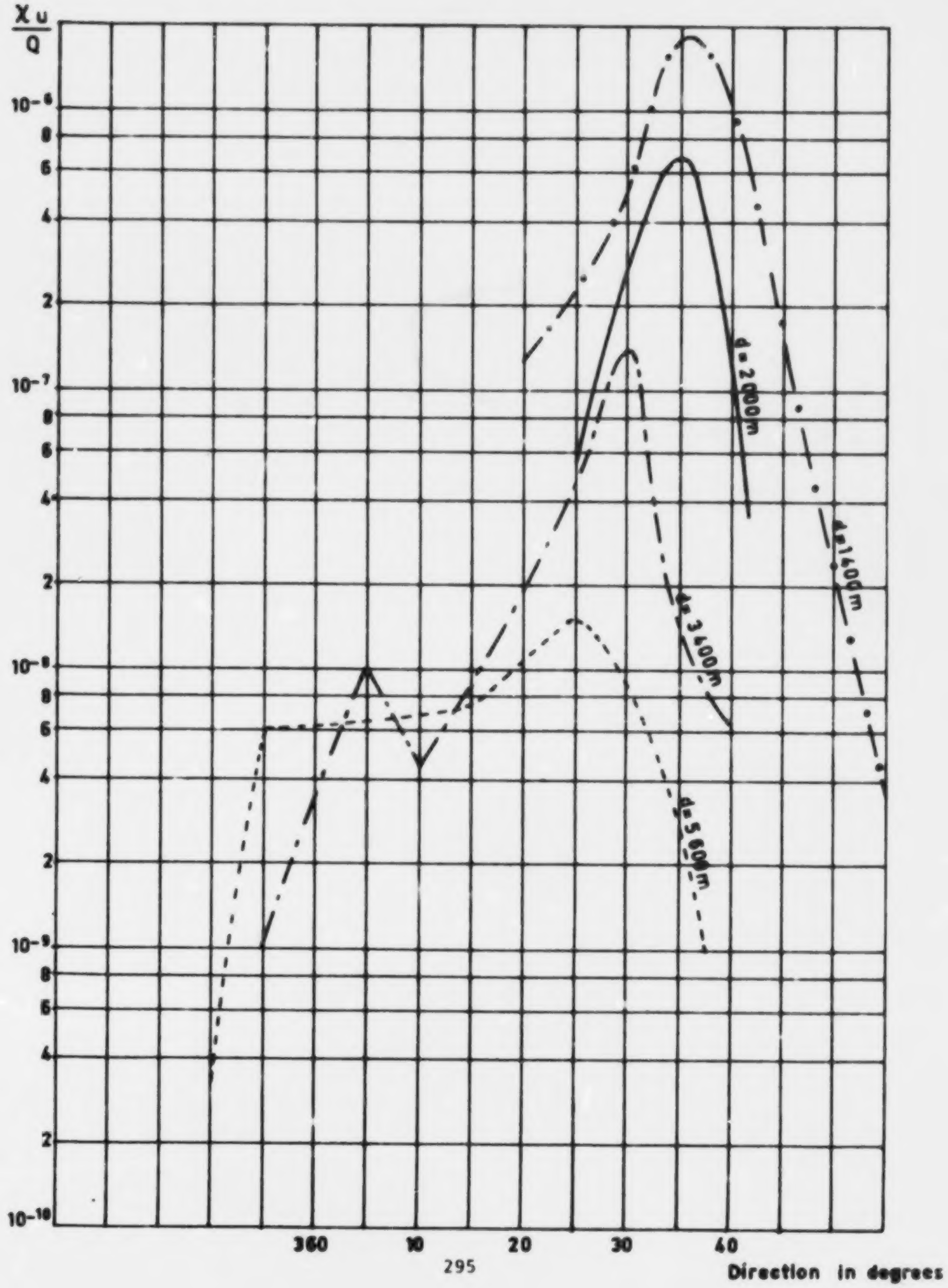

Fig.4 TURNING OF WIND DIRECTION WITH HEIGHT

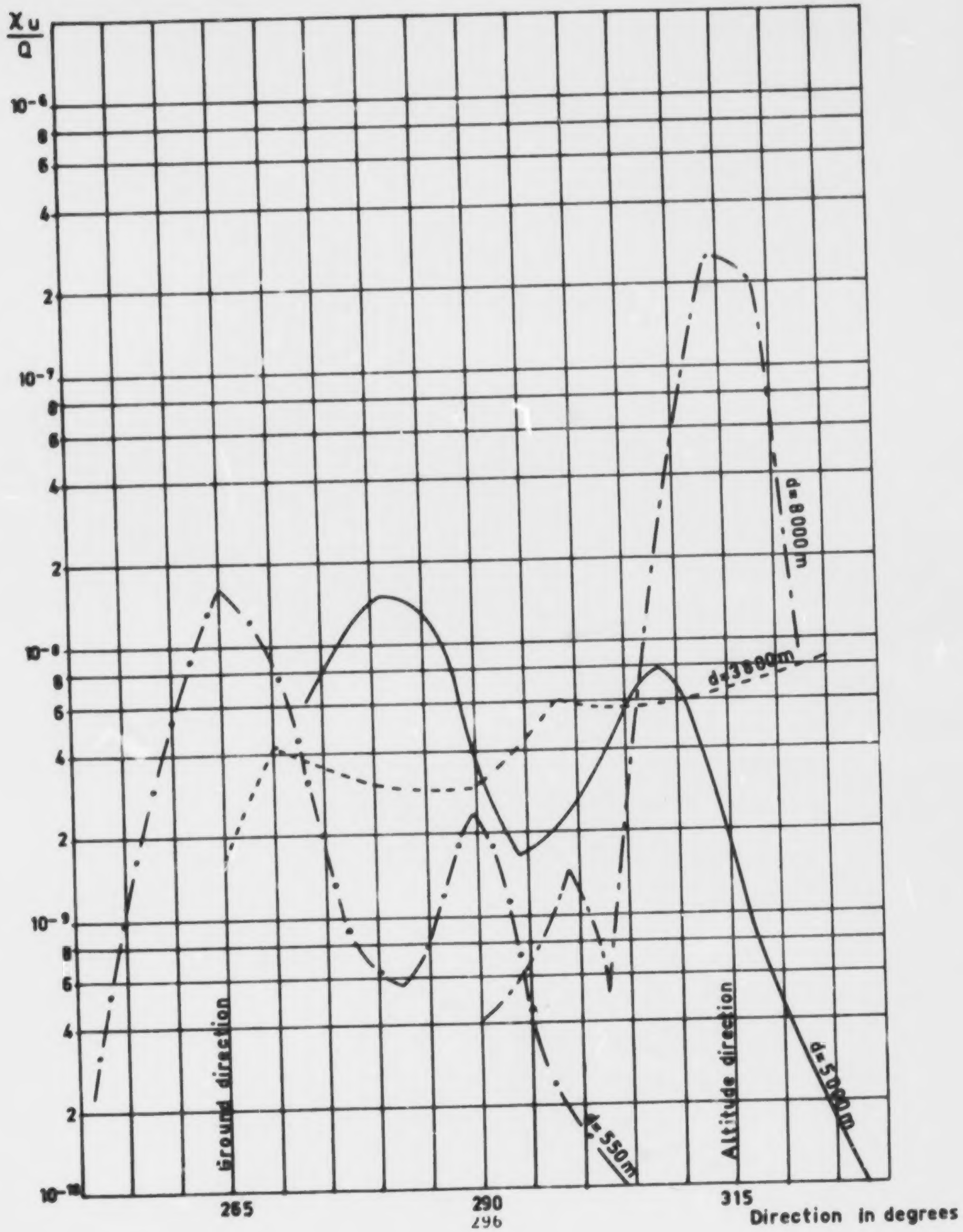

6th NATO/CCMS
International Technical Meeting
on Air Pollution Modeling

Determination of Actual Vertical Windspeed Profiles in the Friction Layer Based on Beforeknown Mean Profiles

by
L.M. MALET
Royal Meteorological Institute
of Belgium

BATTELLE - INSTITUT E.V., Frankfurt/Main
Germany, FR
24-26 September, 1975

1. INTRODUCTION

Vertical windspeed profiles are very often determined by the well known power law :

$$u_2 = u_1 \left(\frac{z_2}{z_1}\right)^m$$

where u_1 = the windspeed observed at the height z_1 above the ground,

u_2 = the windspeed calculated at the height z_2

m = an exponent to be fixed experimentally.

If one goes through the abundant litterature related to the determination of this exponent, it soon appears that the mean values of m obtained by the different authors vary considerably from one another and, furthermore, that the standard deviations of the actual m values around their means often compare with these means themselves.

This is mainly due to the fact that m depends on a number of factors differing from site to site :

- the height z_1 at which the lower windspeed u_1 is measured,
- the height z_2 at which the higher windspeed u_2 is calculated,
- the windspeed u_1 at z_1 level,
- the thermal statification of the atmosphere and
- the roughness of the underlying surface.

Mean values of m are generally proposed as functions of the mean vertical potential temperature gradient. This gradient is considered as remaining constant though the whole layer at the limits of which it is measured ; experience shows that it is very seldom the case and this causes the great variability of m values around their means.

This rapid discussion of the power law comes to the conclusion that its use may lead to considerable errors on wind aloft parameters introduced in air pollution models, especially the short term ones.

As other known means of determination of vertical windspeed profiles, either theoretical or empirical, have not shown much success, a new one is here proposed which is based on the beforeknown mean profiles.

It should however be well understood that this new empirical method is only a tentative and that, if it proves promising, it should be submitted to a sufficient number of field tests.

2. PRINCIPLE OF THE METHOD

As said before, the method is based on the knowledge of mean windspeed profiles determined in an atmospheric layer, the thickness of which is H(m) counted from the ground, in function of fixed classes of values of the potential temperature gradient characterizing the thermal stability of the layer.

For instance, P_j will be the mean profile corresponding to the class j of potential temperature gradient defined by $x \leq \partial\theta/\partial z \leq y$ where x and y are given in °C/100 m.

To compute such mean profiles, it is of course necessary to have at hand a great number (1.000 or more) of simultaneous observations of the wind speed (ten minutes means) made at least at three levels within the layer concerned in the thermal conditions requested.

When the zero plane displacement d characterizing the roughness of the site underlying surface is known, one gets a supplementary point to determine the mean windspeed profile as $\bar{u}_0 = 0$ at height $z = -d$.

So, for each class j of thermal stability one disposes of a series of mean windspeed values : $\bar{u}_0 = 0$ at height $z = -d$, $\bar{u}_1$ at height z_1 $\bar{u}_2$ at height z_2, $\bar{u}_3$ at height z_3 and so on, and it is then possible to describe the profile P_j either graphically or by an expression $\bar{u} = f(z)$.

These mean profiles P_j are obviously the mean of a great number of actual profiles (ten minutes mean for instance).

To determine an actual windspeed profile p_j (in the thermal condition j) knowing the windspeed u_i at one single level z_i and the mean windspeed profile P_j, a fundamental hypothesis is made : the windspeed at any level z of the actual profile p_j is proportional to the windspeed at the same level on the mean profile P_j and the proportionality coefficient k is constant all along the height range within which the thermal condition j is respected. This hypothesis is true when the atmospheric layer is in state of adiabatic equilibrium ($\partial\theta/\partial z \simeq 0$); it has been assumed true for all cases of diabaticity ($\partial\theta/\partial z \neq 0$).

On this assumption, the method to be applied is then simple u_i being the windspeed measured at level z_i (the only one available) on the actual profile p_j and V_i being the windspeed at the same level z_i on the mean profile P_j, the proportionality coefficient k comes from :

$$k = \frac{u_i}{V_i}$$

The windspeed at any level z lower or higher than z_i on the actual profile p_j is then given by

$$u(z) = kV(z)$$

where V(z) is the value of the windspeed at level z on the mean profile P_j.

This latter relation is valid in the height range around z_i where the thermal condition j is fulfilled.

3. APPLICATION OF THE METHOD ON THE SITE OF MOL (BELGIUM)

3.1. The site of MOL belongs to the Belgian Nuclear Research Centre. A meteorological mast, 120 m high, is erected right in the middle of the site which is a flat sandy field planted with pine trees about 14 m high.

Any building on the site is at a distance from the mast greater than eight times its height; the higher, 40 m, stands at 450 m in the South-East direction.

Among other instruments, the meteorological mast is equipped with anemometers at 24, 49, 78 and 114 m and with thermocouples at 8 and 114 m.

At the end of every hour, ten minutes means of the windspeed and of the temperature at these different heights are recorded on a magnetic support.

Using at least 3.000 wind profiles measured in adiabatic conditions, the roughness parameter characterizing the site has been computed; one has found :

$$d = -2,41 \text{ m}$$

The data which have been used to get the mean windspeed profiles in the various thermal conditions j are those collected hourly from January 1966 to December 1973.

They consist of ten minutes mean windspeeds at the 24, 49, 78 and 114 m heights and of ten minutes mean potential temperature gradients calculated between 8 and 114 m by the relation :

$$(\partial\theta/\partial z)_{8.114} \simeq \frac{\overline{T}_{114} - \overline{T}_{8}}{114 - 8} . 100 + 0.98 \ (°C/100 \text{ m})$$

3.2. From the whole set of data, the values of the mean windspeed at different heights corresponding to fixed classes j of potential temperature gradient, have been computed; they are given in table 1.

In a system of rectangular coordinates, with $\ln(z+d+e)$ as abcissa and $\overline{u}$ as ordinate, an adjusting curve of the points corresponding to each class j has been computed. The constant e has been added to z+d under the log sign in order to get $\ln(z+d+e) = 1$ when $z = -d = 2.41$ m; z is of course the geometrical height above the ground surface.

TABLE 1.-

Class j	limits of class $\partial\theta/\partial z$ (°C/100 m)	$\overline{u}$.(m.s^{-1})				
		Level				
		z=d=2.41m	24 m	49 m	78 m	114 m
1	≤-0.9	0	4.05	4.91	5.45	5.68
2	-0.7 to-0.5	0	3.95	4.92	5.49	5.79
3	-0.4 -0.2	0	3.85	4.84	5.50	5.91
4	-0.05 0.05	0	3.82	4.96	5.78	6.39
5	0.2 0.4	0	3.86	5.15	6.17	6.99
6	0.5 0.7	0	3.81	5.31	6.56	7.69
7	0.9 1.1	0	3.46	5.03	6.43	7.74
8	1.3 1.5	0	2.98	4.51	5.85	7.16
9	1.7 1.9	0	2.77	4.32	5.67	6.97
10	2.1 2.3	0	2.61	4.15	5.54	6.81
11	2.5 2.7	0	2.60	4.23	5.60	6.76
12	2.9 3.1	0	2.55	4.20	5.57	6.70
13	3.35 3.65	0	2.53	4.19	5.31	6.49
14	3.8 4.2	0	2.43	4.05	5.39	6.22
15	4.7 5.3	0	2.31	3.86	5.03	5.57
16	≥6.0	0	2.22	3.84	4.81	5.17

Using the adjusting curves equations,the mean values of windspeed in the range of geometrical heights going from 10 to 210 m have been calculated and the results divided in each case by $\overline{u}_{10}$ to get the reduced mean windspeeds

$$\overline{u}_r = \frac{u}{u_{10}}$$

That is these reduced mean windspeeds which have been used to replace the mean profiles P_j by the more praticable adjusted reduced mean profiles $P_{r,j}$.

Figure 1 represents the sixteen $P_{r,j}$ found on the MOL site. Each curve is a fraction of second order parabola except when $j=4$ $(-0.05 \leq \partial\theta/\partial z \leq 0.05°C/100\ m)$ for which it is a fraction of a straight line. All the lines should go through the point of coordinates $(\ln(10-2.41+e),\ \bar{u}=1)$ and start at $(\ln e=1,\ \bar{u}=0)$ which is actually not strictly the case due to the adjustment.

Table 2 gives the values of $\bar{u}_r$ from 10 to 210 m high every 20 m for each class j and Table 3 gives the values of the coefficients of the increasing powers of ln(z+d+e) in the equations :

$\bar{u}_{r,j} = a_0 + a_1 \ln(z+d+e) + a_2 \ln^2(z+d+e)$ representing the adjusted reduced mean profiles $P_{r,j}$

TABLE 2.- REDUCED MEAN WINDSPEED $\bar{u}_r$ $(m.s^{-1})$

Class j	Height above the ground surface (m)										
	10	30	50	70	90	110	130	150	170	190	210
1	1.00	1.61	1.83	1.96	2.04	2.10	2.15	2.18	2.21	2.23	2.25
2	1.00	1.65	1.90	2.05	2.15	2.22	2.28	2.33	2.37	2.40	2.43
3	1.00	1.69	1.98	2.16	2.29	2.39	2.46	2.53	2.58	2.63	2.68
4	1.00	1.80	2.18	2.43	2.62	2.76	2.89	2.99	3.09	3.17	3.24
5	1.00	1.90	2.35	2.66	2.90	3.09	3.25	3.39	3.51	3.62	3.72
6	1.00	2.09	2.68	3.11	3.44	3.72	3.95	4.16	4.35	4.51	4.67
7	1.00	2.32	3.11	3.68	4.14	4.52	4.85	5.15	5.41	5.65	5.87
8	1.00	2.52	3.46	4.16	4.72	5.20	5.61	5.98	6.31	6.60	6.88
9	1.00	2.67	3.73	4.52	5.16	5.71	6.18	6.60	6.98	7.32	7.64
10	1.00	2.82	3.99	4.87	5.59	6.20	6.73	7.20	7.63	8.02	8.38
11	1.00	2.76	3.88	4.72	5.40	5.98	6.49	6.94	7.34	7.71	8.05
12	1.00	2.79	3.93	4.79	5.49	6.08	6.60	7.05	7.47	7.85	8.19
13	1.00	2.66	3.71	4.49	5.13	5.66	6.13	6.54	6.91	7.25	7.57
14	1.00	2.65	3.69	4.46	5.08	5.61	6.07	6.48	6.85	7.18	7.49
15	1.00	2.42	3.27	3.90	4.41	4.83	5.20	5.52	5.81	6.08	6.32
16	1.00	2.27	3.00	3.54	3.96	4.31	4.62	4.89	5.13	5.35	5.55

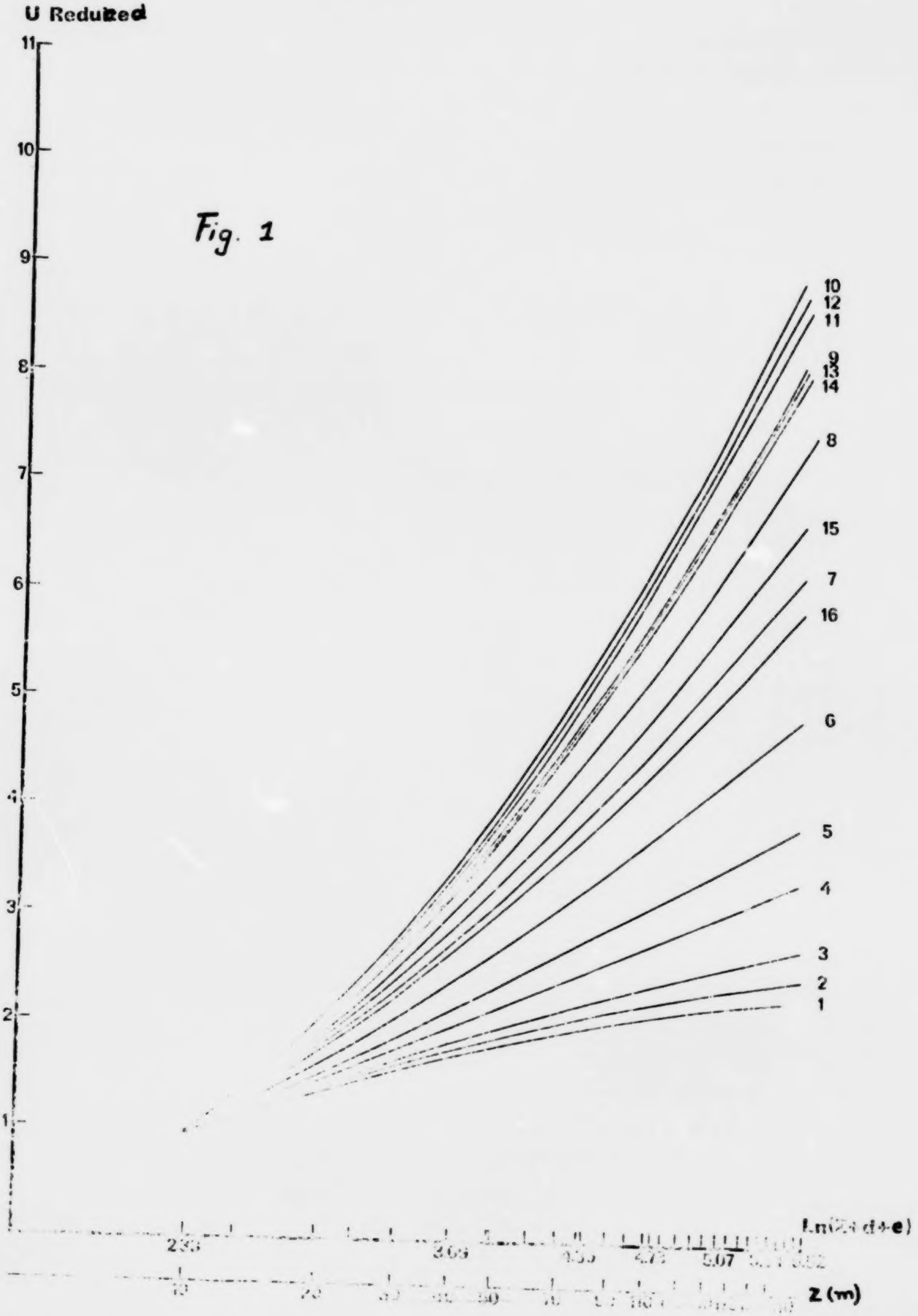

Fig. 1

U Reduced
11
10
9
8
7
6
5
4
3
2
1
10
12
11
9
13
14
8
15
7
16
6
5
4
3
2
1
Ln(Z+d+e)
2.33
3.69
4.73
5.07
Z (m)
10
20
50
100

TABLE 3.- COEFFICIENTS OF THE INCREASING POWERS OF $\ln(z-2.41+e)$

Class	a_o	a_1	a_2
1	-928.10^{-3}	101.10^{-2}	-771.10^{-4}
2	-897.10^{-3}	961.10^{-3}	-633.10^{-4}
3	-853.10^{-3}	899.10^{-3}	-447.10^{-4}
4	-740.10^{-3}	740.10^{-3}	-
5	-665.10^{-3}	631.10^{-3}	354.10^{-4}
6	-496.10^{-3}	391.10^{-3}	107.10^{-3}
7	-281.10^{-3}	836.10^{-4}	199.10^{-3}
8	-102.10^{-3}	-172.10^{-3}	276.10^{-3}
9	291.10^{-4}	-363.10^{-3}	334.10^{-3}
10	158.10^{-3}	-549.10^{-3}	390.10^{-3}
11	885.10^{-4}	-459.10^{-3}	364.10^{-3}
12	111.10^{-3}	-494.10^{-3}	375.10^{-3}
13	-818.10^{-5}	-330.10^{-3}	326.10^{-3}
14	-277.10^{-4}	-307.10^{-3}	320.10^{-3}
15	-246.10^{-3}	-288.10^{-5}	230.10^{-3}
16	-395.10^{-3}	200.10^{-3}	170.10^{-3}

3.3. The reduced mean profiles mentionned hereabove have been used to compute the actual profiles observed on the MOL site during the course of 1974. Using the windspeed at 24 m, the windspeeds at 49, 78 and 114 m have been calculated and compared to the observed values. The difference between the mean of all calculated data and the mean of all observed data for each class j has been evaluated together with the standard deviation of the individual differences.

The same comparison has been made using data computed by the power law with exponents m determined in a previous study.

Table 4 summarizes the results of these comparisons.

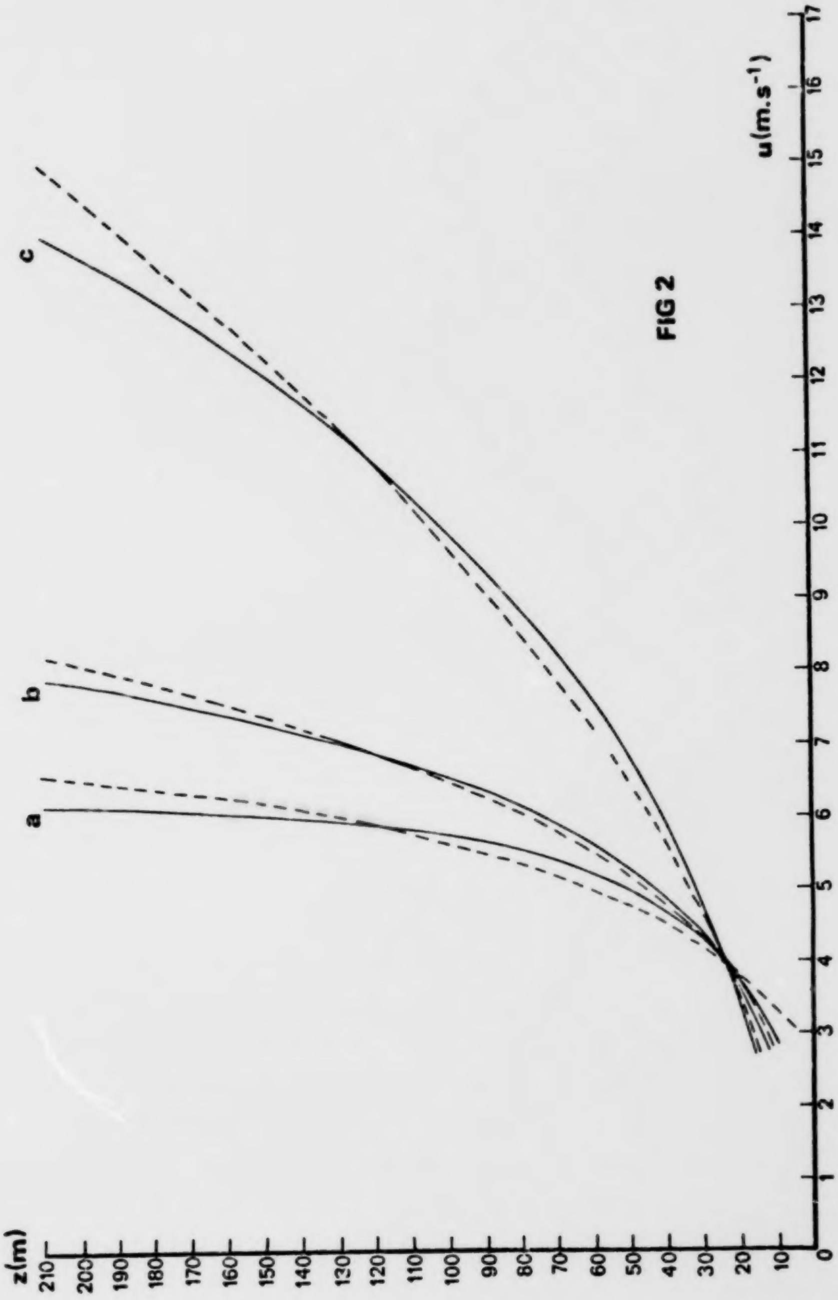
z(m)
210
200
190
180
170
160
150
140
130
120
110
100
90
80
70
60
50
40
30
20
10
0
1
2
3
4
5
6
7
8
9
10
11
12
13
14
15
16
17
u(m.s^{-1})
a
b
c

FIG 2

TABLE 4.-

LEVEL	Mean profiles		Power law	
	$\overline{u}_{cal} - \overline{u}_{obs}$ $(m.s^{-1})$	σ_Δ $m.s^{-1}$	$\overline{u}_{cal} - \overline{u}_{obs}$ $(m.s^{-1})$	σ_Δ $m.s^{-1}$
49	-0.02 to 0.02	0.5	-0.1 to -0.6	0.5
78	-0.05 to 0.1	0.7	-0.2 to -0.5	0.7
114	-0.03 to 0.03	1.0	-0.03 to 0.03	1.0

Table 4 clearly shows that the mean profile method gives real profiles which is not the case for the power law which leads to systematic errors when it is applied for heights smaller or greater than the one used to fix the m exponent.

Fig. 2 illustrates this point. It shows profiles computed for

a) $-0.7 \leq \partial\theta/\partial z \leq -0.5°C/100\ m$
b) $-0.05 \leq \partial\theta/\partial z \leq 0.05°C/100\ m$
c) $2.9 \leq \partial\theta/\partial z \leq 3.1\ °C/100\ m$

with $u_{24m} = 4\ m.s^{-1}$,

using the mean profile method (plain line) and the power law (dashed line) with m exponents fixed between 24 and 114 m.

As regards the variability of the calculated data, both methods lead to similar results. This is due to the fact that in both cases the potential temperature gradients have been measured between 8 and 114 m and assumed constant in this range, which is rarely the case in actual thermal profiles.

It must be pointed out that if the thermal stratification of a given atmospheric layer is known, the mean profile method can be applied strate by strate. This is not the case for the power law because the value of the exponent to be used varies greatly namely with the limits of the layer for which it has been estimated.

4. APPLICATION OF THE MEAN PROFILE METHOD ON OTHER SITES

The reduced mean profiles $P_{r,j}$ depend on anything else but the roughness parameter characterizing the site. For very rough surfaces as on the MOL site, the profiles proposed in the present work coulu be used as such with a good approximation. However it would be far better to find a means of taking roughness differences into account.

If it could be accepted to say that changes in roughness parameter do not affect appreciably the form of the reduced mean profiles, as it is the case for an adiabatic atmosphere,then a simple transformation of coordinates (translation and rotation) might be sufficient to get the result aimed at.

This will make the subject of a further study.

I.R.M.-UCCLE-SEPTEMBER 1975

Rapporteur's Report, Topic II, September 25, 1975
by C. A. Velds

Chairman: K. L. Calder

K. L. Calder, chairman of the sessions for Topic II, in opening the session, draws the attention of the participants on the 7th International Technical Meeting on Air Pollution Modeling, which will be held in the United States, September 7 - 10, 1976. It is the policy of the organization to put into the agenda as many different topics concerning air pollution modeling as possible. To be sure that no points of interest will be overlooked, the participants are asked to send a list of topics for the next year's agenda to D. Jost before the end of this meeting.

K. H. Müller: Dispersion Characteristics via Tracer Techniques

Discussion:

After the presentation the chairman remarks that he was very interested in this paper because the same sort of work is being done in the United States. It seems possible to extract from the data on emissions and air quality a general description of meteorological dispersion. In Müller's paper this dispersion is given as a Green's function. During the last meeting in Risø it came out already that it is feasible to derive empirically the meteorological dispersion which is the basis for source-oriented models. H. Fortak gives his formal comments on the paper as follows: First of all I appreciated very much that you apply fundamental knowledge of statistical physics, i. e. Liouville's equation and others. Secondly I agree with you that for tracer-experiments the solutions of the telegraphic equations seem to be the only useful ones instead of solutions of the parabolic equations which are essentially Gaussian. Many cross-section flights through cooling tower plumes which I performed with light-weight aircraft showed sharp discontinuities of vapour pressure and temperature at the lateral boundaries of the plumes even in far down-wind distances. This indicates, that only solutions of the telegraphic equation are able to explain the actual behaviour of such and similar plumes.

The use of Green's functions by you gives me the opportunity to present shortly the basis of a new time-dependent multiple source urban dispersion model. Assuming arbitrarily distributed, time-dependent sources at the ground, in space and in the height of an inversion layer for a given meteorological time step, in which all meteorological parameters are kept constant in time (and space) an analytical solution is obtained for this time step. The solution is used as an initial condition for the integration during the next meteorological time step in which all meteorological parameters can be charged. The model gives a steady transition for windless conditions and vice versa. Programming of the model for application in the Frankfurt area is not quite completed. I do hope to be able to present the first results during the next CCMS meeting in Washington 1976.

M. Kwizak asks whether the wind data can be forecasted with the model, especially in inhomogeneous terrain.

K. H. Müller: Wind speed and wind direction are no input data but they follow from the measured trajectories.

M. Ribon: Some Features of turbulent Diffusion Process resulting from experimental Field Tests.

Discussion:

W. B. Johnson: How long were the release periods for the sulfur-hexafluoride emissions?

M. Ribon: Between 30 minutes and 2 hours.

L. M. Malet: Determination of actual vertical Wind Speed Profiles in the Friction Layer based on beforeknown mean Profiles.

Discussion:

K. L. Calder asks if the speaker has tried to interprete the measured profiles using the Morin-Obukhov lenght.

L. M. Malet: no.

6 th NATO/CCMS
International Technical Meeting
on Air Pollution Modeling

MODELS OF TEMPERATURE PROFILES UNDER CONVECTIVE AND INVERSION CONDITION, CONNECTED TO AIR POLLUTION.

P. Bacci [+], A. Longhetto [++], D. Anfossi [+++]

[+] Laboratorio Ricerca Ambientale - ENEL - Trino Vc., Italy
[++] Laboratorio Ricerca Ambientale - ENEL - Trino Vc., Italy
and Istituto Fisica Generale dell'Università, Torino, Italy
[+++] Laboratorio di Cosmo-geofisica del CNR, Torino, Italy

BATTELLE - INSTITUT E.V., Frankfurt/Main
Germany, FR
24 - 26 September, 1975

INTRODUCTION.

In the past few years, an increasing area of interest has been directed towards more or less generalized and complex air pollution models, describing space and time distribution of airborne pollutants.

All of these models, from the simplest and straighforwards ones (box-type diffusion models, or urban Gifford-Hanna model (1970))to the most complex ones, like that developed by Shir and Shie (1974), share the common need to have, as input data, reliable meteorological information, in addition to source emission inventory. As motion of air is very complex and data acquisition inadequate, this information for the imput is not available generally; thus one has recourse to various approaches, of statistical or phenomenological type, or to arbitrary assumptions, and the most proper application of these models is towards long-term air prediction or management planning.

However, if a pollution model is to be used as short-term predictive tool of relationships between levels of pollution concentration and emissions for the various sources, it must be given correctly not only the above information, but also and mostly, the time evolution of meteorological field, or at least, a few of its main elements, like mixing height, depth of lower stable layers and their stability, wind field, eddy diffusivity, and so on; in other words, the temporal variation of the vertical structure of the lower half of the planetary boundary layer.

Due to the practical impossibility of a continous monitoring of this vertical structure, the development of forecasting models, based on relationships existing between surface values of main meteorological elements (temperature, radiation, wind speed, humidity, and so forth, ...), seems to be the most promising approach to follow.

We are aware that such an approach doesn't have general applicability, in that several situations in which atmospheric layers at several heights are not connected each other exist, forbidding any relationship to exist between surface values and those at higher levels (Delage, 1974). However, a lot of more homogeneous conditions occur in lower layers, which allow such an attempt to be successful (Anfossi et al. 1974 and 1976).

Large scale meteorological conditions supporting the establishment of this kind of situations are those of weak anticyclonic circulation, which in turn bring about low diluition rates and smoke trapping with subsequent fumigation processes.

Topographical and geographical conformation of the Po Valley, where urban agglomerates, vehicular traffic and industrial settling attain their highest values in Italy, are such as to induce (Santomauro, 1972) a climatology of the above-mentioned kind in at least fifty per cent of cases. Under these conditions, we noticed the feasibility of inferring vertical distribution of air temperature in lower layers as far as the top of radiative inversion, during clear nights with light winds, from sunset to dawn, on the basis of the temperature trend measured near ground (at screen level).

Prediction of temperature profile and time evolution of inversion depth are of use not only in evaluating dispersion of pollutants during nighttime periods, but they represent a fundamental information in forecasting the morning development and growth of the unstable convective layer; in fact, all of models describing thermal erosion of stable layer, i. e. Lilly (1968), Deardoff and Willis (1969), Ball (1960), Betts (1973), Carson (1973), Kranz and Hoult (1973), Stull (1973), Rayment and Readings (1974), require the bulk stability of the first few hundred meters of atmosphere, which is given by the temperature profile at dawn.

The height of unstable convective layer, on one hand, plays a major role in qualitative forecasting of abatement to the ground of pollution trapped at high levels and of behaviour of smoke plume ("break-up" effects described by Csanady (1973) and Kranz and Hoult); on the other hand, it represents a fundamental meteorological input to air pollution models; for example, in the Gifford-Hanna model it represents an height scale, with respect to which vertical concentration distributions are to be similar, while in the Shir and Shie model it is the upper level where boundary conditions of diffusion equation are set.

We whish now to describe briefly the forecasting model of nocturnal temperature profile, we developed by using new boundary conditions obtained in previous field experiments (Anfossi et al., 1974) on growth of radiative inversion depths, and then to show a few examples of its application to model predicting thermal erosion of stable layers.

THE NOCTURNAL TEMPERATURE PROFILE MODEL.

The assesment of vertical distribution of temperature during clear night-time from temperature trend at screen height has been considered for long time by Taylor, Sutton, Brunt, Moeller and others (see Sutton, 1953 and Haltiner-Martin, 1957); their classical work gave us the well-known radiative model, by which one can estimate air temperatures at any time from sunset to dawn in the lower layers of atmosphere. Now, the above model considers atmosphere as a semiinfinite medium and a comparison between its predictions and experimental data shows departures which, in proximity of the inversion top z_i, may become as large as 3 - 4 degrees. A forecasting of morning air temperature from this model is then misleading.

We reconsidered the problem of forecasting temperature profiles, by assuming a model of radiative type (Anfossi et al., 1976) like that proposed by the above authors, with a radiative heat exchange coefficient K_H constant in time and height. The new solution to the problem has been obtained by introducing, when integrating the differential equation for heat transfer, a new set of boundary conditions, prescribed on the ground of a few characteristic features observed experimentally (Anfossi et al., 1974) during nocturnal phenomena of cooling of terrestrial surface and the resulting development of temperature inversion. These boundary conditions can be summarized as follows:

$$\begin{aligned} f\,(0,\quad t) &= f_o \\ f\,(z_i,\quad t) &= 0 \\ z_i = (4\,K_H\,t)^{1/2} &= 70\,t^{1/2} \end{aligned} \qquad (1)$$

The first one is the same as in the classical treatment; the third condition expresses the time evolution of the top z_i of radiative inversion depth, the numerical value 70 $m/h^{1/2}$ having been determined by our experimental measurement; the second condition, this also derived from experimental observations, makes heat flux become zero at the level z_i.

With this set of conditions, our solution to heat transfer equation reads:

$$T(z,t) = T(0,0) - \Big[T(0,0) - T(0,t)\Big] \cdot$$

$$\cdot \left\{ \exp\left[-\left(\frac{z}{z_i}\right)^2\right] - \frac{z}{z_i}\,(\pi)^{1/2}\,\mathrm{erfc}\left(\frac{z}{z_i}\right) + 0.278\,\frac{z}{z_i} \right\} \qquad (2)$$

where t represent the time past from sunset (in hours).

Accounting for applications to problems described in the next section, for which the relevant information becomes the temperature difference between ground surface and the level z_i, equation (2) gives (Anfossi et al., 1976):

$$T(z_i, t) - T(0, t) = 0.63 \left[T(0, 0) - T(0, t) \right]$$

The reliability of our model in giving morning lapse rates as far as z_i showed satisfactory (within a 20% error) in a lot of situations (fig. 1), provided water vapour condensation or strong winds didn't occur; when these last had happened, the model error could rise as far as 100% or more.

As above said, the solution we obtained to the radiative nocturnal profile of temperature has been used as input datum in models describing erosion of stable layers.

DESCRIPTION OF MIXING LAYER HEIGHT MODELS.

Among all of models, we shall consider here only the simplest two, proposed and developed by Carson and Kranz-Hoult respectively; in fact, our chief aim is that of testing the reliability of as simple as possible relationships, to be used both in qualitative evaluations of harmful pollution conditions and in quantitative models for forecasting of pollutant concentrations.

In short, the main features of the above two models are the following. Kranz-Hoult consider a simple thermal balance in a stable air layer $\left[(d\vartheta/dz)_{\text{morn.}} = \text{const} > 0 \right]$ heated from below, in which a well-mixed sub-layer develops and grows, whose depth L and potential temperature ϑ_0, constant with height, increase as solar radiation proceeds in the morning; the forcing function in this model is the net radiation, R_N, which corresponds to $\simeq 0.55\ Q_r$, where Q_r indicates the surface instantaneous incoming radiation. An experimental test of this relationship carried out by us is shown in fig. 2.

On the other hand, Carson considers, in the same layer, the conservation of potential heat and of mass under an entrainment assumption; his model, in which the forcing function is the vertical divergence of the sensible eddy heat flux, shows more generality and completeness than the previous one, in that not only it accounts for large-scale subsidence motions and for entrainment of air at the inversion base down into the mixed layer, but also introduces two distinct temperature gradients, γ_o and γ_1, respectively under and above the surface inversion z_i (as far as 500-600 m).

In the first stage (below z_i) of development of the unstable layer, Carson assumes no entrainment of air at the upper boundary; this makes things easier and, by assuming no subsidence as well, the model simply becomes:

$$L\ (t) = \sqrt{\frac{2}{\varrho\, c_p\, \gamma_o} \int_o^t H(0, \tau) d\tau} \qquad (3)$$

an expression very similar to that obtained by Kranz-Hoult under different enough assumptions:

$$L\ (t) = \sqrt{\frac{2}{\varrho\, c_p\, \gamma_o} \int_o^t R_N\ (\tau)\ d\tau} \qquad (4)$$

the only difference being in the meaning of heat flux (sensible beat flux in the first one and net radiative flux in the second one).

Above z_i, the Carson model changes its expression, in that it accounts for a $\gamma_1 \neq \gamma_o$ lapse rate; it reads:

$$L\ (t) = \sqrt{z_i^2 + \frac{2}{\varrho\, c_p\, \gamma_1} \int_{t_{z_i}}^t H\ (0, \tau)\ d\tau} \qquad (5)$$

where $z_i \equiv L(t_{z_i})$.

APPLICATION OF MIXING LAYER HEIGHT MODELS TO EXPERIMENTAL DATA.

Experimental data which the models described in the previous section have been compared to, were collected during two field experiments, the first one at a flat country in the Po Valley and the other one at a costal site on the Northen Tyrrenian Sea; data belonging to this last refer to winds blowing from land, before the onset of sea breezes, what assures air didn't experience any surface discontinuity). All of measurement were carried out under anticyclonic weak circulations, clear sky or feeble cloudiness (less than 4/8), by employing a captive balloon with thermosonde (accuracy 0.2 °C) and a net radiometer by Middleton; pilot balloons, tracked by theodolites, were also used to evaluate wind profiles, but their data didn't enter in this analysis at the present stage.

First, a run by run comparison between observed heights of mixed layers and those expected by Carson and Kranz-Hoult model has been performed in which experimentally observed morning lapse rates were used and figgs 3 and 4 show an example. As one can see, the Carson model fits better with experimental observations than the Kranz-Hoult model does, during the first 3 - 4 hours after the onset of the phenomenon. Afterwards, they seem pratically to coincide; this could be due to the constant thermal gradient introduced by Kranz-Hoult, which exceeds the value γ_1 used by Carson above z_i and could perhaps counterbalance the larger heat flux used by Kranz-Hoult. However, if forecasting curves of the two models are extrapolated to following hours, they diverge again. Although we didn't have got any experimental data, it is reasonable assume a better fitting of Carson model, whose expected data are larger than those by Kranz-Hoult, as a consequence of its more realistic value of temperature gradient above z_i.

From the above arguments, we retained the Carson model as the better one and then the bulk of our experimental data has been compared to it (Figgs. 5 and 6). In the first stage (under z_i), both morning lapse rates calculated by our radiative model (fig. 1) and experimentally measured have been introduced; in the second stage (above z_i) an average experimental value of $\gamma_1 = 8 \cdot 10^{-3}$ °C m^{-1} was used; these figures differ a bit from the typical ones assumed by Carson. Some what fortuitously, introducing our calculated morning temperature gradients, the agreement of the model with experimental mixing heights improves, as figs5 and 6 show.

With reference to sensible heat fluxes used all over this analysis, we have had resort to indirect estimates on the ground of easier measured physical quantities, like solar radiation Q_r, owing to difficulties in direct evaluation of $H(0,t)$. Following the classical figures given by Pasquill (1949), who evaluated experimentally the thermal balance near ground surface, we assumedthe eddy sensible heat flux to be $\simeq 0.25\ Q_r$; this simple and broad assumption showed not too far from the reality, as the agreement of Carson model with our experiments confirms.

As to the measured mixing heights, at last, one can observe that there is not any significant difference between mixed layer rise at two sites climatologically so different like Trino Vercellese (Po Valley) and La Spezia (Northen Tyrrhenian Sea).

CONCLUDING REMARKS.

A simple radiative model for predicting morning air temperature profiles has been developed, which proved to give reliable stability information as far as 300 m.

This information has been used as input datum in two simple theories describing the development and growth of mixed layers due to thermal convection.

The Carson theory showed better fitting to experimental data we collected at two Italian sites, La Spezia and Trino Vercellese, very different from a climatological point of view.

In conclusion, we have got useful elements to be used both as an input datum in models for prediction or control in real time of concentration distributions of pollutants, and as climatological factor of forecasting the time of breakdown of the nocturnally established inversion and the onset of fumigation processes (fig. 7). Of course, all the above results are to be considered valid for the Northen Italy climatology.

REFERENCES

D. Anfossi, P. Bacci and A. Longhetto (1974) - Atmospheric Environment - 8, pp 537-541

D. Anfossi, P. Bacci and A. Longhetto (1976) - Quart. Journ. R. Met. Soc. - 102 (in press)

F.K. Ball (1960) - Quart. Journ. R. Met. Soc. - 86, pp. 483-494

A.K. Betts (1973) - Quart. Journ. R. Met. Soc. - 99, pp. 178-196

D.J. Carson (1973) - Quart. Journ. R. Met. Soc. - 99, pp. 450-467

G.T. Csanady (1973) - Atmospheric Environment - 7, pp. 1-17

J.W. Deardoff, G.E. Willis and D.K. Lilly (1969) - J. Fluid Mech - 35, pp. 7-31

Y. Delage (1974) - Quart. journ. R. Met. Soc. - 100, pp. 351-364

F.A. Gifford and S.R. Hanna (1970) - Int. Air Poll. Conf. of Int. Union of Air Poll. Prevention Assocs - Washington

C.J. Haltiner and F.L.Martin (1957) - Dynamical and Physical Meteorology - Mc Graw Hill

W.T. Kranz and P.D. Hoult (1973) - Fluid Mech. Laboratory Publication N 73-3, M.I.T.

D.K. Lilly (1968) - Quart. Journ. R. Met. Soc. - 94, pp. 292-309

F. Pasquill (1949) - Proceedings R. Soc. - 198, pp. 116-140

R. Rayment and C.J. Readings (1974) - Quart. Journ. R. Met. Soc. - 100, pp. 221-234

L. Santomauro (1972) - III Meeting of Panel on Modeling of the Nato CCMS (V-1) Paris

C.C. Shir and L.J.Shieh (1974) - J. Appl. Met. - 13, pp. 185-204

R.B. Stull (1973) - J. Atm. Sci - pp. 1092-1099

0.G. Sutton (1953) - Micrometeorology - Mc Graw Hill

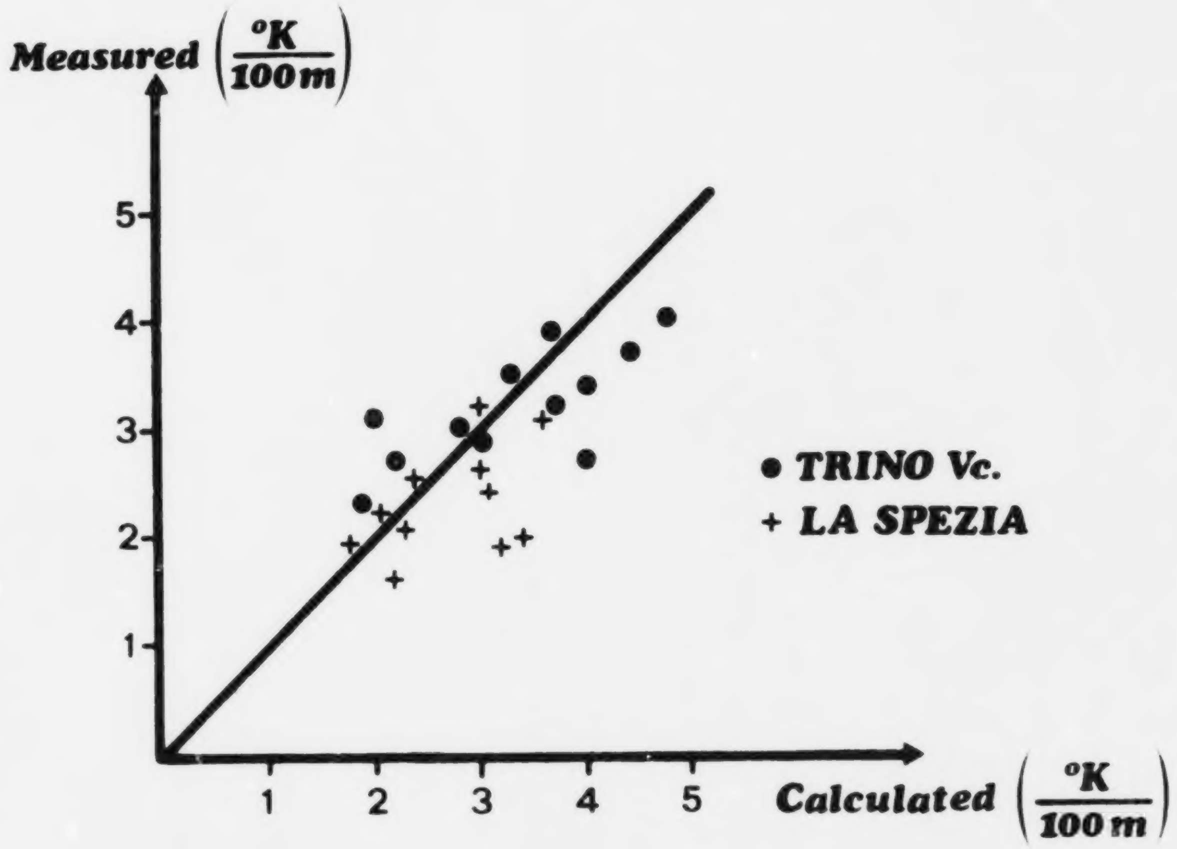

FIG. 1 · *Comparison between measured and calculated* $\left(\frac{\Delta\theta}{\Delta Z}\right)$

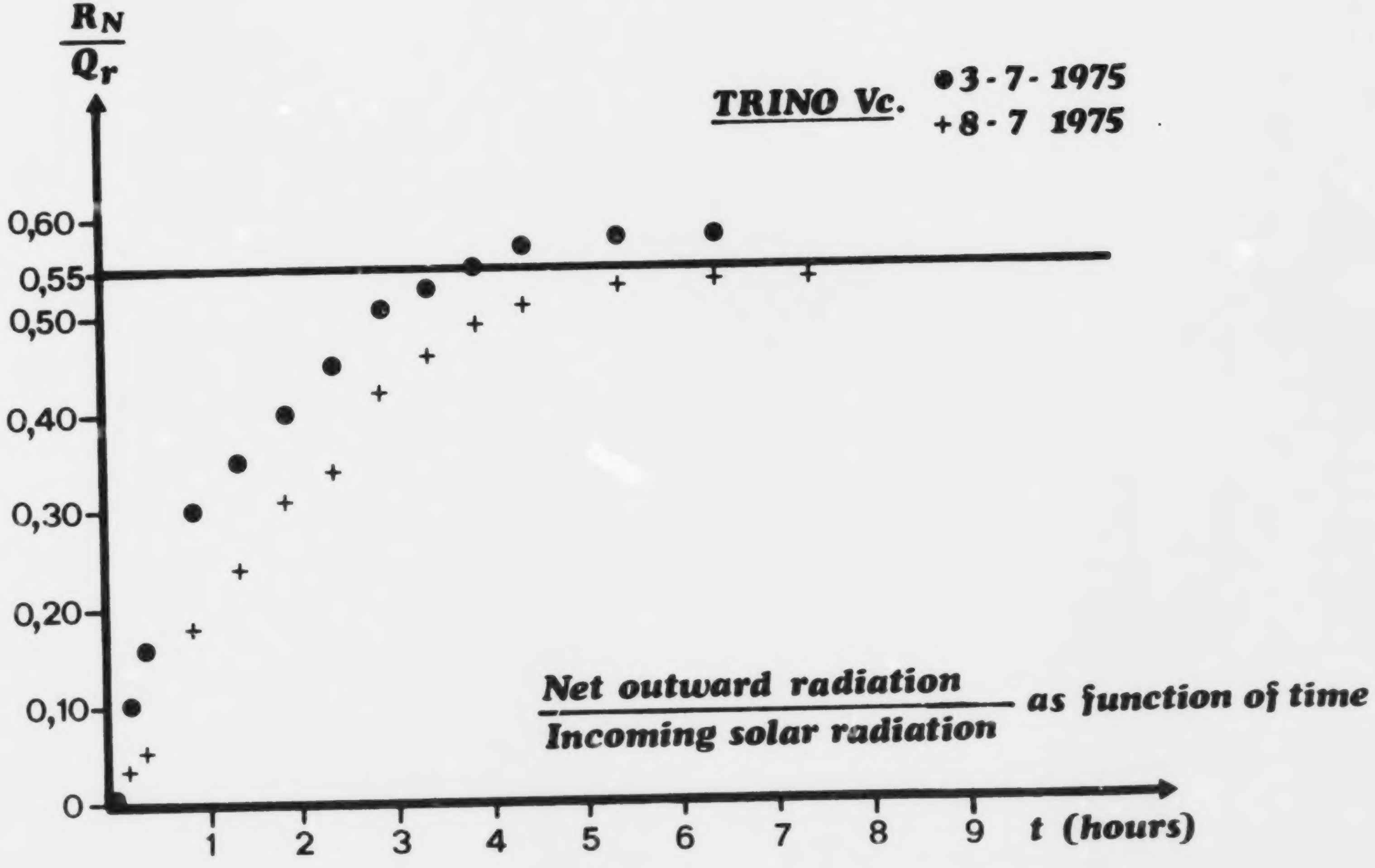$\frac{R_N}{Q_r}$
TRINO Vc.
● 3-7-1975
+ 8-7 1975
0,60
0,55
0,50
0,40
0,30
0,20
0,10
0
1
2
3
4
5
6
7
8
9
t (hours)
Net outward radiation / Incoming solar radiation as function of time

FIG. 2

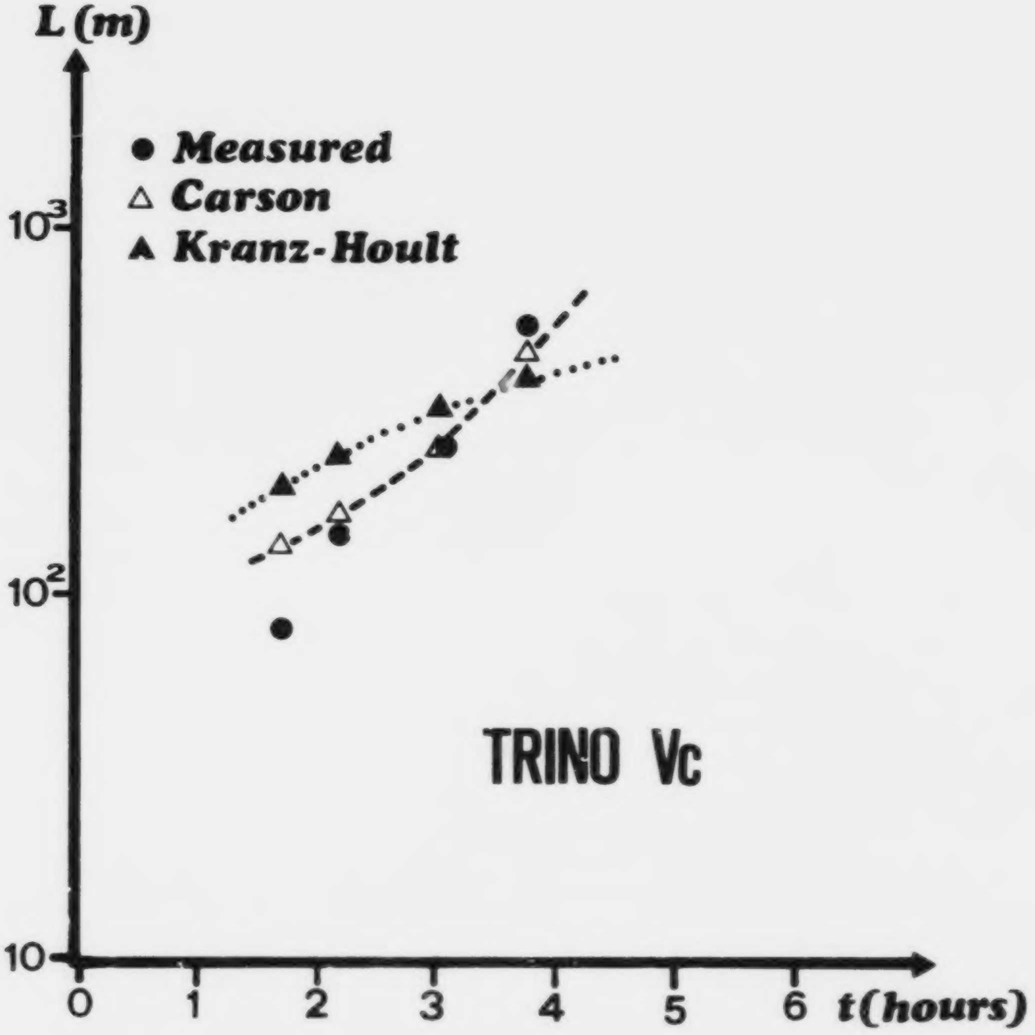
L (m)
● Measured
△ Carson
▲ Kranz-Hoult
10³
10²
10
TRINO Vc
0
1
2
3
4
5
6
t(hours)

FIG. 3

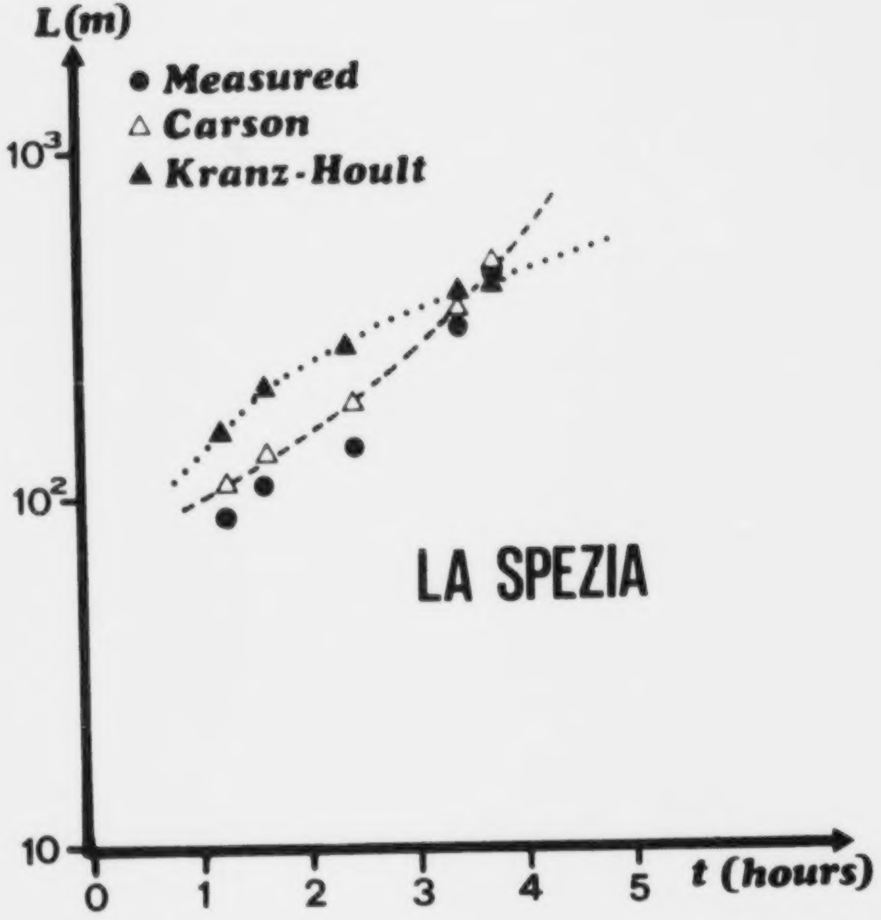
L(m)
10^3
10^2
10
● Measured
△ Carson
▲ Kranz-Hoult
LA SPEZIA
0
1
2
3
4
5
t (hours)

FIG. 4

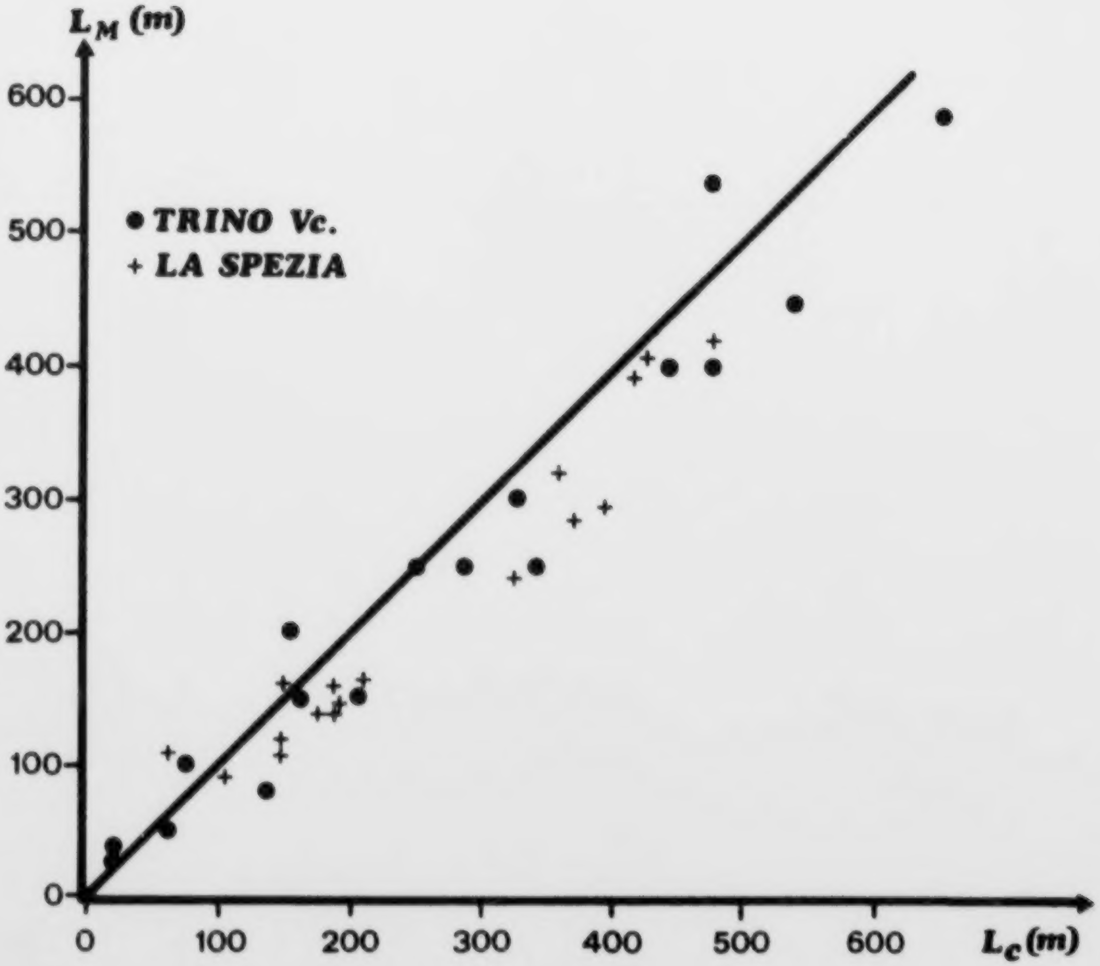

FIG. 5 · Comparison between measured and calculated L
$\left(\frac{\Delta\vartheta}{\Delta Z}\right.$ experimental$\left.\right)$

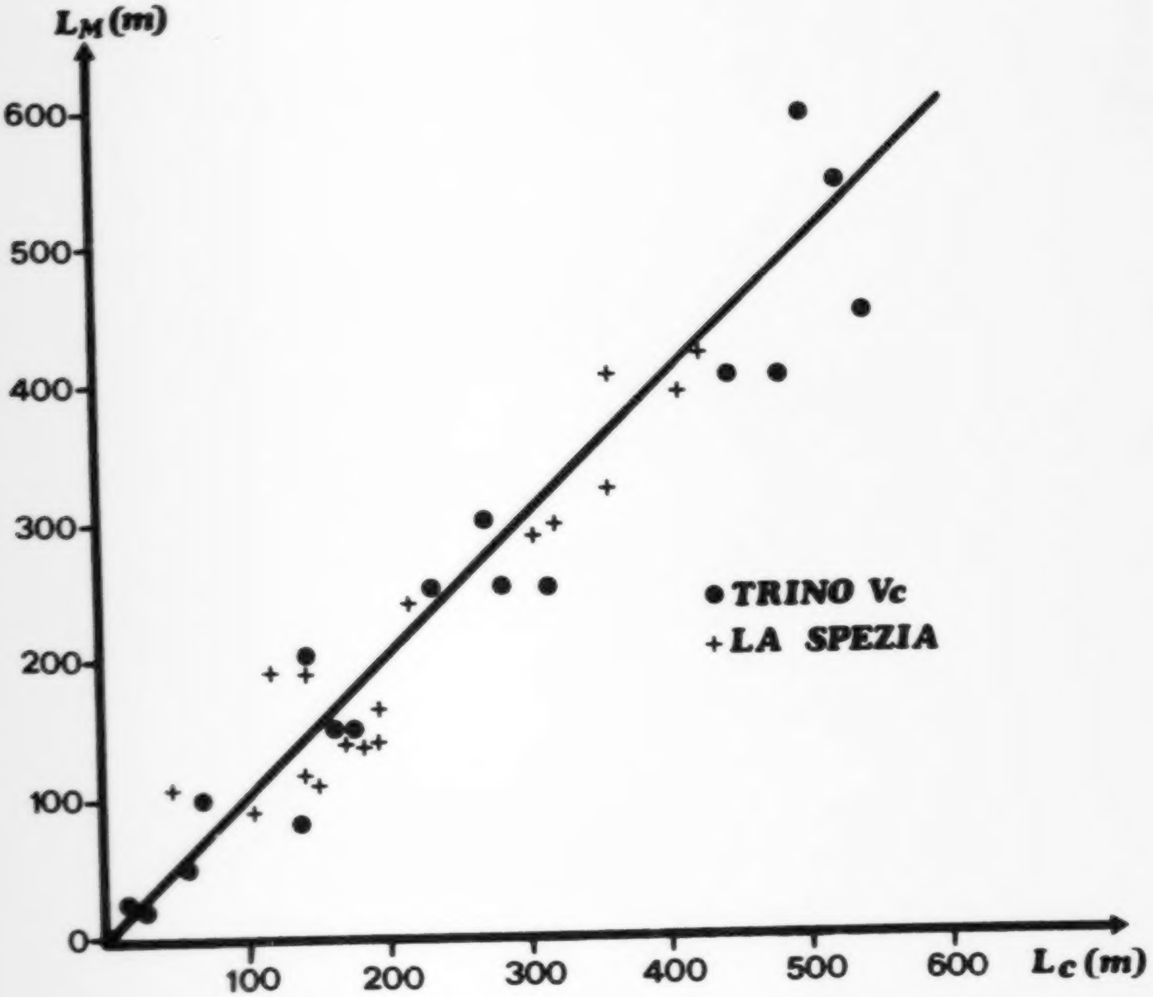

FIG. 6 - Comparison between measured and calculated L $\left(\frac{\Delta\theta}{\Delta Z}\right.$ from our model$\left.\right)$

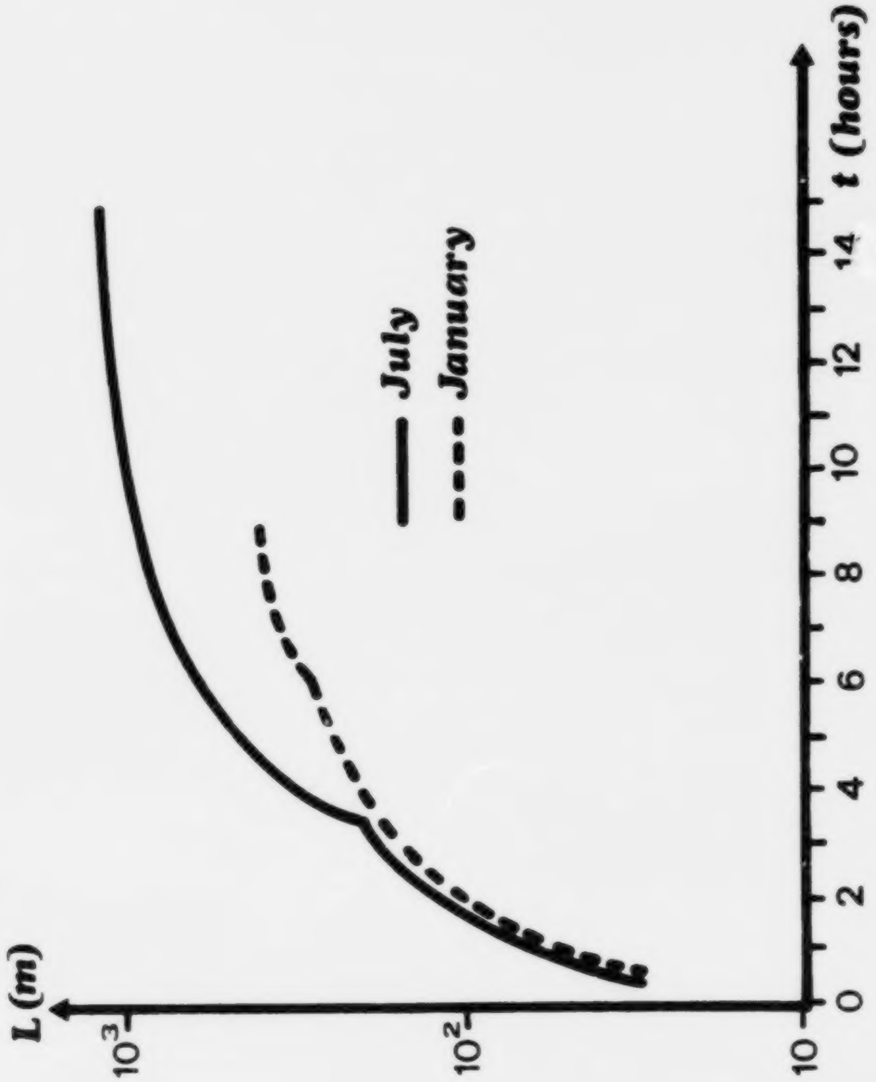

FIG. 7

6th NATO/CCMS
International Technical Meeting
on Air Pollution Modeling

AIR QUALITY MEASUREMENTS IN TURIN

1971-1974

by

Pier Paolo Gaddo, Franco Corazzari, Luigi Giacomelli

FIAT Central Research Laboratories, Orbassano (Turin) ITALY

BATTELLE - INSTITUT E.V., Frankfurt/Main
Germany, FR

24 - 26 September, 1975

ABSTRACT

The fundamental aspects of air pollution in Turin are examined in relation to its urban structure, anemologic situation and main emission sources.

The results of the air quality measurements made in 1971 to 1974 by means of a monitoring network set up by Fiat are also reported.

An analysis is made of the primary pollution data measured at ground and elevated levels under normal operative conditions of pollution sources and under particular conditions deriving from the governmental restrictions of traffic on Sundays and other holidays (4 months). The photochemical transformation reactions of pollutants in the atmosphere are also evaluated.

Some conclusions are drawn on pollution extent and the relevant responsability of the single sources.

The highest pollution levels occur in winter in concurrence with unfavourable weather conditions and the full activity of all the emission sources (in particularly the heating plants).

Critical values are found for sulphur dioxide and particulates, which are responsible for pollution conditions extended in space and time.

Pollution from carbon monoxide, on the contrary, is limited to restricted areas and is ascribable to critical traffic situations, but it remains at acceptable levels.

Pollution from nitrogen oxides and hydrocarbons, which, in the absence ot other terms of reference, is evaluated as a function of the transformations that these pollutants undergo in the atmosphere, does not seem so High. The contribution of vehicular traffic to this last type of pollution was contained within 20 - 30%.

SUMMARY

An outline is made of the fundamental aspects of air pollution in Turin by examining its urban structure, anemologic situation and main emission sources.

The results of the air quality measurements made in 1971 to 1974 by means of a monitoring network set up by Fiat are also shown.

An analysis is made of the primary pollution data measured at ground and elevated levels in normal operative conditions of pollution sources and in particular conditions ensuing from traffic restrictions and the photochemical transformation reactions of pollutants in the atmosphere are evaluated.

Some conclusions are drawn on pollution extent and the relevant responsability of the single sources.

The highest pollution levels occur in winter in concurrence with unfavourable weather conditions and the full activity of all the emission sources (in particular the heating plants).

Critical values are found for sulphur dioxide and dust, which are responsible for pollution conditions extended in space and time.

Pollution from carbon monoxide, on the contrary, is limited to restricted areas referable to critical traffic situations, but it remains at acceptable levels.

Pollution from nitrogen oxides and hydrocarbons, which, in the absence of other terms of comparison, is evaluated as a function of the transformations that these pollutants undergo in the atmosphere, does not seem to be so high. The contribution of car circulation to this type of pollution resulted to be restricted within 20-30%.

The more significant results are shown on :

- page 12 for the concentration trend of primary pollutants at ground level;

- page 18 for measurements made without private car traffic;

- page 20 for pollutant stratification in the atmosphere;

- page 22 for reactions of photochemical smog formation.

FOREWORD

The problems connected with the planning of air pollution control are so different and sometimes contrasting that it is difficult and hazardous to face them without the support of a deep and comprehensive knowledge.

The difficulty originates from the impossibility to find the optimum solution of a problem without knowing all its implications; its hazardousness comes from a possible improper approach, which could lead to inadeguate solutions as far as costs are concerned: too high a cost versus too poor results.

In fact, planning of pollution control is acceptable only if conditions leading to unfavourable effects on environment take place.

It comes out that a deep knowledge of air pollution is requested both in general, in order to frame it in its exact position without distorsions due to erroneous interpretations or ignorance and in detail in order to emphasize its composition by ascribing the real contribution to the single components.

This can be done only through a systematic investigation of air quality consequential not only of primary pollutants from stationary and mobile sources but also of the transformations they undergo to produce secondary reaction products.

The attainment of these goals is particularly advantageous in large urban centres, where many emission sources concentrated in small areas facilitate the occurrence of the worst effects of pollution.

Hence, the present study aims at evaluating air quality conditions in a modern urban centre.

Turin was chosen as subject of this investigation, owing to its extremely variable climatology and the presence in it of all the factors that are peculiar to the large European industrial centres.

Characterization of Turin as a typical specimen for investigation.

A. Description of the town from the point of view of emission and climatological situation.

The urban area of Turin is 130 square kilometres wide and 1,186,566 inhabitants live on it. Its density is 9,000 inhabitants/square Km and it is comparable to that of the other large European towns.

The town can be divided into a central business area including the old town centre and a typically industrial suburban area, where the main metal working, iron metallurgy and manufacturing plants are located.

The old town centre, where narrow (5 to 8 meter roadway) one-way roads run, is connected with the residential and industrial quarters through large multi-lane roads, while the highways, where most of the truck traffic flows, run tangentially to the urban centre.

The total length of the roads is 1,037 Km, 250 of which are devoted to the primary traffic with elevated density.

As far as car traffic density is concerned, Turin is among the European towns having the highest inhabitants/car ratio (2.6 inhabitants/car). The circulating fleet consists approximately of 522,000 private cars, 2000 buses and 25,000 industrial vehicles. The resulting traffic, considering the road network structure and car density, is characterized, especially in the centre, by an alternation of short running periods and frequent stops. This fact is confirmed by the relatively low commercial speed (°), which is 20 to 25 Km/h.

The situation in the suburban areas, on the contrary, is considerably less liable to change and more regular.

As to the climatologic situation, Turin presents various and very significant aspects due to its location on a flat zone behind a hilly region and at the confluence of the Alps valleys (Fig. 1).

The resulting anemologic situation is characterized by low West prevailing winds (1 to 2 m/sec.) from the Alps, North--West winds of katabatic origin from hills, and South-West winds : these wind directions facilitate the accumulation of pollutants in the urban centre.

In addition, the feeble ventilation and long-lasting calm air conditions, particularly in winter, concur in originating air stagnation.

(°) The commercial speed is the real speed at which a distance is covered including the stop times, which, on the contrary, are not considered in mean speed calculation.

From the point of view of thermodynamics, since the town is in a region with a typically continental climate, temperature undergoes considerable variations in the daily averages (from -3 to +4°C in winter, 28 to 32°C in summer), while the relative humidity keeps on high average values both in winter (80 to 90%) and in summer (60 to 70%). A summary of the climatologic situation in Turin from 1971 to 1974 is in appendix 1.

B. Air pollution sources.

Considering the orographic position and the urban structure of Turin, the most different air pollution sources can be found : heating plants for residential buildings, industrial plants for manufacture and power production, private and public vehicle traffic.

A significative estimate of the most polluting emissions could be made on the grounds of the specific fuel consumptions of each source and its emission factors.

A summary of the total emissions shown in table 1 indicates the quantity of pollutants emitted in Turin (°)

(°) Diesel vehicle emissions are not indicated because only bus traffic is allowed in town centre and buses are 1% of the heavy vehicle fleet.
Emissions of industrial plants are also ignored because they are hardly quantifiable.

These figures are calculated by using emission factors from :

- First report on environmental conditions of Italy - A 73 Tecneco;
- U.S. - E.P.A. Manual.

The emission values indicated above, however, are sufficient neither to quantify the real air conditions not to determine the responsability of the single sources. In fact, a global evaluation of air quality cannot leave out of consideration the many and various factors affecting pollution : climatology, emission mode (ground, level), emission dislocation in time and in space, scattering properties and chemical reactivity of the single pollutants.

C. Description of the monitoring system

A systematic investigation of air quality in Turin was made by Fiat which set up a monitoring network operating since 1971. It is arranged so that the statistical data of primary and secondary pollution are available in spots which are representative of the different urban areas.

It consists of:

- three stations equipped to determine fully the primary pollutants and the metereological parameters. The significance of the data measured in these stations is related to their location :

- in Via Lagrange, in the middle of the business centre, normally with a lot of traffic (17,000 vehicles/day with peaks of 1,700 vehicles/hour) slackned by traffic lights; it is a typical instance of roads canyon, 5.50 m roadway, running between 25 to 30 m high buildings;
- at Mirafiori and Ironworks Plant, contiguous to strong industrial concentrations and large road junctions (51,000 vehicles/day with peaks of 4,700 vehicles/hour at Mirafiori; 34,000 vehicles/day with peacks of 3,300 vehicles/hour at Ironworks Plants); (°)

- two stations for monitoring carbon monoxide only placed in the very central zones of Porta Nuova (77,000 vehicles/day with peaks of 6,600 vehicles/hour) and Piazza Statuto (60,000 vehicles/day with peaks of 4,500 vehicles/hour);

- one station for the complete determination of primary and secondary pollutants placed on the Mole Antonelliana, in old town centre, at 93 m height with the possibility of monitoring air at 93 m and 145 m heigh. This station was made operative early in 1974 (Figure 2);

- eight stations for monitoring lead at 1.50 m from ground level, placed in zones significative of the urban traffic (confluence of roads, centre and suburban throughfares)(°°)

(°) In September 1973 the monitoring station at Mirafiori, for technical reasons, was moved to a zone which was less exposed to emissions of industrial and heating plants; it is near great traffic streams (at the crossing Corso Agnelli//Corso Settembrini).

(°°) Data of lead pollution will be dealt with in a specific report of FEEMAS work group.

Analitycal equipment of each Fiat station is listed in Table 2; appendix 2 shows the technical characteristics of the individual instruments.

Fiat monitoring network, to which some automatic stations are designed to be added, is supported by the municipal (air pollution monitoring service) and provincial networks (°) (Figure 3).

The statistical processing of the data collected form January 1971 to June 1974 makes it possible to :

- follow pollution progress at ground level from primary pollutants (SO_2, dust, NO_x, HC and CO);
- determine vehicle contribution to primary pollution from considerations based on the progress diagrams referring to days with or without vehicular traffic (December 1973 to March 1974);

(°) Location and analytical equipment of municipal stations :

- Via della Consolata 10	SO_2, CO, NO_x, oxidants , Pb, Fe, Cu, V, Zn.
- C.so Vercelli, 236	SO_2, CO, dust.
- Str.dell'Aeroporto, 9	Dust, Pb, heavy metals
- C.so Racconigi/V.Moretta	SO_2, dust, Pb, heavy metals

Location and analytical equipment of provincial stations :

- Via Braccini, 11	SO_2
- Via Ponchielli, 56	SO_2
- C.so Venezia, 29	SO_2

- evaluate pollutants diffusion in the atmosphere by means of measurements at elevated levels;
- examine the rate of primary and secondary pollutant transformation as a consequence of photosynthetic reactions.

Statistical data processing is shown in appendix 3.

Distribution of primary pollution at ground level and its progress in 1971 to 1974.

A. Sulphur dioxide

The statistical distribution of the pollution levels was recorded from October to April, during which the heating plants, which are the main pollution sources, are operating. During this period the maximum per-hour concentrations are 50% between 0.15 and 0.50 ppm and 30% between 0.50 and 0.90 ppm while the mean per-day concentrations are 70% between 0.05 and 0.30 ppm; 10% data are between 0.40 and 0.90 ppm (table 3).

This pollution is homogeneously distributed on the whole urban area, it reaches the maximum values in December and January (0.30 to 0.50 ppm per-month concentration) in coincidence with the maximum operation of the heating plants. During the summer months the total pollution level decreases by 90% both in the urban centre and in the industrial areas (see figure 4) (mean per-month concentrations of 0.03 to 0.04 ppm in June to August).

The greater decrease noticed in winter 1973 at Mirafiori station as compared to that occurring at Ironworks Plant and in Via Lagrange is to be attributed to the fact that the monitoring station in September 1973 has been moved to a more open zone, which was, therefore, less subject to the emissions of the urban aggregations and industrial plants.

During the years of investigation a mean 20% per-year increase was noticed in 1971 to 1972 and in 1972 to 1973. A 29% decrease took place during the first six months of 1974, owing to the lower fuel consumption caused by oil crisis.

B. Dust

The distribution of pollution levels from dust, produced essentially by heating and iron metallurgy plants, allows us to point out that the maximum per-hour concentrations are 60% between 0.20 and 0.50 mg/mc and 25% between 0.50 and 0.80 mg/mc. On the contrary, the mean per-day concentrations are 70% between 0.10 and 0.30 mg/mc; 15% values exceed 0.30 mg/mc (table 5).

The maximum pollution level is found in winter (0.30 mg/mc in November and December.

A 60% decrease occurs in summer; this proves a fundamental contribution of heating plants.

During the years under investigation considerable decreases (-18%) were noticed in 1972 in comparison to 1971 as a consequence of the installation of proper purification systems in Fiat iron metallurgy plants located in the northern area of Turin (figure 5).

In the following years dust pollution course was similar to that of SO_2: it underwent an increase in 1973 and a decrease in 1974 (Figure 6).

Nitrogen oxides

The maximum per-hour concentrations of nitrogen oxides from various sources (heating plants, industrial plants and vehicular traffic) are 50% between 0.20 and 0.40 ppm.

The remaining 50% values are homogeneously scattered according to a standard distribution between 0.05 and 0.20 ppm, 0.40 and 1 ppm.

The mean per-day concentrations are 50% between 0.05 and 0.15 ppm only 7% values exceed 0.50 ppm (Table 7).

The course of the nitrogen oxides pollution is similar to these of sulphur dioxide and dust. In fact, it undergoes a 60% decrease in summer (the mean per-month values are 0.31 ppm in December and January, and 0.12 ppm in July and August) (fig. 6).

A continuous increase was noticed from 1971 to 1974.

The 10% mean per-year increase that occurred in 1971 to 1972 and in 1972 to 1973 can be due to sulphur dioxide increase, therefore to fuel consumption in heating plants in the same period, and to increase of the circulating fleet (table 8).

Early in September 1974 the increase (18% approx) is not attributable to the same causes; on the contrary, it could be a consequence of particular meteorological conditions. For instance, it was noticed that a high relative humidity contribute to stagnation of nitrogen oxides in the atmosphere. Since in this period of time the relative humidity values were constantly high and exceeding those measured in the same period in the preceding years (70 to 86% in 1974 versus 58 to 73% in 1973), this phenomenon could be ascribed to the above-mentioned causes.

D. Carbon monoxide

The maximum per-hour concentrations of carbon monoxide, the main source of which was found to be vehicular traffic, are 65% between 5 and 20 ppm and only 7% data exceeds 40 ppm.

The maximum per-day values measured during periods of 8 and 12 consecutive hours (°) are 75% between 5 and 15 ppm.

Only 3% values exceed 30 ppm, while the majority of mean per-day values (85%) are lower than 15 ppm (table 9).

The pollution levels measured in the centre and in the suburban areas are virtually the same, only in some zones of exceedingly intense traffic (more than 77,000 cars/day), such as Porta Nuova e Piazza Statuto the pollution levels are higher (Figure 7).

In 1972 the pollution levels during the years under investigation decreased on an average by 9% as compared to those

---

(°) The analysis was restricted to 8 to 12 hours to include in a single period the hours of the most intense traffic.

of 1971. In 1973 and 1974, on the contrary, 5% and 9% decreases were respectively noticed (table 10).

The decrease in 1973 as compared to the values measured in 1972 is to be related to antiemission measures adopted in cars. In fact, as circulating fleet of Turin is renewed almost completely (70 to 80) in 3 to 5 years, it can be concluded that the antiemission regulations issued in 1970 had their effect since 1973. This is even more significant considering that in the same period the circulating fleet increased by 10% approx and the Mirafiori station was moved to a some where circulation was greater by 30% approx.

The decrease measured in 1974 is obviously imputable, in addition to the above mentioned measures, also to a traffic reduction resulting from oil crisis.

E. Total hydrocarbons

As regards hydrocarbons, which originate from different sources (industrial and thermal plants, vehicular traffic, natural sources), a complete investigation is not possible yet; the available data, in fact, refer only to one station and to a limited period of time (December 1973 to June 1974).

Only for this period it was noticed that the maximum per-hour concentrations of total hydrocarbons are 60% between 2 and 5 ppm, 2% over 6 ppm, while the mean per-day values are 80% between 1 and 3 ppm (table 11).

Since methane , which is 65 to 70% of the total content, is not considered a pollutant, particularly significative for air pollution are the values of total hydrocarbons, methane excepted.

The maximum per-hour concentrations of total hydrocarbons, methane excepted, are 70% between 0.5 and 2 ppm. No value exceeds 6 ppm. The mean per-day concentrations are 95% lower than 1 ppm (table 12).

Particular pollution situations

A. Primary pollution in the absence of private vehicle traffic (December 1973 to March 1974).

Owing to oil crisis, private vehicular traffic was suspended in all the country on holidays from December 1973 to March 1974. On these days only the public service (in some cases it was reinforced) was operative.

The pollution data collected in these occasions were compared with data collected on week-days when all the emission sources are regularly working (figures 8 and 9 - tables 13 and 14).

Significative indications can be drawn from this comparison to determine the vehicle contribution to air pollution from carbon monoxide, nitrogen oxides, hydrocarbons.

It was noticed that carbon monoxide decreases on holidays without traffic by :

- 70% in suburban areas
- 50% in the central area, where public vehicle traffic is more intense.

Nitrogen oxides, which originates from many sources, decreases by 40 to 60% on holidays without traffic.

Since nitrogen oxides decrease, on an average, by 10 to 20% already on holiday eves, when operation of heating plants of factories and office buildings is limited, it can be deduced that private vehicular traffic contributes to 30% pollution.

Heating plant contribution is illustrated in figure 10.

It can be pointed out that on a typical winter day without private vehicular traffic, while carbon monoxice concentration is virtually constant on the lowest values, nitrogen oxides follow exactly the curves of sulphur dioxide and reach higher levels in the hours when heating plants are in full operation.

Hydrocarbons, the sources of which are less specifiable than those of nitrogen oxides, have a curve similar to that of nitrogen oxides. In fact, on holidays without traffic a 32% decrease was noticed, with a 12% decrease already in holiday eves; this indicates a 20% contribution from vehicles.

Sulphur dioxide and dust, which are of non-vehicular origin decreased about 20%.

This situation, however, is not attributable to traffic restriction but to the limited operation of industrial and heating plants occurring both on holiday eves and on holidays.

All the values recorded from December 1973 to March 1974 are shown in Appendix 3.

B. Stratification of pollutants

In order to investigate the pollutant diffusion in the urban atmosphere a monitoring programme at elevated level (93 and 145 m) has been carried out at the Mole Antonelliana station placed at 93 m above ground level.

Then the mean ground pollution values of urban area have been compared with those measured at elevated level (see fig. 11 and 12 - tables 15 and 16) and the primary pollutants resulted to have different diffusion characteristics.

In particular, it was observed that, in winter period from February to March, when the pollution level is the highest in the urban centre :

- sulphur dioxide values at that height remain elevated and they are comparable with those measured at ground level;
- dust, for which no data at 145 m height are available, remain at elevated concentration levels even at 93 m height (0.095 mg/mc versus 0.15 mg/mc at ground level) in spite of its peculiar tendency to deposit on ground;
- carbon monoxide, on the contrary, decreases by 80% at elevated level and remains at minimum values (2 to 3 ppm) which are ordinary pollution conditions of the town;
- nitrogen oxides diffuse less rapidly than carbon monoxide; in fact it decreases by 55% at 93 m height and by 70 at 145 m height;

- total hydrocarbons reach their maximum concentration at 93 m height (mean per-day values of 1.3 to 1.4 ppm at elevated level versus 0.8 to 1 ppm at ground level), while they decrease by 43% at 145 m height.

In summer months (June and July), when urban area pollution is the lowest, a similar behaviour can be observed for sulphur dioxide and dust, i.e. pollution values that can be compared at ground and elevated levels, while carbon monoxide and nitrogen oxides present a higher dispersion coefficient (CO decreasing by 90% and NO_x by 80%).

The continuous maximum concentration of hydrocarbons at 93 m height in winter and at 145 m height in summer would lead to consider the contribution to this type of pollution due to non-urban sources (industrial and natural), the emissions of which would be driven by the wind over the town.

In conclusion, though only short grounded data were available, this investigation made possible to emphasize a marked tendency of SO_2 and dust to stagnate in urban atmosphere. This phenomenon is particularly serious in winter months (November to April), when both pollutants are at the highest concentration.

Carbon monoxide, on the contrary, owing to its high diffusion properties, presents no tendency to accumulation, therefore this proves that CO pollution is closely restricted to the area with strong emissions and to ground level.

Nitrogen oxides,behaviour, owing also to their dual origin of emission sources, stationary plants (emissions at elevated level) and vehicular traffic (emissions at ground level) is intermediate between sulphur dioxide and carbon monoxide.

It is plain that the maximum decreases between ground level and elevated level concentrations occur during summer months when the stationary plant contribution is less effective.

C. Secondary pollutant formation reactions and photochemical smog formation.

Primary pollutants, in particular atmospheric conditions, undergo chemical transformations causing secondary reaction products.

The changes caused in air pollutants of towns by sun radiation are particularly important for the ecologists.

This phenomenon, which is know as photochemical smog, originates a series of complex radical reactions resulting in highly oxidizing components, among which : O_3, PAN, aldehydes (a scheme is shown on figure 13).

This atmospheric reactivity effects both the subjects and air transparency. As it is known; hydrocarbons and nitrogen oxides are responsible for these phenomena.

Only some hydrocarbons in the atmosphere (the so-called reactive HC) take part in photochemical reactions. Similarly, among NO_x only nitrogen dioxide can originate transformation reactions in primary pollutants.

The investigation programme to ascertain the occurrence of photochemical smog formation in Turin and to evaluate its extent was, therefore, drawn up as follows :

- determination of nitrogen oxide and dioxide concentrations at ground and elevated levels; nitrogen dioxide results from photochemical oxidation reactions of nitrogen oxide;
- determination of the total hydrocarbons at ground and elevated levels and subsequent separation and investigation via gascromatography;
- measurement of the secondary reaction products : ozone, peroxyacetilnitrate, aldehydes.

At present the experimental results are not all available. The first data on the determination of nitrogen dioxide and ozone, however, enable us to draw some preliminary information about the extent of this phenomenon.

It was possible to observe, in fact, that, in spite of the high NO_x contents measured in the atmosphere, the component of dioxide is considerably limited. This is proved by the mean concentration of dioxide in the urban centre, which resulted to be only of 0.044 ppm versus 0.173 ppm of NO_x all over the year (tables 17-18-19).

In particular the nitrogen dioxide contents at ground level are highest from March to August (monthly average from 0.04 to 0.07 ppm) and the lowest in winter months (mean con centrations between 0.02 and 0.03 ppm). It is clear that this behaviour differs from that of the total nitrogen oxides.

The oxidation reaction, therefore, results to be indipendent of monoxide concentration and in winter it is probably hindered on the high content of sulphur dioxide.

The concentration levels of NO_2 are constantly minimum at the higher atmosphere layers (at 93 m and 145 m above ground level) (mean monthly concentrations from 0.007 to 0.015 ppm). The maximum hourly concentrations do not exceed 0.04 to 0.08 ppm (table 20).

Since the photochemical reactions originate from nitrogen dioxide photolysis, it is reasonable to infer that the NO_2 levels observed cannot cause photochemical smog fenomena of considerable amount.

On the other hand, the measurements of ozone content made uninterruptedly at 93 m and 145 m levels and desultorily at ground level pointed out that the concentration levels are virtually similar at ground and elevated levels and this would lead to believe that O_3 contents are independent of those of nitrogen dioxide (table 21).

Moreover, the ozone concentrations at elevated level (table 22) in summer (March to August) are higher than those of NO_2 (figure 13). As ozone concentrations of photochemical origin higher than those of NO_2 does not seem to be explainable, it could be concluded that the ozone measured does not originate only from secondary transformation reactions.

In fact, the situations of typical photochemical smog origin are characterized by a progressive decrease of nitrogen monoxide and a simultaneous increase of NO_2 . Then the latter decreases as ozone levels rise.

These situations can normally be found in Los Angeles atmosphere when photochemical phenomena occur.

The comparison between the results of the measurements made in Turin and Los Angeles (Figures 14 and 15) points out that the photochemical phenomena in Turin are to be considered limited in time and, in any case, of very small amount.

FIG. 1 - GEOGRAPHIC POSITION OF TURIN

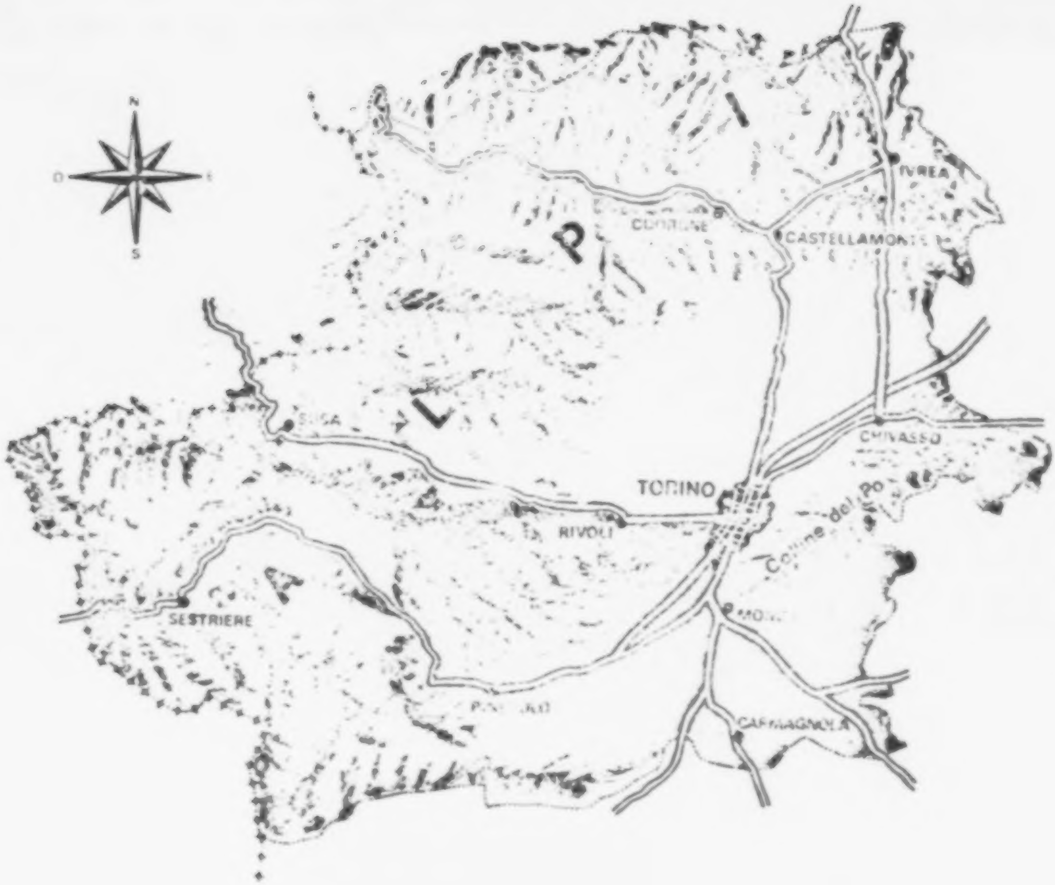

TABLE 1

EMISSION SOURCES IN TURIN ATMOSPERE (*)							
SOURCES	F U E L	Consump. tons/year (1973)	EMISSION - tons/year				
			SO_2	particulates	NO_x (°)	CO	THC
Home heating plants	fuel oil gasoil	560.000 800.000	33.600 12.800	1.400 1.120	1.820 2.600 (°)	304 520	196 280
Industrial thermal plants	Heavy fuel Oil	440.000	26.400	1.513	2.860 (°)	277	193
Cars	Gasoline	230.000	119	460	4.300	112.400	9.200

(*) Calculated using A73 Tecneco emission factors

(°) Calculate using U.S. E.P.A. Air Pollution Engineering Manual

FIG. 2 - STATION ON MOLE ANTONELLIANA

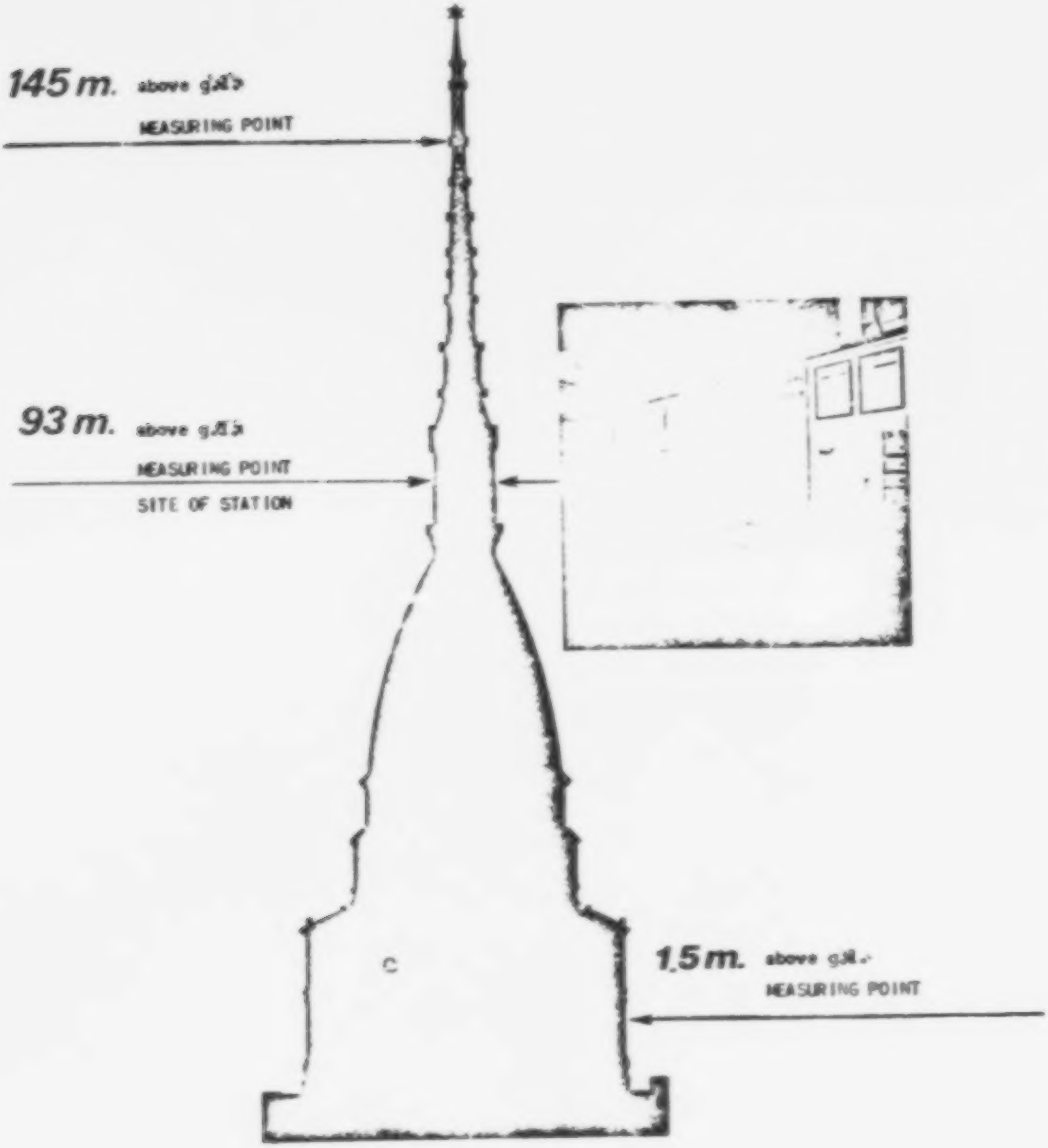

TABLE 2 - FIAT MONITORING NETWORK IN TURIN

MEASURED PARAMETERS	MONITORING STATIONS					
	V.Lagrange	Mirafiori	Ferriere	Mole Antonelliana	Porta Nuova	Piazza Statuto
SO_2	X	X	X	X		
Particulates	X	X	X	X		
NO_x	X	X	X	X		
NO_2	X			X		
CO	X	X	X	X	X	X
THC	X			X		
CH_4	X			X		
Ozone				X		
P.A.N.				X		
Temperature	X	X	X	X		
Humidity	X	X	X	X		
Wind direction	X	X	X	X		
Wind speed	X	X	X	X		

TABLE 3

PERCENT DISTRIBUTION OF DAILY AVERAGES AND MAXIMUM HOURLY VALUES RECORDED FROM 1971 TO 1974.

Number of valid data : 1991

SO_2 content, ppm	Average values, %	Max hourly values, %
0 - 0.02	2.1	0.2
0.02 - 0.05	9.9	2.0
0.05 - 0.10	22.7	8.8
0.10 - 0.15	17.5	10.9
0.15 - 0.20	11.2	9.8
0.20 - 0.30	18.8	18.7
0.30 - 0.40	8.4	12.6
0.40 - 0.50	5.2	10.5
0.50 - 0.60	1.1	7.2
0.60 - 0.70	2.2	7.1
0.70 - 0.80	0.4	3.2
0.80 - 0.90	0.45	3.0
> 0.90	0.05	5.0

FIG. 3 - TURIN AIR POLLUTION MONITORING NETWORK

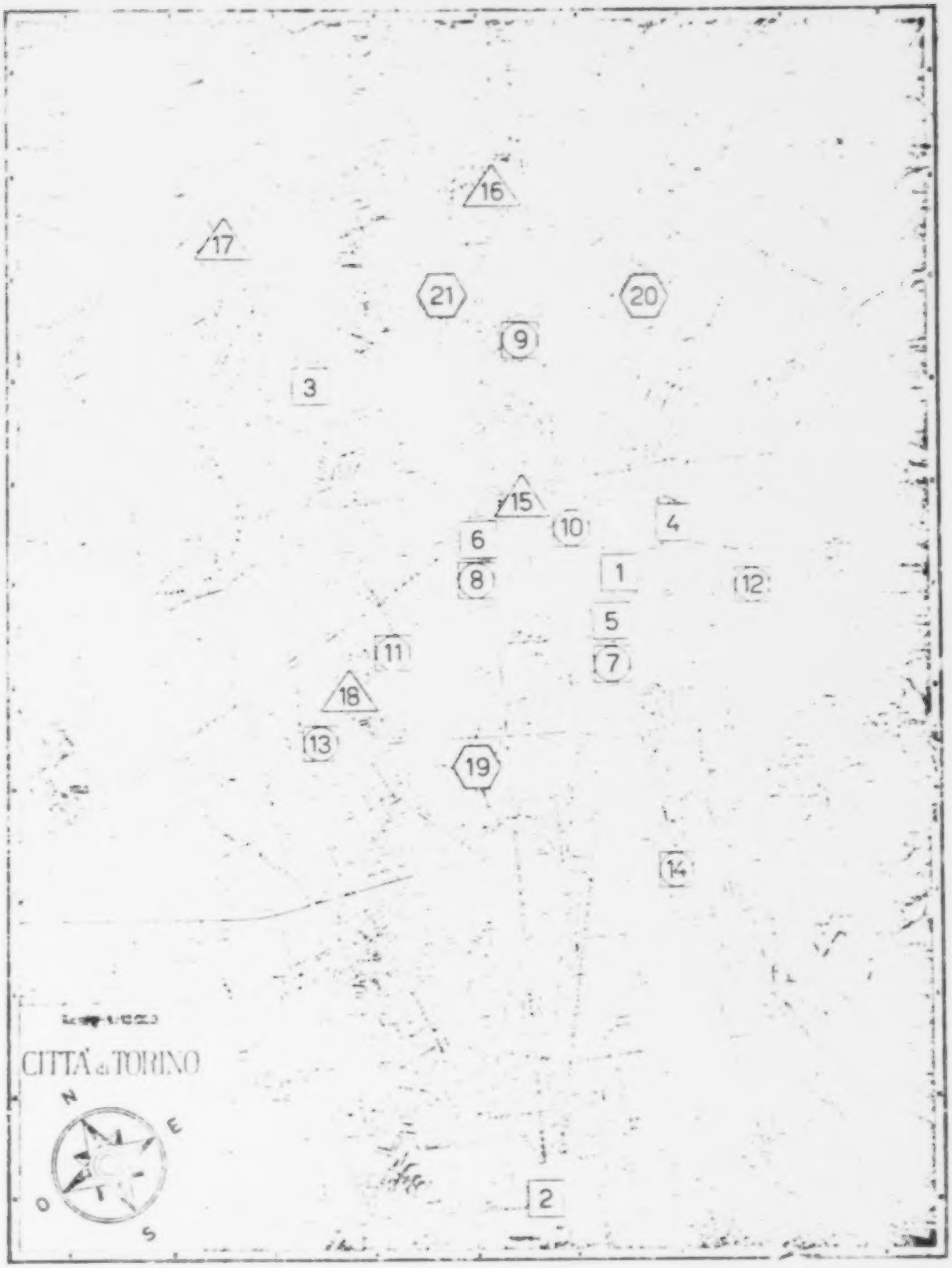

FIAT STATIONS

1) V. Lagrange

2) Mirafiori

3) Ferriere

4) Mole Antonelliana
5) Porta Nuova (CO)
6) P.za Statuto (CO)
7÷14 Pb sampling points.

MUNICIPALITY STATIONS

15) V. Consolata, 10

16) C. Vercelli, 236

17) Str. Aeroporto 9

PROVINCE ADM. STATIONS

19) V. Braccini, 11

20) V. Ponchielli, 56

21) C. Venezia, 29

Preceding page blank

FIG. 4 - SULPHUR DIOXIDE

Seasonal variations

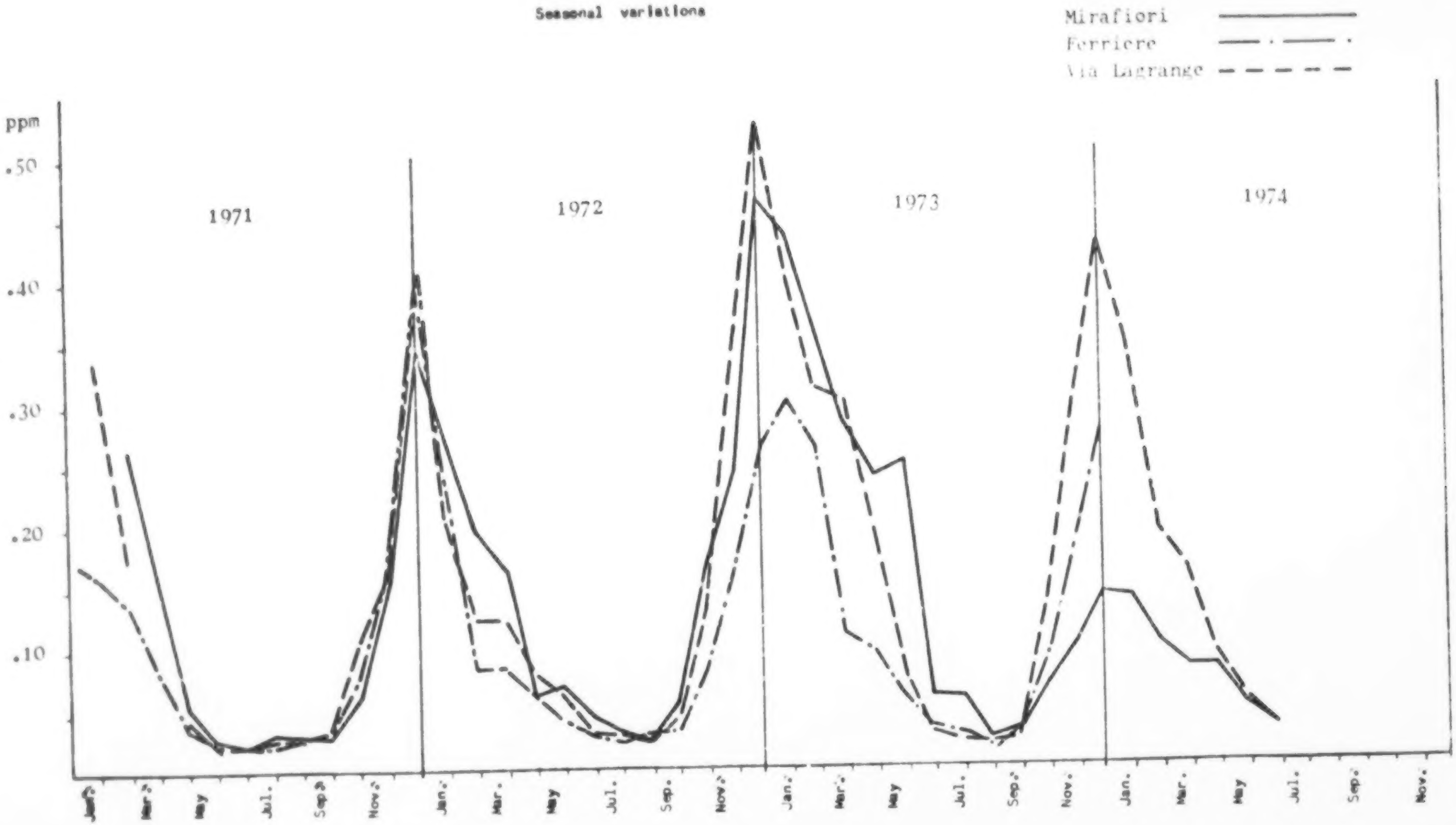

TABLE 4

SULPHUR DIOXIDE PATTERN 1971 TO 1974						
Yearly averages ppm				% variations		
1971	1972	1973	1974	71-72	72-73	73-74
0.104	0.125	0.158	0.112	+20.2	+26.4	-29.0

TABLE 5

PERCENT DISTRIBUTION OF DAILY AVERAGE AND MAXIMUM HOURLY VALUES RECORDED FROM 1971 TO 1974;		
Number of valid data : 3125		
Particulate content, mg/m^3	Average values , %	Max hourly values, %
0 - 0.05	0.3	0.1
0.05 - 0.10	11.1	0.6
0.10 - 0.15	26.5	7.6
0.15 - 0.20	15.2	11.6
0.20 - 0.30	29.0	28.8
0.30 - 0.40	8.5	17.1
0.40 - 0.50	3.7	13.8
0.50 - 0.60	1.6	7.2
0.60 - 0.70	0.5	5.0
0.70 - 0.80	0.1	3.0
> 0.80	0.2	5.3

FIG. 5 - PARTICULATES

Seasonal variations

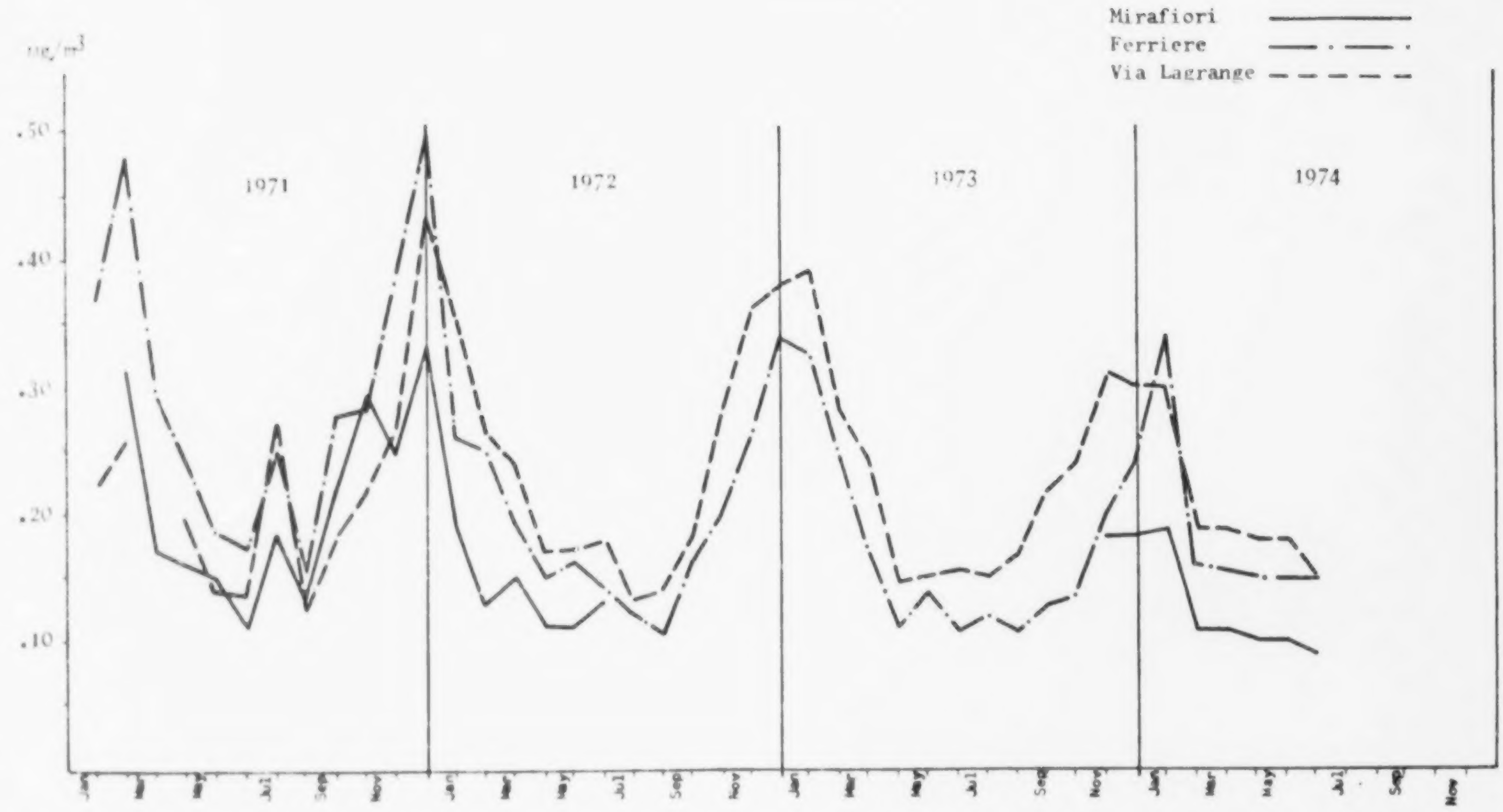

TABLE 6

PARTICULATES PATTERN 1971 TO 1974						
YEARLY AVERAGES Mg/m^3				% VARIATIONS		
1971	1972	1973	1974	71-72	72-73	73-74
0.233	0.190	0.198	0.190	-18.5	+ 4.2	- 4.1

TABLE 7

PERCENT DISTRIBUTION OF DAILY AVERAGE AND MAXIMUM HOURLY VALUES RECORDED FROM 1971 TO 1974		
Number of valid data : 3245		
NO_x content, ppm	Average values, %	Max hourly values, %
0 - 0.05	2.6	0.1
0.05 - 0.10	21.0	3.2
0.10 - 0.15	30.8	7.6
0.15 - 0.20	9.1	11.0
0.20 - 0.30	20.1	23.1
0.30 - 0.40	9.4	22.7
0.40 - 0.50	4.6	7.6
0.50 - 0.60	1.7	8.0
0.60 - 0.70	0.6	6.0
0.70 - 0.80	0.1	2.9
0.80 - 0.90	-	3.0
0.90 - 1.0	-	1.9
> 1.0	-	2.5

FIG. 6 - NITROGEN OXIDES

Seasonal variation

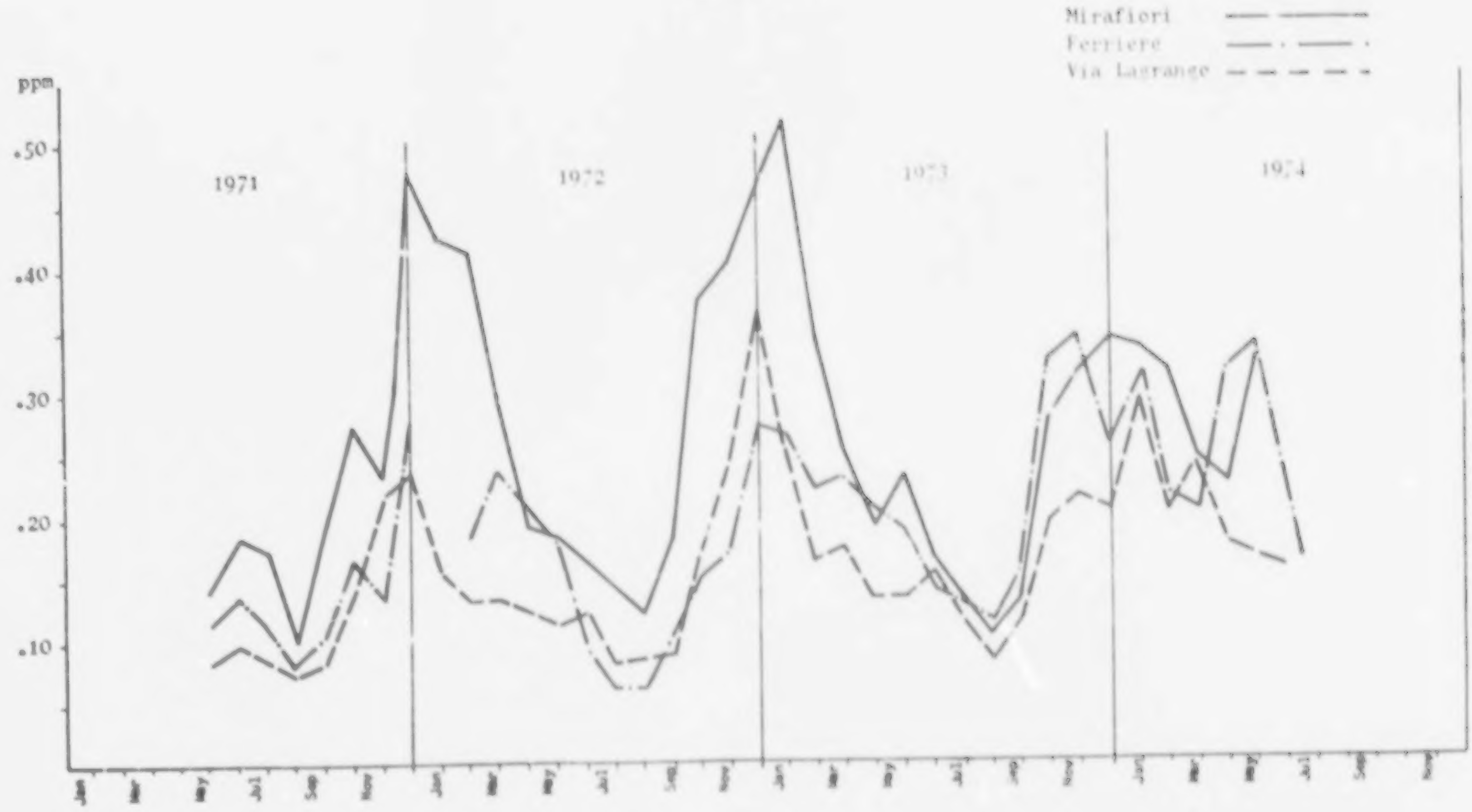

TABLE 8

NITROGEN OXIDES PATTERN 1971 TO 1974

Yearly averages ppm				% variations		
1971	1972	1973	1974	71-72	72-73	73-74
0.172	0.193	0.205	0.242	+12.2	+ 6.2	+ 18

PERCENT DISTRIBUTION OF DAILY AVERAGE, MAXIMUM HOURLY VALUES AND MAXIMUM VALUES OF 8 AND 12 12 HOUR PERIODS RECORDEND IN 1971 - 1974.

Average daily and max hourly values			Max values of 8 and 12 hour periods		
Number of valid data : 4329			Number of valid date : 4354		
CO content ppm	Percent of recorded average values	Percent of recorded max hourly values	CO content ppm	Percent groups max 8 hours	Percent groups max 12 hours
0 - 5	14.9	1.3	0 - 5	4.4	5.0
5 - 10	49.2	18.6	5 - 10	39.2	43.6
10 - 15	19.6	26.8	10 - 15	27.4	26.0
15 - 20	8.2	19.0	15 - 20	11.5	11.0
20 - 30	7.7	14.5	20 - 30	12.5	11.4
30 - 40	0.4	11.8	30 - 40	4.1	2.6
40 - 50	-	4.8	40 - 50	0.8	0.15
50 - 60	-	1.6	50 - 60	0.05	0.05
> 60	-	0.7	> 60	0.05	-

FIG. 7 - CARBON MONOXIDE

Seasonal variations

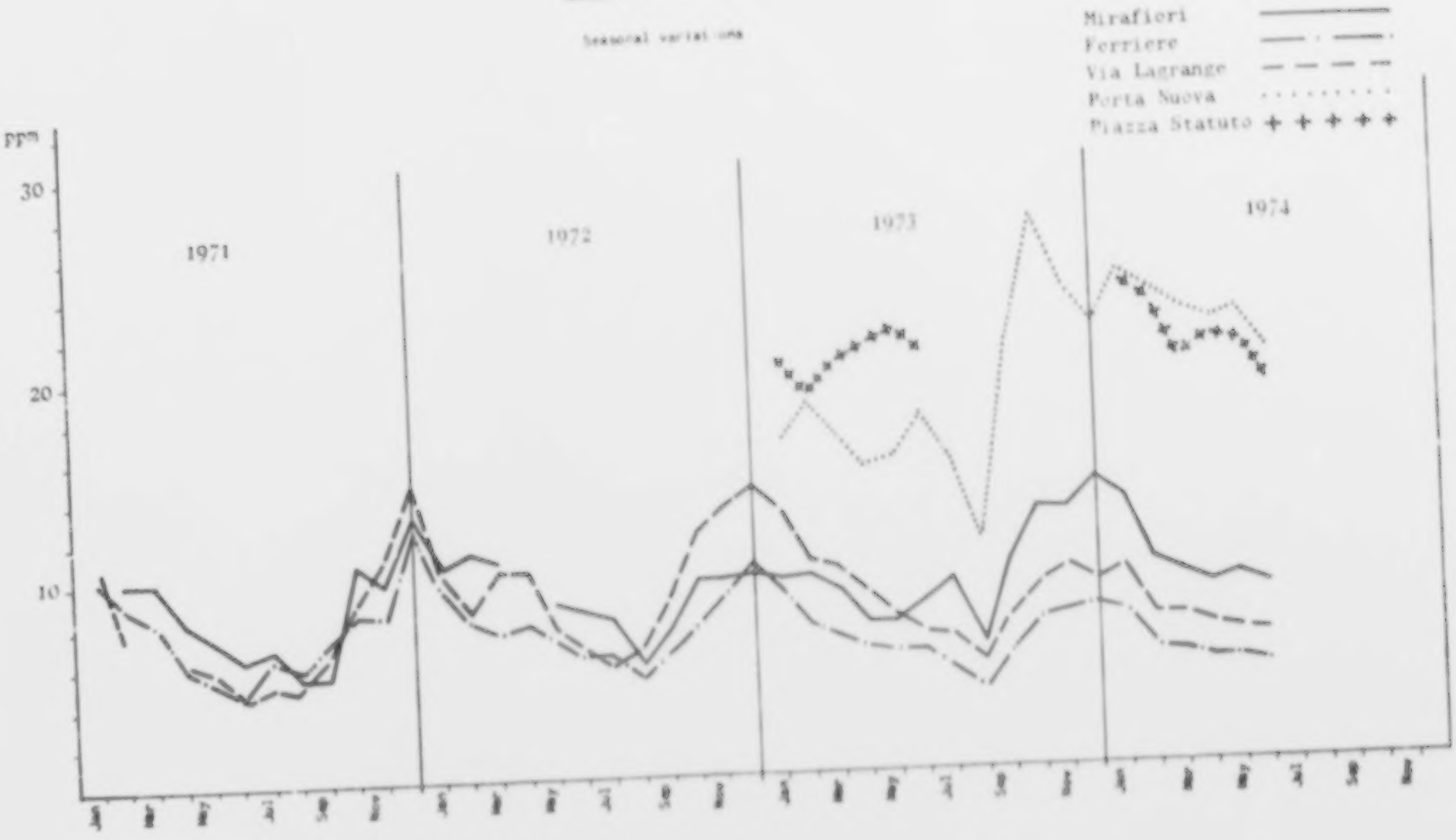

TABLE 10

CARBON MONOXIDE PATTERN 1971 TO 1974						
Yearly averages ppm				% variations		
1971	1972	1973	1974	71-72	72-73	73-74
7.8	8.5	8.1	7.4	+ 9.0	- 4.7	- 8.5

TABLE 11

PERCENT DISTRIBUTION OF DAILY AVERAGE AND MAXIMUM HOURLY VALUES MEASURED AT V. LAGRANGE STATION IN THE FIRST HALF OF 1974.		
Number of valid data : 181		
THC content, ppm	Average values, %	Max hourly values, %
0 - 0.25	0	0
0.25 - 0.5	1.1	0
0.5 - 1.0	8.3	2.8
1.0 - 2.0	38.7	11.1
2.0 - 3.0	43.6	25.9
3.0 - 4.0	7.7	30.4
4.0 - 5.0	0.6	16.5
5.0 - 6.0	-	11.1
> 6.0	-	2.2

TABLE 12

PERCENT DISTRIBUTION OF DAILY AVERAGE AND MAXIMUM HOURLY VALUES MEASURED AT V. LAGRANGE STATION IN THE FIRST HALF OF 1974.

Number of valid data : 181

HC Content, ppm	Average values, %	Max hourly values, %
0 - 0.25	3.9	0
0.25 - 0.5	33.1	6.6
0.6 - 1.0	55.3	21.0
1.0 - 2.0	6.0	49.2
2.0 - 3.0	1.7	17.1
3.0 - 4.0	-	3.3
4.0 - 5.0	-	2.2
5.0 - 6.0	-	0.6
> 6.0	-	-

FIG. 8 - TYPICAL POLLUTION PATTERN DEC 73 - MAR 74 RECORDED IN WEEKDAYS, HOLIDAY EVES AND HOLIDAY WITHOUT TRAFFIC

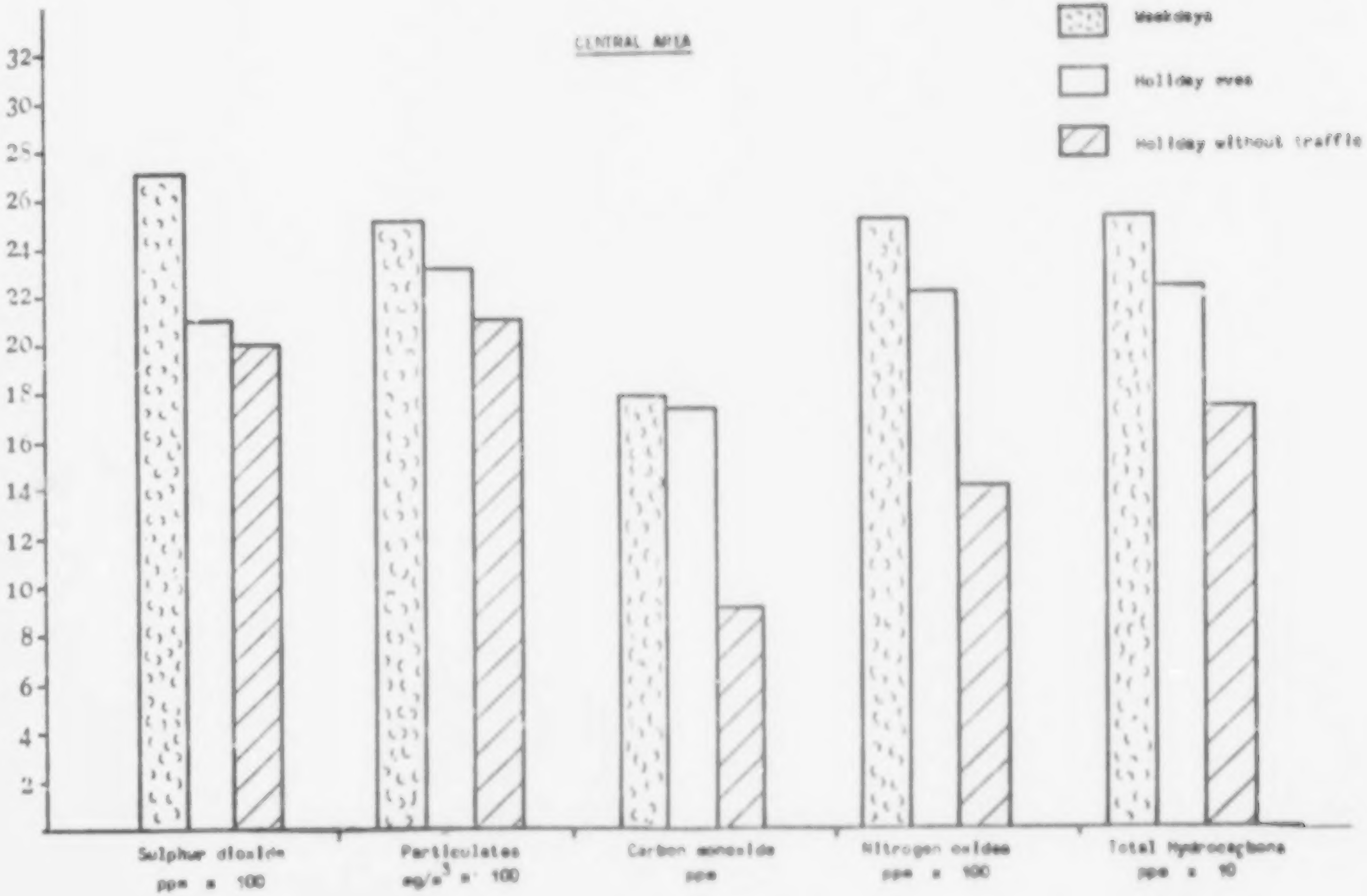

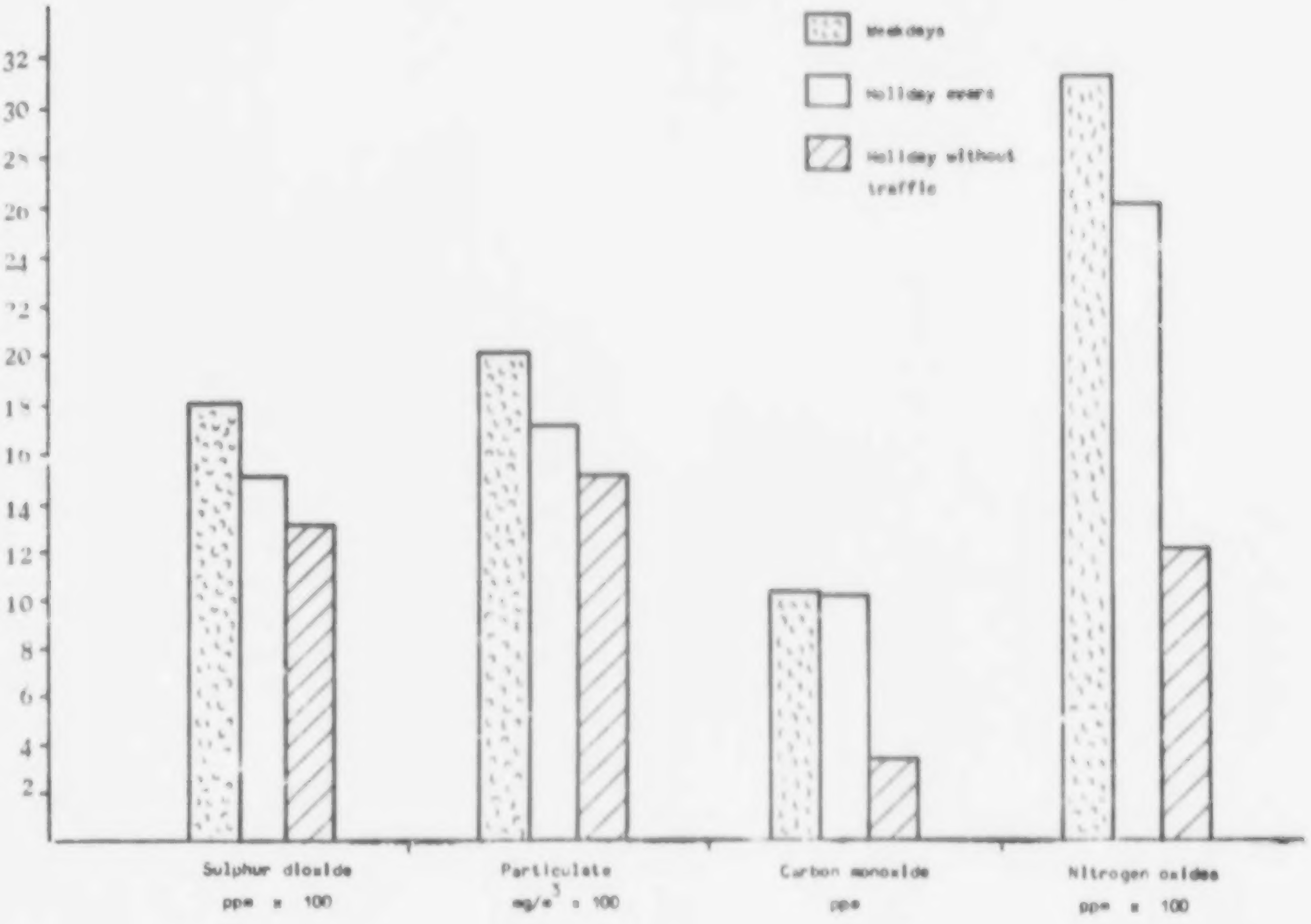

FIG. 9 - TYPICAL POLLUTION PATTERN DEC/73 - MAR/74 RECORDED IN WEEKDAYS, HOLIDAY EVERS, AND HOLIDAY WITHOUT TRAFFIC.

TABLE 13

PERCENT VARIATIONS OF POLLUTIONS ON WEEK-DAYS, HOLIDAY EVES AND HOLYDAYS WITHOUT TRAFFIC (CENTRAL AREA)

POLLUTANTS		DAYS				
		Week-days	Holiday eves	Holidays	Week-days / holidays	Week-days / holiday eves
SO_2	ppm	0.27	0.21	0.20	- 24.[illegible]	- 22.2
PARTICULATES	mg/m^3	0.25	0.23	0.21	- 16.0	- 8.0
CO *	ppm	17.6	17.2	9.0	- 48.9	- 2.3
NO_x	ppm	0.25	0.22	0.14	- 42.8	- 14.0
THC	ppm	2.5	2.2	1.7	- 32.0	- 12.0

TABLE 14

Percent variations of pollution on week-day, holiday ever and holidays without traffic (Suburban and industrial areas)>

POLLUTANTS		DAYS				
		Week-days	Holiday eves	Holidays	Week-days / holidays	Week-days / holiday-eves
SO_2	ppm	0.18	0.15	0.13	- 27.8	- 16.7
PARTICULATES	mg/m^3	0.20	0.17	0.15	- 23.1	- 12.5
CO	ppm	10.2	10.1	3.3	- 67.7	- 1.0
NO_x		0.31	0.26	0.12	- 60	- 15.2

FIG. 10 - VIA LAGRANGE STATIONS

Typical pollution pattern in a holiday without traffic (Sunday 10th February 1974)

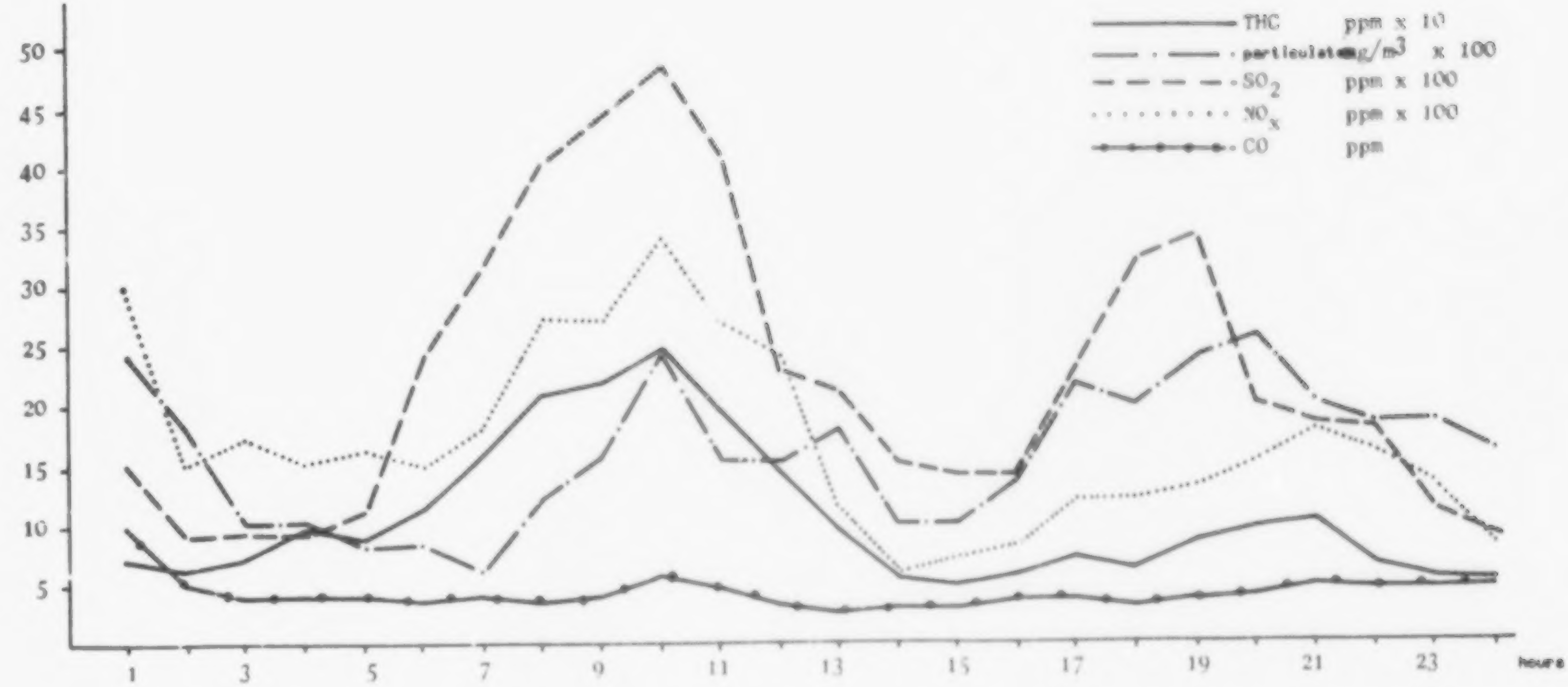

FIG. 11 - PERCENT VARIATION OF POLLUTION AT ELEVATED LEVELS REFERRED TO MEAN CONCENTRATION AT GROUND LEVEL.

- WINTER MONTHS -

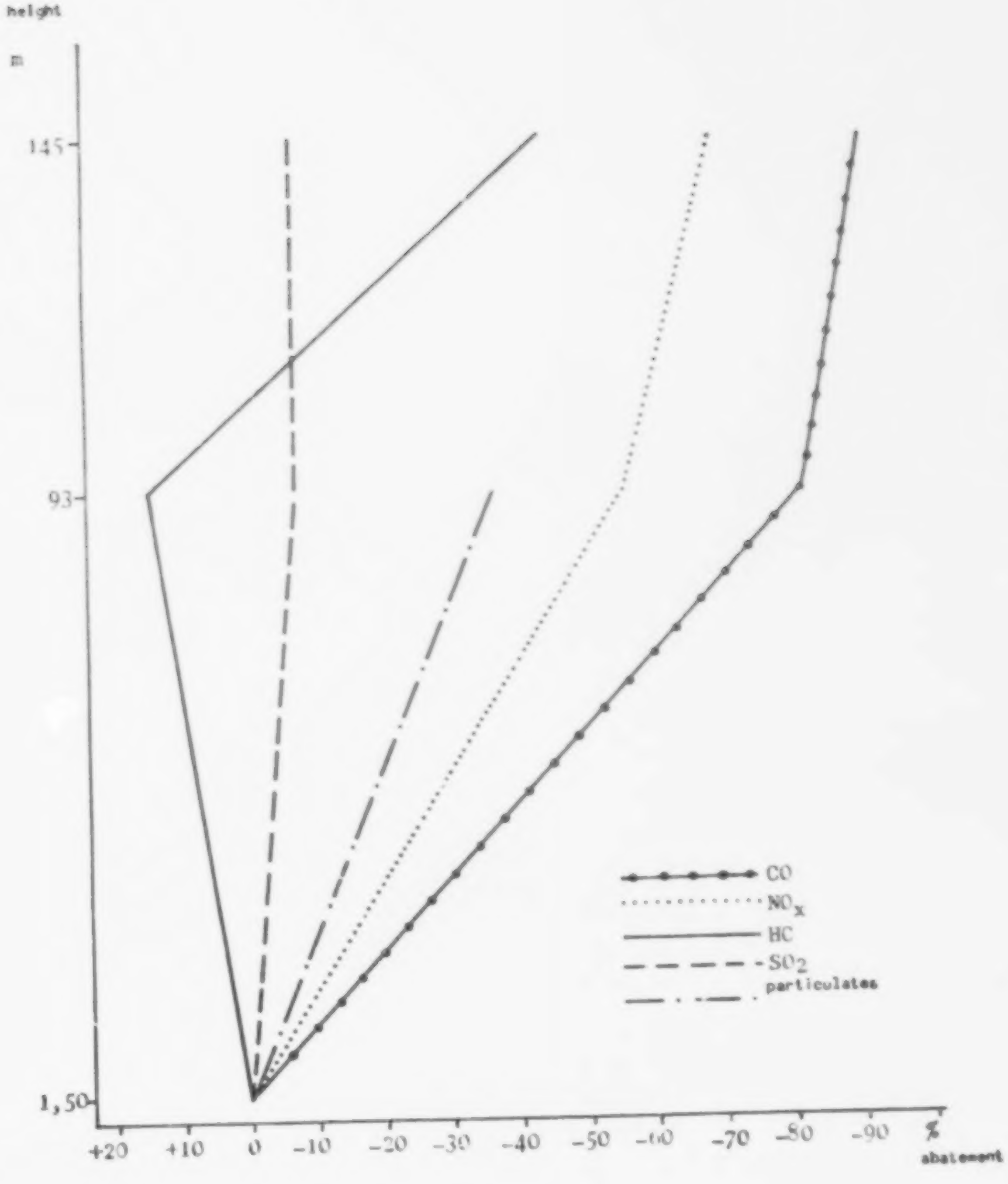

FIG. 12 - PERCENT VARIATION OF POLLUTION AT ELEVATED LEVELS REFERRED TO MEAN CONCENTRATION AT GROUND LEVEL #

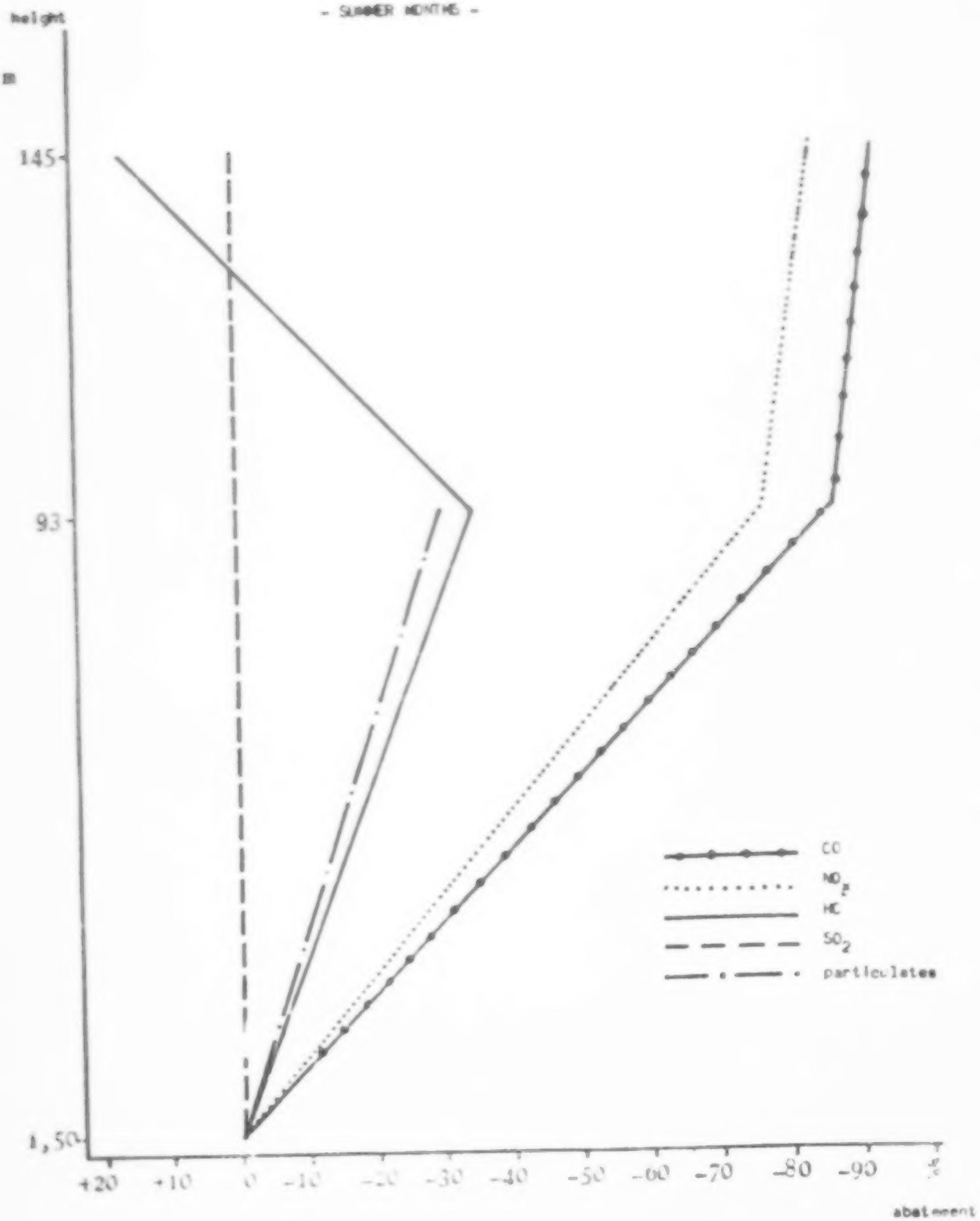

TABLE 15

POLLUTION LEVELS MEASURED AT GROUND AND ELEVATED LEVELS (Months : FEBRUARY - MARCH)

Sampling point	POLLUTANTS				
	CO ppm	NO_x ppm	HC ppm	SO_2 ppm	Polveri mg/m^3
1,50 m *	13.2	0.23	0.7	0.13	0.15
93 m	2.3	0.10	0.8	0.12	0.095
145 m	2.1	0.07	0.4	0.12	–

* Average value recorded in the whole urban area

TABLE 16

POLLUTION LEVELS MEASURED AT GROUND AND ELEVATED LEVELS (Months : JUNE - JULY)

Sampling point	POLLUTANTS				
	CO ppm	NO_x ppm	HC ppm	SO_2 ppm	Polveri mg/m^3
1,50 m	11.7	0.12	0.6	0.03	0.14
93 m	1.5	0.02	0.4	0.03	0.085
145 m	1.0	0.03	0.7	0.03	–

* Average value recorded in the wole urban area

FIG. 13

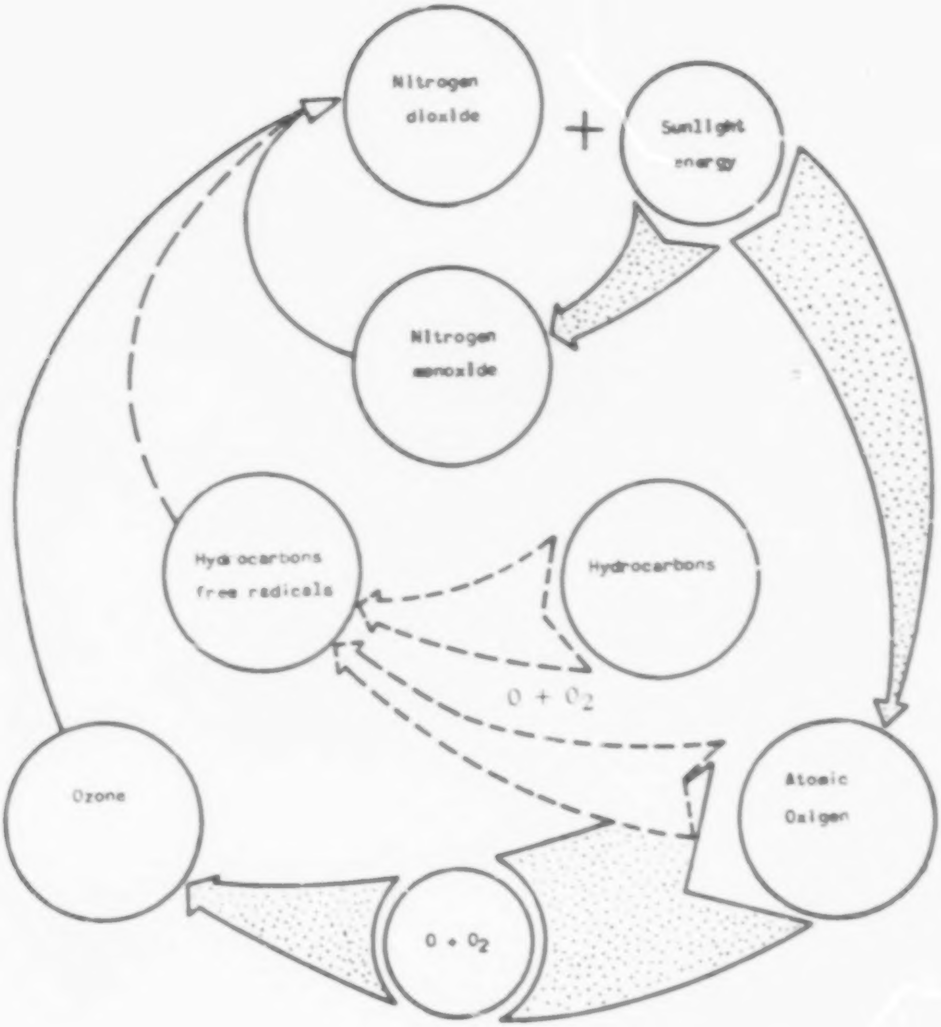

from : Air Quality Criteria for Photochemical Oxidants and Related Hydrocarbons n° 29 - NATO CCMS

NO_x and NO_2 CONCENTRATIONS RECORDED AT GROUND LEVEL V. LAGRANGE STATION

MONTHLY AVERAGES

Table 17

Pollutant	Months 1973					
	July	August	September	October	November	December
NO_x ppm	0.11	0.08	0.11	0.19	0.21	0.20
NO_2 ppm	0.048	0.043	0.038	0.034	0.032	0.029

Table 18

Pollutant	Months 1974					
	January	February	March	April	May	June
NO_x ppm	0.29	0.20	0.24	0.17	0.16	0.15
NO_2 ppm	0.027	0.026	0.068	0.075	0.066	0.043

Table 19

Pollutant	NO_x ppm	NO_2 ppm
Yearly average (July 73 – June 74)	0.173	0.044

TABLE 20

NO_2 POLLUTION CONCENTRATIONS MEASURED AT GROUND AND ELEVATED LEVELS.

Months	February	March	April	May	June
Ground measurements (V. Lagrange station) ppm	0.026	0.046	0.075	0.067	0.044
Measurements at elevated levels (Mole Antonelliana stat) ppm	0.015 *	0.011 **	0.012 *	0.013 **	0.007 *

* Measurements at 93 m a.g.

** Measurements at 145 m a.g.

TABLE 21

COMPARISON BETWEEN VALUES MEASURED AT GROUND AND ELEVATED LEVELS AT STATIONS ON MOLE ANTONELLIANA.

DATE	HOUR	Hourly averages ppb	
		Ground level (m. 1.60)	Height above ground (93 and 145 m)
5-6-74	9,00 - 10,00	10	10
5-6-74	14,00 - 15,00	36	38,2
7-6-74	9,00 - 10,00	15,5	16
7-6-74	14,00 - 15,00	43	45
12-6-74	9,00 - 10,00	1,5	1.5
12-6-74	14.00 - 15,00	79	80
1-7-74	9,00 - 10,00	3	3
1-7-74	14,00 - 15,00	98	100
11-7-74	11,00 - 12,00	54,3	55,0
12-7-74	11,00 - 12,00	68,4	70,0
22-7-74	15,00 - 16,00	93,0	95
23-7-74	17,00 - 18,00	106	110
21-8-74	16,00 - 17,00	153	155
26-8-74	9,00 - 10,00	4	4
26-8-74	15,00 - 16,00	89	90
28-8-74	16,00 - 17,00	50,5	52

TABLE 22

Ozone ppb

Pollution concentrations recorded at elevated levels on Mole Antonelliana stations

1974	Monthly average	Maximum daily average	Minimum daily average	Maximum hourly values	Minimum hourly values
February *	7.8	18.2	1.5	33	0.2
March **	12.3	22.5	4.3	50	1
April *	20	29	7	60	2
May **	16.5	27	9	48	2
June *	26.6	48	7	90	2
July **	33.6	54	20	115	2
August *	43.1	65	20	155	2

* Measurement at 93 m a.g.

** Measurement at 145 m a.g.

FIG. 14 - COMPARISON BETWEEN O_3 AND NO_2 MONTLY AVERAGES RECORDED AT ELEVATED LEVELS

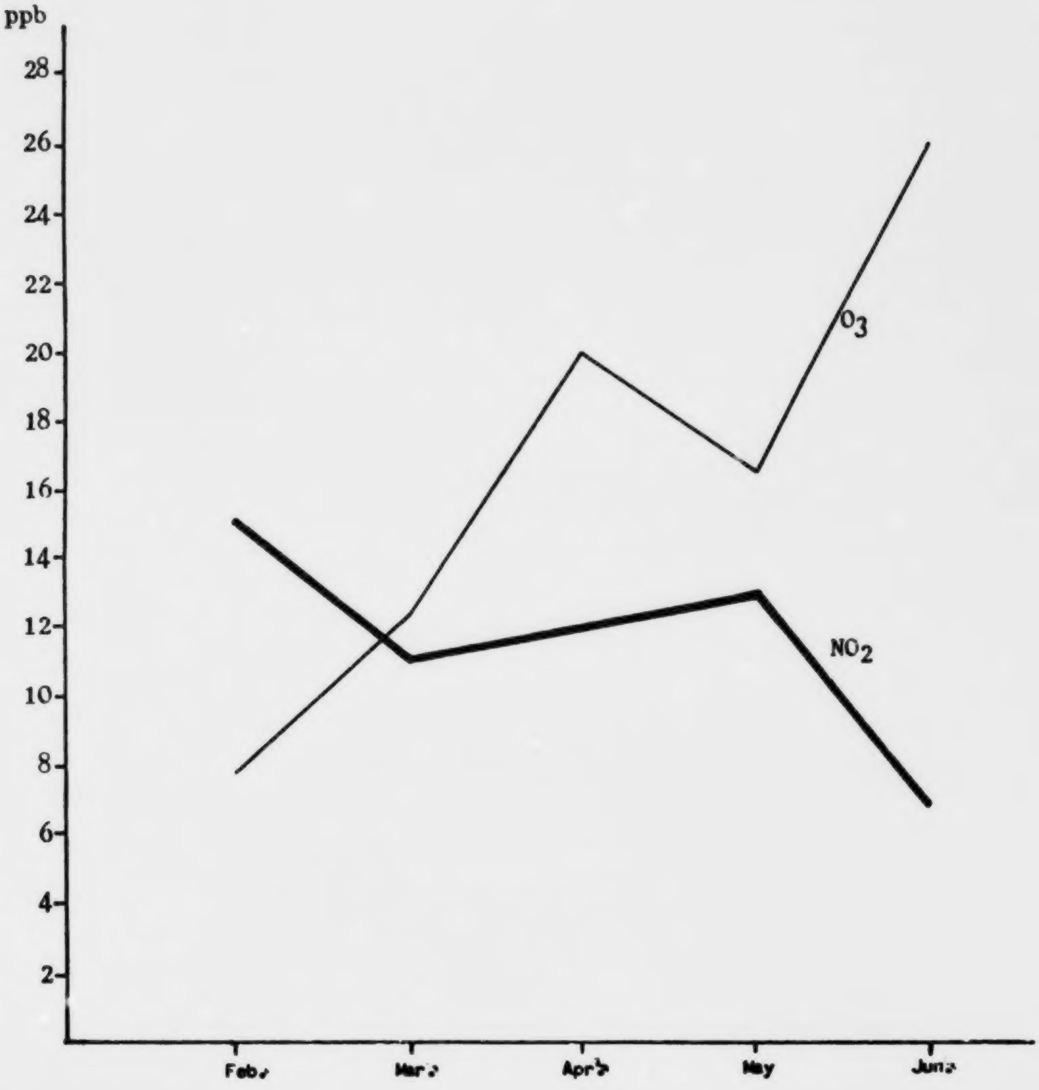

FIG. 15 - TYPICAL PATTERN OF NO, NO_2 AND O_3 IN TURIN ATMOSPHERE

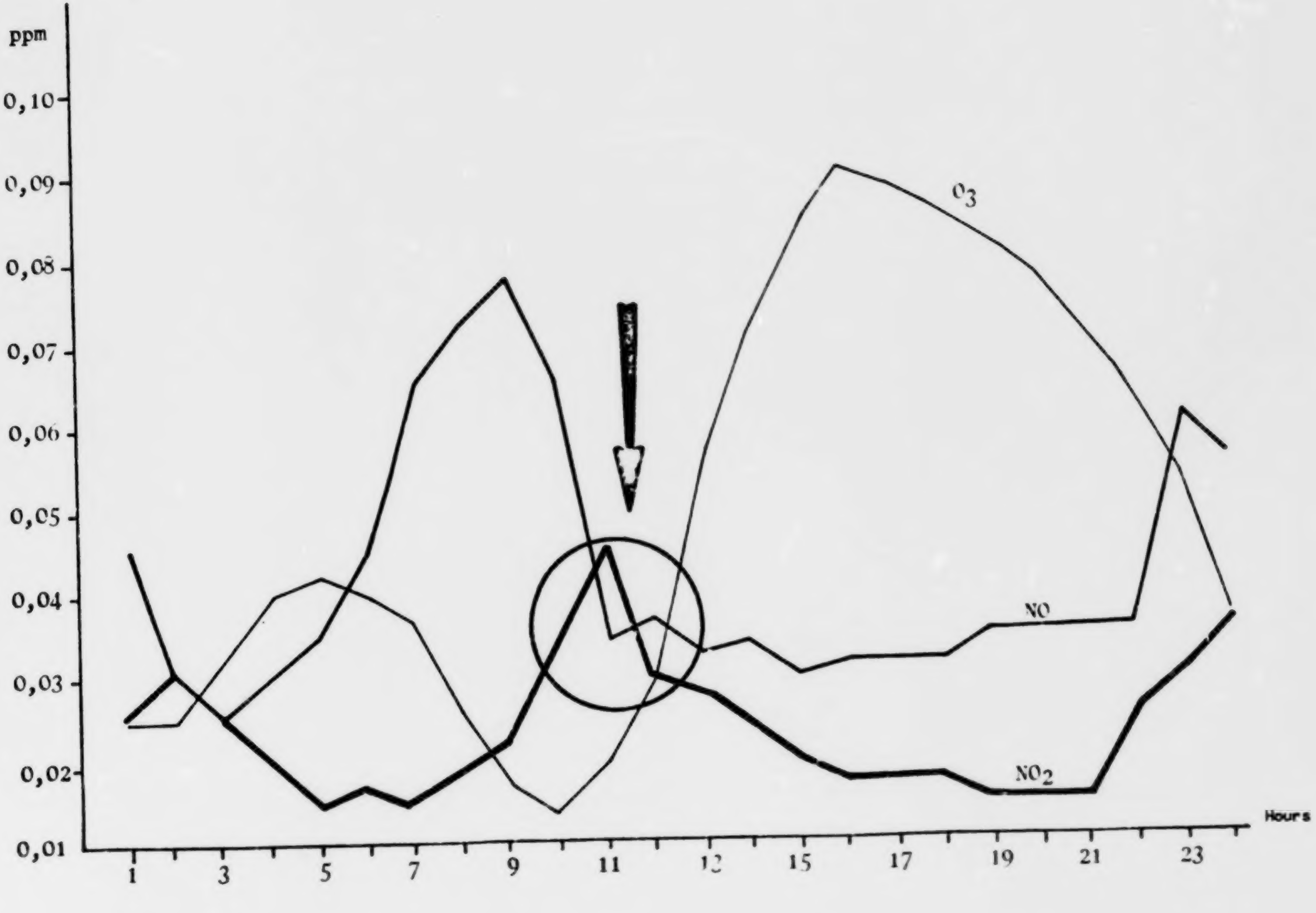

FIG. 16 - TYPICAL PATTERN OF NO, NO_2 AND O_3 IN LOS ANGELES ATMOSPHERE

(from CCMS - Air quality criteria for Photochemical Oxidants n° 29)

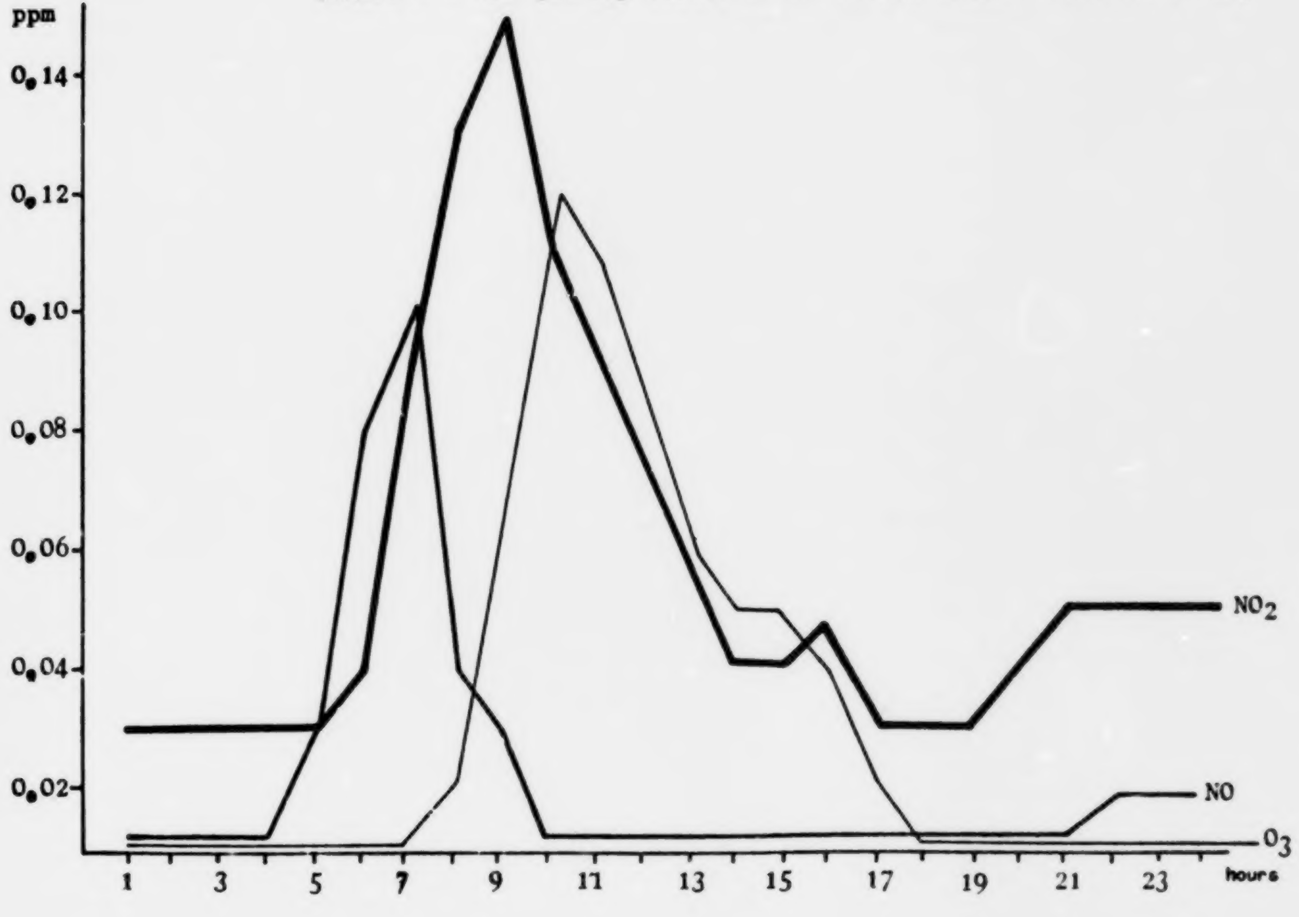

ENCL 5

MONTHS	TEMPERATURE (°C)											
	1971			1972			1973			1974		
	Mean	Min.	Max	Mean	Min.	Max	Mean	Min.	Max	Mean	Min.	Max
January	2,5	- 6,7	10,2	3,8	1,3	8,2	4,5	- 1,3	10,0	5,0	- 1,96	12,73
February	6,7	2,6	11,8	7,8	3,7	12,1	8,0	3,7	12,1	6,8	- 0,35	12,58
March	6,9	- 1,7	14,0	9,9	2,9	16,9	11,7	4,9	17,6	9,4	- 0,03	15,92
April	15,7	9,7	22,2	11,6	6,7	20,3	13,5	5,3	19,5	12,9	7,04	17,59
May	17,6	11,1	24,2	15,3	10,3	25,5	19,8	12,8	25,4	17,8	9,03	26,16
June	21,4	13,9	27,5	20,3	14,1	26,9	23,7	12,3	29,9	22,2	15,67	27,27
July	24,3	19,1	29,6	25,2	16,7	30,6	25,7	18,3	33,0	-	-	-
August	24,4	21,8	28,1	24,8	18,1	30,6	26,1	18,5	30,9	-	-	-
September	19,9	15,1	25,1	20,2	9,8	22,2	21,0	13,0	27,2	-	-	-
October	12,5	8,3	18,6	14,3	11,3	18,8	13,9	5,1	20,1	-	-	-
November	9,6	1,4	13,5	9,4	4,2	16,6	7,9	- 1,2	14,4	-	-	-
December	5,7	0,5	9,7	5,2	- 1,7	11,7	3,4	- 0,6	10,6	-	-	-

ENCL. 2

MONTHS	RELATIVE HUMIDITY (%)											
	1971			1972			1973			1974		
	Mean	Min.	Max	Mean	Min.	Max	Mean	Min.	Max	Mean	Min.	Max
January	75,7	42,6	98,8	76,5	65,6	97,6	87,2	51,0	99,0	86,0	50,1	100
February	64,8	[illegible]	97,5	78,0	35,1	98,6	63,0	32,9	94,8	80,3	37,5	100
March	71,5	44,7	95,0	69,5	41,8	96,4	61,8	41,6	90,6	79,0	40,0	100
April	70,6	40,0	93,1	57,2	37,8	96,4	56,8	32,8	100	70,7	44,0	99,4
May	76,6	56,1	95,7	51,0	31,5	93,0	71,8	34,7	97,7	67,9	20,7	93,3
June	68,9	42,1	89,2	68,3	49,4	95,2	71,0	48,0	98,0	66,0	38,1	94,9
July	67,5	49,9	83,4	56,0	45,8	82,7	70,0	50,2	98,2	-	-	-
August	72,0	57,3	88,5	59,2	37,7	95,8	75,0	65,5	90,6	-	-	-
September	72,6	49,7	92,7	67,5	38,7	96,9	78,7	56,7	96,0	-	-	-
October	69,0	57,6	82,1	70,5	43,8	99,2	79,4	60,1	100	-	-	-
November	79,0	25,9	96,4	76,0	35,2	98,8	80,3	40,1	100	-	-	-
December	76,5	52,0	99,8	79,0	64,4	99,0	78,6	31,2	100	-	-	-

MONTHS	WIND SPEED						(m/s)					
	1971			1972			1973			1974		
	Mean	Min	Max	Mean	Min.	Max	Mean	Min.	Max	Mean	Min.	Max
January	1,4	0,7	2,6	1,4	0,8	2,6	1,2	0,6	2,1	1,3	0,73	3,12
February	1,5	0,3	3,5	1,4	0,6	3,1	1,8	0,7	8,7	1,6	0,90	3,40
March	1,6	0,9	4,1	1,6	1,0	5,9	1,6	0,8	3,4	1,5	0,96	2,40
April	1,5	0,8	3,1	1,7	0,9	4,8	1,8	0,9	4,7	1,6	0,90	2,80
May	1,4	0,8	3,1	1,5	0,8	4,8	1,5	0,9	2,6	1,8	1,1	4,0
June	1,4	0,9	2,5	1,3	0,5	2,4	1,6	1,0	3,6	1,7	1,2	3,8
July	1,5	1,0	2,8	1,4	0,9	2,8	1,4	0,5	2,4	-	-	-
August	1,4	0,7	2,1	0,9	0,5	1,4	1,2	0,6	1,9	-	-	-
September	1,4	0,3	3,1	1,4	0,9	3,5	1,2	0,8	2,6	-	-	-
October	0,9	0,5	2,1	1,2	0,7	2,5	1,2	0,7	2,2	-	-	-
November	1,5	0,8	4,1	1,2	0,6	4,0	1,2	0,6	2,2	-	-	-
December	1,1	0,3	2,4	1,1	0,6	2,4	1,5	0,6	6,3	-	-	-

ENCL. 4 - WIND DIRECTION

Miraflori Station

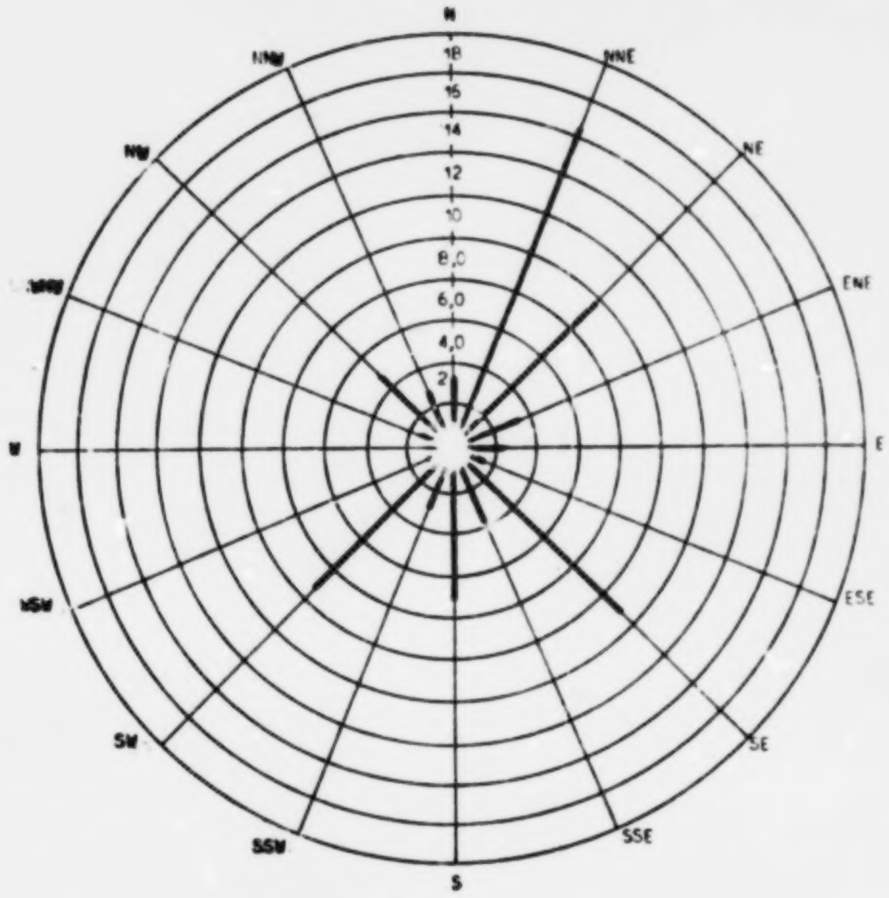

Variable direction : 18,9 %

[illegible] ≥ 5 - WIND DIRECTION

Ferriere Station

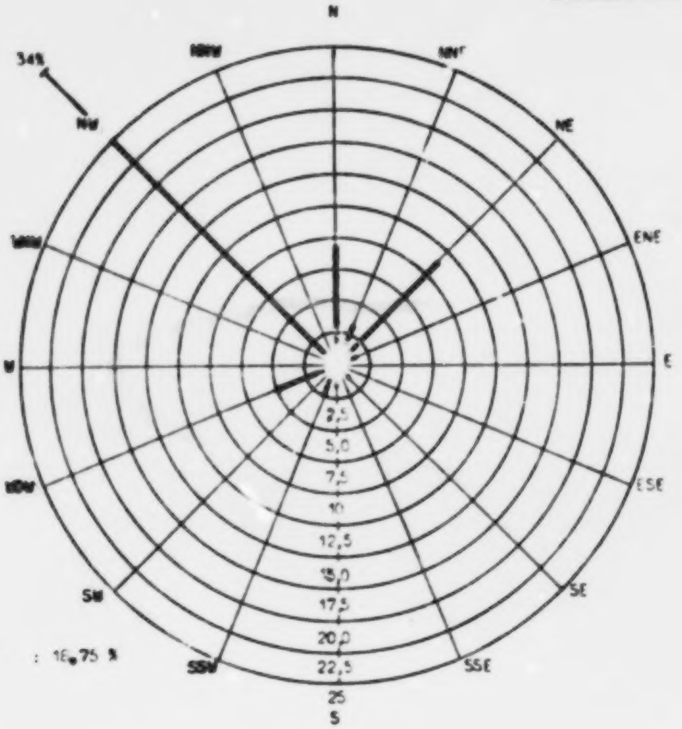

Variable direction : 18,75 %

V> Lagrange station

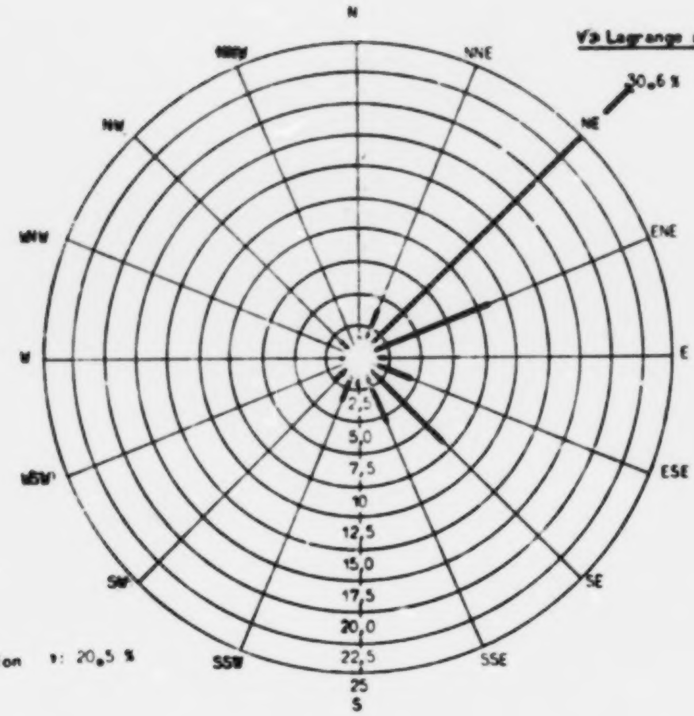

Variable direction : 20,5 %

MONTHS	SULPHUR DIOXIDE ppm - MONTHLY AVERAGES											
	V. Lagrange station				Miraflori station				Ferriere station			
	1971	1972	1973	1974	1971	1972	1973	1974	1971	1972	1973	1974
January	0,320	0,200	0,429	0,340	-	0,260	0,430	0,141	0,156	0,230	0,296	-
February	0,170	0,120	0,307	0,190	0,258	0,190	0,350	0,099	0,131	0,080	0,258	-
March	-	0,120	0,295	0,160	0,144	0,160	0,280	0,079	0,080	0,080	0,105	-
April	0,040	0,076	0,185	0,094	0,050	0,060	0,236	0,081	0,036	0,060	0,091	-
May	0,020	0,058	0,073	0,052	0,025	0,065	0,246	0,051	0,023	0,038	0,056	-
June	0,019	0,027	0,029	0,029	0,020	0,041	0,057	0,029	0,021	0,026	0,031	-
July	0,021	0,026	0,022	-	0,028	0,026	0,054	-	0,019	0,022	0,025	-
August	0,022	0,033	0,018	-	0,027	0,022	0,023	-	0,027	0,024	0,017	-
September	0,026	0,043	0,025	-	0,025	0,050	0,023	-	0,025	0,028	0,031	-
October	0,100	0,130	0,136	-	0,060	0,160	0,099	-	0,074	0,080	0,096	-
November	0,150	0,350	0,295	-	0,150	0,240	0,130	-	0,170	0,160	0,184	-
December	0,390	0,520	0,324	-	0,340	0,460	0,170	-	0,380	0,260	0,280	-

ENCL. 7

MONTHS	SULPHUR DIOXIDE (ppm) - Monthly averages of maximum hourly values											
	V. Lagrange station				Miraflori station				Ferriere station			
	1971	1972	1973	1974	1971	1972	1973	1974	1971	1972	1973	1974
January	0,560	0,348	0,727	0,540	-	0,501	0,718	0,240	0,290	0,435	0,519	-
February	0,380	0,220	0,669	0,370	0,590	0,343	0,662	0,200	0,280	0,149	0,467	-
March	-	0,121	0,585	0,350	0,390	0,160	0,511	0,180	0,180	0,160	0,243	-
April	0,080	0,150	0,405	0,210	0,110	0,285	0,472	0,180	0,090	0,167	0,210	-
May	0,024	0,093	0,131	0,110	0,030	0,104	0,334	0,110	0,040	0,056	0,082	-
June	0,020	0,037	0,060	0,060	0,028	0,061	0,105	0,060	0,030	0,027	0,046	-
July	0,026	0,034	0,052	-	0,030	0,033	0,093	-	0,020	0,032	0,038	-
August	0,027	0,030	0,038	-	0,030	0,032	0,041	-	0,031	0,032	0,029	-
September	0,030	0,075	0,050	-	0,030	0,090	0,063	-	0,030	0,044	0,057	-
October	0,200	0,250	0,290	-	0,170	0,315	0,211	-	0,150	0,154	0,205	-
November	0,290	0,600	0,540	-	0,320	0,443	0,275	-	0,360	0,316	0,343	-
December	0,660	0,772	0,590	-	0,610	0,774	0,346	-	0,680	0,453	0,458	-

MONTHS	SULPHUR DIOXIDE (ppm)						Maximum daily average					
	V. Lagrange station				Miraflori station				Ferriere station			
	1971	1972	1973	1974	1971	1972	1973	1974	1971	1972	1973	1974
January	0,740	0,380	0,713	0,490	-	0,460	0,847	0,240	0,510	0,690	0,570	-
February	0,270	0,180	0,534	0,310	0,540	0,270	0,535	0,160	0,280	0,120	0,410	-
March	-	0,170	0,469	0,300	0,260	0,310	0,452	0,110	0,160	0,120	0,164	-
April	0,080	0,110	0,294	0,160	0,150	0,100	0,365	0,160	0,070	0,080	0,180	-
May	0,050	0,080	0,157	0,080	0,070	0,110	0,284	0,080	0,050	0,060	0,084	-
June	0,030	0,040	0,044	0,050	0,030	0,060	0,096	0,050	0,040	0,030	0,045	-
July	0,030	0,050	0,034	-	0,040	0,040	0,078	-	0,030	0,030	0,036	-
August	0,030	0,040	0,033	-	0,050	0,030	0,040	-	0,050	0,040	0,031	-
September	0,050	0,090	0,044	-	0,040	0,060	0,040	-	0,040	0,060	0,046	-
October	0,240	0,240	0,370	-	0,110	0,310	0,230	-	0,170	0,140	0,230	-
November	0,250	0,670	0,480	-	0,340	0,420	0,221	-	0,410	0,300	0,270	-
December	0,720	0,950	0,560	-	0,620	0,870	0,313	-	0,690	0,590	0,600	-

ENCL.: 9

MONTHS	SULPHUR DIOXIDE (ppm) Maximum hourly values											
	V. Lagrange station				Mirafiori station				Ferriere station			
	1971	1972	1973	1974	1971	1972	1973	1974	1971	1972	1973	1974
January	1,060	0,670	1,031	0,860	-	0,920	1,520	0,480	0,950	1,300	1,088	-
February	0,570	0,360	1,069	0,500	0,950	0,950	1,088	0,340	0,530	0,340	0,775	-
March	-	0,360	1,012	0,690	0,950	0,570	0,909	0,340	0,530	0,270	0,382	-
April	0,190	0,340	0,650	0,351	0,270	0,240	0,720	0,450	0,210	0,220	0,496	-
May	0,050	0,200	0,350	0,213	0,110	0,210	0,440	0,200	0,140	0,110	0,141	-
June	0,050	0,060	0,103	0,080	0,050	0,140	0,210	0,110	0,060	0,050	0,084	-
July	0,050	0,060	0,107	-	0,070	0,050	0,160	-	0,040	0,050	0,068	-
August	0,070	0,050	0,153	-	0,090	0,070	0,214	-	0,050	0,050	0,057	-
September	0,070	0,280	0,092	-	0,090	0,400	0,191	-	0,050	0,120	0,095	-
October	0,670	0,440	0,840	-	0,270	0,620	0,530	-	0,480	0,360	0,634	-
November	0,570	1,120	1,100	-	0,080	0,810	0,570	-	0,940	0,630	0,630	-
December	1,150	1,740	1,180	-	1,030	1,680	0,650	-	1,050	1,170	1,010	-

ENCL. 10

MONTHS	PARTICULATES (mg/m³) Montly averages											
	V.ª Lagrange station				Mirafiori station				Ferriere station			
	1971	1972	1973	1974	1971	1972	1973	1974	1971	1972	1973	1974
January	0,223	0,350	0,385	0,300	-	0,190	-	0,170	0,363	0,260	0,323	0,340
February	0,260	0,260	0,280	0,180	0,315	0,130	-	0,110	0,478	0,250	0,235	0,160
March	-	0,240	0,242	0,180	0,171	0,150	-	0,110	0,292	0,190	0,167	0,180
April	0,195	0,170	0,145	0,170	0,162	0,110	-	0,100	0,241	0,150	0,111	0,150
May	0,140	0,170	0,150	0,170	0,150	0,110	-	0,100	0,188	0,160	0,134	0,150
June	0,136	0,180	0,154	0,150	0,110	0,130	-	0,090	0,175	0,140	0,105	0,150
July	0,272	0,130	0,148	-	0,184	-	-	-	0,250	0,120	0,119	-
August	0,128	0,140	0,166	-	0,134	-	-	-	0,153	0,106	0,107	-
September	0,185	0,180	0,219	-	0,219	-	-	-	0,277	0,160	0,127	-
October	0,217	0,280	0,240	-	0,297	-	-	-	-	0,200	0,134	-
November	0,268	0,360	0,310	-	0,248	-	0,180	-	0,312	0,260	0,200	-
December	0,436	0,380	0,300	-	0,332	-	0,180	-	0,496	0,340	0,240	-

MONTHS	PARTICULATES (mg/m^3) - Monthly averages at maximum hourly values											
	V. Lagrange station				Miraflori station				Ferriere station			
	1971	1972	1973	1974	1971	1972	1973	1974	1971	1972	1973	1974
January	0,390	0,614	0,614	0,480	-	0,312	-	0,290	0,650	0,503	0,670	0,630
February	0,500	0,467	0,508	0,300	0,520	0,234	-	0,190	1,030	0,523	0,490	0,310
March	-	0,426	0,468	0,320	0,330	0,271	-	0,190	0,630	0,431	0,340	0,370
April	0,370	0,302	0,307	0,290	0,320	0,192	-	0,190	0,570	0,384	0,296	0,300
May	0,270	0,345	0,268	0,300	0,270	0,195	-	0,160	0,410	0,342	0,275	0,320
June	0,250	0,309	0,289	0,250	0,220	0,145	-	0,140	0,390	0,280	0,190	0,300
July	0,280	0,273	0,273	-	0,330	-	-	-	0,510	0,300	0,256	-
August	0,210	0,264	0,276	-	0,230	-	-	-	0,260	0,223	0,185	-
September	0,310	0,359	0,355	-	0,390	-	-	-	0,620	0,390	0,241	-
October	0,400	0,519	0,420	-	0,510	-	-	-	-	0,482	0,243	-
November	0,270	0,677	0,470	-	0,430	-	0,310	-	0,678	0,562	0,380	-
December	0,660	0,631	0,490	-	0,530	-	0,280	-	0,940	0,740	0,551	-

ENCL. 12

MONTHS	PARTICULATES (mg/m³)	-	Maximum daily average									
	V. Lagrange station				Miraflori station				Ferriere station			
	1971	1972	1973	1974	1971	1972	1973	1974	1971	1972	1973	1974
January	0,54	0,51	0,62	0,56	-	0,32	-	0,35	0,67	0,43	0,69	0,62
February	0,45	0,42	0,57	0,32	0,53	0,26	-	0,16	0,94	0,39	0,53	0,24
March	-	0,39	0,44	0,29	0,31	0,38	-	0,15	0,50	0,28	0,29	0,28
April	0,31	0,27	0,29	0,29	0,25	0,17	-	0,17	0,36	0,25	0,16	0,24
May	0,26	0,24	0,26	0,27	0,22	0,15	-	0,14	0,33	0,21	0,17	0,22
June	0,20	0,35	0,24	0,27	0,16	0,18	-	0,11	0,23	0,19	0,15	0,23
July	0,25	0,22	0,22	-	0,31	-	-	-	0,38	0,21	0,20	-
August	0,19	0,25	0,25	-	0,25	-	-	-	0,24	0,15	0,15	-
September	0,25	0,33	0,29	-	0,41	-	-	-	0,54	0,27	0,17	-
October	0,39	0,59	0,36	-	0,58	-	-	-	-	0,44	0,18	-
November	0,30	0,55	0,43	-	0,48	-	0,31	-	0,51	0,52	0,31	-
December	0,87	0,67	0,51	-	0,69	-	0,39	-	1,37	0,97	0,46	-

MONTHS	PARTICULATES (mg/m^3) - Maximum hourly values											
	V. Lagrange station				Miraflori station				Ferriere station			
	1971	1972	1973	1974	1971	1972	1973	1974	1971	1972	1973	1974
January	0,850	1,150	1,050	0,920	-	0,480	-	0,700	1,530	1,100	1,750	1,360
February	0,750	0,880	0,950	0,500	0,780	0,480	-	0,340	2,250	0,960	1,500	0,500
March	-	0,820	0,840	0,500	0,630	0,680	-	0,300	2,430	0,850	0,500	1,200
April	0,640	0,590	0,650	0,460	0,770	0,310	-	0,310	1,100	1,450	0,800	0,570
May	0,700	0,850	0,630	0,520	0,450	0,380	-	0,320	1,1500	0,800	0,650	0,560
June	0,430	0,650	0,450	0,480	0,360	0,320	-	0,220	0,660	0,550	0,380	0,620
July	0,480	0,700	0,470	-	0,600	-	-	-	1,100	0,700	0,510	-
August	0,450	0,420	0,550	-	0,570	-	-	-	0,600	0,440	0,400	-
September	0,540	0,700	0,650	-	0,700	-	-	-	1,250	0,930	0,480	-
October	1,080	1,190	0,700	-	0,750	-	-	-	-	1,440	0,400	-
November	0,700	1,240	0,750	-	0,860	-	0,570	-	1,050	1,220	0,700	-
December	1,350	1,070	0,800	-	0,950	-	0,520	-	2,800	2,400	0,800	-

ENCL.: 14

MONTHS	CARBON MONOXIDE (ppm)				-				Monthly averages			
	V.: Lagrange station				Mirafiori station				Ferriere station			
	1971	1972	1973	1974	1971	1972	1973	1974	1971	1972	1973	1974
January	10,7	9,8	12,9	8,8	-	10,4	9,4	13,0	10,1	9,0	8,7	7,7
February	7,3	8,1	10,4	6,7	10,0	11,0	9,6	9,9	8,6	7,6	7,1	6,0
March	-	10,1	9,9	7,0	10,0	10,6	8,8	9,2	7,6	7,0	6,5	5,8
April	6,1	10,1	8,7	6,6	8,1	-	7,3	8,6	5,7	7,4	5,9	5,0
May	5,5	7,2	7,6	6,3	7,0	8,5	7,1	9,1	4,9	6,5	5,7	5,0
June	4,2	6,4	6,6	6,1	6,1	8,1	8,1	8,4	4,5	5,8	5,7	4,8
July	4,9	5,4	6,5	-	6,6	7,6	9,3	-	6,5	5,9	4,7	-
August	4,6	6,4	5,3	-	5,1	5,5	6,0	-	5,2	4,8	3,7	-
September	6,6	8,7	7,5	-	7,2	7,3	9,8	-	6,8	6,1	5,6	-
October	8,8	11,8	9,2	-	10,7	9,6	12,4	-	8,2	7,4	7,2	-
November	9,7	13,2	9,9	-	9,7	9,3	12,3	-	8,0	8,8	7,5	-
December	14,1	14,1	8,8	-	12,7	9,8	12,8	-	12,4	10,3	7,8	-

ENCL. 15

MONTHS	CARBON MONOXIDE (ppm) - Monthly averages of maximum hourly values											
	V. Lagrange station				Mirafiori station				Ferriere station			
January	23,1	20,4	21,9	16,8	-	21,2	19,0	33,9	20,0	15,8	15,5	15.8
February	19,6	16,0	17,9	12,8	19,0	22,1	23,8	26,9	18,9	15,4	13,9	12,3
March	-	22,6	20,4	12,4	23,0	25,2	19,7	24,8	15,4	13,6	12,4	10,9
April	13,7	19,3	15,6	13,0	20,0	-	14,8	25,0	11,7	13,4	10,4	9,0
May	11,7	14,0	14,4	12,8	14,5	18,0	17,5	27,9	10,5	12,1	11,1	9,1
June	10,2	14,6	12,2	10,4	13,3	17,2	24,9	23,7	8,9	4,9	10,3	8,9
July	9,5	10,9	10,7	-	14,4	15,6	30,6	-	12,3	10,9	8,6	-
August	8,0	10,9	8,5	-	9,5	9,9	17,4	-	8,5	8,0	6,3	-
September	13,4	16,9	14,0	-	15,4	15,6	27,0	-	12,4	11.1	10,2	-
October	18,8	23,6	18,6	-	23,3	21,3	32,0	-	18,7	14,2	14,4	-
November	21,4	26,1	18,9	-	19,5	20,9	35,8	-	17,2	16,0	14,9	-
December	31,4	26,9	20,1	-	29,3	21,0	31,4	-	24,3	16,5	14,8	-

MONTHS	CARBON MONOXIDE (ppm) - Maximum daily average											
	V. Lagrange station				Mirafiori station				Ferriere station			
	1971	1972	1973	1974	1971	1972	1973	1974	1971	1972	1973	1974
January	16,7	13,5	17,9	14,1	-	14,5	16,4	26,3	14,2	14,0	13,5	14,7
February	11,8	11,7	18,5	8,9	14,1	13,5	16,0	16,6	15,1	12,3	12,2	8,6
March	-	17,5	15,2	11,9	13,8	13,1	12,3	14,0	12,7	9,0	9,6	7,7
April	10,6	15,5	13,8	9,2	13,6	-	12,7	14,1	7,8	9,5	8,7	6,7
May	9,7	9,5	15,1	8,3	9,3	11,0	9,1	12,0	6,6	7,3	8,0	6,2
June	7,0	9,0	8,4	7,4	8,4	9,5	14,2	12,9	7,0	6,6	6,5	5,6
July	5,8	7,9	7,6	-	9,2	10,2	14,2	-	8,8	7,4	5,9	-
August	6,1	10,5	7,6	-	8,3	8,4	14,6	-	7,6	6,5	6,1	-
September	9,2	12,0	8,8	-	10,2	10,6	14,7	-	8,2	7,2	6,7	-
October	15,3	16,1	14,4	-	19,3	13,4	23,4	-	12,8	10,5	10,4	-
November	15,2	18,6	13,0	-	14,2	14,6	18,3	-	10,2	12,4	11,4	-
December	26,4	24,5	14,3	-	18,2	14,8	27,4	-	20,6	18,7	14,9	-

<table>
<tr><th rowspan="3">MONTHS</th><th colspan="12">CARBON MONOXIDE (ppm) - Maximum hourly values</th></tr>
<tr><th colspan="4">V. Lagrange station</th><th colspan="4">Miraflori station</th><th colspan="4">Ferriere station</th></tr>
<tr><th>1971</th><th>1972</th><th>1973</th><th>1974</th><th>1971</th><th>1972</th><th>1973</th><th>1974</th><th>1971</th><th>1972</th><th>1973</th><th>1974</th></tr>
<tr><td>January</td><td>48,0</td><td>38,0</td><td>39,5</td><td>35,0</td><td>-</td><td>30,5</td><td>34,5</td><td>79,0</td><td>30,0</td><td>28,0</td><td>31,0</td><td>44,0</td></tr>
<tr><td>February</td><td>40,0</td><td>35,5</td><td>30,0</td><td>18,0</td><td>40,0</td><td>30,5</td><td>39,5</td><td>58,0</td><td>30,0</td><td>31,0</td><td>30,0</td><td>21,0</td></tr>
<tr><td>March</td><td>-</td><td>45,7</td><td>38,0</td><td>27,0</td><td>39,0</td><td>38,0</td><td>35,0</td><td>42,0</td><td>22,0</td><td>22,0</td><td>19,0</td><td>18,0</td></tr>
<tr><td>April</td><td>26,0</td><td>41,0</td><td>26,5</td><td>33,0</td><td>50,0</td><td>-</td><td>23,0</td><td>45,0</td><td>19,0</td><td>18,0</td><td>17,0</td><td>16,0</td></tr>
<tr><td>May</td><td>21,0</td><td>23,0</td><td>29,0</td><td>25,0</td><td>26,0</td><td>24,0</td><td>31,0</td><td>43,0</td><td>14,0</td><td>14,0</td><td>16,5</td><td>13,5</td></tr>
<tr><td>June</td><td>18,0</td><td>25,0</td><td>18,5</td><td>22,0</td><td>23,0</td><td>26,0</td><td>42,0</td><td>38,5</td><td>12,0</td><td>15,5</td><td>14,0</td><td>14,0</td></tr>
<tr><td>July</td><td>14,5</td><td>25,0</td><td>15,5</td><td>-</td><td>35,0</td><td>22,0</td><td>60,0</td><td>-</td><td>20,0</td><td>16,5</td><td>12,5</td><td>-</td></tr>
<tr><td>August</td><td>13,0</td><td>20,0</td><td>13,5</td><td>-</td><td>25,0</td><td>23,5</td><td>52,0</td><td>-</td><td>18,0</td><td>14,5</td><td>12,5</td><td>-</td></tr>
<tr><td>September</td><td>20,0</td><td>29,0</td><td>24,0</td><td>-</td><td>45,0</td><td>33,0</td><td>50,0</td><td>-</td><td>20,0</td><td>15,0</td><td>13,0</td><td>-</td></tr>
<tr><td>October</td><td>47,5</td><td>58,5</td><td>34,0</td><td>-</td><td>57,0</td><td>31,0</td><td>60,0</td><td>-</td><td>37,0</td><td>19,0</td><td>24,0</td><td>-</td></tr>
<tr><td>November</td><td>42,0</td><td>50,5</td><td>38,0</td><td>-</td><td>37,0</td><td>34,0</td><td>60,0</td><td>-</td><td>36,0</td><td>28,0</td><td>30,0</td><td>-</td></tr>
<tr><td>December</td><td>73,0</td><td>60,5</td><td>46,0</td><td>-</td><td>45,0</td><td>41,0</td><td>55,0</td><td>-</td><td>52,0</td><td>37,0</td><td>27,0</td><td>-</td></tr>
</table>

MONTHS	CARBON MONOXIDE (ppm) – Pollution levels recorded at Porta Nuova and Piazza Statuto Station															
	Monthly averages				Monthly aver.of mas hourly values				Max daily average				Max hourly value			
	1973	1974	1973	1974	1973	1974	1973	1974	1973	1974	1973	1974	1973	1974	1973	1974
January	16,3	24,1	20,1	23,9	37,2	47,5	34,5	39,6	27,3	34,0	30,1	34,5	64,0	95,0	68,0	72,0
February	18,1	23,4	18,5	22,6	39,2	43,9	33,0	37,1	29,5	31,3	29,3	33,0	58,0	63,0	66,0	60,5
March	16,6	22,1	19,9	19,2	33,2	38,5	32,1	31,6	24,9	30,4	28,6	31,5	55,0	53,5	49,5	47,0
April	15,2	21,8	20,9	20,7	29,8	38,6	33,0	32,6	21,9	26,0	27,1	26,5	48,0	64,5	53,0	53,5
May	15,7	22,0	21,4	20,5	30,5	39,1	32,8	31,8	21,5	28,3	29,2	26,5	41,5	54,0	46,0	44,5
June	17,3	20,3	20,5	18,6	36,3	34,7	32,4	27,6	22,3	25,0	25,3	24,0	45,5	46,0	40,5	37,5
July	15,3	-	-	-	30,5	-	-	-	18,5	-	-	-	42,0	-	-	-
August	11,2	-	-	-	20,8	-	-	-	15,0	-	-	-	34,0	-	-	-
September	23,2	-	-	-	38,1	-	-	-	27,6	-	-	-	45,0	-	-	-
October	26,1	-	-	-	48,4	-	-	-	32,6	-	-	-	72,0	-	-	-
November	27,5	-	-	-	47,5	-	-	-	31,7	-	-	-	84,0	-	-	-
December	27,8	-	-	-	43,3	-	-	-	34,6	-	-	-	75,0	-	-	-

MONTHS	CARBON MONOXIDE (ppm) - Maximum daily values of 8 hour periods															
	V. Lagrange station				Miraflori station				Ferriere station				Porta Nuova station		Piazza Statuto station	
	1971	1972	1973	1974	1971	1972	1973	1974	1971	1972	1973	1974	1973	1974	1973	1974
January	27,9	21,5	26,6	23,0	-	21,3	23,5	37,0	18,4	17,6	16,5	20,4	46,3	64,8	44,6	52,3
February	19,9	18,7	23,5	12,1	19,4	17,7	24,1	26,7	20,1	20,6	15,4	10,7	55,3	47,3	43,5	40,1
March	-	29,6	23,9	18,2	22,5	18,9	16,9	20,9	13,7	12,1	12,2	10,1	38,7	42,9	37,6	38,6
April	16,6	23,6	18,1	17,6	17,6	-	15,1	22,1	10,5	12,9	10,5	10,1	33,3	38,8	40,1	40,2
May	14,5	15,3	21,2	14,3	12,9	14,0	13,6	19,2	9,8	10,6	12,0	8,6	28,9	43,0	36,2	38,1
June	10,4	14,1	12,0	10,4	10,4	12,1	25,9	20,9	7,7	9,8	9,3	8,6	34,7	31,2	31,7	29,7
July	8,0	11,9	10,2	-	13,2	13,1	24,1	-	12,7	9,9	8,7	-	27,3	-	-	-
August	8,2	15,0	9,4	-	10,6	12,2	16,3	-	9,2	9,3	8,7	-	22,4	-	-	-
September	14,3	17,3	13,1	-	14,7	14,1	23,1	-	11,0	10,6	8,6	-	35,1	-	-	-
October	28,9	30,2	24,6	-	30,4	19,3	40,5	-	21,0	12,9	13,1	-	50,2	-	-	-
November	27,2	27,9	21,8	-	21,5	23,4	26,6	-	17,5	17,4	18,1	-	49,0	-	-	-
December	44,4	37,4	24,6	-	27,9	23,2	41,1	-	35,8	23,0	19,9	-	49,0	-	-	-

MONTHS	CARBON MONOXIDE (ppm) - Maximum daily value for 12 hour periods															
	Via Lagrange station				Mirafiori station				Ferriere station				Porta Nuova station		Piazza Statuto station	
	1971	1972	1973	1974	1971	1972	1973	1974	1971	1972	1973	1974	1973	1974	1973	1974
January	25,2	18,8	21,6	20,1	-	18,6	21,5	36,2	16,9	15,9	14,5	20,4	34,1	51,6	36,5	45,2
February	16,8	14,9	21,4	10,9	15,4	16,8	20,0	24,8	16,8	17,3	15,1	9,9	41,9	43,4	36,7	38,5
March	-	25,4	20,2	16,7	20,6	18,6	14,7	18,1	11,8	10,5	12,7	9,7	30,8	38,1	32,3	35,2
April	15,5	20,5	15,9	14,3	17,2	-	14,3	19,9	9,0	11,8	10,1	8,3	28,2	33,2	34,9	36,1
May	13,9	13,1	20,4	12,1	10,8	13,2	12,7	15,3	8,5	9,3	11,3	7,7	27,4	38,0	33,1	36,0
June	10,1	11,8	10,9	9,5	9,8	11,3	19,6	18,0	7,0	8,5	8,3	7,7	32,4	29,0	26,3	25,1
July	7,2	10,6	9,3	-	12,1	12,3	21,2	-	11,1	8,9	7,5	-	23,5	-	-	-
August	7,6	13,3	9,2	-	9,7	11,4	20,6	-	8,4	8,3	7,9	-	18,5	-	-	-
September	14,2	15,0	11,3	-	14,8	12,6	20,1	-	11,0	9,2	8,0	-	32,6	-	-	-
October	24,5	24,3	19,9	-	25,5	16,6	34,7	-	17,2	12,0	12,3	-	42,2	-	-	-
November	21,8	23,4	17,5	-	18,0	18,5	26,4	-	14,3	15,0	15,2	-	41,1	-	-	-
December	39,2	31,8	20,2	-	23,1	19,5	37,3	-	30,7	20,7	15,6	-	46,5	-	-	-

ENCL. 21

MONTHS	NITROGEN OXIDES (NO_x ppm) - Monthly averages											
	V. Lagrange station				Mirafiori station				Ferriere station			
	1971	1972	1973	1974	1971	1972	1973	1974	1971	1972	1973	1974
January	-	0,150	0,250	0,290	-	0,420	0,510	0,330	-	-	0,260	0,210
February	-	0,130	0,160	0,270	-	0,410	0,340	0,310	-	0,180	0,220	0,210
March	-	0,130	0,170	0,240	-	0,220	0,250	0,240	-	0,230	0,230	0,200
April	-	0,120	0,130	0,170	-	0,190	0,190	0,220	-	0,200	0,200	0,310
May	0,080	0,110	0,130	0,160	0,140	0,180	0,230	0,320	0,110	0,170	0,180	0,330
June	0,095	0,120	0,150	0,150	0,180	0,160	0,160	-	0,130	0,090	0,140	0,230
July	0,080	0,080	0,110	-	0,170	0,140	0,130	-	0,110	0,060	0,130	-
August	0,070	0,060	0,080	-	0,100	0,120	0,100	-	0,080	0,060	0,110	-
September	0,080	0,090	0,110	-	0,190	0,180	0,130	-	0,100	0,110	0,160	-
October	0,140	0,170	0,190	-	0,270	0,370	0,270	-	0,160	0,150	0,320	-
November	0,210	0,240	0,210	-	0,230	0,400	0,310	-	0,130	0,170	0,340	-
December	0,230	0,360	0,200	-	0,470	0,460	0,340	-	0,270	0,270	0,250	-

MONTHS	NITROGEN OXIDES (NO_x ppm) - Monthly averages of minimum hourly values											
	Via Lagrange station				Mirafiori station				Ferriere station			
	1971	1972	1973	1974	1971	1972	1973	1974	1971	1972	1973	1974
January	-	0,256	0,421	0,510	-	0,787	0,938	0,730	-	-	0,466	0,590
February	-	0,229	0,310	0,410	-	0,899	0,786	0,710	-	0,372	0,464	0,470
March	-	0,251	0,330	0,520	-	0,556	0,556	0,560	-	0,506	0,456	0,430
April	-	0,237	0,268	0,350	-	0,401	0,417	0,460	-	0,393	0,407	0,680
May	0,130	0,223	0,257	0,350	0,280	0,391	0,500	0,750	0,220	0,332	0,335	0,780
June	0,190	0,207	0,307	0,320	0,430	0,376	0,388	-	0,260	0,186	0,268	0,570
July	0,170	0,169	0,247	-	0,390	0,338	0,315	-	0,240	0,137	0,282	-
August	0,130	0,114	0,155	-	0,240	0,294	0,277	-	0,170	0,135	0,241	-
September	0,180	0,172	0,234	-	0,420	0,350	0,310	-	0,180	0,214	0,332	-
October	0,280	0,330	0,360	-	0,490	0,220	0,580	-	0,250	0,284	0,651	-
November	0,380	0,445	0,370	-	0,460	0,826	0,800	-	0,240	0,294	0,626	-
December	0,380	0,586	0,400	-	0,740	0,853	0,800	-	0,510	0,458	0,503	-

ENCL. 23

MONTHS	NITROGEN OXIDES (NO_x - ppm) - Maximum daily average											
	Via Lagrange station				Mirafiori station				Ferriere station			
	1971	1972	1973	1974	1971	1972	1973	1974	1971	1972	1973	1974
January	-	0,230	0,368	0,500	-	0,710	0,715	0,640	-	-	0,400	0,520
February	-	0,180	0,303	0,330	-	0,520	0,664	0,600	-	0,210	0,380	0,360
March	-	0,220	0,244	0,530	-	0,480	0,370	0,410	-	0,310	0,330	0,320
April	-	0,160	0,196	0,260	-	0,280	0,320	0,360	-	0,270	0,280	0,480
May	0,130	0,140	0,174	0,240	0,260	0,330	0,190	0,520	0,210	0,260	0,250	0,470
June	0,250	0,130	0,212	0,230	0,260	0,230	0,300	-	0,170	0,150	0,190	0,340
July	0,110	0,120	0,162	-	0,250	0,230	0,224	-	0,170	0,080	0,168	-
August	0,110	0,100	0,121	-	0,160	0,220	0,182	-	0,120	0,100	0,165	-
September	0,100	0,190	0,161	-	0,310	0,310	0,193	-	0,140	0,150	0,193	-
October	0,240	0,280	0,370	-	0,370	0,550	0,550	-	0,160	0,200	0,600	-
November	0,330	0,310	0,360	-	0,530	0,620	0,500	-	0,190	0,230	0,480	-
December	0,400	0,630	0,500	-	0,590	0.730	0,740	-	0,460	0,580	0,520	-

ENCL. 24

MONTHS	NITROGEN OXIDES (NO_x ppm) - Maximum hourly values											
	Via Lagrange station				Mirafiori station				Ferriere station			
	1971	1972	1973	1974	1971	1972	1973	1974	1971	1972	1973	1974
January	-	0,44	0,63	0,84	-	1,20	1,68	1,96	-	-	0,84	0,98
February	-	0,39	0,60	0,72	-	2,20	2,10	1,44	-	0,46	0,95	0,98
March	-	0,50	0,54	0,98	-	0,96	0,84	1,10	-	0,98	0,70	0,84
April	-	0,37	0,43	0,54	-	0,66	0,76	0,70	-	0,62	0,65	1,20
May	0,16	0,32	0,36	0,50	0,58	0,64	0,66	1,40	0,52	0,50	0,44	1,50
June	0,90	0,26	0,49	0,60	0,75	0,68	0,72	-	0,44	0,23	0,46	1,08
July	0,30	0,30	0,44	-	0,70	0,86	0,56	-	0,41	0,22	0,42	-
August	0,24	0,16	0,28	-	0,56	0,52	0,66	-	0,28	0,31	0,40	-
September	0,30	0,40	0,42	-	0,66	0,56	0,50	-	0,28	0,30	0,48	-
October	0,46	0,50	0,70	-	0,75	1,20	1,30	-	0,36	0,41	1,36	-
November	0,57	1,05	0,66	-	0,80	1,46	1,30	-	0,42	0,47	1,24	-
December	0,80	0,94	0,88	-	1,30	1,64	1,56	-	1,10	1,06	0,94	-

ENCL.n 25

MONTHS	TOTAL HYDROCARBONS, METHANE, NON-METHANE HYDROCARBONS (Via Lagrange stations - 1974)											
	Monthly averages			Monthly averages of max hourly values			Max daily average			Max hourly values		
	THC	CH_4	HC	THC	CH_4	HC	THC	CH_4	HC	THC	CH_4	HC
January	1,7	1,1	0,6	3,1	1,7	1,5	4,3	2,4	2,5	9,2	3,6	5,3
February	1,9	1,2	0,7	3,3	2,3	1,5	3,9	2,7	1,3	9,4	5,2	5,0
March	2,3	1,6	0,7	4,0	2,8	1,7	3,2	2,3	1,2	7,8	5,2	4,0
April	2,2	1,5	0,7	3,8	2,6	1,6	3,1	2,2	1,0	5,7	4,5	3,0
May	2,3	1,5	0,8	4,0	2,6	2,0	3,3	2,3	1,7	6,5	5,0	5,0
June	1,8	1,2	0,6	2,9	2,0	1,2	2 7	1,8	1,0	5,4	3,3	2,4

ENCL. 26

STATIONS	MONTHS	SULPHUR DIOXIDE (ppm) Daily averages recorded during the period Dec. 73 - Mar. 74 characterized by limitation in private vehicular traffic.																														
		1	2	3	4	5	6	7	8	9	10	11	12	13	14	15	16	17	18	19	20	21	22	23	24	25	26	27	28	29	30	31
Via Lagrange	December	.29	.13 ☆	.23	.36	.45	.43	.66	.30 ☆	.33 ☆	.30	.37	.39	.24	.21	.11	.26 ☆	.53	.52	.42	.25	.19	.21	.15 ☆	.14	.15	.18	.40	.41	.41	.44 ☆	.47
	January	.25	.18	.22	.30	.24	.22	.42	.46	.25	.31	.44	.22	.28 ☆	.46	.32	.49	.29	.31	.24	.24 ☆	.35	.43	.38	.39	.40	.12	.33 ☆	.44	.47	.44	.27
	February	.16	.13	.15 ☆	.17	.15	.10	.09	.11	.23	.22 ☆	.31	.19	.20	.29	.23	.17	.11 ☆	.13	.18	.29	.28	.19	.18	.15 ☆	25	16	.22	.19			
	March	.13	.11	.14 ☆	.20	.27	.23	.20	.17	.15	.12 ●	.17	.27	.26	.30	.14	.14	.14 ●	.16	.11 ☆	.09	.12	.17	.12	.13 ●	.13	.08	.10	.13	.12	.12	.09 ●
Miraflori	December	.16	.07 ☆	.12	.14	.28	.26	.26	.20 ☆	.15 ☆	.21	.24	.28	.16	.18	.10	.14 ☆	.22	.31	.24	.12	.12	.14	.12 ☆	.10	.05	.07	.15	.16	.21	.24 ☆	.19
	January	.08	.07	.10	.13	.11	.09	.24	.23	.19	.17	.18	.17	.18 ☆	.23	.12	.22	.13	.12	.14	.09 ☆	.16	.18	.23	.14	.11	.06	.05 ☆	.07	.10	.12	.11
	February	.11	.09	.05 ☆	.09	.14	.12	.14	.18	.17	.11 ☆	.16	.09	.11	.09	.12	.07	.06 ☆	.06	.09	.11	.12	.13	.11	.07 ☆	.14	.06	.06	.06			
	March	.07	.05	.07 ☆	.06	.10	.07	.11	.08	.07	.07 ●	.10	.11	.11	.10	.11	.07	.08 ●	.11	.09 ☆	.06	.06	.10	.08	.07 ●	.08	.05	.05	.06	.07	.08	.06 ●
Ferriere	December	.23	.10 ☆	.19	.31	.37	.39	.60	.23 ☆	.31 ☆	.24	.32	.36	.20	.20	.15	.21 ☆	.45	.42	.36	.21	.18	.19	.15 ☆	.12	.13	.15	.35	.33	.38	.40 ☆	.40
	January	.19	.14	.17	.25	.19	.16	.34	.35	.22	.27	.37	.20	.24 ☆	.39	.26	.43	.25	.25	.21	.20 ☆	.29	.37	.31	.30	.28	.27	.25 ☆	.33	.41	.35	.21
	February	.14	.11	.11 ☆	.14	.15	.16	.13	.16	.21	.18 ☆	.30	.16	.19	.25	.22	.16	.11 ☆	.12	.16	.26	.24	.17	.17	.14 ☆	.23	.17	.20	.15			
	March	.12	.10	.08 ☆	.14	.19	.15	.14	.17	.13	.10 ●	.14	.21	.22	.25	.15	.13	.12 ●	.12	.08 ☆	.06	.10	.09	.10	.08 ●	.09	.06	.07	.10	.08	.08	.08 ●

☆ Holiday without traffic

● Holiday with traffic at alternate number-plates

ENCL. 27

PARTICULATES Mg/m^3

Daily averages recorded during the period Dec. 73 - Mar. 74 characterized by limitation in private vehicular traffic.

STATIONS	MONTHS	1	2	3	4	5	6	7	8	9	10	11	12	13	14	15	16	17	18	19	20	21	22	23	24	25	26	27	28	29	30	31
Via Lagrange	December	.24	.21 ☆	.21	.32	.49	.46	.43	.20 ☆	.25 ☆	.23	.32	.51	.32	.24	.14	.20 ☆	.33	.48	.40	.23	.26	.26	.20 ☆	.15	.12	.16	.32	.37	.41	.44 ☆	.40
	January	.19	.13	.17	.20	.23	.20	.33	.42	.25	.23	.34	.34	.34 ☆	.43	.32	.48	.32	.31	.28	.21	.36	.49	.56	.38	.23	.21	.29 ☆	.22	.27	.21	.19
	February	.25	.18	.13 ☆	.15	.18	.20	.16	.14	.32	.16 ☆	.25	.18	.17	.18	.19	.13	.11 ☆	.14	.17	.20	.26	[illegible]	.19	.14 ☆	.13	.13	.13	.15			
	March	.19	.16	.16 ☆	.16	.20	.21	.21	.17	.17	.15 ●	.15	.21	.26	.24	.13	.19	.22 ●	.29	.25 ☆	.13	.16	.22	.16	.19 ●	.18	.16	.17	.18	.19	.14	.10 ●
Miraflori	December	.11	.08 ☆	.10	.12	.22	.26	.39	.27 ☆	.18 ☆	.16	.38	.27	.17	.14	.08	.12 ☆	.18	.26	.23	.13	.12	.13	.10 ☆	.09	.07	.10	.16	.20	.21	.16	.26
	January	.12	.13	.11	.13	.14	.12	.18	.21	.15	.14	.17	.21	.18 ☆	.25	.12	.23	.16	.11	.16	.11	.18	.27	.34	.27	.17	.15	.17 ☆	.17	.17	.17	.14
	February	.12	.10	.06 ☆	.10	.13	.13	.08	.10	.16	.12 ☆	.15	.10	.10	.09	.11	.07	.06 ☆	.11	.08	.12	.16	.16	.13	.08 ☆	.12	.09	.09	.08			
	March	.10	.10	.10 ☆	.08	.11	.10	.12	.12	.10	.10 ●	.12	.13	.14	.14	.10	.11	.10 ●	.15	.14 ☆	.08	.10	.12	.09	.10 ●	.10	.10	.09	.11	.11	.09	.07 ●
Ferriere	December	.22	.13 ☆	.18	.24	.35	.43	.47	.31 ☆	.17 ☆	.21	.22	.29	.20	.20	.10	.15 ☆	.27	.34	.30	.18	.17	.17	.14 ☆	.13	.09	.11	.23	.30	.43	.35	.42
	January	.16	.16	.21	.28	.33	.28	.57 ☆	.60	.32	.26	.47	.44	.41 ☆	.55	.42	.62	.35	.30	.28	.16	.36	.48	.49	.36	.21	.29	.23 ☆	.22	.28	.24	.16
	February	.23	.14	.07 ☆	.15	.22	.18	.12	.14	.22	.16 ☆	.22	.17	.17	.15	.17	.10	.08 ☆	.15	.16	.22	.19	.23	.20	.10 ☆	.17	.13	.12	.16			
	March	.17	.14	.12 ☆	.13	.24	.23	.21	.18	.16	.13 ●	.18	.26	.26	.24	.14	.21	.19 ●	.28	.22 ☆	.19	.19	.22	.13	.12 ●	.16	.14	.13	.16	.15	.15	.09 ●

☆ Holiday without traffic

● Holiday with traffic at alternate number-plates

ENCL. 28

CARBON MONOXIDE ppm

Daily averages recorded during the period Dec. 73 - Mar. 74 characterized by limitation in private vehicular traffic

STATIONS	MONTHS	1	2	3	4	5	6	7	8	9	10	11	12	13	14	15	16	17	18	19	20	21	22	23	24	25	26	27	28	29	30	31
Via Lagrange	December	14,7	8,0 ☆	10,0	12,3	13,7	10,8	14,0	3,8 ☆	3,9 ☆	9,5	8,8	9,2	8,3	3,6	4,4	3,9 ☆	11,3	9,6	10,0	9,6	10,6	9,3	4,6 ☆	7,4	7,0	7,1	12,4	11,2	11,9	4,6 ☆	9,8
	January	6,8	7,1	8,0	9,1	9,7	8,0	10,0	10,0	9,5	11,4	12,4	11,2	6,3 ☆	10,0	8,5	9,9	8,2	9,2	11,1	4,2 ☆	14,0	12,5	9,3	7,3	8,3	7,3	4,3 ☆	7,7	7,7	6,4	7,4
	February	8,3	7,3	3,1 ☆	7,9	8,4	6,1	4,6	—	—	3,9 ☆	7,6	6,8	7,6	8,8	7,4	7,1	3,3 ☆	6,8	7,6	9,5	9,4	8,0	7,1	3,4 ☆	6,0	6,2	7,0	7,0			
	March	6,7	7,5	3,9 ☆	10,0	8,3	11,9	7,5	6,2	5,6	4,3 ●	6,3	7,5	7,6	9,4	7,3	7,9	5,9 ●	7,2	4,0 ☆	7,3	7,6	9,6	7,2	5,7 ●	6,8	5,5	8,0	7,7	6,7	8,9	4,8 ●
Miraflori	December	15,0	4,4 ☆	10,4	13,4	19,0	17,4	27,0	2,7 ☆	2,6 ☆	15,1	16,3	16,3	15,6	9,8	13,0	4,2 ☆	15,9	23,0	19,7	16,3	22,3	15,5	4,0 ☆	11,8	6,3	7,8	10,6	13,2	11,7	5,1 ☆	9,7
	January	5,9	9,8	10,4	15,8	8,2	7,1	14,2	15,1	17,6	19,2	19,0	19,7	4,8 ☆	14,7	9,2	14,7	8,5	19,9	25,4	4,1 ☆	24,4	18,2	18,9	12,9	13,8	7,9	2,7 ☆	9,5	14,0	11,7	10,0
	February	11,5	6,8	2,4 ☆	12,1	14,6	10,8	10,4	16,4	14,5	3,0 ☆	9,7	9,6	11,6	11,8	10,6	6,5	1,6 ☆	8,3	10,6	13,8	16,2	10,7	8,5	2,2 ☆	16,1	6,6	5,7	6,3			
	March	12,1	7,2	2,6 ☆	10,6	10,2	11,9	14,2	12,4	6,1	4,2 ●	8,8	11,9	12,4	11,2	13,2	13,0	5,2 ●	11,0	2,6 ☆	8,3	8,9	12,9	8,4	4,8 ●	8,3	8,8	10,6	9,9	10,6	9,3	4,7 ●
Ferriere	December	8,5	3,5 ☆	7,0	8,9	7,9	10,1	14,9	2,7 ☆	2,6 ☆	8,1	9,5	9,9	7,8	7,1	6,5	3,4 ☆	11,2	12,3	10,6	7,3	8,0	8,3	3,5 ☆	5,9	4,6	5,6	10,4	12,2	10,8	3,6 ☆	9,5
	January	5,3	5,7	6,0	7,7	7,4	6,0	6,5	8,2	8,3	9,4	10,8	9,1	4,5 ☆	9,1	6,5	7,8	6,0	10,7	13,8	5,0 ☆	14,7	13,7	9,0	6,1	6,0	7,0	2,8 ☆	4,8	6,7	6,1	6,3
	February	6,2	6,0	2,6 ☆	6,4	7,7	6,3	6,6	7,6	8,3	2,6 ☆	6,1	6,1	6,3	5,6	6,8	4,9	2,3 ☆	4,6	6,2	8,1	6,9	7,0	5,8	3,2 ☆	8,5	5,7	6,5	5,0			
	March	6,3	5,5	3,8 ☆	5,5	6,7	7,5	7,1	5,3	5,2	3,7 ●	5,4	7,3	6,0	7,7	7,1	7,7	5,4 ●	5,6	2,8 ☆	4,6	5,1	7,1	5,9	4,8 ●	5,2	5,0	6,0	6,2	5,6	6,1	4,1 ●

☆ Holiday without traffic

● Holiday with traffic at alternate number-plates

ENCL. 29

STATIONS	MONTHS	CARBON MONOXIDE ppm Daily averages recorded during the period Dec. 73 - Mar. 74 characterized by limitation in private vehicular traffic																														
		1	2	3	4	5	6	7	8	9	10	11	12	13	14	15	16	17	18	19	20	21	22	23	24	25	26	27	28	29	30	31
Porta Nuova	December	20,5	8,7 ☆	16,8	16,1	24,3	22,7	34,6	13,0 ☆	10,8 ☆	20,6	17,3	22,1	18,2	16,0	17,6	9,6 ☆	26,1	27,3	27,8	27,9	31,1	21,2	15,5 ☆	26,5	25,4	23,6	31,4	32,5	25,2	14,7 ☆	21,8
	January	22,4	26,3	26,5	23,0	21,3	20,0	24,3	24,0	30,1	27,3	30,4	26,5	15,4 ☆	24,5	22,6	25,7	22,6	28,9	32,9	13,1 ☆	34,0	33,6	27,3	23,6	17,6	16,6	13,3 ☆	17,0	22,3	24,6	27,7
	February	21,5	23,1	15,3 ☆	23,9	29,9	22,9	17,5	22,1	29,0	12,5 ☆	23,4	26,9	30,3	19,8	27,6	25,9	15,0 ☆	29,2	30,6	29,1	31,7	20,8	23,5	11,8 ☆	22,7	21,3	21,5	26,0			
	March	25,0	20,0	12,0 ☆	24,0	20,0	20,0	23,0	19,0	23,0	16,0 ●	22,0	23,0	22,0	22,0	20,0	22,0	20,0 ●	20,0	13,0 ☆	23,0	24,0	22,0	22,0	19,0 ●	24,0	29,0	30,0	30,0	28,0	23,0	22,0 ●
Piazza Statuto	December	21,5	7,2 ☆	13,6	13,3	19,8	17,6	26,3	8,8 ☆	7,6 ☆	16,5	15,8	20,3	13,9	10,5	9,2	7,5 ☆	17,5	22,8	20,7	23,0	26,2	20,0	9,0 ☆	19,3	11,2	13,0	29,5	27,7	21,6	8,6 ☆	17,4
	January	19,8	27,5	25,3	21,8	19,5	16,5	23,7	22,9	28,2	23,7	26,5	25,6	12,2 ☆	19,7	16,8	18,5	15,8	21,2	24,5	10,6 ☆	21,6	22,7	21,8	19,6	16,6	14,2	11,9 ☆	14,9	17,2	15,6	18,1
	February	18,6	15,2	8,0 ☆	17,0	17,0	17,0	10,6	12,4	21,3	11,8 ☆	16,1	18,1	18,1	16,4	20,6	16,0	9,8 ☆	21,3	25,5	24,6	27,1	18,2	19,8	8,1 ☆	17,2	16,3	15,8	21,4			
	March	22,5	17,3	9,1 ☆	19,5	16,1	17,1	20,2	15,5	21,6	13,7 ●	20,0	18,9	19,0	18,5	17,3	17,9	16,5 ●	19,2	9,3 ☆	21,1	21,5	17,2	18,3	15,9 ●	21,7	25,4	25,8	26,3	23,7	22,2	16,4 ●

☆ Holiday without traffic

● Holiday with traffic at alternate number-plates

ENCL. 30

NITROGEN OXIDES (NO$_x$ - ppm)

Daily averages recorded during the period Dec. 73 - Mar. 74 characterized by limitation in private vehicular traffic

STATIONS	MONTHS	1	2	3	4	5	6	7	8	9	10	11	12	13	14	15	16	17	18	19	20	21	22	23	24	25	26	27	28	29	30	31
Via Lagrange	December	.10	.05 ☆	.14	.18	.21	.20	.24	.07 ☆	.07 ☆	.13	.16	.18	.10	.10	.08	.10 ☆	.18	.27	.30	.21	.30	.13	.09 ☆	.22	.16	.24	.51	.49	.32	.38 ☆	.36
	January	.20	.20	.24	.36	.34	.25	.39	.45	.33	.42	.50	.40	.28 ☆	.45	.31	.38	.23	.33	.34	.19 ☆	.39	.41	.30	.17	.15	.12	.06 ☆	.16	.23	.20	.20
	February	.24	.15	.05 ☆	.20	.25	.14	.11	.08	.15	.16 ☆	.27	.14	.16	.20	.25	.18	.07 ☆	.19	.24	.33	.34	.23	.22	.12 ☆	.29	.22	.19	.30			
	March	.25	.20	.24 ☆	.28	.29	.31	.26	.19	.17	.12 ●	.27	.38	.34	.35	.24	.26	.20 ●	.29	.10 ☆	.27	.28	.39	.25	.18 ●	.22	.18	.23	.25	.21	.25	.14 ●
Miraflori	December	.12	.06 ☆	.19	.35	.50	.47	.67	.16 ☆	.13 ☆	.53	.58	.48	.22	.21	.32	.15 ☆	.29	.37	.43	.34	.50	.29	.14 ☆	.31	.13	.36	.73	.40	.28	.26 ☆	.52
	January	.21	.25	.31	.45	.27	.19	.36	.38	.38	.49	.47	.38	.11 ☆	.48	.35	.43	.19	.53	.55	.15 ☆	.60	.45	.33	.18	.35	.29	.06 ☆	.32	.41	.39	.37
	February	.36	.28	.06 ☆	.39	.44	.32	.19	.45	.61	.18 ☆	.38	.26	.33	.32	.40	.21	.06 ☆	.22	.31	.49	.61	.47	.29	.10 ☆	.37	.22	.17	.24			
	March	.29	.16	.07 ☆	.26	.25	.26	.30	.27	.17	.12 ●	.33	.41	.31	.37	.35	.25	.17 ●	.38	.08 ☆	.32	.31	.36	.19	.11 ●	.20	.16	.24	.28	.26	.23	.09 ●
Ferriere	December	.19	.04 ☆	.12	.09	.24	.40	.46	.13 ☆	.14	.32	.35	.33	.22	.20	.19	.14 ☆	.30	.29	.29	.24	.29	.29	.12 ☆	.21	.13	.22	.52	.49	.35	.24 ☆	.28
	January	.15	.18	.21	.28	.32	.22	.35	.44	.31	.38	.47	.38	.20 ☆	.44	.35	.44	.26	.43	.45	.17 ☆	.52	.49	.37	.24	.25	.27	.08 ☆	.21	.28	.29	.26
	February	.26	.21	.04 ☆	.24	.32	.19	.16	.23	.24	.09 ☆	.25	.22	.28	.24	.31	.19	.06 ☆	.17	.25	.35	.33	.27	.15	.05 ☆	.21	.15	.14	.15			
	March	.20	.18	.07 ☆	.21	.29	.27	.26	.20	.19	.12 ●	.22	.33	.21	.25	.18	.15	.17 ●	.23	.07 ☆	.18	.14	.27	.21	.14 ●	.20	.18	.19	.17	.23	.32	.16 ●

☆ Holiday without traffic

● Holiday with traffic at alternate number-plates

ENCL. 31

HYDROCARBONS (ppm as CH_4)

Daily averages recorded during the period Dec. 73 - Mar. 74 characterized by limitation in private vehicular traffic

	MONTHS	1	2	3	4	5	6	7	8	9	10	11	12	13	14	15	16	17	18	19	20	21	22	23	24	25	26	27	28	29	30	31
Total hydrocarbons	December	3,07	1,76 ☆	5,30	4,40	4,91	4,32	5,97	2,06 ☆	1,38 ☆	3,13	3,21	3,35	2,41	2,34	2,37	1,68 ☆	5,50	4,82	3,68	3,00	3,65	2,60	1,79 ☆	2,20	1,73	2,06	4,30	5,90	5,30	4,80 ☆	5,10
	January	2,10	4,30	3,50	2,80	3,40	2,70	1,60	1,20	0,90	1,40	1,60	1,60	1,20 ☆	1,40	0,90	1,20	1,50	2,10	2,20	1,80 ☆	2,00	2,00	1,50	1,00	0,90	0,80	0,70 ☆	1,00	1,20	0,80	0,90
	February	1,05	0,70	0,50 ☆	0,90	0,90	0,70	0,50	0,80	1,30	1,03 ☆	1,96	1,90	2,30	2,90	2,40	2,10	1,30 ☆	2,60	2,30	3,60	3,80	2,40	1,70	2,10 ☆	3,20	1,30	1,80	2,20			
	March	1,90	2,10	1,60 ☆	2,00	2,90	3,20	2,40	1,80	1,70	1,20 ●	1,70	2,60	2,40	3,00	2,20	2,70	2,70 ●	1,50	1,60 ☆	2,10	2,50	3,10	2,30	2,60 ●	2,40	2,00	2,00	2,40	2,20	2,40	1,90 ●
Methane	December	2,03	1,35 ☆	3,67	2,75	3,08	2,72	3,56	1,41 ☆	0,86 ☆	1.83	2,30	2,48	1,69	1,82	1,76	1,06 ☆	4,05	3,46	2,62	1,86	2,24	1,92	1,09 ☆	1,39	1,18	1,55	1,70	3,00	2,60	2,30 ☆	2,10
	January	1,30	1,80	1,70	1,60	2,40	1,70	1,10	0,80	0,60	0,80	1,10	1,10	1,00 ☆	0,90	0,60	0,70	0,90	1,20	1,30	1,30 ☆	1,20	1,20	1,10	0,70	0,60	0,50	0,40 ☆	0,60	0,70	0,60	0,60
	February	0,70	0,60	0,30 ☆	0,50	0,70	0,50	0,30	0,50	0,90	0,70 ☆	1,40	1,40	1,60	2,10	1,70	1,50	0,96 ☆	1,50	1,60	2,30	2,70	1,20	1,50	1,20 ☆	2,20	1.30	1,30	1,40			
	March	1,50	1,60	1,40 ☆	1,50	2,00	2,20	1,40	1,10	1,00	0,90 ●	1,00	1,40	1,50	1,90	1,40	2,10	2,10 ●	1,90	1,30 ☆	1,50	1,30	2,30	1,50	2,10 ●	1,60	1,40	1,30	1,70	1,70	1,60	1,50 ●
Non-methane hydrocarbons	December	1,04	0,41 ☆	1,60	1,65	1,83	1,60	2,41	0,65 ☆	0,52 ☆	1,30	0,91	0,87	0,72	0,52	0,61	0,62 ☆	1,45	1,36	1,06	1,14	1,41	0,68	0,70 ☆	0,81	0,55	0,51	2,60	2,90	2,70	2,50 ☆	3,00
	January	0,80	2,50	1,80	1,00	1,00	1,00	0,50	0,40	0,30	0,60	0,50	0,50	0,20 ☆	0,50	0,30	0,50	0,60	0,90	0,90	0,50 ☆	0,80	0,80	0,40	0,30	0,30	0,30	0,30 ☆	0,40	0,50	0,20	0,30
	February	0,35	0,10	0,20 ☆	0,40	0,20	0,20	0,20	0,30	0,40	0,33 ☆	0,56	0,50	0,70	0,80	0,70	0,60	0,34 ☆	1,00	0,70	1,30	1,10	1,20	0,50	0,60 ☆	1,00	0,60	0,50	0,80			
	March	0,40	0,50	0,20 ☆	0,50	0,90	1,00	1,00	0,70	0,70	0,30 ●	0,70	1,20	0,90	1,10	0,80	0,60	0,60 ●	0,60	0,30 ☆	0,60	0,90	0,80	0,80	0,50 ●	0,80	0,60	0,70	0,70	0,50	0,80	0,40 ●

☆ Holiday without traffic

● holiday with traffic at alternate number-plates

ENCL. 32

STATION	MONTHS	NITROGEN DIOXIDE (NO_2 - ppm) Daily averages recorded during the period Dec. 73 - Mar. 74 characterized by limitation in private vehicular traffic.																														
		1	2	3	4	5	6	7	8	9	10	11	12	13	14	15	16	17	18	19	20	21	22	23	24	25	26	27	28	29	30	31
Via Lagrange	December	.043	.031 ☆	.041	.021	.023	.029	.036	.034 ☆	.022 ☆	.037	.037	.035	.027	.008	.015	.015 ☆	.030	.031	.032	.033	.033	.028	.012 ☆	.026	.020	.034	.040	.039	.045	.030 ☆	.030
	January	.030	.020	.019	.024	.032	.024	.042	.035	.029	.033	.034	.037	.033 ☆	.030	.021	.035	.024	.037	.025	.022 ☆	.039	.040	.031	.021	.021	.017	.008 ☆	.016	.025	.017	.024
	February	.022	.017	.016 ☆	.017	.024	.016	.016	.021	.040	.025 ☆	.031	.020	.015	.025	.027	.029	.019 ☆	.022	.031	.028	.039	.039	.029	.031 ☆	.047	.029	.031	.035	.		
	March	.036	.035	.025 ☆	.035	.038	.049	.052	.041	.040	.025 ●	.033	.053	.053	.060	.059	.059	.052 ●	.039	.028 ☆	.050	.038	.034	.048	.038 ●	.047	.046	.064	.063	.066	.077	.068 ●

☆ Holiday without traffic

● Holiday with traffic at alternate number-plates.

6th NATO/CCMS
International Technical Meeting
on Air Pollution Modeling

A STANDARDIZED MODEL FOR THE PROJECTION OF GROUND LEVEL CONCENTRATIONS AND ITS APPLICATION IN THE APPROVAL PROCESS FOR AIR POLLUTING INDUSTRIAL FACILITIES

by

S. Külske
Landesanstalt für Immissions- und Bodennutzungsschutz
Essen

BATTELLE - INSTITUT E.V., Frankfurt/Main
Germany, FR

24 - 26 September, 1975

Preceding page blank

Calculations are necessary to determine ground level concentrations, which are to be expected in the surroundings of industrial facilities. Such calculations are carried out for the implementation of industrial facilities as well as for the extension of existing facilities. We normally use a Gaussian plume model with the usual assumption of a biaxial Gaussian distribution. The model and its application are explained in the following.

The model calculates frequency distributions of ground level concentrations at given receptor points for given point, line, or area sources.

Reproduced from
best available copy.

Line and Area sources are simulated by a number of representative point sources. The edges of the partial sources must not be larger than 20 % of the distance of the middle point of the area to the closest receptor point.

Yearly frequency distributions of the following meteorological parameters are used:

- stability classes by Turner
- wind directions in classes of 10° and the assumption of an equal distribution in steps of 1° within the classes of 10°
- wind speeds in the steps 1, 1.5, 2, 3, 4.5, 6, 7.5, 9, 12 m/s.

The assumption of an equal distribution of the wind directions within the classes of 10° is absolutely necessary as may be seen from fig. 1.

The upper part of the figure shows the north-east sector from the source location. The classification of wind directions in 10° without the assumption of an equal distribution results in concentrations which are higher along the direction beams. The immission field is inhomogeneous. The lower part of the figure shows a homogeneous immission field for the same source with the assumption of equal distribution within the 10° classes.

The plumerise is calculated with the formula of Moses for neutral meteorological conditions:

$$\Delta h = 0.35 \cdot \frac{vd}{\bar{u}} + 5.41 \cdot \frac{Q_H^{1/2}}{\bar{u}}$$

Δh : plumerise in m
v : exhaustion velocity of the waste gas in m/s
d : stack diameter in m
Q_H : termal energy of the waste gas in kcal/s
$\bar{u}$: mean wind velocity averaged over the plumerise interval in m/s

Figure 2 shows a comparison of calculated ground level concentrations in the north-east sector of a 40 m high source as 97.5 % values of the concentration, i.e. 97.5 % of the calculated ground level concentrations are lower values than those shown here. The lower part of the figure shows values calculated with the plumerise formula of Briggs while the upper part shows values calculated with the formula of Moses for neutral meteorological conditions. The Briggs formula calculates a maximum immission load of about 70 % of the maximum immission load, which is calculated with the Moses formula. Using the Moses formula the maximum immission load is about 500 m closer to the source. Lidar measurements at stacks of power plants indicate that the Moses formula gives a more realistic description of the plumerise.

Meteorological stabilities and dispersion parameters σ_y and σ_z are classified according to Turner and not according to Klug, which is usual in the Federal Republic. σ_y and σ_z-values of Mc Elroy-Pooler or Singer-Smith are used depending on the source height of emissions. The following figure 3 explains the use of the σ-values. For stack heights up to 20 m and distances less than 600 m the σ-values of Mc Elroy-Pooler are used, while

For source heights over 100 m the calculation is based on σ-values by Singer-Smith. For source heights between 50 and 100 m σ-values are got by linear interpolation between the values of Mc Elroy-Pooler and Singer-Smith.

The following figures show comparisons of annual averages of calculated ground level concentrations in the surrounding of a 10 m high emitter. The classification of Klug is compared to the classification of Turner and the above mentioned σ are used.

Figure 4: Description of 95 % values of ground level concentrations

a) calculated with Klug classifications
Values over 50 microgram per m^3 may only be found in the northern area of the source. The maximum is 1.14 mg/m^3 in the distance of 600 m.

Reproduced from best available copy.

b) calculated with Turner classification and σ-values by Mc Elroy-Pooler
The field of ground level concentrations is evidently more homogeneous. The maximum of 3 mg/m^3 occurs in the close neighbourhood of the source.

The Turner classification and the use of Mc Elroy-Pooler parameters, therefore, leads to more realistic results.

In order to cover the unsafety of the projection as well as the cases with wind speeds less than 1 m/s, which cannot be calculated, and inversion situations not been taken into consideration, the simulated concentration values are multiplied by a safety factor of 1.5.

The licensing of an industrial facility can only be approved if the total load - which consists of the existing load and the additional load caused by the planned industrial facility - does not exceed immission standards. The existing load is determined by measurements. The difficult task now is to add up the existing load and the additional load to a total load. For the percentage values of the frequency distribution this is done by using the multiplication theoreme of the theory of probability to the distributions of existing and additional load. It may be assumed that the distributions may be approximated by exponential distributions.

An arbitrary percentage ξ_q of the total distribution may be calculated according to the following equation:

$$(\alpha-\beta)\cdot(1-q)=\alpha\cdot e^{-\beta\xi_q}-\beta e^{-\alpha\xi_q}$$

with

$\alpha=\frac{1}{a}$ a: mean value of the 1st distribution

$\beta=\frac{1}{b}$ b: mean value of the 2nd distribution

q: the basic quantic of the distribution

Reproduced from best available copy.

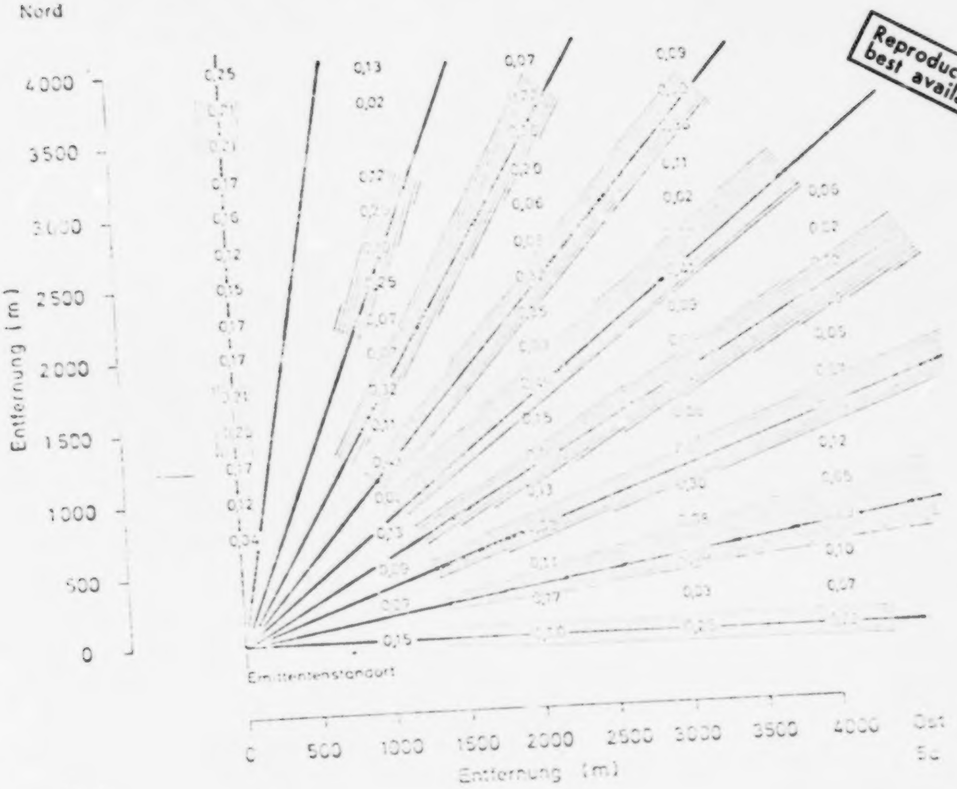

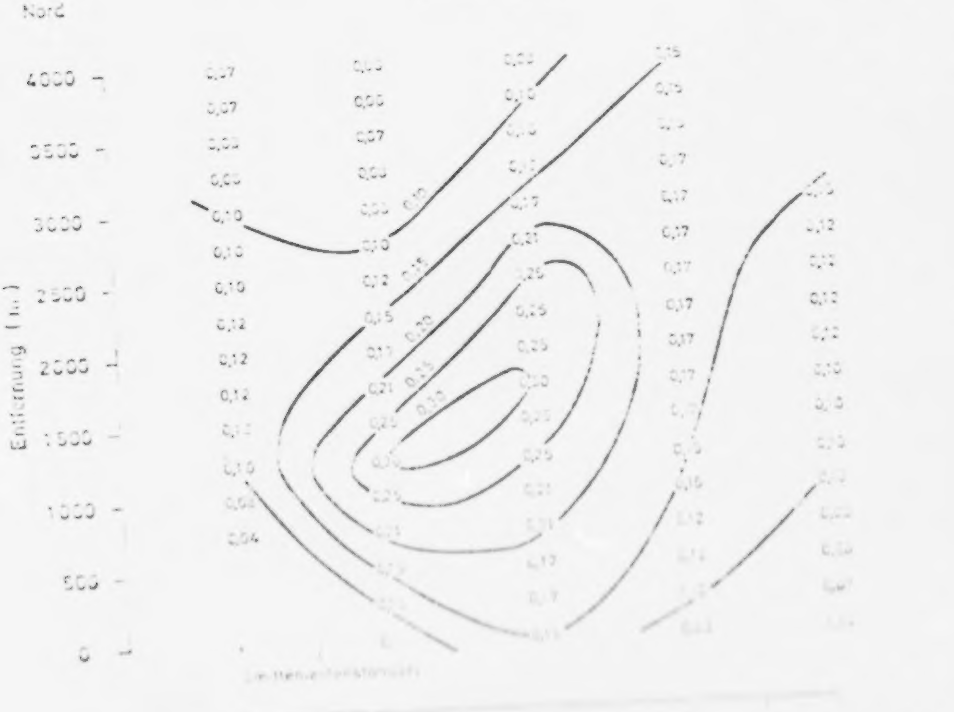

[illegible] in the perib[illegible] sector of the source, [illegible] ^{3}/h ,
[illegible] quantity of waste gas R = 25000 N
[illegible] according to Klug, C- parameters
[illegible] of 10°
[illegible] direction class of 10°

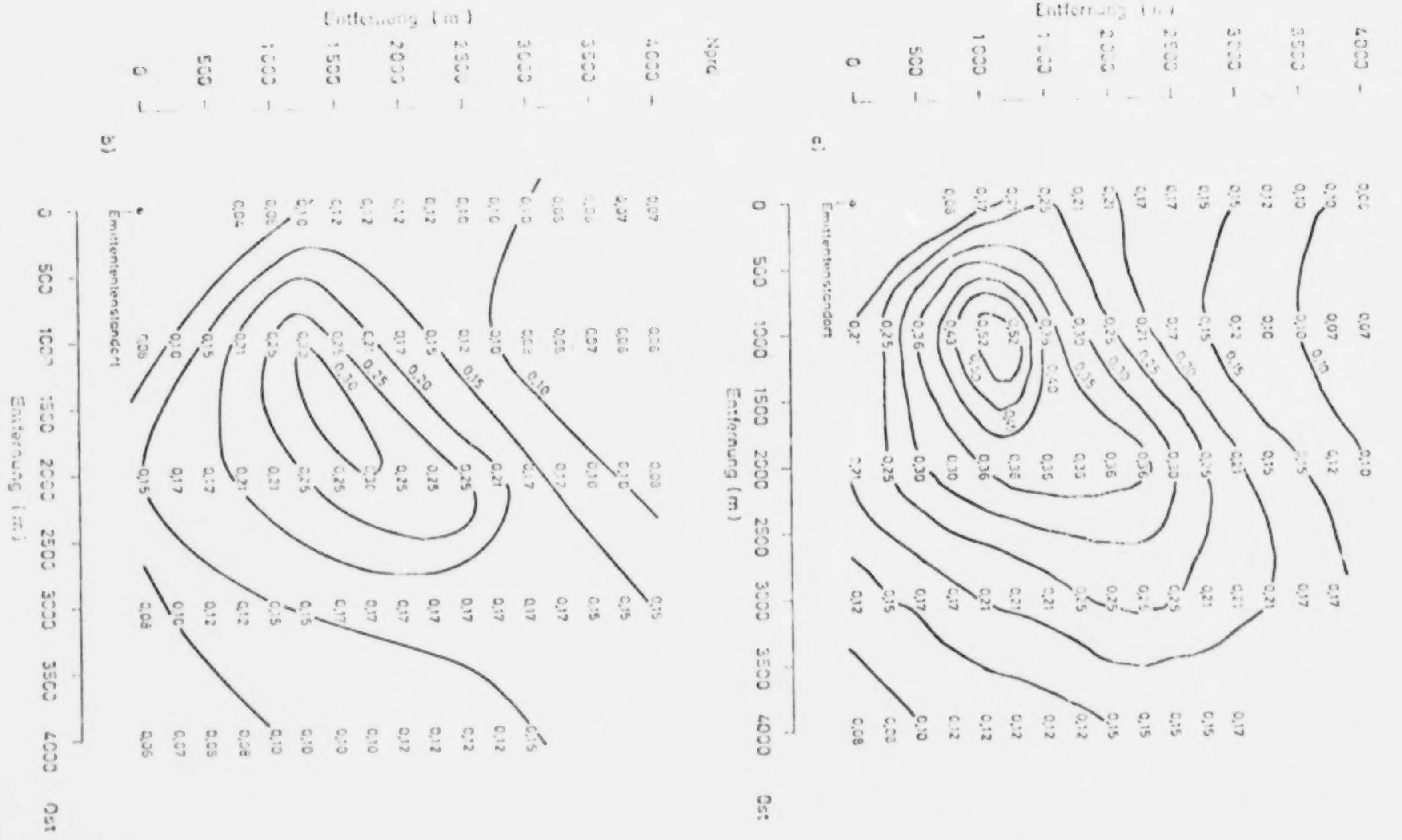

Fig. 2:

97.5 % value of ground level concentrations in mg/m^3 in the north-east sector of the source. Stack height h = 40 m, quantity of emission Q = 500 kg/h, quantity of waste gas R = 25000 Nm^3/h, waste gas temperature T = 120°C. Classification of stability according to Klug, σ-parameters by Klug.

a) calculation with the plumerise formula by Moses for neutral stability

b) calculation with the plumerise formula by Briggs

Use of σ -values

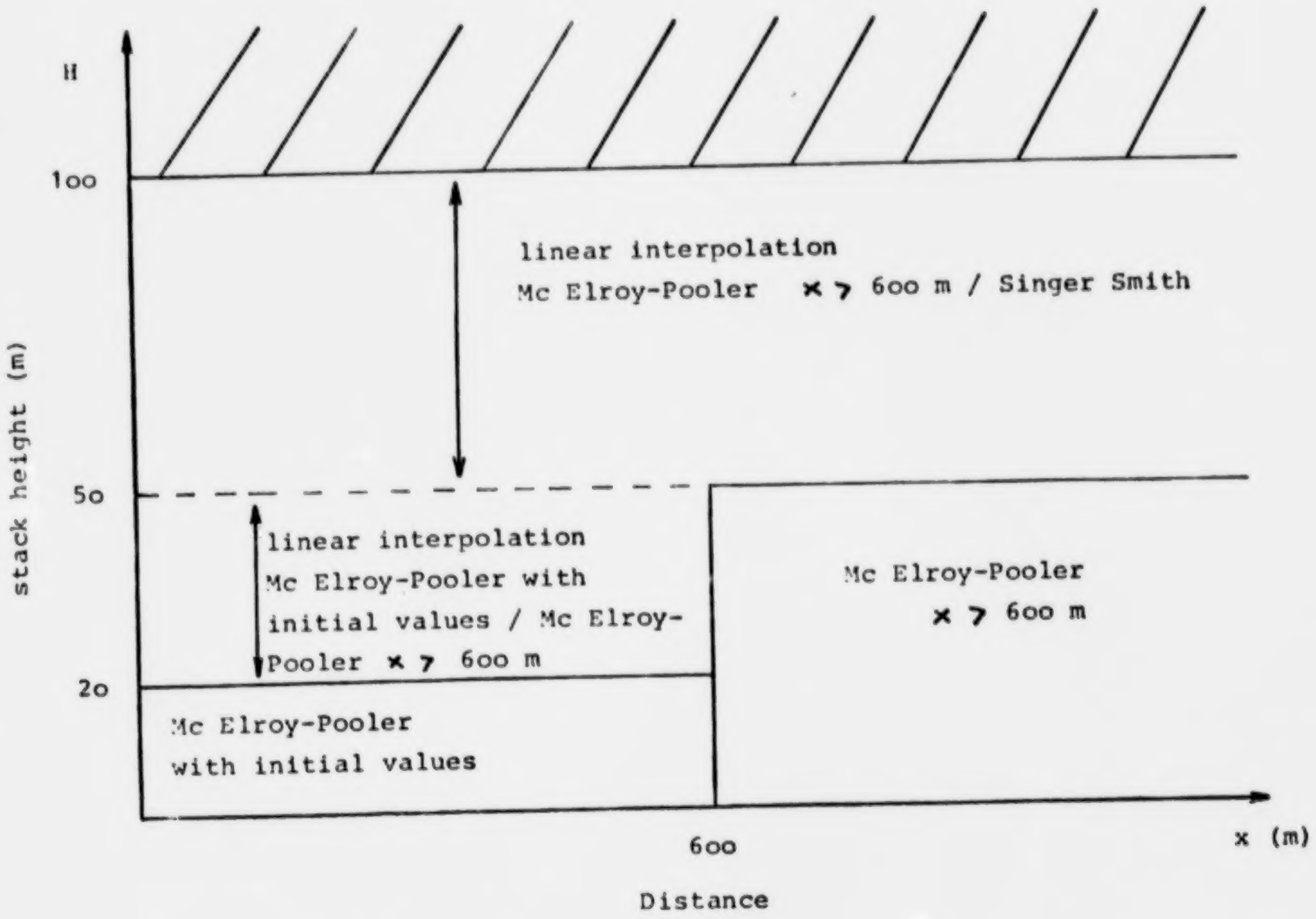
H
100
50
20
stack height (m)
linear interpolation
Mc Elroy-Pooler $x > 600$ m / Singer Smith
linear interpolation
Mc Elroy-Pooler with initial values / Mc Elroy-Pooler $x > 600$ m
Mc Elroy-Pooler $x > 600$ m
Mc Elroy-Pooler with initial values
600
x (m)
Distance

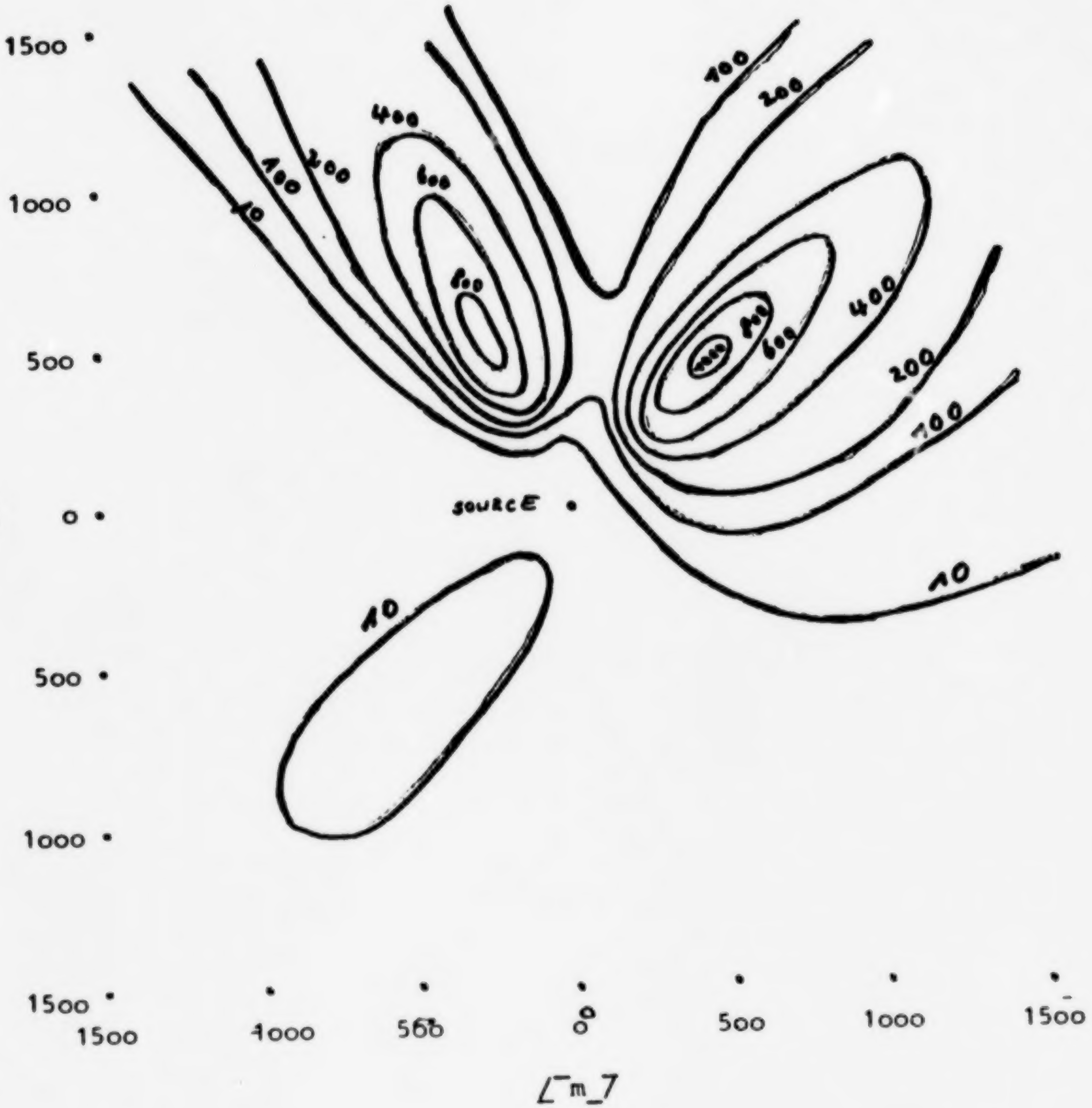

Fig. 4a:

95 % values of ground level concentrations in $/ug/m^3$

H = 1o m

Q = 5oo kg/h

R = 25.ooo m_n/h

Klug-classification

Station: Düsseldorf

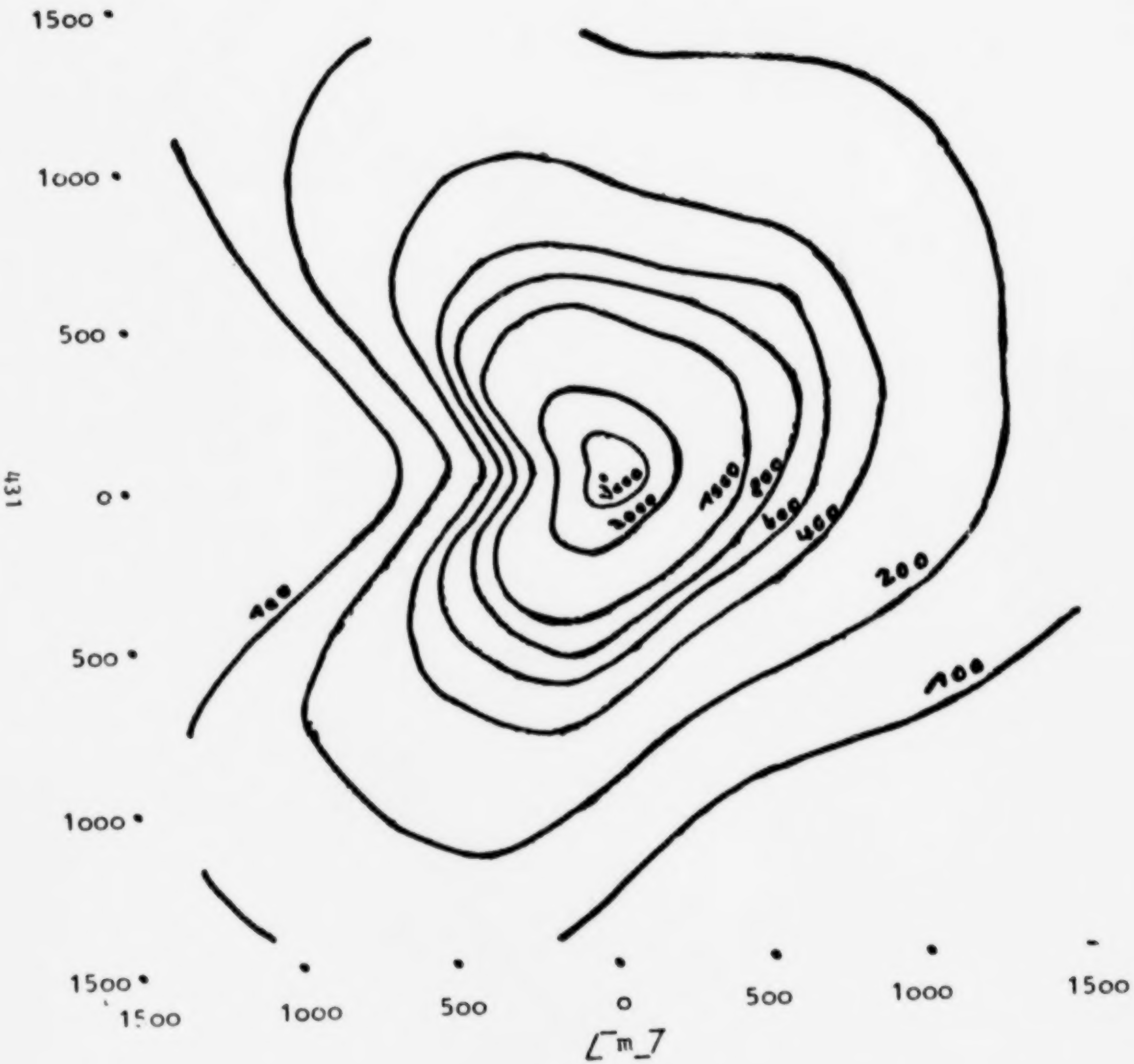

Fig. 4 b:

95 % values of ground level concentrations in $\mu g/m^3$

H = 1o m
Q = 5oo kg/h
R = 25.ooo m_n/h
Station: Düsseldorf
Turner-classification
Sigma: Mc Elroy-Pooler

6th NATO/CCMS
International Technical Meeting
on Air Pollution Modeling

A STANDARDIZED DISPERSION MODEL FOR JUDGING THE PERMISSIBILITY OF AIR POLLUTING INDUSTRIAL FACILITIES

by

MR O.A. Schmitt

Der Minister für Arbeit, Gesundheit und
Sozіales des Landes Nordrhein-Westfalen

BATTELLE - INSTITUT E.V., Frankfurt/Main
Germany, FR
24 - 26 September, 1975

Preceding page blank

1. Administrative View Points of the Application of Dispersion Calculations

The establishing and the operating of air polluting industrial facilities, e.g. facilities of iron and steel industry, chemical and petrochemical processes, are subject to licensing in the Federal Republic. The authorities may deliver a license only if it is proved that no harmful effects on the environment (dangers to health, major molestations, and major disadvantages) are caused by the implementation and operation of such facilities.

Air pollutions, for instance, are qualified as harmful effects on the environment, if certain immission standards are exceeded.

Therefore, the authorities have to calculate - or order the calculation of - expected concentrations of air polluting substances caused by the planned industrial facilities in the surroundings of these facilities in order to make a legal decision.

I do not want to hide that authorities do not always proceed according to this method. In many cases law courts had to revise the decisions of authorities because

> "calculations and investigations on expected air pollutions caused by the facilities subject to licensing"

were missing.

In other cases precalculations were made, but the choice of the calculation methods and parameters was left to the expert so that the same premises led to different results.

Lately a high law court again revised a decision of authorities and requested that normally the additional load which is to be expected from a planned facility may be calculated, but the existing load caused by existing facilities must be determined by measurements in order to get an estimation as exact as possible.

To make sure that the applications for licensing are handled and judged equally, our ministry tried to codify the total material. In the short time available, I only can give a survey of the most important regulations. Mr. Külske will explain important details of the dispersion calculations.

II. The Most Important Regulations

Emission Data

As the quality of the results of dispersion calculations cannot be better than the quality of the emission data, we have developed a system of forms, which shall give us a - time and space dependent - view of the emission situation as realistically as possible. We have made the experience that short-term emissions - which are caused e.g. during starting and stopping conditions of facilities or occur during jam conditions and while loading products - are of greater importance in causing harmful effects to the environment than emissions during normal operating conditions. Therefore, we must be able to calculate with dispersion models high percentages of the yearly frequency distribution in order to determine short-term immissions.

Estimation of Relevant Emission Components

From the emission data for the planned facilities it must be estimated which emission components according to nature - e.g. smelling intensity or toxicity -, amount, derivation conditions, and time dependent distribution may be looked upon as being of decisive importance for the approval process. For those components - normally not more than four - the calculation of immissions has to be done.

Dispersion Model - Choice of Parameters

The dispersion model used by us is a plume model. It is based on the Pasquill equation, but it contains a large number of parameters which include a manifold world-wide experience to a different degree. The model was standardized especially according to the simulation technique of line and area sources, the handling of non-constant emissions, the classification of the wind speed, the choice of the plumerise formula, the choice of dispersion parameters depending on emission height and distance, and the use of a safety factor in order to consider the unsafety of the model and the meteorological situations of wind speeds less than 1 m/s., which cannot be simulated with a plume model.

Application of the Calculation Procedure

The immission load in the surroundings of the planned facilities (so-called additional load) is determined space and time dependently - as is asked for by legal request for the approval process -. As to area sources we choose a polar coordinate system to determine those points for which a calculation of ground level concentrations has to be done (so-called receptor points). Thus, this system guarantees that expense and information are in an optimal proportion. In the neighbourhood of the facilities the receptor points are closer together, while at the boundaries of the area under consideration there are not as many receptor points.

For high point sources (stack heights of power plants) a Cartesian coordinate system is used, as it allows constant grid width even for large distances, which are of major interest in this case.

At all receptor points or - if certain parts of the area under consideration are not interesting - at the decisive receptor points, as e.g. in housing areas, the ground level concentrations have to be calculated for all meteorological dispersion conditions, which may be described by wind direction, wind speed, and stability class. They have to be described as a frequency distribution using the frequency of the meteorological dispersion situation.

The 99 % value has to be calculated from the frequency distribution in order to answer the question if effects which are dangerous to health may be caused by the immissions. In order to judge the permissibility of molesting effects, 98 % to 94 % values have to be determined according to regulations of standards. The results got by this procedure are multiplied by the safety factor of 1.5 in order to take into account of dispersion situations which cannot be calculated as well as eventual uncertainties which may lead to higher concentrations.

According to the safety philosophy used in the Federal Republic this risk has to be carried by the operators of industrial facilities.

Total Load

The final judgment and the decision about the application for licensing are not possible without knowing the existing load in the areas being possibly influenced by the planned facilities. Normally, this existing load has to be measured according to the above cited sentence. The total load, which results from existing and additional load, may be got for each receptor point by adding percentages of equal size of the existing and additional load. The percentages of the existing load are determined according to a distribution-free mathematical test, which garantees a statistic safety of at least 75 %. On the other hand, the addition of percentages of different bases causes difficult problems. But they could be solved by means of the multiplication theoreme of the probability theory, since investigations showed that the distribution functions could be approximated adequately by exponential functions in the range of higher percentages.

Examining of the Total Load

According to the above described legal requirements, licenses may be given only if the comparison of the percentages for the total load to the immission standards shows that these immission standards will not be exceeded if the planned facilities are operated in the later future.

The immission standards are based on effects of air polluting substances which are dangerous or molesting. This differentiation is not only reflected by different standards but also by different exceeding-frequencies allowed.

Rapporteur's Report, Topic II (continued), September 25, 1975
by D. Jost

Chairman: K. L. Calder

A. Longhetto: Models of Temperature Profiles under Convective and Inversion Conditions connected to Air Pollution.

Discussion:

F. B. Smith: In which way is entrainment of energy from above included in the mentioned Carson Model?

A. Longhetto: This entrainment is not taken into account.

O. A. Schmitt: A standardized Model for the Projection of Ground Level Concentrations and its Application in the Approval Process for air polluting industrial Facilities.

Discussion:

W. B. Johnson: What is the interpretation of the differences shown in the two calculated concentration fields?

O. A. Schmitt: The differences are due to the diffusion parameters used according to Klug and Turner. Measurements in the neighbourhood of an aluminum manufactury show the maximum to appear very near to the source, this finding is in accordance with calculations using Turner parameters, whereas Klug parameters lead to more distant maxima.

6th NATO/CCMS
International Technical Meeting
on Air Pollution Modeling

TOPIC III

VALIDATION OF AIR QUALITY SIMULATION MODELS

Battelle - Institut e. V. Frankfurt / M
Germany, FR

24 - 26 September, 1975

6th NATO/CCMS
International Technical Meeting
on Air Pollution Modeling

USING SENSITIVITY ANALYSIS TO DETERMINE DISPERSION MODELING INPUT REQUIREMENTS

by

Mr. Charles C. Masser and Dr. James R. Hammerle
National Air Data Branch, EPA, Research Triangle Park, N. C. 27711

BATTELLE - INSTITUT E.V., Frankfurt/Main

Germany, FR

24 - 26 September, 1975

Preceding page blank

INTRODUCTION

Perhaps the most difficult task in the analysis of regional air pollution studies is the collection and verification of an adequate emissions data base. In practice these data requirements are often difficult to define because of the physical measurements involved and their expense of collection.

This paper will utilize the Climatological Dispersion Model[1] to develop the sensitivity analysis procedure. The resulting techniques are presented such that the accuracy requirements of each parameter can be determined as a function of the remaining parameters and the maximum allowable pollutant concentration. Also, given a complete set of parameters and their accuracy estimates, the resulting maximum possible error in pollutant concentrations can be calculated.

The development of the sensitivity analysis procedure involves three steps. (1) Definition of the error equation and how it relates to air pollutant concentrations, (2) definition of the predictive air pollutant concentration equations and consideration of their inputs, and (3) solution of the error equation using the air pollutant concentrations equations. A single specific example is given where the impact of air pollutant concentration is calculated due to an error in source location.

---

[1] Busse, A. D. and Zimmerman, J. R., Dec. 1973: Users Guide for the Climatological Dispersion Model EPA Report-R4-73-024.

Error Analysis

The first task in the error analysis is the definition of a meaningful measure of the error (e.g., the difference in air pollutant concentration prediction with and without an error in any of the dependent variables). One can recognize that this error can be a function of many parameters: source strength, stack height, stack diameter, gas exit velocity or temperature, lateral and longitudinal receptor position, or atmospheric stability. Since concentrations predicted are a function of atmospheric conditions, the development of this analysis will utilize a worst-case meteorological situation in order to determine the most stringent source-receptor resolution required. However, a single stability category cannot be used to satisfy this criterion because the worst-case stability for a low stack can differ from that for a tall stack. Two stability regimes --slightly stable (Class E) and slightly unstable (Class C) have, therefore, been determined to be useful in most sensitivity calculations. Source strength and stack height are elements of assessment methodology, and thus the individual source features are retained. For the impact of the emission parameters on the calculated air quality at a receptor, two alternatives for the user exist: (1) determination of the error associated with a particular source at one or more specified receptor locations (e.g., air qualtiy monitoring site), or (2) evaluation of the impact of a particular source throughout the study region. Therefore we define as the measure of error the intergral of the error over both the lateral (crosswind) and longitudinal (downwind) directions; the longitudinal distance may be taken as the distance either to the receptor or to the downwind edge of the study region.

The integrated measure of error, due to a variation in the concentration dependant variables, may be defined as:[2]

$$IE = \int_x \int_y \left| \chi - \chi_E \right| dy\, dx \qquad (1)$$

where:

IE = integrated measure of error

χ = reference concentration = $f(x,y)$

χ_E = concentration due to an error in the dependent variables = $f(x,y)$

x = distance to receptor along the mean wind direction from the source (m).

y = crosswind distance to receptor (m)

The sensitivity of any concentration-dependent variable can be studied by solving this equation.

Pollutant Concentration Equations

The basic Gaussian plume formula for atmospheric dispersion is described in detail elsewhere,[3] however the basic assumption assumes the plume spread has a Gaussian distribution in both the horizontal and vertical planes.

---

[2] Littman, F. E.; Rubin, S.; Semrau, K. T.; Dabberdt, W. F: January 1974, A Regional Air Pollution Study (RAPS) Preliminary Emission Inventory. EPA Report 450/3-74-030.

[3] Turner, D. B., 1969: Workbook of Atmospheric Dispersion Estimates. EPA Report No. 999-AP-26.

The concentration is given as:

$$\chi = \frac{Q}{\pi \sigma_y \sigma_z \bar{u}} \exp\left\{-\frac{1}{2}\left[\left(\frac{y}{\sigma_y}\right)^2 + \left(\frac{H}{\sigma_z}\right)^2\right]\right\} \qquad (2)$$

where:

Q = source strength (gm $\sec^{-1}$).

H = plume height (m).

$\bar{u}$ = effective transport wind speed (m $\sec^{-1}$).

$\sigma_y = ax^b$ = horizontal standard deviation of pollutant concentration (m).

$\sigma_z = cx^d$ = vertical standard deviation of the pollutant distribution (m).

a, b, c, d = experimentally determined constants dependent on stability conditions.

The plume height, H, is defined as the height of the plume centerline when it becomes almost horizontal. Thus:

$$H = h^* + \Delta h \qquad (3)$$

where: h^* = stack height (m).

Δh = plume rise (m).

All plume rise formulae consider the rise due to two effects; momentum and buoyancy. The momentum term depends upon physical stack parameters (exit velocity and diameter) and the buoyancy term upon heat parameters (heat emission rate or the difference between effluent and ambient air temperature).

There are over 100 formulae and probably 50 papers published reviewing and analyzing the accuracy and applicability of plume rise equations. Without exception, the investigators have concluded that none predict plume rise accurately under all meteorological conditions. At the present time it seems that the preferred equation of the meteorological fraternity is the one developed by Briggs.[4-6] Briggs concluded that the maximum plume rise was:

$$\Delta h = \frac{1.6 F^{\frac{1}{3}} (3.5 x^*)^{2/3}}{\bar{u}} \tag{4}$$

where: F = Buoyancy flux ($m^4 \sec^{-3}$)

x^* = Distance at which atmospheric turbulence begins to dominate entrainment (m).

For distances less than x^* the final plume rise Δh is:

$$\Delta h = \frac{1.6 F^{1/3} x^{2/3}}{\bar{u}} \tag{5}$$

F is defined as:

$$F = \frac{g d^2 V_s}{4} \left(\frac{T_s - T}{T_s} \right) \tag{6}$$

---

[4] Briggs, Gary A., 1969: Plume Rise USAEC Critical Review Series TID-25075, National Technical Information Service, Springfield, Va. 22151

[5] Briggs, Gary A., 1971: Some Recent Analyses of Plume Rise Observation pp 1029-1032, in Proceedings of the Second International Clean Air Congress, edited by H. M. Englund and W. T. Berry. Academic Press, New York.

[6] Briggs, Gary A., 1972: Discussion on Chimney Plumes in Neutral and Stable Surroundings. Atmos. Environ. 6, 507-510 (Jul 72)

where:

d = stack diameter, (m)
g = gravitational acceleration, (9.7m $\sec^{-2}$)
V_s = stack exit gas velocity (m $\sec^{-1}$)
T_s = stack exit gas temperature, (°K)
T = ambient temperature, (°K)

For stable or neutral conditions:

$$x^* = 14\, F^{5/8} \qquad F \leq 55$$

$$x^* = 34\, F^{2/5} \qquad F \geq 55$$

Combining equations (5) and (6) we have:

$$\Delta h = \frac{1.6\, x^{2/3}}{\bar{u}} \left[\frac{g d^2 V_s}{4} \left(\frac{T_s - T}{T_s} \right) \right]^{1/3} \tag{7}$$

Equation (7) and (3) can be combined:

$$H = h^* + \frac{1.6\, x^{2/3}}{\bar{u}} \left[\frac{g d^2 V_s}{4} \left(\frac{T_s - T}{T_s} \right) \right]^{1/3} \tag{8}$$

and substituted in equation (2) resulting in a general relationship:

$$\chi = f(Q, V_s, T_s, h^*, x, y, \bar{u}, d, T)$$

The effect of an error in any of these parameters (Δ) on the pollutant concentration (calculated χ) can therefore be determined.

Solution of Error Integral

Using equation (2) for χ and modified equation (2) for χ_E in equation (1) the error may result from incorrect estimates of V_s, T_s, h^*, or y, considering Q and $\bar{u}$ as constant over the integration, it is possible to define an integrated normalized (concentration) error[2] INE, where:

$$IE = \frac{Q}{\pi \bar{u}} INE \tag{9}$$

For given values of H, stability, and x the values of Δy(error in y) for various INE (for example have been calculated[2] and are shown in Figures 1 through 8, using the following relationship with equation (2) in equation (1):

$$\chi_E = \frac{Q}{\pi \sigma_y \sigma_z \bar{u}} \exp\left\{-\frac{1}{2}\left[\left(\frac{y+\Delta y}{\sigma_y}\right)^2 + \left(\frac{H}{\sigma_z}\right)^2\right]\right\} \tag{10}$$

where:

Δy = lateral source location error, (m)

This procedure can be repeated for other given parameters to indicate INE as a function of errors in any of the parameters.

---

[2] Ibid.

Example Solution

To determine the allowable source location error, Δy, for given Q, H, $\bar{u}$, x and stability conditions, equation (9) is solved for INE, which is then used to obtain Δy from Figures 1 through 8. However, equation (9) contains two unknowns, IE and INE, therefore a value for IE that represents a tolerable level of concentration error must be specified or chosen.

The error limit for this example is specified on the basis of (1) a reference source strength, $Q_{reference}$, and (2) an allowable source location error for that strength (from which $INE_{reference}$ is found using Figures 1 through 8). Thus, IE in Equation (9) becomes the reference integrated normalized concentration error at downwind distance x for a specific source height and stability.

$$IE = \left(\frac{Q_{reference}}{\pi \bar{u}} \right) INE_{reference} \qquad (11)$$

Using equations (9) and (11), where $IE = IE_{reference}$, since error acceptable is the same regardless of source size when source-receptor distance is the same, yields a relationship for INE (assuming the same wind speed):

$$INE = INE_{reference} \left(\frac{Q_{reference}}{Q} \right) \qquad (12)$$

The permissible resolution error, Δy, is then determined from Figures 1 through 8 on the basis of INE together with atmospheric stability, source height, and the selected downwind distance. Figures 1 through 4 apply to stable atmospheric conditions, while Figures 5 through 8 apply to the unstable. Source heights of 0, 5, 30, and 100 meters are used in the figures, while Δy values are 5, 15, 30, 60, and 100 meters; interpolation must be used for intermediate values. A step-by-step procedural outline and example follow. Note that a minimum Δy of 10 meters is recommended because of the impact of stack diameter and initial mixing in limiting the occurrence of smaller values.

The determination of Δy comprises the following steps:

Step	Task
1.	Select stability category (stable or unstable), stack height (H), downwind distance (x), $Q_{reference}$, and $\Delta y_{reference}$.
2.	Using stability, H, x, and $\Delta y_{reference}$, determine $INE_{reference}$ from Figures 1 through 8.
3.	Select Q, and using it, $INE_{reference}$, and $Q_{reference}$, solve Equation (4) for INE using the selected Q, $INE_{reference}$, and $Q_{reference}$.
4.	Using stability, H, x, and INE, determine Δy from Figures 1 through 8.

For example, considering that the smallest source under consideration ($Q_{reference}$) is to emit at least 100 tons/year, and that the majority of source locations may be determined, using available maps, within ± 100 m ($\Delta y_{reference}$), Figure 3 may be used to determine INE = 409 for a downwind receptor point of 10 km ($x = 10^4$ m) in stable atmospheric conditions and stack height 30 m. Next, consider a source emitting 10,000 tons/year and stack height of 100 m with what precision should this large source be located?

From equation (12)

$$\text{INE} = 409 \quad \frac{100 \text{ tons/year}}{10{,}000 \text{ tons/year}} = 4.09$$

From Figure 4, for stable atmospheric conditions, given the same receptor distance of 10 km (10^4m), Δy = 5m, or, in given the previously mentioned minimum Δy of 10 m , the source location should be specified within ± 10m.

A significant feature of this method is its flexibility: the error measure can be taken to most any selected downwind distance or distance interval. In addition, rather than specifying a single resolution required of all stacks, the method yields a recommended spatial resolution for each source based on the stack height and emission rate of the individual source maintaining the same source-receptor distance. The analysis can also be applied to any of the variables contained in the concentration equation such as stack temperature, height, diameter or exit velocity, providing that the INE figures be replotted for other parameters than Δy.

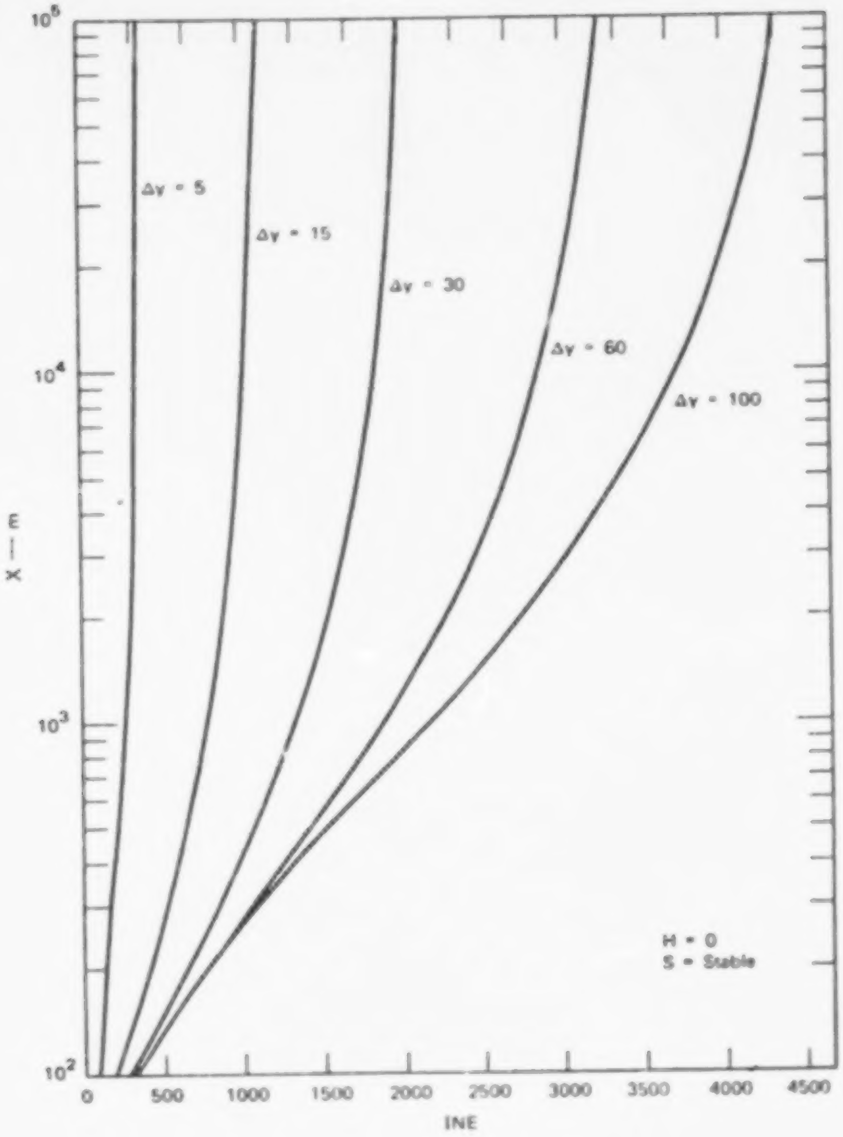

FIGURE 1 VARIATION OF INTEGRATED NORMALIZED ERROR WITH LONGITUDINAL DISTANCE FROM THE SOURCE WHEN SOURCE HEIGHT IS AT THE SURFACE AND ATMOSPHERIC CONDITIONS ARE STABLE

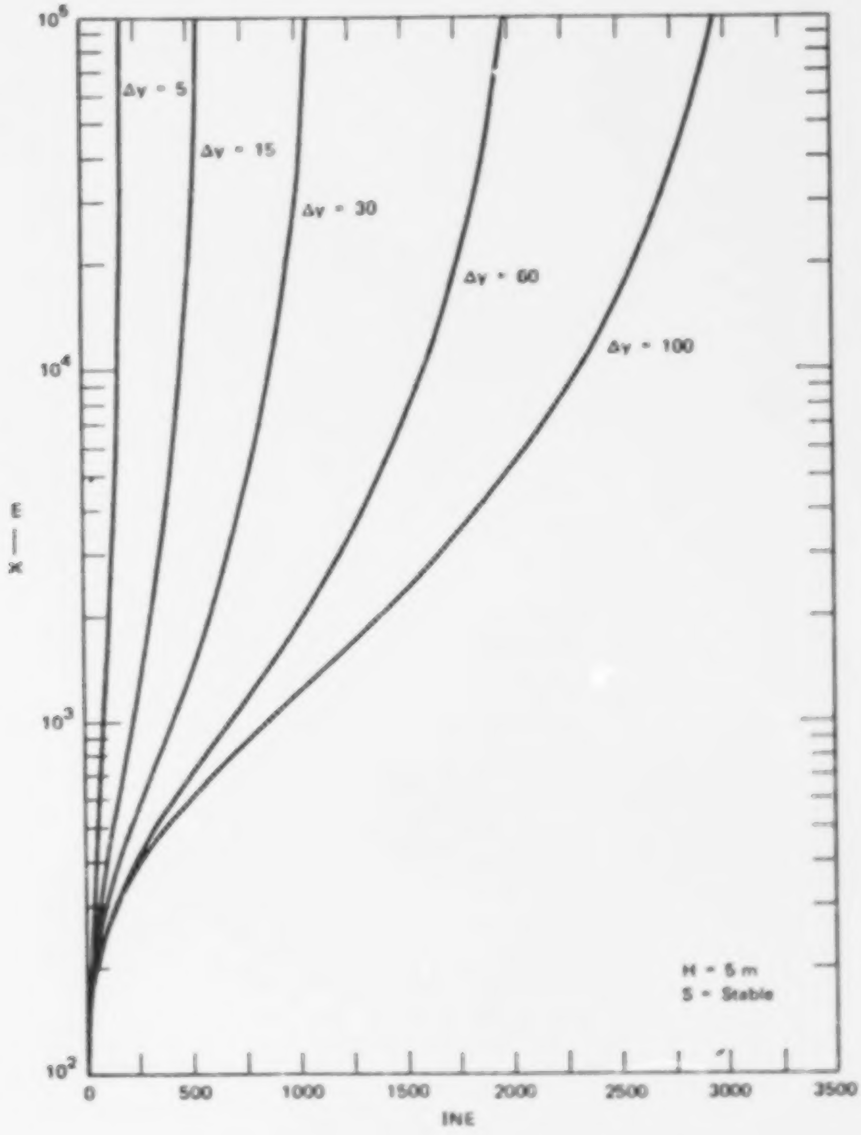

FIGURE 2 VARIATION OF INTEGRATED NORMALIZED ERROR WITH LONGITUDINAL DISTANCE FROM THE SOURCE WHEN THE SOURCE HEIGHT IS FIVE METERS AND ATMOSPHERIC CONDITIONS ARE STABLE

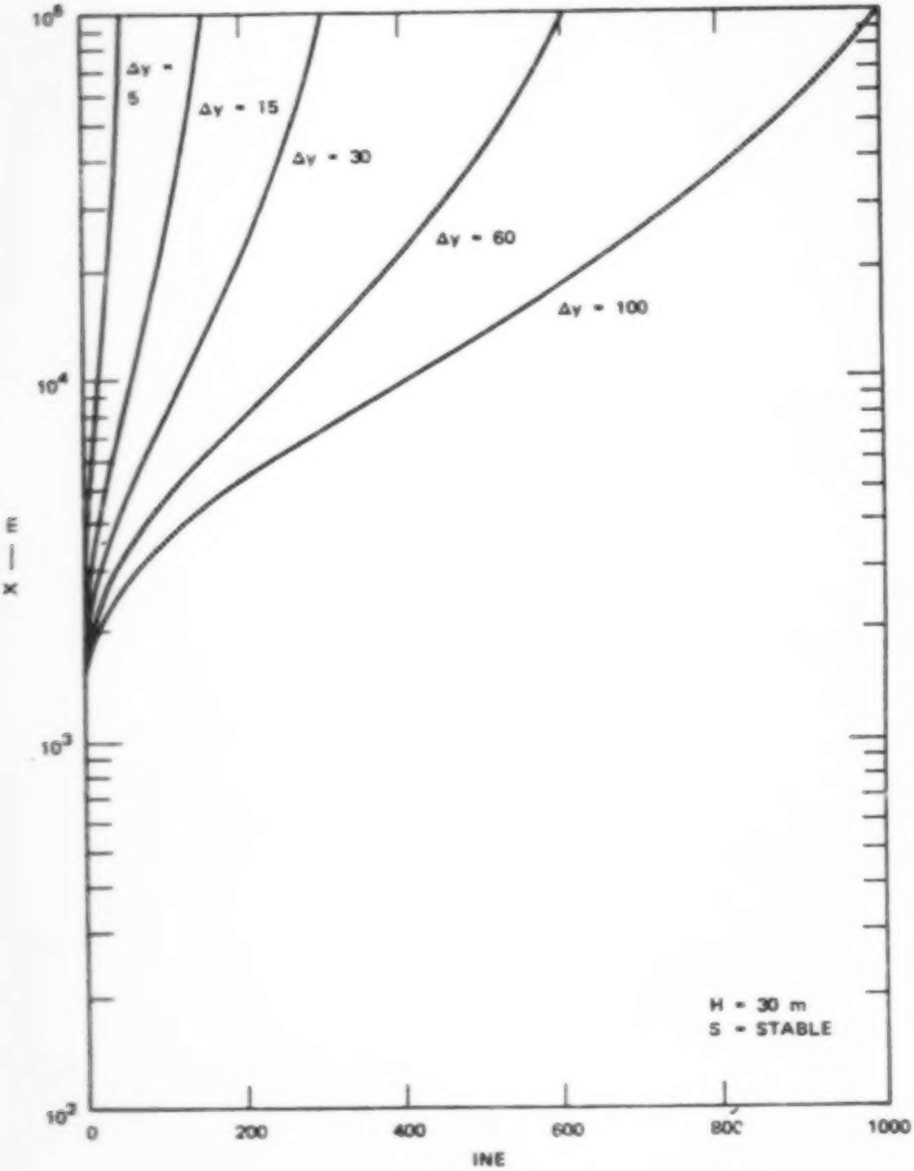

FIGURE 3 VARIATION OF INTEGRATED NORMALIZED ERROR WITH LONGITUDINAL DISTANCE FROM THE SOURCE WHEN SOURCE HEIGHT IS 30 METERS AND ATMOSPHERIC CONDITIONS ARE STABLE

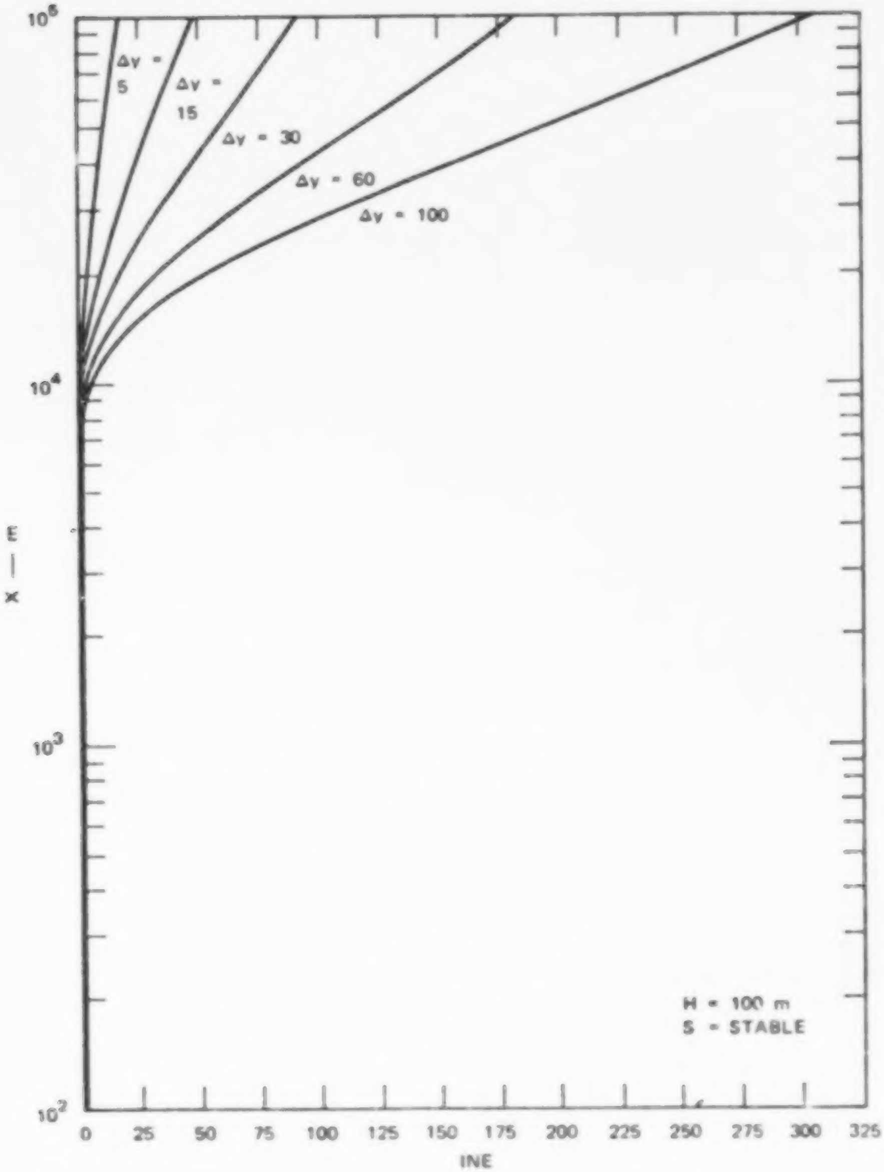

FIGURE 4 VARIATION OF INTEGRATED NORMALIZED ERROR WITH LONGITUDINAL DISTANCE FROM THE SOURCE WHEN SOURCE HEIGHT IS 100 METERS AND ATMOSPHERIC CONDITIONS ARE STABLE

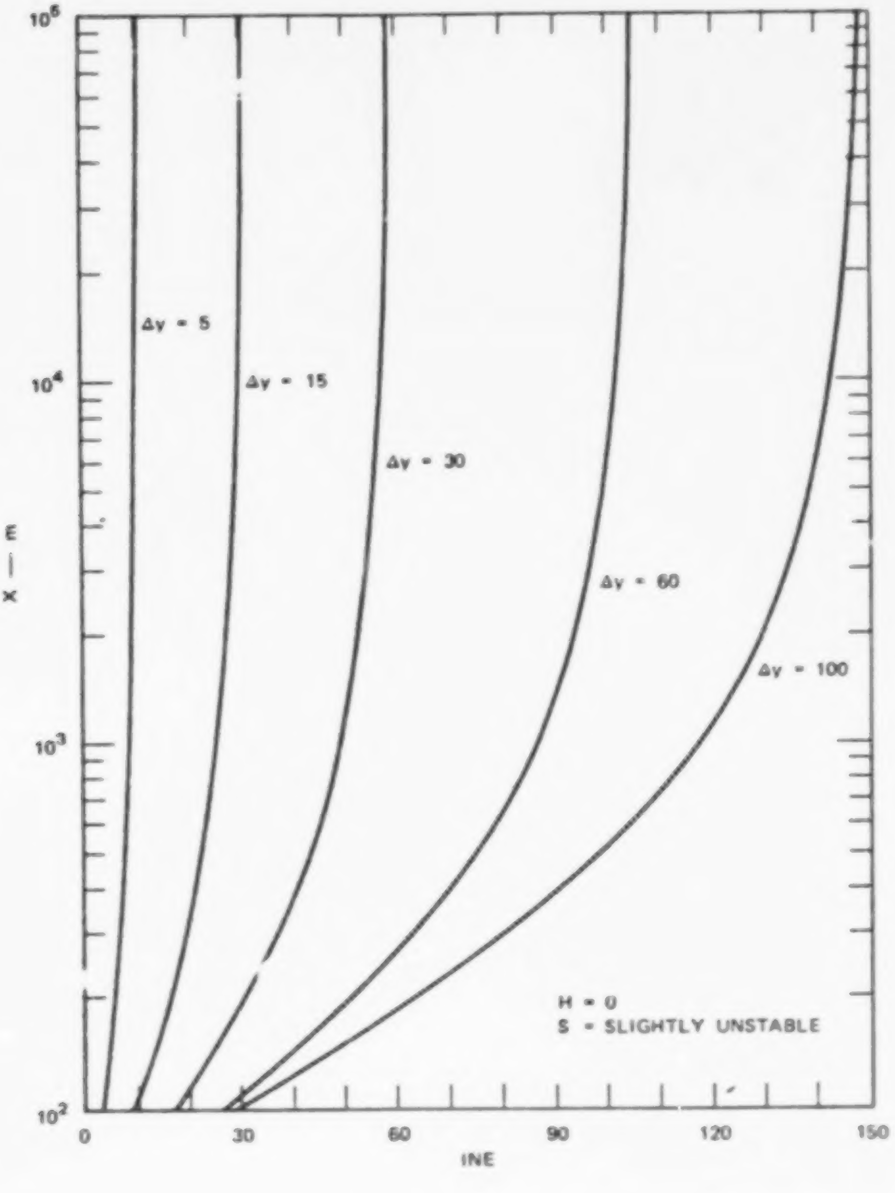

FIGURE 5 VARIATION OF INTEGRATED NORMALIZED ERROR WITH LONGITUDINAL DISTANCE FROM THE SOURCE WHEN THE SOURCE HEIGHT IS AT THE SURFACE AND ATMOSPHERIC CONDITIONS ARE SLIGHTLY UNSTABLE

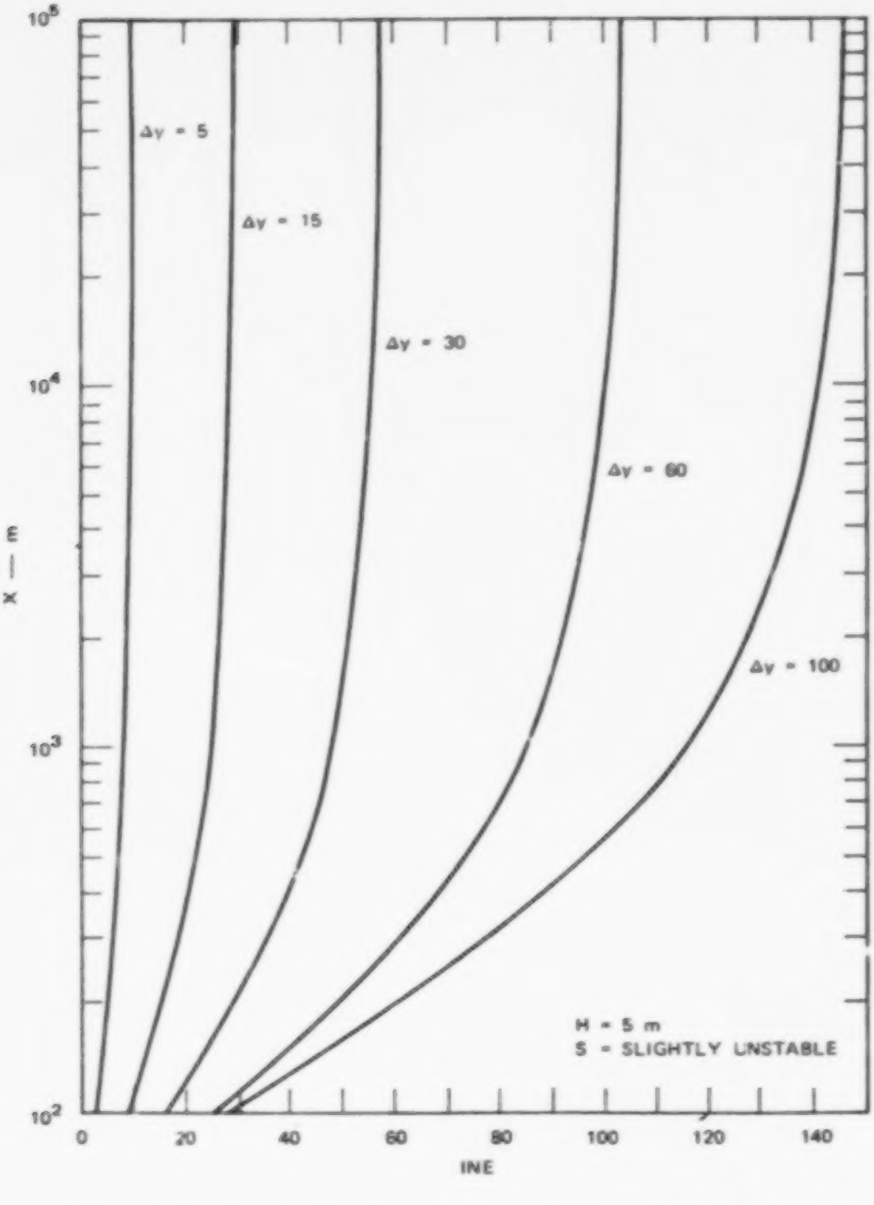

FIGURE 6 VARIATION OF INTEGRATED NORMALIZED ERROR WITH LONGITUDINAL DISTANCE FROM THE SOURCE WHEN SOURCE HEIGHT IS FIVE METERS AND ATMOSPHERIC CONDITIONS ARE SLIGHTLY UNSTABLE

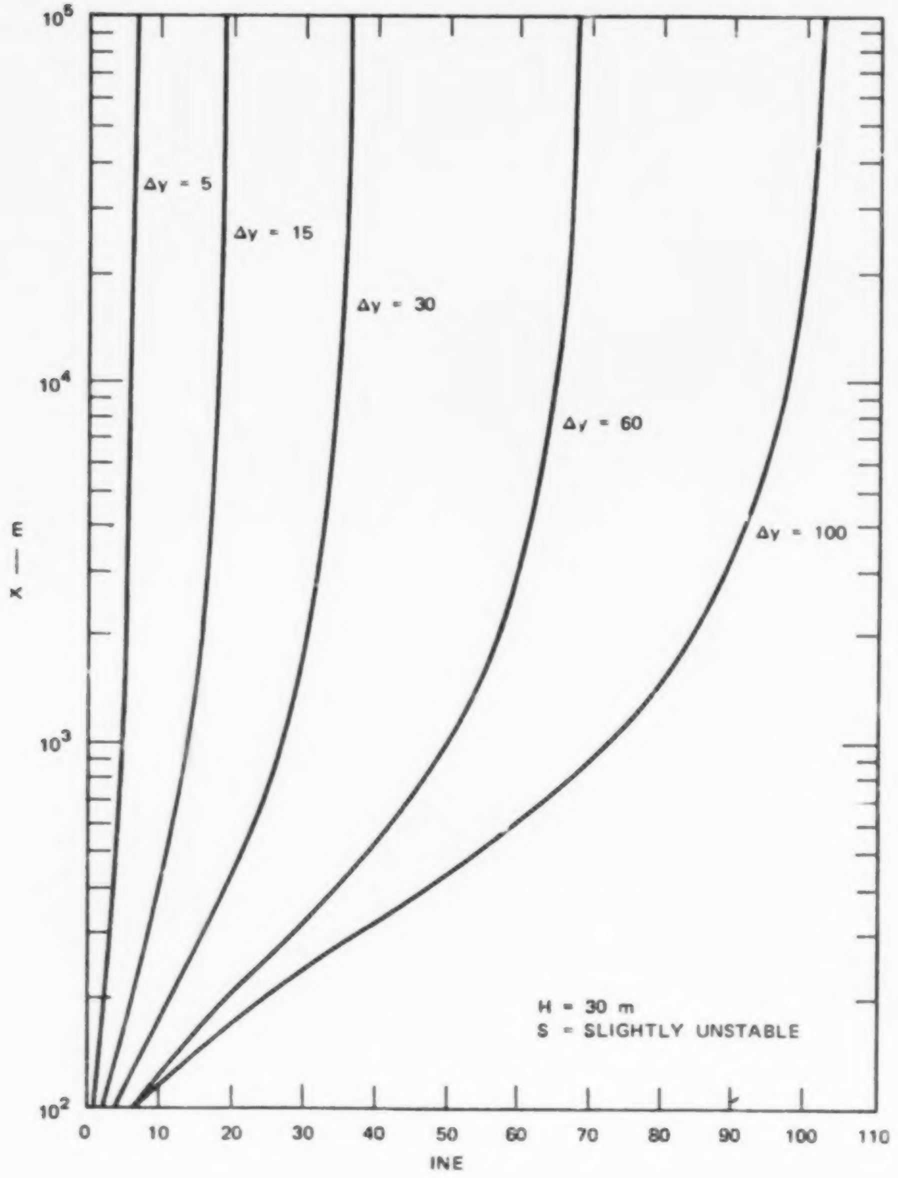

FIGURE 7 VARIATION OF INTEGRATED NORMALIZED ERROR WITH LONGITUDINAL DISTANCE FROM THE SOURCE WHEN SOURCE HEIGHT IS 30 METERS AND ATMOSPHERIC CONDITIONS ARE SLIGHTLY UNSTABLE

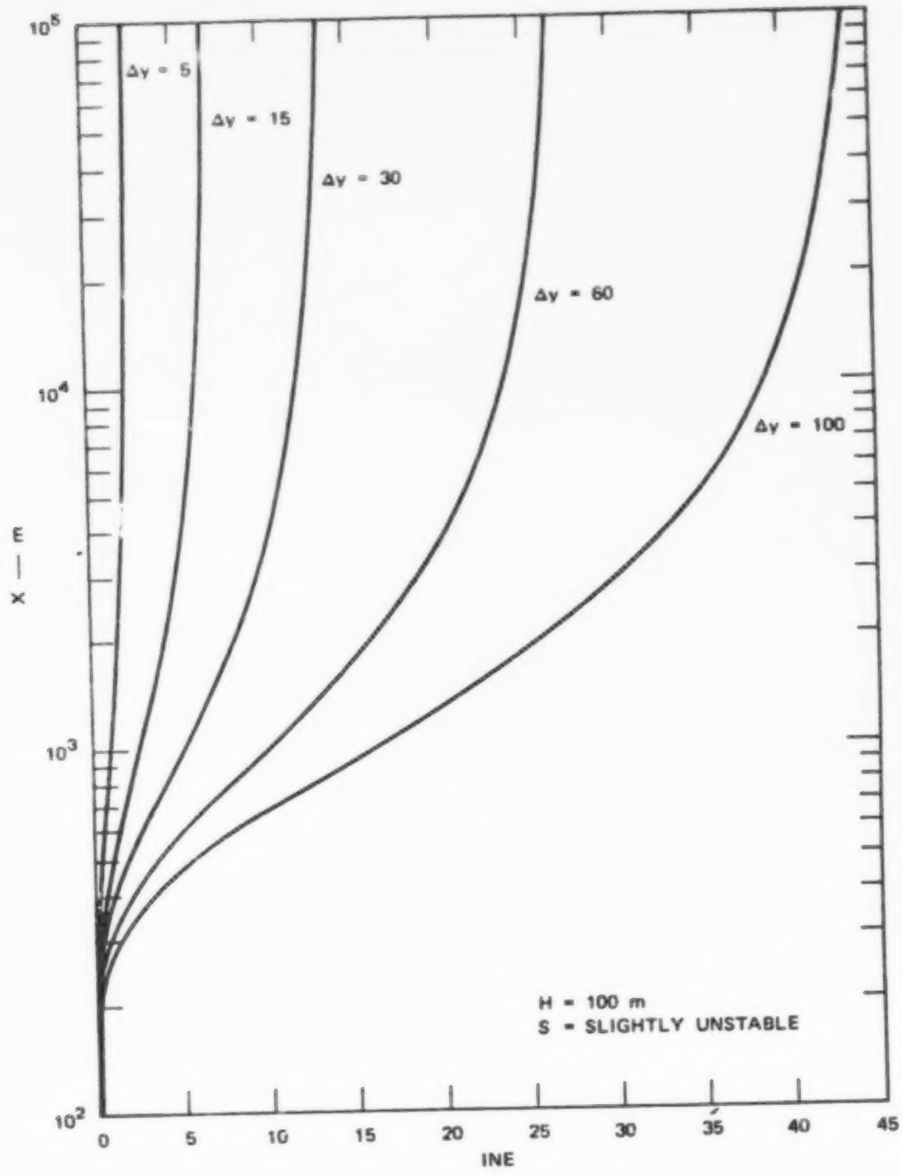

FIGURE 8 VARIATION OF INTEGRATED NORMALIZED ERROR WITH LONGITUDINAL DISTANCE FROM THE SOURCE WHEN SOURCE HEIGHT IS 100 METERS AND ATMOSPHERIC CONDITIONS ARE SLIGHTLY UNSTABLE

6th NATO/CCMS
International Technical Meeting
on Air Pollution Modeling

APM 6/3

Validation of a Single Source Dispersion Model

by

Russell F. Lee
Monitoring and Data Analysis Division
Environmental Protection Agency

and

Michael T. Mills and Roger W. Stern
GCA Corporation

BATTELLE - INSTITUT E.V., Frankfurt/Main

Germany, FR

24 - 26 September, 1975

*On assignment from the National Oceanic and Atmospheric Administration

Preceding page blank

1. INTRODUCTION

BACKGROUND

Estimates of SO_2 concentrations downwind from large power plants are urgently needed to guide environmental and energy related policy decisions. Most mathematical dispersion models for the prediction of SO_2 concentrations provide estimates over averaging times which are either very short (one hour or less) or very long (seasonal or annual). For example, the plume parameters given by Turner[1] and developed principally from earlier work of Pasquill, Cramer and Gifford are based on experimental data, most of which were collected for averaging times of 10 to 30 minutes. Power law relationships, by which concentrations from point sources are linked to averaging times, are generally considered to be valid only over averaging times that range from a few minutes to perhaps one or two hours. The National Ambient Air Quality Standards for SO_2 in the U. S., however, include an averaging time of 24 hours. A method currently favored for estimating 24-hour concentrations is to average concentrations that have been predicted for the component one-hour periods. To date, very few sets of field data have been available to test the adequacy of this estimation technique.

PURPOSE OF STUDY

The purpose of this paper is to describe validation studies of an Environmental Protection Agency dispersion model. The model was designed to estimate 1-hour and 24-hour ground-level concentrations caused by emissions of a single source. Emphasis is placed on the 24-hour value.

The analytical procedures are designed to parallel, to the extent practicable, those used by Klug[2] and Montgomery, et al.[3], in their analyses of TVA data.

MODEL DESCRIPTION

The EPA Single-Source Model (CRSTER) is a Gaussian dispersion model developed by the EPA Division of Meteorology. The procedure calculates maximum daily SO_2 concentrations for a year, identifies the meteorological conditions associated with the maxima, and calculates hourly and daily concentrations for an array of receptor locations. The concentrations are calculated for 180 receptor positions situated at each of 36 directions from the source and at five different distances. The model handles from 1 to 19 sources but assumes all are at the same physical location.

Meteorological inputs to the model consist of hourly surface observations of wind speed (knots), wind direction sector (tens of degrees), temperature (°F), total cloud cover (tenths), and twice daily mixing heights (meters). The format for these data is that used by the National Climatic Center for punched cards of hourly surface observations. The data are input into a preprocessor program which, in turn, writes a tape containing hourly values of stability index, mixing height, temperature, wind speed, flow vector (wind direction plus 180°), and randomized flow vector. The randomized flow vector is equal to the flow vector, plus a random number between -4 and +5 degrees. The randomization procedure prevents excessive concentrations in azimuths which are exact multiples of ten degrees. The preprocessor output tape is then read by the single source model which performs the actual concentration calculations.

The preprocessor program generates hourly mixing heights from the twice daily mixing height measurements according to the interpolation scheme for rural areas described in the Interim User's Guide[4]. Hourly stabilities are determined according to the system given by Turner[1] employing Pasquill's classification scheme with the addition of a stability class 7 (G) for which the assumption is made that the plume does not reach the ground. Wind speeds (u_0) measured at instrument height (h_0) (assumed 7 meters for most weather stations) are adjusted by means of a stability dependent power law ($u = u_0[h/h_0]^p$) to correspond to values one would expect at the stack top (h). Plume rise is calculated on an hourly basis using the method of Briggs[5,6,7]. If the plume rise calculation indicates that the plume height will be above the mixing layer, then a zero concentration is specified. If the plume height is below the top of the mixing layer, the presence of the top of the layer is accounted for by introducing image plumes (see Turner[1]) to satisfy the essentially zero flux conditions at ground level and at the top of the mixing layer.

Source strengths input to the single source model may posses various degrees of temporal resolution. In the seasonal version of the model, an annual average SO_2 source strength is specified along with monthly variation factors. In addition to the monthly factors, the diurnal version of the model employs hourly emission variation factors for each month of the year. A modified version of the model, used in this validation study, allows actual hourly source strengths to be utilized.

2. PLANT DESCRIPTIONS

CANAL PLANT

The Canal Plant and Surroundings

The Canal Plant is located on the south side of the Cape Cod Canal about 1.6 kilometers from the entrance on Cape Cod Bay (Fig. 1). The surrounding terrain is gently rolling with elevations generally below 60 meters above mean sea level. The highest elevations in the area are about 90 meters above sea level in the western end of the Cape. Most of the area is covered with scrub pine forests and low vegetation.

Data for the study were collected in 1971. During that year, the plant consisted of a single oil-fired unit with a generating capacity of 560 megawatts. The top of the stack was about 91 meters above grade and 5.6 meters in diameter. The main power plant structure to the north of the stack totally enclosed the turbine generator and boiler. The roofs of the turbine and boiler rooms were about 30 meters and 59 meters above grade respectively. Stack and boiler data are given in Table 1.

Overview of Monitoring Program

SO_2 concentrations were measured at four locations on a continuous basis with Ultragas SO_2 Analyzers manufactured in Germany by H. Wosthoff. These instruments measure sulfur dioxide by the increase in conductivity

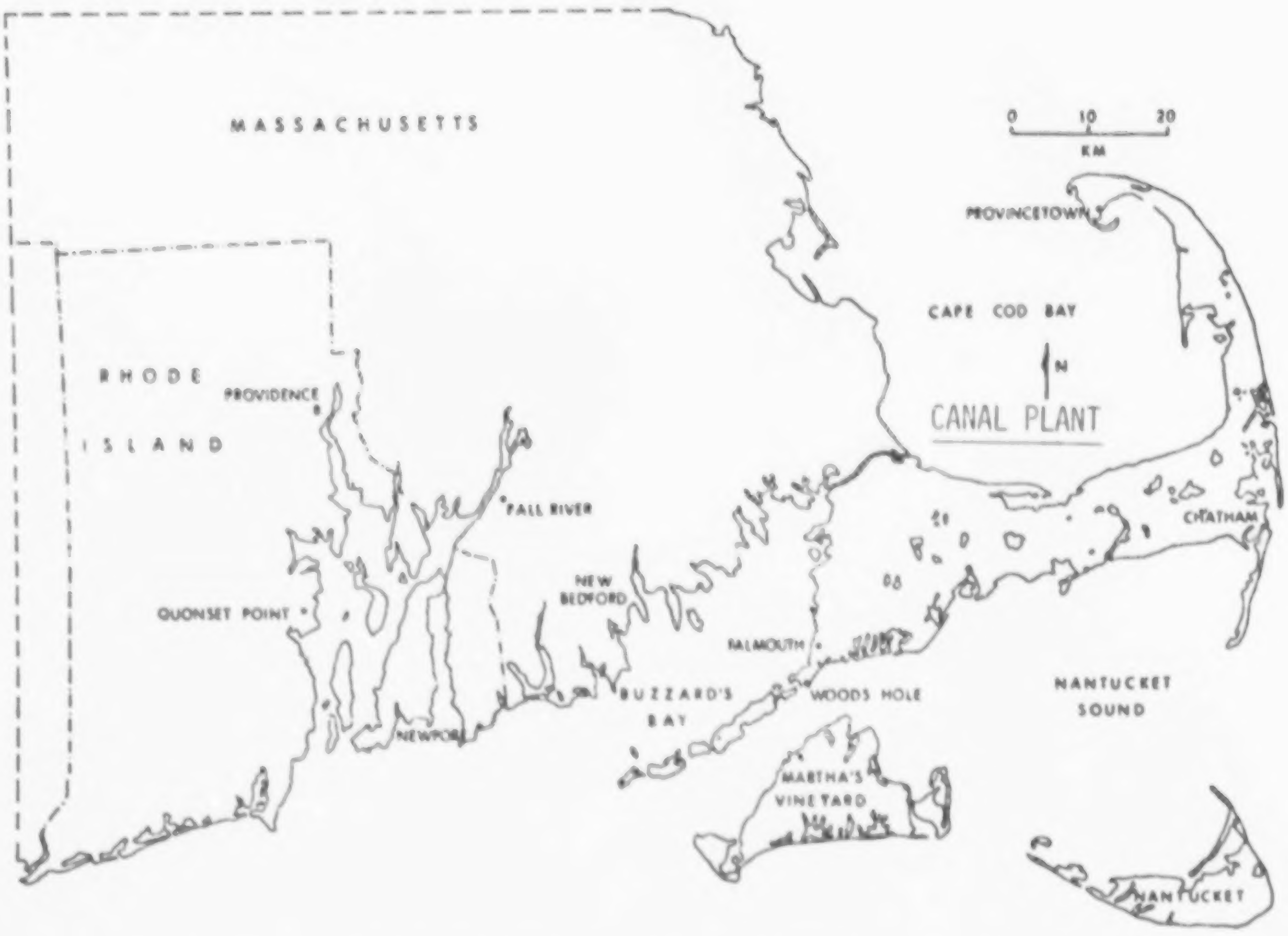

Figure 1. Map of eastern Massachusetts and Rhode Island showing locations of the Canal Plant. Meteorological observations were used from Quonset Point Naval Air Station and Nantucket Island

Table 1. PLANT CHARACTERISTICS

	Plant						
	Stuart	Muskingum		Philo			Canal
	Stacks	Stack	Stack	Stack	Stack	Stack	Stack
Characteristic	all four	1	2	4	5	6	1
Stack height (M)	244	251	251	81	81	84	91
diameter (M)	6.0	7.6	6.7	5.2	3.9	2.6	5.6
velocity (M/S)	22.2	28.5	24.8	4.5	7.7	29	-
temperature (°K)	373	430	425	458	458	433	-
Number of boilers per stack	1 each	4	1	2	2	1	1
Maximum generating capacity per stack (MW)	610	876	591	166	166	125	560
Average per stack (MW)	439	718	487	114	128	84	-
Plant total (MW)	2440	1467		457			560
Plant average (MW)	1318	1235		326			-

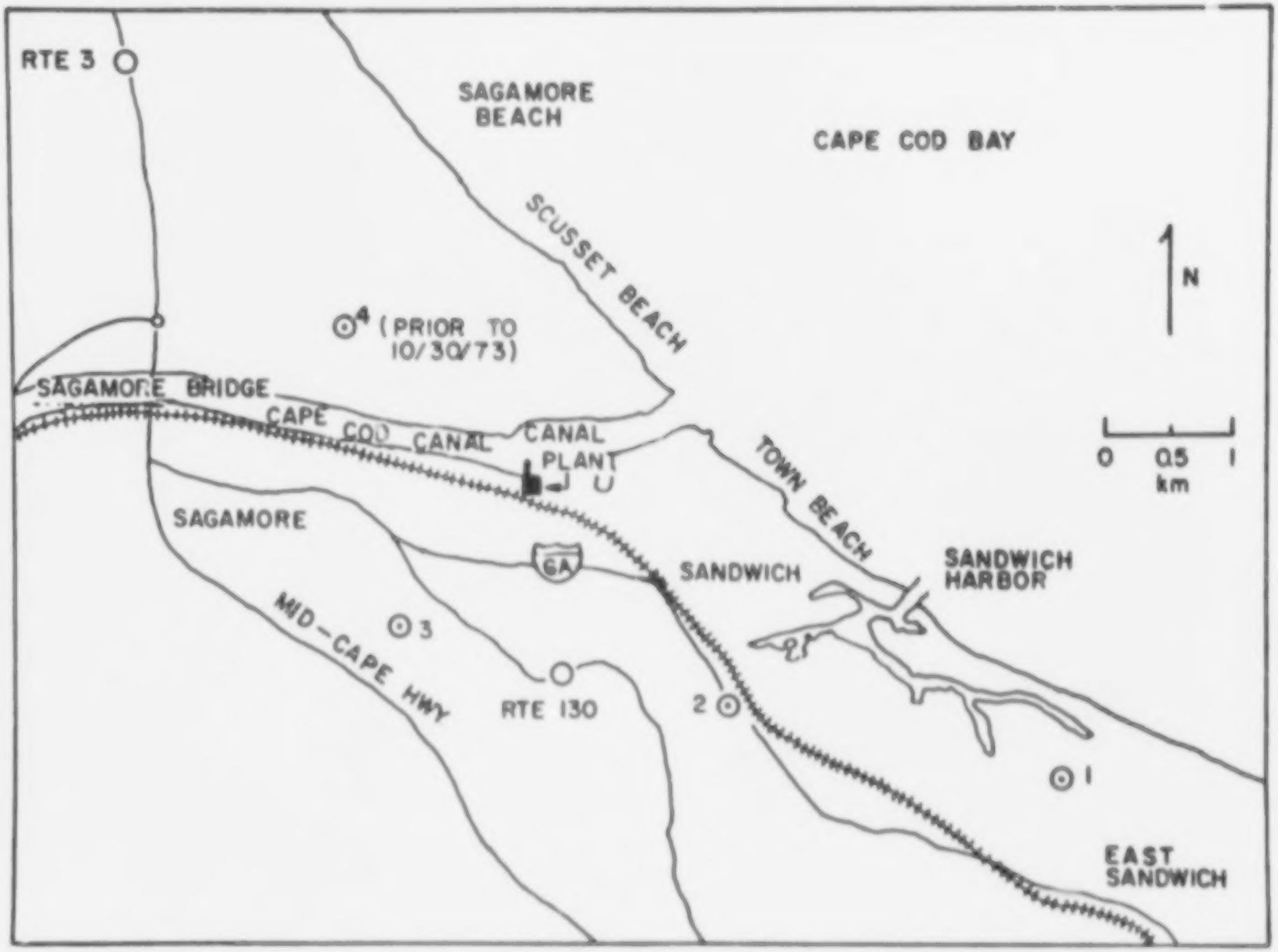

Figure 2. Sketch of the Canal Plant area showing the locations of the four automatic SO_2 stations by the symbol ⊙

of an acidified hydrogen peroxide solution and have a full scale reading of 0.4 ppm. The instruments do not conform to the reference method for sulfur dioxide or to any of the specified equivalent methods[8]. They have, however, been extensively studied and one comparison noted a correlation coefficient of 0.99 with the West-Gaeke method[9]. The instruments used provide a continuous real-time chart trace and a tape printout giving date, time, and average concentration over consecutive 30 minute periods. The locations of the SO_2 monitors with respect to the Canal Plant are given in Figure 2 and Table 2.

Meteorological Data

Bendix-Friez Aerovanes were used to provide local wind speed and direction data. Through July 1971, the principal source of wind data was the Aerovane mounted on a 12.2 meter mast located on the 58.8 m boiler-room roof. After July 1971, wind data were obtained from a second Aerovane installed on a 44 meter tower near the top of Telegraph Hill, approximately 5 kilometers south-southeast of the Canal Plant. Wind data were used to identify the samplers not affected by the plant, for background determination, and for the dispersion modeling. Mixing heights were derived from the Nantucket Island Rawinsonde data.

STUART PLANT

Stuart Plant and Surroundings

The J. M. Stuart plant is located in Southwestern Ohio on the Ohio River, about nine kilometers southwest of Manchester, Ohio,

Table 2. SULFUR DIOXIDE MONITOR STATIONS

Plant	Station No.	Station Name	Distance (km)	Bearing (degrees)	Elevation above stack base (m)
Canal	1		4.7	119	10
	2		2.3	138	4
	3		1.4	224	40
	4		2.0	312	20
	-	Top of stacks	-	-	91
Stuart	1	Boone	2.4	35	115
	2	Brudysville	6.6	15	85
	3	Bentonville	13.4	28	121
	4	Manchester	8.7	49	-7
	5	Maysville	3.8	279	-4
	6	Rectorville	8.4	156	115
	7	Somo	5.0	220	115
	-	Top of stacks	-	-	244
Muskingum	1	Beverly	5.3	140	64
	2	Hackney	4.3	40	82
	3	Rich Valley	8.3	35	101
	4	Caldwell	19.6	35	128
	-	Top of stacks	-	-	251
Philo	1	Philo	1.7	174	3
	2	Fox Run	4.9	166	2
	3	Irish Ridge	5.0	235	99
	4	Duncan Falls	1.3	343	12
	5	Salt Creek	6.0	25	26
	6	Indian Run	4.2	334	63
	-	Top of stacks	-	-	81

and four kilometers east of Maysville, Ohio (Figure 3). It is located near the center of the river valley. The ridges on either side of the valley are about 115 meters above the valley floor and 700 meters from the power plant. The 244-meter stacks rise 130 meters above the surrounding countryside. The data were collected during the one year period from January 1, 1973 to December 31, 1973. The plant consisted of four identical coal fired boilers with a capacity of 610 megawatts each. However, one boiler was under repair during the entire year so that the total generating capacity was only 1830 megawatts. The yearly average generating load was 1318 megawatts, or 72 percent of available capacity. Stack and boiler data are given on Table 1.

Overview of Monitoring Program

The monitoring network consisted of seven sulfur dioxide monitoring stations (Fig. 4 and Table 2). The instruments were electrolytic conductivity devices manufactured by Leeds & Northrup Company. The sample was obtained by passing ambient air, taken from five feet above ground level, through an absorption column along with an absorption solution. Data were taken continuously and listed every hour. Electrical calibration tests were performed weekly for zero and half-scale operations. Overall calibration tests were made every six months at 0.2 ppm using the permeation tube method whose accuracy is traceable to the U. S. Bureau of Standards.

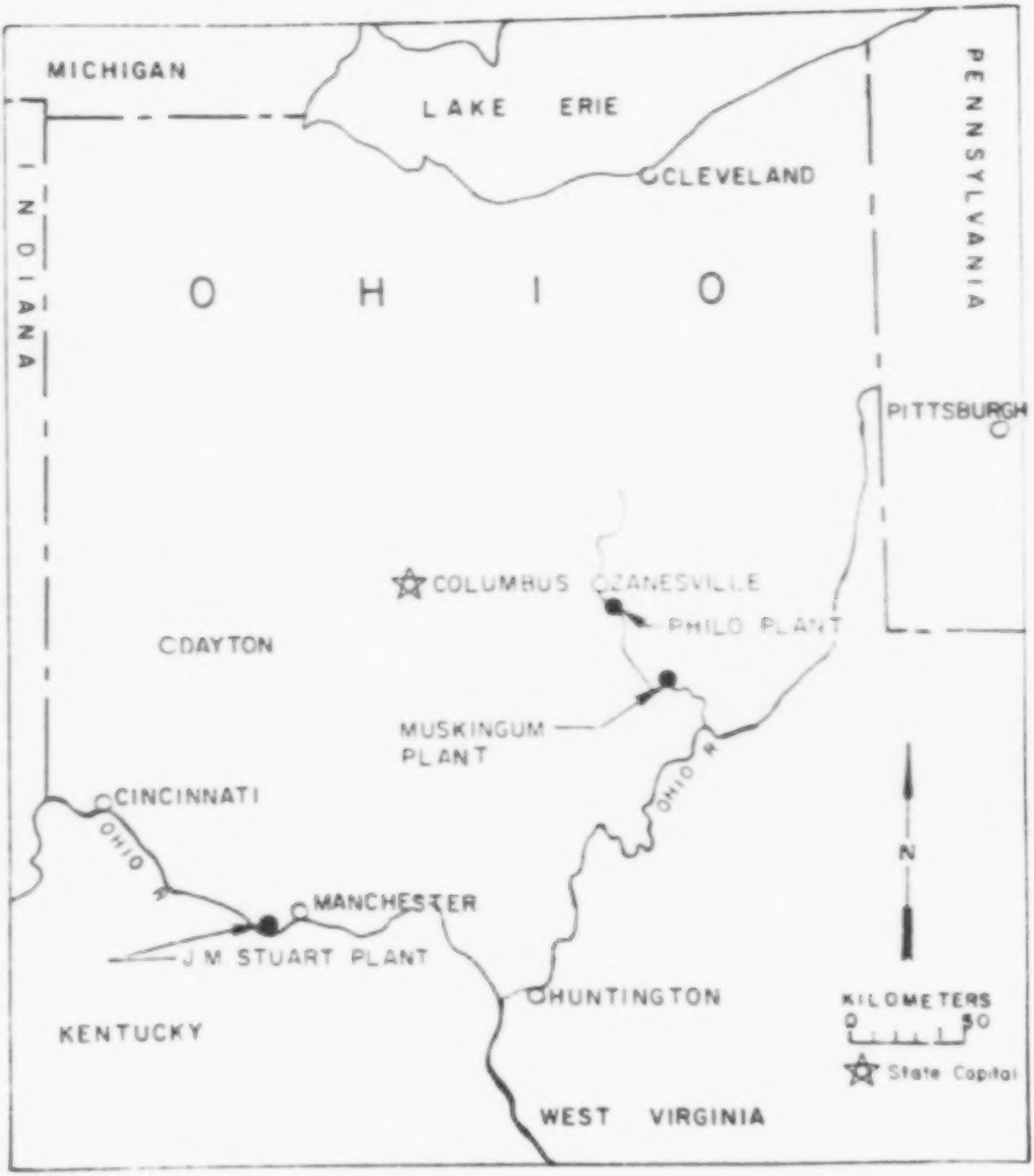

Figure 3. Map of Ohio and surrounding states showing location of J. M. Stuart Plant, Philo Plant, and Muskingum River Plant

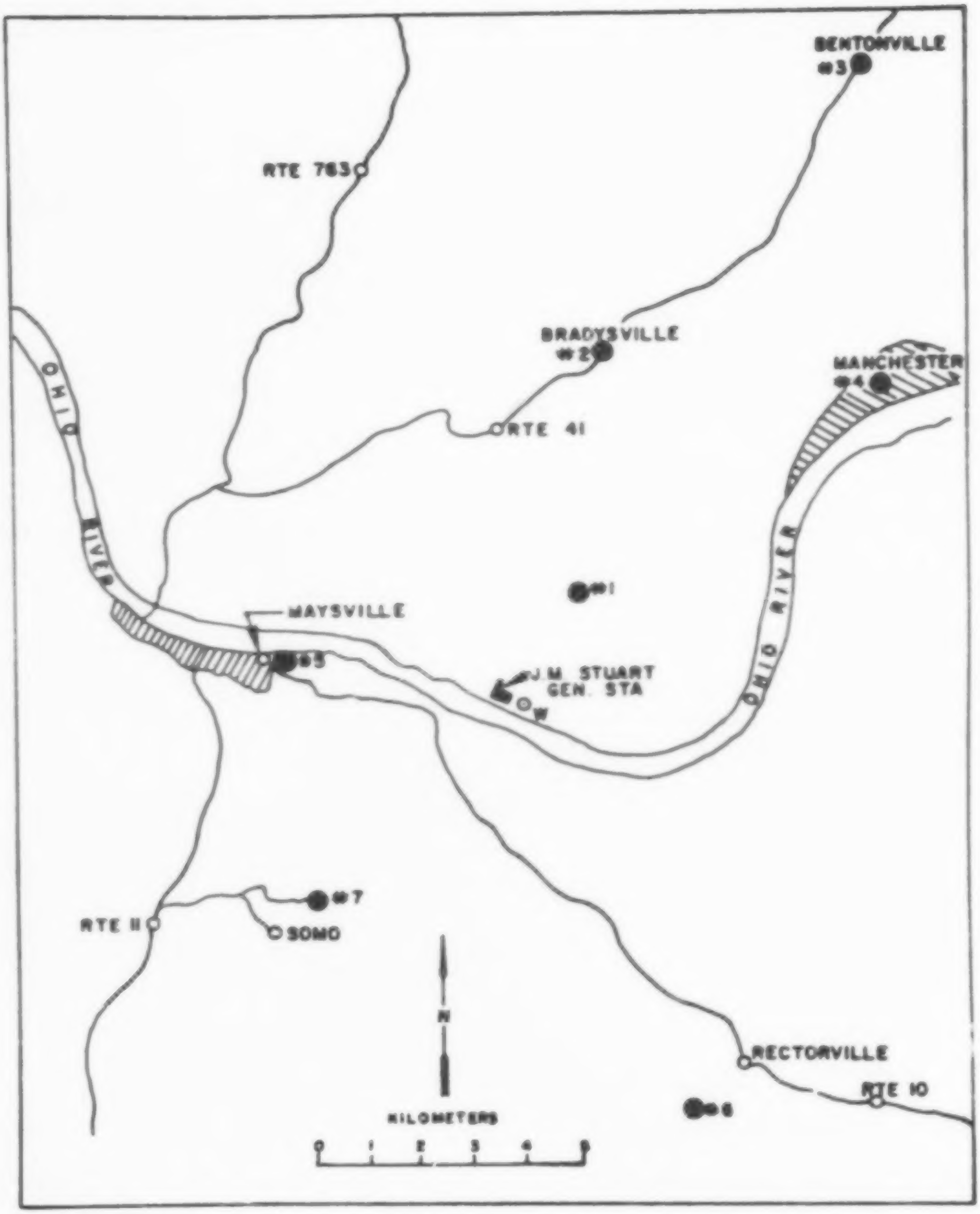

Figure 4. Sketch of the J. M. Stuart Plant area showing locations of seven automatic SO_2 monitoring stations

The monitor at Station 2 was moved to Station 4 on March 10, 1973, and the monitor at Station 7 was discontinued on June 17, 1973. Therefore, no data are available for Station 2 for nine months, Station 4 for three months, and Station 7 for six months. There were some additional hours of missing data due to loss of electrical power, periods of calibration and maintenance, and system failures.

Fuel Analysis

Each barge of coal from a specific vendor was sampled during the unloading process. All samples were analyzed. In the process of determining the caloric value of the coal by bomb calorimeter, the bomb washings were titrated using tetrahydroxyquionone (THQ) to determine the acid content which indicates the sulfur level. The procedure, the THQ colorimetric method, has been shown to be in agreement with the standard ASTM method. It is used as a typical procedure by the Dayton Power and Light Company and the American Electric Power System, and the Ohio Power Company.

Meteorological Data

The meteorological instrumentation at the J. M. Stuart Plant consisted of a Bendix-Friez wind speed and direction device mounted 40 meters above the ground on the coal stacking tower. The plant wind data were used to identify samplers not affected by the plant plume to aid in determining background. The meteorological data collected at the National Weather Service (NWS) Station at Cincinnati, Ohio were used in the model. Mixing heights were derived from rawinsonde data collected at the NWS station at Dayton, Ohio.

MUSKINGUM PLANT

Muskingum Plant and Surroundings

The Muskingum Plant is located in Southeastern Ohio, on the Muskingum River, about six kilometers northwest of the town of Beverly. Figure 5 indicates the location of the plant, the SO_2 monitoring sites, and the surrounding towns. The plant is in the river valley about 500 meters from the valley walls which rise about 75 meters above the valley floor. The two 251-meter stacks are 640 meters apart and extend about 185 meters above the surrounding terrain. During 1973 the plant consisted of five coal fired units with a total capacity of 1467 megawatts (Table 1).

Overview of the Muskingum Monitoring Program

Four sulfur dioxide monitoring stations made up the monitoring network (Fig. 5 and Table 2). The monitoring stations were established in 1969 to monitor the ambient changes when the new stacks were installed[10].

Meteorological Data

There were two wind monitoring stations. Both used Friez Aerovane wind speed and direction devices. One was located at Beverly mounted 33 meters above ground, and the other at the Hackney SO_2 monitoring

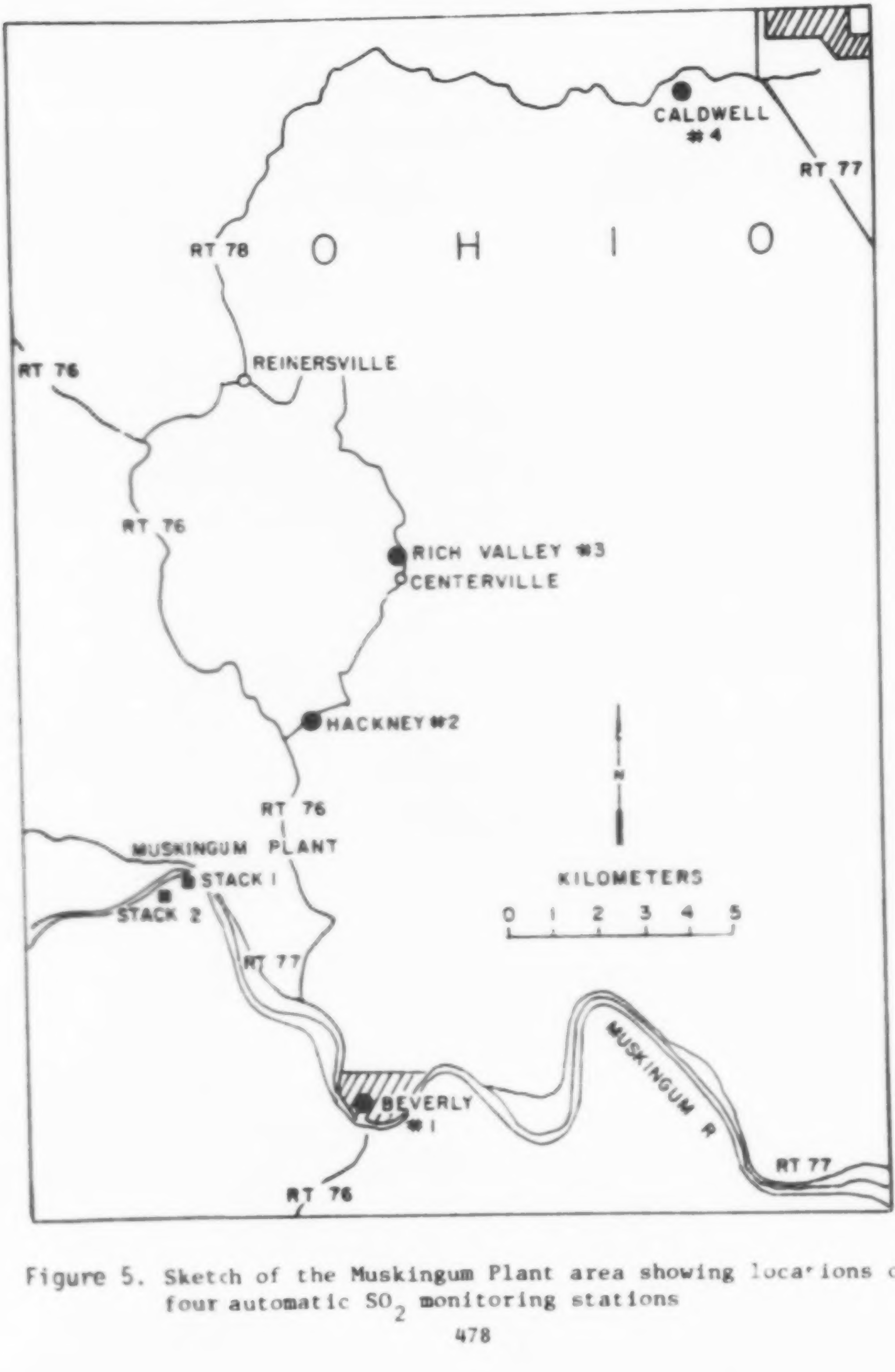

Figure 5. Sketch of the Muskingum Plant area showing locations of four automatic SO_2 monitoring stations

station, on a 22-meter mount. The data from Hackney were used for selecting the "background" stations, but Beverly data were used when the Hackney data were missing.

Weather data used in the modeling were obtained from upper air and surface data collected at the NWS station at Huntington, West Virginia. (See Figure 3).

PHILO PLANT

Philo Plant Description

The Philo plant is a 457 megawatt facility located in eastern Ohio on the Muskingum River in the town of Philo, about 11 kilometers to the southeast of Zanesville, Ohio (Figs. 3 and 6). The plant is roughly 500 meters from the valley walls to the east and west, although the valley widens to the north. The three stacks are approximately 82 meters high and rise about 10 meters above the surrounding terrain. During 1974, the period of this study, the plant consisted of five coal-fired boilers feeding into three stacks (Table 1).

Overview of the Philo Monitoring Program

The monitoring system in 1974 was made up of six Malloy continuous SO_2 samplers, located as shown in Fig. 6 and Table 2. The monitoring system maintenance and data acquisition were performed by the Environmental Research and Technology Company in Lexington, Mass. The instruments were calibrated every six months in Lexington and zeroed every night by computer.

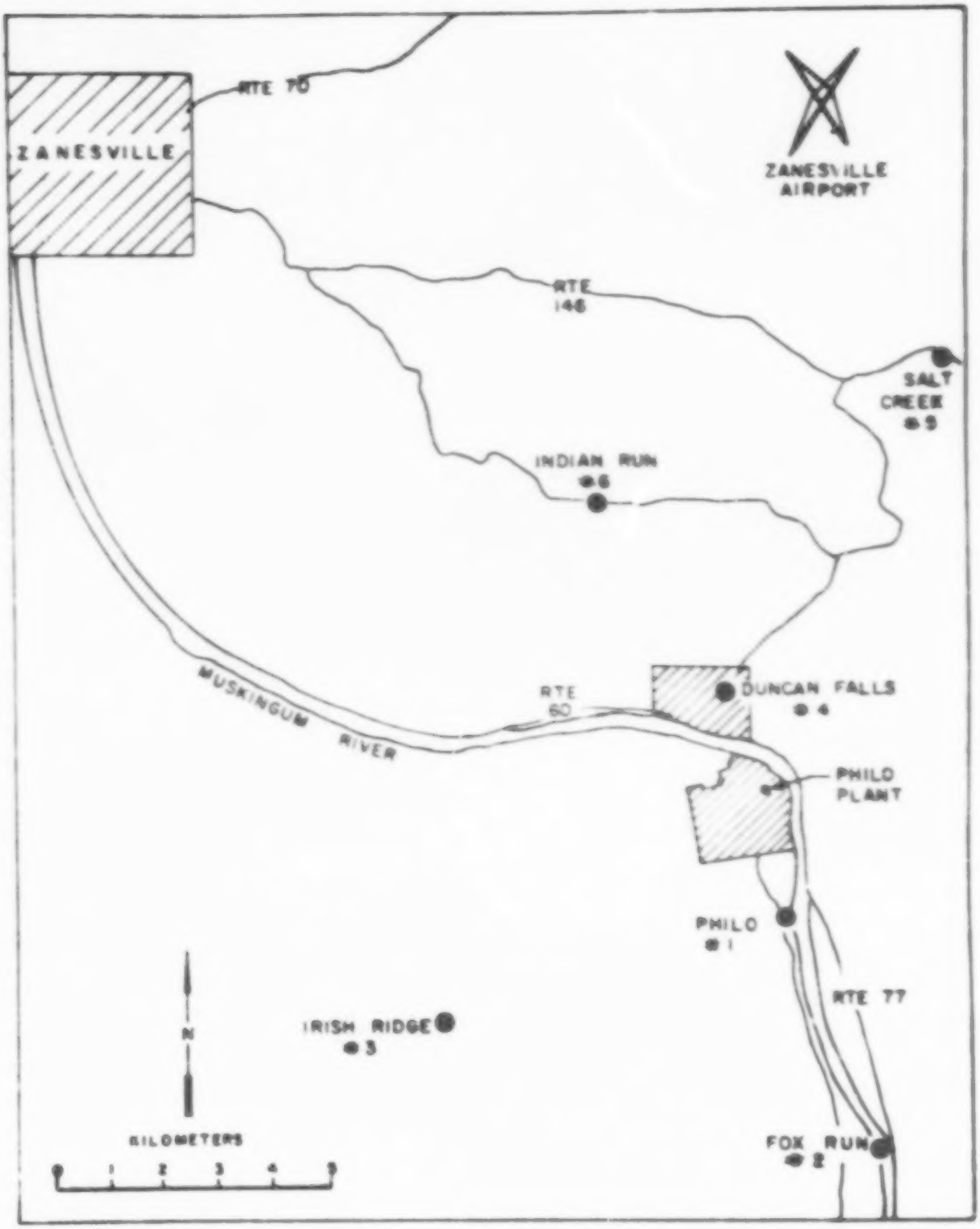

Figure 6. Sketch of the Philo Plant area showing locations of six automatic SO_2 monitoring stations

Data were recorded for all of 1975 except for the following:

Station 1	First 91 days of year
Station 4	First 91 days of year
Station 6	Second 91 days of year

Meteorological Data

There were three meteorological stations:

1. Irish Ridge Upper - elevation 140 meters above plant base, (50 meters above ground). Measured wind speed and direction, temperature, and temperature difference between Irish Ridge Upper and Irish Ridge Lower.
2. Irish Ridge Lower - elevation 104 meters above plant base, (11 meters above ground). Measured wind speed and direction, and temperature.
3. Duncan Falls - elevation 14 meters above plant base, (6 meters above ground). Measured wind speed and direction.

The wind instruments were Climet Anemometers.

The winds from Irish Ridge Upper were used to determine which sites to use to estimate background. When Irish Ridge Upper data were missing, Irish Ridge Lower data were used. When that data were also missing, Duncan Falls data were used. Surface wind and stability data from the National Weather Service Station at Columbus, Ohio were used in the dispersion model. Mixing heights were derived from upper air data collected at Dayton, Ohio.

3. DATA PREPARATION AND PROCESSING

Meteorological Data

The sources of the meteorological data are shown on Table 3. Hourly surface observations from airport log sheets were keypunched on to cards.

Table 3

SOURCES OF METEOROLOGICAL DATA

Plant	Surface Observations Airport	Year	Upper Air Data Airport
Canal	Quonset Point, R. I.	1971	Chatham, Mass.
J. M. Stuart	Cincinnati, Ohio	1973	Dayton, Ohio
Muskingum	Huntington, W. Va.	1973	Huntington, W. Va.
Philo	Columbus, Ohio	1974	Dayton, Ohio

The surface observations included:

- station
- date and time
- ceiling height
- ambient temperature
- wind direction
- wind speed
- percent cloud cover

Table 4

AVERAGE MONTHLY PERCENT SULFUR CONTENT OF FUEL

Month	Canal	Stuart	Muskingum	Philo
January	2.0	1.8	4.9	3.9
February	1.9	1.6	4.8	4.8
March	2.1	1.8	4.8	4.7
April	1.9	1.7	4.5	4.4
May	2.1	1.8	4.7	3.3
June	2.1	1.6	5.0	3.2
July	2.1	1.5	4.7	2.6
August	2.0	1.5	4.7	3.2
September	1.9	1.5	4.3	3.2
October	0.9	1.5	4.6	2.4
November	1.0	1.8	4.5	2.6
December	0.9	2.1	4.4	3.7

Plant Emission Data

The hourly emission rate of SO_2 was computed from the fuel consumption rate and the sulfur content of the fuel. The hourly fuel consumption rate of each of the boilers was summed to obtain the plant fuel consumption rate. The plant fuel rate was then multiplied by the sulfur content and an appropriate conversion factor to obtain the hourly sulfur dioxide emission rate from the plant.

Air Quality Data

The air quality data required for this study were the concentrations of sulfur dioxide (SO_2) attributable to the plant being studied. The samplers measured concentrations, not only from the plant being studied, but from other sources as well. The portion of the concentration due to those other sources is referred to as background in this study. Since there is no accurate way of knowing how much of the total concentration is due to the power plant, this portion of the concentration must be estimated.

The portion of the concentration due to the plant, for each hour, at each sampler, was estimated, first, by estimating the background concentration and, second, by subtracting the background concentration from the concentration measured at each sampler. One background concentration was assumed to be valid for all receptors for one hour. The background concentration was taken to be the average of the concentrations from all samplers that are not located with ± 45° of the downwind direction. The downwind direction is based on the wind direction recorded by the wind vane at the plant. When the wind observation indicated calm, or was missing, the last recorded wind direction was used, with one exception. This exception occurred when a sampler recorded a concentration greater than 0.1 ppm. In that case the downwind direction was taken as the direction from the plant to that sampler.

Quality Control

Particular attention was given to quality control. Emissions, air quality, and meteorological data were each keypunched with the date and time preceding the measured values. All punched cards were verified. A computer program was used to check for missing hours, cards out of chronological order, input data out of range, and unreasonable changes between consecutive data values. The keypunched data were read onto magnetic tape, with each record prefixed by a plant code to prevent the unlikely mixing of data from different plants. All programs which modified the data had internal checking routines to assure that the correct data was read. The output from each program was spot checked by manual calculations.

4. RESULTS OF THE MODEL VALIDATION

Figures 7 through 22 show log-normal plots of cumulative frequency distributions of (1) measured concentrations, (2) measured concentration minus the estimate of "background," and (3) the model-calculated concentration for the same location. Rather than presenting data for all the sampling stations, data are shown for two sites for each plant. In each case, the data presented are from sites where the model gave the best and the poorest predictions, respectively. Tables 5 and 6 show the measured and predicted concentrations at each sampler for selected points on the frequency distributions.

Table 5. 1-HOUR CONCENTRATION DISTRIBUTION STATISTICS FOR MEASUREMENTS AND MODEL VALIDATION RUN (μmg/m^3)

Plant	Sampling Station	Ninety-fifth Percentile[a] M[b]	P[c]	Ninety-ninth Percentile[a] M	P	Second Highest M	P	Highest M	P
Canal	1	25	< 1	101	6	435	253	438	283
	2	14	< 1	72	< 1	553	174	618	179
	3	18	< 1	18	2	446	446	732	509
	4	15	< 1	31	< 1	575	427	638	479
Stuart	1	140	<10	270	400	685	1372	857	1393
	2[d]	80	<10	445	180	685	814	1014	948
	3	74	26	200	240	1022	565	1153	1022
	4	53	<10	180	130	750	515	883	541
	5	28	<10	80	<10	495	823	565	1219
	6	48	<10	135	120	980	595	1053	693
	7[d]	33	<10	102	30	325	976	435	1000
Muskingum R.	1	27	<10	150	160	857	980	925	1083
	2	57	<10	270	150	786	1304	786	1310
	3	130	<10	350	210	996	873	1179	933
	4	72	<10	200	160	735	465	786	645
Philo	1	50	<10	170	98	525	1295	893	1639
	2	37	<10	163	222	735	945	891	1059
	3	47	<10	163	920	745	4049	917	4593
	4	27	<10	190	88	665	1945	695	1981
	5	35	80	134	555	575	1279	675	1344
	6	118	20	253	650	565	2369	595	2482

---

[a] Percentile values given in terms of cumulative percent of concentration less than given values.

[b] Measured concentrations with subtracted background.

[c] Predicted concentrations.

[d] Samplers were in operation for less than half the year. Data not included in subsequent analyses.

Table 6. 24 HOUR CONCENTRATION DISTRIBUTION STATISTICS FOR MEASUREMENTS AND MODEL VALIDATION RUN ($\mu g/m^3$)

Plant	Sampling Station	Ninety-fifth Percentile[a]		Ninety-ninth Percentile[a]		Second Highest		Highest	
		M[b]	P[c]	M	P	M	P	M	P
Canal	1	32	4	52	14	66	16	75	29
	2	15	<1	28	6	36	9	46	11
	3	17	4	46	18	77	38	83	39
	4	15	<1	44	2	63	4	75	16
Stuart	1	83	55	245	128	259	149	277	161
	2[d]	46	28	160	52	63	75	159	98
	3	50	36	110	75	181	91	225	102
	4	40	24	63	41	79	45	83	49
	5	31	5	52	50	63	57	77	75
	6	42	21	135	46	147	69	195	83
	7[d]	45	23	69	60	69	73	77	120
Muskingum R.	1	32	32	100	69	133	81	170	97
	2	55	32	100	80	131	82	137	91
	3	98	31	130	58	165	73	227	74
	4	52	24	95	41	109	45	115	47
Philo	1	45	29	134	139	132	133	133	147
	2	35	39	60	69	67	86	110	104
	3	44	143	92	368	127	471	132	541
	4	41	47	60	111	62	165	158	220
	5	23	81	78	207	87	222	94	226
	6	65	107	121	217	121	282	138	356

---

[a] Percentile values given in terms of cumulative percent of concentrations less than given values.

[b] Measured concentrations with subtracted background.

[c] Predicted concentration.

[d] Samplers were in operation for less than half the year. Data not included in subsequent analyses.

A comparison of the frequency distributions of the model calculations and the observed one-hour concentrations shows that the model predicts the upper percentile fairly well, but significantly under-predicts most of the remainder of the distribution. A similar effect occurs in the frequency distributions of the 24-hour concentrations. Part of the underprediction may be due to sampler errors, as Klug speculates[2], since many of the lower concentrations are measured near the threshold of the sensing device. Also, much of the low concentration end of the distribution does not represent pollution from the plant at all, but rather differences between the estimated background and the actual background at the sampler. For example, if three samplers upwind of the plant recorded concentrations 10, 20 and 24 $\mu g/m^3$, the "background" would be considered the average of the upwind stations, in this case 18 $\mu g/m^3$. This "background" is subtracted from each concentration recorded at that hour, so that, in this case, there is one negative concentration, and two positive concentrations of 2 and 6 $\mu g/m^3$, respectively. Corresponding model predictions would, quite correctly, be zero.

Not all the underprediction can be explained by the above hypotheses, however. Several sampling stations show large underpredictions for high observed concentrations. For example, on the frequency distribution of one-hour concentrations at the Muskingum River sampling station 3, the 98th percentile measured value is well over 200 $\mu g/m^3$, while the model prediction is on the order of 60 $\mu g/m^3$. As Mills, et al.[11] noted, an error of this size could occur if the actual stability differs from the stability as calculated by the computer program.

In the U.S.A., short term (24 hours or less) National Ambient Air Quality Standards, for SO_2 and particulates, are given in terms of concentrations "not to be exceeded more than once per year." Thus, the second highest concentrations are of concern. The ratios of the model prediction to the measured (less background) of the second highest one-hour concentrations range from .3 to 3.0, except for two Philo samplers where the ratios are 4.2 and 5.4. These two samplers were located at elevations 18 meters below and 18 meters above the stack tops, respectively. The geometric mean of the ratios is 1.2. The corresponding ratios for the 24-hour concentrations range from .2 to 2.7, except for one sampler at the Philo plant where the ratio is 3.7 and one at the Canal plant where the ratio is 0.06. The geometric mean of the ratios is 0.7.

The model tends to underpredict the 24-hour concentrations, and slightly overpredict the one-hour concentrations. The degree to which the model overpredicts or underpredicts is a strong function of the plant being studied. For example, at the Canal plant, the second highest one-hour concentrations are underpredicted at three of the four sites, while the corresponding 24-hour concentrations are underpredicted at all four sites. The ratios of predicted to measured concentrations (without background) at the Canal plant range from .3 to 1.0 for 1-hour concentrations, and from less than .1 to .5 for 24-hour concentrations, with geometric means of .6 and .2 respectively (Figure 7). At Philo, however, the second highest one-hour concentrations are overpredicted at all six sites, and the corresponding 24-hour concentrations at five of the six sites.

Table 7

Geometric Means of the Ratios of Predicted to Measured (less background) Second-Highest Concentrations

Plant	1-Hour	24-Hour
Canal	.60	.20
Stuart	.95	.59
Muskingum River	1.01	.51
Philo	2.79	2.06
All Plants	1.23	.68

The ratios of the predicted to measured concentrations range from 1.3 to 5.4 for one-hour concentrations, and from 1.0 to 3.7 for 24-hour concentrations. The geometric means of the ratios are 2.8 and 2.1 respectively.

At the Stuart and Muskingum River plants, the second-highest one-hour concentrations are underpredicted at about as many sites as they are overpredicted. The corresponding 24-hour concentrations are underpredicted at all 11 sites. The ratios of predicted to measured second highest one-hour concentrations range from .5 to 2.0 with a geometric mean of 1.0. The corresponding ratios for 24-hour concentrations range from 0.4 to 0.9, with a geometric mean of 0.6.

The correlation coefficients between the ratio of the predicted to measured (less background) and distance are given in Table 8. The negative correlations of the ratios of predicted to measured with distance indicates a tendency for the model to underpredict more at greater distances. The correlation is highly significant at Stuart, but not statistically significant at the other plants.

The negative correlations between the ratios and distances are consistent with theory[12] and observations[13] which indicate that beyond a few kilometers, the plume width should not be proportional to distance to the 0.9 power as used in this model, but some smaller power.

Table 8. CORRELATION COEFFICIENTS OF RATIOS (predicted/measured) TO DISTANCE

Averaging Time	Plant	Correlation	95% Confidence Interval	Significant to 5% Level
1	Canal	-.41	- .98 to .91	No
1	Stuart	-.91	-.994 to -.14	Significant to 1%
1	Muskingum R	-.78	-.995 to .72	No
1	Philo	.09	- .78 to .84	No
1	All Data	-.29	- .66 to .19	No
24	Canal	-.24	- .98 to .94	No
24	Stuart	-.56	- .97 to .64	No
24	Muskingum R.	-.82	-.996 to .67	No
24	Philo	.33	- .66 to .90	No
24	All Data	-.19	- .59 to .29	No

5. CONCLUSIONS

Based on the analyses of the performance of the Single Source model at four large power plants, several conclusions can be made.

The model predicts the upper percentile of the frequency distribution of one-hour concentrations and of the corresponding distributions of 24-hour concentrations acceptably well. Concentrations over the remainder of the frequency distributions are significantly underpredicted. Part of this underprediction is an apparent one, resulting from the technique used to estimate the concentrations. Another portion of the underprediction is probably due to measurement errors when concentrations are near the threshold level of the instrument. Obviously there are also uncertainties in specifying the appropriate wind direction, wind speed, and stability class.

The following specific conclusions are made.

- The second highest one-hour concentrations are predicted within a factor of 2.0 at two-thirds of the sampling sites. The geometric mean of the ratios of the model prediction to the measured (less background) for all sampling sites is 1.2. The most significant overpredictions occurred around the Philo plant, where the model is less likely to account properly for the terrain influences. These influences are very pronounced because the effluent is emitted from stacks which are little higher than the terrain features themselves.
- The second highest 24-hour concentrations tend to be underpredicted by the model, with the ratio of predicted concentration to measured concentration ranging from about .2 to 2.7 at about 90 percent of the sites.

- The degree to which the model over or underpredicts concentrations is strongly dependent on the factors relating to the plant and its surroundings. For example, at the Canal plant, the model significantly underpredicts the second highest one-hour concentrations at three sampling sites out of four, and the second highest 24-hour concentrations at all four sampling stations. At the Philo plant, however, the model overpredicts the second highest one-hour concentrations at all six sites, and the second highest 24-hour concentrations at five of the six sites. At Stuart and Muskingum River, the second highest one-hour concentrations are underpredicted at three sites out of five and two sites out of four, respectively. The corresponding 24-hour concentrations are underpredicted at all the Stuart sites, and three of the four Muskingum River sites.
- The model tends to underpredict at greater distances, a tendency which is highly significant at one plant. This is consistent with theory[12] and observation[13] in that, at greater distances, the plume width increases with distance to a power rather smaller than the 0.9 power as is assumed in this model.

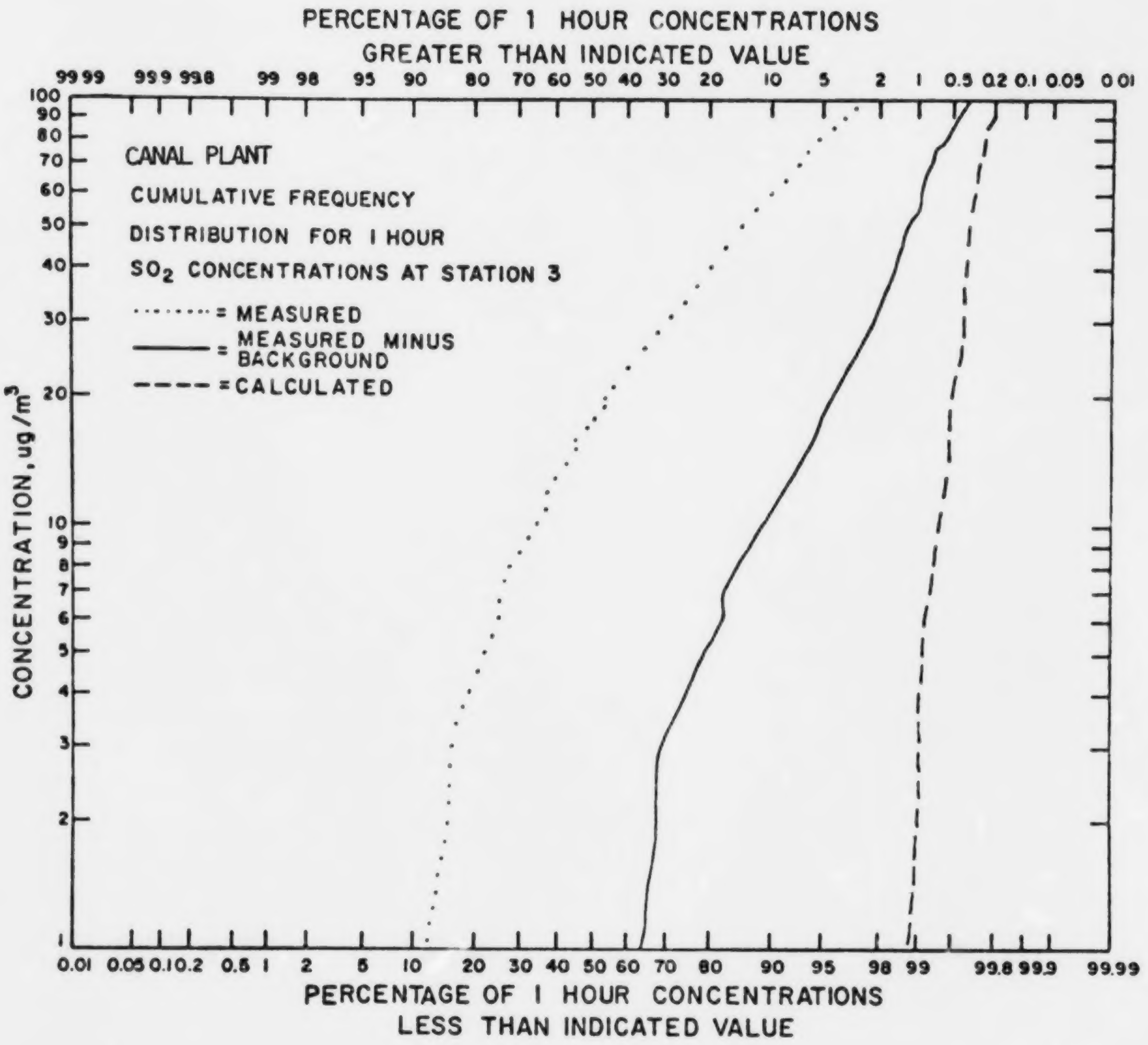

Figure 7. Cumulative frequency distributions for 1 hour SO_2 concentrations at station 3

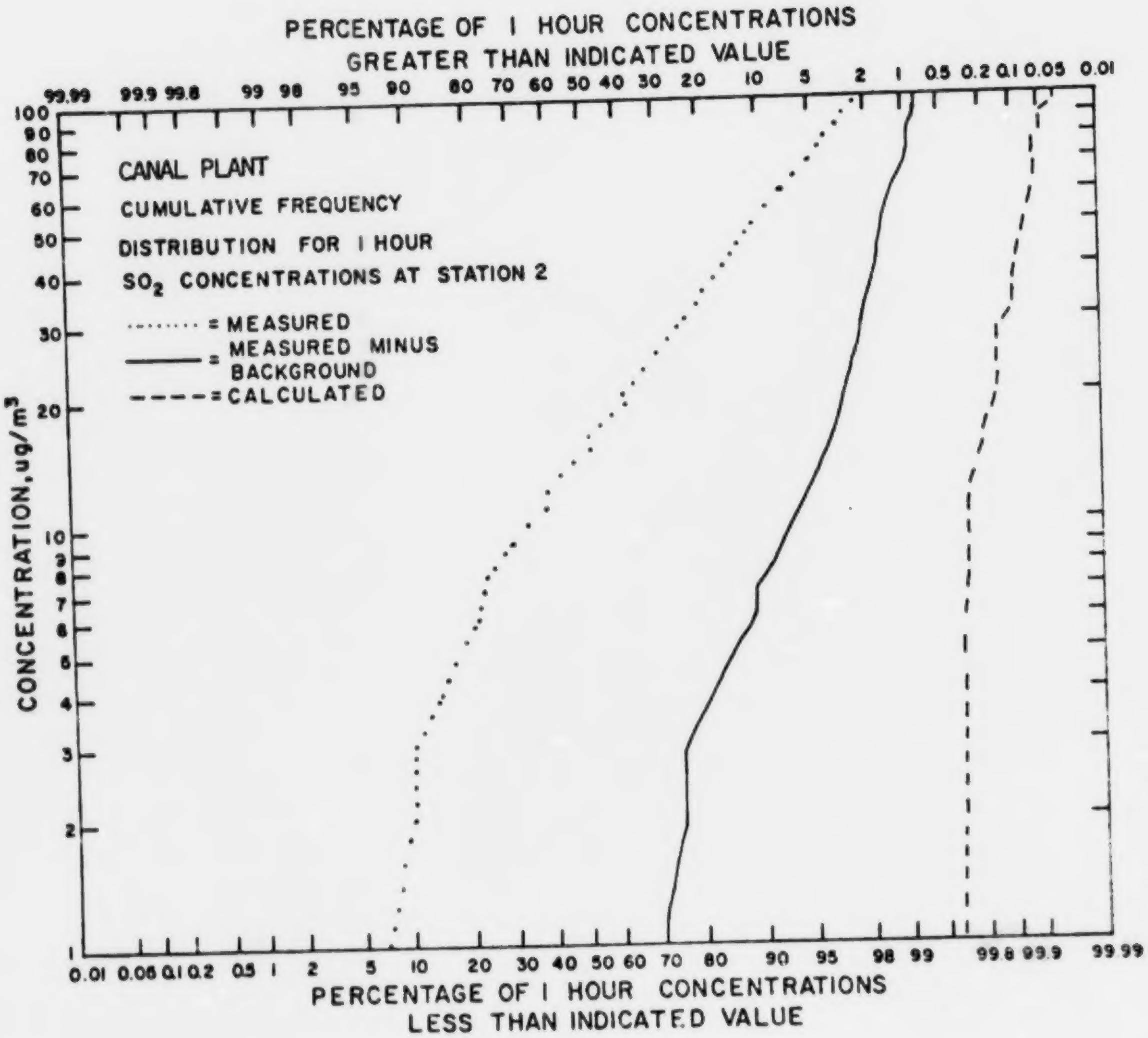

Figure 8. Cumulative frequency distributions for 1 hour SO_2 concentrations at station 2

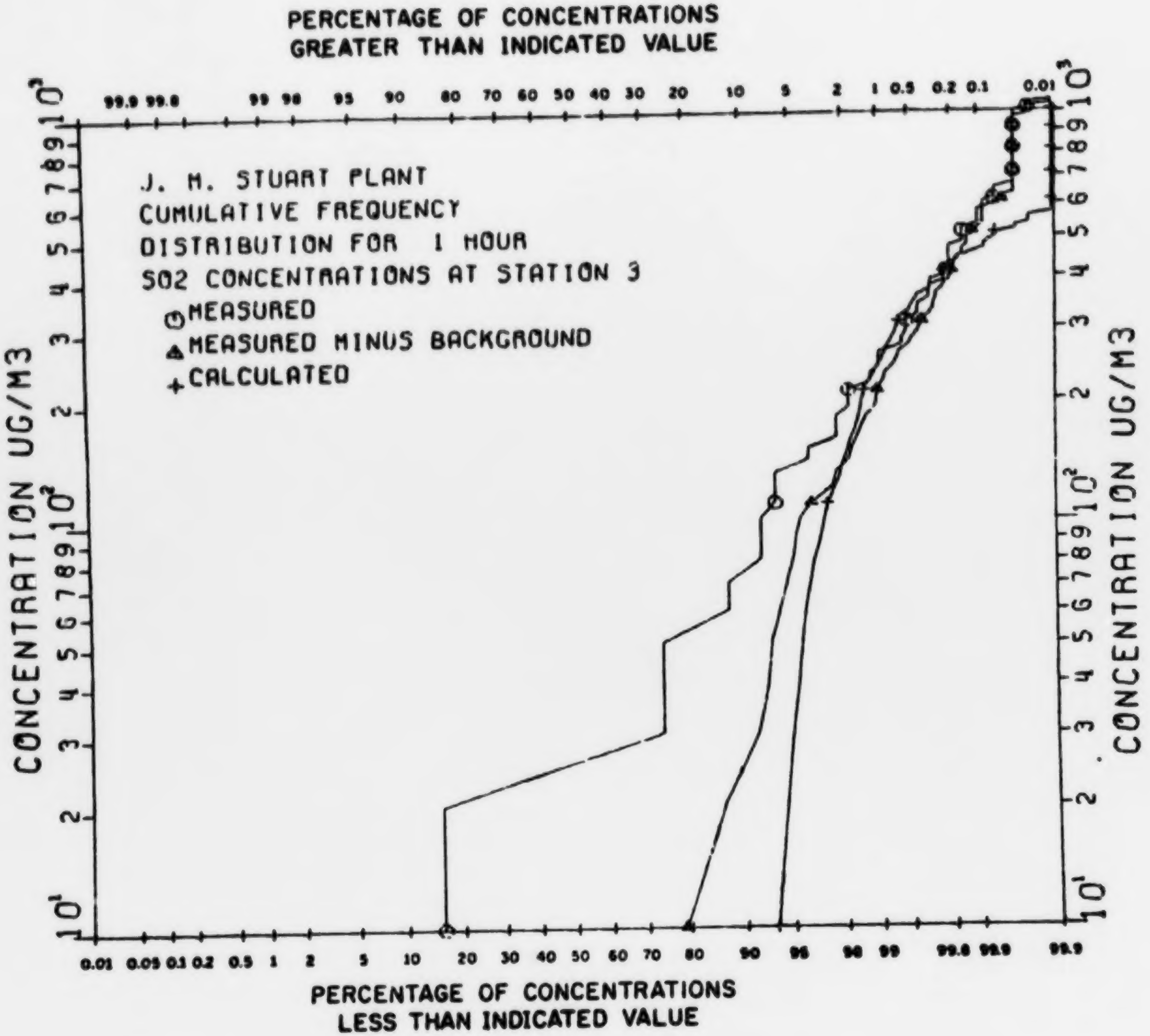

Figure 9. J. M. Stuart plant cumulative frequency distribution for 1-hour SO_2 concentrations at station 3

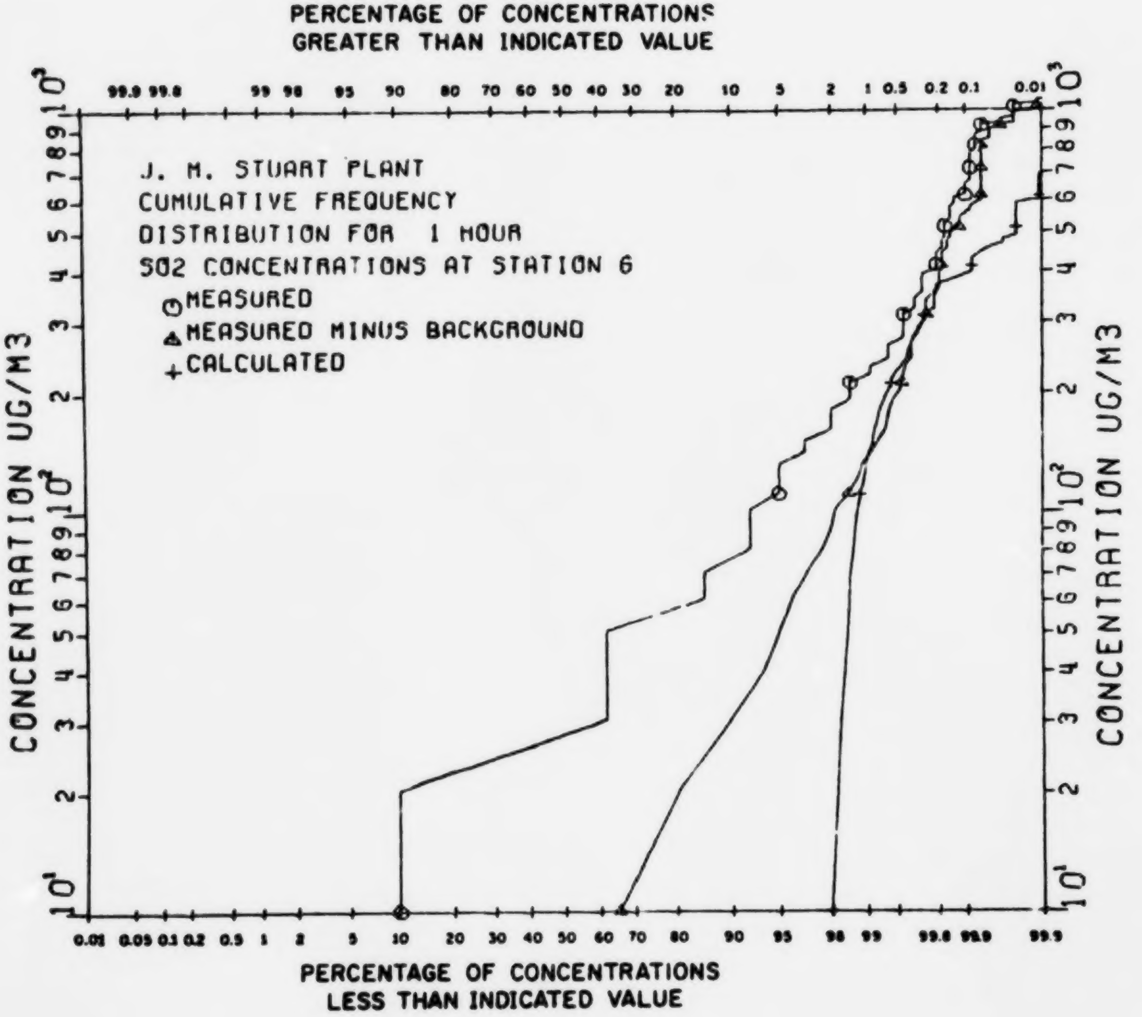

Figure 10. J. M. Stuart plant cumulative frequency distribution for 1-hour SO_2 concentrations at station 6

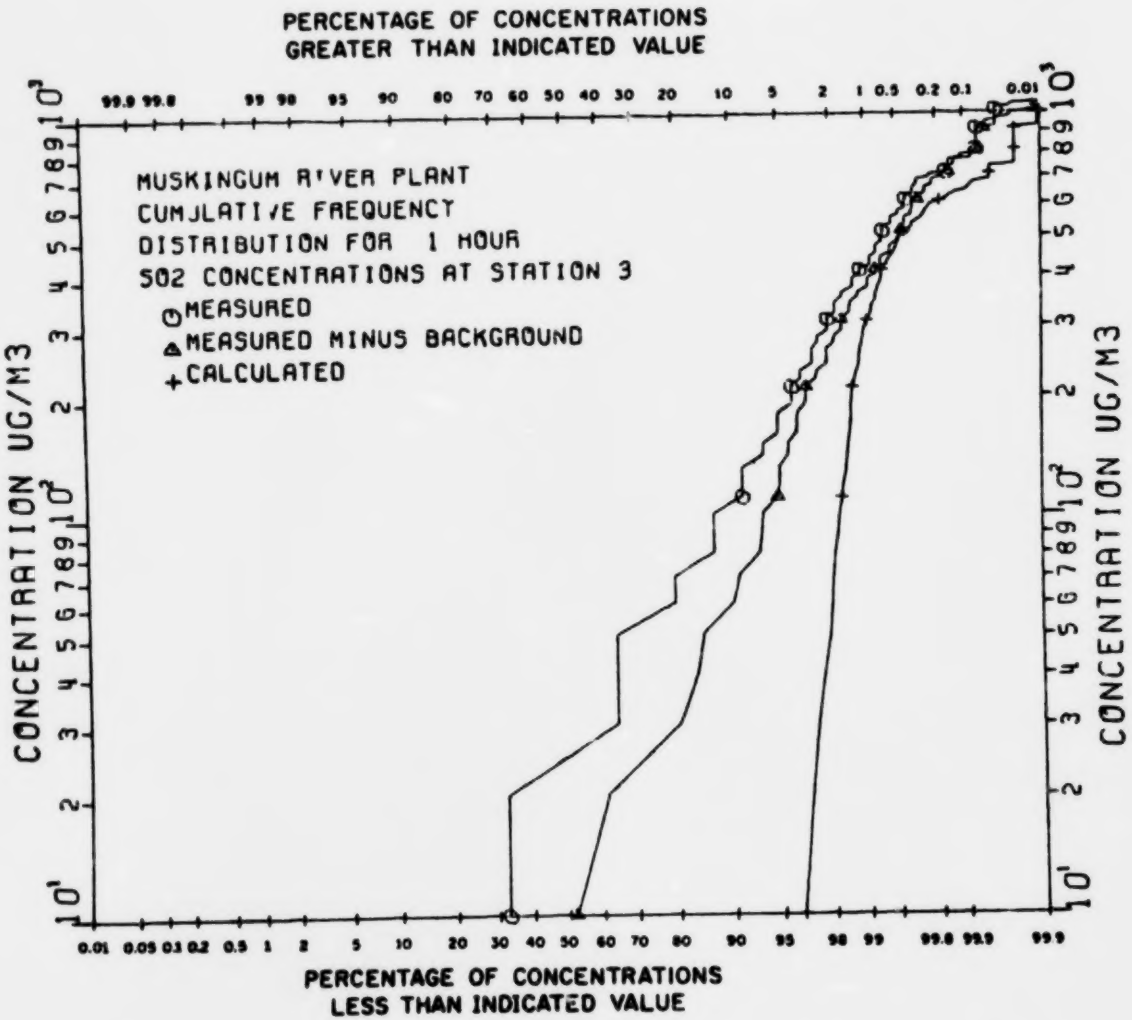

Figure 11. Muskingum River plant cumulative frequency distribution for 1-hour SO_2 concentrations at station 3

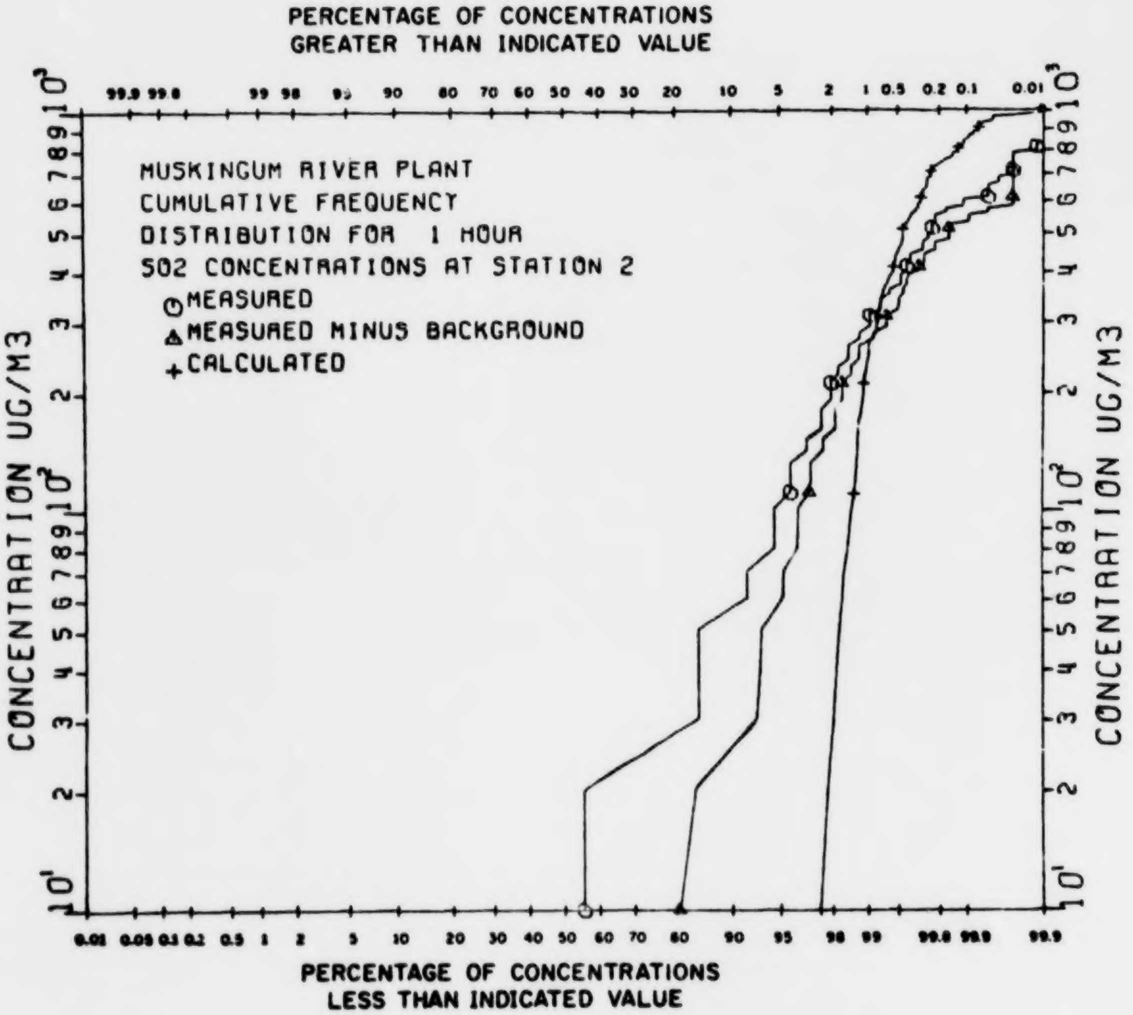

Figure 12. Muskingum River plant cumulative frequency distribution for 1-hour SO_2 concentrations at station 2

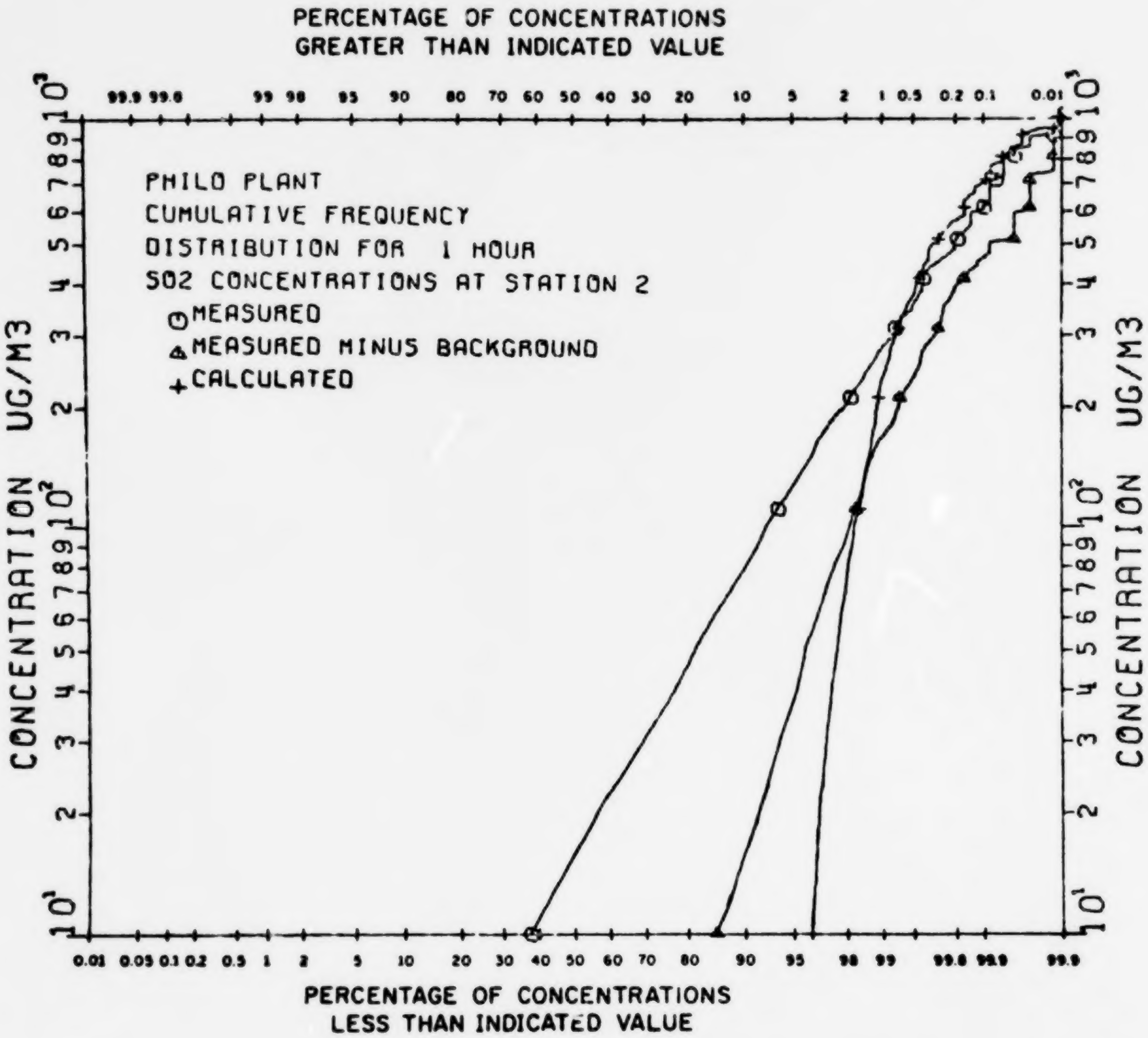

Figure 13. Philo plant cumulative frequency distribution for 1-hour SO_2 concentrations at station 2

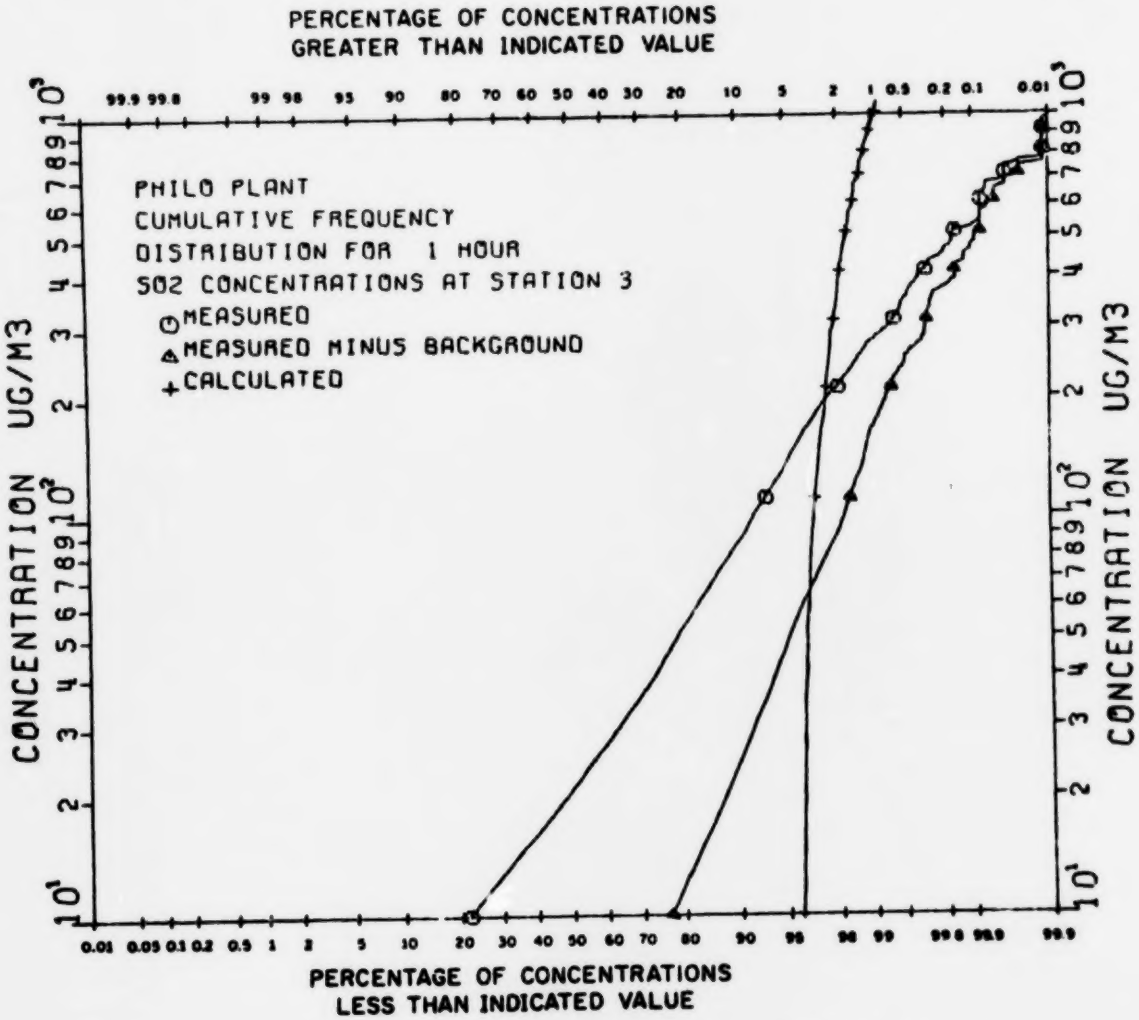

Figure 14. Philo plant cumulative frequency distribution for 1-hour SO_2 concentrations at station 3

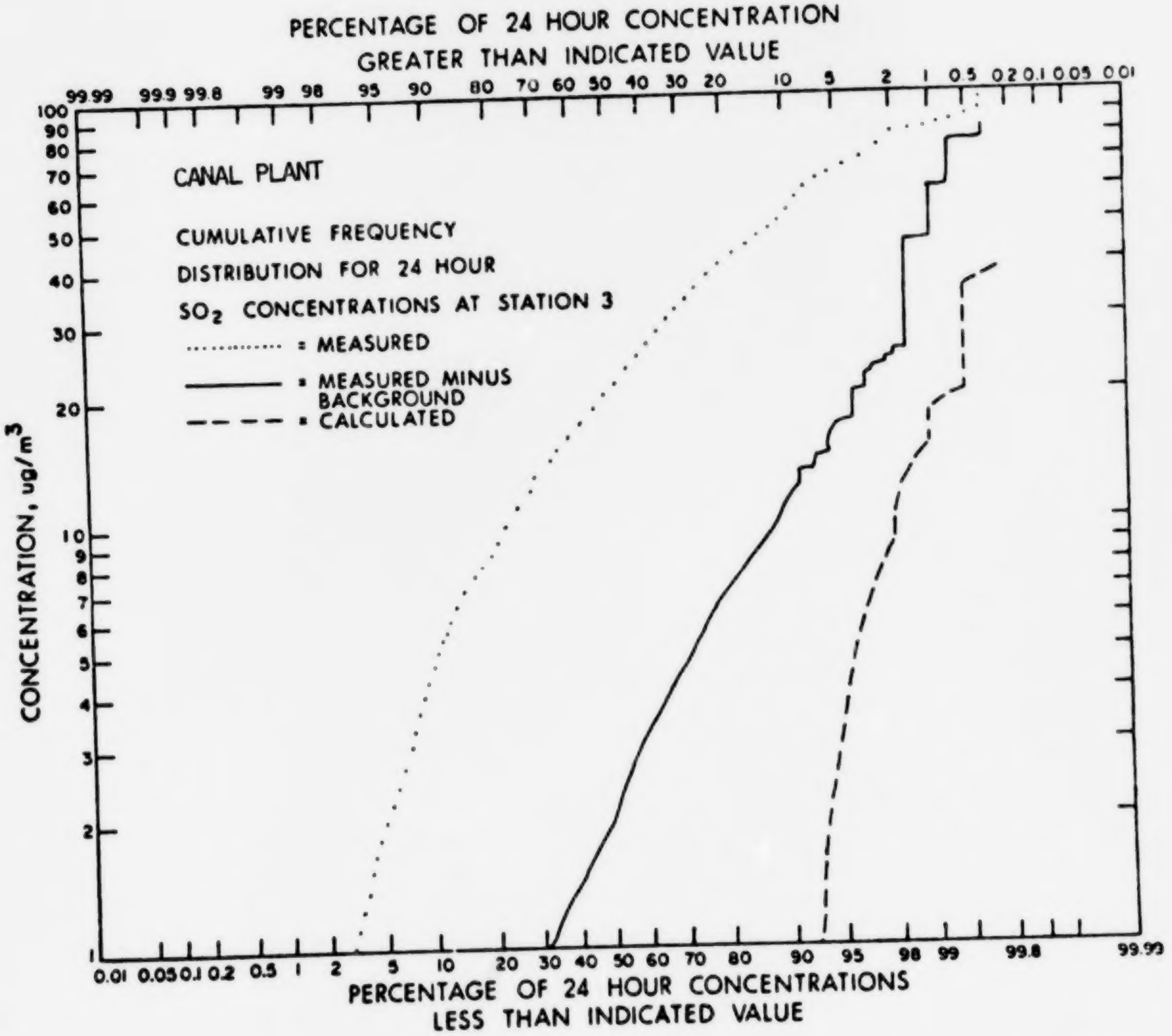

Figure 15. Cumulative frequency distribution for 24 hour SO_2 concentrations at station 3

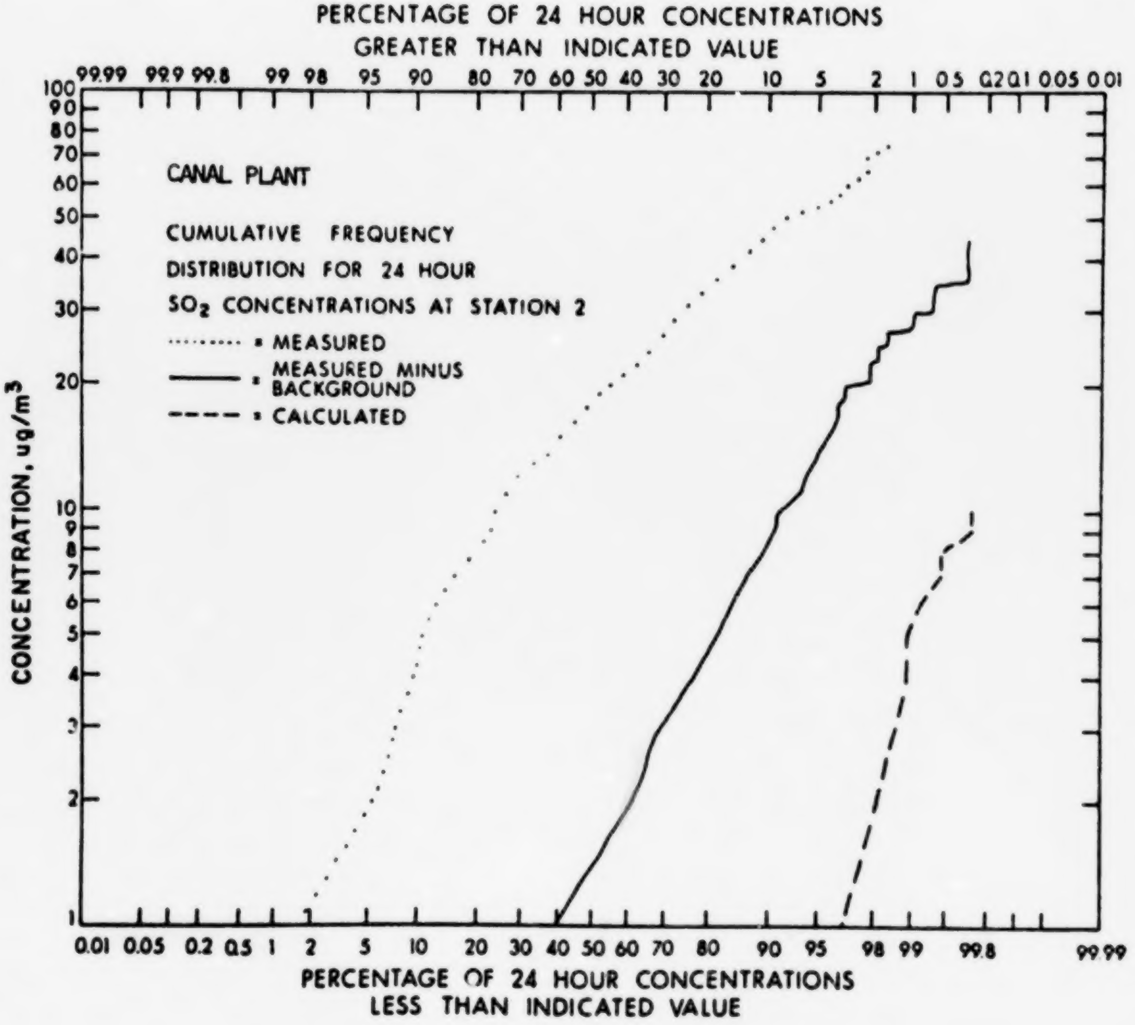

Figure 16. Cumulative frequency distribution for 24 hour SO_2 concentrations at station 2

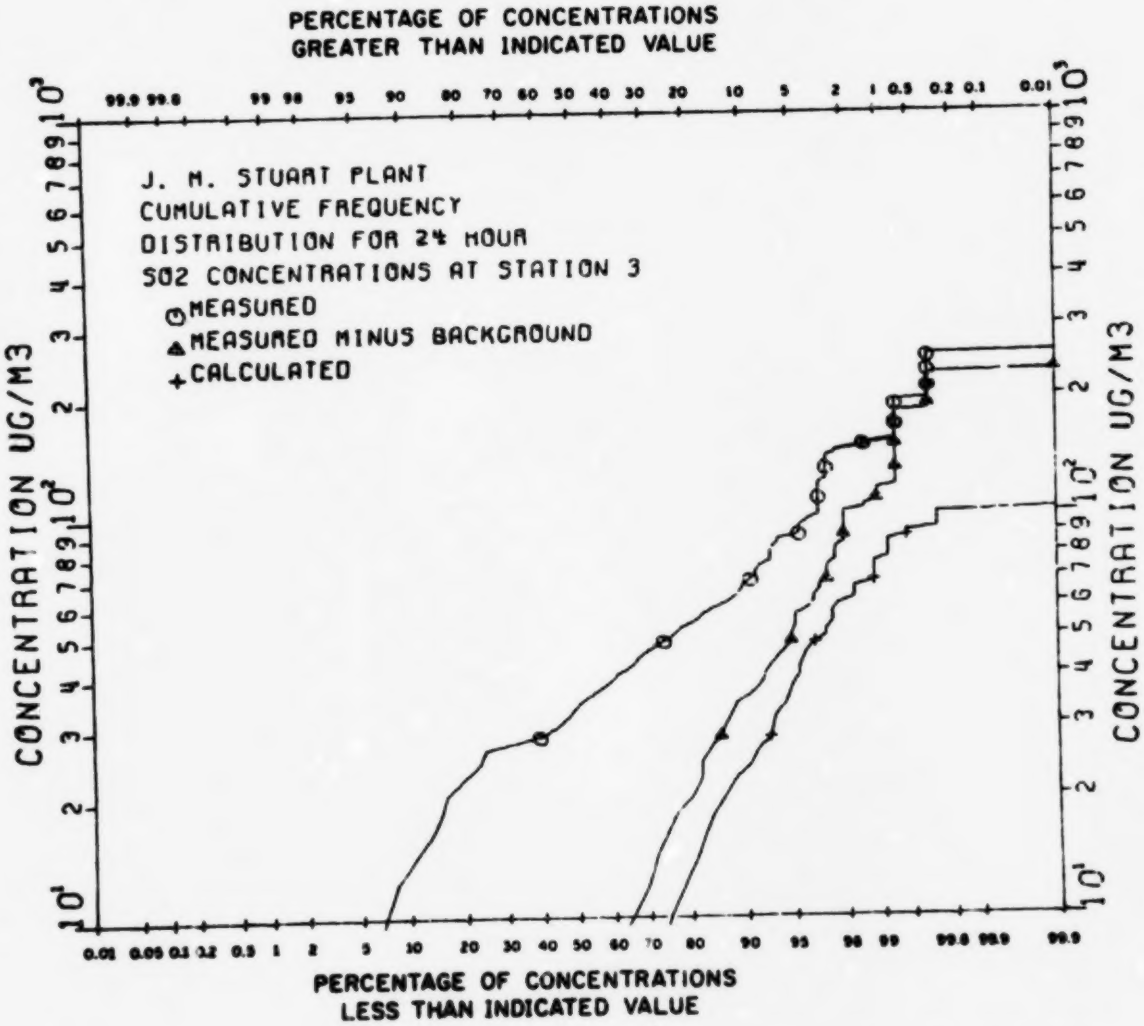

Figure 17. J. M. Stuart plant cumulative frequency distribution for 24-hour SO_2 concentrations at station 3

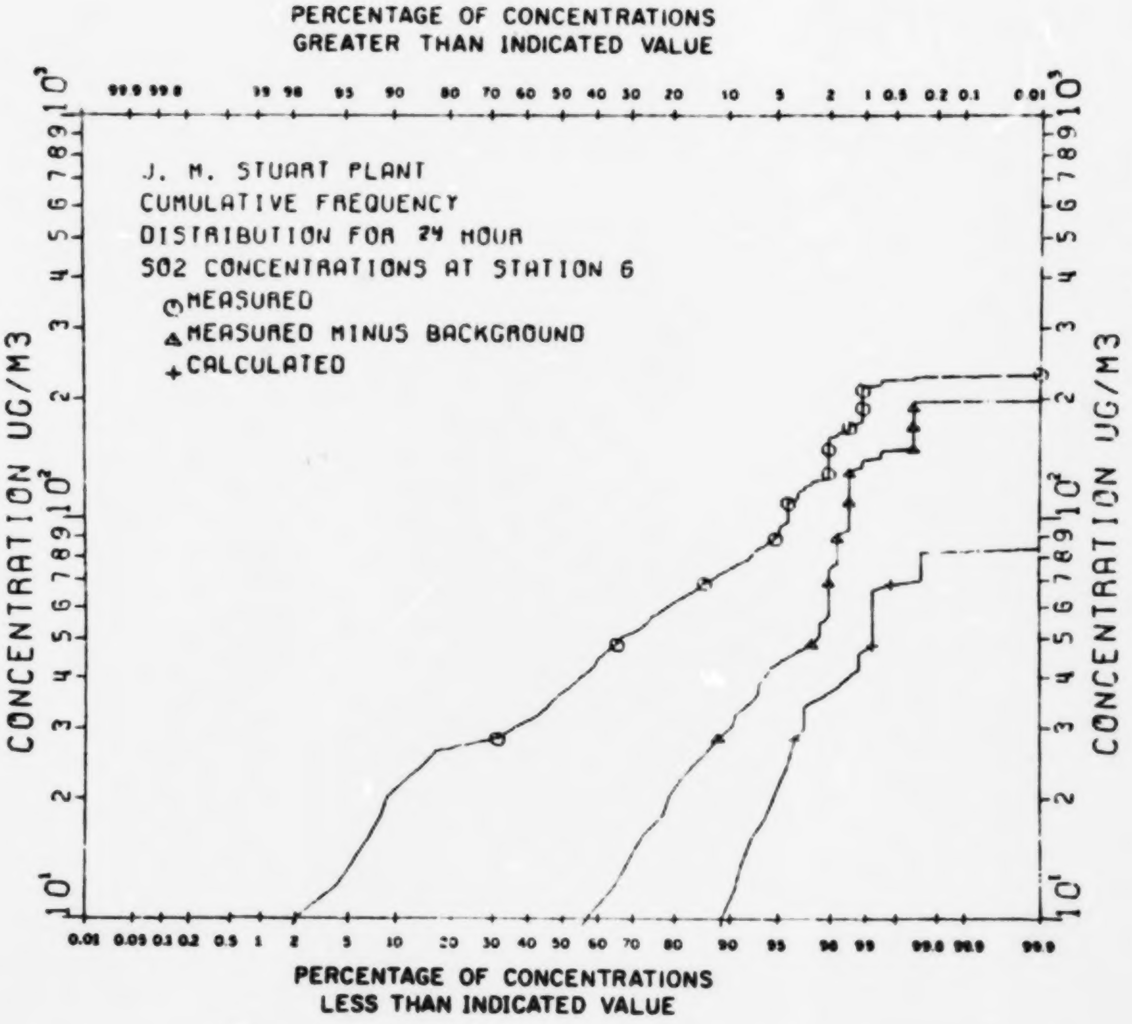

Figure 18. J. M. Stuart plant cumulative frequency distribution for 24-hour SO_2 concentrations at station 6

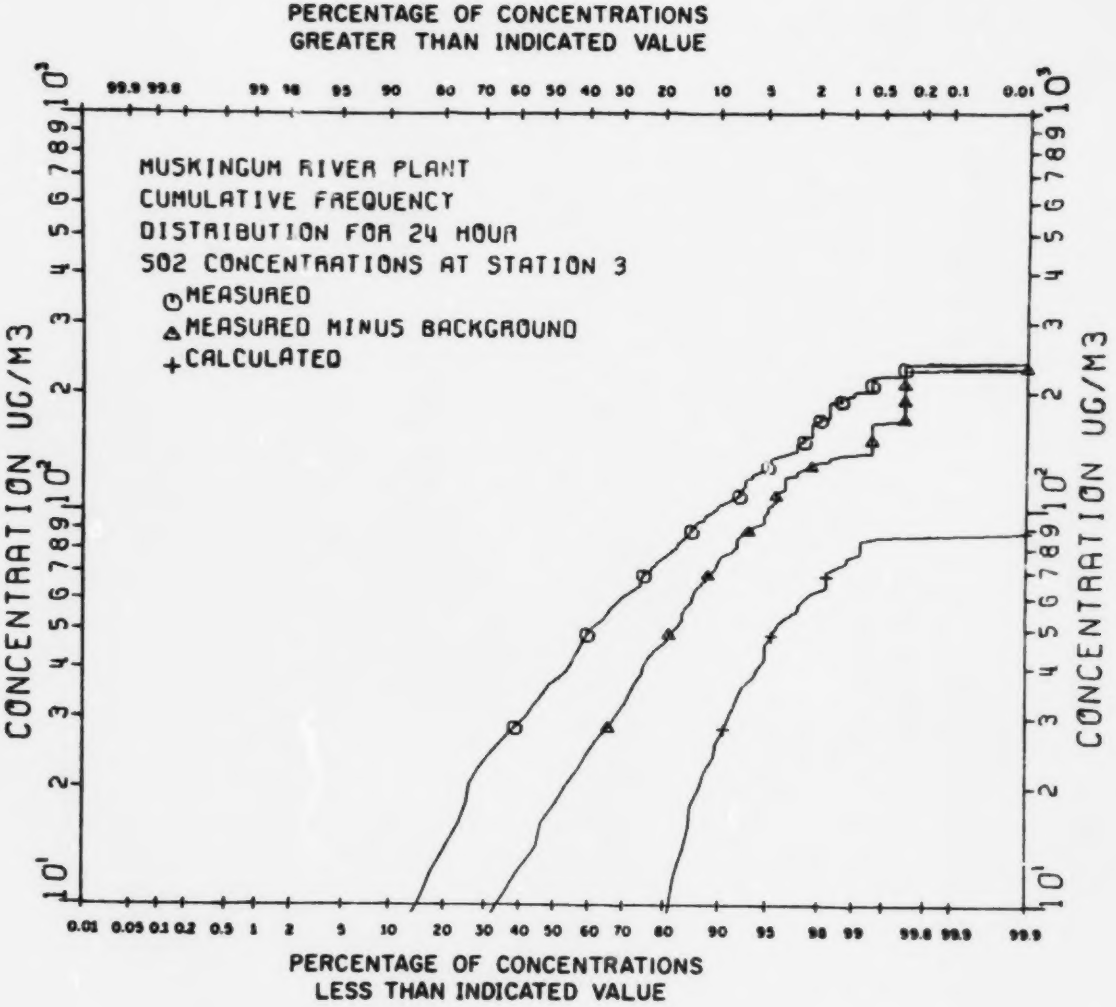

Figure 19. Muskingum River plant cumulative frequency distribution for 24-hour SO_2 concentrations at station 3

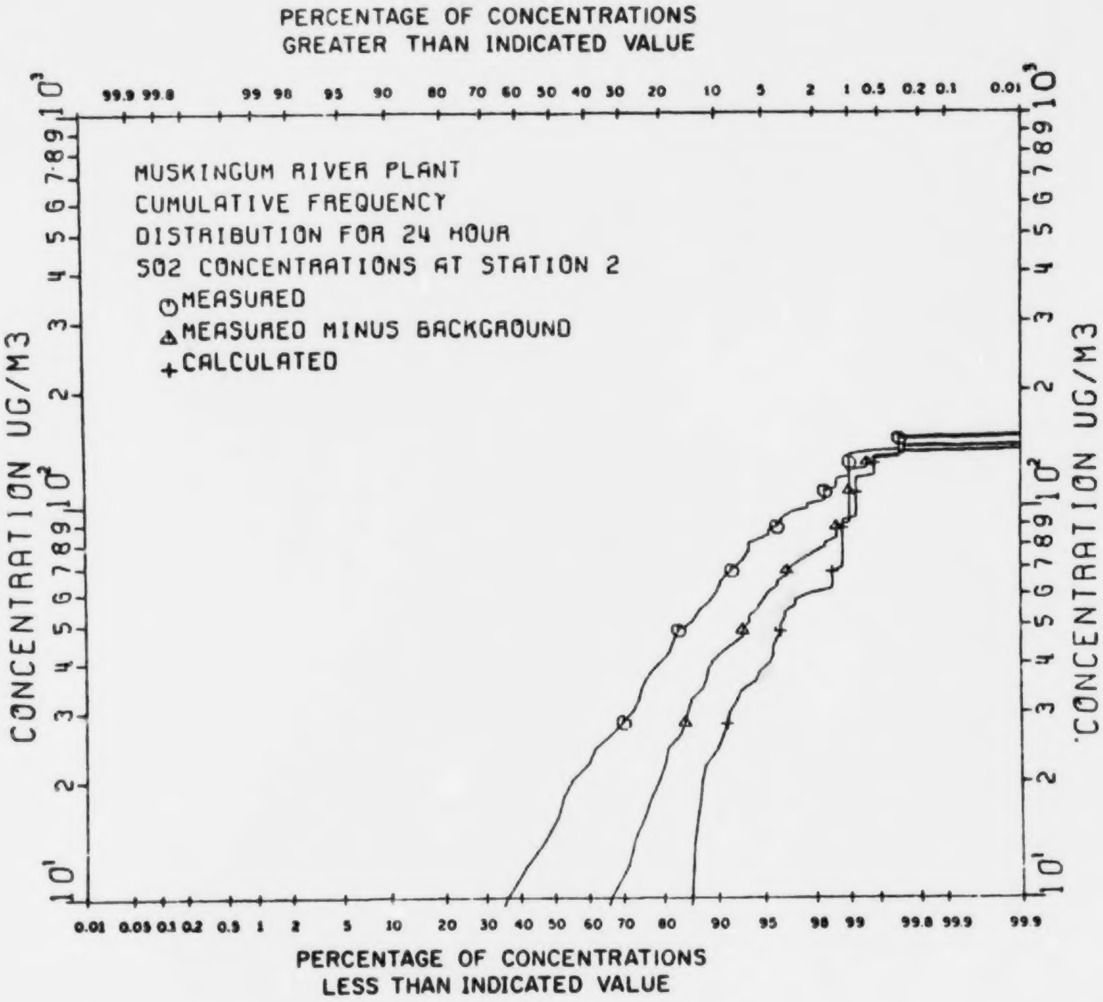

Figure 29. Muskingum River plant cumulative frequency distribution for 24-hour SO_2 concentrations at station 2

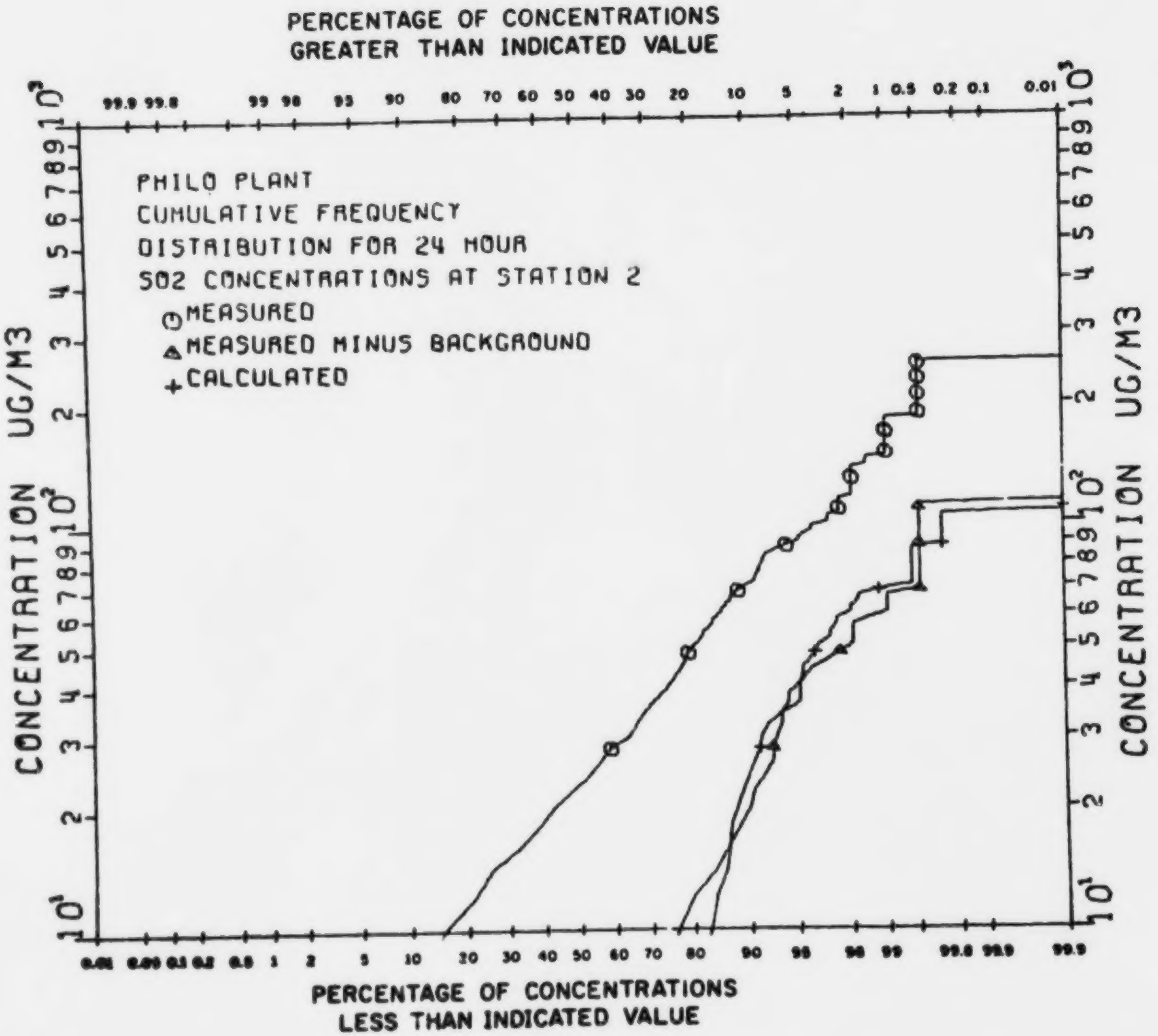

Figure 21. Philo plant cumulative frequency distribution for 24-hour SO_2 concentrations at station 2

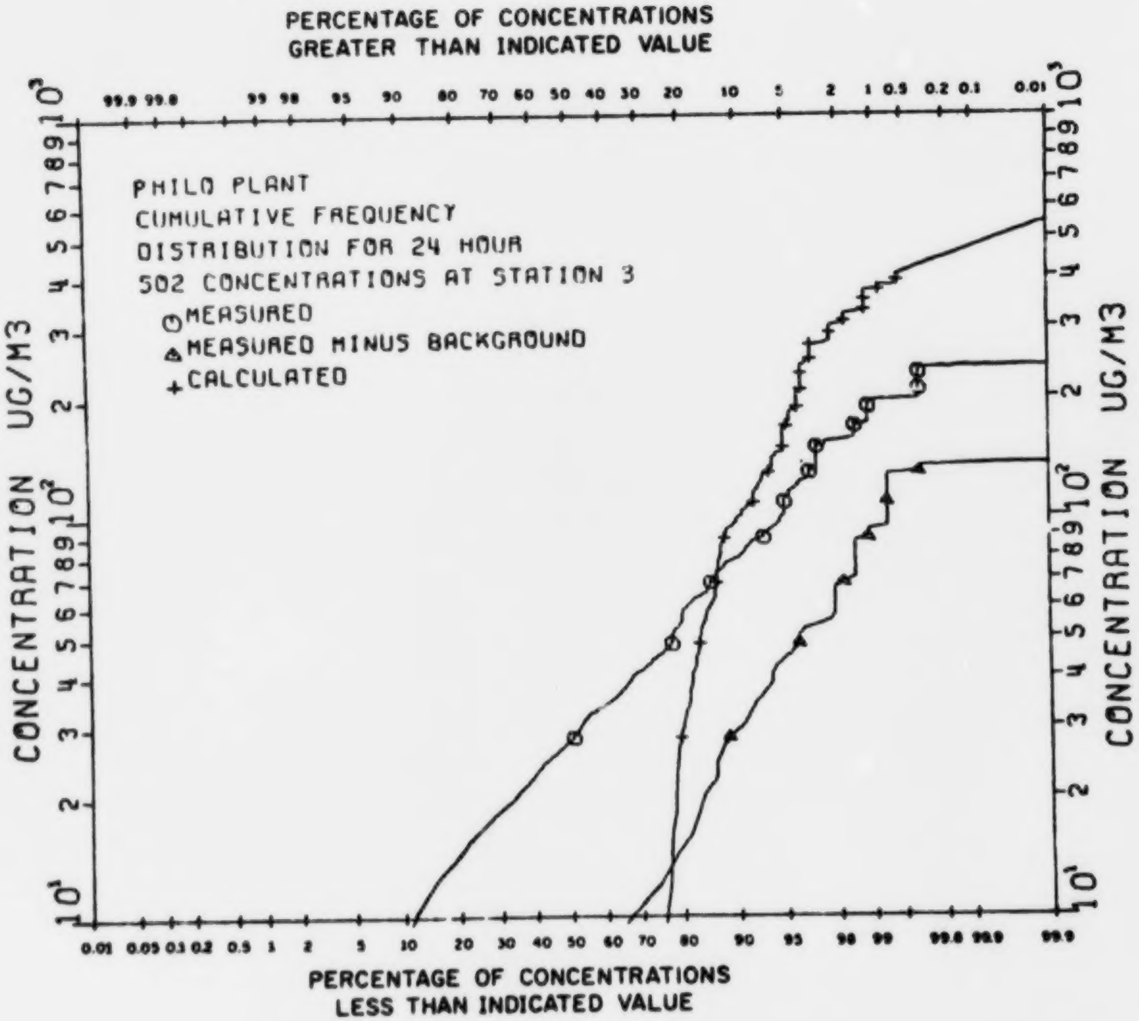

Figure 22. Philo plant cumulative frequency distribution for 24-hour SO_2 concentrations at station 3

References

1. Turner, D.B., Workbook of Atmospheric Dispersion Estimates. U. S. Environmental Protection Agency, Office of Air Programs Publication AP-26, Revised 1970.

2. Klug, Werner, Dispersion from Tall Stacks. U.S. Environmental Protection Agency, Office of Research and Development, Environmental Monitoring Series, Publication EPA 600/4-75-006, October 1975.

3. Montgomery, T.L., S.B. Carpenter and H.E. Lindley, The Relationship Between Peak and Mean SO_2 Concentrations. Conference on Air Pollution Meteorology of the American Meteorological Society in cooperation with the Air Pollution Control Association, Raleigh, North Carolina, April 5-9, 1971.

4. Hrenko, J., D.B. Turner and J. Zimmerman, Interim User's Guide to a Computation Technique to Estimate Maximum 24-Hour Concentrations from Single Sources. U.S. Environmental Protection Agency, Division of Meteorology, October 1972.

5. Briggs, Gary A., Plume Rise. U.S. Atomic Energy Commission Critical Review Series, TID-25075, National Technical Information Service, Springfield, Virginia, 22151, 1969.

6. Briggs, Gary A., Some Recent Analyses of Plume Rise Observations, pp. 1029-1032 in Proceedings of the Second International Clean Air Congress, edited by H.M. Englund and W.T. Berry, Academic Press, New York, 1971.

7. Briggs, Gary A., Discussion on Chimney Plumes in Neutral and Stable Surroundings. Atmospheric Environment 6, 507-610, July 1972.

8. Federal Register, Volume 36, No. 158, August 14, 1971.

9. Preining, D., et al., Staub-Reinhalt Luft, Vol. 29, No. 11, November 1969.

10. Smith, M.E., S. Frankenberg, Improvement of Ambient Sulfur Dioxide Concentrations by Conversion from Low to High Stacks. Journal of the Air Pollution Control Association, 25(6): 595-610, June, 1975.

11. Mills, M.T., and F.A. Record, Comprehensive Analysis of Time-Concentration Relationships and the Validation of a Single-Source Dispersion Model. U.S. Environmental Protection Agency, Publication EPA-450/3/75-083, 1975.

12. Pasquill, F., Atmospheric Diffusion, second edition, pp. 193-197, 362-364, 1974.

13. Csanady, G.T., Crosswind Shear Effects on Atmospheric Diffusion, Atmospheric Environment,

6th NATO/CCMS
International Technical Meeting
on Air Pollution Modeling

Applicability of Meteorological Data to Distant Locations and their Influence on the Calculation of Pollutant Concentrations

by

H. Bresser and Ch. Heger

Technischer Überwachungs-Verein
Rheinland e. V.

BATTELLE - INSTITUT E. V., Frankfurt/Main
Germany, FR

24 - 26 September, 1975

Preceding page blank

Applicability of Meteorological Data to Distant Locations and their Influence on the Calculation of Pollutant Concentrations

I. Introduction

In the Federal Republic of Germany the long-time mean value and the 95-percentile derived from the frequency distribution of the concentration values are often used to determine specific load levels for pollution load. If the frequency distribution of pollutant concentration is not obtained by measurements but by calculation, one must have both a suitable model, and a three dimensional frequency distribution of dispersion conditions i.e. of stability class, wind direction and wind speed. Compilation of such statistics usually requires observations over a considerable time period. These data are normally not available at all concerned locations or they may be insufficient. In the Federal Republic of Germany only the observations of the stations of the German Weather Service are available. The question is, whether it is feasible to apply the meteorological data compiled at an official weather station to a location near-by. One should note that often at certain locations complete meteorological records are not available but there are measurements on wind behaviour.

II. Compared Locations

To test the transfer of the meteorological data of one location to another look at Cologne and Düsseldorf! At the meteorological stations at Cologne and Düsseldorf airport complete data are available i.e. the joint frequency distribution of Turner's stability classes, wind directions and wind speeds over the last five years. Cologne airport is situated in the bay of Cologne, whence the Rhine valley opens to the north and west into the flat country. Düsseldorf airport is 60 kilometers north of Cologne airport. Towards the east the Rhine valley is bordered between

Cologne and Düsseldorf by the mountain ridge of the Bergische Land; north of Düsseldorf the Rhine valley also extends to the east into the flat country. To realize the differences of important meteorological data look at figure 1! It contains the frequency pattern of wind direction. In spite of the relative short distance between Cologne and Düsseldorf a remarkable difference in the wind direction pattern can easily be seen. Now look at figure 2: The relative portions of the Turner classes show a definite dependence on the wind direction but rarely differ between Cologne and Düsseldorf. This fact leads one to conjecture that wind direction pattern is a critical factor even if distances are small, but application ot the data of a station over greater distances becomes possible, if a correction of the frequency of wind direction ist applied.

III. Comparative Calculation

To estimate the size of deviation of such pollutant concentration calculations the following data were used. Firstly the meteorological data of Cologne (indicated by the subscript K) and secondly the meteorological data of Düsseldorf, corrected for the frequency of wind direction, (indicated by the subscript $D \rightarrow K$). According to the statement above the quantities to be compared are the calculated mean value, S_M, and the 95 - percentile, P_{95}. Our model is the standardized model as laid down in the Northrhine-Westphalia regulation on refineries. It has been discussed in detail by Külske and Schmitt. It is mainly characterised by the following key-words;

Gaussian plume model
Plume rise by formula from Moses and Carson
Parameters σ_y, σ_z from McElroy for
low sources and from Singer-Smith for high ones.

We have considered a high source and a low one. Specific details pertaining to these sources are contained in figure 3. The sources constitute the origin of the co-ordinate system. The mean values

S_M and the 95-percentiles P_{95} were calculated for points on five straight lines. These are allocated to directions North, East, South and West and to an additional direction approximately West-North-West, which constitutes the sector of main pollution according to the wind vector diagram of Cologne.

The graphs of the mean value S_M and the 95-percentile P_{95} as functions of the distance from the source are shown in figure 4. They are shown for the direction WNW e.g. and for the high and low source. The distance between the points and the source varies from 200 meters to 10.000 meters.

For this particular research it is important to compare the results derived from the meteorological data of Cologne, identified by K, with the results obtained using the data from Düsseldorf which were corrected for the frequency distribution of the wind direction applicable to Cologne.
The latter indicated by D→K.
The ratios $S_{M,K}/S_{M,D \rightarrow K}$ and $P_{95K}/P_{95,D \rightarrow K}$ are shown in figures 5 to 8 for the high and low source, respectively. To assess the result the graphs shown in figure 4 should be kept in mind.
Figures 5 to 8 exhibit the same general scheme: The abscissa represents the distance from the source at a logarithmic scale whereas the ordinate reflects the above mentioned ratios. The drawings consist of 5 individual diagrams related to directions North, East, South, West and West-North-West. The value concerned is found at top left and the respective source at top right. The maximum values for the mean value $S_{M,K}$ and the 95-percentile $P_{95,K}$ respectively are shown for all directions between distances of 200 meters and 10.000 meters.

Figure 5: High source - mean value

The ratio of calculated mean values varies between 0,9 and 1,1 except in a few cases. These exceptions occur at a distance of 200 meters in directions of South and West-North-West and beyond 5.000 meters in a westerly direction. The values there range from 0,8 to 0,9. Where deviations occur, however, the mean values are already one order of magnitude lower than maximum.

Figure 6: High source - 95 - percentile

In the highly polluted areas in the East and West-North-West the ratio of the 95 - percentiles varies from 0,9 to 1,1. In the direction of North values between 0,9 and 1,2 are found, except for a distance of 200 meters where the 95 - percentile however is still approximately one order of magnitude smaller than maximum. Greater deviations down to 0,5 occur to the west whereas towards the south the 95 - percentile practically reaches zero. In westerly direction the maximum 95 - percentile is still considerably lower than in the directions of high pollution load.

Figure 7: Low source - mean value

The ratio of the mean values lies between 0,9 and 1,1 for all directions other than West - except for one instance in the north. A decrease down to 0,75 is evident towards West.

Figure 8: Low source - 95 - percentile

The ratio of the 95 - percentiles ranges from 0,8 to 1,2 for all directions. One exception is found in the west at distances of 5.000 and 10.000 meters, where the absolute values, however, are already very small.

Whether one looks at high or low sources, mean values, or 95 - percentiles the following statement can be made:
If the long time mean values or the 95 - percentiles of Cologne, derived from the meteorological data of Cologne, are compared with those values obtained from the Düsseldorf data corrected for wind frequency distribution, the deviations in the majority of cases are less than 10 %.
Only a few cases exceed 25 %. Deviations of 25 % and more were only found in areas where the absolute load levels were insignificant. Deviations greater than 50 % did not occur.
In addition to the described results further calculations were made using different combinations of sources.
It was found that deviations further decreased. Deviations of more than 20 % were then not observed.

IV. Summary

When calculations of pollutant concentration have to be computed for a specific location, complete meteorological data, as required for calculation, are frequently not available. If the aim of pollutant concentration simulation is the calculation of frequency distributions and derived therefrom long-time mean values and 95 - percentiles, the following rules apply, based upon previous results:

a) Depending on the geographical situation even a small local move can cause a significant change in the frequency of wind directions. Therefore an uncorrected application of data can lead to great deviations.

b) These deviations can be greatly reduced even if meteorological data are transferred over greater distances (50 kilometers or more). One only has to correct these data for the wright frequency distribution of wind directions leaving all other parameters unchanged. Thus deviations of more than 25 % up to 50 % will only occur in extreme situations in areas of low ground level concentration. Especially in areas of high concentration a deviation of even less than 10 % can be expected.

c) If in an individual case these statements about the accuracy obtained by transferring meteorological data are not sufficient, an investigation should be made using complete data of two neighbouring stations. The same procedures should be applied as laid down as an example in this report.

Figure 1

Frequency of Wind Direction

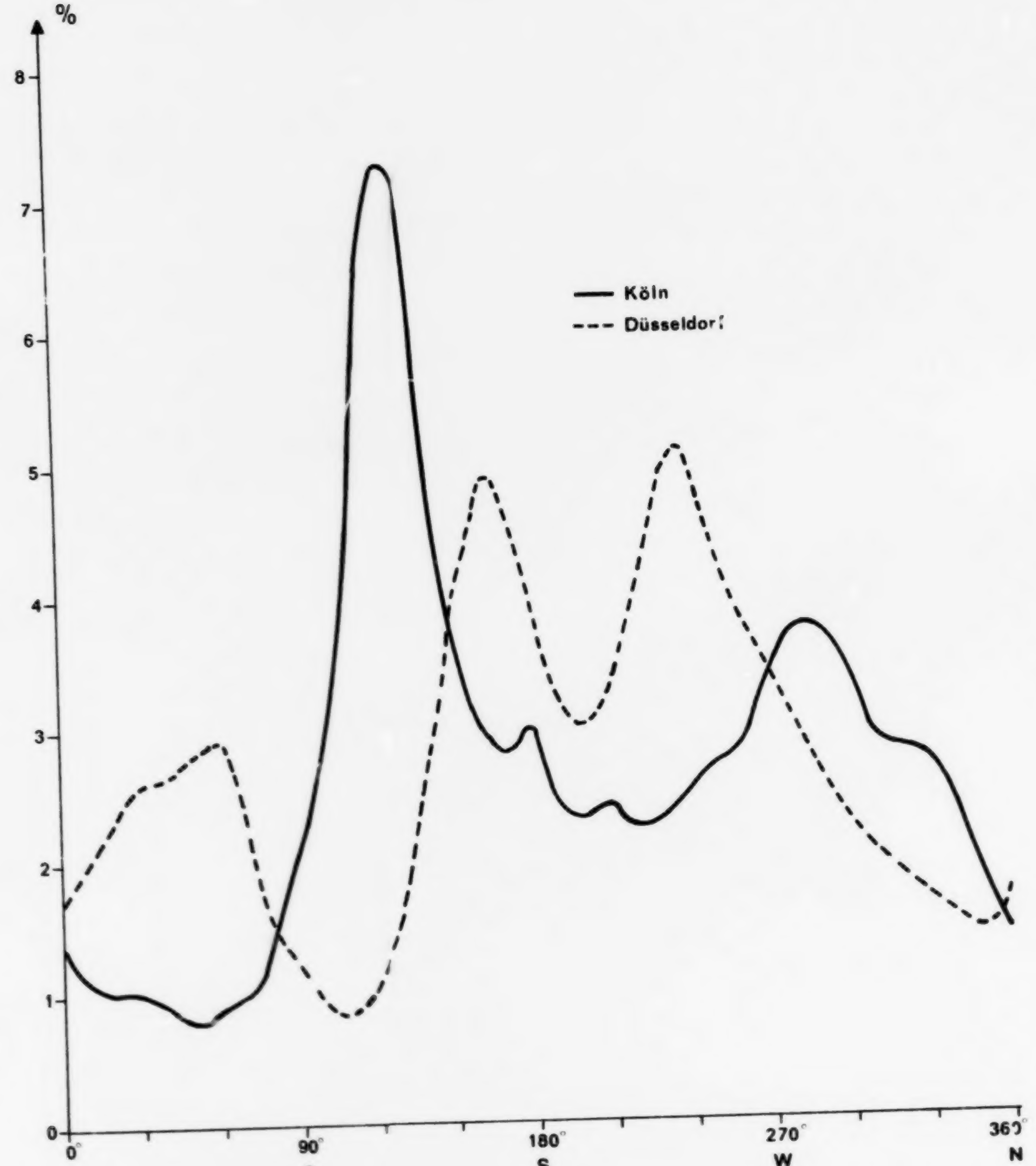

Figure 2

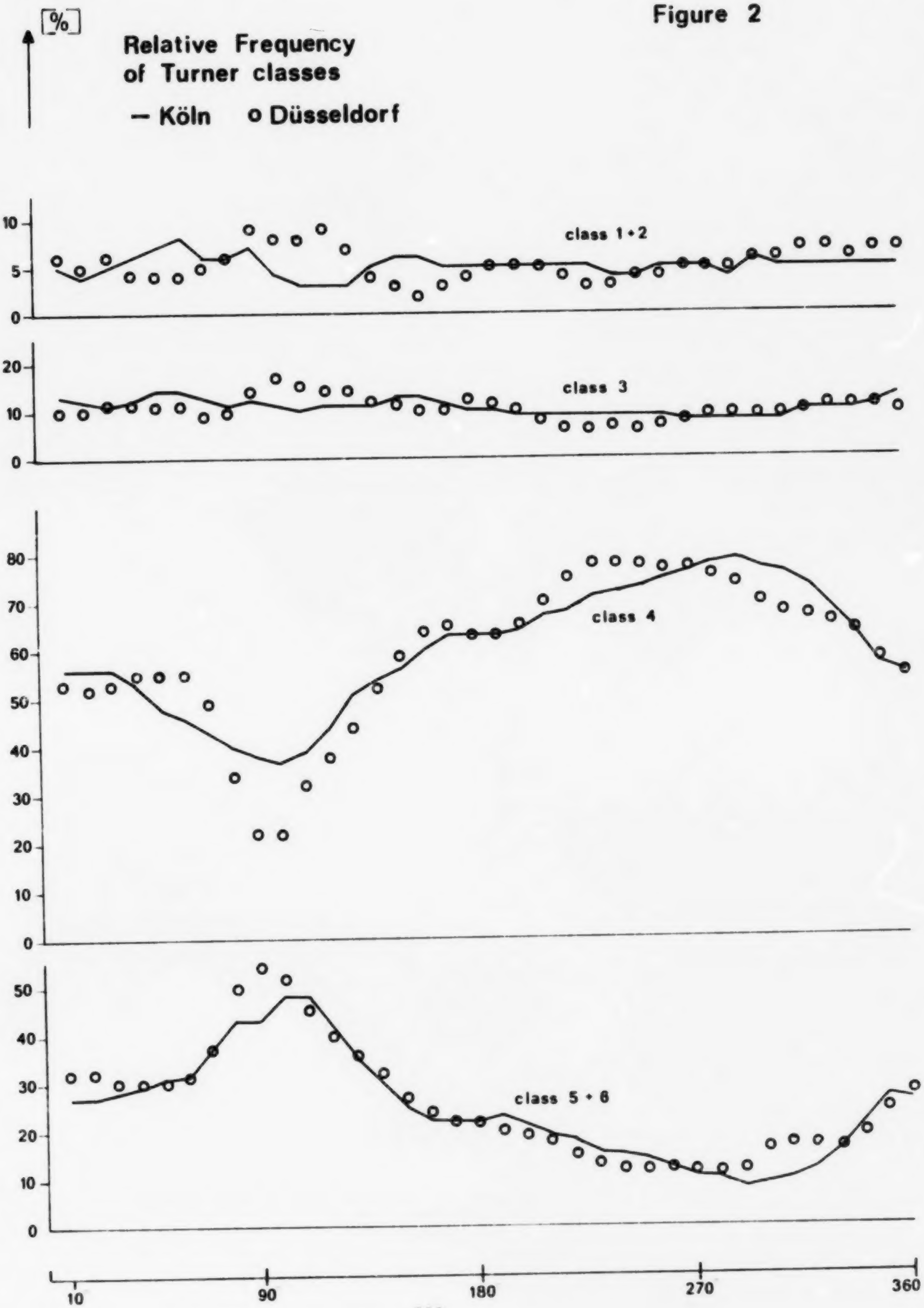
[%]
Relative Frequency
of Turner classes
— Köln o Düsseldorf
10
5
0
class 1 + 2
20
10
0
class 3
80
70
60
50
40
30
20
10
0
class 4
50
40
30
20
10
0
class 5 + 6
10
90
180
270
360

Figure 3

High source

Stack height	100	m
Emission rate	247	kg/h
Stack exit velocity	10	m/s
Stack gas effluent	176 000	Nm^3/h
Stack gas temperature	140	°C

Low source

Stack height	10	m
Emission rate	34,2	kg/h
Stack exit velocity	2	m/s
Stack gas effluent	295	Nm^3/h
Stack gas temperature	250	°C

Figure 4

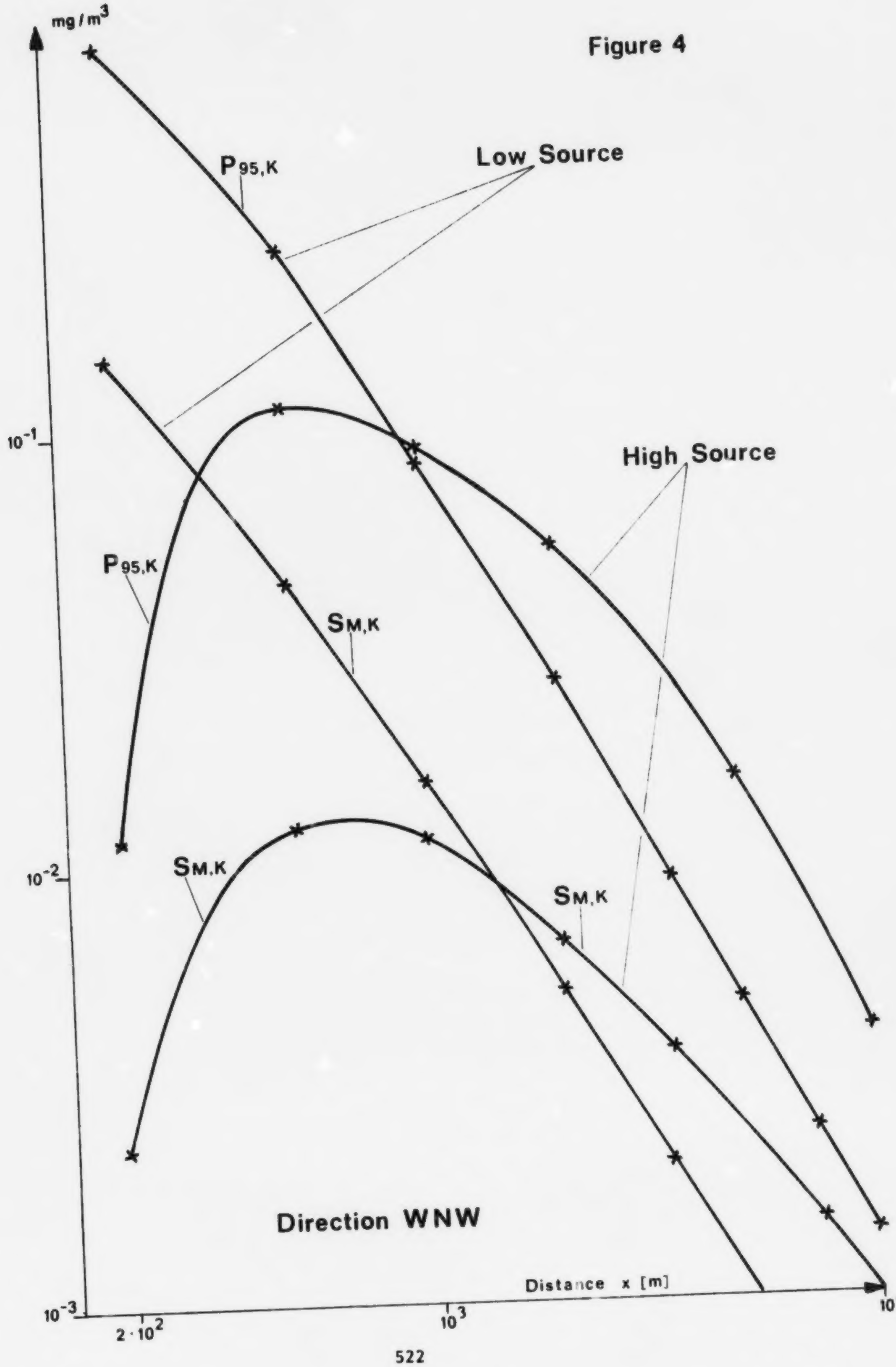
mg / m³
Low Source
P95,K
High Source
P95,K
SM,K
SM,K
SM,K
10⁻¹
10⁻²
10⁻³
2·10²
10³
10⁴
Distance x [m]
Direction WNW

Figure 5

High Source

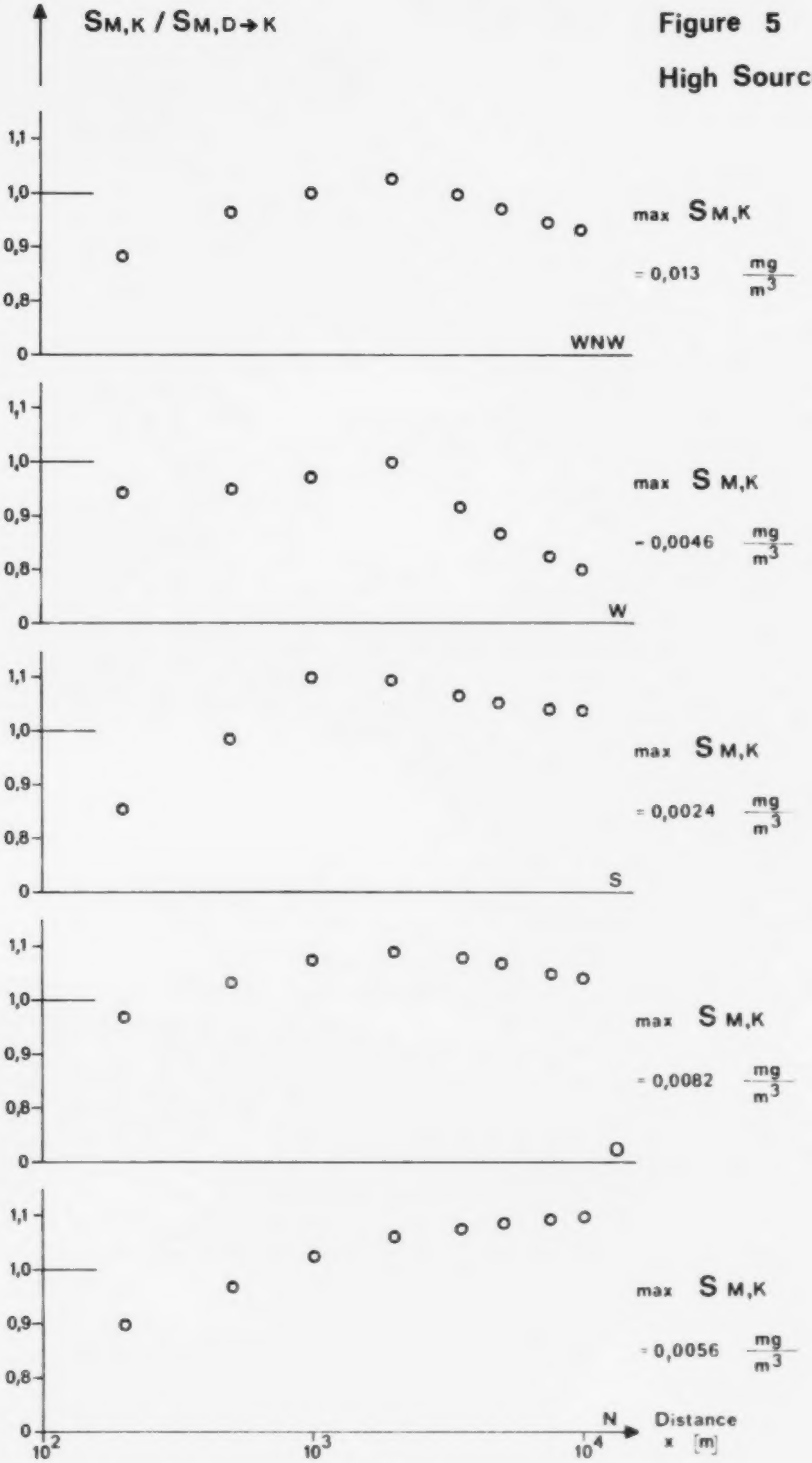

Figure 6

High Source

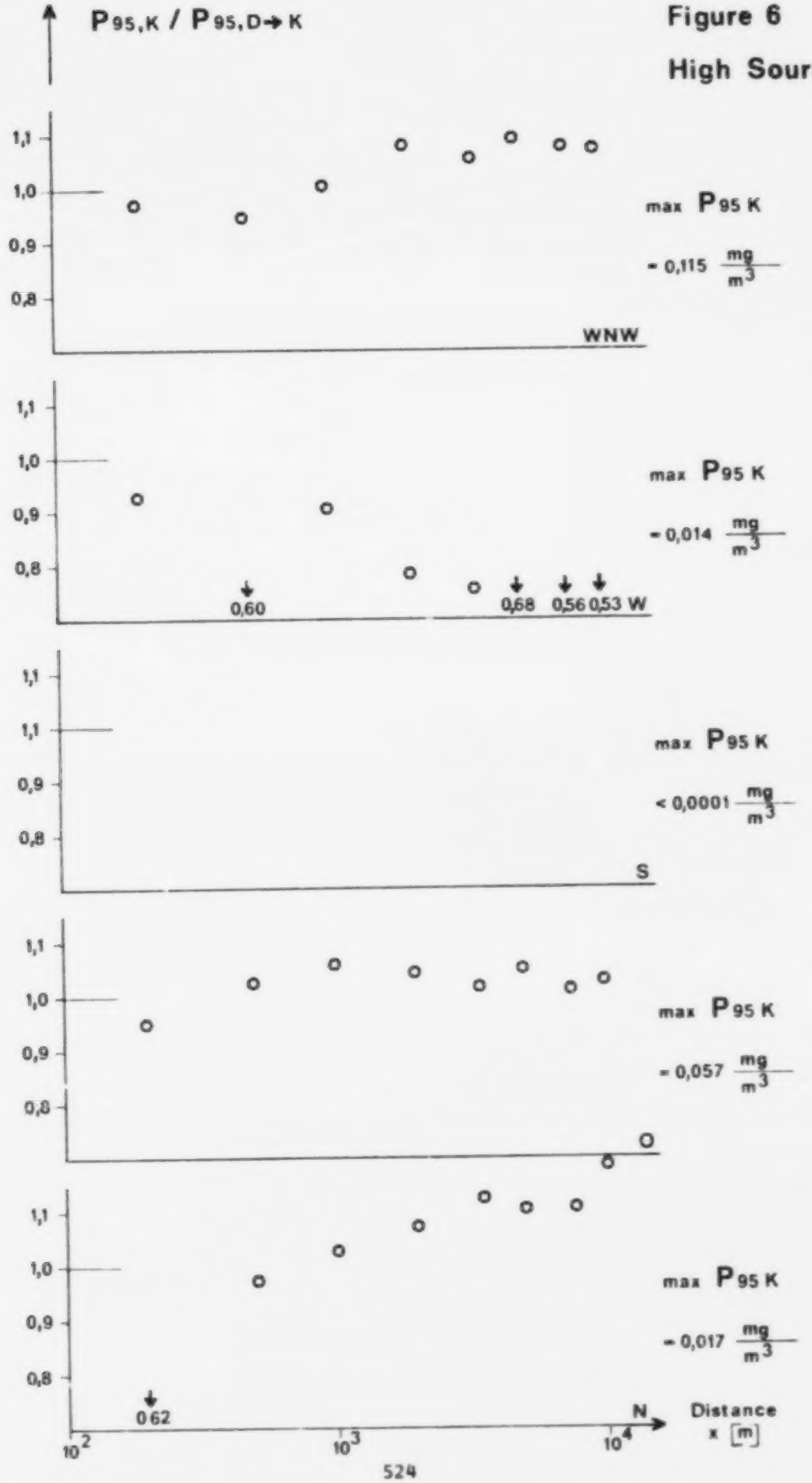

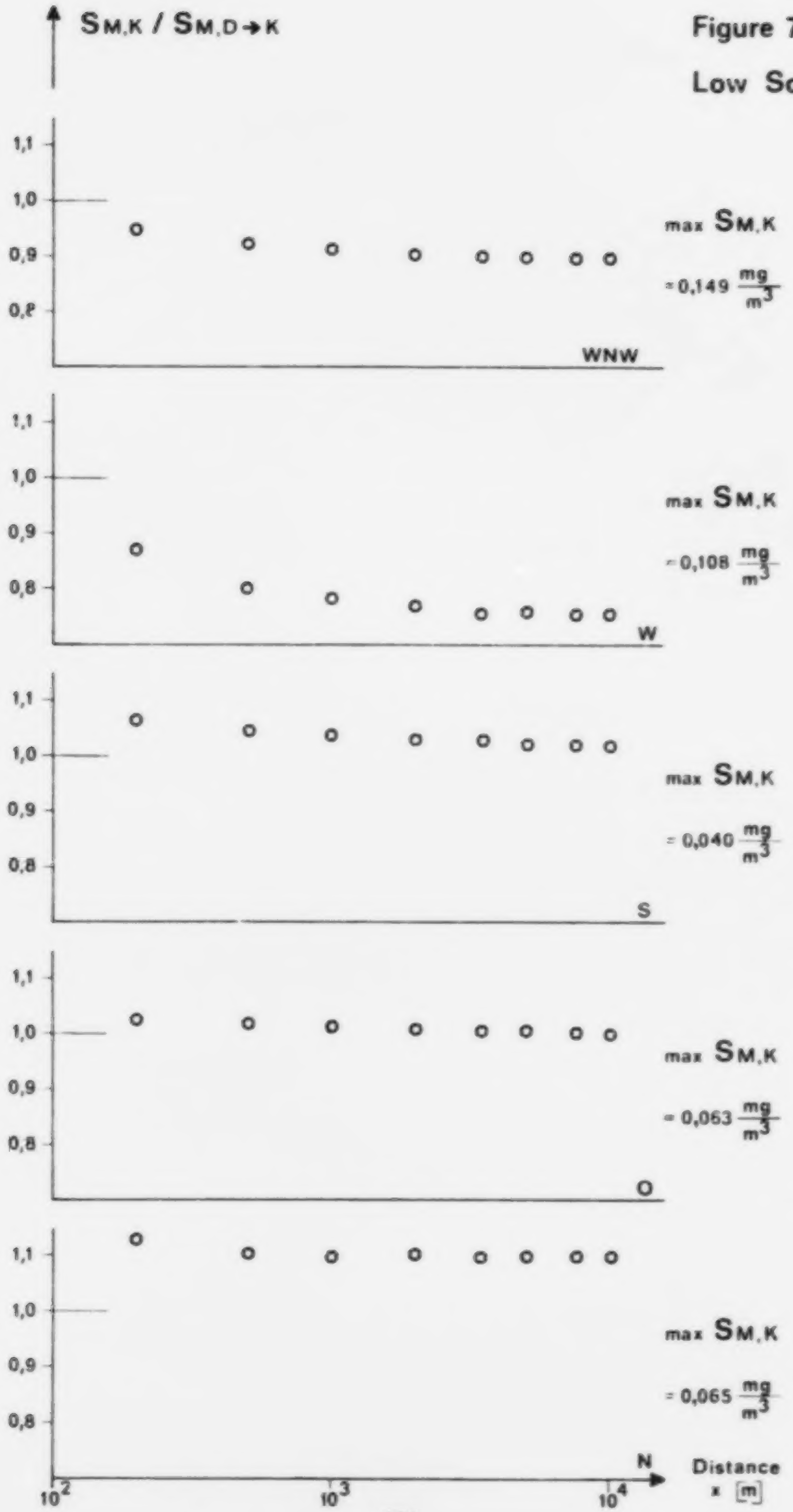

Figure 7

Low Source

Figure 8

Low Source

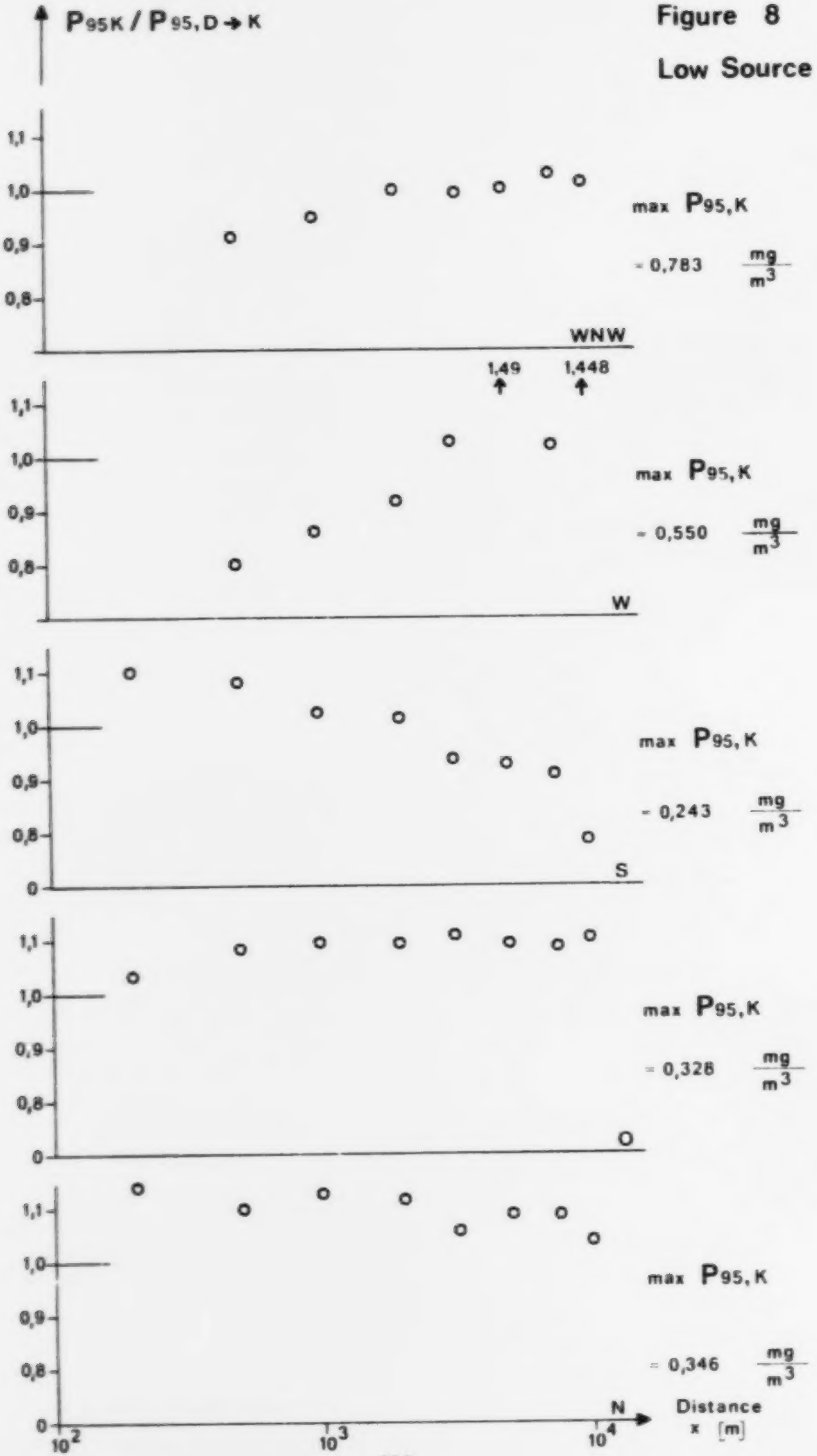

Rapporteur's Report, Topic III, September 25, 1975
by B. Turner

Chairman: W. B. Johnson

The chairman stated that it is important to consider the use of modeling, not just as a mathematical pursuit. In order to ask how useful the models can be, they must be validated by comparison of calculations with measurements.

J. R. Hammerle: Using Sensitivity Analysis to determine Dispersion Modeling Input Requirements

Discussion:

W. B. Johnson: This type of analysis should be extended to other parameters.

R. F. Lee: Validation of a Single Source Dispersion Model

Discussion:

B. Sivertsen: Have you tried another rise formulation to determine the effect upon results?

R. F. Lee: No.

B. Sivertsen: Would you expect the meteorological data to be representative?

R. F. Lee: The data that was available was used. In some cases it may not be representative.

H. van Dop: Have you determined correlations of the calculated and measured concentrations?

R. F. Lee: No, we would not expect the correlations to be very good due to the inability of predicting the direction of the transport wind at plume level.

W. B. Johnson: The field of concentrations for various individual periods would be interesting. What stability classification was used?

R. F. Lee: Basically that of Pasquill.

W. B. Johnson: Do you know why there are few sampling stations to the east of the plants?

R. F. Lee: I do not know. The stations presumably were located considering the wind frequencies.
Some work has been done by making calculations after rotating the wind directions.
Also, there seems to be some systematic changes of the validation with distance from the source.

6th NATO/CCMS
International Technical Meeting
on Air Pollution Modeling

SENSITIVITY ANALYSIS OF PARAMETERS EFFECTING THE RESULTS OF GAUSSIAN MODELS

by

Jürgen K. Strott and W. Christ
Battelle-Institut e.V.
Frankfurt/Main

BATTELLE - INSTITUT E.V., Frankfurt/Main
Germany, FR

24 - 26 September, 1975

1. Introduction

In the Federal Republic industrial facilities are subject to licensing. For the approval process it is necessary to pre-calculate the immissions that will be caused by the facilities under consideration. As these calculations have legal consequences, they have to be as exact as possible. On the other hand, for economic reasons, the model must be as simple as possible. These two requirements, high accuracy and cheapness, i.e. a fast running computer model, are contradictory. To solve this problem it is absolutely necessary to understand the sensitivity of a model's output to its input.

Stimulated by a paper of S.T. Thayer and R.C. Koch we investigated the influence of source location dependent vertical diffusion parameters σ_z and different subdivisions of the wind rose.

2. Model Description

The influence of a source location dependent vertical diffusion parameter σ_z was tested with a modified version of the AQDM model (cf. /4/):

- the area source simulation was left as it was originally, namely simulation by an upwind located virtual point source,
- the plume rise is simulated by the formula of Briggs instead of the originally used one of Holland/Stümke,

- six stability categories are allowed (stability classes by Klug were used),
- mixing heights from stable to unstable were used as: 0, 0, 1200, 1500, 1800, 1800 m.

In addition to this, the model was modified in such a way that for every source (point or area source) and for every wind direction three different sets of σ_z may be used for three pre-defined height classes (in our case 0 - 200 m, 200 - 400 m, and over 400 m). Thus, depending on the source location, different dispersion conditions in the three height classes and in every wind direction from the view of the source may be considered.

For testing the influence of different subdivisions of the wind rose (e.g. using 36 instead of 16 directions), the CDM model was modified in such a way that it allows an arbitrary number of wind directions. For testing the above described model modifications, we used the input data set of the "Test City" of the AQDM model /7/ in order to save computer time.

3. Effect of Source Location Dependent Diffusion Parameters

Two calculations were compared, one using the same set of σ_z for all directions and all heights and one using different sets of σ_z. Figure 1 shows the source distribution and the σ_z-roses used.

The following three different sets of σ_z were applied:

- for effective source heights over 200 m we used modified Pasquill parameters (relevant mainly for source No. 1),
- for wind directions carrying the pollutants towards the city σ_z-values were applied which are used by the TÜV Rhineland /2/ for source heights less than 50 m and distances farther than 600 m from the source,
- for wind directions carrying pollutants towards the open country σ_z-values by Klug (cf. /4/) were used.

Table 1 shows values for these three parameter sets for four different distances and three stabilities. The three parameter sets are extremely different, but the differences between the different sets are by far not as large as the differences between the different stabilities within the sets.

The 21 sources of Test City were classified in six groups as may be seen from figure 1 using six different σ_z-roses.

In the second run the modified Pasquill parameter set was used for all directions and height classes. Figure 3 shows isopleths of the annual mean of the SO_2 concentrations for Test City.

The astonishing result was that for both runs the distribution of annual means brought only slight differences. Figure 4 shows isopleths of the differences between the two runs in percentage of the second run.

Using different σ_z-values we calculated in the center of the city at most 8 % less ground level concentration and upwind the main wind direction (cf. figure 2) at most 6% higher concentrations compared to the run using the modified Pasquill parameter set alone.

It should be noticed that this result is no contradiction to the results of Thayer and Koch. They found that the stability class and the corresponding σ_z are of important influence on the calculated ground level concentration, while our results indicate that the different σ_z functions used are of minor importance. This is confirmed, too, by the values of table 1.

4. Influence of the Number of Wind Directions of the Wind Rose

For testing the influence of the number of wind directions we used the same set of emission data as above but the wind rose of Frankfurt (cf. figure 5). The Frankfurt wind rose has two predominant wind directions, which are nearly opposite. Moreover, the wind rose has nearly exactly the same shape for all stability categories. Thus, if there exists an influence of the number of the wind directions on the results of ground level concentrations, it must be clearly seen by such a wind frequency distribution. Figures 6 and 7 show the results of the two calculations using first 16 and then 36 wind directions. A comparison of the two figures shows clearly a change of the main direction of the isopleths.

The CDM model allows a distinction between concentrations coming from point and area sources. From this splitting we know that concentrations coming from area sources differed in both calculations less than 10 %, while those coming from point sources differed about 30 %. As emissions from point sources sum up to over 80 % for Test City, the differences in figures 6 and 7 are mainly due to the effects of the point sources.

Table 1: Values of Diffusion Function $\sigma_z = a \cdot x^b$

Stability	500 m	1000 m	5000 m	10000 m	
stable	30	45	117	176	
neutral	46	81	302	533	a)
unstable	273	664	5211	12655	
stable	6	8	19	26	
neutral	13	21	68	113	b)
unstable	90 (41)	234 (83)	2162 (430)	5629 (873)	
stable	8	12	35	56	
neutral	22	38	129	218	c)
unstable	75	140	596	1110	

a) Dispersion Parameters for City Centers /2/

b) Dispersion Parameters of Klug,
values in () are for stability class IV

c) Modified Pasquill Parameters

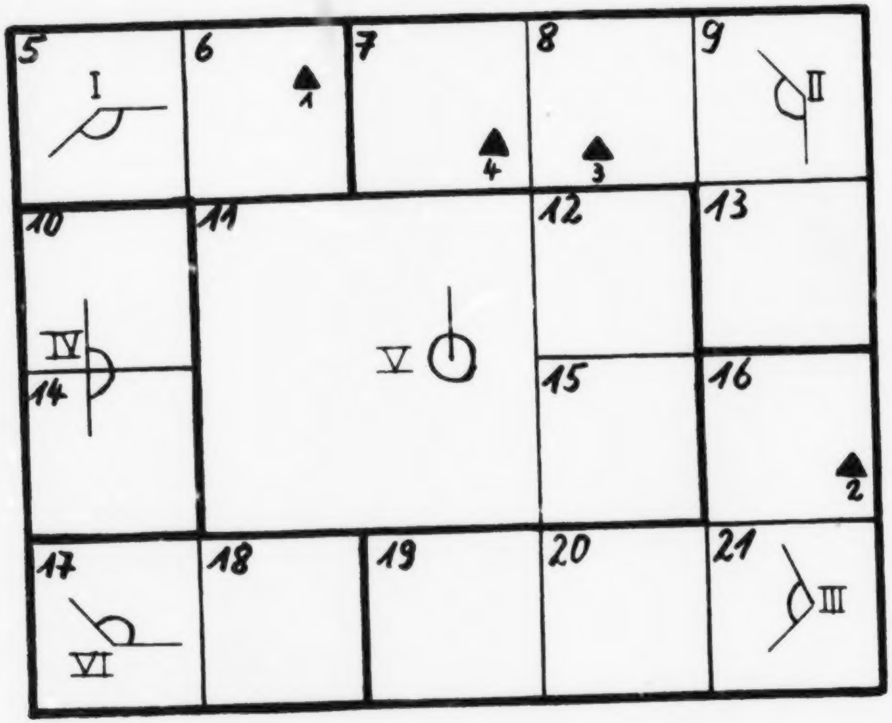

Figure 1: Source Distribution and σ_z-Roses

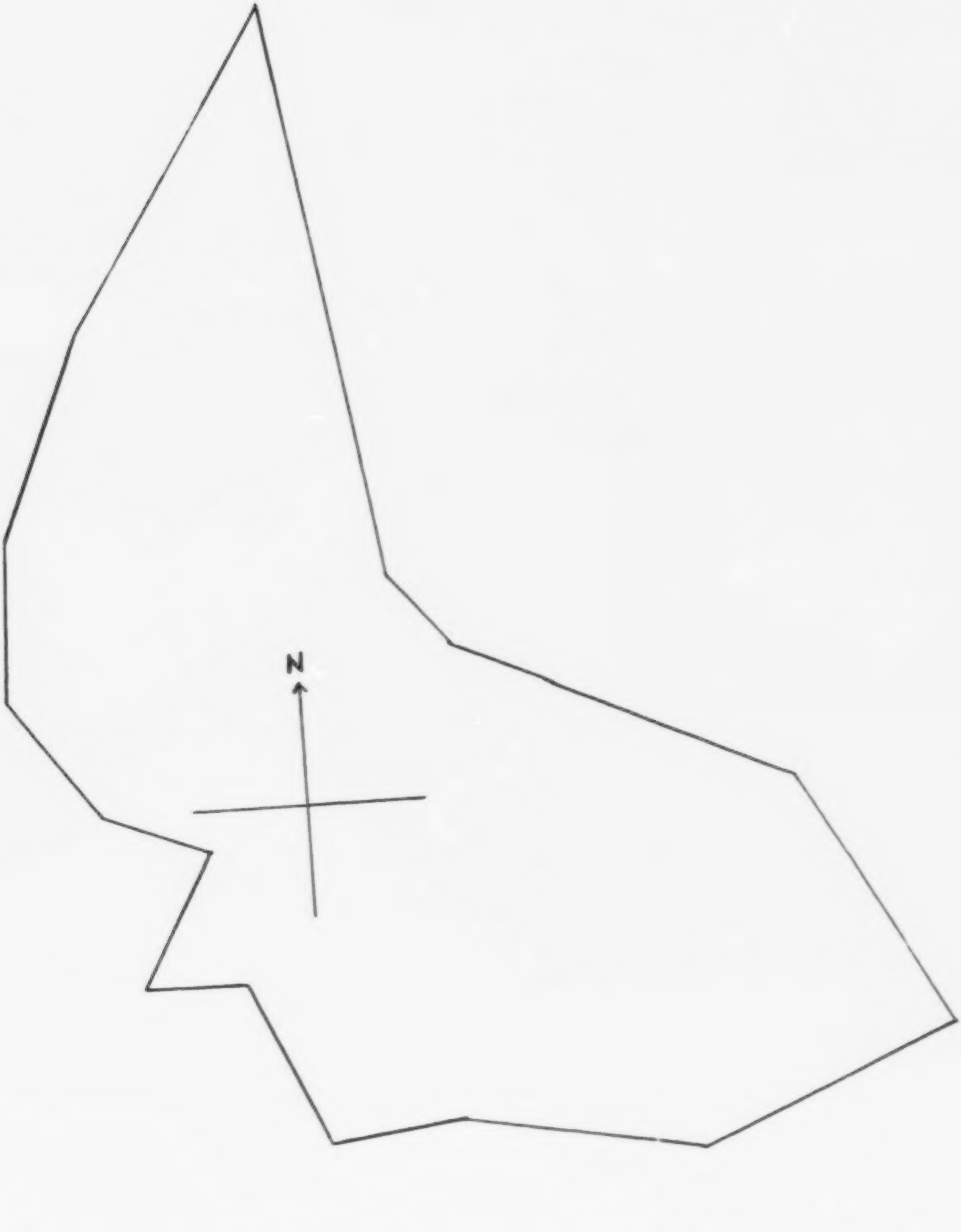

Figure 2: Wind Rose for Test City, 16 Wind Directions

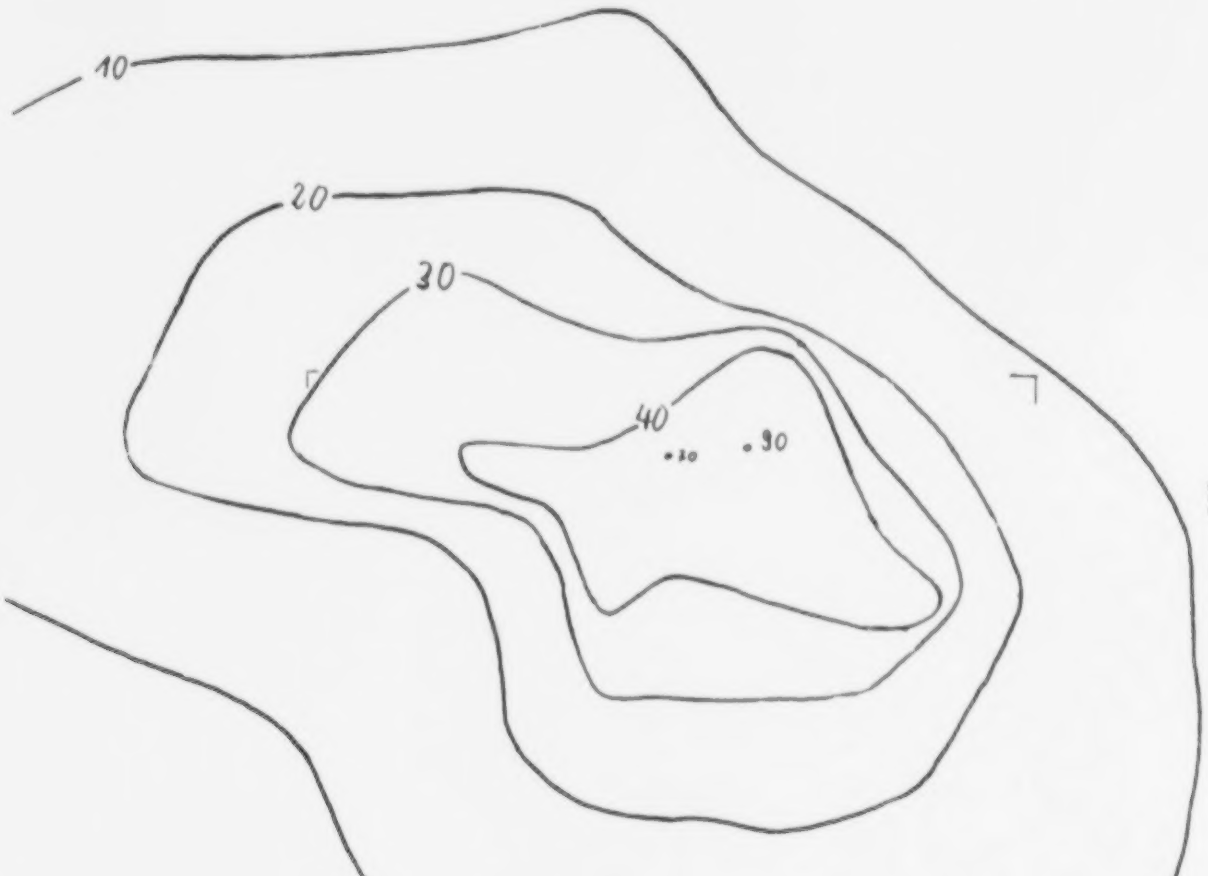

Figure 3: Isopleths of Annual Mean Concentrations of SO_2 ($\mu g/m^3$) Calculated with AQDM

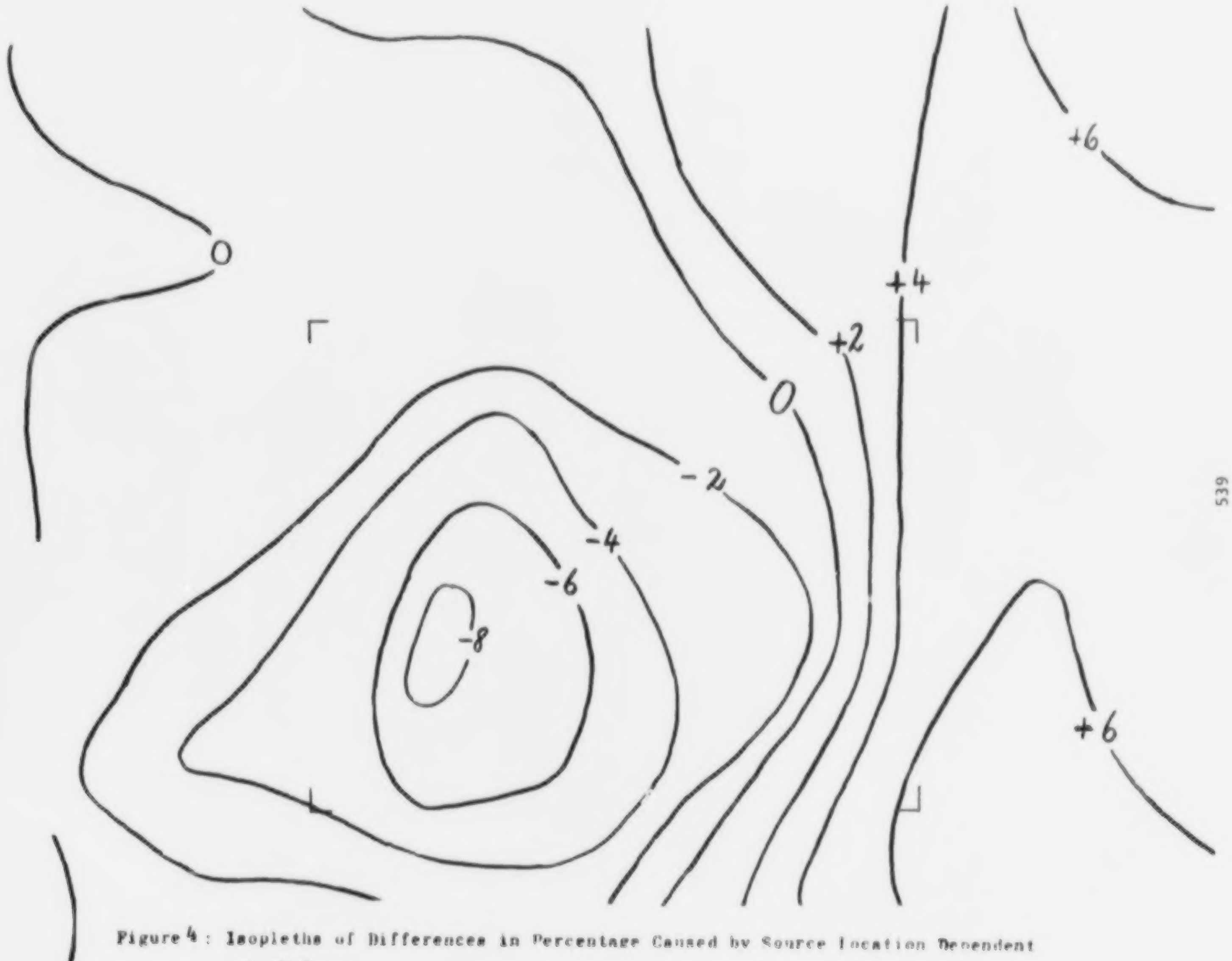

Figure 4 : Isopleths of Differences in Percentage Caused by Source Location Dependent σ_z-Values

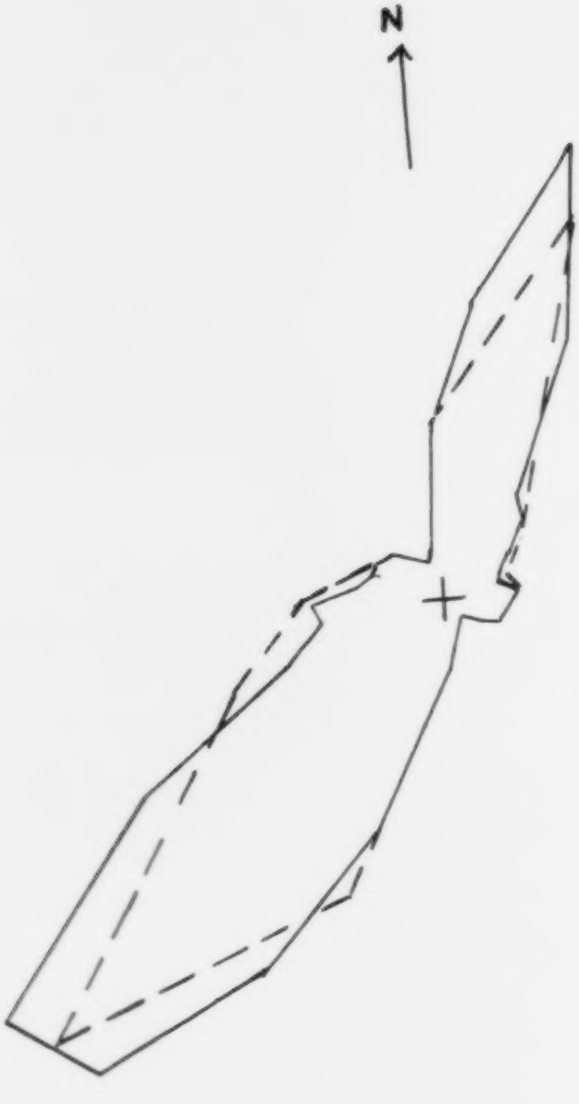

Figure 5: Frankfurt Wind Rose:

—— 36 Wind Directions

- - - 16 Wind Directions

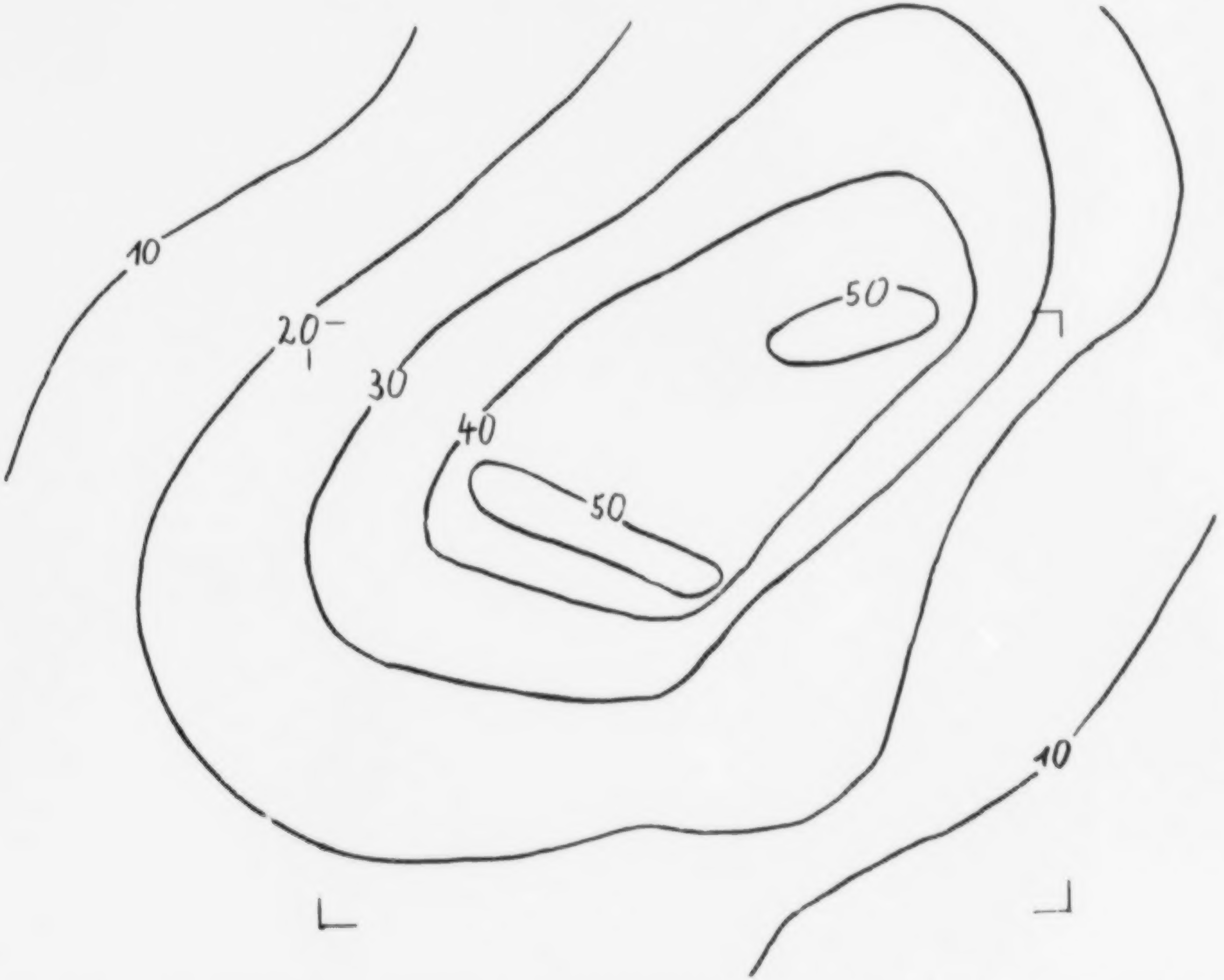

Figure 6: Isopleths of Annual Mean Concentrations of SO_2 ($\mu g/m^3$), Calculated with CDM Using 16 Wind Directions

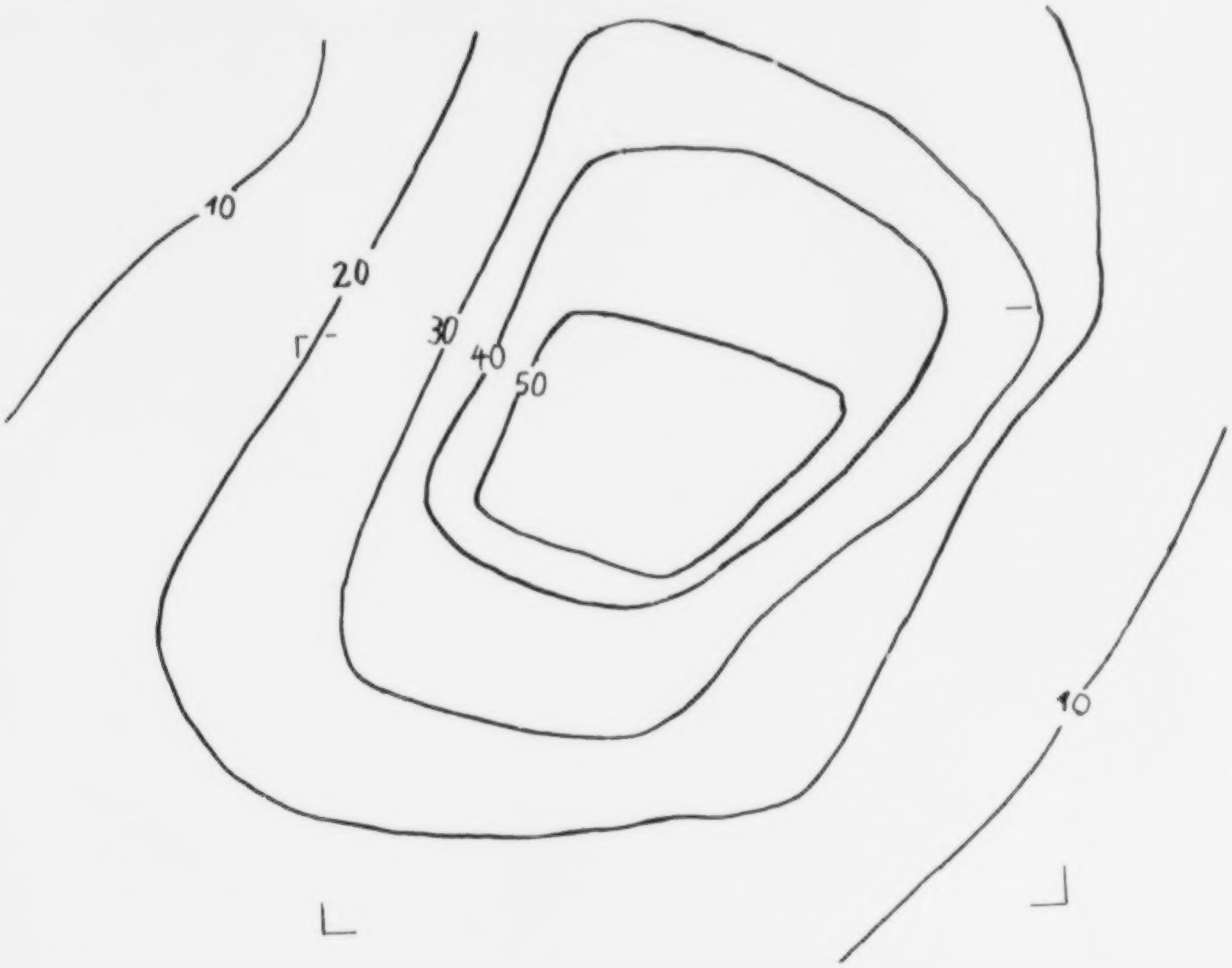

Figure 7: Isopleths of Annual Mean Concentrations of SO_2 (ug/m^3), Calculated with CDM Using 36 Wind Directions

References

/1/ K.L. Calder
A Climatological Model for Multiple Source Urban Air Pollution.
Nat. Air Pollution Control Administration, Division of Meteorology, Raleigh, North Carolina, Sept. 1970

/2/ L. Kropp
Grundlagen der Ausbreitungsrechnung in Immissionsprognose für luftverunreinigende Stoffe, Köln, 1975
Verlag TÜV Rheinland GmbH

/3/ Lufthygienisch-meteorologische Modelluntersuchung in der Region Untermain.
5. Arbeitsbericht, Juni 1974
Regionale Planungsgemeinschaft Untermain

/4/ J.K. Strott, A. Braig, K. Michelmann
Vergleich von Rechenmodellen zur Ausbreitungsrechnung Parts 1 and 2.
Bericht für das Bundesministerium des Innern.
Battelle-Institut e.V., Juni 1974

/5/ S.D. Thayer and R.C. Koch
Sensitivity Analysis of the Multiple-Source Gaussian Plume Urban Diffusion Model,
Conference on Urban Environment and 2nd Conference on Biometeorology, October 31 - November 2, 1972, Philadelphia, Pennsylvania,
reprinted in Proceedings of the 5th Meeting of the Expert Panel on Air Pollution Modeling No. 35

/6/ J.A. Tikvart and D.O. Martin
A General Atmospheric Diffusion Model for Estimating
the Effects of One or More Sources on Air Quality,
Annual Meeting of the Air Pollution Control Association,
June 1968

/7/ TRW Systems Group
Air Quality Display Model (1969)
Contract No. PH 22-68 60 USDHEW
Public Health Service, NAPCA, Washington, D.C.

6th NATO/CCMS

International Technical Meeting
on Air pollution Modeling and its Application

Urban Air Modeling Support

by

K. H. Müller

EURATOM/ Ispra

BATTELLE - INSTITUT E. V. Frankfurt/Main
Federal Republic of Germany
24 - 26 September, 1975

A series of about 50 tracer experiments in city-scale is planned for the period 1976-77 at two differently structured places: Frankfurt /Main and Venice. All these experiments will be performed as a collaboration between different research institutes and local authorities. Frankfurt /M. (Deutscher Wetterdienst, EURATOM, Freie Universität Berlin, local regional and Federal authorities), Venice (CNR, EURATOM, IBM Venezia, local authorities).

Air samples will be drawn (time series) partly on ground level (about 50 - 100 sampling stations with about 10 sequential air samples each), partly via airplane-sampling.

The experiments mainly aim

- to build-up a dispersion data base useful for dispersion parameter determination
- to construct empirical transfer functions which are considered to be reference distributants useful for checking analytical dispersion formulas
- to study the dependence of the transfer functions upon the source position
- to find out a suitable parametrization for surface roughness
- to check the usual classification of meteorological parameters relevant to pollutant dispersion, comparing the concentrations of similar experiments to be performed in Frankfurt and Venice under equal classified meteorological situations.

Rapporteur's Report, Topic III (continued) September 25, 1975

by F. B. Smith

Chairman: W. B. Johnson

J. Strott: Sensitivity Analysis of Parameters effecting the Results of Gaussian Models

Discussion:

W. B. Johnson opened the discussion by asking if it would be fair to summarize the conclusions of the paper by saying that the effects of wind direction errors were more important, in the author's experiment, than the effects of errors in others; to which the speaker agreed.

F. B. Smith asked if this conclusion were not rather heavily dependent on the strongly directional nature of the wind rose used.

J. Strott replied that had a more symmetric wind rose been used, such as that applicable to Bremen, then the effect would not have been so great.

B. Turner enquired whether or not the three σ_z systems quoted had been used separately, to which the author replied that two types of calculation had been made. In the first, the schemes of Klug and Pasquill had been used separately, whereas in the second these schemes had been applied together at different distances for Cologne (Köln).

K. H. Müller /H. Fortak:
Urban Air Modeling Support

Discussion:

After H. Fortak had delivered his description of plans for monitoring pollution over Frankfurt in windless or light wind conditions the Chairman, W. B. Johnson, asked if the main point was to study pollution in light wind situations trapped below elevated inversions.

H. Fortak agreed and added that they were also interested in how theses inversions were broken up, for example by cooling tower plumes.

K. H. Müller then continued the presentation by discussing the type of tracers to be used. Afterwards
K. E. Grønskei enquired as to the nature and variety of meteorological situations to be studied.

H. Fortak said "dangerous situations"!

W. B. Johnson suggested that Freon 12 should be considered as a tracer. Syringe samples suitable for analysis could be collected rapidly by an aircraft, at least 100 such samples were quite feasible, and these could be analysed subsequently by gas chromatography.

K. H. Müller thought it was better to get an on-line real time picture of concetrations not provided by Freon 12.

H. Fortak emphasised that measurements made from aircraft within the mixing layer are easier to interprete than ground level measurements.

6th NATO/CCMS
International Technical Meeting
on Air Pollution Modeling

TOPIC IV

REGIONAL AND INTERREGIONAL DISPERSION MODELS

Battelle - Institut e. V. Frankfurt / M
Germany, FR

24 - 26 September, 1975

6th NATO/CCMS
International Technical Meeting
on Air Pollution Modeling

FEASIBILITY DEMONSTRATION OF AN AIR-BUDGET MODEL FOR THE ASSESSMENT OF TRANSFRONTIER AIR POLLUTION

by

Warren B. Johnson
Daniel E. Wolf
Robert L. Mancuso

Stanford Research Institute
Menlo Park, California, USA

BATTELLE-INSTITUT E.V., Frankfurt/Main
Germany, FR

24-26 September, 1975

Preceding page blank

ABSTRACT

This brief investigation into the feasibility of using an air quality budget concept as the basis for an international air quality management plan in Europe has focussed upon the technical aspects of the problem. A simplified, preliminary version of an air quality budget model has been developed for the Federal Republic of Germany (FRG) that is capable of calculating monthly and annual averages of multinational trans-border fluxes of SO_2, as well as amounts removed by dry and wet deposition processes within individual counties. We have chosen SO_2 for this work because it is the major pollutant in Europe.

For demonstration purposes, the preliminary air budget model has been run with a full year of meteorological and emissions data for 1970, but only for the FRG because of the lack of availability of data for other countries. Among other results, the demonstration calculations gave the following estimates:

- A total of approximately 2,900 kilotons of sulfur compounds* were exported to other countries from the FRG during 1970, distributed as follows:

Austria	12.0%
Czechoslovakia	11.5%
German Democratic Republic	40.0%
Denmark/Baltic Sea	5.9%
North Sea	4.2%
The Netherlands	11.6%
Belgium/Luxembourg	7.0%
France	6.3%
Switzerland	1.5%

---

* In terms of equivalent weight of SO_2.

- Removal processes caused about 675 kilotons of sulfur compounds to be deposited within the FRG from FRG emissions during 1970, 425 kilotons from dry processes, and 250 kilotons from wet processes.

These results from the preliminary model should be considered as rough estimates only. However, the values are reasonable, and the fact that the model is economical to use encourages its application to a wider area of Europe as a feasible next step. When additional emissions data become available for the countries surrounding the FRG, the model could be used to calculate the pollutant imports to, as well as the exports from, the FRG and other European countries.

The availability of a refined operational version of this model should be a significant asset in securing international interest and cooperation in implementing an international air quality management plan.

I INTRODUCTION

A. Nature of the Problem

Air quality management on a national basis is more difficult because of the inability to control pollution "background" concentrations in the air entering the country from upwind.

Certain air pollution control techniques that are beneficial to the nation implementing them may be harmful to neighboring nations downwind. For example, intermittent emission releases from tall stacks during favorable meteorological conditions can be used, taking advantage of atmospheric dispersion in reducing local pollutant concentrations. However, this type of air quality control is of no help to neighboring countries downwind, since the total atmospheric pollutant loading is the same regardless of source height.* Thus, a nation that increases its industrial emissions, but maintains its own air quality at constant levels by releasing the pollutants at greater heights or under more favorable dispersion conditions, will cause the air quality of neighboring nations to deteriorate.

This action violates Principle 21 of the UN Stockholm Conference on the Environment, which states that no nation shall improve its environment at the expense of other nations. Yet at present there is no effective means of preventing this action or of even knowing when it occurs.

---

*In actuality, concentrations far downwind will probably increase as the source height increases, because of the smaller amount of pollutant removal from the higher plume during transport.

B. Related Studies

For several years, air pollution studies have been carried out on an international cooperative basis by the NATO Committee on the Challenges of Modern Society (CCMS). However, almost all of these studies have been concerned with urban air pollution.

The study most relevant to the air quality budget concept is the cooperative OECD program, "Long Range Transport of Air Pollutants," led by the Norwegian Institute for Air Research. This major study involves ten participating countries, extensive field experiments, and several types of transport and diffusion models. This program is research oriented, with emphasis on detailed case studies. A significant development has been the 1972 SO_2 emissions inventory on a 127 × 127 km grid covering Central and Northern Europe. Work is in progress to change the grid to $1/2^{\circ}$ latitude by 1° longitude.

C. Objective

The goal of the air quality budget study is to determine the feasibility of developing a practical and objective method for planning and managing air quality on an international basis. A key element of this method would be an air quality budget for each participating nation, which would involve keeping track of the pollutant "import and export," or trans-border flux, across national boundaries.

This overall goal has been translated into two specific objectives for this project:

- To develop, for demonstration, a simplified air pollution transport model to calculate trans-border fluxes (exports) of sulfur compounds for the Federal Republic of Germany (FRG).

- To develop a scenario or conceptual plan by which a refined version of this model might be applied for air quality budget management and control on an international basis.

Our progress in achieving these objectives is described in subsequent sections.

II DESCRIPTION OF THE DEMONSTRATION MODEL

A. General Rationale and Design Goals

Although development of an optimum model for calculating trans-border pollutant flux was beyond the scope of this study, we felt that a detailed investigation into possible modeling approaches was necessary to determine their feasibility. This investigation revealed a promising modeling approach. To demonstrate the feasibility of this approach, we have developed a simplified version of the model, which is being applied to the FRG.

Major features needed in a model for the FRG application (see Figure 1) are:

- The model must be capable of both assessing current conditions and predicting conditions at some future time.
- The model must be capable of calculating annual averages of trans-border pollutant fluxes as a function of location around the border.
- Because of the need to operate on a year's worth of meteorological data to calculate annual averages, the model must be kept as simple as possible to minimize computer costs.
- Pollutant removal through both wet and dry deposition will be significant and must be included to calculate realistic trans-border pollutant fluxes.
- Pollutant transport is more important than pollutant diffusion for this application and should therefore be given priority.
- Pollutant diffusion can be treated in a simplified manner since computation of concentration fields is not required for this application.
- Pollutant emissions should be considered as variable in both time and space for best accuracy, but as a first approximation can be considered variable only in space.

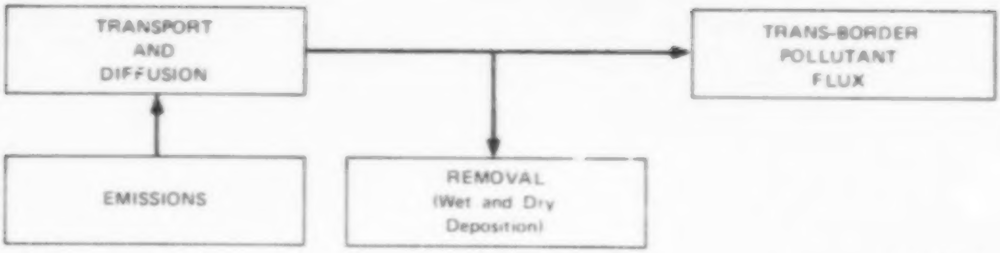

SA-3038-4

FIGURE 1 PRINCIPAL ELEMENTS OF THE AIR BUDGET MODEL

These design criteria have been retained in the demonstration model; however, for expediency, various simplifying assumptions have been incorporated in this initial version of the model. These assumptions and limitations are discussed below.

B. Treatment of Pollutant Emissions

The SO_2 emissions inventory for the FRG for the year 1970 as prepared by NUKEM (1971) has been used as input to the model. As illustrated in Figure 2, the total emissions are divided into area-source cells that are 0.5° in latitude by 1° in longitude, or approximately 55 km N-S by 70 km E-W.

For each of these cells, the annual-average emissions are divided into discrete 12-hour-average emission increments, or "puffs," which are released at 12-hour intervals and tracked at three-hour time steps by the model until they move outside the national boundary. The reason for selecting the 12-hour intervals is that these intervals correspond to the frequency at which synoptic upper-air wind observations are available. Thus, during the course of a year, 730 puffs are tracked for each of the 74 cells, giving a total of 54,020 puffs that are tracked by the model.

C. Treatment of Pollutant Transport

The individual puffs are transported according to the current wind field, as interpolated from the available upper-air wind observations at 850 mb (approximately 1500 m above sea level) for the year 1970. Although it is recognized that significant vertical wind shears occur between the surface and the 1500-m level, especially in winter and at night, we feel that the use of 1500-m winds will demonstrate the technique. Averaging of the available wind observations in the layer between the surface and

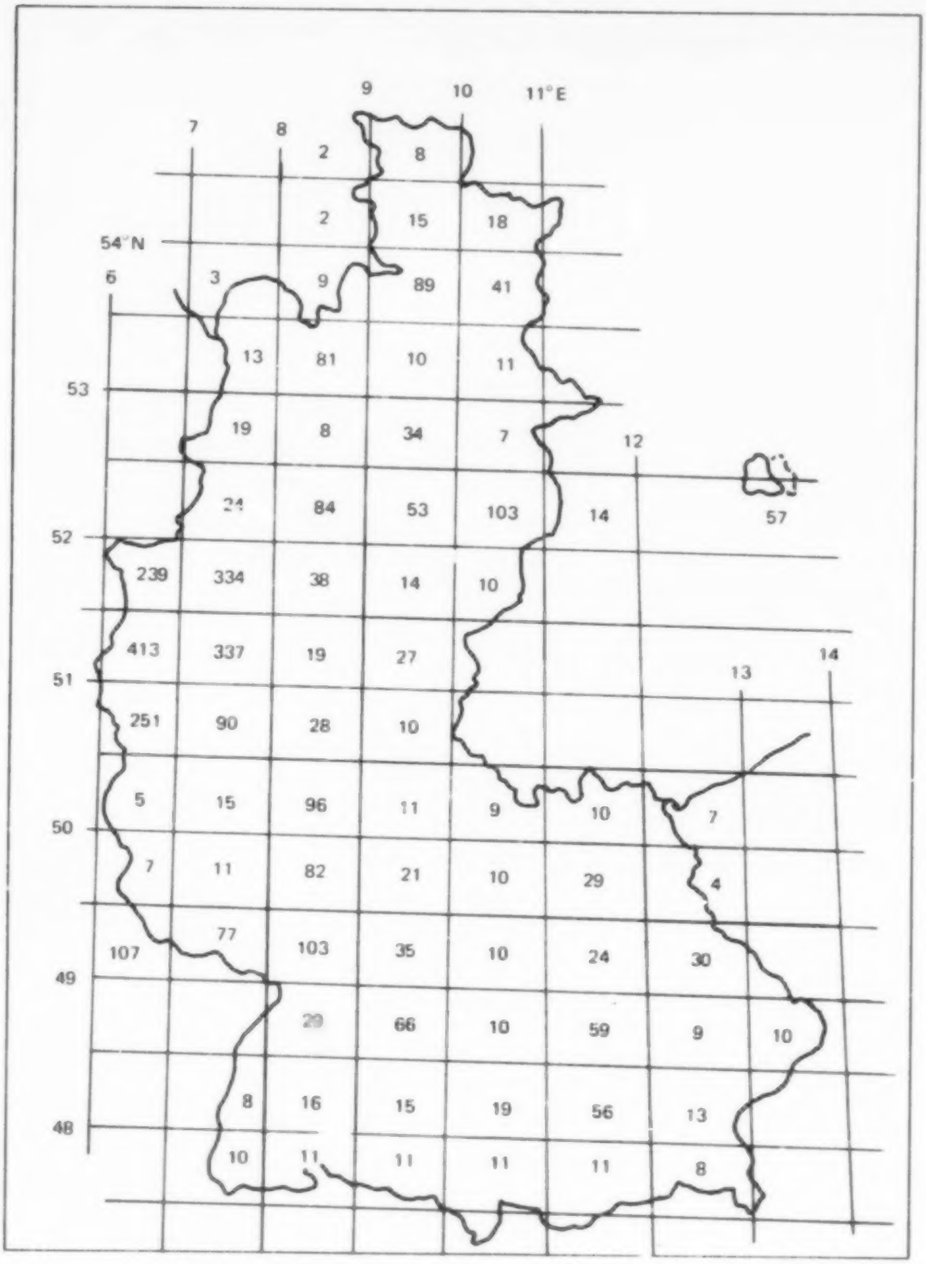

SA-3038-5

FIGURE 2 TOTAL SO_2 EMISSIONS (KILOTONS) IN THE FRG DURING 1970 (GRAND TOTAL, 3.6×10^6 TONS) SOURCE: NUKEM (1971)

1500 m would result in a more realistic simulation. This refinement can be incorporated at a later date.

The upper-air sounding stations used in this analysis are listed in Table 1 and are plotted in Figure 3.

D. Treatment of Pollutant Diffusion

Since the model is not a typical diffusion model in the usual sense of its being used to calculate concentration fields, a simplified treatment of diffusion is possible. As previously mentioned, each SO_2 emissions puff represents an area source of approximately 55 km × 70 km. In the model, the puff is considered to immediately diffuse vertically to give a uniform concentration in the layer between the surface and the 1500-m level. The initial lateral extent of the puff is approximated by a cylinder or disk that is 60 km in diameter. Fickian diffusion is then assumed during the transport of the puff, giving an increase in lateral area proportional to time at a rate K (the lateral eddy diffusivity) of 10^8 cm^2 sec^{-1}, or 36 km^2 hr^{-1}. Thus, we have

$$\begin{aligned} r^2(t) &= r^2(t_o) + Kt \\ &= (30\ km)^2 + (36\ km^2\ hr^{-1})t \quad , \end{aligned}$$

where

r = puff radius

t = time

t_o = initial time

K = lateral eddy diffusivity.

Although more sophisticated diffusion formulas could readily be used, this simplified treatment should be satisfactory for determining the areas

Table 1

LIST OF METEOROLOGICAL STATIONS FOR WHICH
1970 DATA WERE USED FOR INPUT TO THE MODEL

Station Number and Name	Data Type	Latitude	Longitude
1. Wien	Wind (850 mb)	48.25°N	16.37°E
2. München		48.13	11.72
3. Stuttgart		48.83	9.20
4. Idar/Oberstein		49.70	7.33
5. Wahnsdorf		51.12	13.68
6. Essen		51.40	6.97
7. Hannover		52.45	9.72
8. Emden-Wolthusen		53.37	7.22
9. Griefswold		54.10	13.38
10. Schleswig		54.53	9.55
11. Payerne		46.82	6.95
12. St. Hubert		50.03	5.40
13. Helgoland	Precipitation	54.18	7.90
14. Schleswig		54.53	9.55
15. Cuxhaven		53.87	8.72
16. Griefswold		54.10	13.45
17. Bremen		53.05	8.78
18. Lüchow		52.97	11.18
19. Münster		51.97	7.60
20. Gütersloh		51.93	8.33
21. Bad Salzuflen		52.10	8.73
22. Hannover		52.46	9.70
23. Berlin		52.46	13.30
24. Göttingen		51.55	9.95
25. Leipzig		51.42	12.23
26. Köln		50.86	7.13
27. Frankfurt		50.05	8.58
28. Nürnberg		49.50	11.08
29. Freiburg		48.00	7.85
30. München		48.13	11.72

affected by precipitation scavenging (wet deposition) and dry deposition, and of the border length covered by the pollutant as it moves across the national boundary.

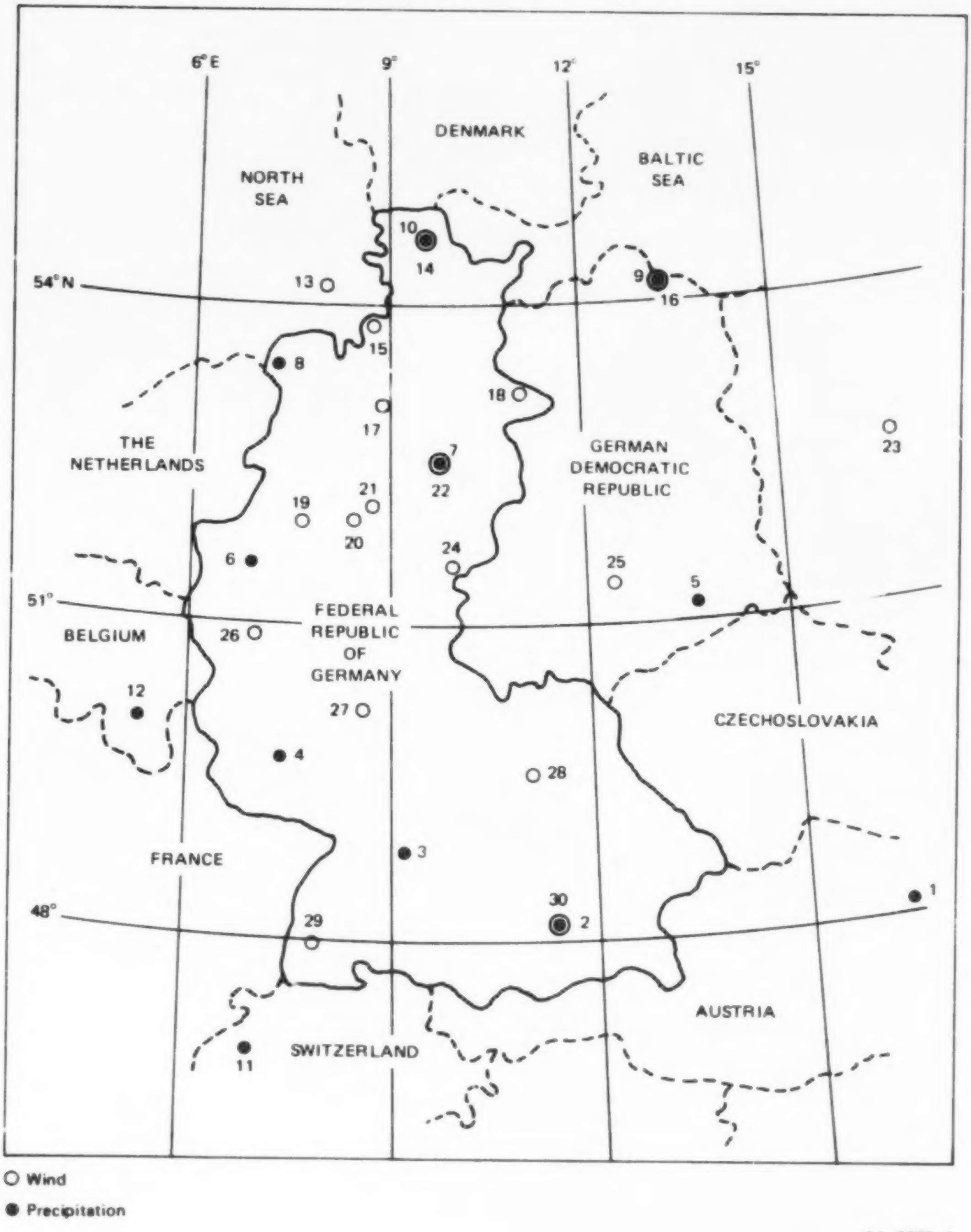

○ Wind

● Precipitation

SA-3038-6

FIGURE 3 LOCATIONS OF METEOROLOGICAL STATIONS FOR WHICH 1970 DATA WERE USED

E. Treatment of Pollutant Removal

The conversion of SO_2 to sulfate aerosol and other compounds, and the subsequent removal of these sulfur compounds from the air by means of cloud droplets (rainout), falling precipitation (washout), and vegetation and soil uptake and other chemical reactions at the surface (dry deposition) together constitute one of the most complex problem areas in the field of air pollution. Recognizing that SO_2 removal is particularly significant over the relatively long transport distances involved in our study, we have attempted to include these effects in the model in a simplified, but hopefully realistic, manner. However, determining the best way to model these removal processes is not a straightforward task, since the current state of knowledge is far from complete, and new results tend to emphasize the large number of variables that enter into the problem.

As an example, studies by Weber (1970a, 1970b, 1971) and Gartrell (1964) show that the half-life of SO_2 in urban areas or near large sources may be as short as 20 or 30 min under certain conditions, while others have estimated SO_2 half-lives to be as long as a week. These results indicate that SO_2 residence time is at least a function of concentration, meteorological conditions (humidity, clouds, rain, fog), and the presence of catalysts and other compounds, such as ammonia (Weber, 1971).

1. Wet Deposition

For the purpose of calculating the SO_2/sulfate removal by wet deposition, daily total precipitation observations during 1970 at a total of 18 stations are input to the model. These stations are listed in Table 1 and their locations are plotted on Figure 3. Interpolated precipitation values are used to calculate the SO_2 mass removed from each puff at each location on the grid during each three-hour time step.

The pollutant removal by wet deposition is calculated using the following conventional relationship:

$$\chi/\chi_o = \exp(-\Lambda R t)$$

where

χ = SO_2 concentration at time t

χ_o = initial SO_2 concentration

Λ = wet deposition rate

$[hr^{-1}(mm\ hr^{-1})^{-1}$, or $mm^{-1}]$

R = precipitation rate (mm hr^{-1} of water)

t = time during which precipitation occurred (hr).

A review of recent field and laboratory studies was conducted to find an appropriate value for the wet deposition rate, Λ. Some of the studies reviewed did not report results directly in the form of values of Λ, but these have been calculated on the basis of the information given. A summary of these results is given in Table 2.

Table 2

SUMMARY OF AVAILABLE DATA ON VALUES OF THE WET DEPOSITION RATE (Λ)

	Λ (mm^{-1})	
	Rain	Snow
Hales et al. (1970)	7.2×10^{-2}	1.4×10^{-3}
Summers and Hitchon (1973)	1.8	1.6×10^{-1}
Bielke and Georgii (1968)	0.9 to 2.8*	---

*Depending upon droplet size.

A wide range of values is indicated, with the values of Hales et al. (1970) considerably lower than the others. However, the values from Summers and Hitchon (1973) may well be overestimates, since they apply principally to convective rains. The laboratory (rain chamber) results of Bielke and Georgii (1968) might also be high, in view of the rather high pollutant concentrations (800 $\mu g/m^3$) used in their experiments. On the other hand, the latter data could be underestimates of the total wet deposition rate, since they do not include rainout effects, while Summers and Hitchon indicate that their results represent mainly rainout processes.

For lack of better estimates, we have used the following values for our initial model runs:

	Λ (mm^{-1})
Summer	1.0
Winter	0.1
Spring and Fall	0.5

The low winter value reflects the nonconvective nature of much of the precipitation, and the fact that some of the precipitation will be in the form of snow. The deposition coefficient could be made dependent upon precipitation type, rather than season. This is a refinement that can be easily incorporated at a later date.

The computer program keeps track of each puff's location and duration of exposure to the variable precipitation intensity, calculates the pollutant mass removed during each time step, and assigns this amount to the appropriate cell (location) in the computation grid.

2. Dry Deposition

To calculate the pollutant removal by dry deposition processes, we have used the relation,

$$Q/Q_0 = \exp(-\lambda t) \quad ,$$

which is essentially identical to the previous equation for wet deposition, except that λ represents the dry deposition rate in units of hr^{-1}. For an appropriate value of λ, we have resorted to estimates by Kellogg et al. (1972) that the average annual ratio of dry to wet deposition over the Northern Hemisphere is approximately 0.3. On the basis of an annual wet deposition rate of 0.5 mm^{-1} calculated from the average of the seasonal values used, and taking into account the annual average precipitation intensity in the FRG of about 750 mm yr^{-1}, we have arrived at an estimate of about 0.01 hr^{-1} for the value of the dry deposition rate.

In the model calculations, pollutant mass is removed at this rate from each puff at each time step and assigned to the appropriate cell in the grid corresponding to the location of each puff.

F. Calculation of Trans-Border Fluxes

As previously mentioned, the model tracks each puff as it moves about the grid in accordance with the observed winds, removes mass from the puff by wet deposition when precipitation areas are encountered and by dry deposition on a periodic basis at each time step, and calculates the position and lateral spread of the puff when it crosses the national boundary. To simplify matters, the national boundary or border of the FRG is approximated by a series of 23 linear segments as indicated in Figure 4. The pollutant mass crossing the border within each of these segments is accumulated for the year, permitting the evaluation of the annual spatial distribution of pollutant flux (or export) to neighboring countries.

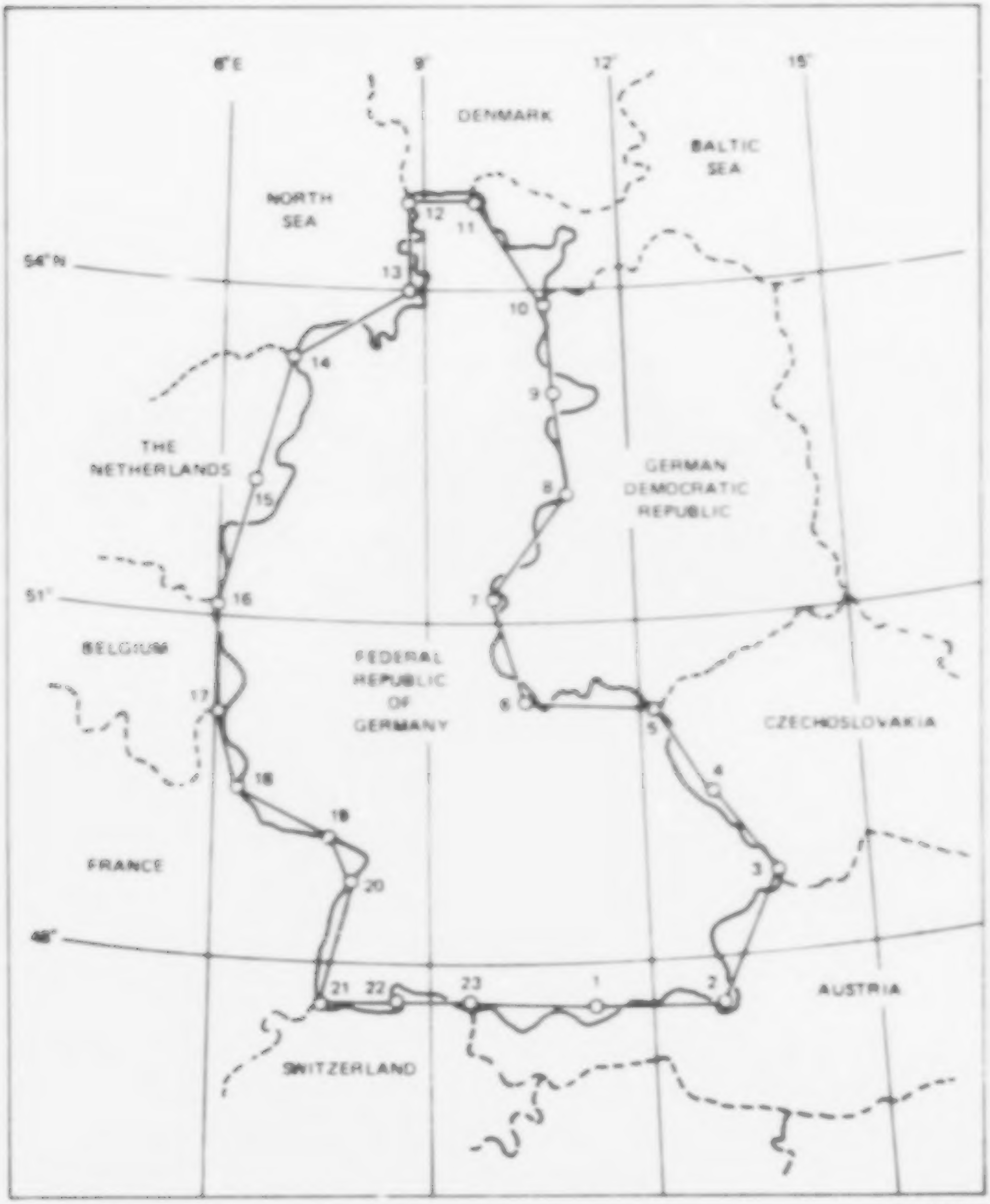

FIGURE 4 APPROXIMATION OF NATIONAL BOUNDARIES OF THE FRG BY MEANS OF LINEAR SEGMENTS

III RESULTS FROM PRELIMINARY MODEL CALCULATIONS

Using a full year of meteorological and SO_2 emission data for 1970 as previously discussed, we have conducted trial runs with the model to calculate monthly and annual averages of trans-border pollutant flux from the FRG, as well as spatial distributions of dry and wet pollutant deposition within the FRG. These results, as presented in this section and in the Appendix, generally speak for themselves. The discussion in this section is thus limited to a few remarks on the nature of the calculations and on the interpretation of the major features shown by the results.

A. Nature and Cost of the Calculations

Since meteorological data were reported only twice each day, 12 hours was used as the basic time interval for changing of the values of the input variables. The annual emissions for each grid cell were simply divided into 730 equal 12-hour values for this purpose. The calculations employed a 3-hour time step, which was chosen--after several trials--as the best compromise between computational accuracy achieved and computer time required.

The calculations were performed on a CDC-6400 computer, with graphics supplied by the CDC-280 system. The total computer run, including the monthly and annual calculations and all computer graphics and special printouts, required 28 minutes of central processor time, at a total cost of $191.00. A more sophisticated version of this model may tend to increase the computer time required, but this increase can be at least partially offset through increased computational efficiency.

B. Trans-Border Flux from the FRG

The monthly and annual distributions of the calculated trans-border pollutant flux are shown in Table 3. These results are also graphically presented in Figure 5 for the annual case, and in the Appendix (Figures A-1 to A-6) for the 12 monthly cases.

Table 3 indicates that East Germany (German Democratic Republic--GDR) received more than three times as much SO_2 sulfates from the FRG during 1970 as did any other country. This is because of the GDR's generally down-wind location (considering annual average winds) and its relatively long common border with the FRG. However, during certain months (such as January, May, and June), pollutant exports were more evenly distributed, and approximately the same amounts were received by the Netherlands and the GDR.

More detailed information on the calculated pollutant flux as a function of perimeter location around the 2400-km border of the FRG are presented in Figure 5 and Figures A-1 to A-6. The minimum values that appear consistently from month to month at border locations of 700, 1400, and 2300 km (counter-clockwise starting from the Bodensee) are caused by the special orientations of the border segments between points 5 and 6, 12 and 13, and 20 and 21, respectively (see Figure 4). The orientation of these segments is such that they are frequently parallel to the transport winds, which results in a small value of pollutant flux per unit length.

Clearly, if additional emissions data were available for the countries surrounding the FRG, the model could be used to calculate the pollutant imports to, as well as the exports from, the FRG and other European countries.

TABLE 1

MONTHLY AND ANNUAL BUDGETS OF SO_2/SULFATES* FOR THE FRG DURING 1970

COUNTRY	EXPORT OF SULFUR COMPOUNDS (KILOTONS)												
	JAN	FEB	MAR	APR	MAY	JUN	JUL	AUG	SEP	OCT	NOV	DEC	ANNUAL
AUSTRIA	18.0	30.0	31.5	16.5	43.1	22.0	28.0	13.9	21.3	35.3	19.0	32.6	345.7
CZECHOSLOVAKIA	21.3	35.6	32.1	42.0	21.0	12.1	31.3	18.8	25.1	30.6	31.5	15.1	330.9
GERMAN DEMOCRATIC REPUBLIC	29.0	107.6	93.1	129.3	40.2	58.3	132.3	28.3	115.0	93.7	132.3	78.0	1144.1
DENMARK-BALTIC SEA	26.0	9.2	13.3	2.1	4.2	11.3	16.9	16.0	30.3	11.5	10.2	5.2	168.3
NORTH SEA	11.7	6.2	14.0	[illegible]	13.0	11.2	6.2	13.0	1.6	3.3	5.7	2.9	128.4
NETHERLANDS	38.1	14.0	39.3	3.1	60.0	54.3	69.9	30.7	19.0	47.8	4.2	30.0	331.0
BELGIUM-LUXEMBOURG	22.4	21.8	13.4	9.0	21.3	29.4	3.1	18.8	11.1	13.0	3.3	11.6	198.3
FRANCE	1.8	20.6	13.1	2.0	15.1	39.0	3.5	9.3	23.1	18.3	3.1	11.7	170.9
SWITZERLAND	2.1	2.3	1.0	1.7	3.0	3.1	3.9	2.8	2.8	1.0	2.6	9.0	11.2
SUBTOTAL	233.0	239.8	213.3	236.0	232.9	231.4	233.2	[illegible]	332.2	239.9	239.9	206.0	2866.2
WET DEPOSITION IN FRG	7.4	5.8	12.0	10.9	38.1	39.3	11.7	43.2	28.4	25.3	23.0	3.6	212.3
DRY DEPOSITION IN FRG	37.8	23.1	33.5	31.6	26.8	12.3	38.3	33.2	38.1	30.9	29.3	22.3	321.3
TOTAL	300.1	273.0	306.1	300.4	300.1	[illegible]	300.1	[illegible]	396.2	300.1	296.4	300.1	3333.2
TOTAL EMISSIONS	300.1	273.0	300.5	296.1	310.1	[illegible]	[illegible]	[illegible]	398.2	300.1	296.1	300.4	3333.0

*In terms of equivalent weight of SO_2.

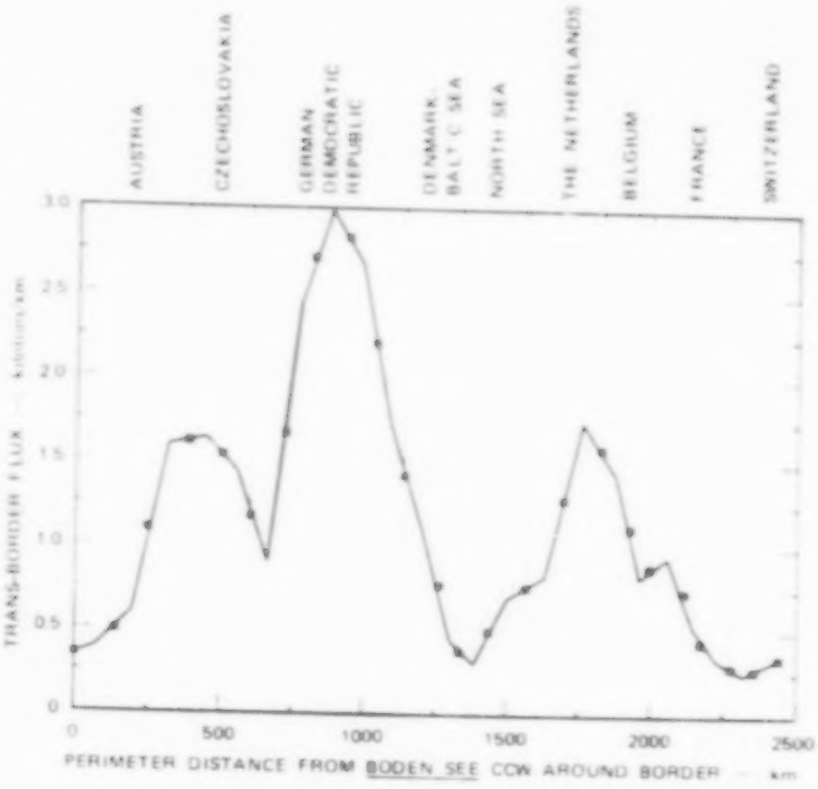

FIGURE 5 TOTAL TRANS-BORDER SO_2/SULFATE FLUX FROM THE FRG DURING 1970 AS A FUNCTION OF BORDER LOCATION (VALUES REFER TO EQUIVALENT WEIGHT OF SO_2)

C. Dry Deposition

Table 3 lists the monthly and annual totals for both dry and wet deposition.

Figure 6 and Figures A-7(a) to A-18(a) illustrate the annual and monthly dry pollutant deposition distributions calculated by the model for 1970. As would be expected, the dry deposition patterns show maxima over the Ruhr industrial area in association with the large emissions there. There are some changes associated with variations in the average wind speed and direction from month to month, but generally the patterns are fairly similar.

D. Wet Deposition

On an annual basis, the wet deposition distribution shown in Figure 7 is quite similar in shape to the dry deposition pattern (Figure 6). This similarity probably reflects the rather uniform annual precipitation received by the various portions of the FRG. However, the monthly patterns depicted in Figures A-7(b) to A-18(b) reveal considerable variation from month to month. This variation is especially noticeable when the results for winter and summer months are compared. It is also noteworthy that the calculations for several months show maxima that are not over the Ruhr area, because of spatial inhomogeneities in the monthly rainfall patterns.

It should be kept in mind, of course, that the calculated dry and wet deposition values are directly dependent upon the deposition rates adopted for the calculations. Since the latter are not known with much precision, the results from these calculations should be considered only as first approximations.

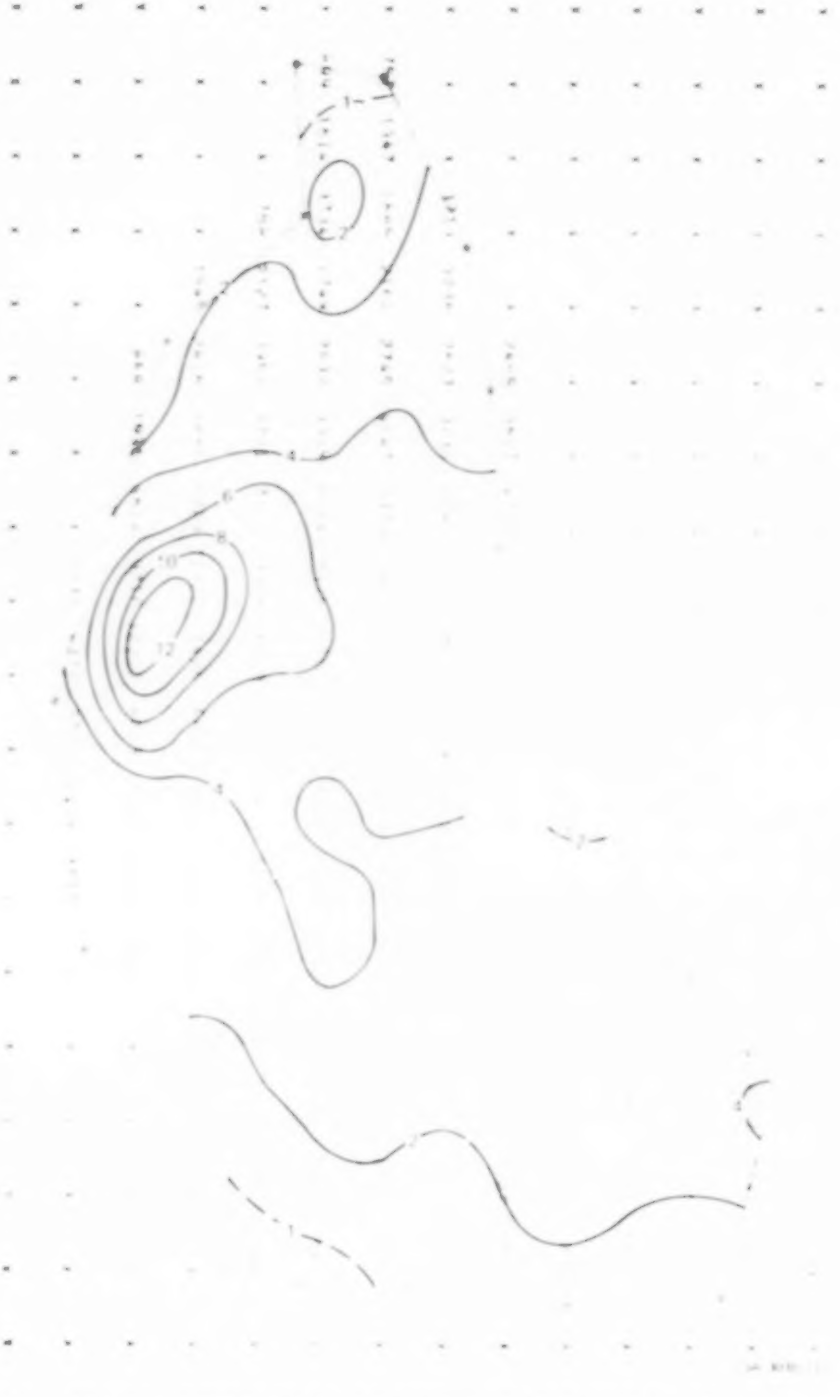

FIGURE 6 SPATIAL DISTRIBUTION OF TOTAL DRY DEPOSITION OF SO_2/SULFATES WITHIN THE FRG DURING 1970 (CONTOURS ARE LABELLED IN KILOTONS OF SO_2 EQUIVALENT WEIGHT)

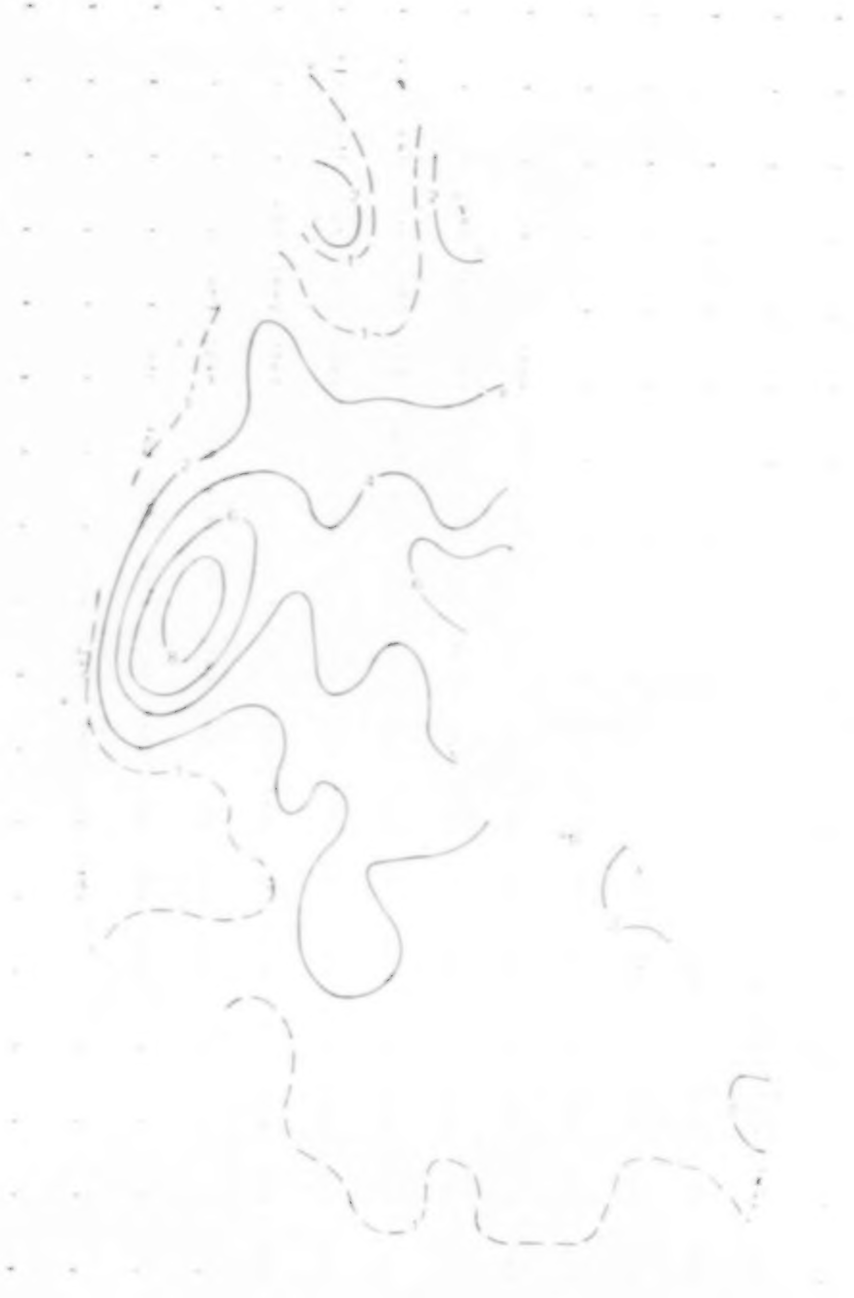

FIGURE 7 SPATIAL DISTRIBUTION OF TOTAL SO_2/SULFATE WET DEPOSITION WITHIN THE FRG DURING 1970 (CONTOURS ARE LABELLED IN KILOTONS OF SO_2 EQUIVALENT WEIGHT)

IV APPLICATION OF THE AIR BUDGET MODEL IN INTERNATIONAL AIR QUALITY MANAGEMENT

If the air budget model were expanded to include all of Central and perhaps Northern Europe, a table similar to Table 3 could be prepared for each of the various nations, but also including pollutant import from, as well as export to, all of the other nations. This could be accomplished not only for the assessment of current or historical conditions, but also for estimating future international air pollution impacts of projected future emissions levels.

Information of this type could form the basis for international agreement among nations on annual air pollution "export quotas" for each nation as applied to every other nation. These quotas could then be factored into the individual national air resource management plans. Using the air budget model, such information could be updated on an annual or more frequent basis. Conceivably, the regulatory system could include cost penalties or credits to nations deviating from their export quotas.

Validation of the air budget model would be difficult, since this would require detailed pollutant concentration measurements at several points between the surface and the 1500-m level or above, at closely spaced locations along all national boundaries. These data, of course, do not currently exist, and would be prohibitively expensive to obtain. However, this should not be considered as a major disadvantage. Since the model is considerably simpler in terms of its output than most diffusion models, the potential for error is significantly reduced. We expect that it will not be difficult to develop confidence in the results from a refined model, particularly when it is used in a relative sense, such as in comparing the results from one year with another.

Although the technical aspects of an international air quality management plan based upon the air budget approach are fairly straightforward, the political aspects of putting such an arrangement into practice are somewhat more difficult. At least five major international organizations with environmental activities exist that could be considered likely candidates for taking the lead in this matter: the Economic Commission for Europe (ECE), the Council of Europe, the North Atlantic Treaty Organization (NATO), the Organization for Economic Cooperation and Development (OECD), and the European Economic Community or Common Market (EEC). According to McLin (1972),

> "...Mobilizing the political will to act at the highest national levels is something which NATO does better than the others. The Council of Europe ... (specializes) in drafting conventions. The EEC may become an effective agency for deciding and enforcing a whole range of regulations at the European level."

If this is an accurate assessment, then it appears that the EEC would be the most effective organization to initiate, regulate, and enforce an international air quality management plan.

V PROPOSED FURTHER MODEL DEVELOPMENT

The preliminary results from the simplified demonstration model have been encouraging. At this stage, the development of a realistic, practical, and objective air budget model for use in an international air quality management plan is not only feasible, but promising. The feasibility of putting such a plan into practice, however, is more difficult to judge, since this depends upon the degree of cooperation that can be achieved among a number of participating nations, and other non-technical political considerations.

Since the need for such an international air quality management plan will become even more acute in future years, this work should be continued to the stage where a satisfactory, operational air budget model has been developed and demonstrated for Central and Northern Europe. The existence of such an objective technique for assessing the international air budget of pollutant imports and exports could be a key factor in securing the agreement of the various nations to participate in an international air quality management plan.

ACKNOWLEDGMENTS

This study was conducted under a contract from the Federal Ministry of the Interior, FRG, to the Stanford Research Institute of Menlo Park, California, USA. The authors gratefully acknowledge the contributions of the following persons: Reg. Dir. Dr. E. Weber of the Federal Ministry of the Interior for arranging the transmittal of the emissions data; Dr. S. P. Blake, Mr. G. D. Hopkins, and Dr. S. Brown of SRI for their comments and encouragement during the course of the research; Miss I. Niemeyer for her rapid translation; Mr. U. F. Pilz for quality control and coordination in the German language; Mrs. E. Molton for typing under extraordinary pressures; and others too numerous to cite individually here.

Appendix A

MONTHLY AVERAGE RESULTS FOR 1970 OF TRANS-BORDER POLLUTANT FLUX FROM THE *FRG*, AND DRY AND WET DEPOSITION WITHIN THE *FRG*

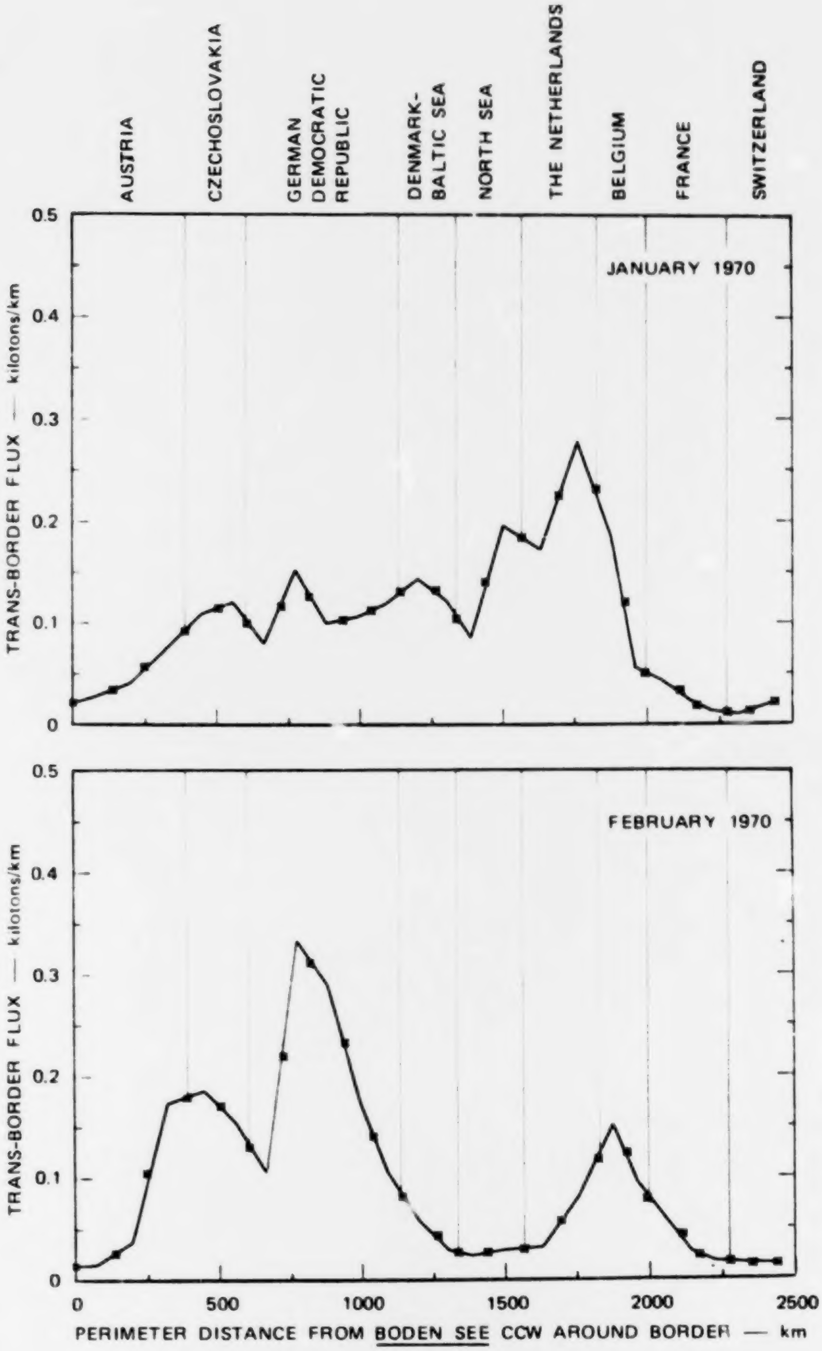

FIGURE A-1 TRANS-BORDER SO_2/SULFATE FLUX FROM THE FRG DURING JANUARY AND FEBRUARY 1970 AS A FUNCTION OF BORDER LOCATION (VALUES REFER TO EQUIVALENT WEIGHT OF SO_2)

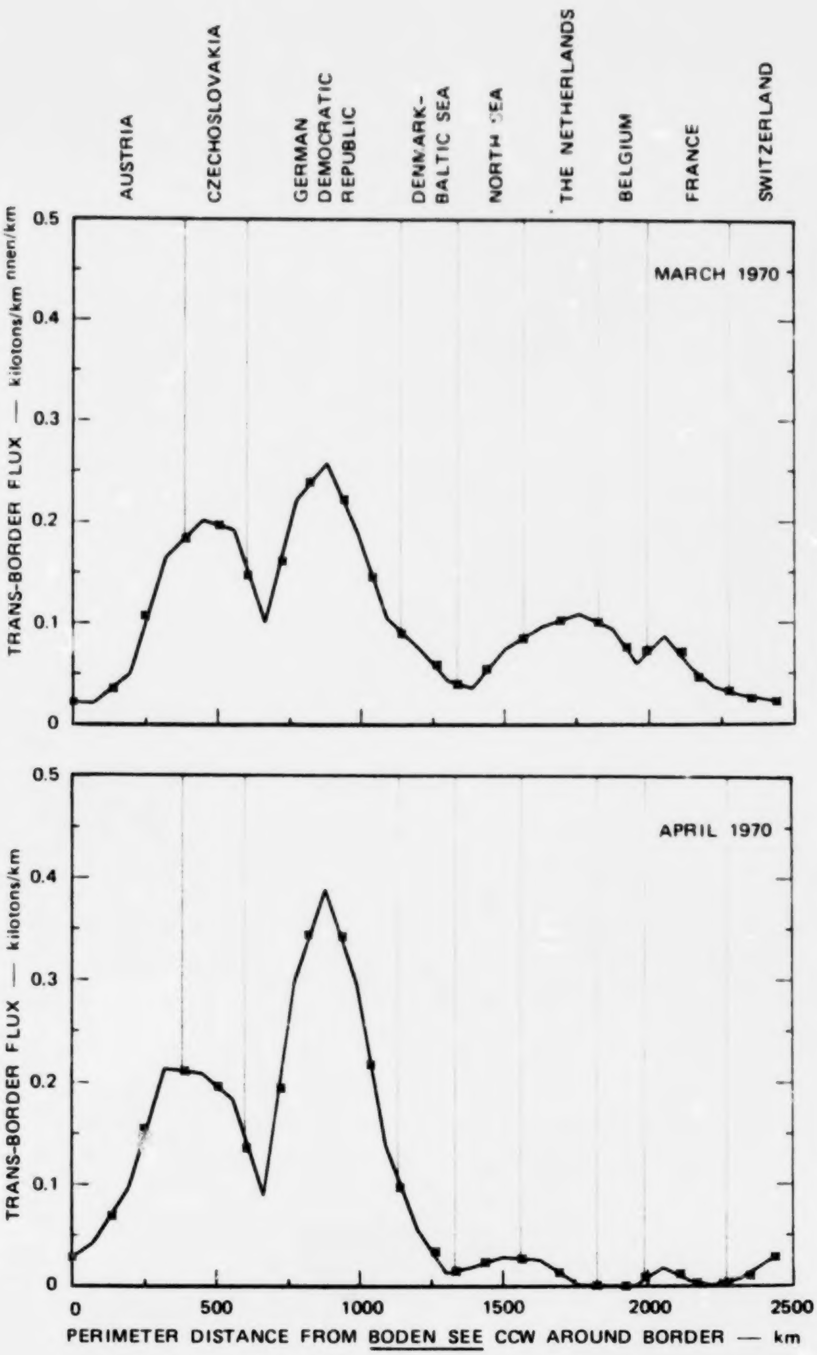

FIGURE A-2 TRANS-BORDER SO_2/SULFATE FLUX FROM THE FRG DURING MARCH AND APRIL 1970 AS A FUNCTION OF BORDER LOCATION (VALUES REFER TO EQUIVALENT WEIGHT OF SO_2)

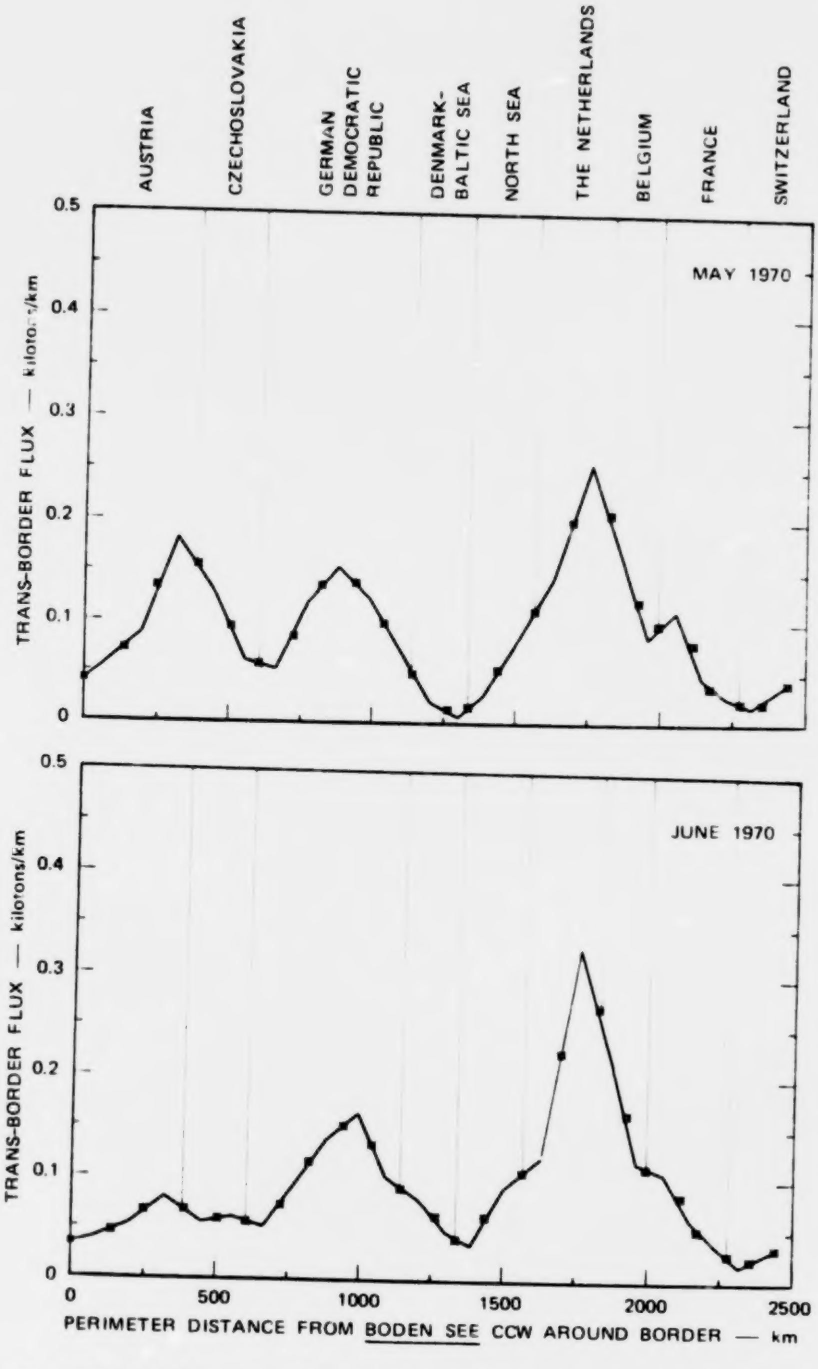

FIGURE A-3 TRANS-BORDER SO_2/SULFATE FLUX FROM THE FRG DURING MAY AND JUNE 1970 AS A FUNCTION OF BORDER LOCATION (VALUES REFER TO EQUIVALENT WEIGHT OF SO_2)

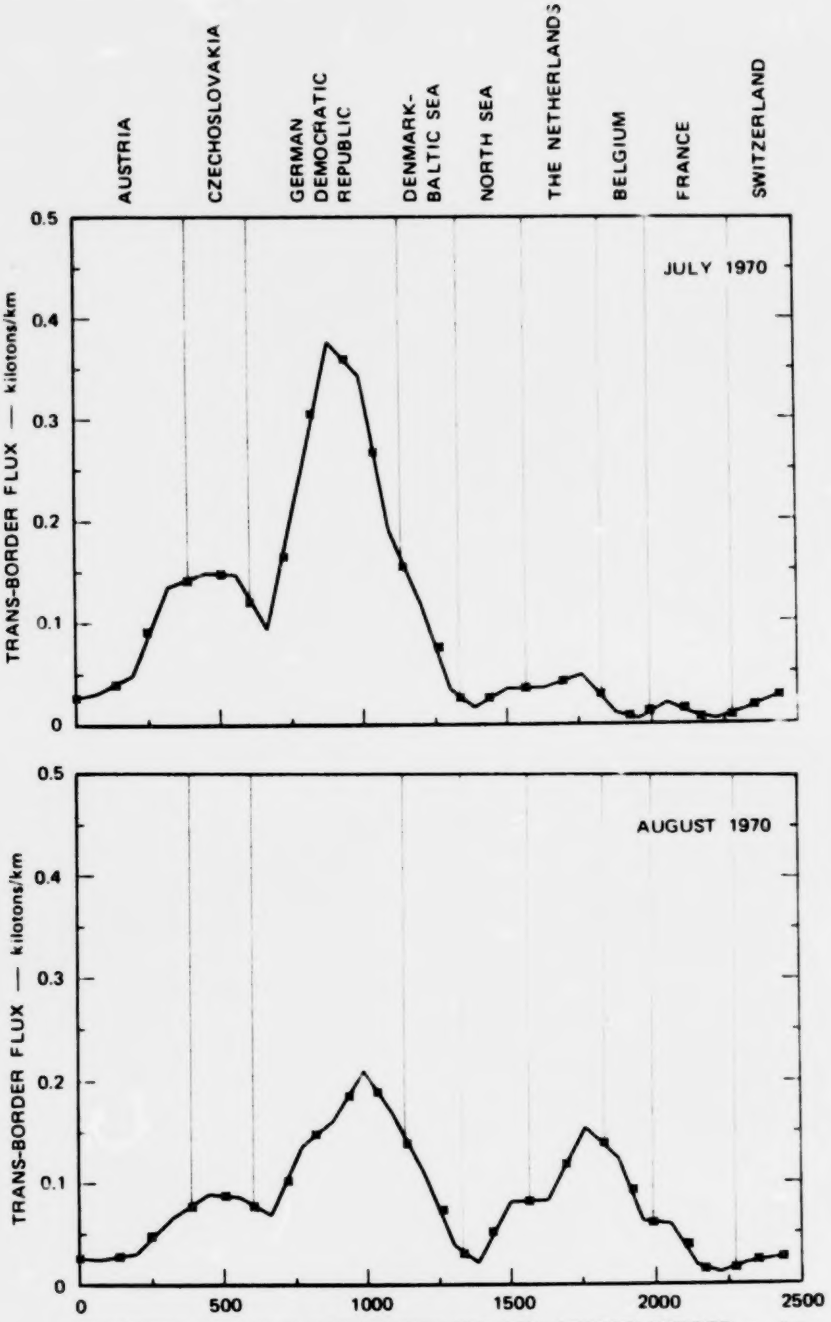

FIGURE A-4 TRANS-BORDER SO_2/SULFATE FLUX FROM THE FRG DURING JULY AND AUGUST 1970 AS A FUNCTION OF BORDER LOCATION (VALUES REFER TO EQUIVALENT WEIGHT OF SO_2)

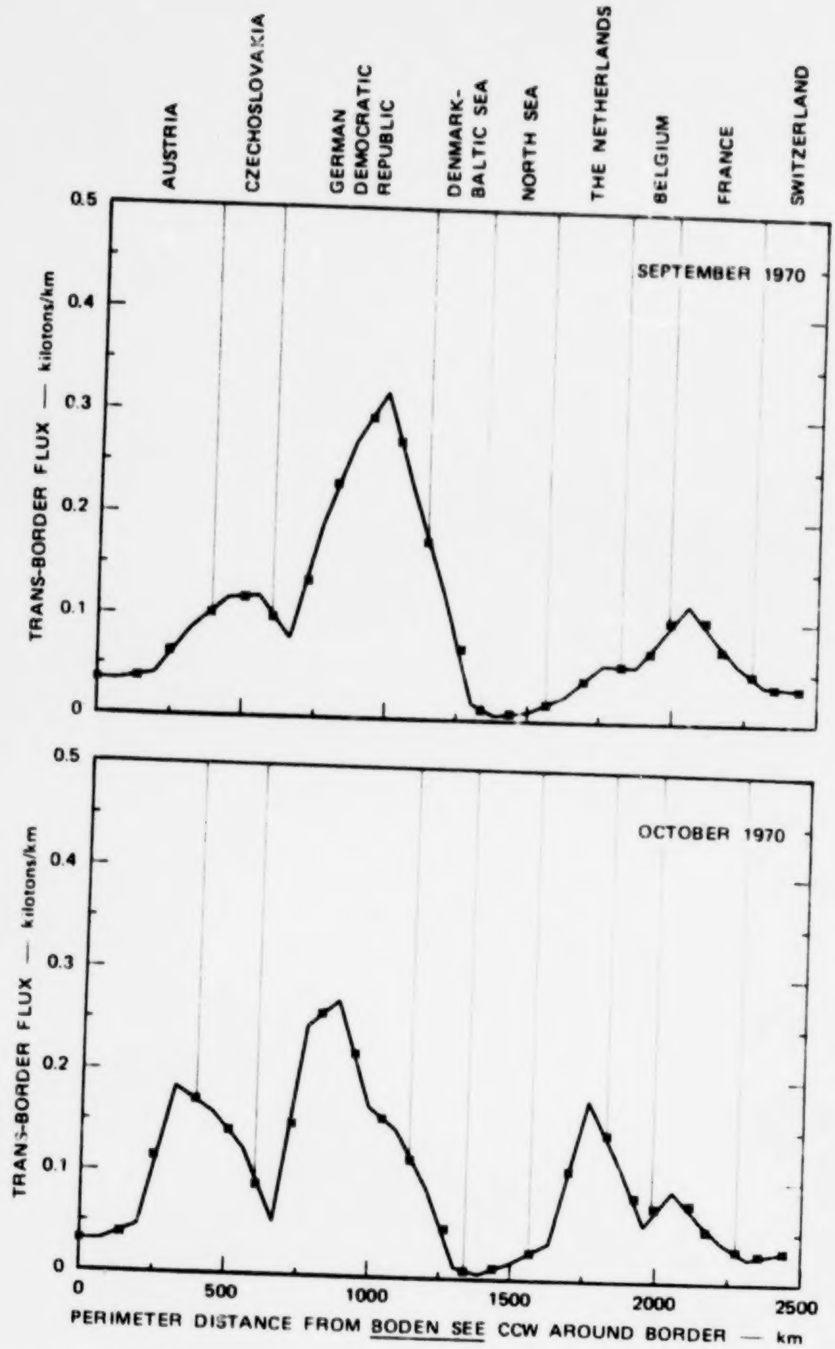

FIGURE A-5 TRANS-BORDER SO_2/SULFATE FLUX FROM THE FRG DURING SEPTEMBER AND OCTOBER 1970 AS A FUNCTION OF BORDER LOCATION (VALUES REFER TO EQUIVALENT WEIGHT OF SO_2)

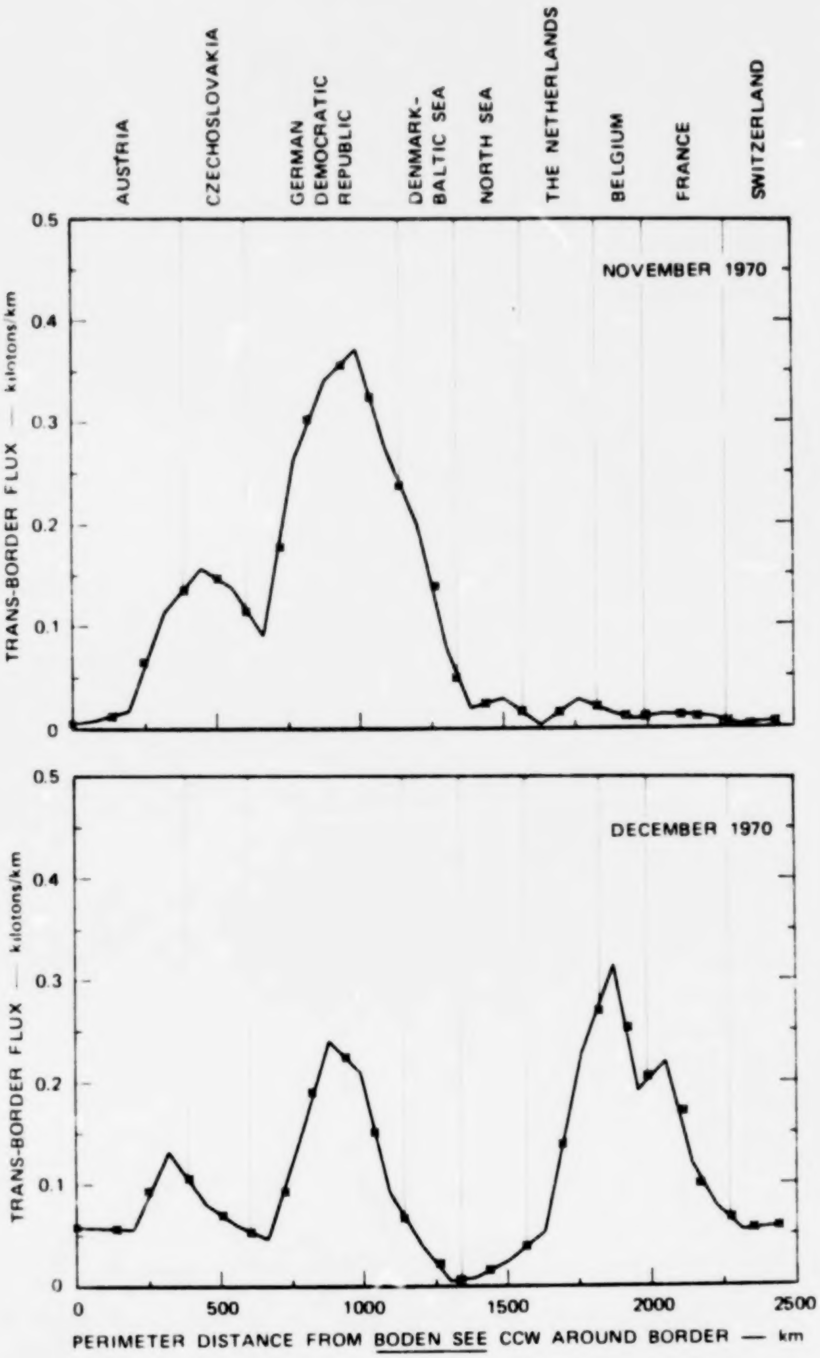

FIGURE A-6 TRANS-BORDER SO_2/SULFATE FLUX FROM THE FRG DURING NOVEMBER AND DECEMBER 1970 AS A FUNCTION OF BORDER LOCATION (VALUES REFER TO EQUIVALENT WEIGHT OF SO_2)

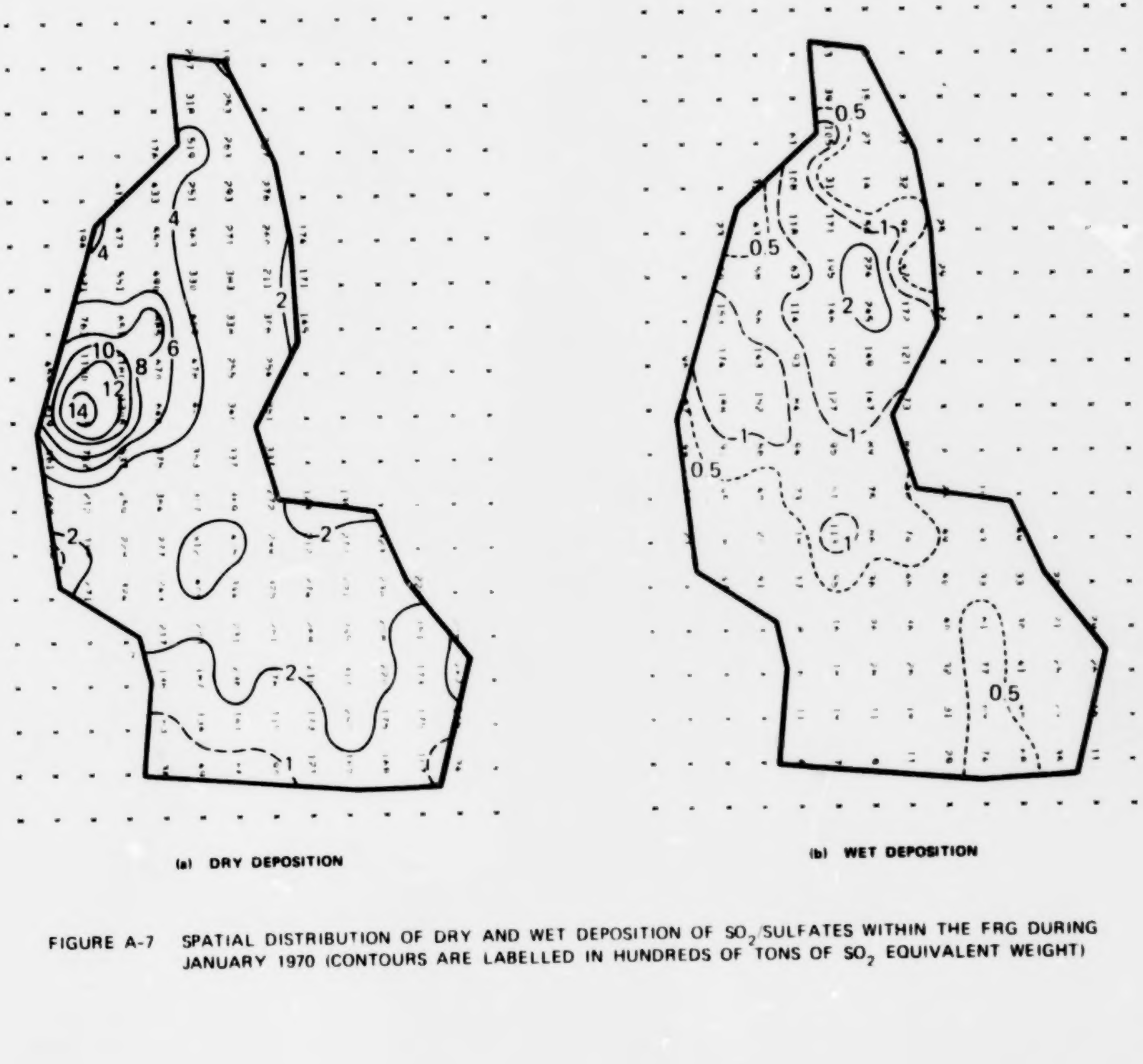

(a) DRY DEPOSITION

(b) WET DEPOSITION

FIGURE A-7 SPATIAL DISTRIBUTION OF DRY AND WET DEPOSITION OF SO_2/SULFATES WITHIN THE FRG DURING JANUARY 1970 (CONTOURS ARE LABELLED IN HUNDREDS OF TONS OF SO_2 EQUIVALENT WEIGHT)

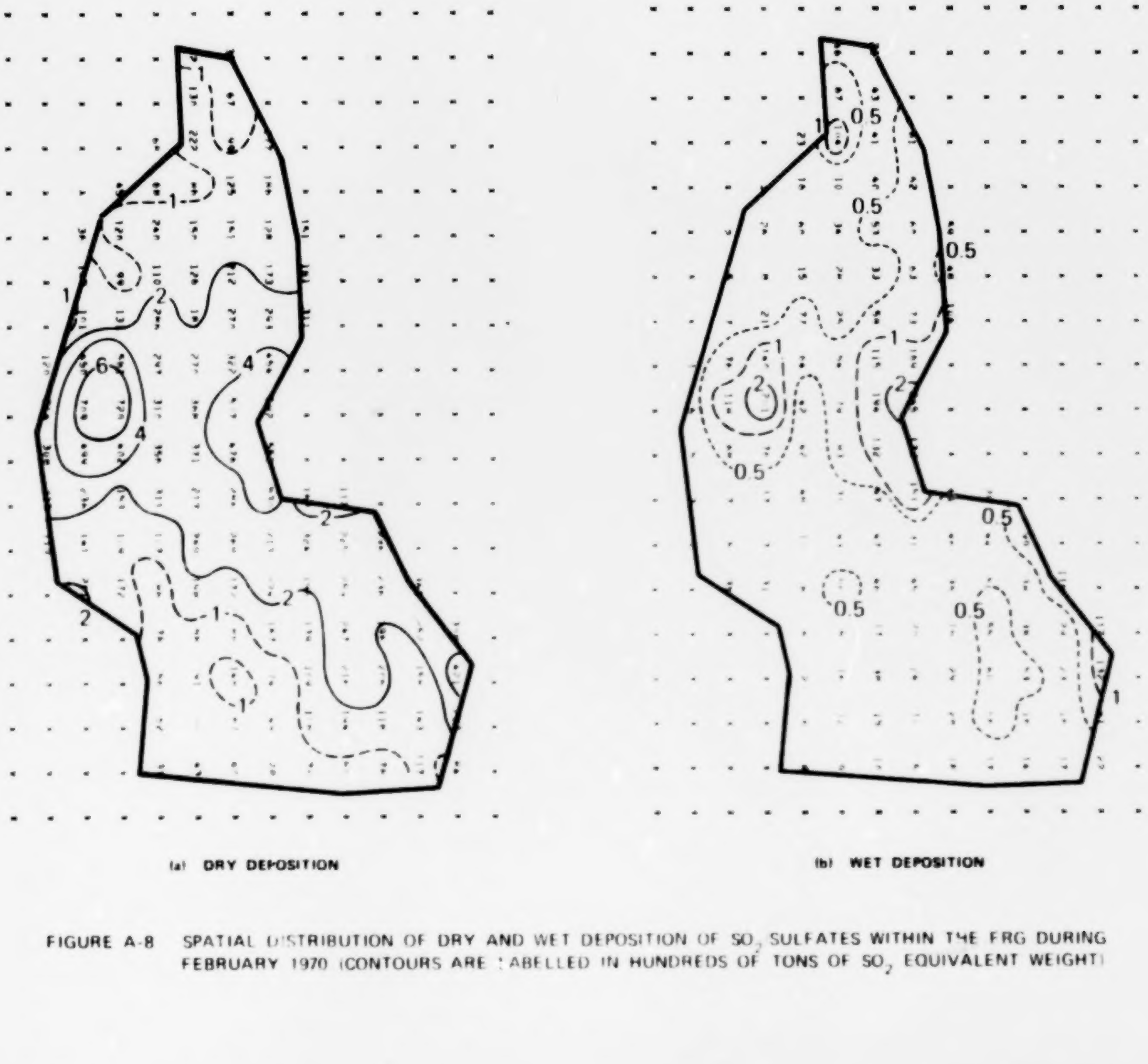

(a) DRY DEPOSITION

(b) WET DEPOSITION

FIGURE A-8 SPATIAL DISTRIBUTION OF DRY AND WET DEPOSITION OF SO_2 SULFATES WITHIN THE FRG DURING FEBRUARY 1970 (CONTOURS ARE LABELLED IN HUNDREDS OF TONS OF SO_2 EQUIVALENT WEIGHT)

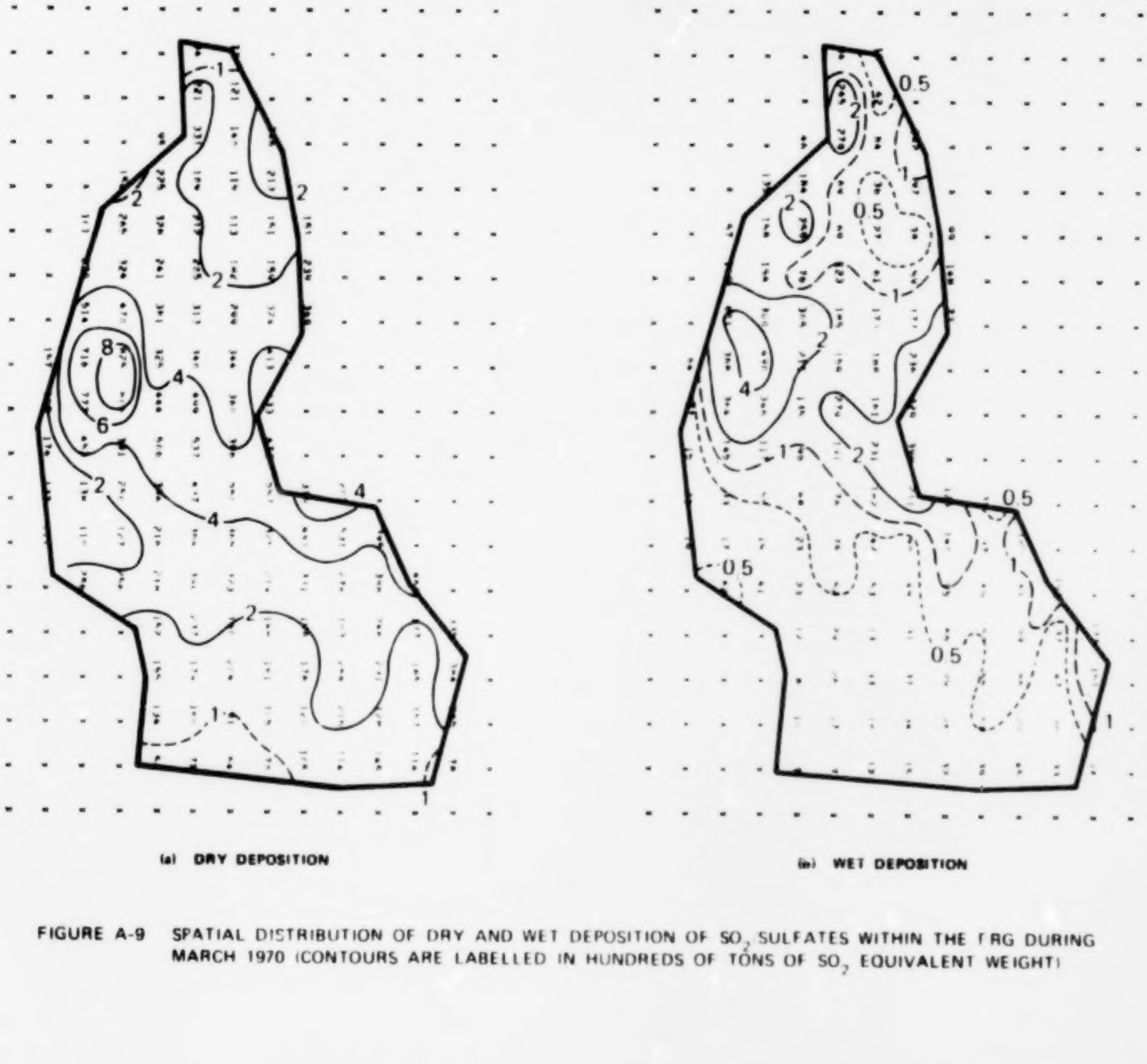

(a) DRY DEPOSITION

(b) WET DEPOSITION

FIGURE A-9 SPATIAL DISTRIBUTION OF DRY AND WET DEPOSITION OF SO_2 SULFATES WITHIN THE FRG DURING MARCH 1970 (CONTOURS ARE LABELLED IN HUNDREDS OF TONS OF SO_2 EQUIVALENT WEIGHT)

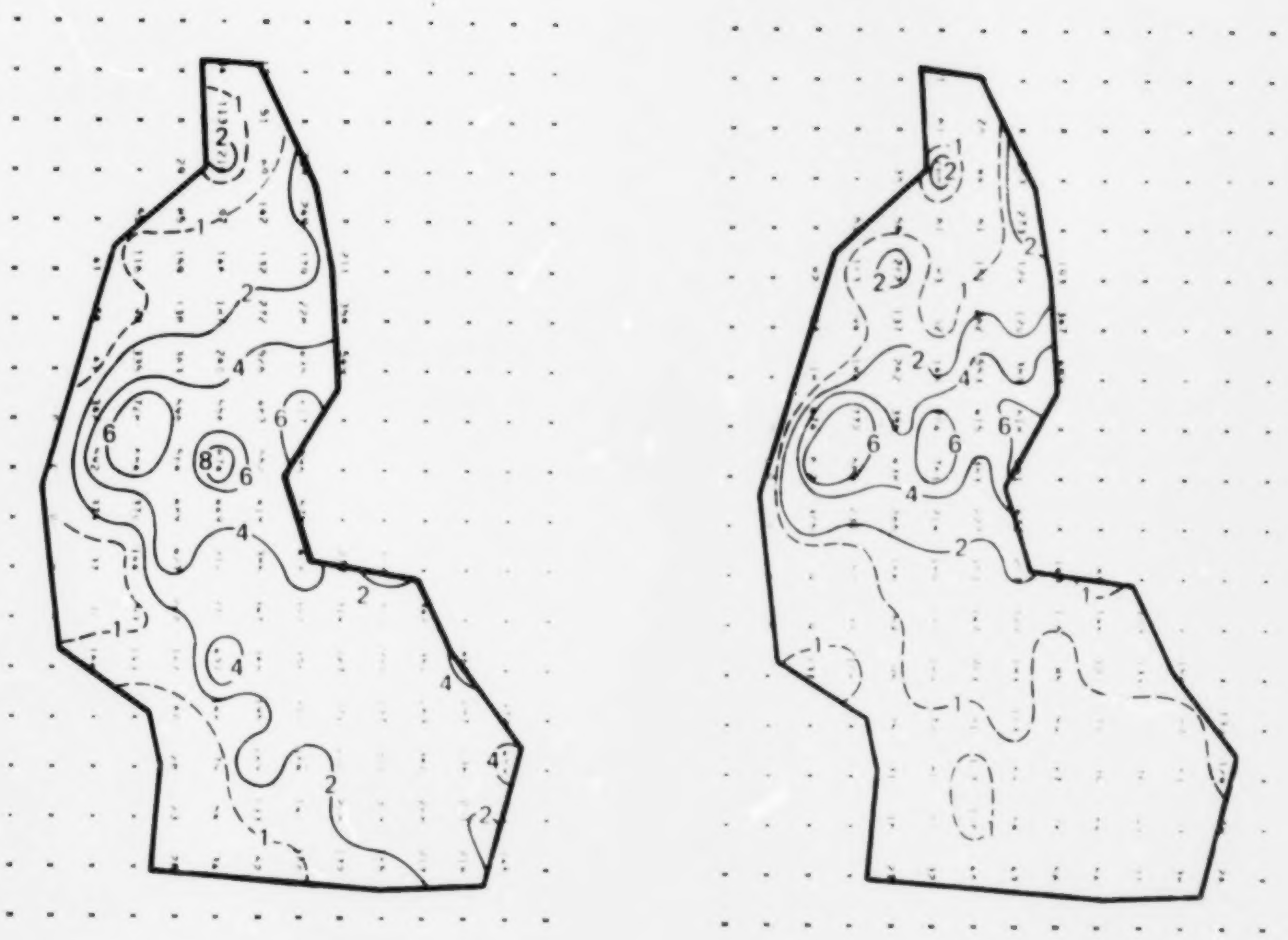

(a) DRY DEPOSITION

(b) WET DEPOSITION

FIGURE A-10 SPATIAL DISTRIBUTION OF DRY AND WET DEPOSITION OF SO_2 SULFATES WITHIN THE FRG DURING APRIL 1970 (CONTOURS ARE LABELLED IN HUNDREDS OF TONS OF SO_2 EQUIVALENT WEIGHT)

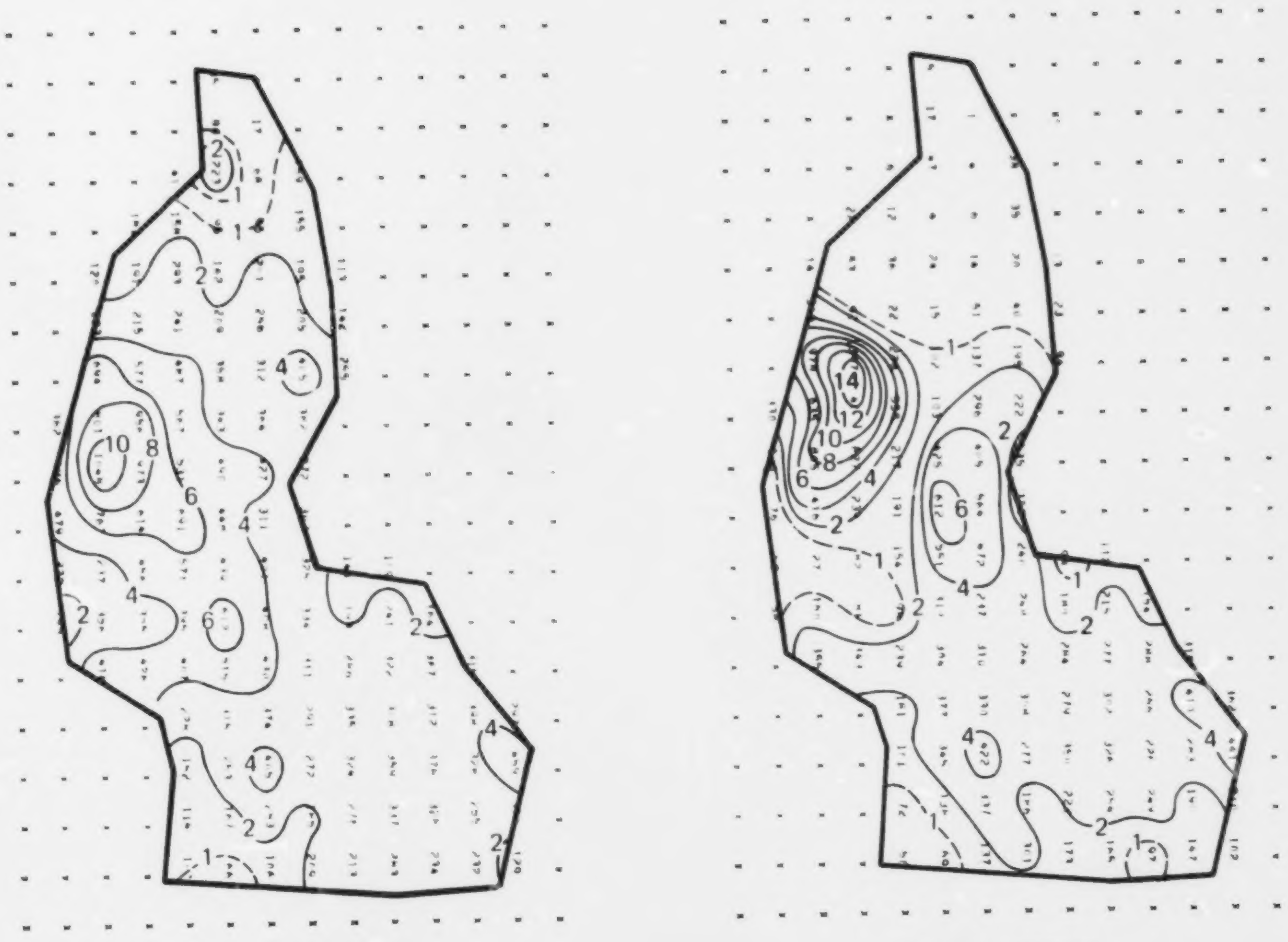

(a) DRY DEPOSITION

(b) WET DEPOSITION

FIGURE A-11 SPATIAL DISTRIBUTION OF DRY AND WET DEPOSITION OF SO_2 SULFATES WITHIN THE FRG DURING MAY 1970 (CONTOURS ARE LABELLED IN HUNDREDS OF TONS OF SO_2 EQUIVALENT WEIGHT)

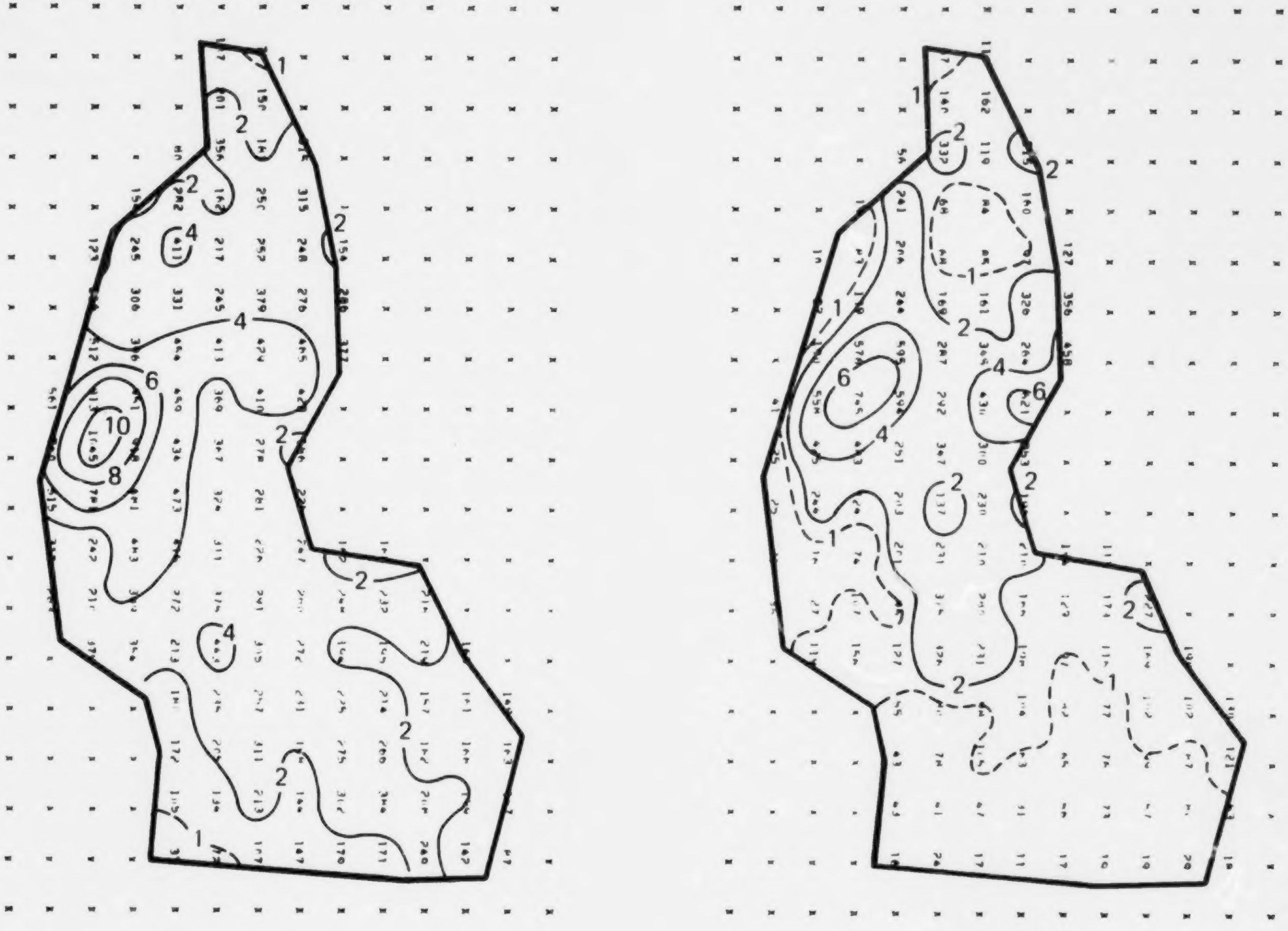

(a) DRY DEPOSITION

(b) WET DEPOSITION

FIGURE A-12 SPATIAL DISTRIBUTION OF DRY AND WET DEPOSITION OF SO$_2$/SULFATES WITHIN THE FRG DURING JUNE 1970 (CONTOURS ARE LABELLED IN HUNDREDS OF TONS OF SO$_2$ EQUIVALENT WEIGHT)

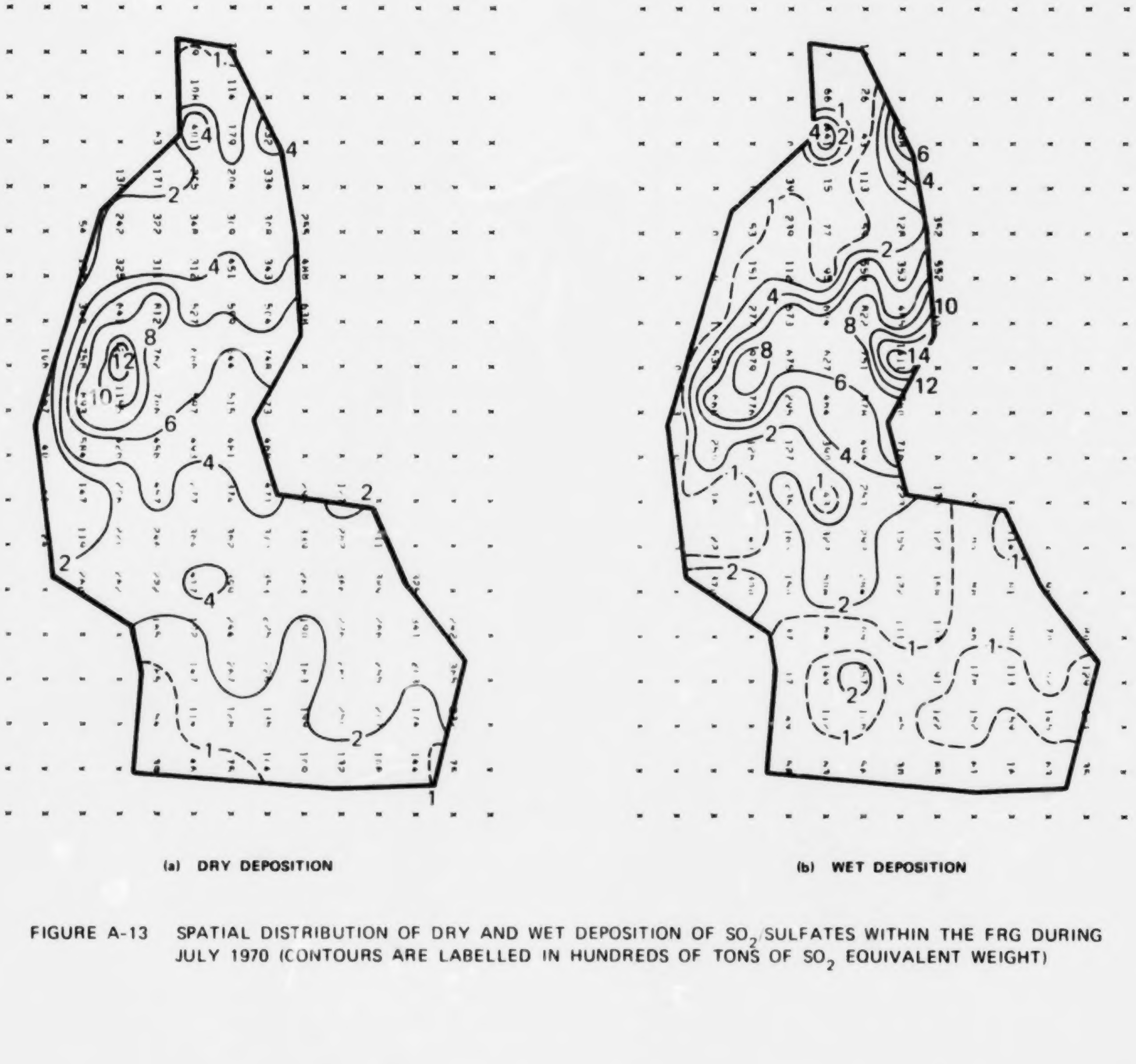

(a) DRY DEPOSITION

(b) WET DEPOSITION

FIGURE A-13 SPATIAL DISTRIBUTION OF DRY AND WET DEPOSITION OF SO_2 SULFATES WITHIN THE FRG DURING JULY 1970 (CONTOURS ARE LABELLED IN HUNDREDS OF TONS OF SO_2 EQUIVALENT WEIGHT)

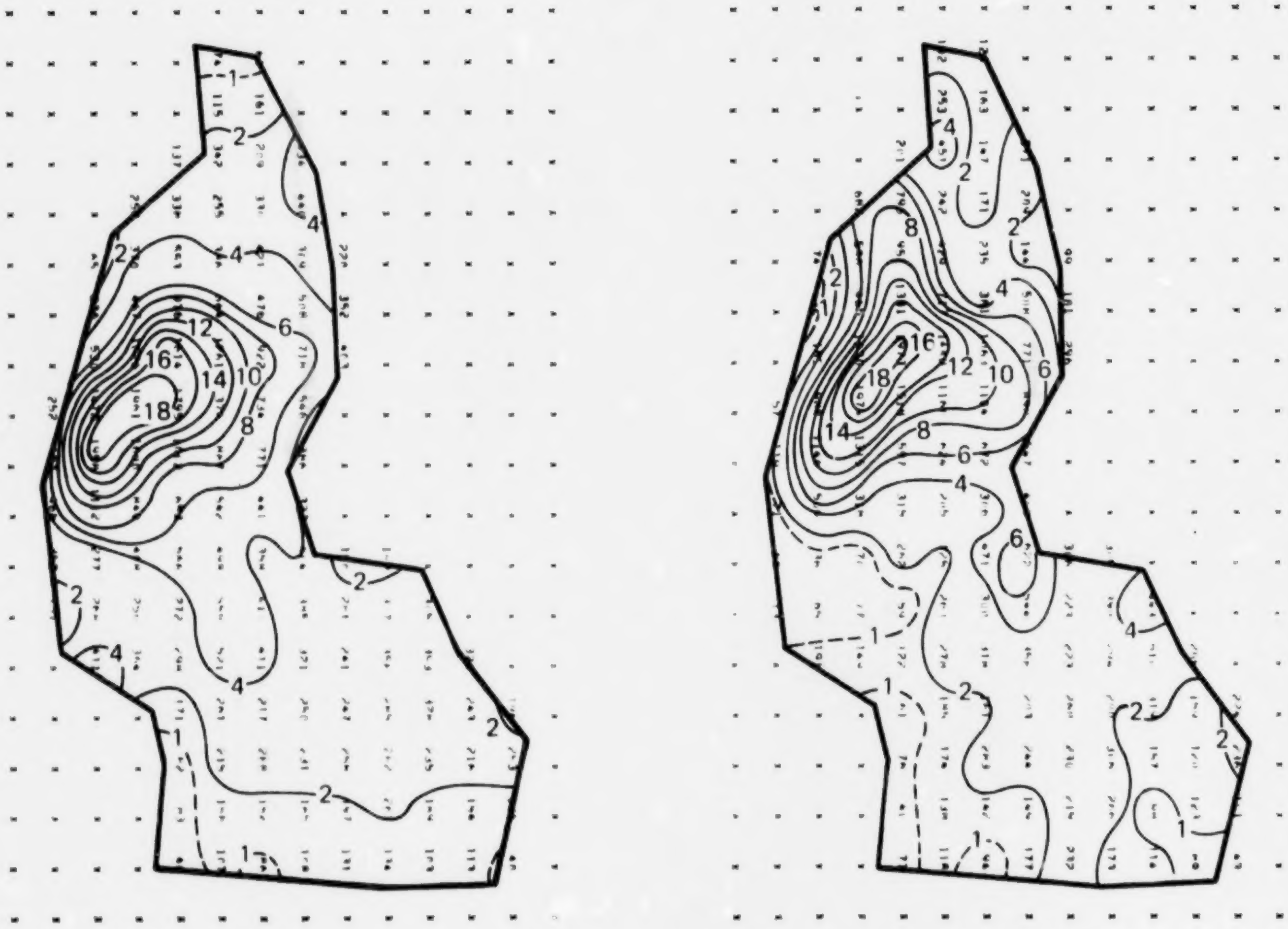

(a) DRY DEPOSITION

(b) WET DEPOSITION

FIGURE A-14 SPATIAL DISTRIBUTION OF DRY AND WET DEPOSITION OF SO_2/SULFATES WITHIN THE FRG DURING AUGUST 1970 (CONTOURS ARE LABELLED IN HUNDREDS OF TONS OF SO_2 EQUIVALENT WEIGHT)

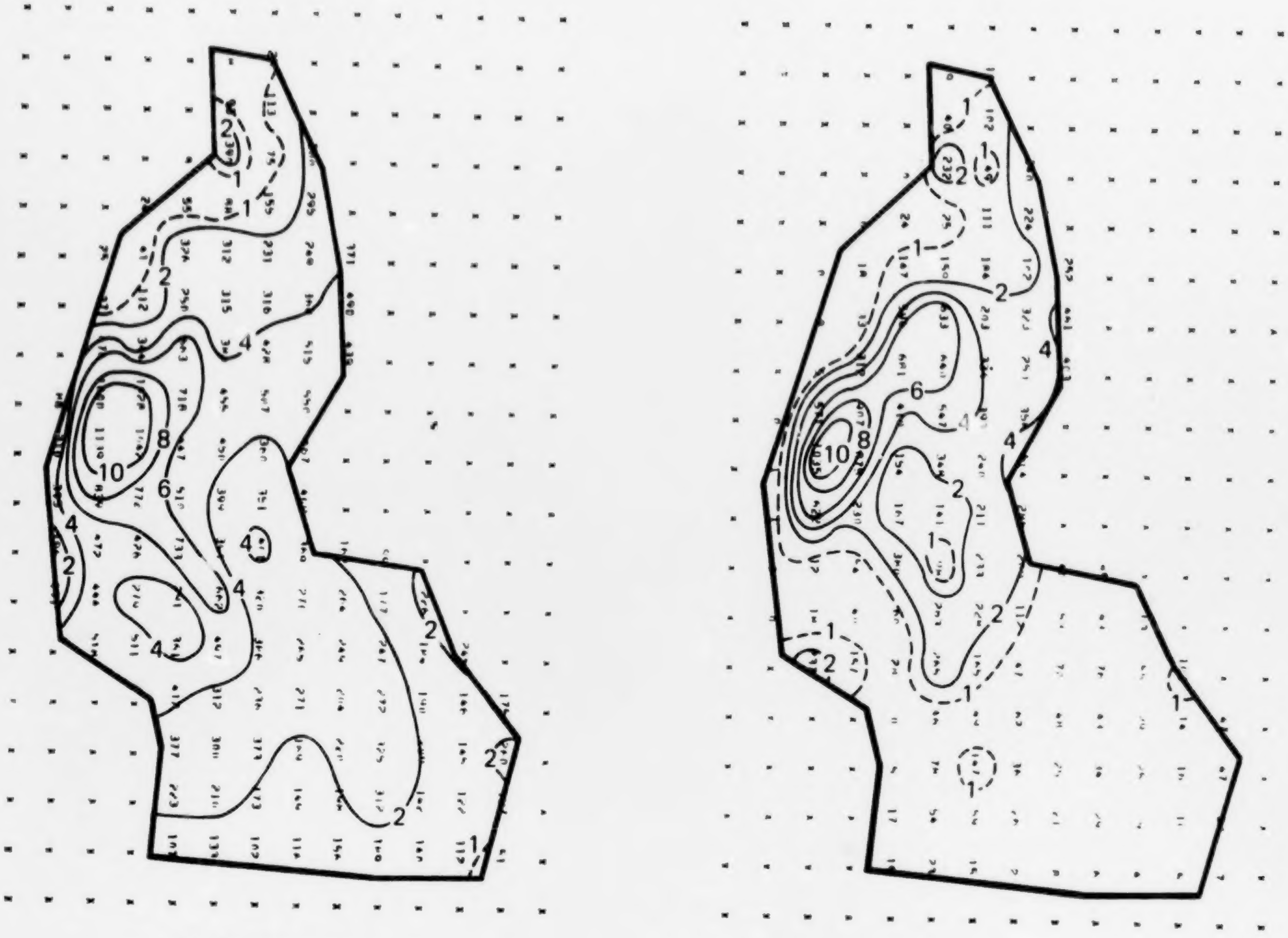

(a) DRY DEPOSITION

(b) WET DEPOSITION

FIGURE A-15 SPATIAL DISTRIBUTION OF DRY AND WET DEPOSITION OF SO_2/SULFATES WITHIN THE FRG DURING SEPTEMBER 1970 (CONTOURS ARE LABELLED IN HUNDREDS OF TONS OF SO_2 EQUIVALENT WEIGHT)

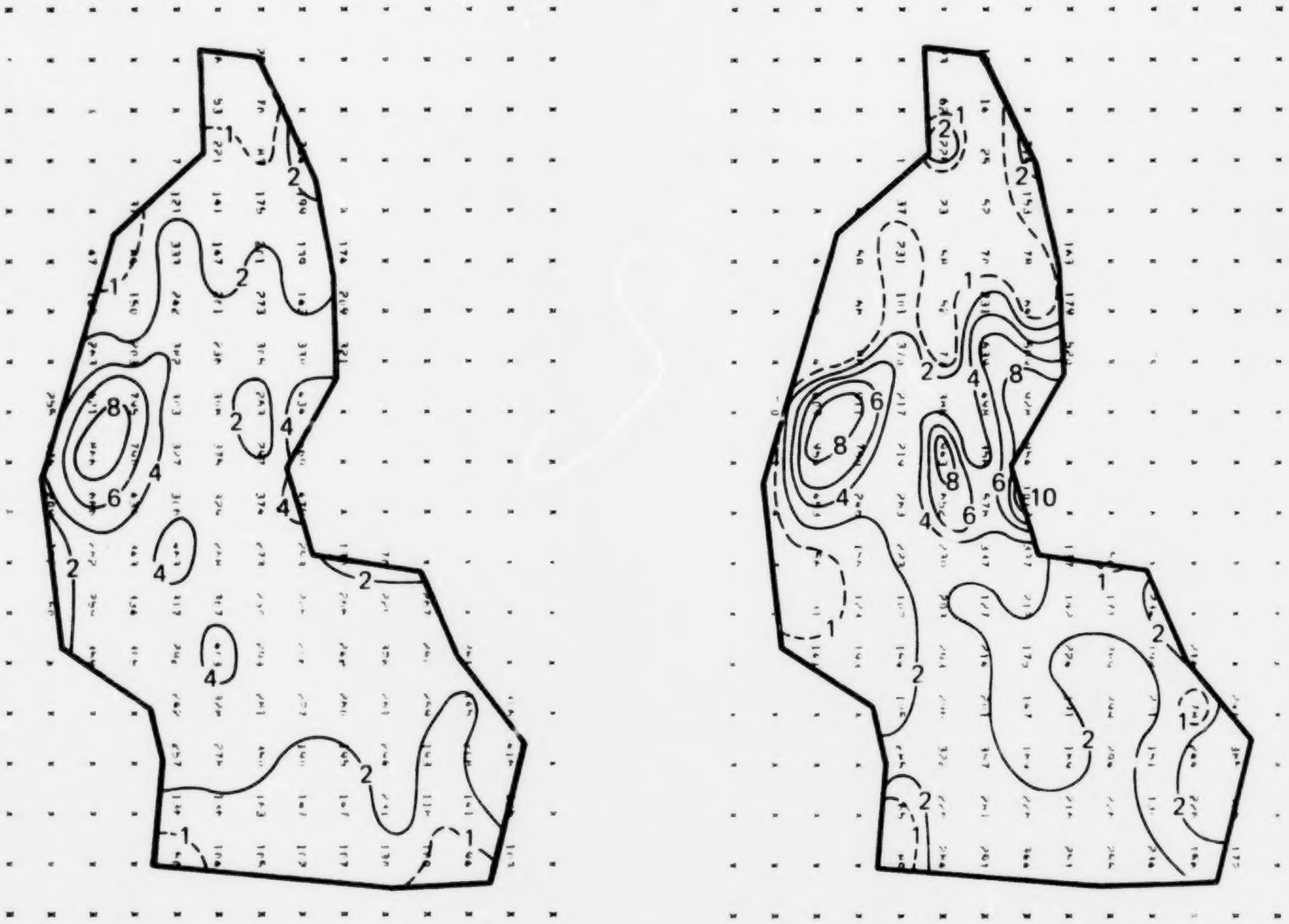

(a) DRY DEPOSITION

(b) WET DEPOSITION

FIGURE A-16 SPATIAL DISTRIBUTION OF DRY AND WET DEPOSITION OF SO_2 SULFATES WITHIN THE FRG DURING OCTOBER 1970 (CONTOURS ARE LABELLED IN HUNDREDS OF TONS OF SO_2 EQUIVALENT WEIGHT)

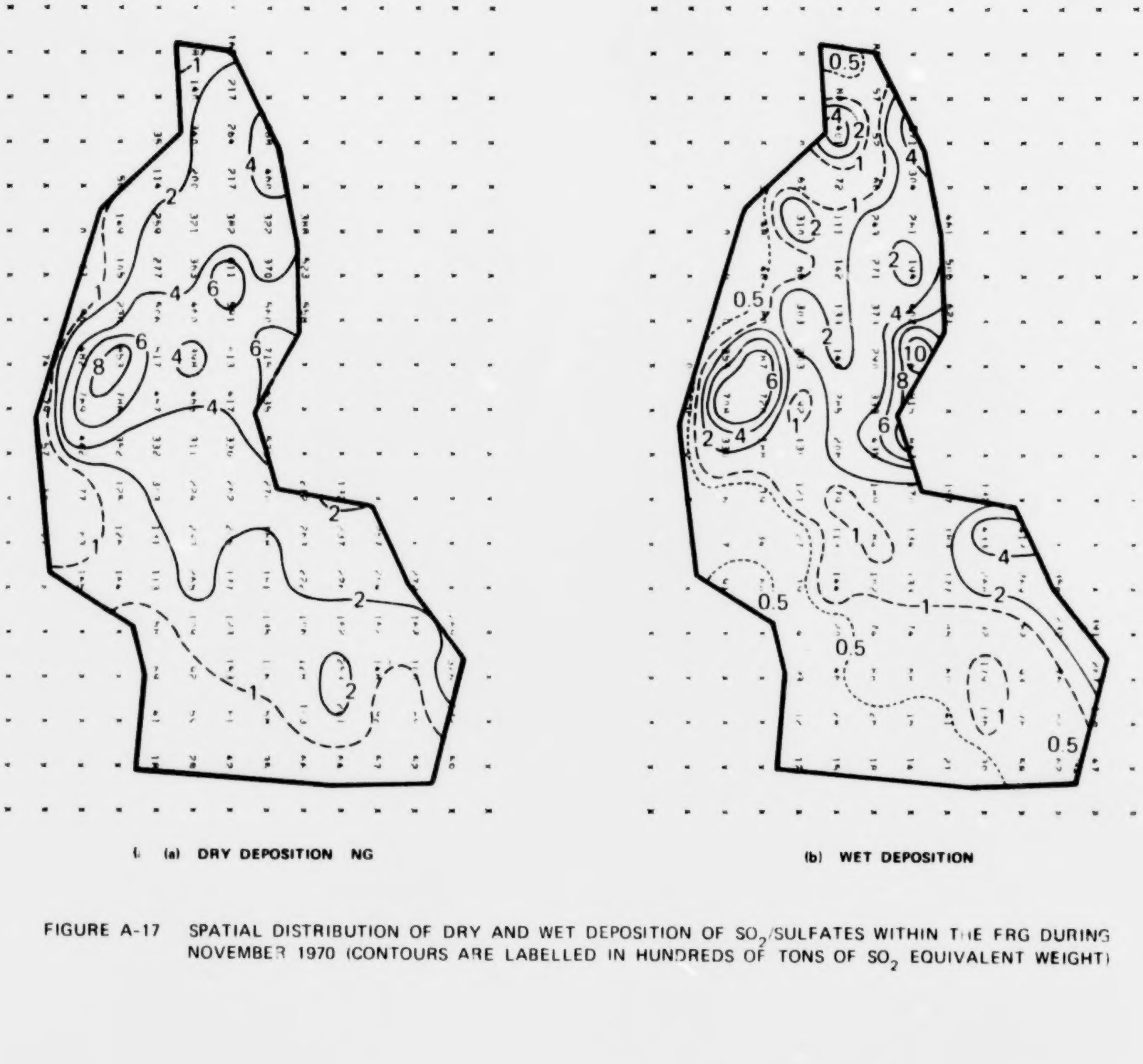

(a) DRY DEPOSITION NG

(b) WET DEPOSITION

FIGURE A-17 SPATIAL DISTRIBUTION OF DRY AND WET DEPOSITION OF SO_2/SULFATES WITHIN THE FRG DURING NOVEMBER 1970 (CONTOURS ARE LABELLED IN HUNDREDS OF TONS OF SO_2 EQUIVALENT WEIGHT)

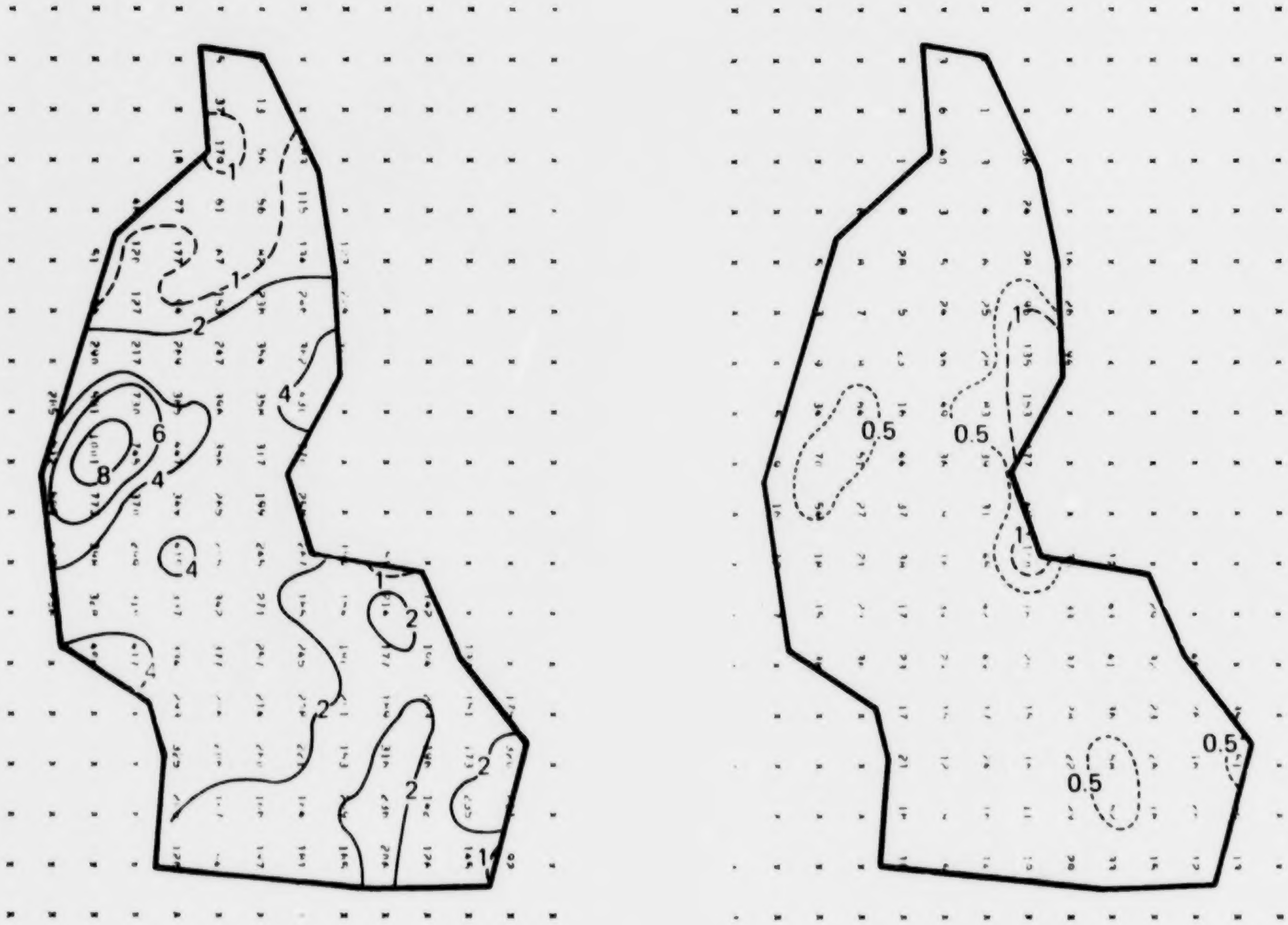

(a) DRY DEPOSITION

(b) WET DEPOSITION

FIGURE A-18 SPATIAL DISTRIBUTION OF DRY AND WET DEPOSITION OF SO_2/SULFATES WITHIN THE FRG DURING DECEMBER 1970 (CONTOURS ARE LABELLED IN HUNDREDS OF TONS OF SO_2 EQUIVALENT WEIGHT)

REFERENCES

Bielke, S., and H. W. Georgii, 1968: Investigation on the incorporation of sulfur dioxide into fog- and rain-droplets. *Tellus*, *20*, No. 3, 435-441.

Gartrell, F. E., L. F. Thomas, and S. B. Carpenter, 1963: Atmospheric oxidation of SO_2 in coal burning power plant plumes. *J. Amer. Ind. Hyg. Assoc.*, *24*, 113.

Hales, J. M., J. M. Thorp, and M. A. Wolf, 1970: Precipitation scavenging (1970). Proc. of Symposium, June 1970, Richland, Wash., USA. U.S. Atomic Energy Commission, Div. of Technical Information.

Kellogg, W. W., R. D. Cadle, E. R. Allen, A. L. Lazrus, and E. A. Martell, 1972: The sulfur cycle. *Science*, *175*, 587-596.

McLin, J., 1972: Stepping across boundaries. *Environment*, *14*, No. 4, 16-28.

NUKEM, GmbH Umwelttechnik, 1973: SO_2 emissions in the FRG. Report No. L-71-104, prepared for the Ministry of the Interior, Referat U II 4.

Summers, P. W. and B. Hitchon, 1973: Source and budget of sulfate in precipitation from Central Alberta, Canada. *J. Air Poll. Contr. Assoc.*, *23*, No. 3, 194-199.

Weber, E., 1970a: Contribution to the residence time of sulfur dioxide in a polluted atmosphere. *J. Geophys. Research*, *75*, No. 15, 2909-2914.

Weber, E., 1970b: Determination of the lifetime of SO_2 by simultaneous CO_2 and SO_2 monitoring. Proc. Second Clean Air Congress, Paper No. CP25F, 477-481.

Weber, E., 1971: Removal of sulfur dioxide from the atmosphere. Proc. of the Second Meeting, NATO CCMS Panel on Modeling, July 1971, Paris, France, Report No. 5, Chapter XII.

6th NATO/CCMS
International Technical Meeting
on Air Pollution Modeling

Validation of a multiple source diffusion model based on the Gaussian plume model

by

F.T.M. Nieuwstadt and H. van Dop
Royal Netherlands Meteorological Institute
De Bilt

BATTELLE - INSTITUT E.V., Frankfurt/Main
Germany, FR
24 - 26 September, 1975

Preceding page blank

Summary

With a dispersion model, based on the Gaussian plume model, the average concentration pattern can be calculated from a given emission. The averaging time considered here is in the order of at least a few months. The area may contain (low and high) point sources and area sources, so that a large source complex can be handled.

In order to test the model it is necessary to have an area available for which sufficiently accurate emission data are known over a long period. Such data became available for a part of the province of Noord-Holland - including the major cities Amsterdam and Haarlem. For the testing period the months January, February, March, October, November and December 1972 were chosen. The pollution component for which the validation was carried out was sulphur dioxide, as this was the most extensively and rather accurately measured component at that time.

The spatial correlation coefficients between the measured and calculated concentrations averaged over the period of six months were about 0.75. The mean relative difference between the two concentrations amounted to only about 5% with a standard deviation of 20%.

-o-o-o-

I. Introduction

Many air pollution models are based on the well-known Gaussian plume model, which is based on a particular solution of the equation of mass conservation under steady and homogeneous conditions. Empirical information is brought into the model through specification of dispersion parameters, which determine the dimensions of the plume. A complete solution of the equation of mass conservation is very complex, so that the use of the Gaussian plume model is preferred for its simplicity.

In the application of the model, however, one should be aware of its limitations: state state and homogeneity.

In order to estimate the performance of the model it is necessary to carry out a so-called validation in which measured and calculated concentration values are compared. It was pointed out by Johnson (1972), that the validation of a model should start with the validation of its elements.

The validation of the Gaussian plume model should start with the calculation of the dispersion from a single point source. A validation for a single source has been reported by Klug (1974): he found that the ratio of observed and calculated concentrations averaged over a year ranges from 0.55 to 1.94 and 0.44 to 1.31 depending on the dispersion parameters used.

Most of the comparisons between model calculations and air pollution measurements have been made for a complex source configuration, which is defined as a region where many, and also many different types of sources are present. The validation of a model, however, in such a region is more difficult.

For short term averaging periods (1-24 hrs) comparisons between calculated and observed concentrations have been made for instance by Turner (1964), Marsh and Withers (1969) and Shieh (1970). The calculations averaged over a short term are also used to construct a frequency distribution. Comparisons with measured frequency distributions have been made by Fortak (1970) and Bringfelt (1974).

The Gaussian plume model is also used to calculate concentrations averaged over a long term (e.g. several months to a year), a.o. by Pooler (1961) and Martin (1971).

Koch and Mayer (1971) have compared calculations of short and long term averaged concentrations with measured data. They concluded that the model performs better for the calculation of long term averaged concentrations. This is probably due to the fact that errors in the short term calculation tend to average out in the long term calculation. Therefore the Gaussian plume model seems more suited for the calculation of long term average concentrations.

An objective validation can be done in many ways (Olssen, 1974) all of which do not seem to be satisfactory, as was pointed out by Corlin (1974) in relation to the use of a correlation coefficient. In this paper much attention will be paid to various forms of model validation, in order to obtain a comprehensive impression of the model performance.

For the validation described here the Gaussian plume model for long term averaged concentrations was used in a complex source region near Amsterdam. The simulation was carried out for the average SO_2 concentrations over the first and last quarter of 1972.

II. The long term averaged Gaussian plume model

a. Model equations

The equation of the long term averaged concentration from the emission of one point source (Calder, 1971) is

$$\chi = \sum_{S} \sum_{N} \frac{2Q}{\sqrt{2\pi}\,\sigma_{z_S} U_N\,\varepsilon r} F(\theta_i, S, N)\, e^{-\frac{H_{N,S}^2}{2\sigma_{z_S}^2}} \qquad (1)$$

The concentration χ [g/m^3] is given by this equation at a distance r [m] from the source with a strength Q [g/s] in a sector of width ε around the direction θ_i+180°. (θ_i is the wind vector). The vertical dispersion of the plume is described by the dispersion coefficient σ_z [m], which is classified according to the so-called stability classes (S). The effective transport velocity of the plume is given by U [m/s], which is subdivided into wind speed classes (N). H [m] is the effective source height.

b. Dispersion coefficients

The dispersion coefficients σ_z are chosen depending on source height. For low sources (up to 50 m) the coefficients of Pasquill-Gifford (Turner, 1969) have been used and for sources over 50 m those of Singer and Smith (1966), in order to model the dependence of the dispersion on the height of the release. The change of the dispersion coefficients at 50 m, which has been somewhat arbitrarily chosen, may be too abrupt from the physical point of view.

The equations of the dispersion coefficients are given in table 1.

Table 1. Dispersion coefficients according to Pasquill-Gifford and Singer-Smith for the different stability classes S.

$$\sigma_z = a r^b + c$$

	Pasquill-Gifford						Singer-Smith			
	r < 1000 m			r > 1000 m						
S	a	b	c	a	b	c	S	a	b	c
A	$9.4\ 10^{-5}$	2.22	16.37	$2.4\ 10^{-4}$	2.09	-9.60	B_2	0.411	0.907	0
B	0.037	1.53	3.19	0.054	1.10	2.54	B_2			
C	0.099	0.93	0.24	0.099	0.93	1.74	B_1	0.326	0.859	0
D(U < 5.5 m/s)	0.21	0.73	-1.37	0.92	0.55	-9.06	B_1			
D(U > 5.5 m/s)							C	0.223	0.776	0
E	0.20	0.69	-1.16	2.34	0.40	-16.32	D	0.062	0.709	0
F	0.098	0.72	-0.32	6.53	0.26	-25.16	D			

Pasquill-Gifford: A $r < 400$ m : $a = 6.0\ 10^{-3}$ $b = 1.55$ $c = 6.27$

c. Stability definition

The dispersion coefficients are classified according to so-called stability classes. For this calculation a modification of Pasquill stability classes has been used (Nieuwstadt, 1972). For each hour the stability class following Pasquill's notation, is determined for each season as a function of time of day, cloud cover and wind velocity. Between the stability classes of Pasquill and those of Singer and Smith a relation has been adopted as shown in table 1.

d. Transport velocity

When the dispersion coefficients of Pasquill-Gifford are used, the wind velocity at the physical stack height is taken as transport velocity. In the case where the Singer and Smith dispersion coefficients are applied the definition of the transport velocity is taken according to Smith and Singer (1966). In order to be able to calculate the transport velocity, it is assumed that the variation of the wind speed with the altitude is described by a power law. Although the power law has no physical justification, it gives a reasonable approximation of the variation of the wind with height. The exponent p in the power is given in table 2 as a function of the stability classes.

Table 2. The value of the exponent p in the wind profile law. $U_2/U_1 = (z_2/z_1)^p$ for the different stability classes S.

S	p
A,B	0.10
C,D	0.16
E,F	0.30

e. The distribution function $F(\theta_i,S,N)$

The function $F(\theta_i,S,N)$ gives the distribution of stability, wind speed and wind direction classes.

In the calculation of $F(\theta_i,S,N)$ periods with wind speeds less than 0.5 m/s (calm), variable winds and fog have been excluded. The influence of these periods on the long term averaged concentration is negligible, because these periods amounted to only a few percent of the total period of six months.

Use has been made of three wind speed classes: 0.5-2.5, 3.0-5.5 and $\geqslant$ 6.0 m/s (the wind speed at 10 m is taken). Three wind speed classes are sufficient, because for wind speeds $\geqslant$ 6.0 m/s the distribution of the stability classes is approximately independent of the wind speed. From a frequency distribution function of wind speeds the representative wind speed $(1/\{1/u\})$ has been determined for each wind speed class: 1.45, 4.0 and 8.0 m/s.

f. Plume rise

The effective stack height H [m] is equal to the sum of the physical stack height h [m] and the plume rise Δh [m]. The plume rise formulas of Briggs (Briggs, 1971) and Concawe (Concawe, 1966) have been used in these calculations depending on the heat output Q_H [Mwatt] of the source.

g. Area source description

The dispersion from an area source has been modelled by a so-called virtual point source in the centre of the area source. The equation for the virtual point sources is identical to (1) except for an extra term in the denominator. This term is needed to model the initial dilution by the area source. A fixed effective source height of 10 m is used.

The virtual point source will lead to unacceptable results for the concentration inside the area source itself. This problem is avoided when the area sources are chosen to coincide with the calculation grid.

Because of a lack of data no mixing height has been applied in these calculations. Also the effect of decay and deposition, which are assumed to be of little importance for the calculation of long term averages, has been neglected.

III. Input parameters

a. Emission inventory

The region, for which the validation is carried out, consists of an area of 25x20 km near Amsterdam (figure 1). The location of the area and point sources has been indicated in figure 1.

The point source data are given in table 3. Some large sources outside the region of computation have also been included in the calculations; they are also indicated in figure 1. The region is situated near two large bodies of water (the North Sea and the Ysselmeer). Because of these inhomogeneities the region is not ideally suited for an application of the Gaussian plume model.

Table 3. The physical stack height (h), and the heat output Q_H of the point sources.

h [m]	Q_H [Mwatt]
40	1.8
50	0
100	15
90	0.1
26	8.2

b. Meteorological data

For the validation period in 1972 the distribution function $F(\theta_i N, S)$ has been calculated from meteorological parameters, which are routinely measured at Schiphol Airport. Although this station is situated a few kilometres south of the validation area, the data are considered to be representative, for the meteorological situation in this region. However, the description of the meteorological situation by one station in an inhomogeneous region as described above is open to question.

c. Grid specifications

The calculations have been performed on a square grid of 20x25 km with a grid size of 1 km (figure 1). The area sources have been subdivided into squares of 1x1 km, which coincide with the grid squares.

IV. Emission data

a. Concentration measurements

The SO_2 concentrations have been measured in and around the computation region at the points shown in figure 2.

The SO_2 immission is determined by taking 24-hour air samples, which are chemically analyzed by means of the pararosalinin method. From these 24-hour averages an average over the validation period has been calculated.

In figure 2 a concentration pattern has been drawn from the concentrations in the measuring points. This was done because the measured concentrations can be heavily influenced by local emission conditions, which cannot be described by the model. By designing a pattern by means of the measured values these local influences might be smoothed out.

The deviation in the 24-hour average concentration is estimated to be 15%. If it is assumed that the sampling errors are neither correlated nor systematic, this will lead to a negligible deviation of ~ 1% in concentrations averaged over six months.

b. Background concentration

The background concentration can be defined as the concentration in the region caused by sources outside the region, which are not included in the calculations.

An estimate of this concentration has been obtained by selecting periods of 24 hours during which the wind direction is in a sector of 90° north, east, south and west. For these periods the concentrations in measuring points on the upwind side of the validation region are assumed to be representative for the background pollution transported in the direction of these wind directions.

It was observed that these concentrations were high for wind directions from the east sector and south sector and low from the other sectors, because the air for these wind directions is transported primarily over sea. When the background concentration for each wind direction is multiplied by the distribution function of wind directions $\sum_N \sum_S F(\theta_i, S, N)$ the total background concentration is found to be: $\chi_b = 33\ \mu gr/m^3$.

This number has been added to all the calculated results. We realize that this is a very crude way to obtain a background concentration. Other meteorological factors except wind direction may have a large influence on the background concentration. Therefore validation results, in which the background concentration plays a role, should be considered with proper care.

V. Validation methods

Various validation methods have been tried in order to obtain more detailed information on the performance of the model. The validation has been carried out for three different cases:

A The concentrations calculated at the measuring points or at receptor points are compared with the measured concentrations.

B From the measured concentration pattern (figure 2) the concentrations at the grid points have been obtained by interpolation. These concentrations were then compared with the calculated concentrations at the grid points.

C The geographical source pattern will influence both the measured and the calculated concentration in a similar way: high concentrations are to be found near the sources, both in the measured and calculated concentrations. So the spatial correlation between the observed and calculated concentrations is to a certain extent determined by the source configuration. In order to estimate this bias in the validation a test has been performed in which it was assumed that the concentration was directly proportional to the local emission. Thus transport from neighbouring sources is neglected. This procedure is essentially equal to the simple model of Gifford and Hanna (1973) and is described in appendix I.

The validation for the cases A, B and C has been performed by calculating several statistical parameters:

I The correlation coefficient calculated from the points where both the measured and calculated concentrations were known.

II The rank correlation coefficient calculated for the same points as mentioned in I. The advantage of the rank correlation is that it can be applied to non-Gaussian distributions.

III The frequency distribution of the measured and calculated concentrations over all points where these are known.

IV The average and standard deviation of the absolute and relative difference between the observed and calculated results.

From the correlation coefficients is found how well the spatial concentration pattern is described. The frequency distribution indicates whether the distribution of concentration over all receptor points is properly simulated. The statistics of the differences indicate how well the model may be assumed to perform at an arbitrary point.

VI. Results

The results of the calculations are shown in figure 3. The validation for the three cases A, B, C described in chapter V is explained hereafter. One should note that in this section the calculated concentration at a point means an average concentration over the validation period of six months.

A Receptor points

In table 4 the average and the standard deviation of the calculated and observed concentrations (respectively χ_c and χ_o) over the receptor points are given.

Table 4. Results of the validation in the receptor points (55 points). The mean (m) and standard deviation (σ) of the observed and calculated concentrations: χ_o and χ_c over these points; the correlation coefficient and the rank correlation coefficient: r and r_k; the mean (m), standard deviation (σ) and range (r) of the absolute relative difference: $\chi_c - \chi_o$ and $(\chi_c - \chi_o)/\chi_o$.

	χ_c [$\mu g/m^3$]	χ_o [$\mu g/m^3$]	$\chi_c - \chi_o$ [$\mu g/m^3$]	$\frac{\chi_c - \chi_o}{\chi_o}$
mean	58.4	64.2	-6.0	-0.05
s.d.	13.6	21.3	13.6	0.20
range	-	-	74	1.0

correlation	0.78
rank correlation	0.80

The mean overall grid points of the calculated concentration χ_c is slightly lower than the mean of the measured concentration χ_o. However, this result is directly dependent on the background concentration.

The standard deviation of the calculated concentrations over the grid points is less than the standard deviation of the observed concentrations. Apart from model defects two other effects might be responsible for this. First, the standard deviation of the observed concentrations is largely affected by very high concentrations measured in the city of Amsterdam; these are due to local sources, which are not resolved by the model. Second, the emissions have been estimated from average fuel consumption over a large area (figure 1). More detail, which undoubtedly is present in this emission pattern, will increase the standard deviation of the calculated results.

The correlation coefficient r and the rank correlation coefficient r_k are also given in tabel 4. As might be expected, r_k is slightly higher than r. A scatter diagram of the measured and calculated concentrations in the receptor points is shown in figure 4, together with the linear regression line. The correlations are reasonably good.

Next, in table 4, the results concerning the absolute difference $\chi_c - \chi_o$ and the relative difference $\chi_c - \chi_o / \chi_o$ are given. The mean value, the standard deviation and the range, which is the difference between the maximum and minimum value, for both differences have been calculated from the results in the receptor points.

The mean value may be considered a systematic error in the calculated results. Once more it must be said that this value is directly dependent on the background concentration.

The standard deviation and the range are representative for the non-systematic errors. From these standard deviations a confidence limit can be constructed for the calculated results.

The frequency distribution of the calculated and observed results over all measuring points is shown in figure 5. The correspondence between the two frequency distributions is satisfactory. The larger variance of the measured concentrations is also apparent from this figure.

B Grid points

The results as discussed in section A above are for this case given in table 5 and figure 6.

Table 5. Results of the validation in the grid points (122 points). See caption of table 4 for the meaning of the symbols.

	χ_c [$\mu g/m^3$]	χ_o [$\mu g/m^3$]	$\chi_c - \chi_o$ [$\mu g/m^3$]	$\frac{\chi_c - \chi_o}{\chi_o}$
mean	53.6	55.4	-1.8	0.0
s.d.	9.7	14.9	9.7	0.17
range	-	-	48	0.87

correlation	0.77
rank correlation	0.77

From these results it follows that the standard deviation of the measured concentration has decreased. The same is true, however, for the calculated concentration. So that also in this case the conclusion is that the spatial variance of the calculated results is too low.

Both correlation coefficients did not change significantly. The standard deviations of the absolute and relative difference have decreased. The agreement between the frequency distribution of the measured and calculated concentrations in the grid points is fair.

In figure 7 the isopleths of constant difference between measured and calculated concentrations are shown.

We may, therefore, conclude that for this situation validation at the grid points does not add many different aspects to the results of the validation on the receptor points.

C Influence of source configuration

The validation in this case has been performed with a model in which the concentration is directly proportional to the local emission. (Appendix I).

As this model describes only area sources, the contribution of the point sources to the concentration has to be subtracted. The contribution from the point sources is estimated with the Gaussian plume model (1). The error caused by this procedure is presumably small, as the relative contribution of the point sources is small.

The results obtained by means of this simple model are shown in table 6 and figure 8. They are comparable to those obtained by means of the Gaussian plume model.

Table 6. Results of the validation in the receptor points (55 points) with the simple model described in appendix I. See caption of table 4 for the meaning of the symbols.

	χ_c [$\mu g/m^3$]	χ_o [$\mu g/m^3$]	$\chi_c - \chi_o$ [$\mu g/m^3$]	$\frac{\chi_c - \chi_o}{\chi_o}$
mean	52.3	56.9	-4.6	-0.06
s.d.	10.4	14.8	10.4	0.16
range	-	-	48	0.66

correlation	0.71
rank correlation	0.79

VII. Discussion and conclusions

The results of section A and B of chapter VI indicate that a long term averaged concentration can be reasonably calculated by means of the Gaussian plume model.

From the correlation coefficient, which is about 0.8, follows that about 60% of the spatial variance is explained.

The problem remains that the Gaussian plume model has been applied in this case to a complex source region. It is virtually impossible to infer from this validation the performance of the Gaussian plume model for a single source.

Another problem related to the complex source region is the fact that the source configuration influences both the measured and the calculated validation results in a similar way. It follows from the results of section C, chapter VI, in which the concentrations have been calculated from a simple model based on direct proportionality between emission and concentration, and on neglecting transport, that this influence may be very important.

It is difficult to estimate if and how much the Gaussian plume model improves upon the simple model. The results of the simple model compared with the measurements are at least as good as the results of the Gaussian plume model.

However, from the calculation with the Gaussian plume model it follows that the concentrations calculated in the neighbourhood of Haarlem can for 33% be ascribed to the area source of Amsterdam, which is in direct contradiction to the simple model.

A choice between the two models on the results presented is not possible. From a physical point of view, however, the Gaussian plume model is to be preferred to the simple model, because the latter model totally neglects the transport of pollution.

References

Briggs, G.A. Some recent analyses of plume rise observation. Proc. of the Second International Clean Air Congress (1971), pp. 1029-1032.

Bringfelt, B., Hjorth, T. and Ring, S. A numerical air pollution dispersion model for central Stockholm. Atm. Env. (1974), Vol. 8, pp. 131-148.

Calder, K.L. A climatological model for multiple source urban air pollution. NATO-CCMS, Proceedings 2nd Meeting (1971), pp. I-1, I-33.

Concawe The calculation of atmospheric dispersion from a stack (1966).

Corlin, A. The User's need for precise description and verification of a model. NATO-CCMS, Proceedings 5th Meeting (1974), pp. 15-1, 15-4.

Fortak, H.G. Numerical simulation of temporal and spatial distributions of urban air pollution concentration. Proc. Symp. on Multiple-Source Urban Diffusion Models (1970), EPA-AP-86.

Gifford, F.A., Hanna, S.R. Modeling urban air pollution. Atm. Env. (1973), Vol. 7, pp. 131-136.

Johnson, W.B. Validation of air quality simulation models. NATO-CCMS, Proceedings 3rd Meeting (1972), pp. VI-1, VI-9.

Klug, W. Dispersion from tall stacks. NATO-CCMS, Proceedings 5th Meeting (1974) pp. 36-1, 36-8.

Koch, R.C., Thayer, S.D. Validation and sensitivity analysis of the Gaussian plume multiple-source urban diffusion model (1971), Geomet report No. EF-60.

Marsh, K.J. Withers, V.R. An experimental study of the dispersion of the emissions from chimneys in Reading, III The investigation of dispersion calculations. Atm. Env. (1969), Vol. 3, pp. 281-302.

Martin, D.O. An urban diffusion model for estimating long term average values of air quality. J.A.P.C.A. (1971), Vol. 21, No. 1, pp. 16-19.

Nieuwstadt, F.Th.M. Stability categories and dispersion coefficients.
Royal Netherlands Meteorological Institute (1975),
W.R. 75-3 (in Dutch).

Olssen, L.E.
Ring, S.
Validation of urban air pollution models.
NATO-CCMS, Proceedings 5th Meeting (1974),
pp. 25-1, 25-12.

Pooler, F.
A prediction model of mean urban pollution for
use with standard wind roses.
Int. J. Air and Water Poll. (1961), Vol. 9,
pp. 199-211.

Shieh, L.J.
Davidson, B.
Friend, J.P.
A model of diffusion in urban atmosphere:
SO_2 in greater New York.
Proc. Symp. on Multiple-Source Urban Diffusion
Models (1970), EPA-AP-86.

Singer, I.A.
Smith, M.E.
Atmospheric dispersion at Brookhaven National
Laboratory.
Int. J. Air and Water Poll. (1966), Vol. 10,
pp. 125-135.

Smith, M.E.
Singer, I.A.
An improved method of estimating concentrations
and related phenomena from a point source
emission.
J. Appl. Met. (1966), Vol. 5, pp. 631-639.

Turner, D.B.
A diffusion model for an urban area.
J. Appl. Met. (1964), Vol. 3, pp. 432-438.

Turner, D.B.
Workbook of atmospheric dispersion estimates.
U.S. Dept. of Health, Education and Welfare,
No. 999-AP-26.

-o-o-o-

Acknowledgement

The supplying of emission data by the "Provinciale Waterstaat Noord Holland" is gratefully acknowledged. The concentration measurements were provided by the "Zaanse Commissie voor hygiëne van het milieu" and the "Centrale Coördinatiecommissie meting luchtverontreiniging Noorzeekanaalgebied". The authors wish to thank Mr. E.H.J. Vermaas for the writing of computer programs, and Mr. S. Kruizinga for the discussions on statistical problems. Mr. C.A. Engeldal assisted in a very helpful way during the calculations. The authors are indebted to the director in chief of the Royal Netherlands Meteorological Institute, dr. M.W.F. Schregardus, for his permission to undertake this study.

-o-o-o-

Appendix I

Simple area source model of Gifford and Hanna (1973)

In this model it is assumed that the concentration in an area source of about 1x1 km can be determined by the following equation:

$$\chi = c \frac{q}{U} \qquad \text{I.1}$$

where $\chi\,[\mu g/m^3]$ is the concentration inside the area source with a strength of $q\,[\mu g/m^2 s]$. The wind at 10 m is chosen as the transport velocity $U\,[m/s]$. The dimensionless constant of proportionality c is chosen to be 50. (Gifford and Hanna, 1973).

From I.1 the concentration averaged over the total validation period can be calculated when a representative U for this period is substituted. This value of U is found from the distribution function $\sum_{\theta_i}\sum_{S} F(\theta_i, S, N)$ of wind speed classes.

The concentration averaged over the total period is then only directly proportional to the local area source strength. Thus transport from other area sources is neglected.

The background concentration is added to the results calculated with I.1.

-o-o-o-

Captions to the figures

Figure 1. Point source and area source configuration. The point sources are indicated by dots. Also is shown the coordinate axes and the coordinate centre. Distances in km.

Figure 2. The measured concentration pattern averaged over the validation period of six months. Concentrations are in $\mu g/m^3$. The sampling stations and the average measured concentrations are indicated.

Figure 3. The calculated concentration pattern averaged over the validation period. Concentrations are in $\mu g/m^3$. The receptor points located at the sampling station are indicated together with the average calculated concentration.

Figure 4. Scatter diagram of calculated and observed concentrations in the receptor points.

Figure 5. The cumulative spatial frequency distribution of the measured and calculated concentrations over the receptor points.

Figure 6. The cumulative spatial frequency distribution of the measured and calculated concentrations over the grid points.

Figure 7. Isopleths of constant difference between measured and calculated values: $\chi_o-\chi_c$.

Figure 8. The cumulated spatial frequency distribution of the measured and calculated concentrations over the receptor points for the validation with the simple model described in appendix I.

FIG.1

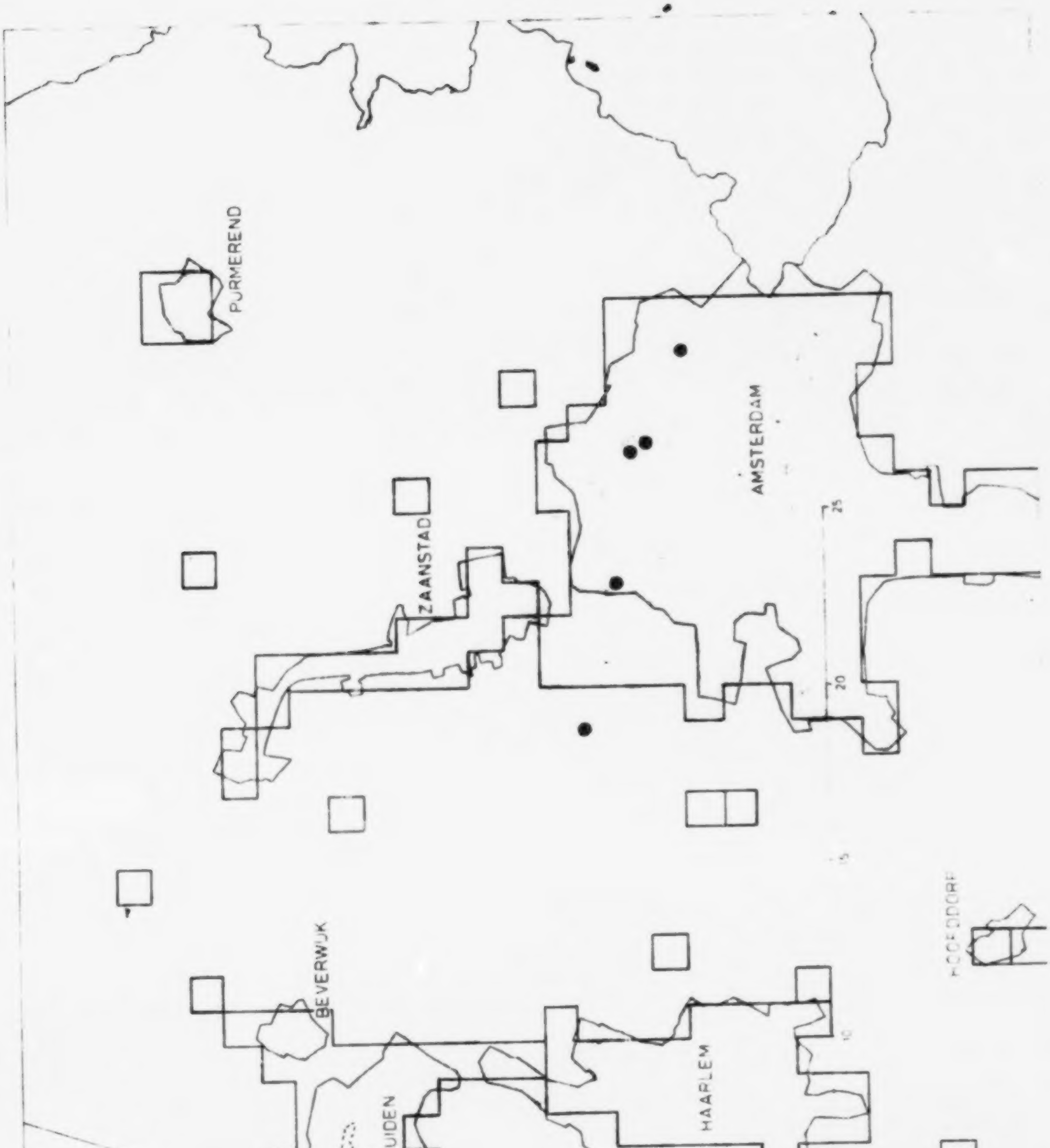
N
PURMEREND
ZAANSTAD
AMSTERDAM
BEVERWIJK
IJMUIDEN
HAARLEM
ZANDVOORT
HOOFDDORP
20
15
10
5
0
10
15
20
25

FIG. 2

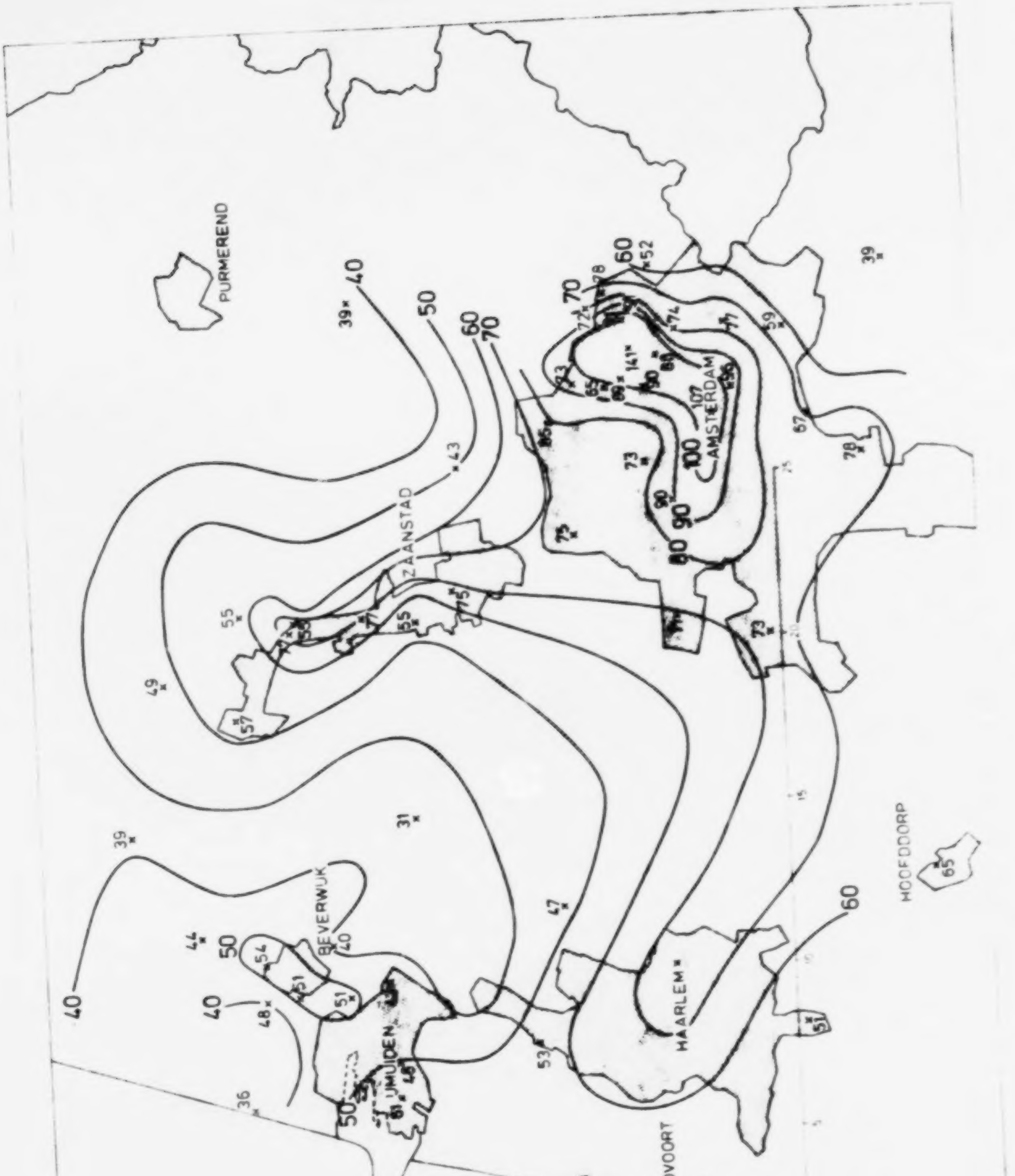
N
PURMEREND
ZAANSTAD
AMSTERDAM
BEVERWIJK
IJMUIDEN
HAARLEM
ZANDVOORT
HOOFDDORP
40
50
60
70
80
90
100
0
5
10
15
20
25

FIG 3

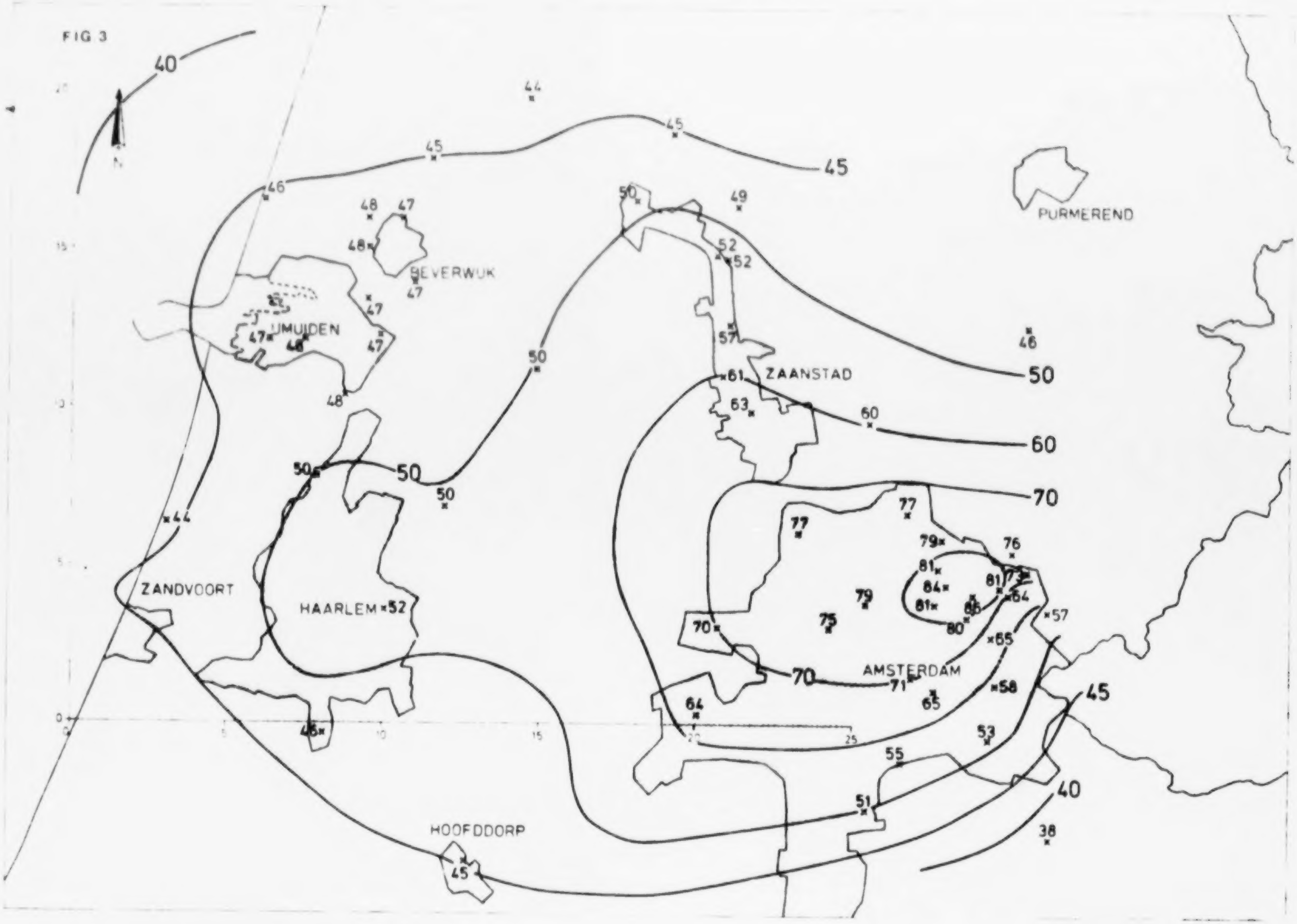
N
PURMEREND
BEVERWIJK
IJMUIDEN
ZAANSTAD
ZANDVOORT
HAARLEM
AMSTERDAM
HOOFDDORP
40
45
50
60
70
0
5
10
15
20
25

FIG.4

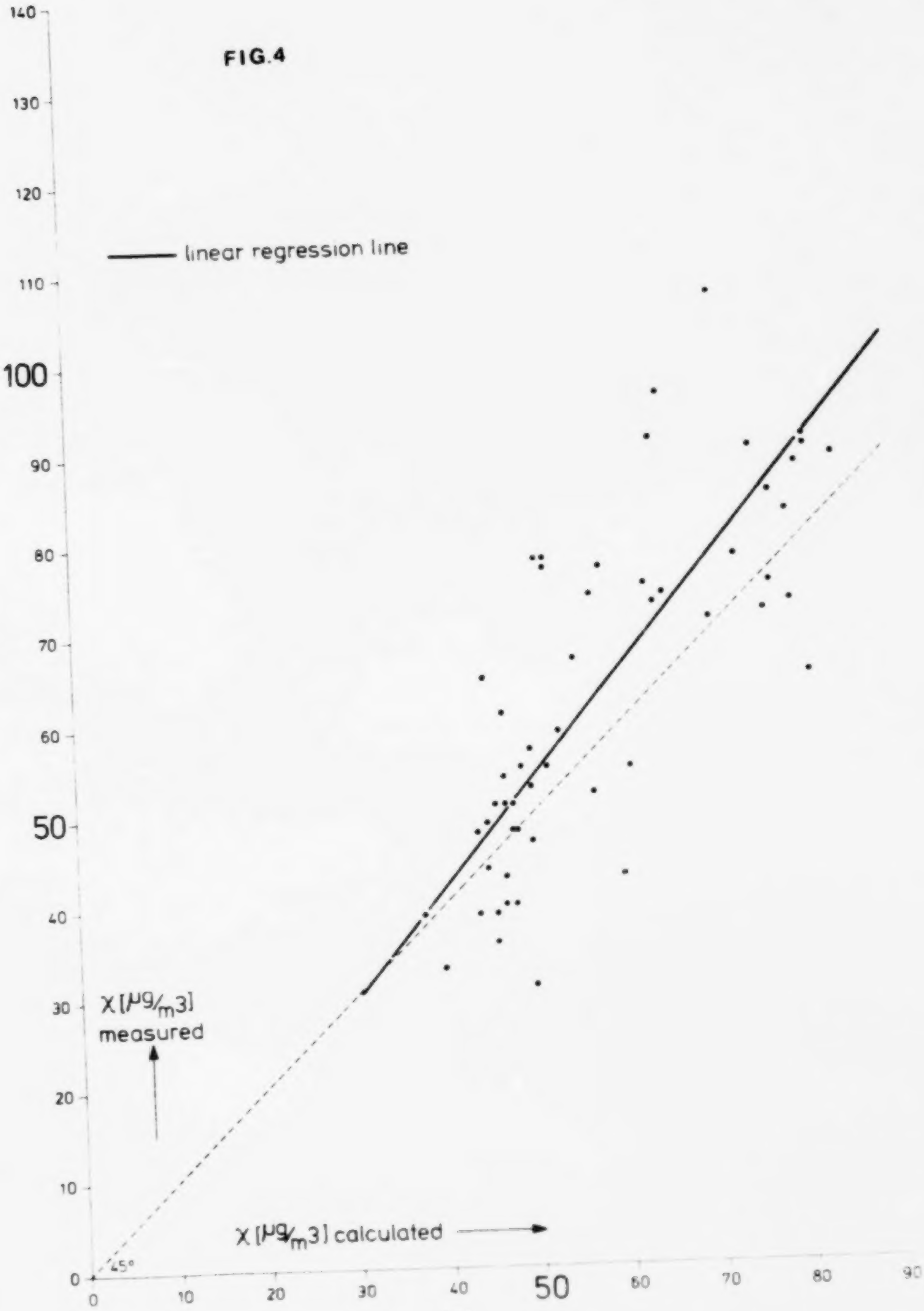
140
130
120
110
100
90
80
70
60
50
40
30
20
10
0
linear regression line
χ [μg/m3] measured
χ [μg/m3] calculated
45°
0
10
20
30
40
50
60
70
80
90

FIG.5

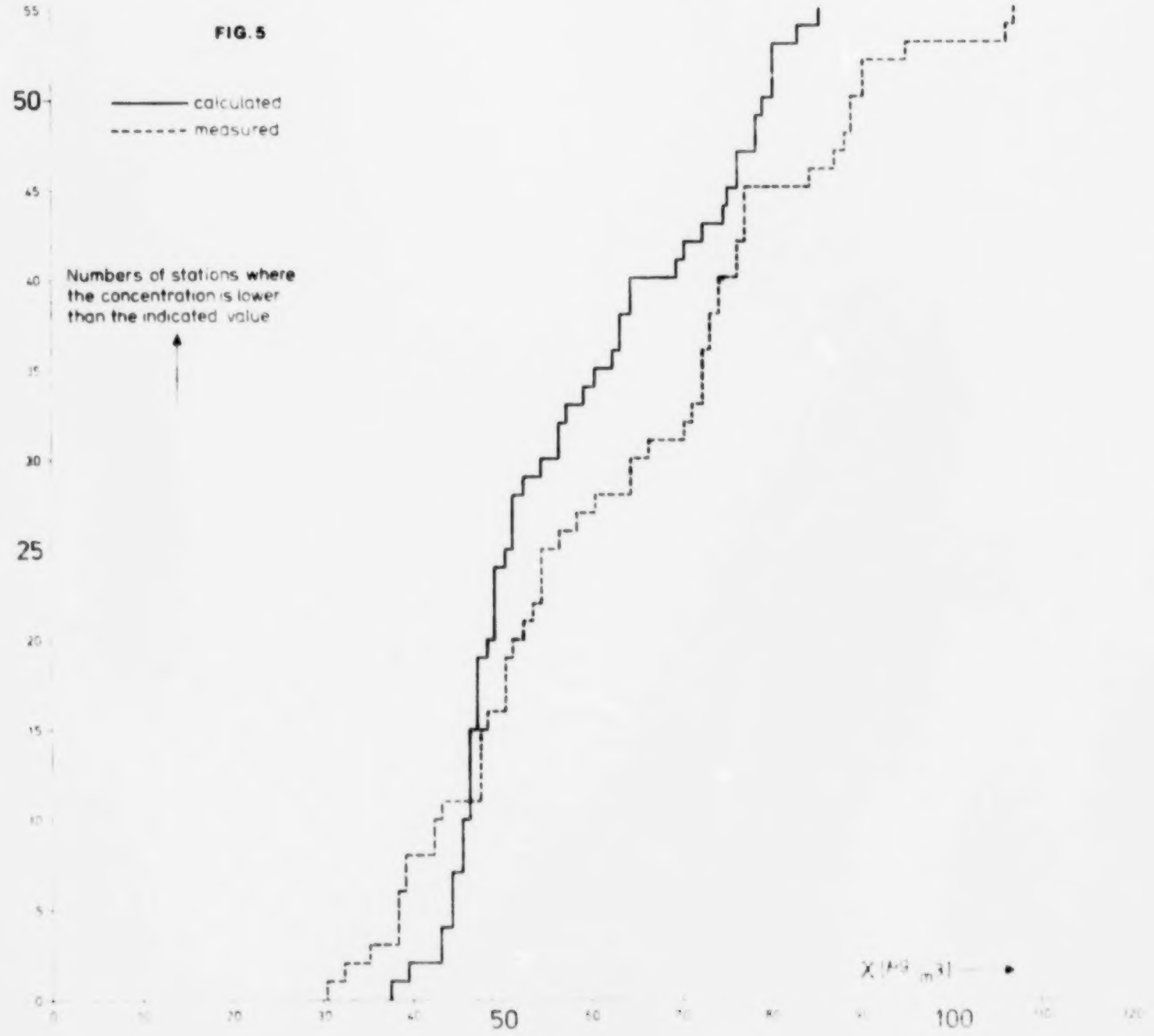
calculated
measured
Numbers of stations where the concentration is lower than the indicated value
55
50
45
40
35
30
25
20
15
10
5
0
0
10
20
30
40
50
60
70
80
90
100
110
120
X (µg/m³)

FIG.6

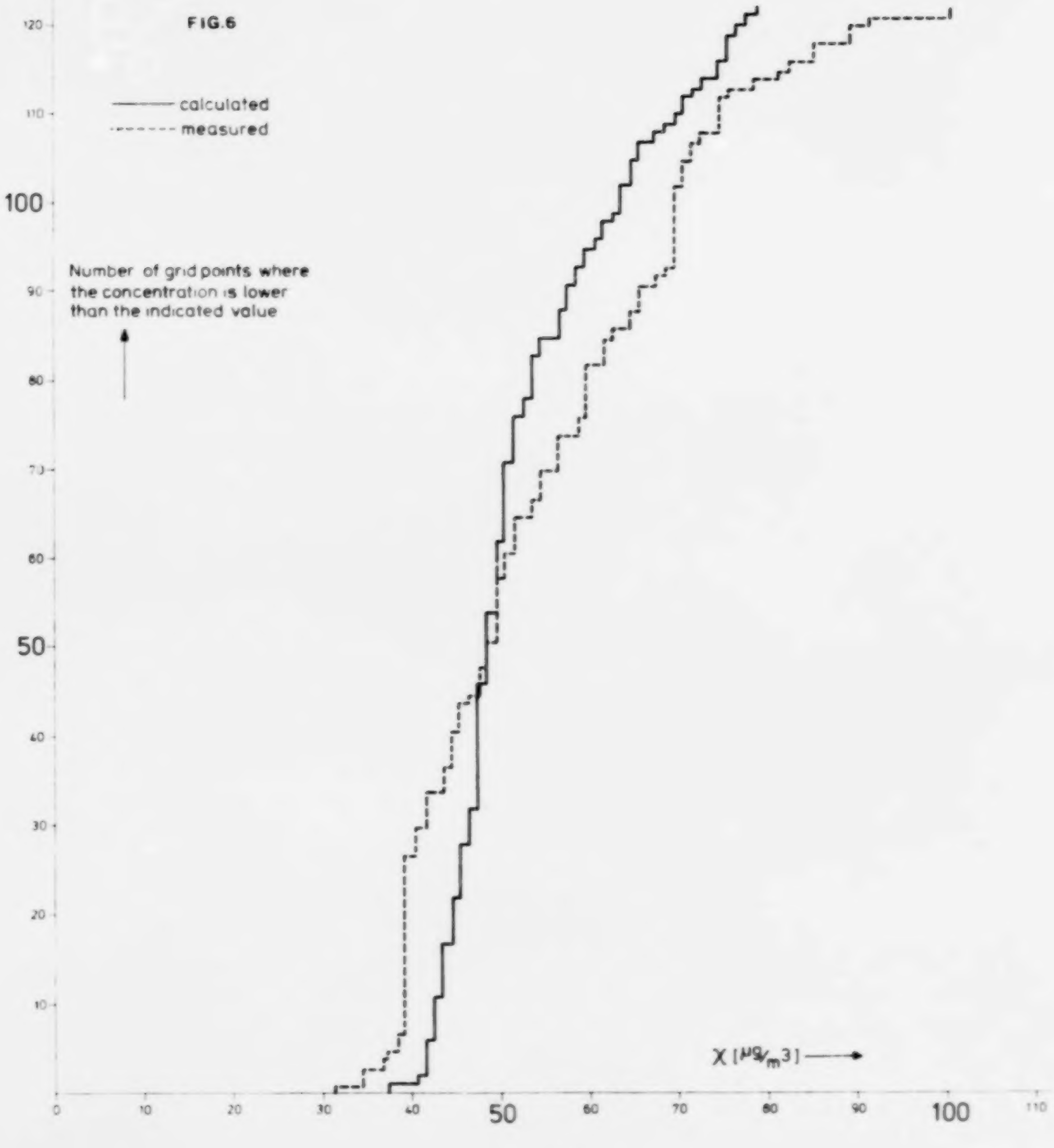

120
110
100
90
80
70
60
50
40
30
20
10
calculated
measured
Number of grid points where the concentration is lower than the indicated value
χ [µg/m3]
0
10
20
30
40
50
60
70
80
90
100
110

FIG.7

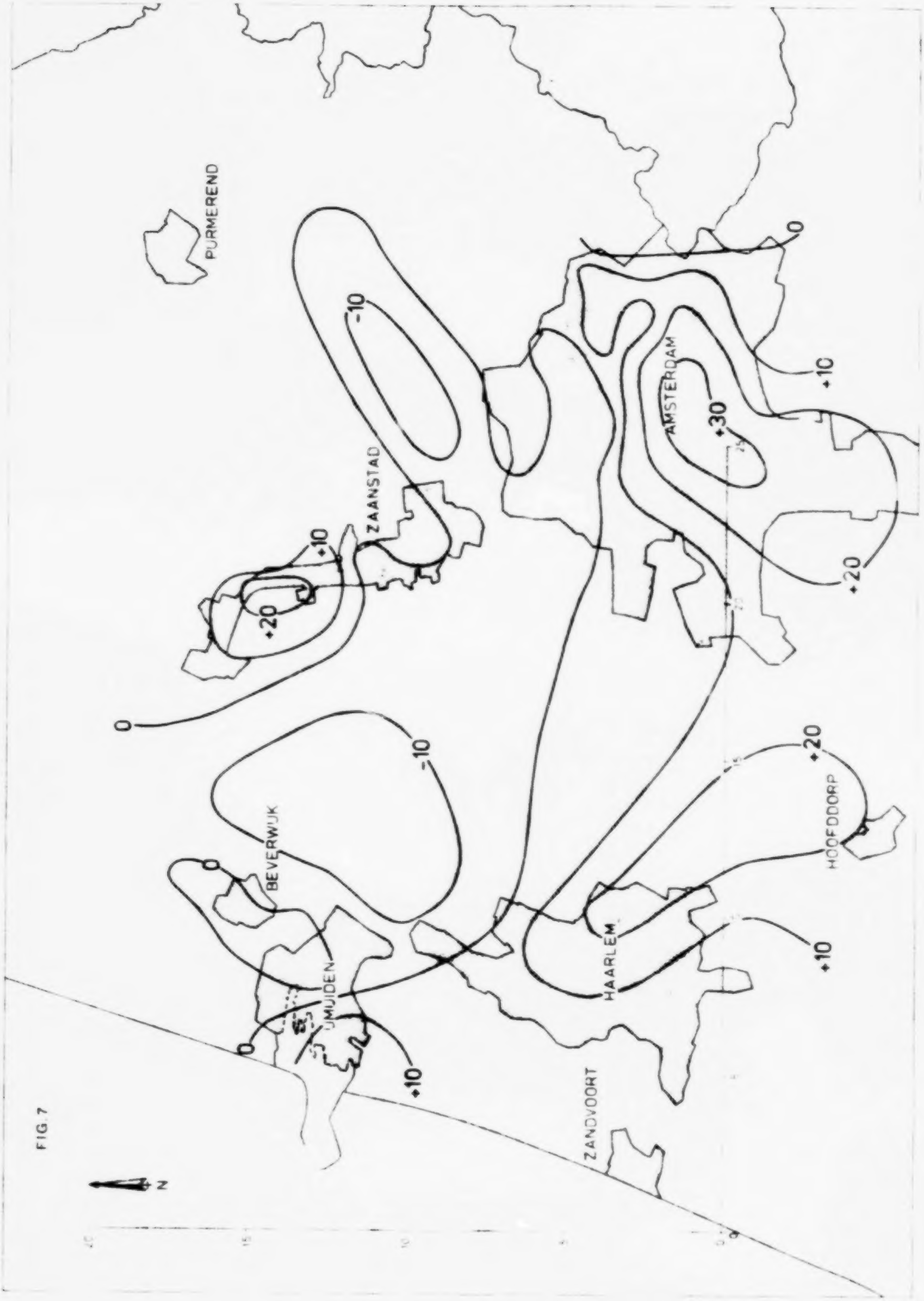
N
PURMEREND
ZAANSTAD
AMSTERDAM
BEVERWIJK
IJMUIDEN
HAARLEM
HOOFDDORP
ZANDVOORT
0
-10
+10
+20
+30
-10
0
+20
+10
0
+10
+20
+10
0
+10
0
5
10
15
20

FIG.8

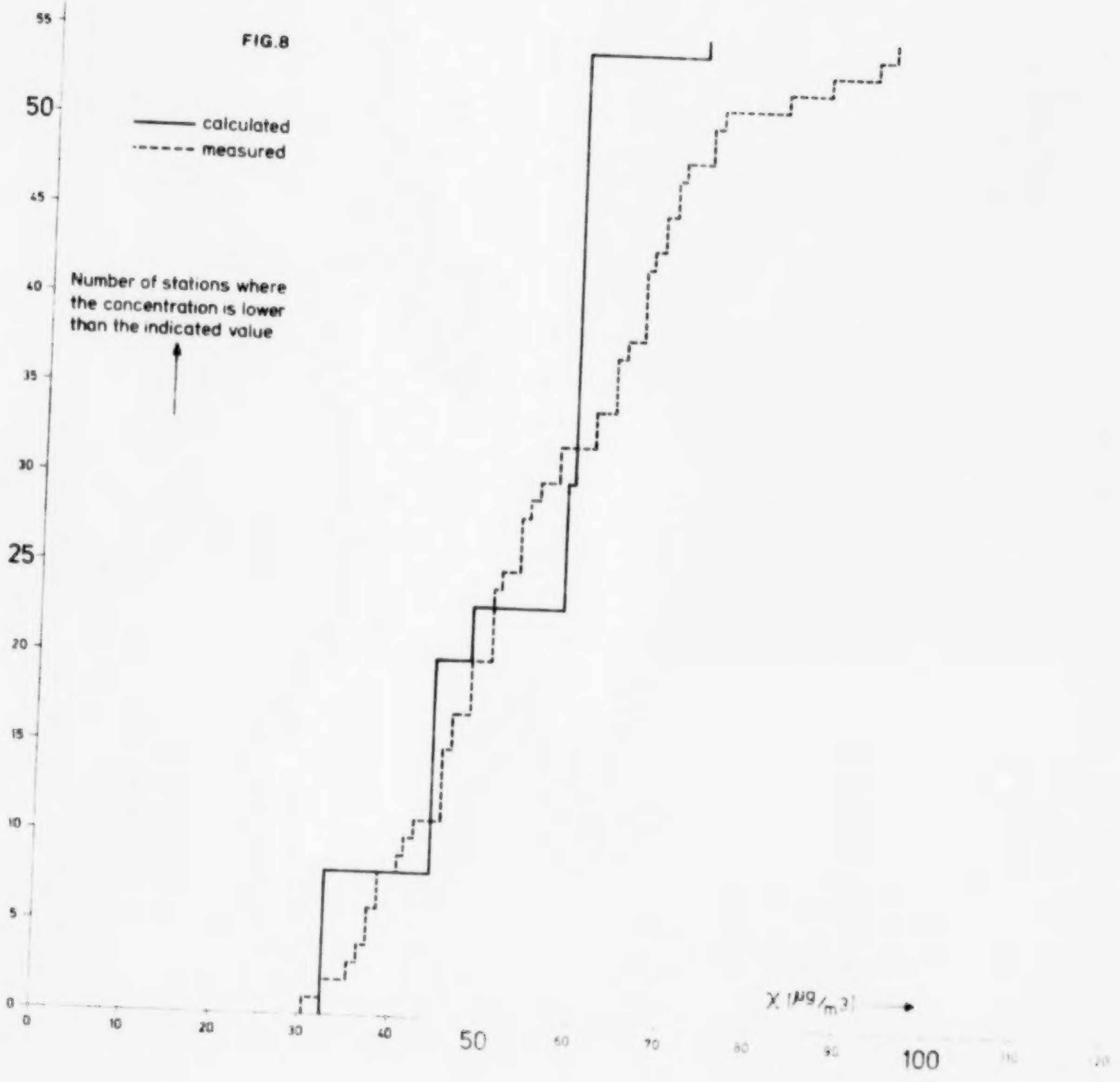
calculated
measured
Number of stations where the concentration is lower than the indicated value
55
50
45
40
35
30
25
20
15
10
5
0
0
10
20
30
40
50
60
70
80
90
100
110
120
χ ($\mu g/m^3$)

Rapporteur's Report, Topic IV, September 26, 1975

by C. F. Barrett

Chairman: M. Kwizak

In his opening remarks the Chairman expressed some disappointment at the lack in the papers presented at the meeting, of new models as distinct from the application of existing models, sometimes with modifications, to new cities. He hoped that Canada would in the next year contribute to the development of new regional and possibly urban models and report to the next meeting.
He remarked that there was no agreement on the distinction between global, regional and urban models. Some workers considered distances of 80 - 100 km from the source to be the province of regional models; the OECD regarded distances of greater than 150 km as implying long-range transport, but the criterion used was probably whether the pollution crossed frontiers and the chairman regarded this as unsatisfactory. He thought regional problems were those that do not involve an impact on (reasonably) nearby ground-level receptors. On this definition a local problem can be changed into a regional problem by increasing the stack height and he gave as an example, illustrated by slides, the Sudbury IWCO plant which emitted 2,9 x 10^6 tons/year of SO_2 from two nearby stacks. For many years three relatively low stacks were used and the countryside up to 30 km away was devastated. In the fall of 1972 a 380 m stack with high exit velocity was installed which removed the local problem. The behaviour had been extensively studied with photographs, airplane traverses of the plume and satellite photographs. The plume now travels distances of order 120 miles before losing its identity and thus large quantities of SO_2 are transported far afield so that there was now concern about acid rain i. e. a regional problem. In so far as the acidity of the soil may contribute to the emission of N_2O from fertilizers which where transported upwards is destructive of the ozone layer (as suggested by Mc Elroy to be far more important than freons and supersonic transports) this SO_2 contributes to a global problem.

B. Turner: An efficient Gaussian-Plume Multiple-Source Air Quality Algorithm.

Mr. D. B. Turner presented a paper on an efficient Multiple-Source Air Quality Algorithm.

In answer to Mr. Grønskei Mr. Turner said that the maximum distance to which the model could be applied was limited by the knowledge of the dispersion parameters and ultimately by the assumption of a steady state. In answer to Mr. Braig he thought that poor knowledge of dispersion parameters was the major cause of the tendency of models of this type to overestimate. Another problem raised by Mr. Slater lays in the need for hourly values of the mixing height. Mr. Turner said that these were input data external to the model. In the USA they were obtained by interpolation between the twice daily radiosondes.

W. B. Johnson: Feasibility Demonstration of an Air Budget Model for the Assessment of Transfrontier Air Pollution.

Mr. W. B. Johnson presented paper (b) on a feasibility demonstration of a "buff" model for transfrontier pollution. Mr. Grønskei thought that case studies were better for studying effects particularly when damage is confined to particular episodes, but Mr. Johnson considered that there was a need to study long-term effects as well as episodes. The same speakers agreed that the treatment of dry deposition in the model needed improvement.

A discussion between Mr. Johnson and Mr. Slater concluded that for validation vertical mapping of the pollution was required and that remote sensing would probably provide the best means of obtaining it.

Mr. Scholberg remarked that the figure of $ 190 for the cost ofcalculations and output was misleading because the cost of input of the data would be much greater. Mr. Johnson said that the data were already on mag tape from a previous investigation.

H. van Dop: Validation of a Multiple Source Diffusion Model, based on the Gaussian Plume.

Dr. van Dop presented a paper on validation of a multiple source diffusion model. Dr. Sivertsen questioned the use of the CONCAWE plume rise formula.

Dr. Vogt made the general remark that there was insufficient information on dispersion parameters in rough terrain.

6th NATO/CCMS
International Technical Meeting
on Air Pollution Modeling

TOPIC V

NEW MODELING TECHNIQUES

Battelle - Institut e.V. Frankfurt / M
Germany, FR
24 - 26 September, 1975

6th NATO/CCMS
International Technical Meeting
on Air Pollution Modeling

SIMULATION OF SO_2-DISPERSION IN THE VENETIAN AREA

by

Runca, E. - Melli, P. - Zannetti, P.

Centro Ricerca IBM, Venezia, Italy

BATTELLE - INSTITUT E.V., Frankfurt/Main
Germany, FR
24-26 September, 1975

Preceding page blank

Abstract

This study tests the possibility of describing the dispersion of atmospheric pollutants, in a complex coastal zone such as the Venetian area, by means of a diffusion model. The simulation of SO_2 - dispersion is carried out by developing two different models. One is a Gaussian type diffusion model, the other one is based on the numerical -integration of the diffusion equation written according to the K-theory. The Gaussian model is based on the assumption that the pollutant has a Gaussian distribution along the vertical and is uniformly distributed crosswind in each sector of the wind rose.
With the use of meteorological data recorded on an hourly-basis and average evaluations of urban and industrial emissions, SO_2 three-monthly average concentrations were computed for the period Feb.'73-Feb. '74. The results were compared with the concentration values recorded at ten monitoring stations during the same period. In this comparison a correlation coefficient equal to 0,718 for the year '73 and to 0,798 for the year '74 were obtained. The general agreement between the model results and the measured data proved the validity of the applied technique for simulating long term average concentrations in the Venetian area and its applicability for land planning purposes.
The model based on K-theory integrates the time dependent diffusion-concentration equation according to the method of fractional-steps. The implemented numerical technique allows for variable grid spacing and time steps. Comparison between numerical and analytical solutions proved satisfactory. The model has not, as yet, been applied to the real phenomena because of unsatisfactory input data. It has been designed with the purpose of simulating short term SO_2 - average concentrations and complementing the Gaussian model.

Introduction

Many attempts have been made in the last two decades to simulate SO_2 concentration fields in areas affected both by industrial and urban emissions (Pooler 1961, Turner 1964, Shieh 1971, Calder 1971, Martin 1971, etc.). The models developed for such a purpose have proved to work well in situations in which the parameters affecting the dispersion were rather uniform over the whole area. In more complicated areas, on the contrary, further implementations of diffusion models up to now realized are needed in order to formulate a satisfactorily precise idea of their reliability as well as of their limits.

Venice and its surroundings are a typical example of an area in which the dispersion of the atmospheric pollutants is greatly affected by the non-uniformity of its geographic characteristics. In this area the presence of different types of adjacent surfaces (land, lagoon and Adriatic Sea, see fig.1) induces a local circulation which interacts with the synoptic wind making it very difficult to identify the dispersion patterns of a pollutant.

On the other side the study of Air Pollution problem in Venice is made urgent by the damages that pollution causes to its priceless artistic patrimony.

In order to give a practical contribution to this problem an application of diffusion models is being carried out.

The problem was tackled by applying, as a preliminary attempt, a Gaussian type model, by which three montly average concentrations as well as the annual ones were simulated for the years 1973 and 1974. The discussion of the obtained results constitutes the essential part of this article. Later, a diffusion model based on numerical integration of the diffusion equation, written according to the K-theory, will be briefly analyzed. Such a model was built in order to take into account the local characteristics which cannot be included in the previous model.

Application of the Gaussian model

Since the region under investigation shows the presence of a large industrial area (situated in the mainland) as well as three densely populated urban areas (Marghera and Mestre on the mainland, Venice on the islands at the center of the Lagoon, see fig. 1) both industrial and urban pollution must be taken into account in the model.

Data concerning industrial sources were taken from an inventory carried out by the Local Government in 1972 according to the National Law about Pollution promulgated in April 15th, 1971. Such an inventory showed the presence of 74 stacks with a total emission rate of 160000 tons/year and a range of heights from 10 to 120 m.

The knowledge of the average strength of sources introduces in the model computations a certain inaccuracy, which otherwise is somewhat reduced by the fact that long term averages are calculated.

The evaluation of the spatial distribution of domestic heating emissions was made on the basis of the last national general census, taken in 1972, which furnished a great mass of information not only about the distribution of the population but also about the state of buildings and their facilities (e.g. domestic heating plants).

For the 272 sections, in which the urban districts of the Venetian Area were subdivided, the consumptions of polluting fuels and therefore the yearly emissions of SO_2 were computed.

As for the definition of the emission rates (variable throughout the different periods of the year), it was achieved by using the concept of day/degree, defined as:

$$dd = T_b - \frac{\sum_{i}^{24} T_{h,i}}{24}$$

where T_b is the temperature at which heating starts and T_{hi} is the average hourly temperature at i-th hour of the day.

In Venice T_b is equal to 15,5 C. The total yearly emission was distributed over the whole "cold period", proportionally to the days/degree, as shown in fig. 2.

The above calculated fractions of the total yearly emission were then used to calculate the emission rates for each of the 272 above mentioned sections. Every area emissions was finally introduced in the model as an equivalent constant strength point source, located in the barycenter of the corresponding section.

The height of the urban emissions, including plume rise, was estimated to be about 30 m in the historical center of Venice (whose buildings are generally old and low) and around 45 m. in the urban areas of the mainland, which have developed in the last three decades and show taller buildings. Meteorological data as well as SO_2-concentration data were supplied by the network that Tecneco installed in Venice by appointment of the Istituto Superiore di Sanità (Superior Institut for Health). It consists of one meteorological station situated in the historical center of Venice and of 24 monitoring sensors (fig. 1).

The meteorological station records on an hourly basis wind speed, wind direction according to the eight sectors of the wind rose, temperature, pressure, rainfall, humidity, cloudiness and fog. Concentration data recorded by the 24 monitoring sensors are transmitted to a small computer which elaborates the data and prints the hourly average values as well as daily statistics. Besides that, every time the 30 minutes average SO_2- concentration "standard" (.30 ppm) imposed by the Italian law is exceeded in a station the computer gives an alert. Since only 10 stations were regularly operating from February 1973, the model has been tested on the data recorded by them in the period February 1973 - January 1975. Anyway some results will also be given for the other operating sensors in the year 1974.

Diffusion equation

The equation used for the computation is the classical Gaussian plume formula (Pasquill 1962), written according to the modifications introduced by Martin (1971) and Calder (1971). For a single point source the concentration at a receptor point P is given by:

$$C_P = \frac{n}{\Pi^{3/2}} \frac{Q}{\sqrt{2}} \cdot \sum_{\substack{iw=1\\ is=1\\ it=1}}^{6.6.4} \frac{F(id,iw,is,it)}{U_{iw} D_P S_z(D_P,is)} exp\left[\frac{-h^2(iw,is,it)}{2S_z^2(D_P,is)}\right]$$

where:

n	number of wind rose sectors $(n=8$, in our computation)
Q	source emission rate (Kg/s)
F (id,iw,is,it)	denotes the relative frequency of winds blowing into the given 45 - wind direction sector (id), for a given wind speed class (iw), atmospheric stability class (is) and temperature class (it).
U_{iw}	average wind speed for the iw - class at source height (m/s)
D_P	projection along the wind direction of the distance between the receptor point P and the point source
S_z	vertical standard deviation obtained from Gifford's plots (Slade, 1968) (m)
h	source effective height (m)

The above mentioned hourly meteorological data were used to determine the joint frequency distribution of meteorological conditions. As to wind speed the following six classes were used: 0 → 1,57, 1,57 → 3,14, 3,14 → 5,24, 5,24 → 8,38, 8,38 → 11 and greater than 11 m/s; the representative speed U_{iw} was computed as the arithmetic mean of the measured values belonging to the iw- - class. In order to take into account the variation of the wind speed with the height an esponential law was used, whose exponent was assumed equal to .25 for unstable and neutral classes and .5 for stable ones. Though low wind speed were the most frequent ones, frequencies of calms were so low that it was decided to disregard them. Wind directions were grouped into 8 classes corresponding to the standard 8 compass directions (N, NE, ..., NW). Atmospheric stabilities were grouped into 6 classes, according to Pasquill's criteria. Finally, in order to take into account the influence of temperature on the plume rise, the following classes were intro-

duced: less than 0, 0 → 10, 10 → 20, and greater than 20 C; the representative temperature has been evaluated as the arithmetic mean of the measured values belonging to the it class.
The plume rise has been evaluated according to the Concawe formula (Détrie, 1969). Since no suitable information was available neither the height of the inversion layer nor the decay of SO_2 were introduced in the model.

Results

The monitoring stations were divided into three groups according to their geographical location. Figs. 3-4-5 show measured three-monthly average concentration as well as the calculated one for two stations chosen out of each group. Fig. 3 refers to sensors 6 - 30, located at the southern edge of the Industrial Area, while stations 10-29 (fig.4) are situated between the Industrial Area and the urban centers of Mestre and Marghera and finally fig. 5 shows the results for sensors 16 - 22 located in Mestre and in Venice respectively.
The model simulates fairly well the observed values for all the stations but 10 and 29. This is an expected result since the areas in which they are located show discontinuities (i.e. variations in surface roughness, and land-lagoon transition) greater than elsewhere. To this it must be added that they are very close to the strongest point sources and therefore much more affected by possible inaccuracies in the evaluation of their mutual locations.
All the results have been summarized in figs. 6-7, which also show the regression lines for 1973 and 1974 respectively. The correlation coefficients are .72 for the year 1973 and .8 for the year 1974.
The model was also used to calculate SO_2 - annual average concentration for the years 1973 and 1974; the relative results are plotted with the experimental ones in figs. 8-9. As it was expected, the model proved to give better results if the period of calculation was extended. The encouraging results obtained by applying the model

led to extend the calculations over the whole area of interest in order to get a visible description of the spatial distribution of the pollutant. This made it possible to draw the isolines of concentration, shown in figs. 10-11, for the periods June-August 1973 and December 1973-February 1974 respectively. By comparing the two maps a conclusion can easily be drawn that because of the local meteorological conditions (Runca and Zannetti, 1973), in summer SO_2 "keeps away" from the historical center, and concentrates itself near the industrial sources. In the winter, the different meteorology prevailing over the area as well as the presence of urban emissions causes a wider spread of the SO_2 and consequently raises the pollution level in the urban center of Venice.

Description of the numerical model

The application of a model based on Gaussian plume formula has a few severe limitations. This approach can give erroneous results in low wind conditions. In addition it cannot incorporate the complex effects induced by the local geography and their influence on the distribution of pollutants. Though the Gaussian formulation has the above limitations it is nevertheless widely used. First, because it offers a practical method for calculation and secondly, because the present availability and accuracy of input data is generally inadequate to develop a more sophisticated model. On the other hand if the diffusion of atmospheric pollutants has to be described in detail the model must accomodate temporal and spatial variations of meteorological parameters, effects of the inhomogeneous surface conditions and other features. Since models based on the numerical integration of the diffusion concentration equation, such as those developed by Randerson 1970, Sklarew 1970, Lamb 1971, Shir and Shieh 1973, proved capable of dealing with the previosly mentioned features, the study which is being carried out tests the application of a model of this kind for simulating short term SO_2 - average concentration in the Venetian area.

The basic assumption of the model is that the equation governing local changes in SO_2 in the atmosphere can be written, disregarding the decay term, as follows:

$$\frac{\partial C}{\partial t} + u\frac{\partial C}{\partial x} + v\frac{\partial C}{\partial y} + w\frac{\partial C}{\partial z} = \frac{\partial}{\partial x}\left(K_x\frac{\partial C}{\partial x}\right) + \frac{\partial}{\partial y}\left(K_y\frac{\partial C}{\partial y}\right) + \frac{\partial}{\partial z}\left(K_z\frac{\partial C}{\partial z}\right) + S \qquad (1)$$

where:

C	mean concentration of SO_2 in Kg/m^3;
u, v, w	horizontal and vertical components of the wind velocity in m/s;
Kx, Ky, Kz	coefficients for eddy diffusion along the x, y, z, directions in m^2/s;
S	source of SO_2 in Kg/m^3 sec.

Equation (1) is numerically solved with the method of fractional steps (Yanenko, 1971) in a three dimensional grid system with the x-axis oriented S-N, the y-axis oriented W-E and the z-axis extended vertically to the height of the mixing layer.
At present the grid system consists of 21x21x15 points.
Along the x-and y-axes the grid points are spaced 100 m.apart. The vertical grid sizes depend on the height of the mixing layer. As yet a final decision on the vertical subdivision has not yet been taken. In this preliminary and testing phase the model runs with a mixing height of 280 m. and a constant vertical grid size of 20 m. The orientation of the grid system is such that the industrial emissions as well as the

urban emissions are as far as possible from the edges of the grid framework. Boundary conditions for the vertical diffusion range are specified, assuming that ground and mixing layer base are impermeable to the SO_2, as follows:

$$K_z \frac{\partial C}{\partial z} = 0 \qquad z = 0, H(t)$$

where H (t) is the mixing height. The lateral boundary conditions cannot be well posed. At present the model is testing a few different boundary conditions which are not discussed here; the simplest one assumes that inflow and outflow of SO_2 due to horizontal diffusion can be neglected. Anyway it results that if the grid framework is large enough computation is not affected by the lateral boundary conditions. As far as the initial conditions are concerned, since the computation shows (Shir and Shieh 1973) that the observed concentration values are reached within two hours under average wind speed conditions, the concentration field at the beginning of the simulation can be set to zero over the whole region.

Numerical scheme

According to the method of fractional steps the concentration field at the time t+Δt is obtained from that at the time t by separating the contribution due to the source, convection and diffusion terms ef equation (1). Hence at every time step the equation $\frac{\partial c}{\partial t} = S$ and the remaining six one-dimensional time dependent equations

(3 for the convection and 3 for the diffusion) are solved separately by a finite-difference technique. The numerical scheme applied to the convection equations is the one devised by B. Carlson (Richtmyer and Morton 1967) and it is illustrated for convection along the x-axis, in fig. 12. The diffusion equations are solved with an implicit space-centered difference scheme allowing for a variable grid spacing. With respect to the x-axis the difference equation is:

$$\frac{C_i^{t+\Delta t} - C_i^{t}}{\Delta t} = \frac{2}{\Delta x_i\,(\Delta x_i + \Delta x_{i-1})} \left\{ \theta\, D[C_i^{t+\Delta t}] + (1-\theta)\, D[C_i^{t}] \right\}$$

with

$$D[C_i] = \frac{\Delta x_i}{\Delta x_{i-1}} K_{x_{i-1/2}} C_{i-1} - \left(\frac{\Delta x_i}{\Delta x_{i-1}} K_{x_{i-1/2}} + K_{x_{i+1/2}} \right) C_i + K_{x_{i+1/2}} C_{i+1}$$

where ΔX_i is the interval between the i and i+1 grid point and θ is a parametric constant. This method is always stable for $\frac{1}{2} \leq \theta \leq 1$. Since Carlson's scheme is unconditionally stable, assuming $\frac{1}{2} \leq \theta \leq 1$, the choice of the time step and grid spacing in solving equation (1) is limited only by accuracy. With the application of Carlson's scheme it is not necessary to observe the stability condition $u \Delta t \leq \Delta x$, therefore allowing for a time step such that $u \Delta t = \Delta x$ in the area of maximum concentration gradients. The numerical scheme has been tested by comparing analytical with numerical solutions of equation (1), obtained respectively from the explicit relation used by Roberts to represent the diffusion of a puff of smoke (Sutton, 1953) and from calculations with the proposed method Fig. 13 shows some of the obtained results.

Application of the numerical model

As a preliminary investigation the model has been applied with the same input data used in the Gaussian model and with rough assumptions such as constant mixing height, no surface discontinuities, vertical exchange coefficient expressed by a power law and constant emission rate (urban sources enter the model as point sources, see the Gaussian model). This application showed some agreement between the observed and the computed hourly values as far as their orders of magnitude were concerned. As expected the agreement between the time evolution of observed and expected values was very unsatisfactory.

Since the model was not built to be applied with the input data used in the Gaussian model, the obtained results are not worth being discussed here. An application of the model is being developed in which the meteorological factors affecting SO_2 - dispersion are described by experiments carried out by CNR (Italian National Research Council). This application will be the subject of a future article.

Conclusions

The application of a Gaussian-type model to compute long term SO_2 - average concentration in Venice and its surroundings has been presented. Although it is difficult to describe the local meteorology, the choice of characterizing the atmospheric stabilities according to Pasquill's categories as well as the assumptions concerning height variation of the wind and the plume rise proved to be satisfactory. Since the obtained results showed that the seasonal patterns of SO_2 - concentration can be described by the model, it has been used to illustrate the influence of seasonal climate on the SO_2 dispersion over the area and the contributions of urban and industrial emissions to the pollution level in the historical center of Venice.

Improvements can be brought to the model by introducing in it a proper definition of the atmospheric stabilities on the basis of a more detailed knowledge of the local meteorology as well as by better defining the industrial emissions rates and locations.
In such a way the model could become a valid tool for land planning purposes and for optimizing the monitoring network.
In addition, a model based on the diffusion concentration equation has been briefly described. The devised numerical scheme allows for variable grid spacing and time step. Since the model's spatial resolution can be increased in the areas where the emissions are located and the advection distance per time steps can be made equal to the grid spacing in the region of maximum concentration gradient, a substantial reduction in numerical errors should result. The application of this model with the same data used in the Gaussian model showed their adequacy in describing the average aspects of the phenomena, but not its time evolution. Better results are expected from an application which is being developed with a set of more appropriate data.

Acknowledgements

The authors are indebted to Tecneco, Regione Veneta, Coses and Veneziana Gas which supplied the basic data in this study.

References

Calder, K.L. A climatological model for multiple source urban air pollution - Nato Committee on the Challenges of Modern Society, Air pollution n. 5, 1971

Detrie, J.P. La Pollution Atmosphérique - Dunod, 1969

Gifford, F.A. Atmospheric diffusion in an urban area - II IRPA Conference, Brighton, England, 1970

Martin, D.O. An urban diffusion model for estimating long term average values of air quality - Journal of Air Pollution Control Association, january, 1971

Pasquill, F. Atmospheric diffusion - D. Van Nostrand, 1962

Pooler, F. A prediction model of mean urban pollution for use with standard wind roses - Intern. J. Air and Water Pollution, 4, 199-211, 1961

Runca, E. and Zannetti, P - A Preliminary Investigation of the Air Pollution Problem in the Venetian Area - IBM Technical Report CRV007/513-3524, December 1973, Venice Scientific Center, Italy

Shieh, L.J. et al. The IBM air quality diffusion model with an application to New York City - Palo Alto Scientific Center IBM, 1971

Slade, D.H. Air Pollution - Academic Press vol. 1, 1968

Turner, D.B. A diffusion model for an urban area - Journ. of Applied Meteorology, 3, 1964

Lamb, R.G. and Neiburger, M. - An interim version of a generalized urban air pollution model. Atmospheric Environment, 5, 239-264, 1971;

Randerson, D. A numerical experiment in simulating the transport of sulfur dioxide through the atmosphere. Atmospheric Environment, 4, 615-632, 1970;

Richtmyer, R.D. and Morton, K.W. - Difference methods for initial value problems - Interscience Publishers, New York, 1967;

Shir, C.C. and Shieh, L.J. - A generalized urban air pollution model and its application to the study of SO_2 distributions in the St. Louis metropolitan area. Tech.Rep. RJ 1227, IBM San Jose Res. Cent., Cal., 1973;

Sklarew, R.C. Preliminary report of the S^3 urban air pollution model simulation of carbon monoxide in Los Angeles. Systems, Science and Software Inc., La Jolla, Cal., 1970;

Sutton, O.G. Micrometeorology. Mc Graw-Hill, New York, 1953;

Yanenko, N.N. The method of fractional steps. Springer Verlag, Berlin Heidelberg New York, 1971.

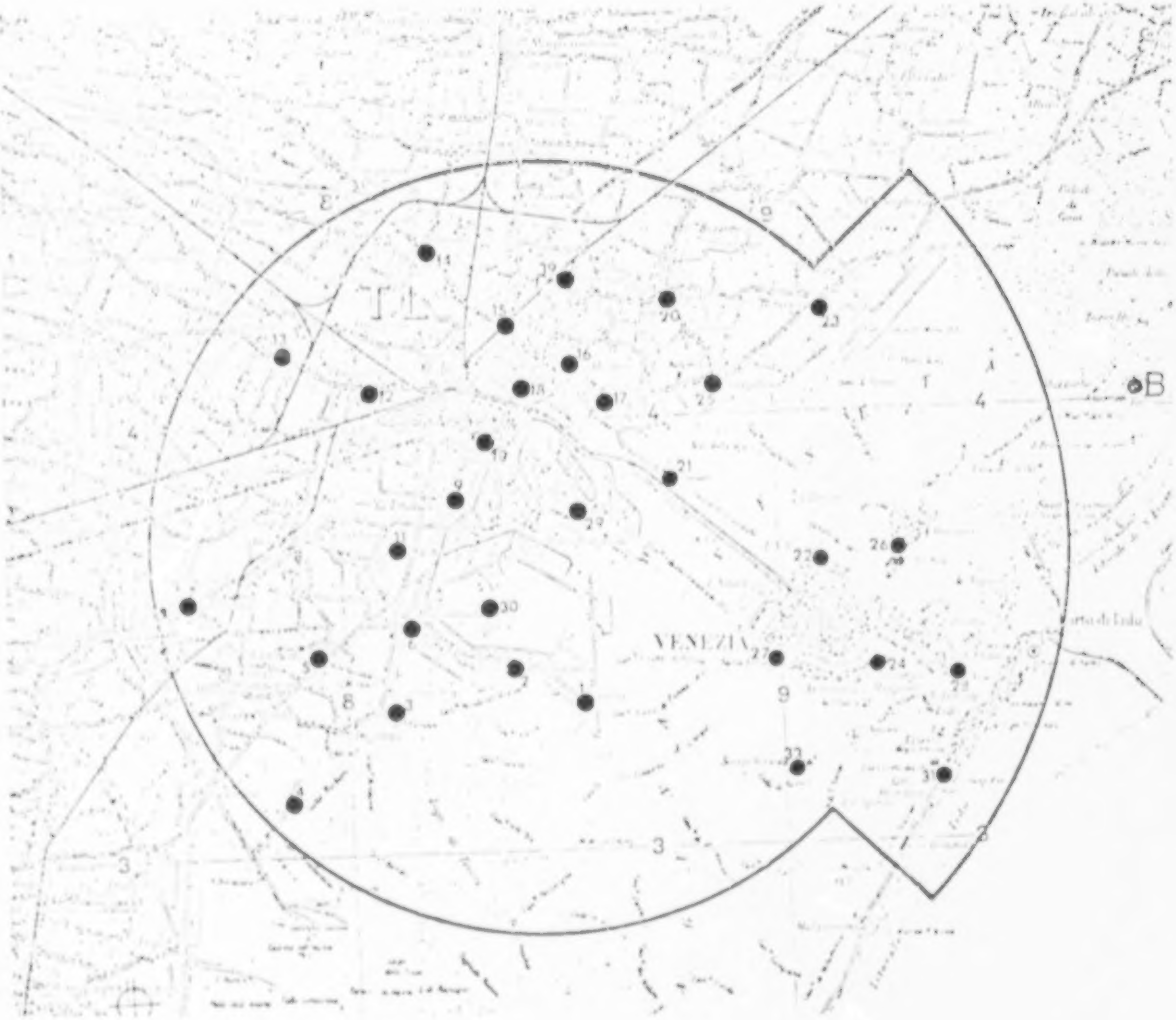

Fig. 1 Venetian Area - Dots indicate the location of the SO_2 monitoring stations (2,6,9,10,16,17,22,24,29,30 were operating since Feb. '73)

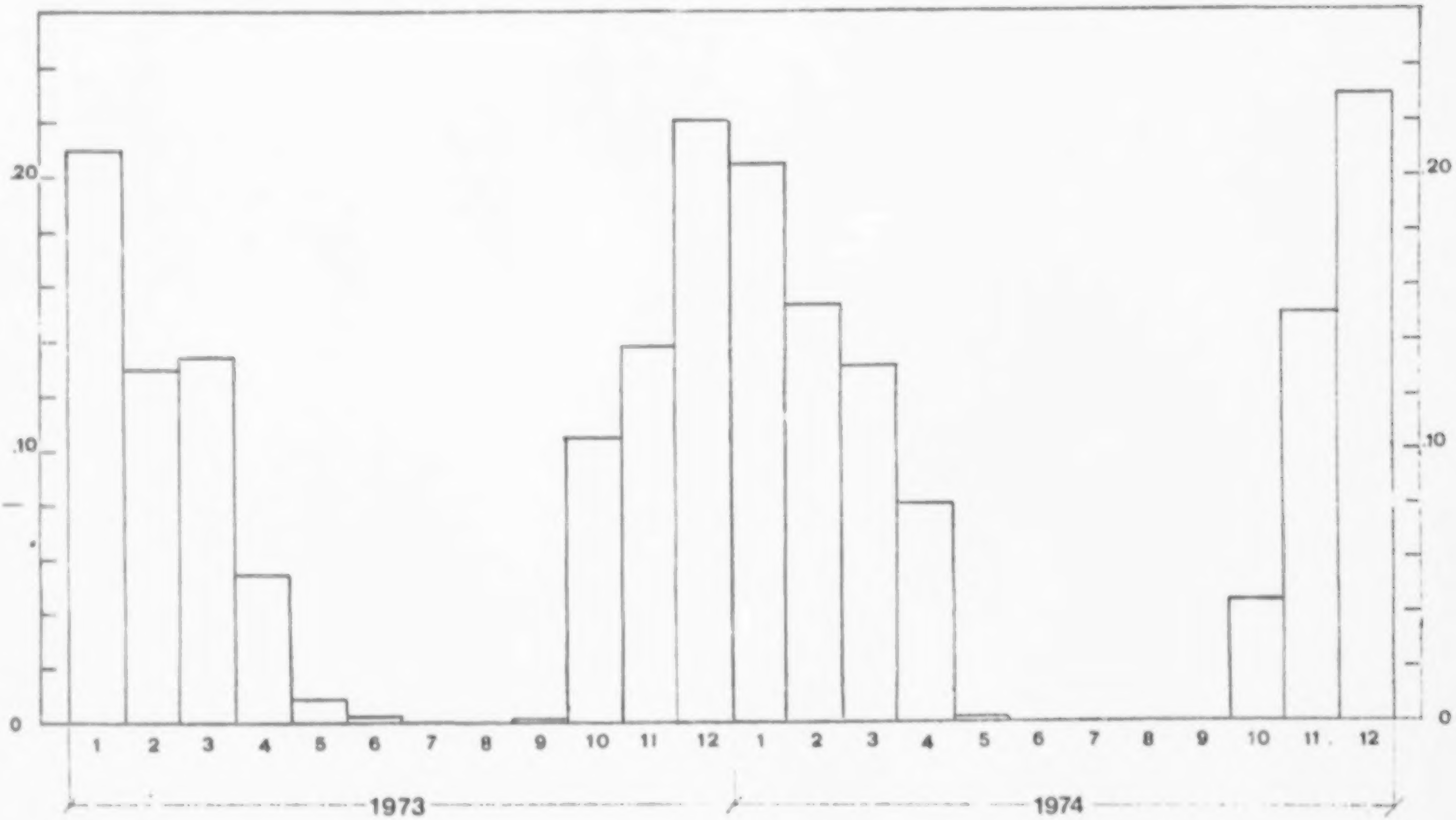

Fig. 2 Histogram of domestic heating emissions distribution throughout the years 1973 and 1974.

SO_2-SEASONAL AVERAGE CONCENTRATION

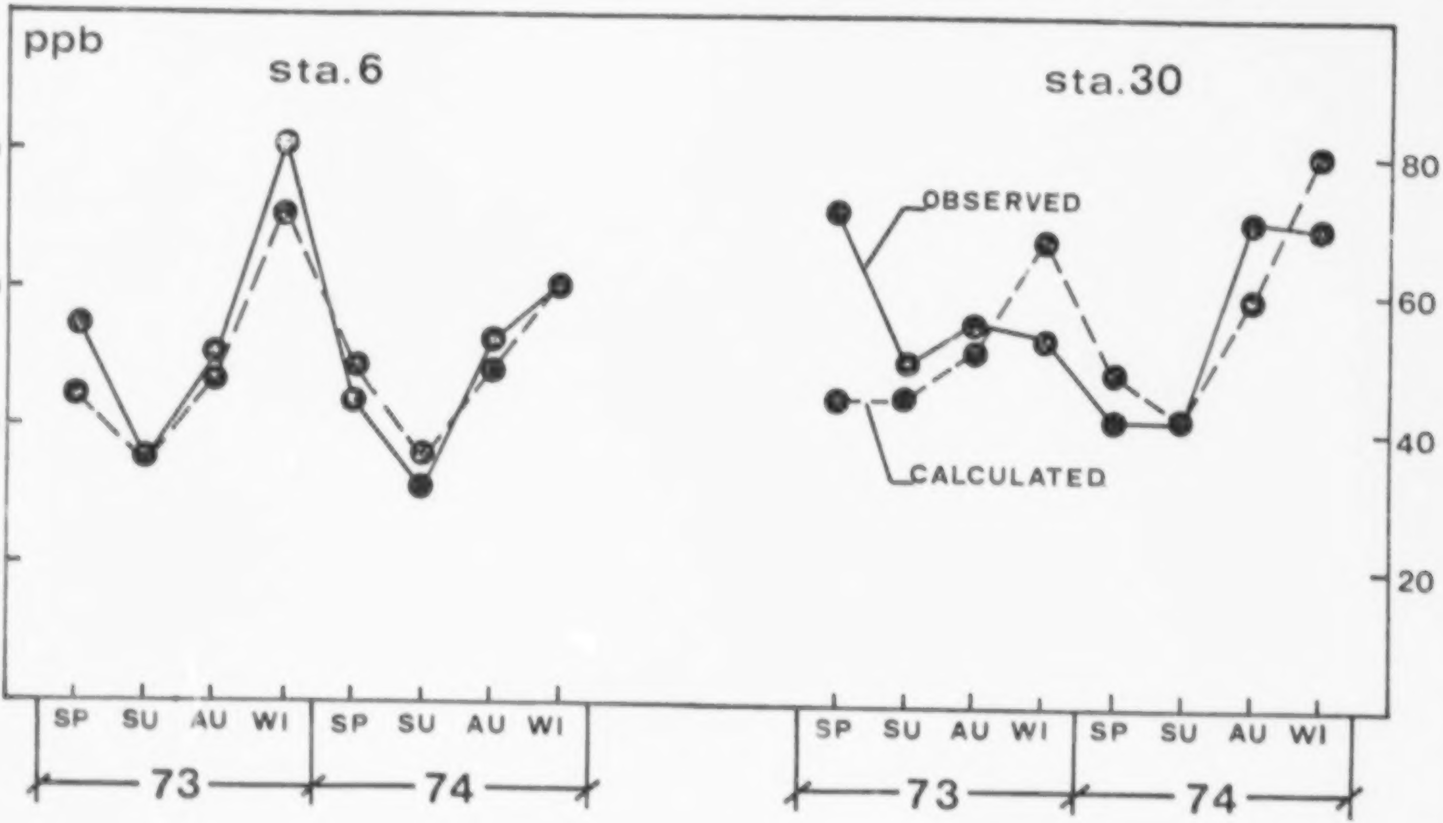

Fig.3

SO_2-SEASONAL AVERAGE CONCENTRATION

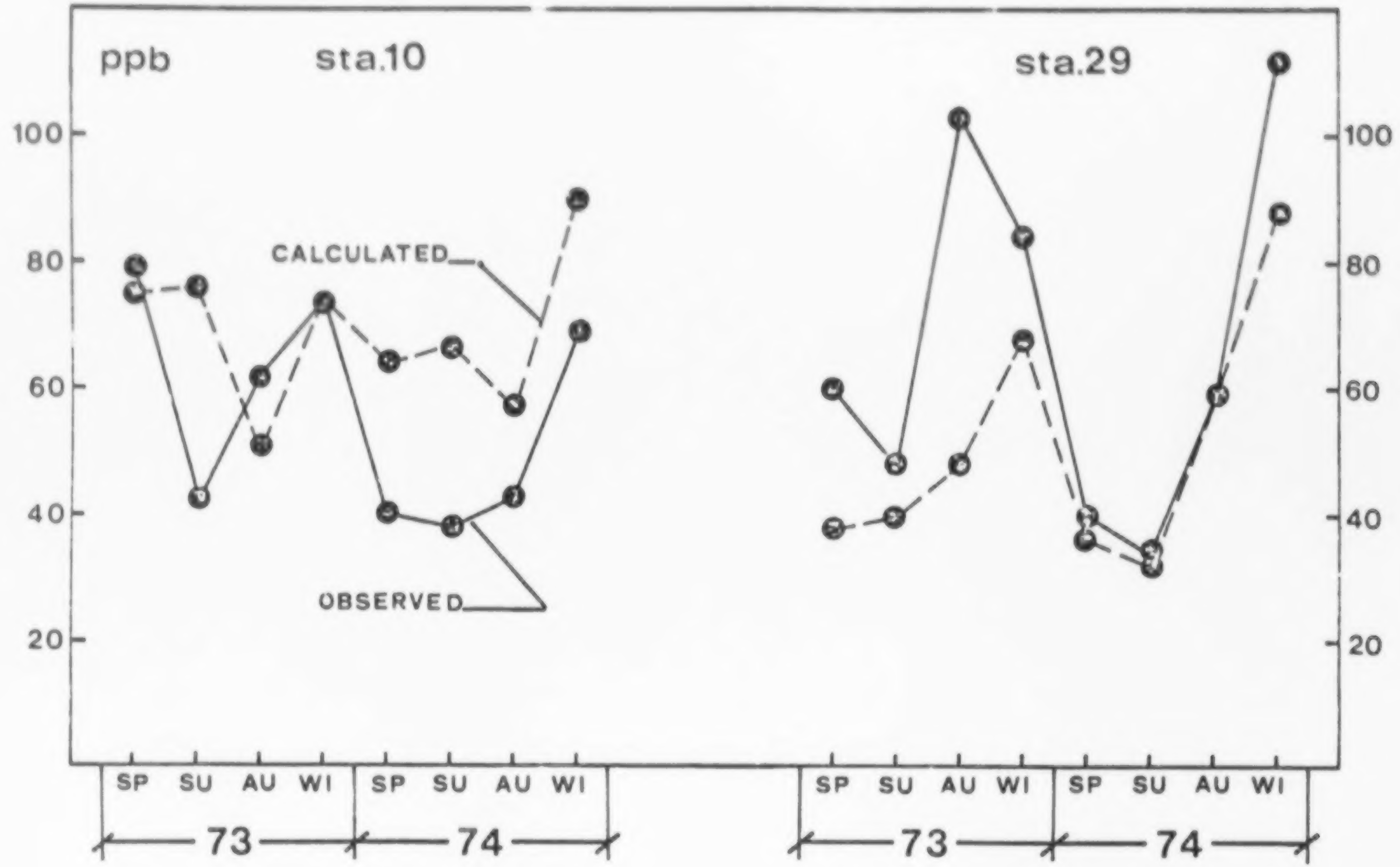

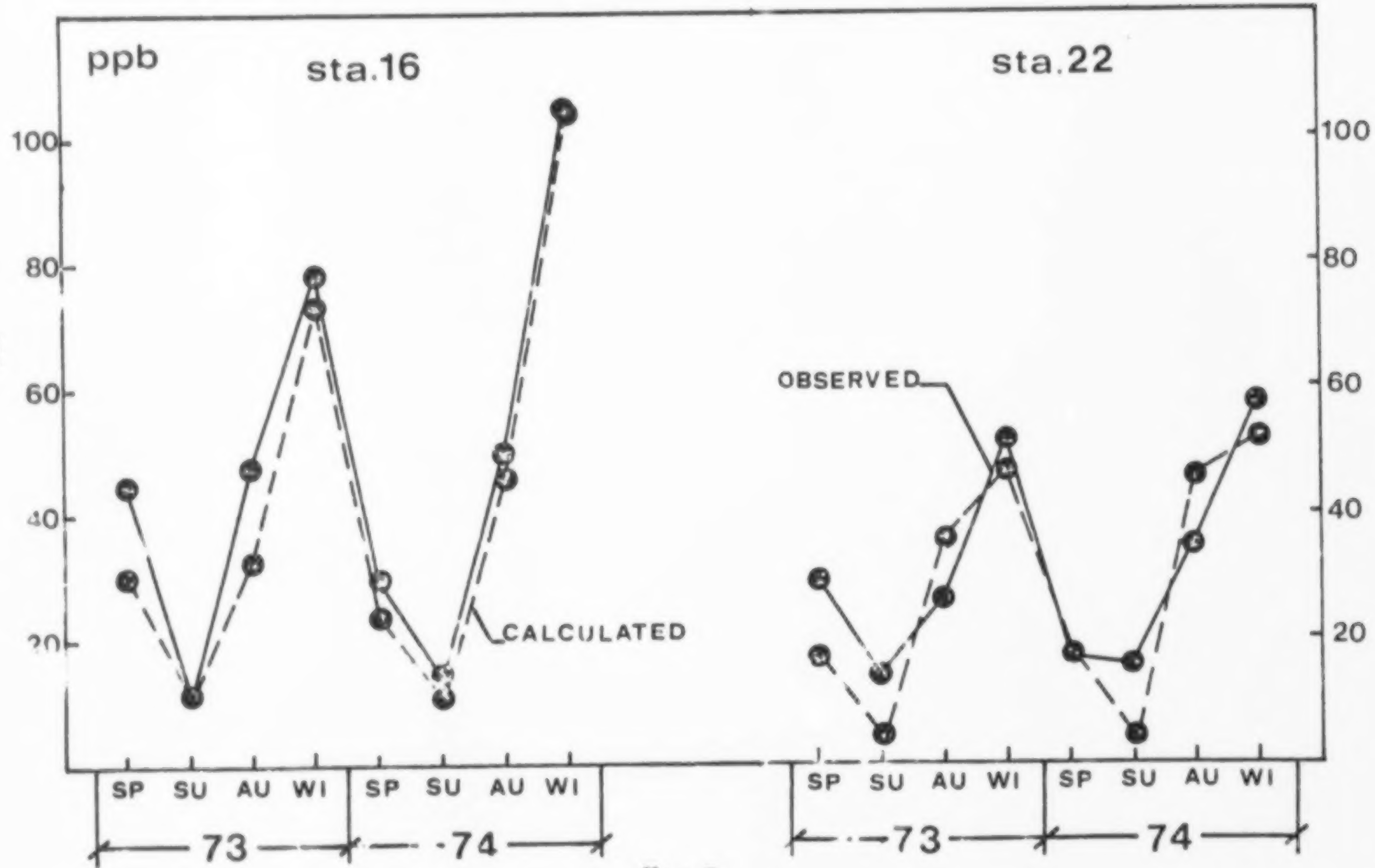

SO$_2$-SEASONAL AVERAGE CONCENTRATION

Fig.5

Fig. 6 Regression line of observed versus calculated average SO_2 concentration (ppb) for three-monthly periods from Feb. '73 to Jan. '74.

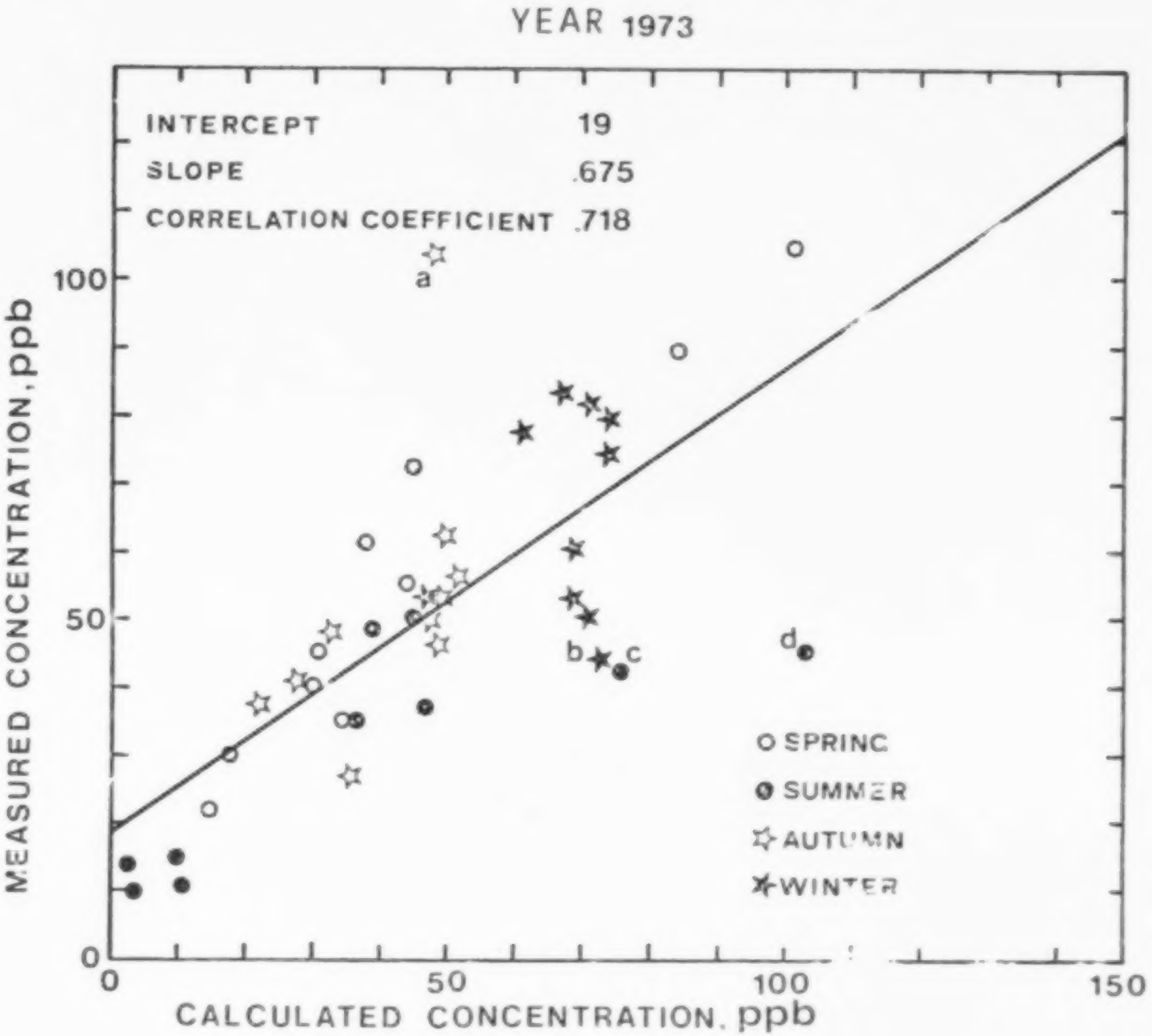

Fig. 7 Regression line of observed versus calculated average SO_2 concentration (ppb) for three-monthly periods from Feb. '74 to Jan. '75.

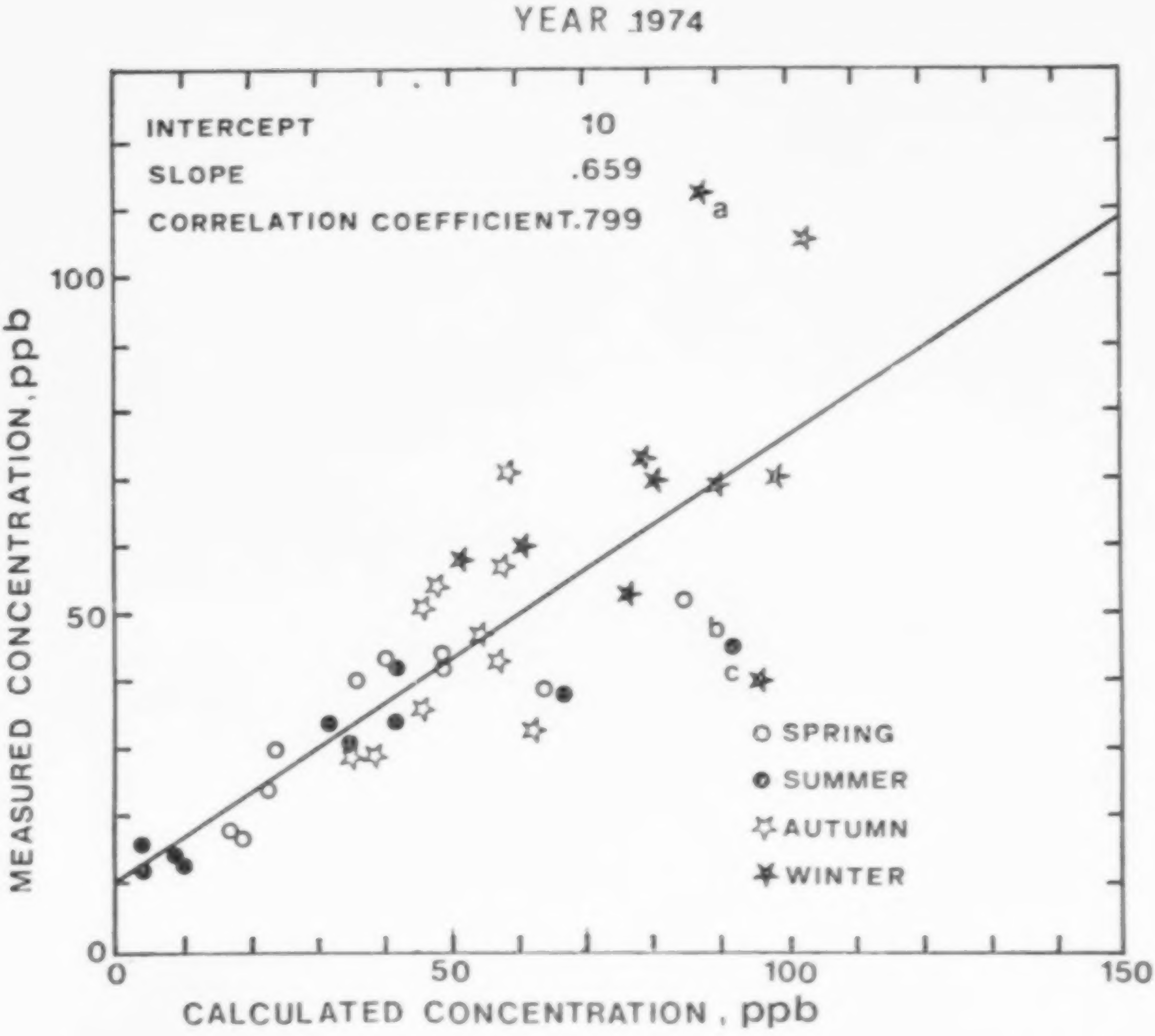

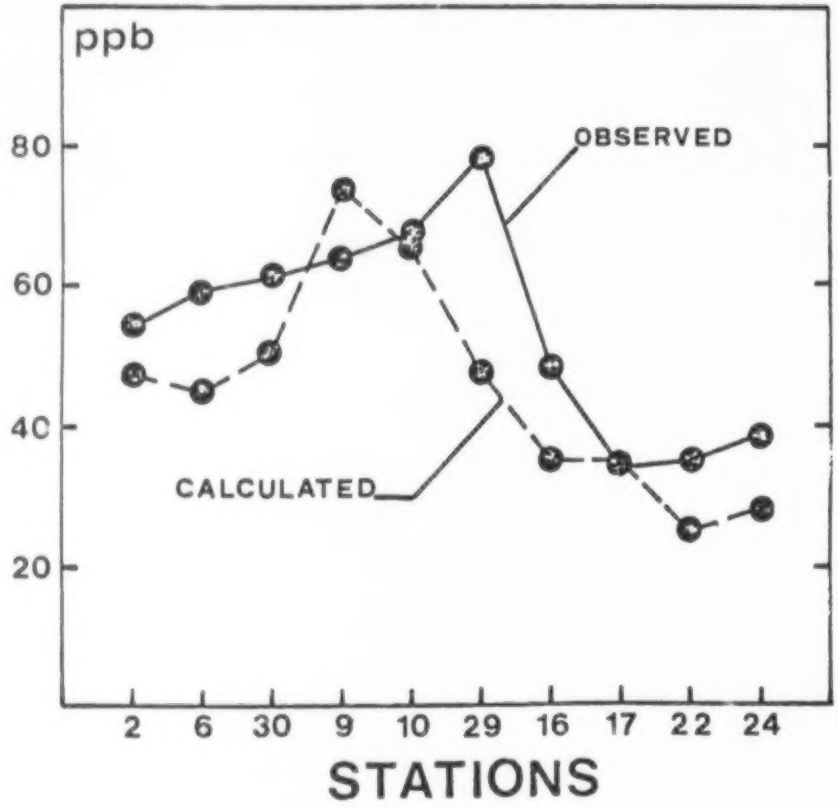

SO_2 - ANNUAL
AVERAGE CONCENTRATION
1973

Fig.8

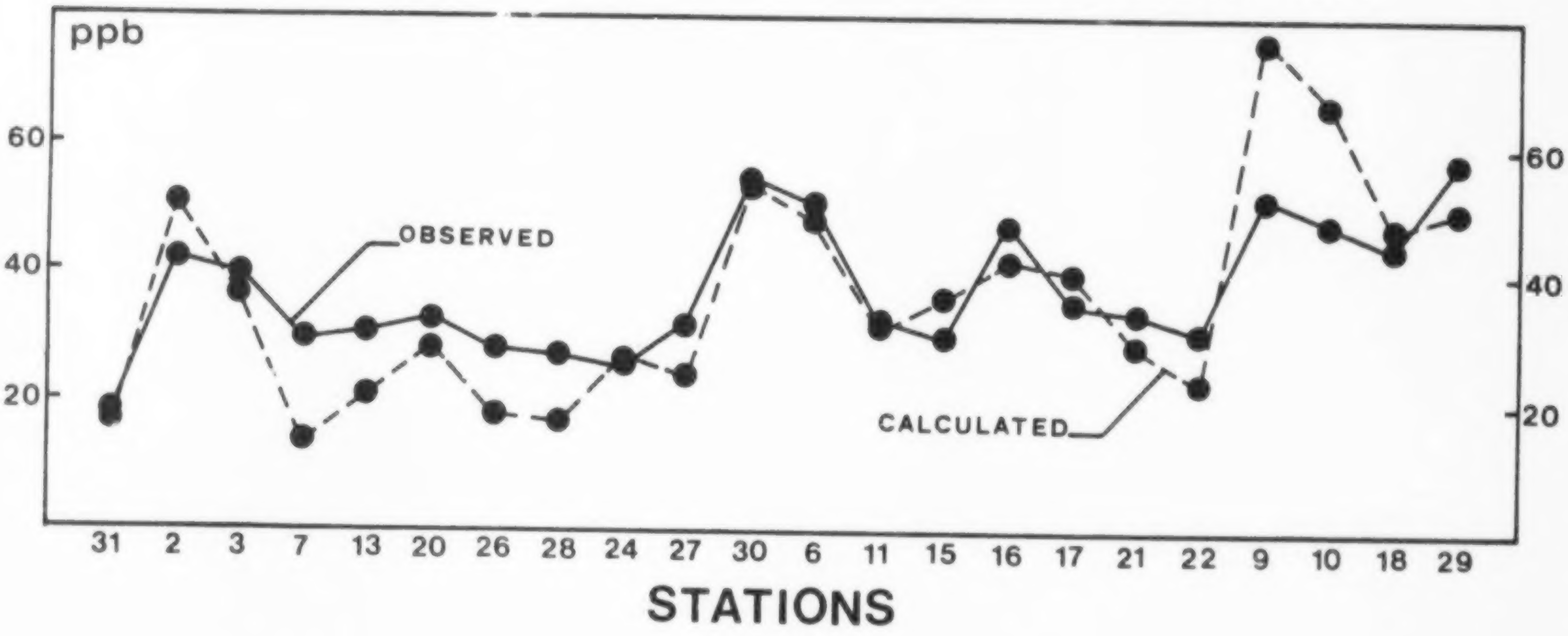

SO$_2$-ANNUAL AVERAGE CONCENTRATION 1974

Fig.9

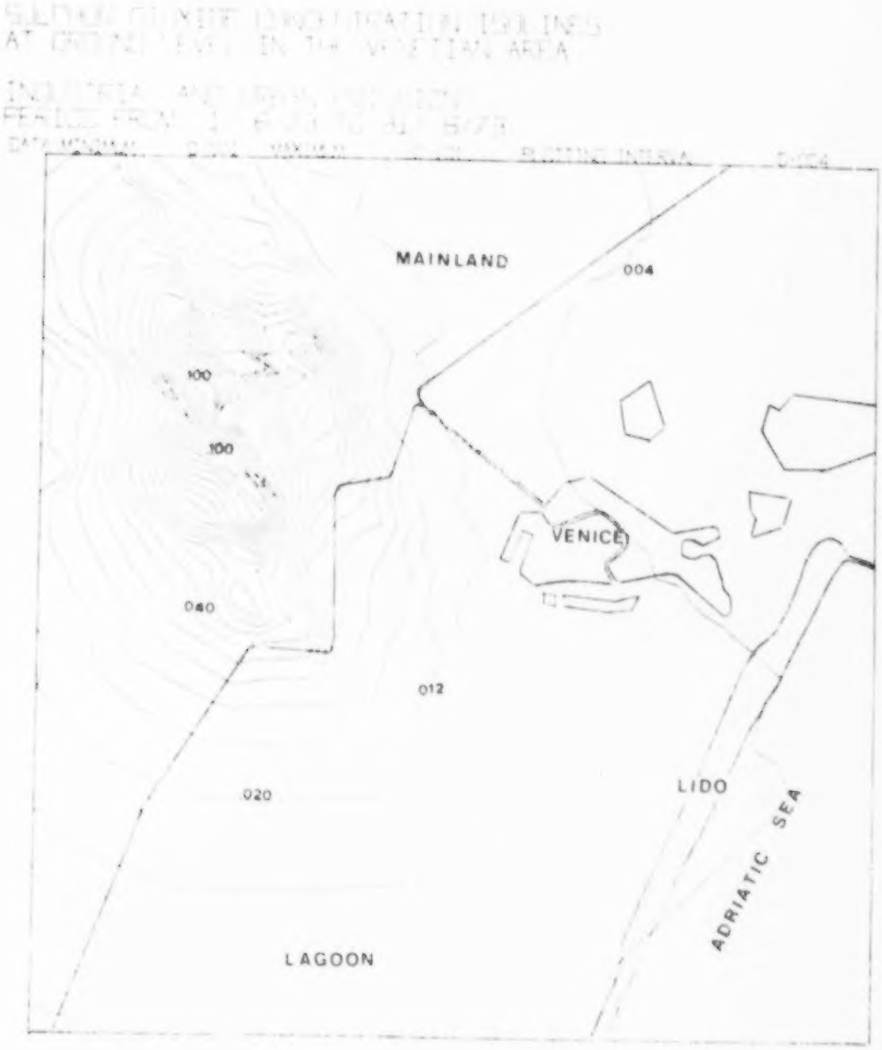

[illegible] CONCENTRATION ISOLINES
AT GROUND LEVEL IN THE VENETIAN AREA
INDUSTRIAL AND URBAN [illegible]
PERIOD FROM [illegible]
DATA MINIMUM [illegible] MAXIMUM [illegible] PLOTTING INTERVAL [illegible]
MAINLAND
004
100
100
040
012
020
VENICE
LIDO
ADRIATIC SEA
LAGOON

Fig. 10 Concentration values are in ppm.

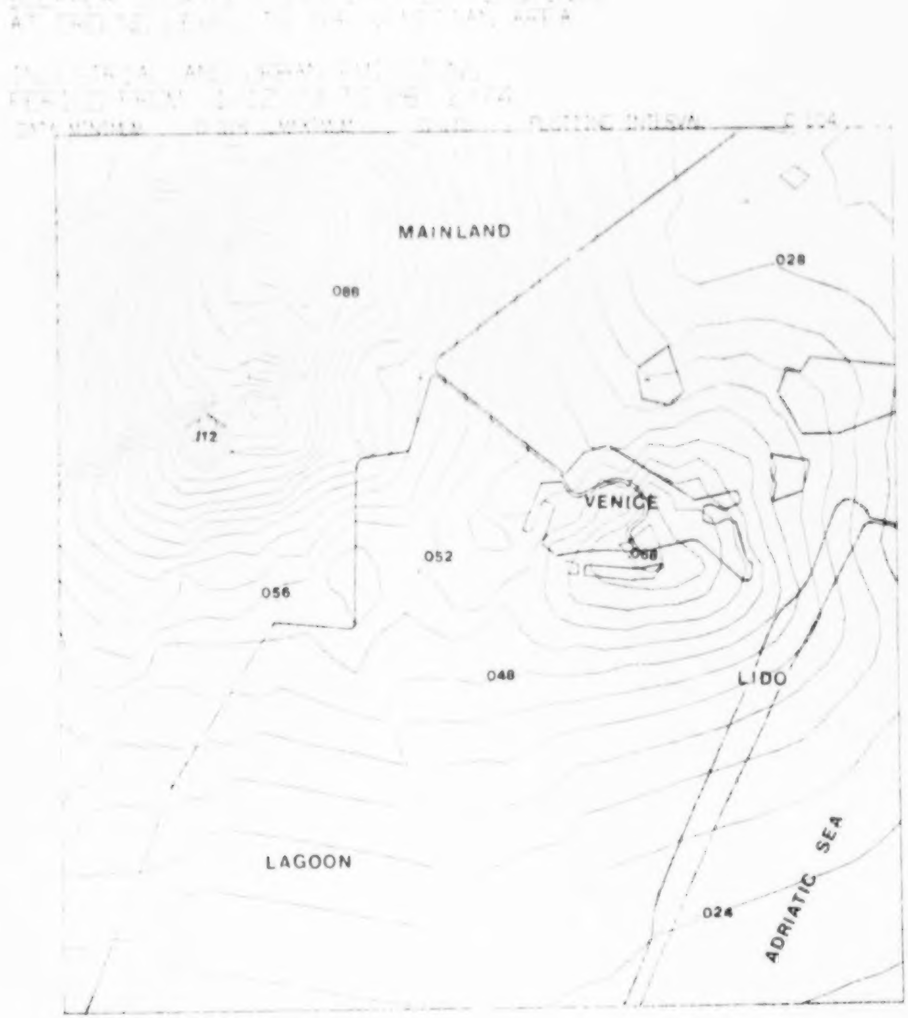

Fig. 11 Concentration values are in ppm.

FIG. 12 - CARLSON'S scheme applied to convection along x-axis

characteristic a $\quad u\Delta t < \Delta x \quad C_i^{t+\Delta t} = \dfrac{C_i^t \cdot (\Delta x - u\Delta t) + C_{i-1}^t u\Delta t}{\Delta x}$

characteristic b $\quad u\Delta t > \Delta x \quad C_i^{t+\Delta t} = \dfrac{C_{i-1}^t \Delta x/u + C_{i-1}^{t+\Delta t} \cdot (\Delta t - \Delta x/u)}{\Delta t}$

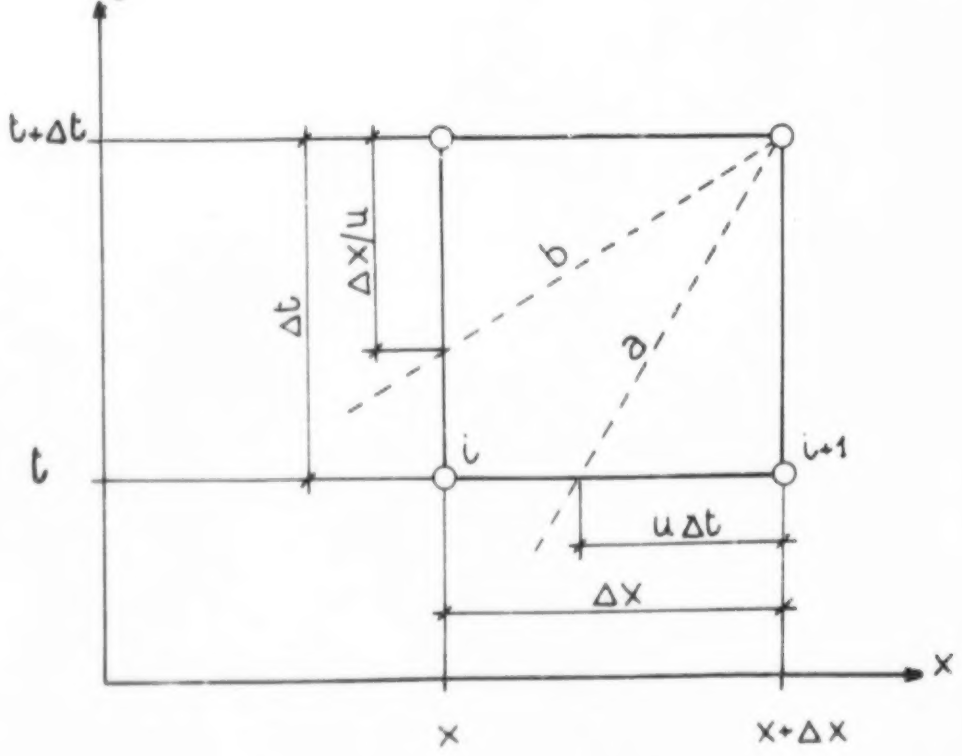

$K_x = K_y = K_z = 500\ m^2/s$

$U = 2\ m/s\ ,\ V = W = 0$

$\Delta X = \Delta Y = \Delta Z = 1000\ m$

$\Delta T = 500\ sec\ ,$ Instantaneous source = 1 Kg

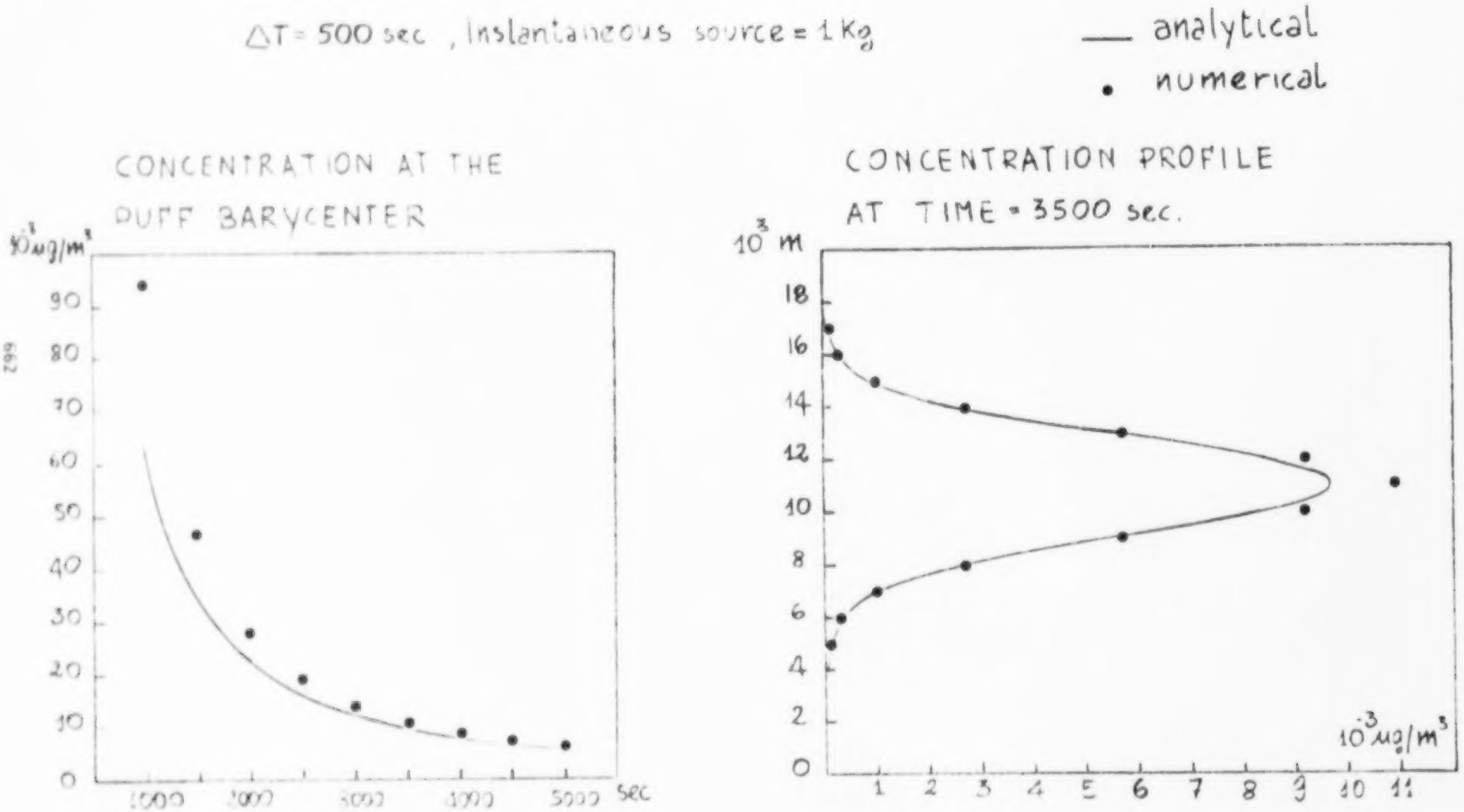

FIG. 13 Comparison of analytical with numerical solution

6th NATO/CCMS
International Technical Meeting
on Air Pollution Modeling

A GAUSSIAN MODEL IN COMPLEX TOPOGRAPHICAL SURROUNDINGS

A Case Study of the Dispersion of Fluorine from an Aluminium Plant

by

André Scholberg
SEDE S.A.
Midi 33
CH 1800 VEVEY
SWITZERLAND

BATTELLE - INSTITUT E.V., Frankfurt/Main
Germany, FR
24-26 September, 1975

A GAUSSIAN MODEL IN COMPLEX TOPOGRAPHICAL SURROUNDINGS

A Case Study of the Dispersion of Fluorine
from an Aluminium Plant

I - INTRODUCTION

Martigny is situated at a sharp right-angled bend of the Rhone valley at a point where the meteorological features of the valley change. The valley widens slightly above Martigny and the growing of fruit there, mainly pears, apples, apricots and grapes, is of great economical importance. In 19[illegible], an aluminium factory was founded at Martigny-Bourg south of the main town. Considerable damage to the apricot crops was observed around the factory. In 1952, a new plant was established at Martigny-Ville. Damages around that plant appeared. In 1956, the Bourg plant ceased activity and damage around that plant disappeared. In 1965, filtering devices were installed. Since then, there appears to be considerably less damage, however this may be due to the fact that most of the apricot trees around the factory were uprooted in favor of more hardy crops, and some of the land was simply bought up by the plant. Nevertheless, there is a strong feeling among the farmers that fluorine is responsible for most of the poor harvests experienced.

Since 1954, the state authorities disposed all along the valley a network to measure the amount of fluorine in the air, and that deposited on the leaves of the fruit trees. Though the pattern showed that the fluorine was found mainly around the factories, no strong correlation could be directly observed between the damage to the apricot trees and the fluorine.

Two other factories with a large aluminium production are situated 40 and 55 km up the valley from Martigny at Chippis and Steg. Though the amount of fluorine emitted is probably some 5 times greater, complaints have been less numerous because there are no apricot trees or other sensitive crops around these plants.

In 1973, we were asked to conduct a meteorological study to determine [illegible] the extent of the polluted areas.

Figure 1 is a map of the valley bend. The position of the Martigny aluminium plant is indicated by the arrows.

II - Meteorological measurements

The wind speed and direction were measured at 9 locations (see figure 1). Temperature, humidity, sunshine and rainfall were also recorded. We also used the usual meteorological maps and daily weather reports from the Swiss Meteorological Institute.

Recordings of the wind direction and velocity provide statistical data regarding the wind pattern in the valley bend.

Valley breezes dominate the wind pattern in summer; a strong wind rises around 11 a.m., reaches typically 8 m/s at 4 p.m. and decreases in the evening. Around midnight or a little after, a slight breeze blows down the valley (typically 1 m/s).

However, the breezes in the small confluent valley south-west of Martigny follow their own different rhythm, and complicate the situation in the bend considerably.

The general flow patterns observed in the Martigny bend are summarized in figure 2.

No measurements of stability were directly available. We attempted to gather data on this parameter in two ways:

- from the measurement of the variability of the wind direction,
- by correlating the directions recorded by two anemometers.

Neither of these methods gave any satisfactory results. This was mainly due to inadequate instrumentation. Also, we have yet to improve our understanding of the relationship between vertical and horizontal dispersion as a function of the flow pattern in the valley bend.

A certain number of soundings were made with free lift balloons to gather some information about the wind structure. During the day, the upslope showed a considerable increase in speed with altitude as well as a substantial directional shear (figure 2). The flow curves fairly quickly at ground level. At higher levels, the line of flow takes the bend later and a sort of reflection of the flow lines against the valley wall is observed. No soundings were made in the streams flowing down the valley at night.

III - FLUORINE MEASUREMENTS

A Harding static absorbing apparatus is shown in figure 3. Static absorbers have been in use around Martigny since 1958 and have proved cheap and rugged. Moreover, there is good correlation between the measurements and the amount of fluorine found in the leaves of trees (figure 4).

The amount of fluorine absorbed by the paper is determined by chemical analysis. Results are expressed in arbitrary units, i.e. µg F^- per dm^2 of paper per month. We were faced with the problem of determining what parameter was measured by the Harding absorber and with what accuracy.

A sample of 20 coupled measurements showed a somewhat Gaussian distribution of their relative differences, and the dispersion evaluated from that sample was 15%. This would mean that for some 90% of the measurements, the relative error would be less than 25%.

We first thought that the Harding absorber was giving a measurement of average concentrations. However, calculations showed an abnormally low correlation (.50) between measurements and calculated concentrations. Realising that the Harding absorber was very sensitive to ventilation, it was assumed that the Harding absorber apparatus actually measured the flux of fluorine going through it. The hypothesis was first proved by a set of qualitative experiments. Subsequently, correlations between calculated flux and Harding measurements climbed to a rewarding 0.90 .

In 1973, a large network of 65 stations was set up around the plant. The Harding absorbers were sampled consistently every two weeks over a period of 4 months. Figure 5 shows the network, and figure 6 represents the distribution of the 496 measurements obtained.

IV - MODELING

Modeling was attempted in order to establish a correlation between the concentration of fluorine measured and the emission of the plant. The model would also provide the isopleths of polluted areas.

The plant operates night and day. The emission is due to the ventilation of the factory floor and is considered to be fairly constant. The emission rate, probably underestimated, was assumed to be 1 g/s.

Numerical Model

This was believed necessary to simulate the boundary conditions and the effect of the wind sheer. However, computing time increased dramatically with the number of cells used and the resolution obtained was poor. This attempt did show that the effect of wind sheer was reasonably small.

Gaussian Model

The hypothesis was made that dispersion was Gaussian along the flow lines. The Gaussian model was then adapted so that the flow lines were hyperbolas, the asymptotes running parallel to the two branches of the valley. Reflections on the walls of the valley can be easily simulated in such a model (see figure 8). Lines of flow were calculated from the wind data for each wind direction and for low or high wind speeds and their parameters included in the model. The model could calculate either the average concentration $\overline{C}$ or the average flux $\overline{\phi} = \overline{C.u}$

V - RESULTS

Figures 9 and 10 show typical computer outputs of fluxes calculated in the valley around the plant.

Correlation between calculations and measurements

2 week averages

The correlation coefficients between calculated and measured data (2 week averages) are the following:

- upper network, 292 measurements : 0.87
- lower network, 197 measurements : 0.67

- entire network, 489 measurements : 0.88

Summer mean

Calculated and measured fluxes (summer mean) along two sections of the network along and across the upper part of the valley are compared in figures 11 and 12. Correlation is very high; 0.94 and 0.99 respectively.

Figures 13 and 14 compare calculated and measured fluxes (summer mean) along and across two sections of the lower part of the valley. Correlation coefficients are much lower; 0.38 and 0.46 respectively. Indeed, considering figure 14, it would seem almost surprising that the coefficient is positive.

Over the entire network, the correlation coefficient for the summer mean data is nevertheless 0.98.

The explanation of the discrepancies in the lower part of the valley is found in the action of the small confluent valley situation south-west of the plant. The wind blowing down this valley does not significantly perturbe the lines of flow above the Martigny plant during the strong upwinds that blow most of the time. However, the light winds blowing down both valleys at night meet head on and highly complicated patterns of flow result. This would explain the wave like appearance of the fluxes measured below the Martigny plant.

Figure 15 shows the rose of the winds between 3 a.m. and 6 a.m. during the summer of 1973. The rose shows that separate stable patterns of flow are established at night according to the relative strength of the breezes descending the main valley and its confluent.

Regression between calculations and measurements

The high values of the correlation coefficients show that a direct linear relationship can be established between the calculated fluxes of fluorine and the measurements. This relationship would be:

$$\Gamma_{\text{measured}} = \alpha\Gamma_{\text{calculated}} + F_o$$

α can be identified as a capture ratio of the absorber

F_o is a constant that could be identified as background pollution

α and F_o are determined by regression analysis of the 489 measurements:

$$\alpha = \frac{1}{1060}$$

The capture ratio of the Martigny static absorber exposed during 14 days would be of the order of 10^{-3}. This figure is only an order of magnitude since there is considerable uncertainty regarding the actual emission of the plant and the lack of measurements concerning dispersion parameters. The statistical error here is small (5%).

We also find:

$$\Gamma_o = 81\ \mu g\ \text{(arbitrary units)} = 3\ \mu g/m^2/d$$

The average background pollution during the summer of 1973 was thus established. However, the statistical error is important, and at a level of confidence of 90%:

$$7\ \mu g < \Gamma_o < 155\ \mu g\ \text{(arbitrary units)}$$

Origin of the Background Pollution

The high figure found for the background pollution was unexpected. We tried to discover whether the Chippis and Steg aluminium factories higher up the valley would not produce a fluorine flux of that order. The Gaussian plume equation can be integrated in a valley where lateral diffusion is limited by the valley slopes on either side:

$$\bar{\phi} = \sqrt{\frac{2}{\pi}}\ \frac{Q}{L\,\sigma_z}$$

where L is the width of the valley,

Q the emission rate.

The breezes descending the valley at night are generally stable. Corresponding value of σ_z is of the order of 300m for a distance of 50 km. Some authors give lower figures. If the total emission of the Chippis and Steg plants is assumed 5 g/s, i.e. 5 times that of the Martigny plant, we find an average flux of the order of 25 to 50 μg arbitrary units, i.e. of the same order of magnitude as the background flux calculated by regression analysis.

VI - CONCLUSIONS

A Gaussian plume model adapted to curved flow lines gave satisfactory results in determining the polluted areas above the Martigny plant. This seems to be due to the fact that the average flow lines are rather stationary. The high density of measuring stations and the 2 week averaging time helped smooth out statistical errors and the correlation between calculation and measurement was high. The model was not so successful below the plant in the confluence of the main Rhone valley and the small tributary valley. Background pollution was traced to the aluminium plants at Chippis and Steg 50 km away.

An interesting result concerns the Harding absorber apparatus. It seems that this apparatus measures the flux of pollutant rather than the concentration. The distinction between flux and concentration revealed in the study is generally ignored: as a rule, attention is primarily directed to the concentration of pollutants in the air. This is normal since the amount of pollutant inhaled by human beings is proportional to the concentration. However, plants and trees seem to act as filters to retain the pollutants in the wind, and concentration is less pertinent than the flux of those pollutants. We are led to believe that the sensitivity of plants to pollutants expressed in terms of concentration may not be quite relevant; studies conducted to determine these sensitivities and ignoring the problem of ventilation may be misleading. In our opinion, attention should be given to these considerations when the impact of air pollution on plants and trees is of main concern.

sede sa

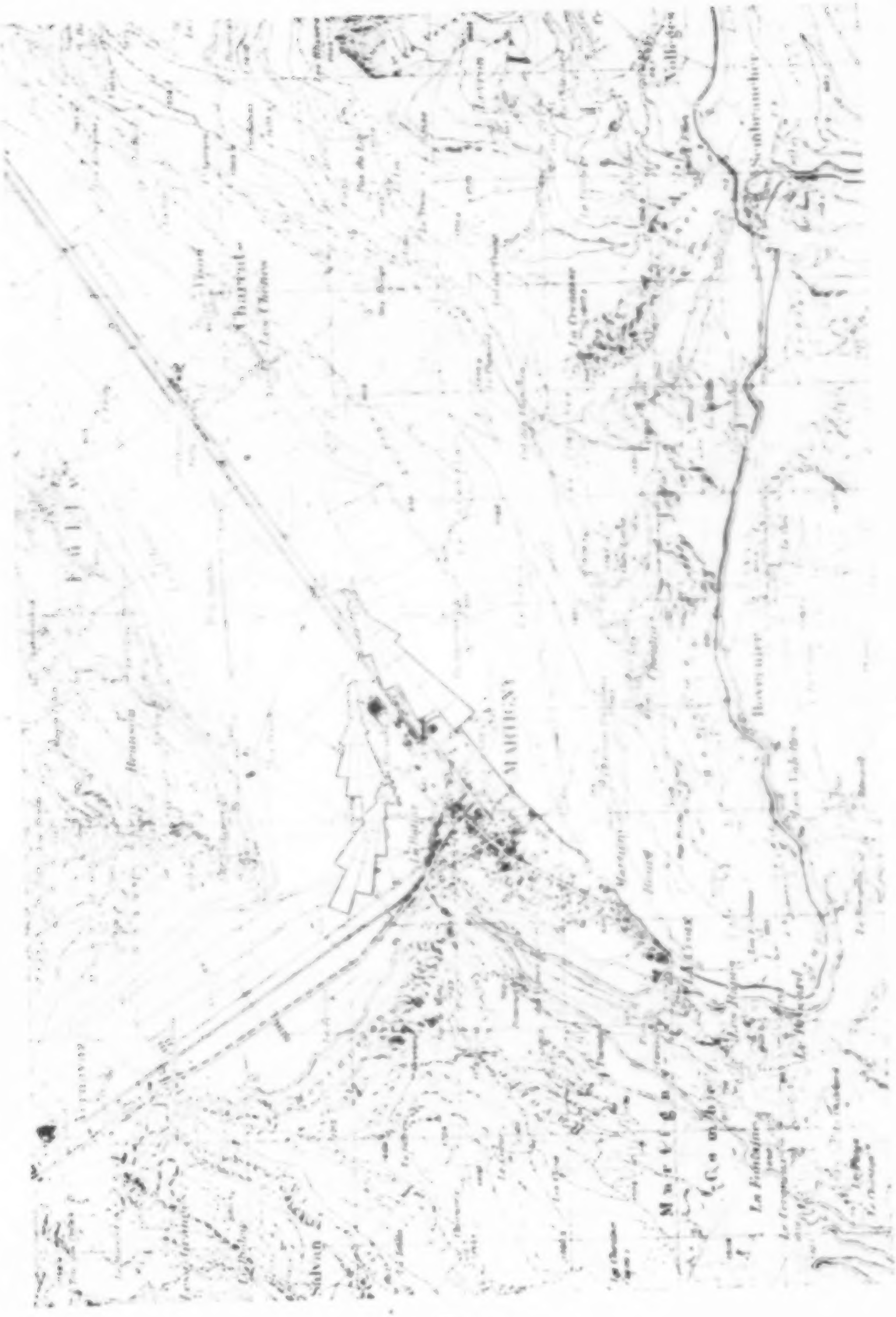

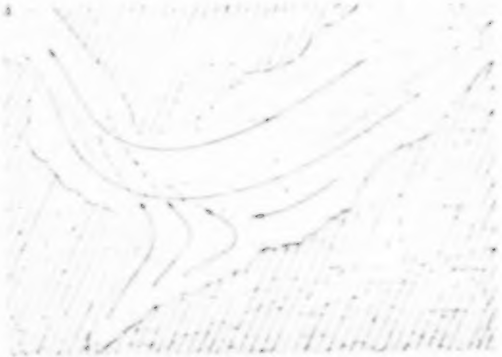

Fig.2a from [illegible] to [illegible]

The [illegible] flowing down the main valley and its contiguous [illegible] [illegible].

Reproduced from best available copy.

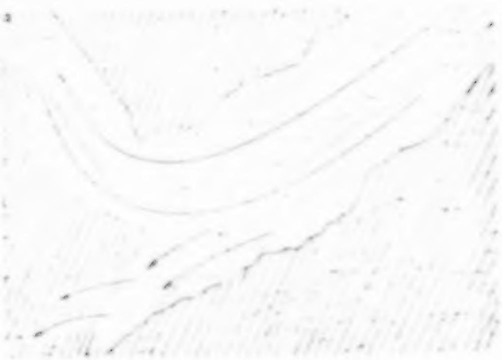

Fig.2b from [illegible] to 1100 h

The morning sun warms up the slopes facing South East. The breeze continues in the tributary valley.

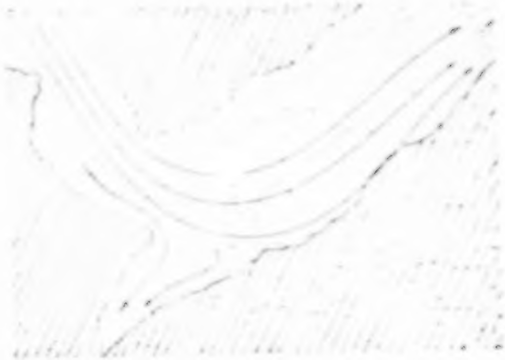

[illegible] from [illegible] to [illegible]

A strong [illegible] wind [illegible] up the main valley [illegible] [illegible] [illegible].

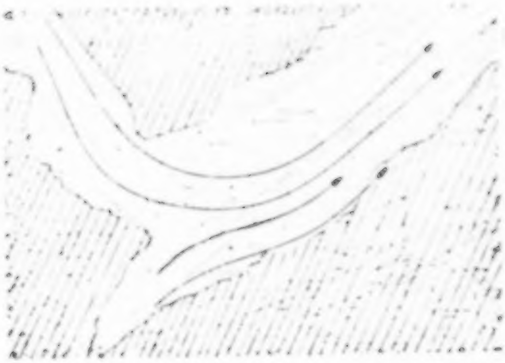

Fig.2d from [illegible] to [illegible]

A cold katabatic breeze starts flowing down the tributary valley and smoothly joins the main flow.

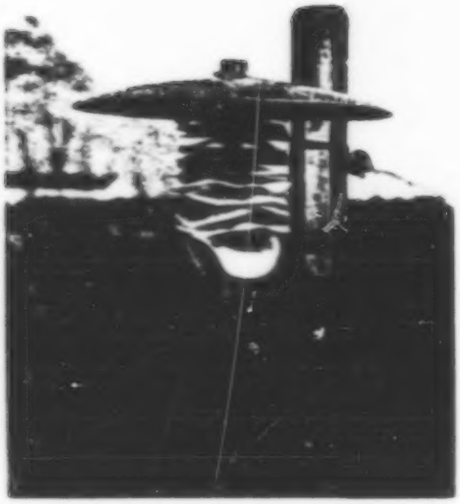

Fig. [illegible] Harding station
Harding apparatus

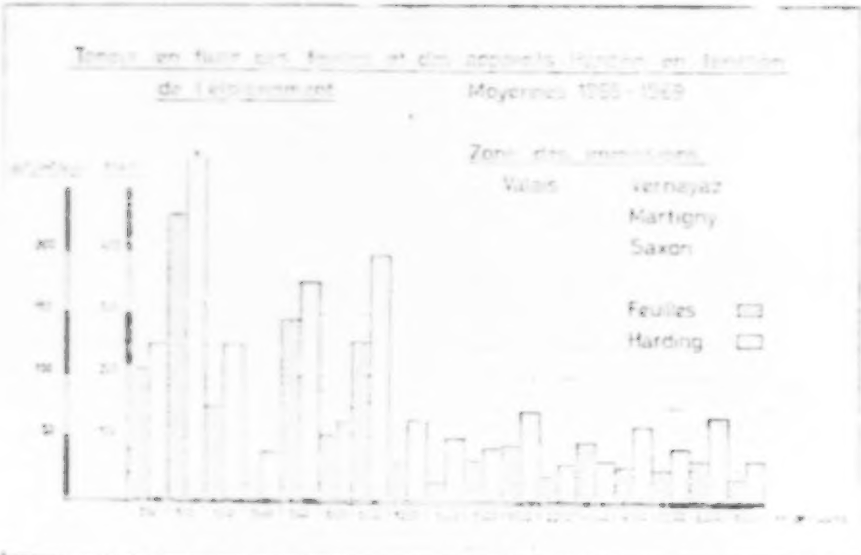

Fig. [illegible] Fluorine in the leaves of the trees and Harding measurements
as a function of the distance from the aluminium factory

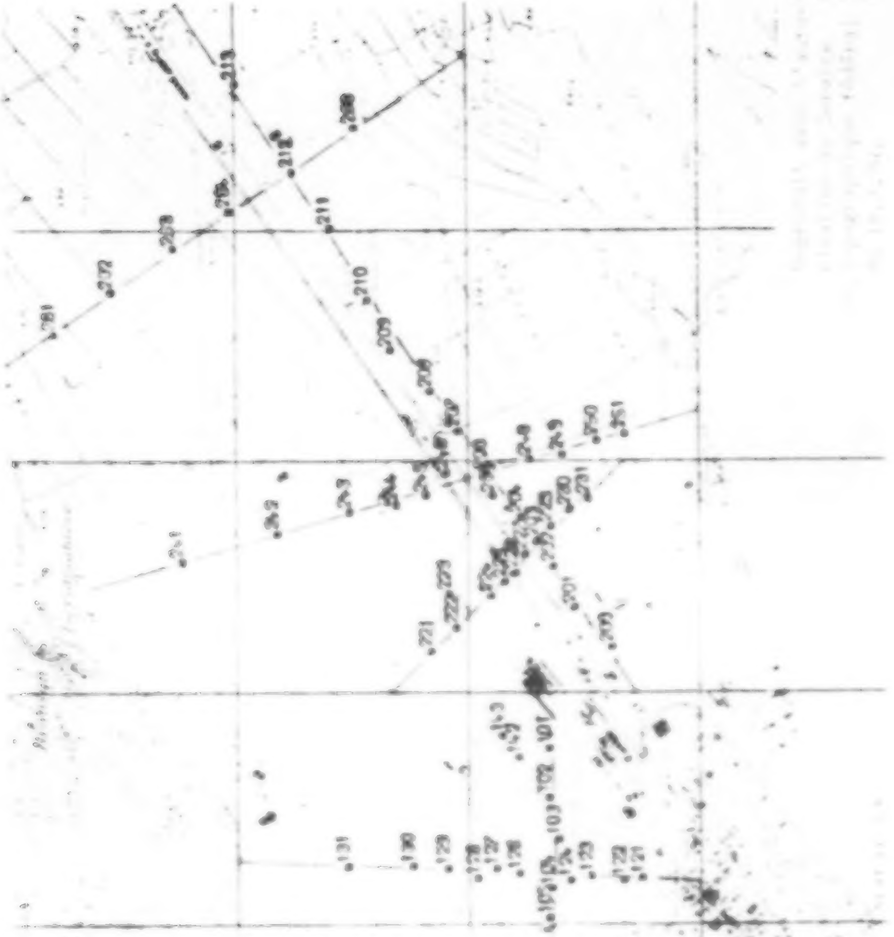
213
212
211
210
209
208
110
111
112
101
102
103
105
107
108
109
121
122
123
126
127
128
129
130
131
221
222
223
241
242
243
244
248
249
250
251

sede sa

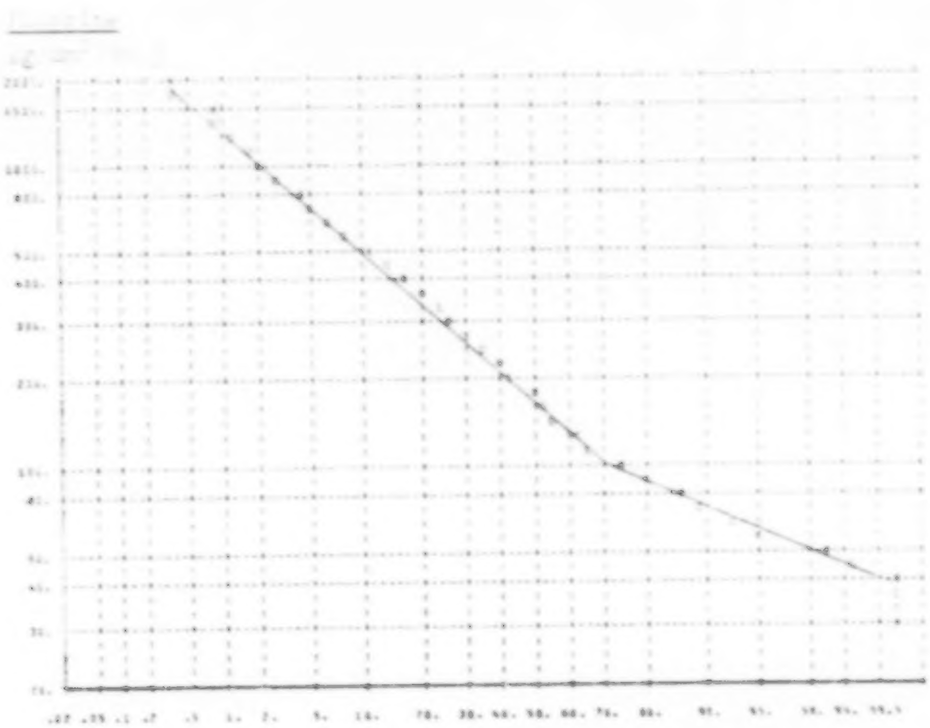

Fig. [illegible] Distribution of [illegible] [illegible] measurements
(expressed in arbitrary units)

sede sa

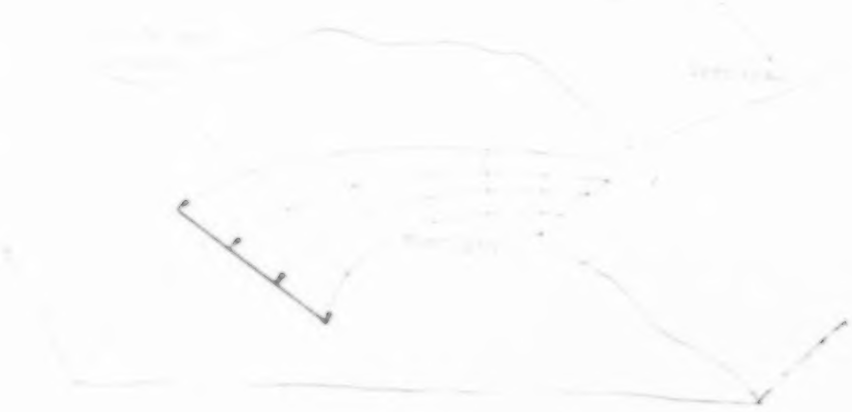

Fig. 4: Wind shear

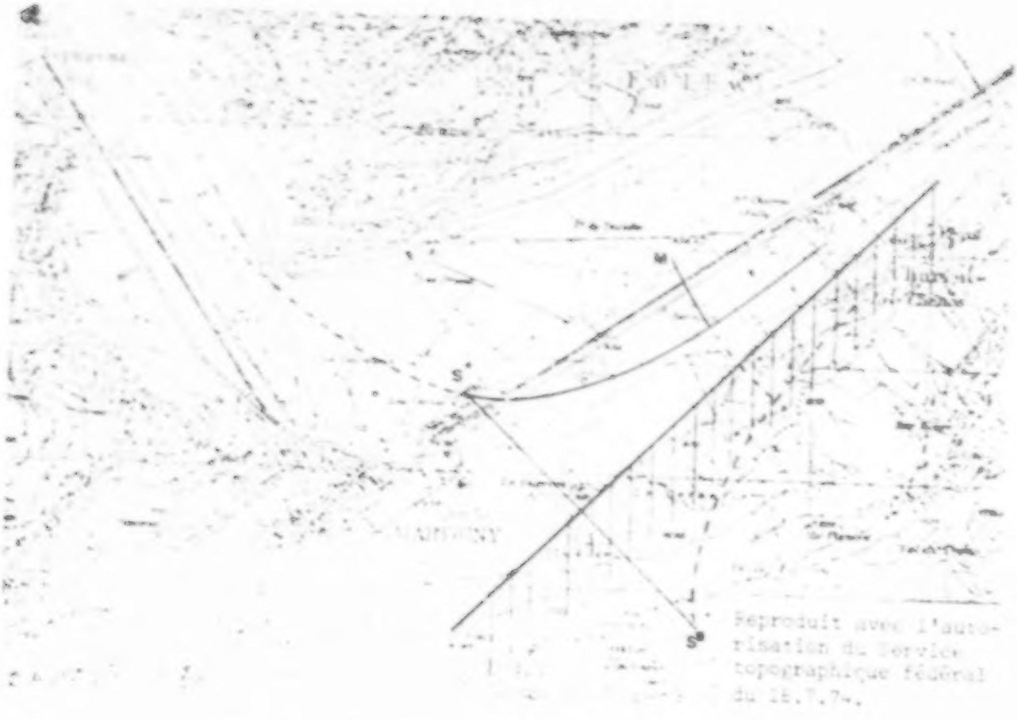

Reproduit avec l'autorisation du Service topographique fédéral du 18.7.74.

Fig. 5: Flow lines in the model

Flow lines are hypothetical. An image source S* and image flow lines are introduced to account for a reflection on the valley wale.

sede sa

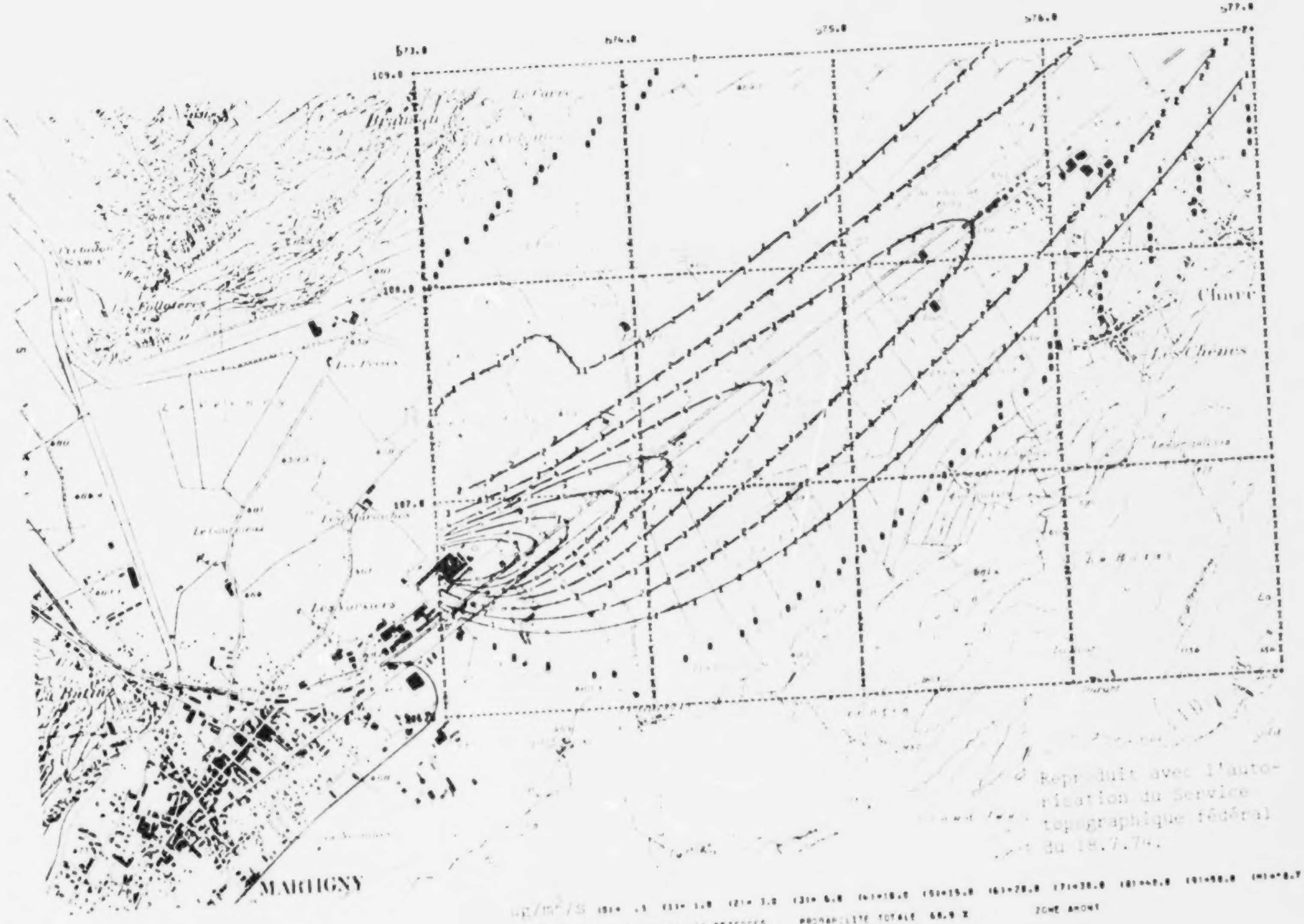
573.0
574.0
575.0
576.0
577.0
109.0
108.0
107.0
Chœx
Les Chênes
Les Follaterres
MARTIGNY
ug/m²/S (0)= .1 (1)= 1.0 (2)= 3.0 (3)= 6.0 (4)=10.0 (5)=15.0 (6)=20.0 (7)=30.0 (8)=40.0 (9)=50.0 (M)=80.7
GROUPE 1 MOYENNE DE 16 EPISODES PROBABILITE TOTALE 68.9 % ZONE AMONT

Reproduit avec l'autorisation du Service topographique fédéral du 18.7.74.

Fig. 9 : Average summer flux of fluorine (upper valley)

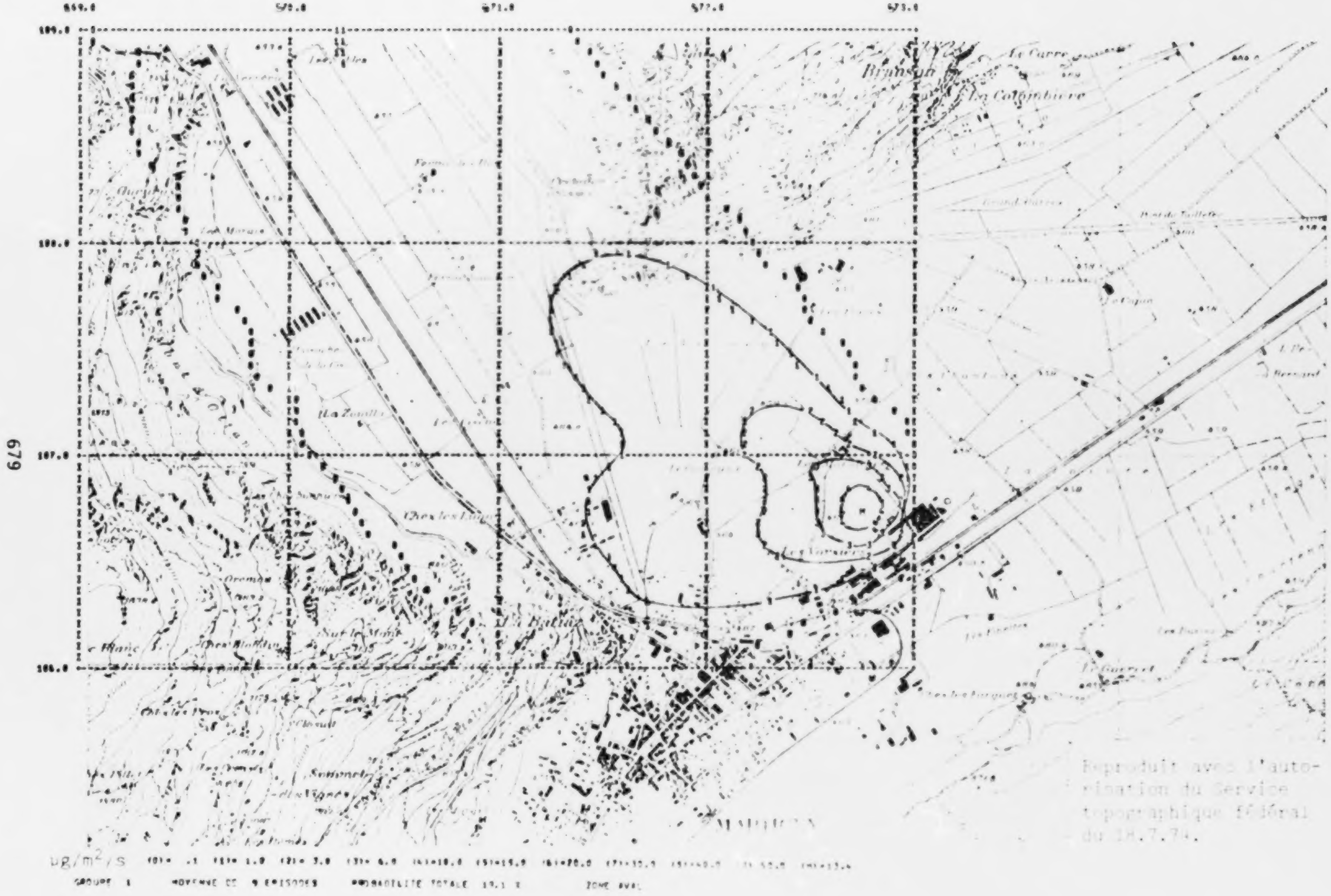

Reproduit avec l'autorisation du Service topographique fédéral du 18.7.74.

Fig. [illegible] Average [illegible] flux of [illegible] ([illegible] valley)

sede sa

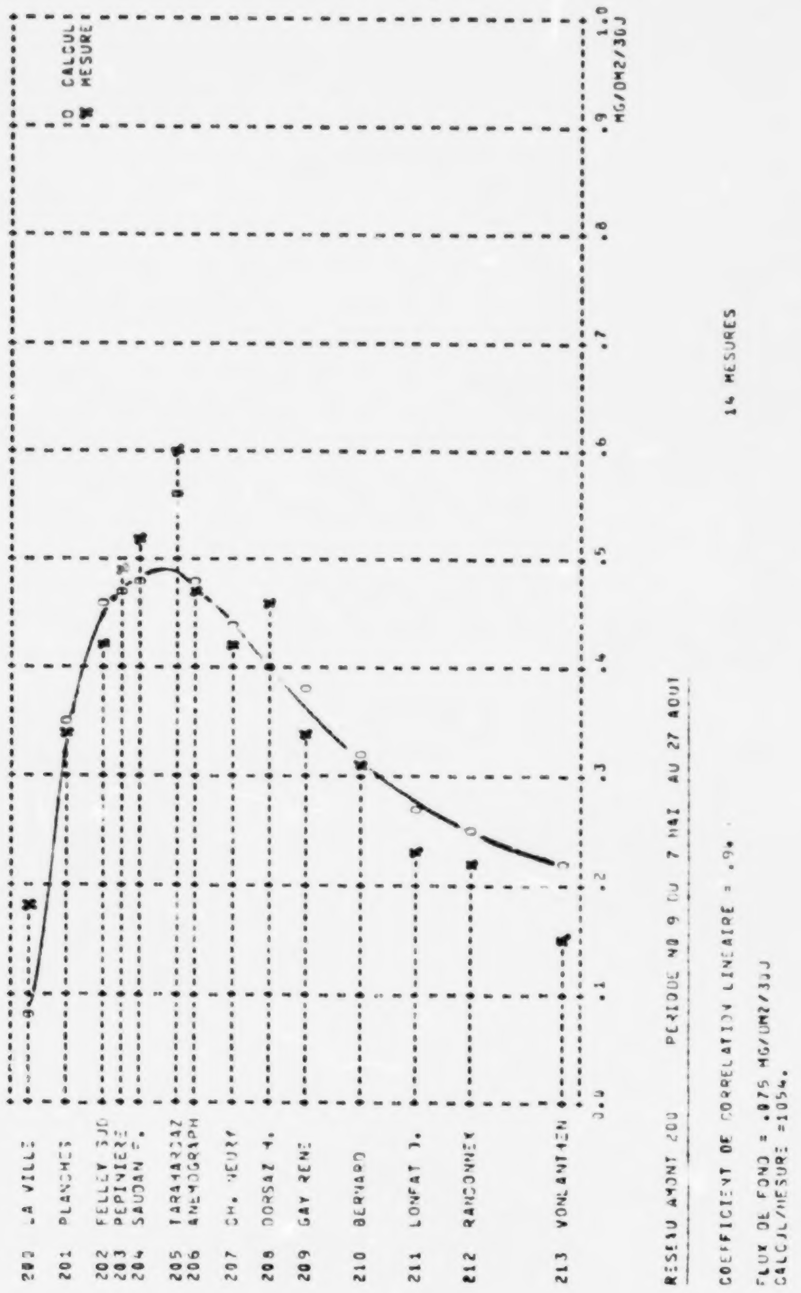

Fig. 11 Calculated fluxes and Harding measurements along the upper valley (summer means)

sede sa

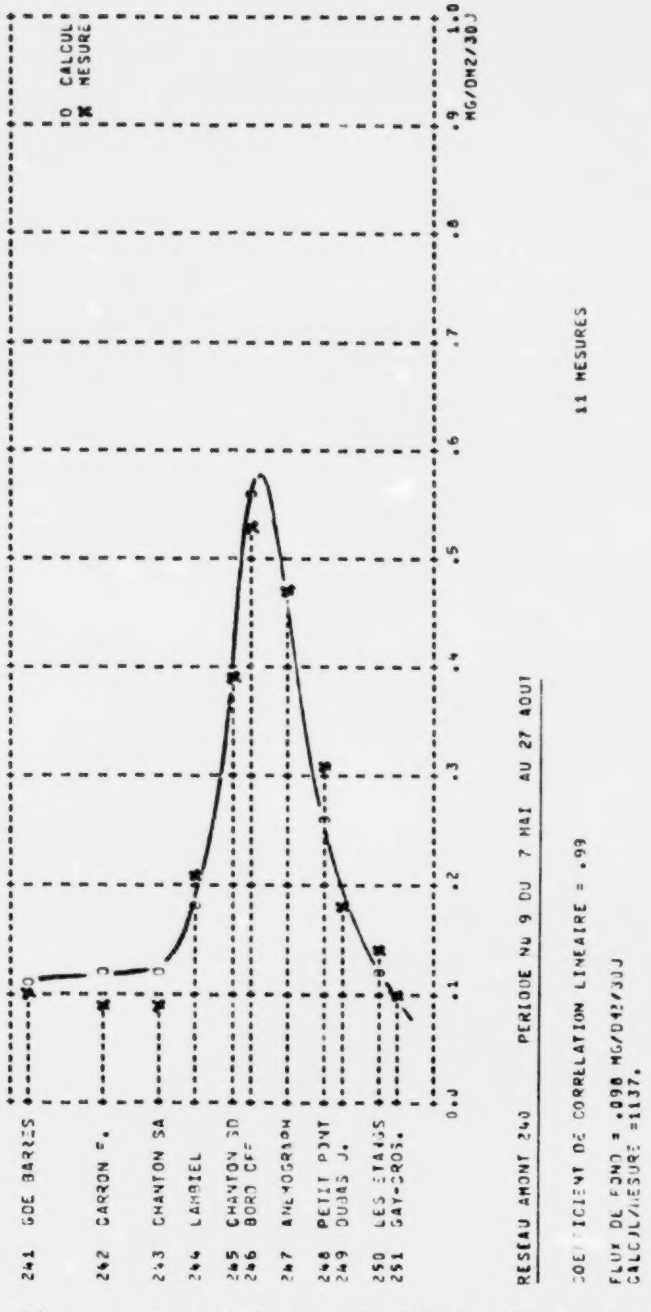

Fig. 12 Calculated fluxes and Harding measurements across the upper valley (summer means)

sede sa

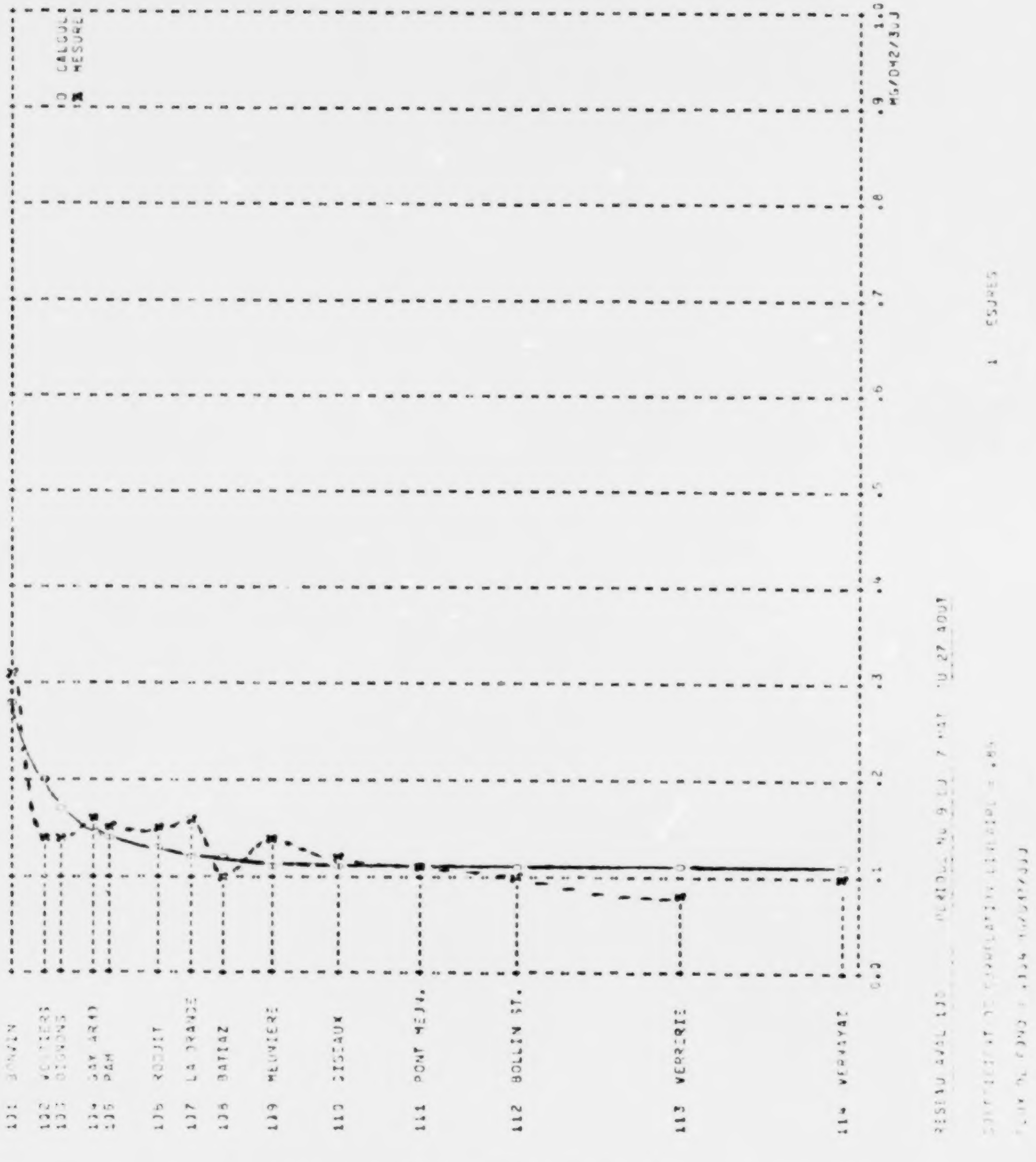

Fig. 14 Calculated fluxes and Harding measurements along the lower valley (summer means)

sede sa

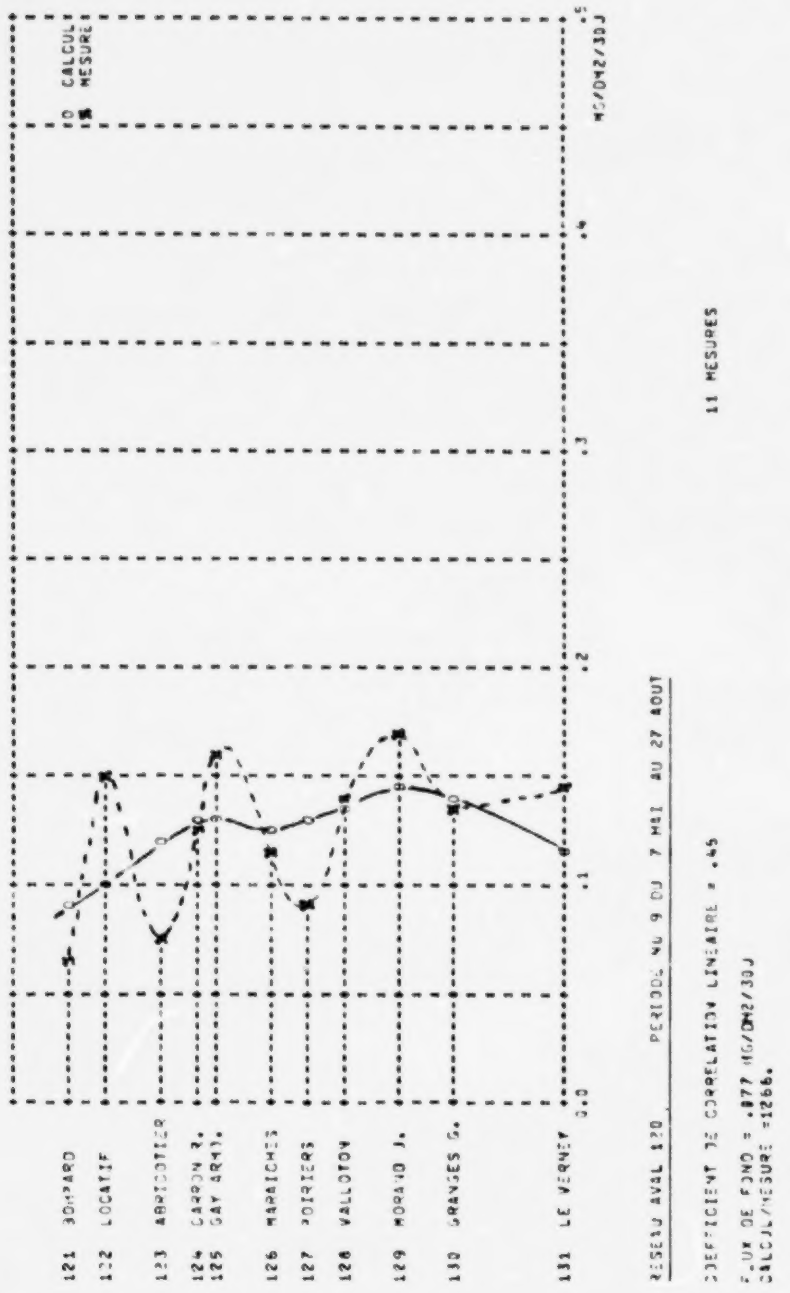

```
RESEAU AVAL 120        PERIODE NO 9 DU  7 MAI  AU 27 AOUT

COEFFICIENT DE CORRELATION LINEAIRE = .45                          11 MESURES

FLUX DE FOND = .077 MG/DM2/30J
CALCUL/MESURE =1266.
```

Fig. 14 Calculated fluxes and Harding measurements across the lower valley (summer means)

sede sa

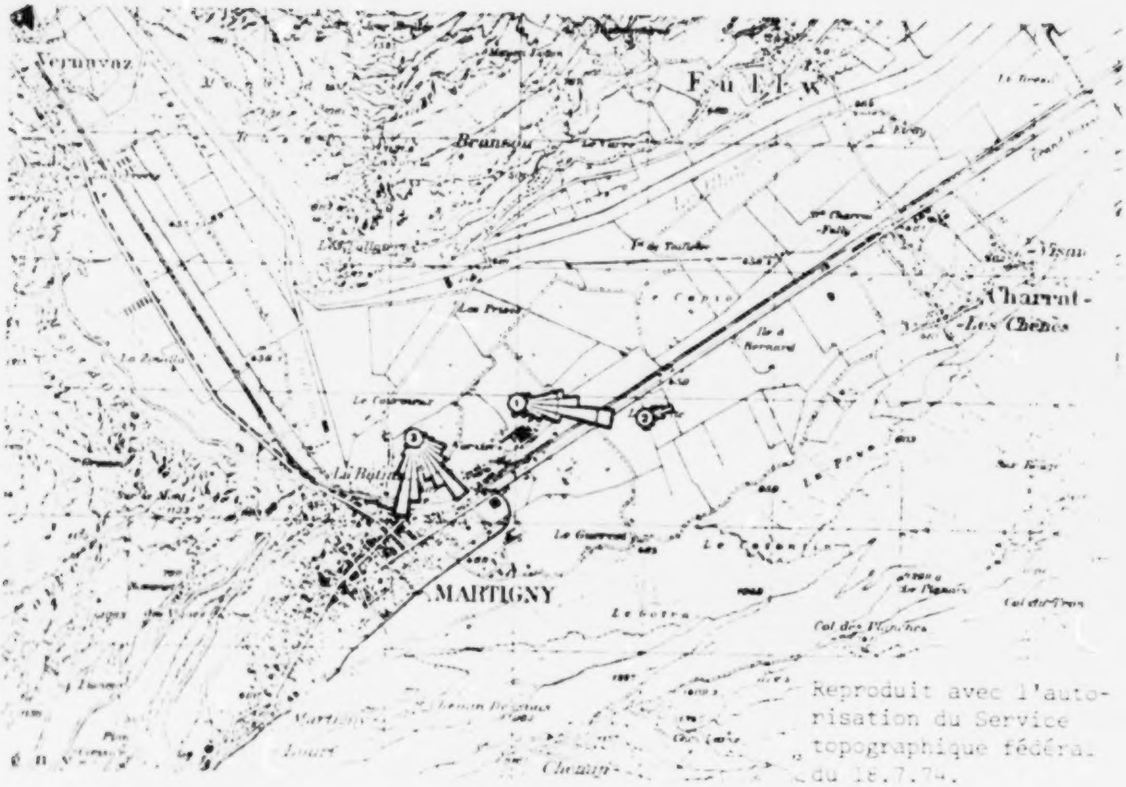

Reproduit avec l'autorisation du Service topographique fédéral du 18.7.74.

Fig. 15 Rose of the winds between 300 am and 600 am

6th NATO /CCMS
International Technical Meeting on Air Pollution Modeling

The Role of Wind-Tunnel Modeling in Predicting Dispersion

C. F. Barrett
Warren Spring Laboratory
Gunnels Wood Road
Stevenage
Hertfordshire, UK
SG1 2BX

Battelle-Institut e. V. Frankfurt/M
Germany, FR
24 - 26 September, 1975

The Role of Wind-Tunnel Modeling in Predicting Dispersion

INTRODUCTION

In the second of this series of meetings, Snyder gave a valuable discussion of similarity criteria for fluid modelling which was subsequently published (ref 1). At the last (fifth) meeting (Chapter 31 of the Proceedings) a paper by the same author was devoted to the fluid modelling programme of the meteorology laboratory at the EPA. This further contribution on wind-tunnel modelling does not pretend to be an exhaustive survey but is based on the author's own experience, which is confined to non-stratified wind tunnels, and is intended to stimulate discussion. More rigorous discussion will be found in references 1 and 2.

SIMILARITY CRITERIA

Similarity criteria are discussed in reference 1. The discussion here will be confined to some points of interest or difficulty. A fundamental point quoted from reference 1 is "All modellers recognize that rigorous modelling with significant reduction in scale is impossible". Hence in every experiment choices must be made of which parameters need to be matched and which ones can be sacrificed.

REYNOLDS NUMBER

It is impossible to match full scale Reynolds Numbers in a wind tunnel. Not only is there a considerable reduction in the length scale (typically of order 1/500) but velocities are also frequently reduced (typically by a factor of 5) because it is desired to simulate buoyancy. Hence Reynolds Numbers are typically three orders of magnitude smaller in the model than at full scale. The question arises: what is the minimum tolerable Reynolds Number? Snyder points out that the main effect on the flow is in the restriction of the high frequency end of the turbulence spectrum. Specifically the ratio of the Kolmogoroff microscale to a characteristic length in the flow is expected to vary as $Re^{\frac{3}{4}}$. With no reduction in wind-speed the typical value of 1 mm for this microscale in the lowest 100 m of atmosphere becomes the equivalent of 10 cm in the model. Allowing for a speed reduction by a factor of 5, this becomes the equivalent of 35 cm. Most problems of interest relate to much larger scales and difficulty due to this cause is unlikely. An exeption is the diffusion of puffs and also problems where concentrations over short periods are of interest, notably odours. Care in the use of models in these problems is clearly necessary and further work is called for.

The effect on the flow around buildings has been much discussed, though little work has been done. For sharp-edged structures, a critical Reynolds Number of 11 000 appears to be indicated and this not very restrictive. For rounded structures the position is less satisfactory. Some recent visualizations of the flow around large oil-storage tanks, (ref 2) showed changes in the boundary layer separation over range of Reynolds Number from 4.0×10^6 to 2.7×10^7. The modelling of rounded structures can therefore be uncertain.

SCHMIDT NUMBER

The Schmidt Number is the ratio of momentum diffusivity to mass diffusivity. It appears in the non-dimensionalised Navier-Stokes equation in the form of the product of Reynolds Number and Schmidt Number. For gases Schmidt Number is near to one (as is the corresponding number for diffusion of heat). By sacrificing Reynolds Number matching we are implying that molecular processes can be neglected and therefore we are also justified in ignoring differences in diffusitivities for gases and heat. However for particles of radius 1 µm the Schmidt Number is 10^6 and for radius 0.1 µm, 70 000. Hence if smoke is to be used quantitatively in a model experiment care may be necessary.

ROUGHNESS LENGTH

Geometrical similarity of model and prototype is required, but since Reynolds Number is not duplicated, fine detail is not required, and the surface can be represented by roughness length z_0. However if the roughness Reynolds Number $U^* z_0/v$ (where U^* is the friction velocity) falls below some critical value dependent on the geometry the flow becomes aerodynamically smooth and Reynolds Number dependent. For sand grains the critical values is 2.5, but this is certainly too low in many other cases. For small sparsely arranged blocks a value of around 10 seems to be adequate, but no general statement can be made at present.

Aerodynamically smooth flow is not an adequate representation of the atmosphere and so it is often necessary to increase the value of z_0 in the model over the full scale value. Fortunately atmospheric diffusion is not sensitively dependent on the value of z_0.

BOUNDARY-LAYER HEIGHT

Reference 1 says "Boundary-layer heights must, of course, correspond with the geometrical scale ratio". It is not clear to the author whether the full scale height referred to is $0.2\ U^*/f$ or z_i to use conventional notation.

The upper part of the boundary layer in wind-tunnel models is not in equilibrium. In any case it will be different from the atmospheric equivalent because there is no change in direction with height in the tunnel. (In most cases also it will be stably stratified). It is only the lower part of the boundary layer that can be modelled with some certainty. It therefore seems to the author that simulation is not likely to be sensitively dependent on the boundary layer height. In practical cases the full scale value will often not be known, which would raise difficulties if the suggested insensitivity is not valid.

The failure to model the upper part of the boundary layer implies that problems involving diffusion in this region may not be successfully modelled. Thus there may be some question about modelling effluent from high power station chimneys and also about diffusion over considerable distances. In the latter case the problem will show itself in the influence of the turning of the wind with height. The limiting distance seems to be somewhere greater than 5 km but is not known with certainty.

EQUIPMENT

A summary of many of the tunnels used in simulation of the boundary layer may be found in the report on a recent Euromech conference devoted to this subject (ref 4). The opinions given there were that 1/500 is the minimum scale possible if buoyant effects are to be modelled and that the test section should be 20 m long to allow sufficient fetch for boundary layer growth, and at least 3 m wide to avoid any effects of walls. Too large a tunnel "is undesirable as it takes too long to change models and conduct experiments". (The one the author works with has dimensions 20 m long x 1.5 m high x 4.3 m long).

Most workers use a system devised by Counihan to produce an artificially thickened boundary layer; this system has three components: a barrier, vorticity generators and surface roughness. This gives a region sufficiently slowly developing to be suitable for modelling experiments beyond about seven boundary-layer heights.

It is clear that quite substantial installations are required. In addition a good deal of time and effort has to go into instrumentation particularly for the measurement of concentration for which suitable instrumentation is not available commercially. At Warren Spring Laboratory we use methane as a tracer gas and determine its concentration with equipment based on the flame ionization detector. This system has a time constant of about 0.5 second; for faster response an infra-red system has been devised but we have little experience of its use so far.

A few wind tunnels have means for producing stable stratification. This requires even more engineering and the author has no direct experience of it.

Reproduced from
best available copy.

VERIFICATION

The verification of wind-tunnel modelling will not be discussed in detail. Very realistic plumes in the unobstructed flow can be obtained, whose spread agrees well with published data, e.g. the well-known Brookhaven figures. We can therefore assume that the concentrations obtained correspond approximately to 1-hour mean values. To the author's knowledge no full scale data have been compared with measurements made in a fully developed boundary layer. Measurements have been conducted mainly in tunnels with uniform flow or, if the wind shear was present, the turbulence levels were far too low. Nevertheless the results obtained are encouraging and do not cast any doubt on the results of model experiments. Clearly more work needs doing in this area.

USES OF MODEL EXPERIMENTS

The brochure reproduced in Chapter 31 of the proceedings of the fifth of these meetings (reference 5) summarizes the uses that can be made of fluid models. Broadly they find their major application in regions where there are large obstructions to the flow, such as buildings or hills. Among the jobs to which the Warren Spring wind tunnel has been applied are:

- Selecting suitable heights for chimneys close to large buildings.
- Placing of ventilation intakes to avoid contamination.
- Study of an "air-rights structure" i.e. where a building is situated over a vehicle underpass.
- Dispersion in a valley.
- Study of the possibility of fog formation on a trunk road due to water vapour emission from a large works.
- Dispersion of exhausts from motor vehicles.

Dispersion of dense explosive gases.
Performance of particulate samplers.

These are perhaps sufficient to indicate the range of problems considered by one group.

Lastly, fluid models have a demonstrative (or educational) value in convincing architects, planners etc. of the need for unwelcome decisions on chimney height or fuel usage.

REFERENCES

1 Snyder, W. H. Similarity Criteria for the Application of Fluid Models to the Study of Air Pollution Meteorology. *Boundary Layer Meteorology*, 1972, *3*, 113-34.

2 Plate, Erich J. *Aerodynamic Characteristics of Atmospheric Boundary Layers*, US Atomic Energy Commission, 1971.

3 Probert, S. D., Hasson, M. A. and Lee, T. S. Boundary layer separation for winds flowing around large fixed-roof oil-storage tanks with small aspect ratios. *Atmos Environ*., 1973, *7*, 651-4.

4 Hunt, J.C.R. and Fernholz, H. Wind-tunnel simulation of the atmospheric boundary layer; a report on Euromech 50. *J. Fluid Mech*., 1975, *70*, 543-59.

5 Snyder, W. H. Fluid modeling program of the Meteorology Laboratory, US Environmental Protection Agency. Chapter 27 of Proceedings in the fifth meeting of the expert panel on air pollution monitoring, 1974.

6th NATO/CCMS
International Technical Meeting
on Air Pollution Modeling

PREVISIONAL MODEL OF GASEOUS POLLUTANT DISTRIBUTION FOR OPTIMAL CONTROL OF EMITTING SOURCES

by

G.L. Marziano, A. Sutera, L. Gianolio, M. Ciprian
Istituto Ricerche "G. Donegani", Montedison S.p.A.
Via del Lavoro 4, 28100 Novara, Italy

BATTELLE - INSTITUT E.V., Frankfurt/Main
Germany, FR

24 - 26 September, 1975

ABSTRACT

In this paper a managing model for optimal control of industrial pollutant emitting sources in the area of Venice (Italy) is presented.

This model, presently under development, will consist of the following three parts, mutually interacting:

i) a meteorological model, able to predict the meteorological situation with at least twelve hours' advance.

ii) an air quality simulation model, which calculates the distribution of gaseous pollutants, when the emitting sources and the meteorological parameters are specified.

iii) an optimization program, able to choose the most economical way to reduce the emissions, so that the pollutant concentration might be everywhere less than a prefixed value.

The equations and the numerical methods of solution used in the first two models are presented; a detailed flow-chart of the third model is also reported.

Finally, as a first application, SO_2 concentration distributions calculated by the air quality simulation model in the Venice area are presented. Results are analysed and compared with experimental data.

1. Foreword

As the problem of air pollution becomes every year more and more important, many methods have been proposed in order to solve it, at least in the sense of maintaining the pollutant concentration at ground level lower than a prefixed value. However this objective cannot be reached in a convenient way without a good knowledge of the relations between pollution and the factors that influence it. Among these the most important appear to be,as the experience shows, the intensity, the characteristics and the distribution of the emitting sources, and the meteorological conditions as well. It is not necessary to precise, as everybody knows, that the meteorological conditions are very much influenced by the geographical situation of the region under consideration, so that this too is playing a very important role in the problem.
From the previous statements it is easy to understand that the factors governing the air pollution in a given area are so many and so deeply interrelated, that, in order to solve the problem, either one relies on empirical criteria, which however balance their low cost with a complete lack of reliability and rationality or has to develop a model, which may account, in the most reasonable way, for at least the most important influencing factors.

Although many problems are still to be solved, expecially as far as atmospheric turbulence is concerned, one might say that in the present state of the art, in the field of air quality simulation models, exist various models that can give a reasonable picture of the way in which the diffusion of pollutant products in the atmosphere occurs. It appears that now the main reason why many air quality simulation models don't check so well with experimental results lies in the degree of uncertainty which affects the input data. It is evident, in fact, that the more a model is sophisticated,the more detailed must be the input data in order to get reasonable results. This is the price which has to be paid if one wants a better resolution, either in space or in time, of the results of the model.

For the reasons listed above, in the present paper no new air quality simulation model is presented; rather, a more complex model, which includes as one of its parts an already existing diffusion model, is presented.

This is a managing model that, on the base of meteorological previsions and the results of an air quality simulation model, may allow to control in an optimal way the industrial emitting sources in order to keep the pollutant concentration less than a prefixed value.

The forementioned managing model is still being developed, however some informations about it can already be given. Moreover, to be shure that the model will have a good probability of working efficiently, a preliminary evaluation of the reliability of the chosen air quality simulation model has been performed, using available data related to the area to which the model first is going to be applied.

2. The structure of the managing model

The managing model we are dealing with in this paper, will consist of the following three parts, mutually interacting:

i) a meteorological model, able to predict the meteorological situation with at least twelve hours'advance;

ii) an air quality simulation model, which calculates the predicted distribution of pollutants, on the base of the predicted values of the emissions and of the meteorological parameters;

iii) an optimization program, able to choose the most economical way to reduce the emissions in order to keep the pollutant concentration everywhere less than a prefixed value.

The area to which this model will be applied is the urban and industrial area of Venice, in Italy. Of course, the model is being developed in the most general way, so that it should be possible to apply it to other places, however it has to be considered that, as the factors which have to be accounted for in a meteorological model depend on the area under consideration, still the meteorological part of our model refers mainly to Venice.

Up to now, only theoretical work has been done on the meteorological model, namely the mathematical formulation of the problem: as to the choice of the numerical methods of solution, tests are still made in order to get a good one considering the predictive nature of the model. As far as the optimization program is concerned, the control strategy has already been chosen, in principle: however no practical application has yet been performed, as the necessary data couldn't yet be acquired.

As to the air quality simulation program, it has been preliminarly verified with available data in the Venice area for the period 15th-28th February 1975.

The managing model is presently restricted to the pollution due to SO_2, because this pollutant is the only one for which consistent data are or may become available in Venice: obviously no difficulty, in principle, stands against the extension of the model to other gaseous pollutants, provided data on their emission and the possibility of their control can be obtained.

3. The meteorological model

3.1. The physical problem

In order to study the local circulation, intended as the meteorological field in a closed region with the horizontal dimension of some hundred Kilometers and the vertical dimension of a few thousand meters, we can start from the consideration that local motions of atmosphere are the result of the interaction between more motions generated in a different way. For the purpose of this note it is advantageous to consider two distinct motions that are defined for two different scales.

If we set M the meteorological field in a local motion, we assume that it is given by:

$$M = M_1 + M_2 \qquad (3.1)$$

where:

M_1 - represents the meteorological field due to large scale flow patterns;

M_2 - represents the meteorological field due to the response of atmosphere to the presence of inhomogeneities of the earth's surface in a assigned region.

Each of the two M represents any of the dependent variables u, v, w, θ, q.

(The introduction of humidity in this model is done to allow the introduction in it of radiative effects).

The topographic characteristic of the Venice area allows us to assume M_2 as the meteorological field of a breeze-motion. This particular local motion is known from a theoretical point of view to be the response of atmosphere to an horizontal thermal gradient produced by the temperature difference between land and sea.

As a result of turbolent diffusion the heat flows towards the higher layers of atmosphere and produces these horizontal gradients.

The breeze circulation is confined in the lower layers of atmosphere, practically in the planetary boundary layer. This layer is turbolent and consequently the principal mechanism of energy exchange in a breeze-motion is turbolent diffusion. Since the scale of turbolence is a subgrid scale with respect to the motion in question we shall perform the appropriate parameterization for turbolent diffusion coefficients.

3.2. The synoptic variables

The observation studies of synoptic motion suggest that this state is changing slowly with time. Then, it is no longer necessary to consider the dynamics of the synoptic motion. We assume thus:

$$\frac{\partial}{\partial t} M_1 \equiv 0 \qquad (3.2)$$

This assumption is also in accordance with the following scale analyses. The synoptic motion has an advective time of about 10^5 sec, while the breeze has an advective time of about 10^4 sec. This implies that the synoptic variables change very little during the evolution of breeze-motion. Furthermore, the (3.2) implies also that the synoptic variables can be introduced as initial condition respect to breeze-motion.

Another consideration about the synoptic state is that we must consider this motion in planetary boundary layer and therefore it is modified by torbolent nature of this layer. The modification, due to turbolent diffusion, generally involves changes in the velocity, temperature and moisture in the synoptic state. Actually, these changes depend also on the properties of the earth surface.

If we assume that the surface inhomogeneities don't modify the synoptic flow, we can use an one-parameter model for modelling this motion.

This means that synoptic state in the planetary boundary layer is given by:

$$\frac{\partial}{\partial z}\left(K_z^{(m)}\frac{\partial}{\partial z}\hat{u}\right)+f\left(\hat{v}-v_g\right)=0 \tag{3.3}$$

$$\frac{\partial}{\partial z}\left(K_z^{(m)}\frac{\partial}{\partial z}\hat{v}\right)+f\left(u_g-\hat{u}\right)=0 \tag{3.4}$$

(3.5) $$\frac{\partial}{\partial z}\left(K_z^{(\theta)}\frac{\partial}{\partial z}\hat{\theta}\right) = 0$$

(3.6) $$\frac{\partial}{\partial z}\left(K_z^{(q)}\frac{\partial}{\partial z}\hat{q}\right) = 0$$

Moreover, we assume that synoptic state is a barotropic state without vertical motion. With this assumption we can put:

(3.7) $$\frac{\partial}{\partial x}\hat{u} = \frac{\partial}{\partial x}\hat{v} = \frac{\partial}{\partial x}\hat{\theta} = \frac{\partial}{\partial x}\hat{q} = 0$$

(3.8) $$\frac{\partial}{\partial y}\hat{u} = \frac{\partial}{\partial y}\hat{v} = \frac{\partial}{\partial y}\hat{\theta} = \frac{\partial}{\partial y}\hat{q} = 0$$

(3.9) $$\hat{w} = 0$$

3.3 The predictive equations

In order to obtain the equations for the prediction of breeze motion from the general equations of hydrothermodynamics we assume that:

a) there are no radiation effects in breeze-motion;

b) there are no moisture phase change effects in the dynamics or thermodynamics equations;

c) the synoptical and local horizontal diffusion coefficients are set to zero;

d) the lower layers of atmosphere are considered as incompressible;

e) the perturbations are considered as hydrostatics;

f) the products between pressure perturbations are neglected.

In order to justify the assumptions d, e, f we have used the conclusions of Dutton's paper (Dutton e Fichtl 1969); while the assumptions a, b are due to the necessity to simplify the model equations.

With these assumptions we obtain a prognostic set of equations:

(3.10)
$$\frac{\partial}{\partial t}\tilde{u} + (\tilde{u}+\hat{u})\frac{\partial}{\partial x}\tilde{u} + (\tilde{v}+\hat{v})\frac{\partial}{\partial y}\tilde{u} + \tilde{w}\frac{\partial}{\partial z}(\tilde{u}+\hat{u}) = -\theta\frac{\partial}{\partial x}\tilde{\pi} -$$
$$- f v_g \tilde{\theta}/\hat{\theta} + \frac{\partial}{\partial x}\left[\tilde{K}_x^{(m)}\frac{\partial}{\partial x}\tilde{u}\right] + \frac{\partial}{\partial y}\left[K_y^{(m)}\frac{\partial}{\partial y}\tilde{u}\right] + \frac{\partial}{\partial z}\left[(\tilde{K}_z^{(m)}+\hat{K}_z^{(m)})\frac{\partial}{\partial z}(\tilde{u}+\hat{u})\right] +$$
$$+ f\tilde{v}$$

(3.11)
$$\frac{\partial}{\partial t}\tilde{v} + (\tilde{u}+\hat{u})\frac{\partial}{\partial x}\tilde{v} + (\tilde{v}+\hat{v})\frac{\partial}{\partial y}\tilde{v} + \tilde{w}\frac{\partial}{\partial z}(\tilde{v}+\hat{v}) = -\theta\frac{\partial}{\partial y}\tilde{\pi} +$$
$$+ f u_g \tilde{\theta}/\hat{\theta} + \frac{\partial}{\partial x}\left[\tilde{K}_x^{(m)}\frac{\partial}{\partial x}\tilde{v}\right] + \frac{\partial}{\partial y}\left[\tilde{K}_y^{(m)}\frac{\partial}{\partial y}\tilde{v}\right] + \frac{\partial}{\partial z}\left[(\tilde{K}_z^{(m)}+\hat{K}_z^{(m)})\frac{\partial}{\partial z}(\tilde{v}+\hat{v})\right] -$$
$$- f\tilde{u}$$

$$(3.12)\quad \frac{\partial}{\partial t}\tilde{\theta} + (\tilde{u}+\hat{u})\frac{\partial}{\partial x}\tilde{\theta} + (\tilde{v}+\hat{v})\frac{\partial}{\partial y}\tilde{\theta} + \tilde{w}\frac{\partial}{\partial z}(\tilde{\theta}+\hat{\theta}) =$$

$$\frac{\partial}{\partial x}\left[\tilde{K}_x^{(\theta)}\frac{\partial}{\partial x}\tilde{\theta}\right] + \frac{\partial}{\partial y}\left[\tilde{K}_y^{(\theta)}\frac{\partial}{\partial y}\tilde{\theta}\right] + \frac{\partial}{\partial z}\left[(\tilde{K}_z^{(\theta)}+\hat{K}_z^{(\theta)})\frac{\partial}{\partial z}(\tilde{\theta}+\hat{\theta})\right]$$

$$(3.13)\quad \frac{\partial}{\partial t}\tilde{q} + (\tilde{u}+\hat{u})\frac{\partial}{\partial x}\tilde{q} + (\tilde{v}+\hat{v})\frac{\partial}{\partial y}\tilde{q} + \tilde{w}\frac{\partial}{\partial z}(\tilde{q}+\hat{q}) =$$

$$\frac{\partial}{\partial x}\left[\tilde{K}_x^{(q)}\frac{\partial}{\partial x}\tilde{q}\right] + \frac{\partial}{\partial y}\left[K_y^{(q)}\frac{\partial}{\partial y}\tilde{q}\right] + \frac{\partial}{\partial z}\left[(\tilde{K}_z^{(q)}+\hat{K}_z^{(q)})\frac{\partial}{\partial z}(\tilde{q}+\hat{q})\right]$$

where $f = 2\Omega\sin\phi$ and $f_c = 2\Omega\cos\phi$
and the diagnostic equations:

$$(3.14)\qquad \frac{\partial}{\partial z}\tilde{w} = -\left(\frac{\partial}{\partial x}\tilde{u} + \frac{\partial}{\partial y}\tilde{v}\right)$$

$$(3.15)\qquad \frac{\partial}{\partial z}\tilde{\pi} = g\,\tilde{\theta}/\hat{\theta}^2$$

The set (3.10) - (3.15) forms a system of six equations for the six unknown $\tilde{u}$, $\tilde{v}$, $\tilde{w}$, $\tilde{q}$, $\tilde{\theta}$, $\tilde{\pi}$. This is a close set if we know the functional form of diffusion coefficients. Moreover, in order to solve the preceding equations we must assign the appropriate boundary conditions.

The synoptical diffusion coefficient is assumed as if the atmosphere were neutral, while the local one must be able to simulate also the stable and convective cases.

4. The Air Quality Simulation Model

4.1 General Remarks

The air quality simulation model is the one developed by C.C. Shir and L.J. Shieh [1]. Fundamentally it is based on the assumption that the concentration C of pollutant gas, which is function of time and space, is solution of the differential equation:

$$\frac{\partial C}{\partial t} + \vec{V}\nabla C = K_H \nabla_H^2 C + \frac{\partial}{\partial z}\left(K \frac{\partial C}{\partial z}\right) + Q + R \qquad (4.1)$$

where:

$\vec{V}$: wind velocity (which cartesian components are U, V, W), that is considered function of space and time

∇ : gradient operator $\left(\frac{\partial}{\partial x} + \frac{\partial}{\partial y} + \frac{\partial}{\partial z}\right)$

K_H : horizontal turbulent diffusion coefficient

K : vertical turbulent diffusion coefficient, which is assumed function of z and of the atmospheric conditions

$\nabla_H^2 C = \frac{\partial^2 C}{\partial x^2} + \frac{\partial^2 C}{\partial y^2}$: horizontal laplacian of C

Q : emitting sources intensity

R : chemical reaction rate

In equation (4.1) the term $\vec{V}\nabla C$ represents the advection, while the first two terms on the right hand side represent the turbulent diffusion in the horizontal and the vertical respectively. It's worthy to note that the equation is of turbulent type, which means that the concentration $C(x,y,z,t)$ is not to be considered an instantaneous value, but a value averaged on a time interval sufficiently large to eliminate the rapid oscillations of the corresponding instantaneous variable and small enough that the temporal derivative itself doesn't loose sense.

The boundary conditions are:

$$K \frac{\partial C}{\partial z} = 0 \qquad \text{at } z = 0 \text{ and } z = H$$

$$\frac{\partial^2 C}{\partial x^2} = 0 \qquad \text{at } x = 0 \text{ and } x = x_{max} \qquad (4.2)$$

$$\frac{\partial^2 C}{\partial y^2} = 0 \qquad \text{at } y = 0 \text{ and } y = y_{max}$$

where H is the mixing height, which is assumed dependent of time, according to the meteorological conditions.

4.2 The Physical Parameters of the Model

The integration of equation (4.1) requires that values for H, $\vec{V}$, K_H, K, Q, R are supplied as functions of time.

- The chemical reaction rate R is assumed proportional to C according to equation:

$$R = -k_a \, C \tag{4.3}$$

with $k_a = 10^{-4} \sec^{-1}$, when the pollutant is SO_2

- K is assumed depending on height (z), surface roughness and meteorological conditions (expecially stability, which is considered a continuous function of wind speed and insolation - the latter depending on sky cover and time of the day, once the place and the season are specified -)

- $\vec{V}$ is interpolated, at ground level, using data obtained at meteorological stations. Its variation with height is assumed a power law of the type

$$|\vec{V}| = |\vec{V}_g|(z/z_g)^p \tag{4.4}$$

where p is computed using two values of upper wind according to the relation:

$$p = \ln\,(|V_2|/|V_1|)/\ln(z_2/z_1) \tag{4.5}$$

and the subscript g refers to ground level (z_g is assumed equal to 10 m). Also the variation with height of the wind direction is accounted for.

- K_H is assumed related to K according to the formula

$$K_H = 100 \, K_{max} \cdot \frac{z}{z_s} \exp \left[-0.004 \, (z - z_s) \right] \tag{4.6}$$

with the constraint that K_H be not less than 100 and not larger than 500 m^2/sec.

For fuller details refer to the paper by Shir and Shieh (1974).

4.3 The Numerical Solution

The differential equation (4.1) is integrated using a finite difference scheme. More precisely, the advection and horizontal diffusion terms are approximated by second order central difference, and the Crank-Nicholson formula was used for the vertical diffusion term; furthermore, a time splitting method was applied in the discretization of the advective part of the concentration equation.

5. The application of the air quality model to the Venice area

An application of the air quality simulation model briefly described in 4. has been made to the Venice area for the period 15th-28th February 1975. One has to consider that this was the first time that an attempt was made to apply an air quality model to that area using short term (1 hr) averaged values and not climatological data.

This is the reason why for many sources it was impossible to get emission values averaged over so short a period: in fact, for some of them no more than yearly average values could be collected, and, as far as residential heating emissions were concerned, their distribution in space and time had to be assumed in the most reasonable way starting just from a global value of fuel consumption in the whole area. Another study is presently being developed, with data referring to the period 28th July - 11th August 1975, so that the influence of residential heatings may be cut off: moreover this study will possibly allow to evaluate the effects of breeze motions, which up to now cannot yet be accounted for, on the concentrations calculated by the model.

5.1 Input Data

A rectangular area of 22.5 x 30 kilometers, with longer side parallel to the North-South direction and shorter side parallel to the East-West direction, including the urban and industrial areas of Venice, Mestre and Porto Marghera, was chosen. It was then divided into 30x40 square grids of 750 m side each, that was the base of the numerical solution of equation (4.1).

As to the vertical grids, fourteen of them where considered, with size increasing with height from 20 to 140 meters at maximum. As the top of the model is assumed variable with the mixing height, ranging from 500 to 1000 m, the last five grids' sizes were assumed variable with time according to the meteorological conditions.

For each surface grid a value of surface roughness was determined, according to its morphological characteristics as they could be desumed from the map of the considered area. From the urban characteristics, as they could be determined from the map, the 24 hr average values of area source emissions were computed for each grid, starting from the value of global fuel consumption in the whole area. A diurnal pattern of area source emissions was assigned, in the lack of any information about it, based on reasonable assumptions on the way in which residential heating plants are operated.

In the considered area 60 stacks of industrial plants were located. For some of them it was possible to get hourly averaged SO_2 emission values, for some other only longer term (up to one day) average values, and for the remaining ones just an yearly average value.

As to the meteorological conditions, values of surface wind speed and direction every half an hour were given by two meteorological stations located within the considered area: these values were used to get hourly average values of wind speed and direction which then were interpolated to get corresponding values at every surface grid. In the lack of experimental observations, the upper wind values at 70 and 200 m were calculated from the value of geostrophic wind desumed from the meteorological charts, using the so called "Taylor's spiral" formula.

As values of geostrophic wind were supplied every twelve hours, the intermediate values were determined by linear interpolation, so that hourly values of upper wind could be obtained.

The mixing height at every hour of simulated time was computed using the following formula:

$$H = \left(\alpha_o + \frac{3}{4}\pi\right) \sqrt{\frac{2K}{f}} \qquad (5.1)$$

where α_o depends on stability and surface roughness, f is Corioli's parameter and K is the value of eddy diffusivity assumed constant in Taylor's spiral formula.

At one of the two forementioned meteorological stations (Tessera Airport), among other variables, also the sky cover, the temperature and the pressure were determined. The first one was supplied every hour to the model, to allow computation of continuous stability class in the way explained in the paper by Shir and Shieh.

There are, especially in winter, two particular meteorological situations, which origin in the area of interest a kind of local circulation for which the assumptions made before about upper wind values and mixing height become completely unreasonable: they are the fog and the bora wind.

When there is fog, synoptic conditions are such that a strong low inversion is present over the area: in such situation it's reasonable to assume that the height of the mixing layer coincides with the height of the fog stratus; in the lack of better information about the height of the fog stratus, an average value of 200 meters was assigned to the mixing height when fog was present: moreover no variation of wind speed was assumed with height.

When bora wind blows one may assume that the wind speed is constant up to roughly 800 meters: so, when the surface wind speed at ground level was greater than 6 m/sec and its direction was comprised between 0 and 90 degrees, a uniform wind field in the whole area was assumed and the mixing height was set up to 800 meters.

5.2 Results

The air quality simulation model computed the hourly average of surface concentration of SO_2 at every grid point. The SO_2 concentration was also measured at monitoring stations located over the area. Comparison was made between the one hour average values of the concentration measured at the stations and the values computed by the model for the grids in which the stations were located. This comparison is obviously not so meaningful, as it is made between local values and values which should be considered as averages made over a relatively large volume: however, keeping in mind this fact, it still can give a reasonable evaluation of the accuracy of the model. In figures 1+21 the diagrams of one hour average concentrations computed by the model and detected at three monitoring stations for all the 14 days considered are presented. As it can be seen, the model simulates, on the average, the concentration patterns both in the case of high and low concentrations. However it doesn't follow the sharp variations of the detected concentration,both because of the rather high uncertainty in the input data (not well known temporal variation of emitting sources intensity, as explained in 5.1, and not enough accurate values of meteorological parameters) and because of the fact, already explained, that the model gives volume averages while the monitoring stations detect local values, which can be influenced by local factors that are accounted for by the model only on an average base.

In figures 22+28 the comparison between observed and computed 24 hr averages of concentration at seven stations are presented. As it can be observed, the points don't lie so distant from the diagonal, showing a sufficiently good correlation between computed and observed data.

Fuller analysis of the results is still being performed, so no exact values of statistical indexes (for example correlation coefficients) are available. Roughly the correlation coefficient between 1 hr observed and computed average concentrations can be said to be not far from 0.5 using logarithmic scale and 0.32 using linear scale. The correlation coefficient for spatial averages (obtained averaging over the stations), still using 1 hr average values, is roughly 0.25 in linear scale and 0.38 in logarithmic scale. However it must be considered that these values were obtained using also detected values at stations that later appeared not to be working properly in that period. So, after a deeper analysis of detected values, the correlation coefficients listed above should probably rise; but also if they didn't rise so much, they should still be considered fairly good in view of the errors affecting input data.

In figure 29 the comparison between the whole period average computed and detected concentrations at seven stations is presented. Again, a good correlation between computation and observation appears.

6. The process control

6.1 General remarks

While the real time management of the emissions that occur in an industrial area is not the only scope of the previously presented models, still it represents their most logical application.

The development of a managing program for gaseous pollutant emissions in an industrial area is very interesting from an economical point of view. Such a program, in fact, where its development is technically possible, can grant a more rational temporal planning of the emissions, allowing a greater release of pollutants when the meteorological situation is favourable, and, on the other hand, suggesting a reasonable reduction of them when it's necessary. This results also in a better management of the pollution control facilities, in the sense that it can give optimal criteria for their project and utilization. The management of the emissions must evidently account for the legal limits, that, for SO_2 in Italy, are, for urban areas, 0.15 ppm on a 24 hr average and, for industrial areas, 5 ppm on an 8 hr average. Moreover these limits are going to be diminished, so that a rational management of emissions becomes even more necessary. A managing model is practically a method of determining, on the base of economical and technical considerations, the maximum allowable emission for every stack in order to keep the ground concentration below a prefixed value at the lowest possible cost.

The development of a managing model has to account for the following factors:

a) the method must be precise and rapid as well;

b) for a given plant there are many methods to reduce the pollutant emissions:

  b-1) variations (substantially always reductions) in the production;

  b-2) use of fuels containing a lower sulfur percentage (when the emission is due to combustion);

  b-3) abatement of SO_2 before the stack;

  b-4) variation of the release (heating of the gases, forced circulation, etc.);

c) some plants influence other plants, so that load variations affect both profit and emissions of the other plants;

d) if the control is made by changing the plant load, additional costs rise during the transient periods, as the relationship between load and profit is then more complex;

e) costs must be accurately evaluated according to the characteristics of each plant and of the industry operating it;

f) other variables, very difficult to evaluate, concern the relationships within an industry or between industries.

Because of the reasons listed above, an accurate preliminary analysis of all the technical, economical and strategic factors present in the considered area is necessary. This greatly limits the development of a managing model of more general applicability.

6.2 The method of the influencing factors

The emission management implies the optimization of an economical objective function of the emissions, with the constraint that the ground level SO_2 concentration be less than a given value. This would, in principle, require the use of an air quality simulation model at each iteration of the optimization cycle, just for the verification of the constraints. It's evident that such a policy would be unreasonable if the air quality simulation model previously described were applied (probably the results would be acquired too late for their practical application) and still too expensive even if a more simplified diffusion model (for example a gaussian one) were used. So another way has been chosen, based on the consideration that every surface grid's SO_2 concentration is mainly influenced by a small part of the total number of stacks, depending on meteorological conditions, and that, furthermore, it may be assumed that each of the influencing stacks contributes to its part of the SO_2 concentration proportionally to its emission intensity: this way is what we call the method of the "influencing factors". Let's define with F(i, j, m, n) the percentage by which stack n contributes to the SO_2 concentration of surface grid (i, i) under the m-th set of meteorological conditions and standard emission intensity: we call F the "influencing factor" of stack n over the grid i, j under meteorological conditions m. It is evident that, using the air quality simulation model in a parametric way, one can compute once for all a set of influencing factors (i, j, m, n) for a reasonable number of meteorological situations. So, when, by means of the meteorological predictive model, the meteorological situation has been determined, and, using the air quality simulation model, the predicted SO_2 concentrations at ground level have been computed, the values of i, j, m for the grids in which the concentration exceeds the allowed maximum can be immediately determined. By consequence, the proper values of the influencing factors F(i, j, m, n) can be chosen in the set of the precedently computed ones: optimization of emissions will then be performed just for those stacks whose influencing factors are significant, which greatly simplifies the solution; moreover, in the iterations of the optimization cycle, the computation of constraints will be done just using the influencing factors. The air quality simulation model will then be used again, after optimization has been performed, just for verification purposes. It's easy to understand that this method can grant a sufficiently fast optimization, while the precision mainly depends on the detail with which influencing factors are computed (namely the number of sets of meteorological conditions which have been considered). On the other hand, when dealing with control processes the rapidity in decision making can compensate to a certain degree a loss in precision. Moreover one has to consider that, at least during the winter period, the surface SO_2 concentration is also due to residential heatings, whose emissions neither are controllable nor are even known with sufficient precision: so a certain degree of imprecision is inevitable, if nothing because of the uncertainty by which residential emissions are known, and this imprecision is surely greater than that due to the method of influencing factors.

6.3 The control scheme

In figure 30 is reported a block diagram which better explains the relationships, for control purposes, among the various models previously described.

Starting from the present meteorological conditions, the meteorological model computes the predicted values of meteorological parameters, which are fed, with the predicted values of emissions, to the air quality simulation model. The computed values of ground level SO_2 concentration are then analysed to verify whether they exceed the limits fixed by the law. Using the influencing factors, the values of which are chosen, in the proper file, according to the meteorological conditions, the plants to be controlled are determined.

The objective function is expressed as the summation of the costs of changing the plants' operating conditions, which are related to the emissions through the plant models. This objective function is then minimized with the constraint for the surface SO_2 concentration to be less than the legal limits. The verification of the constraint is performed, during the optimization iterations, by means of the influencing factors, as previously said.

Once the optimal configuration of the operating conditions of the plants is computed, it is verified by feeding back the new emission values to the air quality simulation model.

7. Conclusions

In this paper a managing model for optimal control of gaseous pollutant emissions in industrial areas is proposed. This model consists in the coupling of an already existing air quality simulation model with a meteorological predictive model and a process control program. Because of the great importance of local factors, only in principle it is of general applicability. So the study is presently restricted to the control of SO_2 concentration at ground level in the area of Venice (Italy), and is still under development. As the possibility of practical use of such a tool lies in the reliability of the results it gives, contemporarily to the theoretical work on the meteorological and the control models, a preliminary evaluation of the capability of the air quality simulation model to describe the pollution in the chosen area has been performed. The results show that the model, previously tested only in St. Louis, is applicable to Venice too: actually it clearly appears that the precision of results is quite correlated to the detail with which input data have been provided. An application for control purposes, however, requires a more detailed analysis of the capability of the model to simulate the sharp variations in concentration, which implies a better knowledge of the time and space trend of emission intensities and meteorological parameters. For the considered area is quite complex from a meteorological point of view and densely industrialized too, the acquisition of very detailed data is rather difficult. So, although it's possible to say that, in principle, the proposed model is feasible and its development is going on satisfactorily, a lot of work is still to be done before a practical application can be satisfactory.

8. References

1) C. C. Shir, L. J. Shieh: A Generalized Urban Air Pollution Model and Its Application to the Study of SO_2 Distributions in the St. Louis Metropolitan Area.
Journ. of Applied Meteorology 13, 2 (1974), pp. 185-204.

2) J. E. Fromm, Numerical Solution of the Navier-Stokes Equations at High Reynolds Numbers and the Problem of Discretization of Convective Derivates. IBM Research Report.

3) L. Collatz, The Numerical Tratment of Differential Equations (Springer 1960).

4) Dutton-Fichtl (1969): "Approximate equations of motion for gases and liquids" J. Appl. Meteor. 11, pg. 91-115.

5) Estoque M.A. (1961): "A theoretical investigation of the sea breeze". Quart. J. Roy. Meteor. Soc., 87, 136-146.
(1962): "The sea breeze as a function of prevailing synoptic situation" J. Atmos. Scie. 19, 224-250.

6) Magata (1965): "A study of the Sea-Breeze by the numerical experiment" J. Meteor. Soc. Japan 16, 23-36.

7) Malkus, Joannes S., Witt G. (1959): "The evolution of a convective element. A numerical calculation". The Atmosphere and Sea in Motion, New York, The Rockfeller Institute Press, pp. 425-439.

8) Mc Pherson, R.D. (1970): "A numerical study of the effect of a coastal irregularity" J. Appl. Meteor., 9, 767-777.

9) Molekamp, C.R. (1868): "Accuracy of finite difference methods applied to the advection equation" J. Appl. Meteor., 7, 160-167.

10) Leith, C. E. (1969): "Two dimensional eddy viscosity coefficients". Proc. WHO/IUCA Simposium on Numerical Weather prediction in Tokio, Nov. 26-Dec. 4, 1968. Japan Meteorological Agency, Tokyo, pp. I-41, I-44.

11) Lilly, Douglas K. (1962): "On the numerical simulation of buoyant convection" Tellus, 14, 148-172.

12) O'Brien, J.J. (1970): "A note on the vertical structure of the eddy exchange coefficient in the planetary boundary layer", J. Atm. Scie., 27, 1213-1215.

13) Pielke, R. A. (1974): "A three-dimensional Numerical model of the Sea-Breezes over South Florida" Mon. Wea. Rev., 102, 115-139.

14) Yamamoto, G. and Shimanuki A. (1964): "Turbulent transfer in diabatic condition" J. Meteor. Soc. Japan, 44, 301-307.

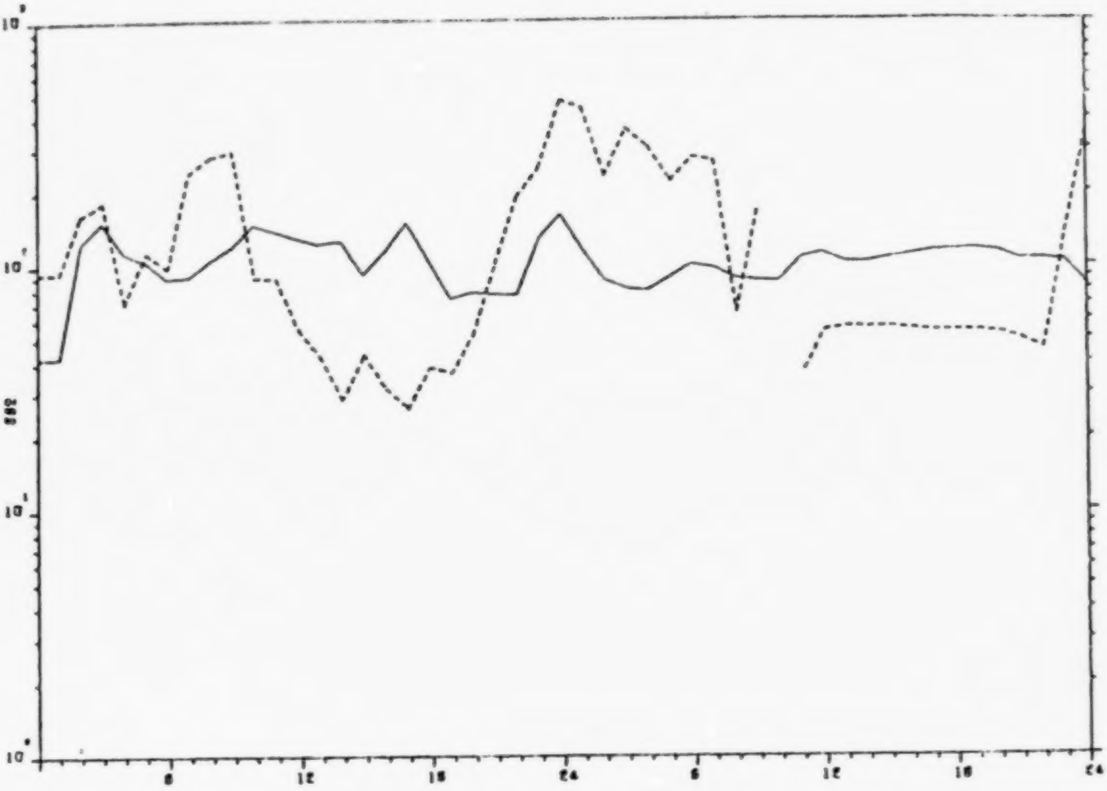

FIG. 1 - Computed (solid line) and observed (dashed line) SO_2 concentrations at station n. 4 for the days February 15th-16th 1975 (SO_2 concentrations are in arbitrary units).

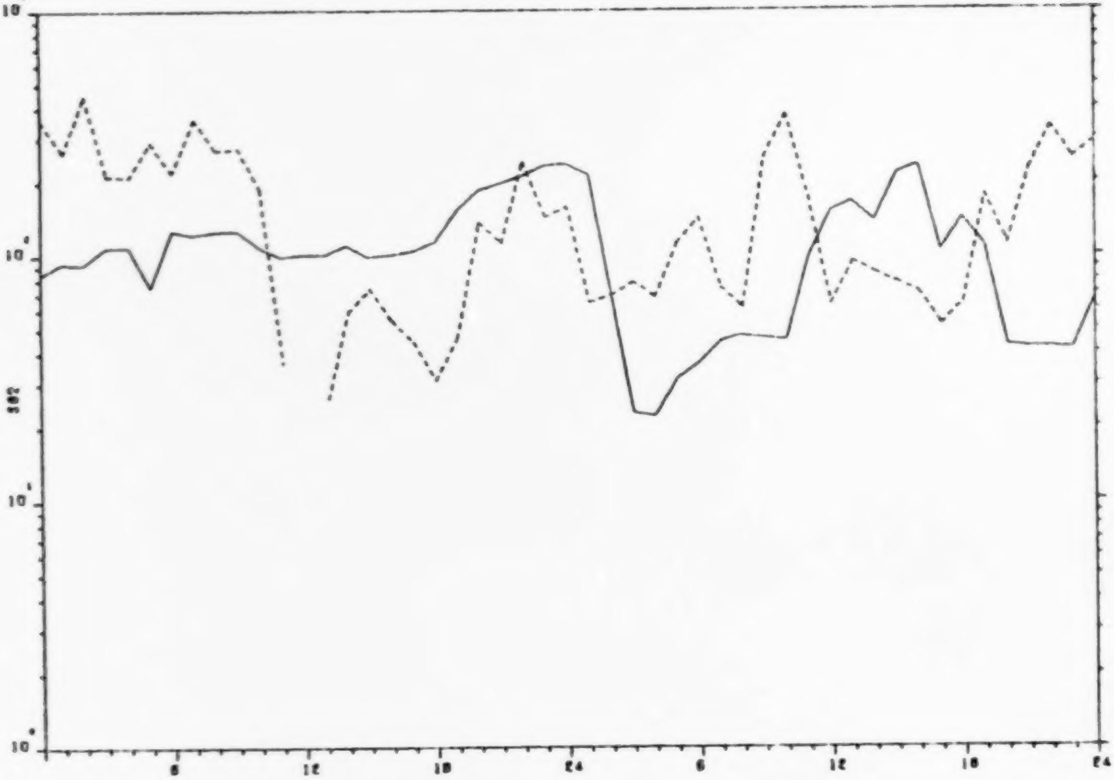

FIG. 2 - Computed (solid line) and observed (dashed line) SO_2 concentrations at station n. 4 for the days February 17th-18th 1975 (SO_2 concentrations are in arbitrary units).

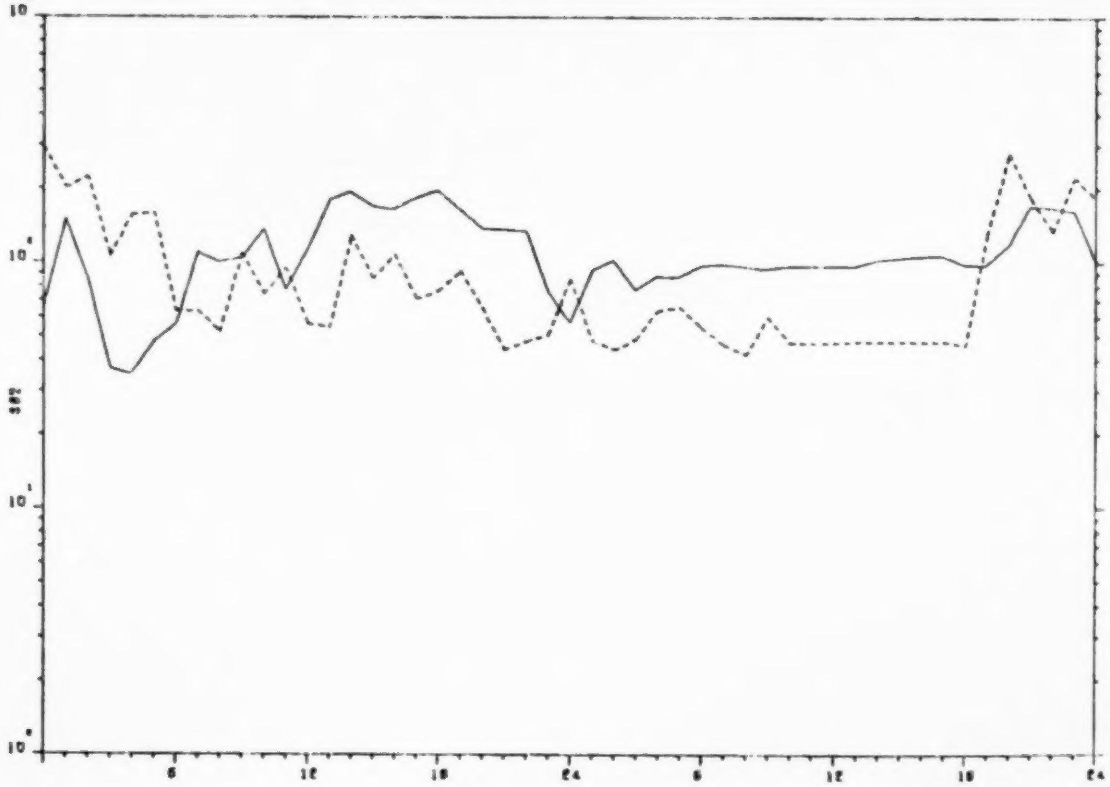

FIG. 3 - Computed (solid line) and observed (dashed line) SO_2 concentrations at station n. 4 for the days February 19th-20th 1975 (SO_2 concentrations are in arbitrary units).

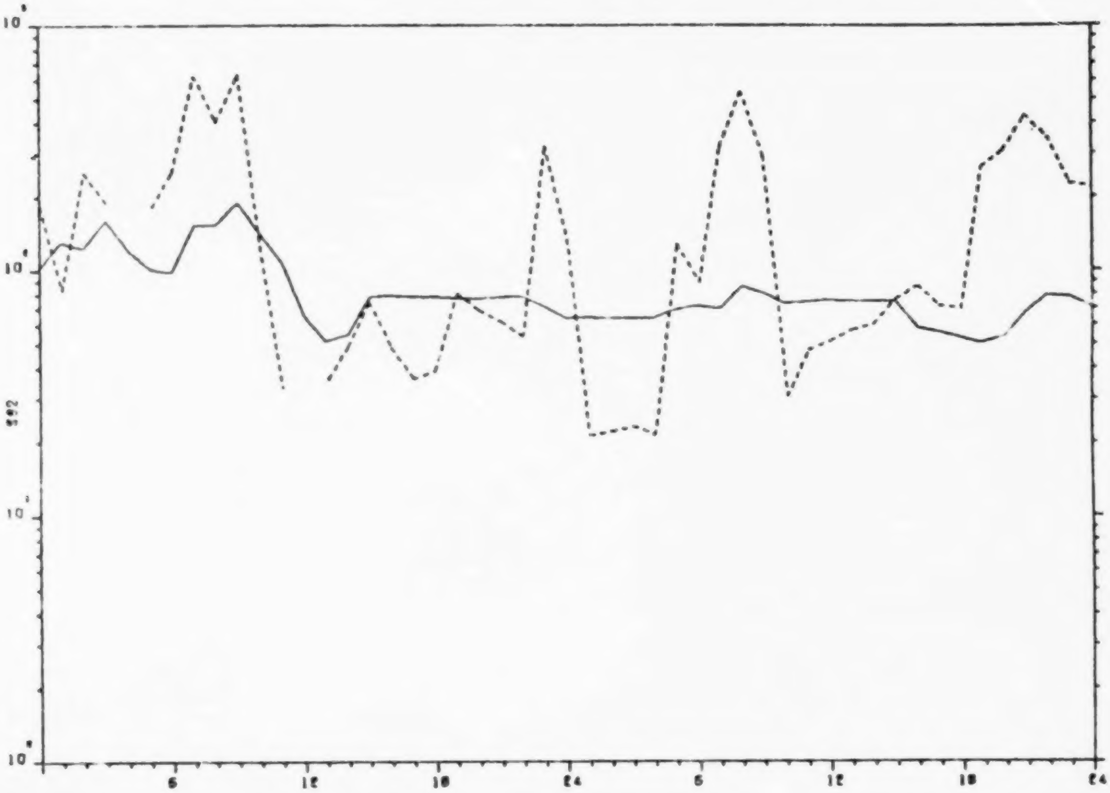

FIG. 4 - Computed (solid line) and observed (dashed line) SO_2 concentrations at station n. 4 for the days February 21st-22nd 1975 (SO_2 concentrations are in arbitrary units).

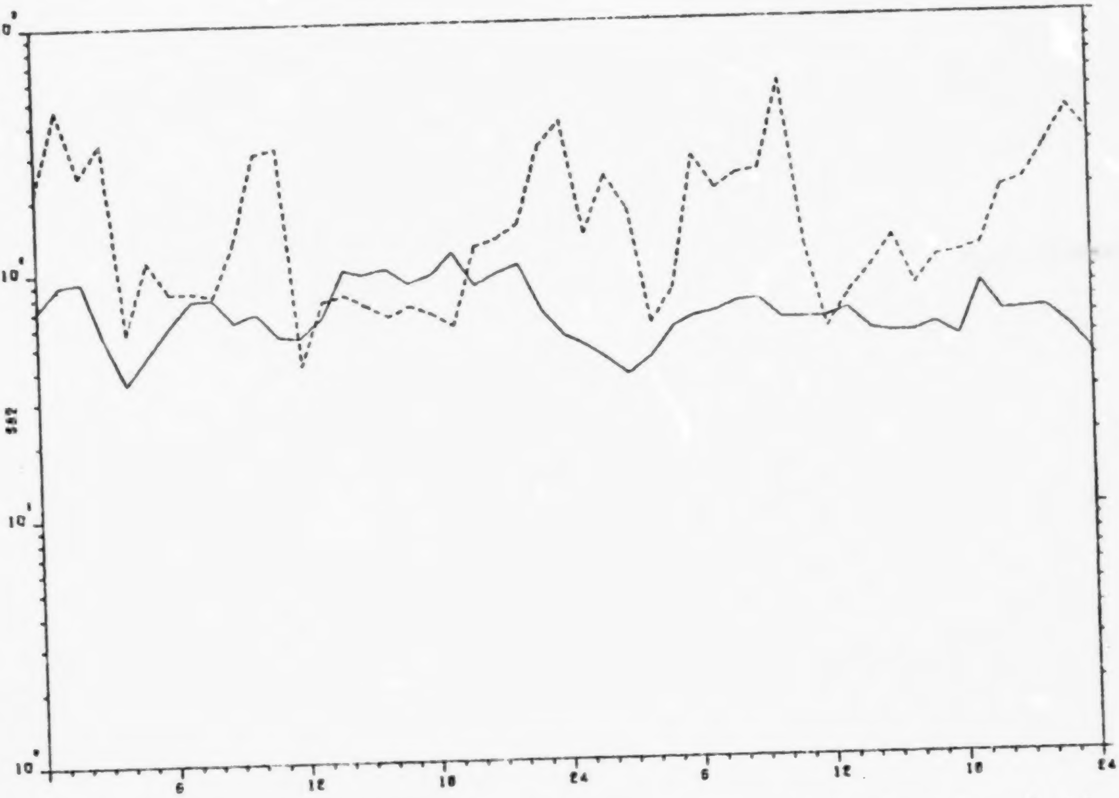

FIG. 5 - Computed (solid line) and observed (dashed line) SO_2 concentrations at station n. 4 for the days February 23th-24th 1975 (SO_2 concentrations are in arbitrary units).

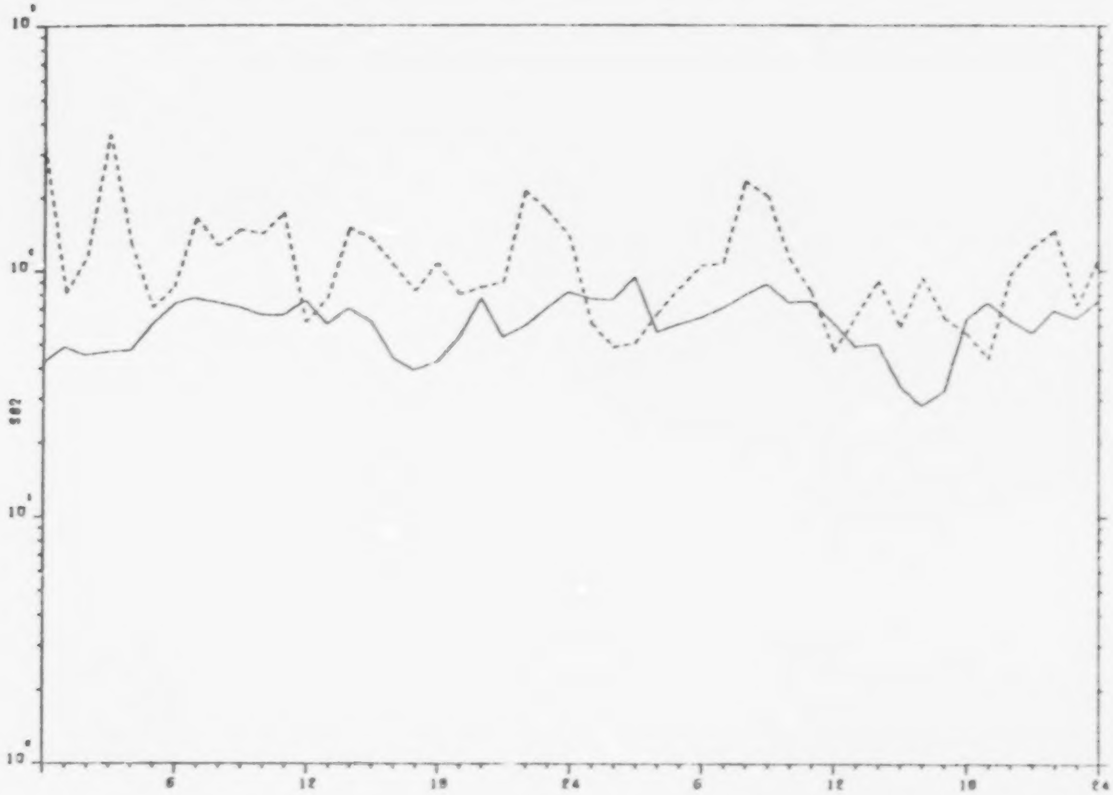

FIG. 6 - Computed (solid line) and observed (dashed line) SO_2 concentrations at station n. 4 for the days February 25th-26th 1975 (SO_2 concentrations are in arbitrary units).

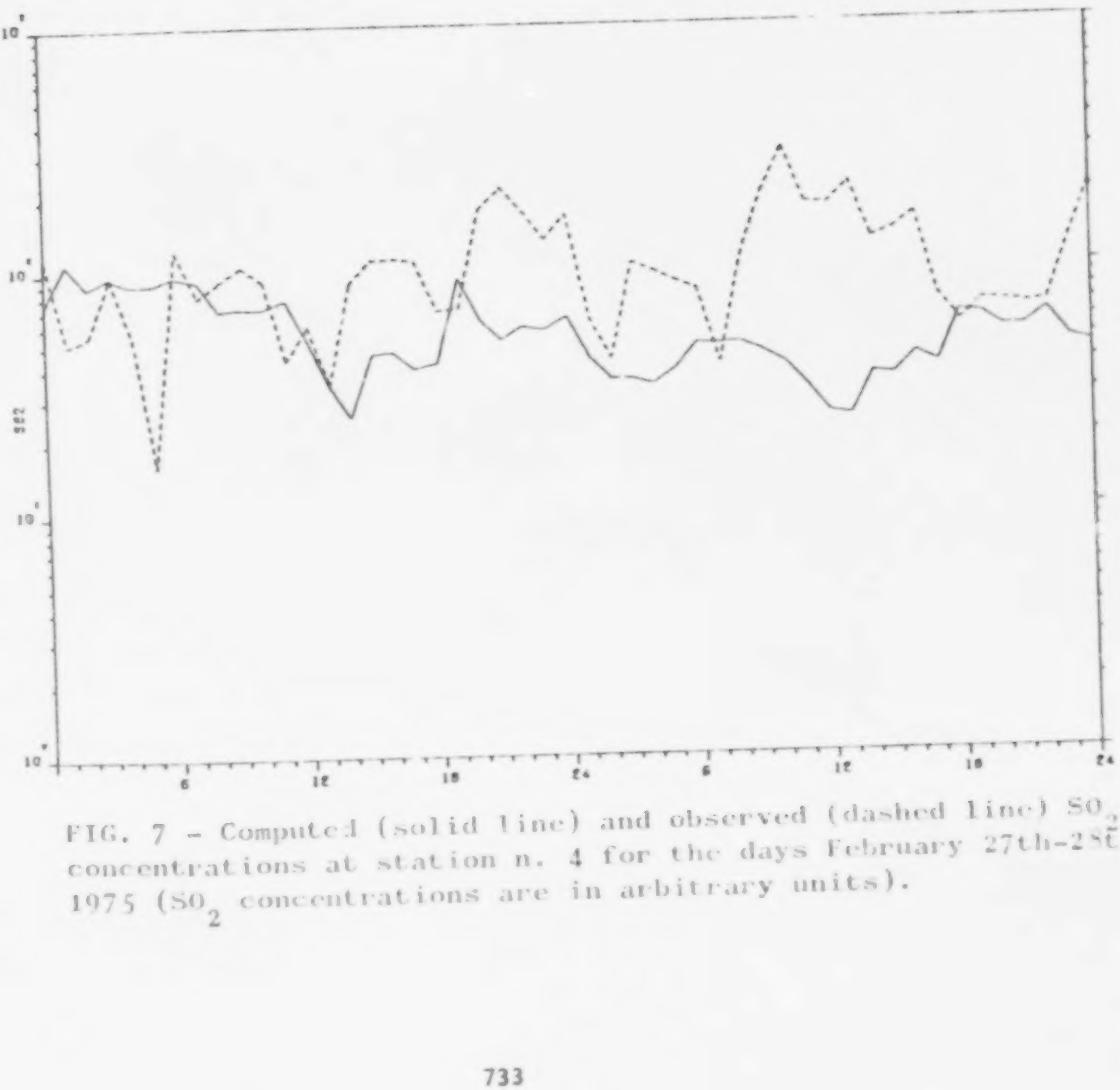

FIG. 7 - Computed (solid line) and observed (dashed line) SO_2 concentrations at station n. 4 for the days February 27th-28th 1975 (SO_2 concentrations are in arbitrary units).

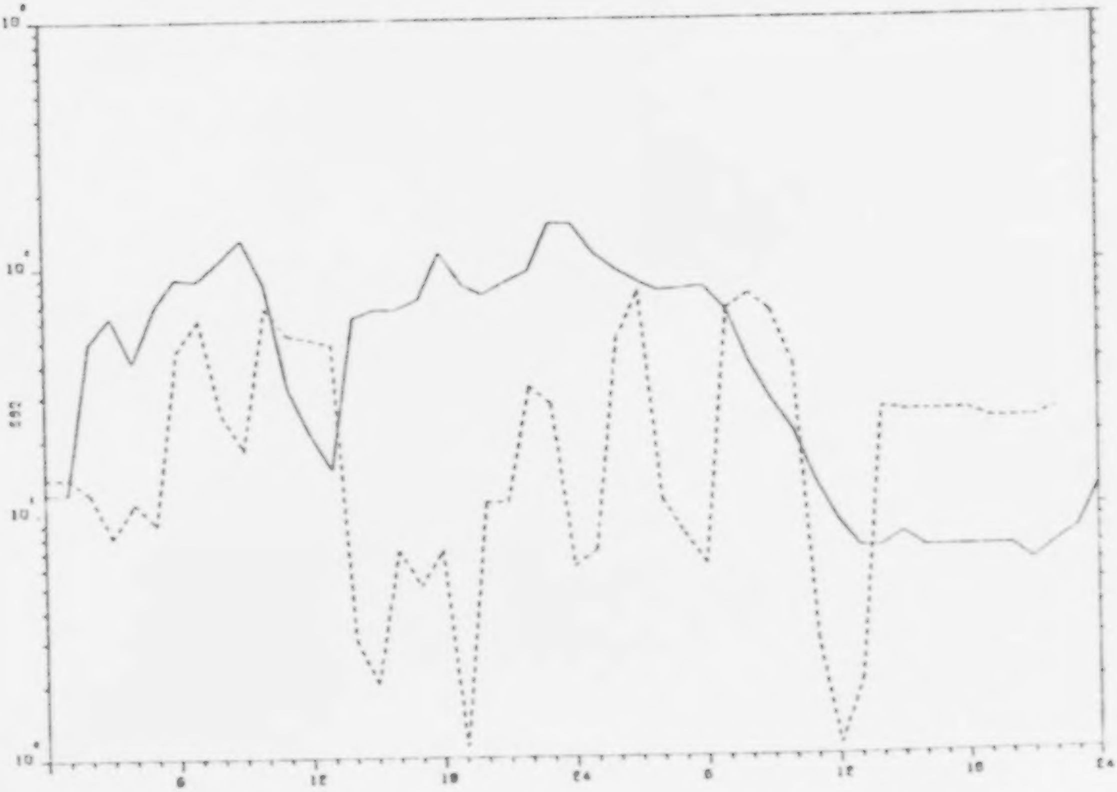

FIG. 8 - Computed (solid line) and observed (dashed line) SO_2 concentrations at station n. 9 for the days February 15th-16th 1975 (SO_2 concentrations are in arbitrary units).

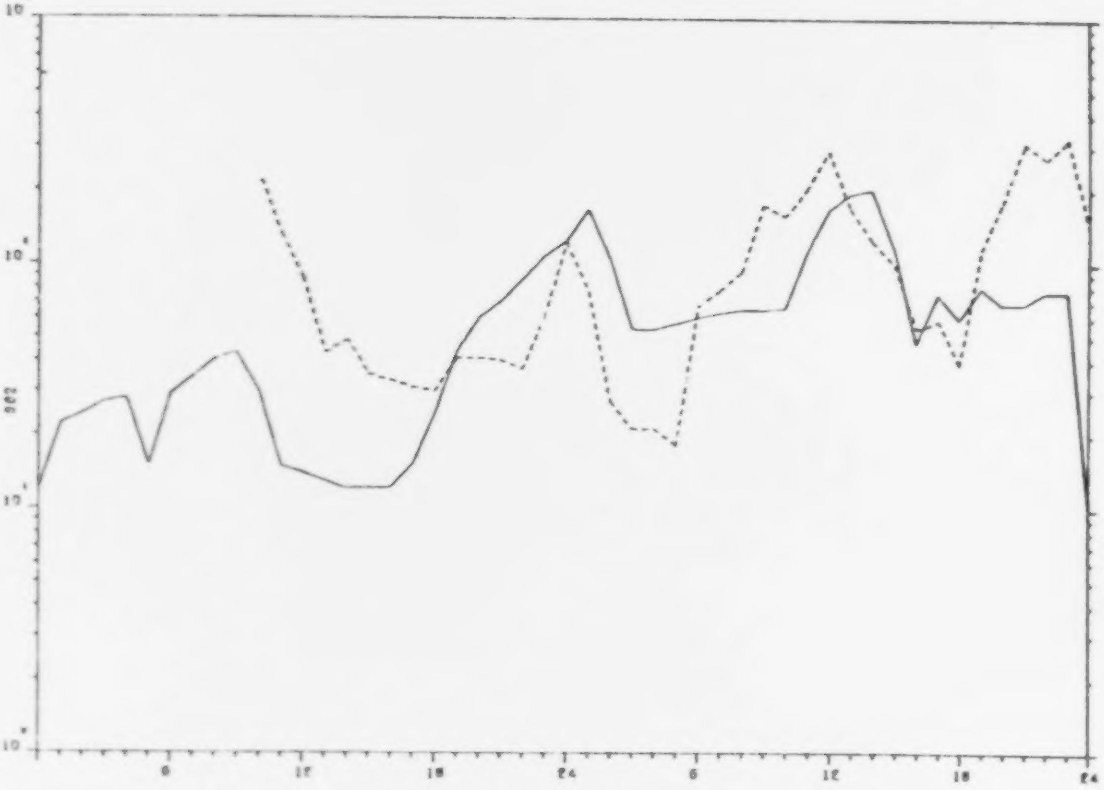

FIG. 9 - Computed (solid line) and observed (dashed line) SO_2 concentrations at station n. 9 for the days February 17th-18th 1975 (SO_2 concentrations are in arbitrary units).

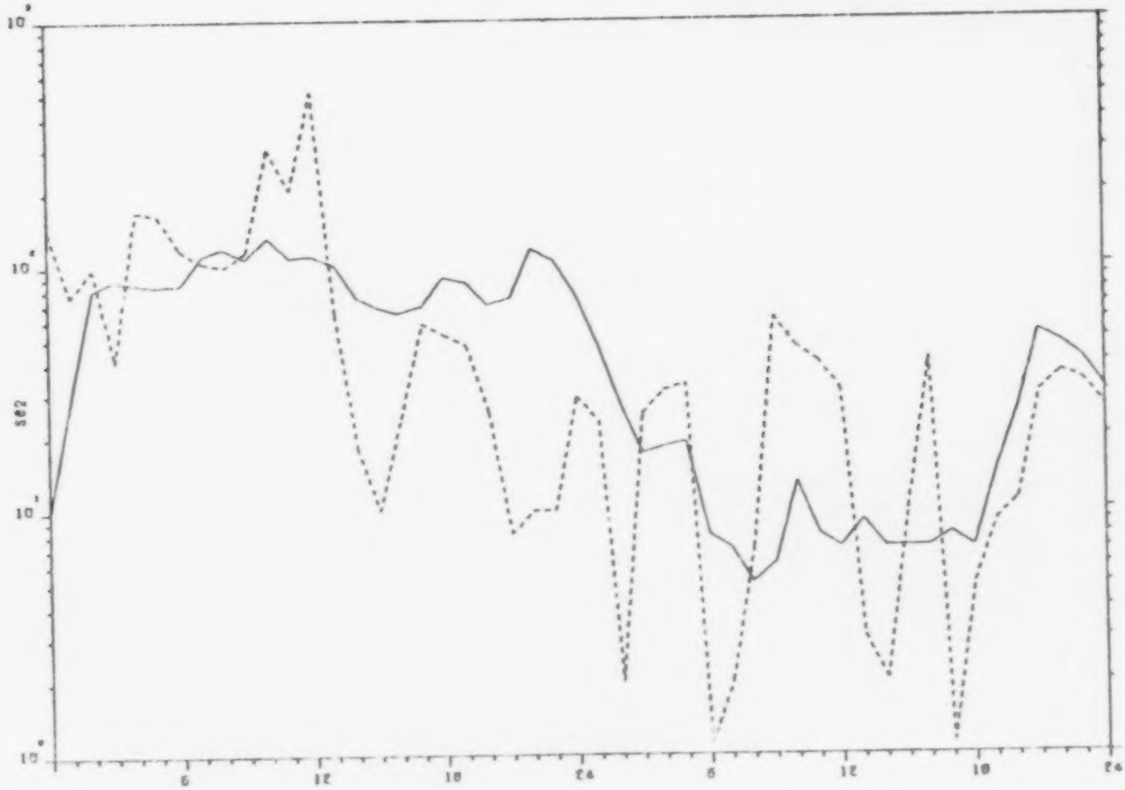

FIG. 10 - Computed (solid line) and observed (dashed line) SO_2 concentrations at station n. 9 for the days February 19th-20th 1975 (SO_2 concentrations are in arbitrary units).

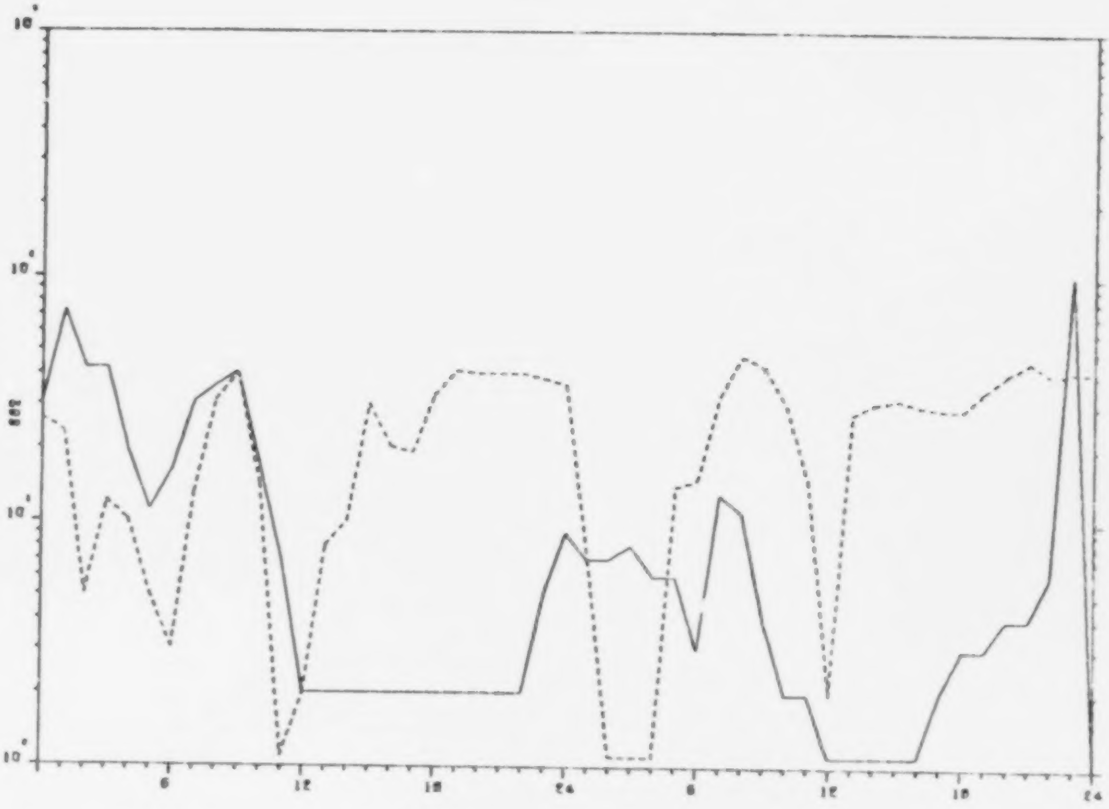

FIG. 11 - Computed (solid line) and observed (dashed line) SO_2 concentrations at station n. 0 for the days February 21st-22nd 1975 (SO_2 concentrations are in arbitrary units).

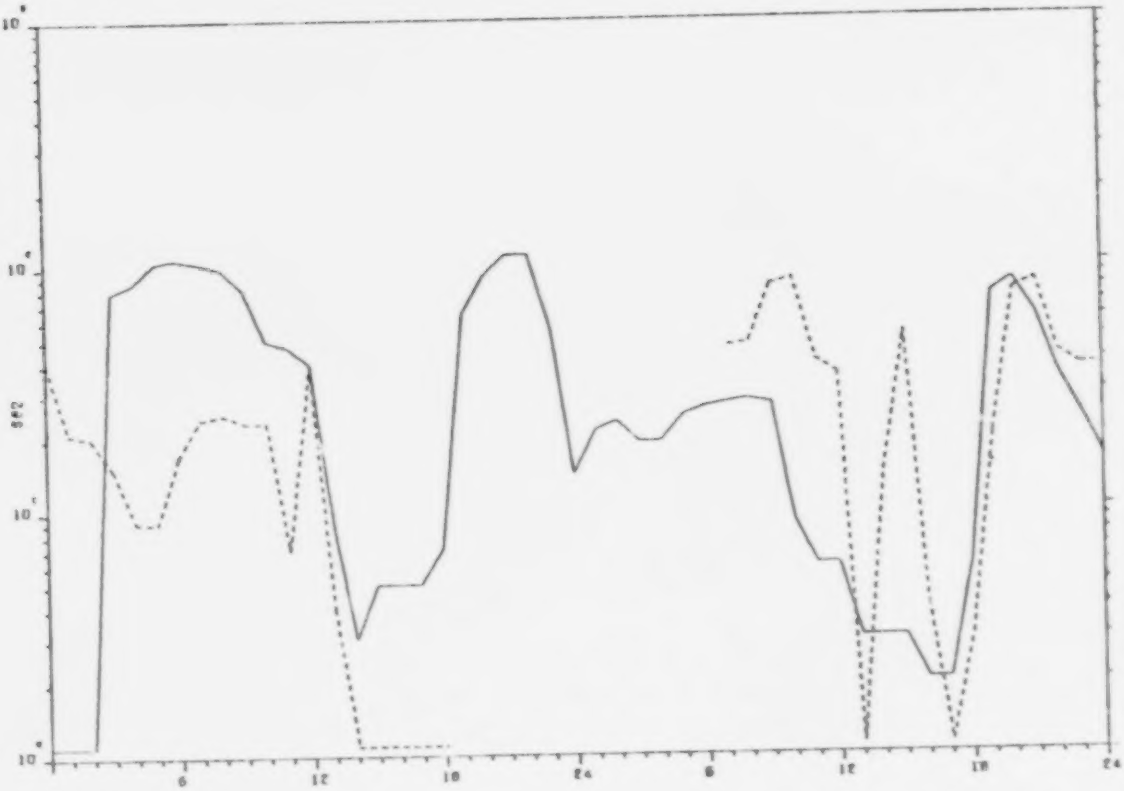

FIG. 12 - Computed (solid line) and observed (dashed line) SO_2 concentrations at station n. 9 for the days February 23rd-24th 1975 (SO_2 concentrations are in arbitrary units).

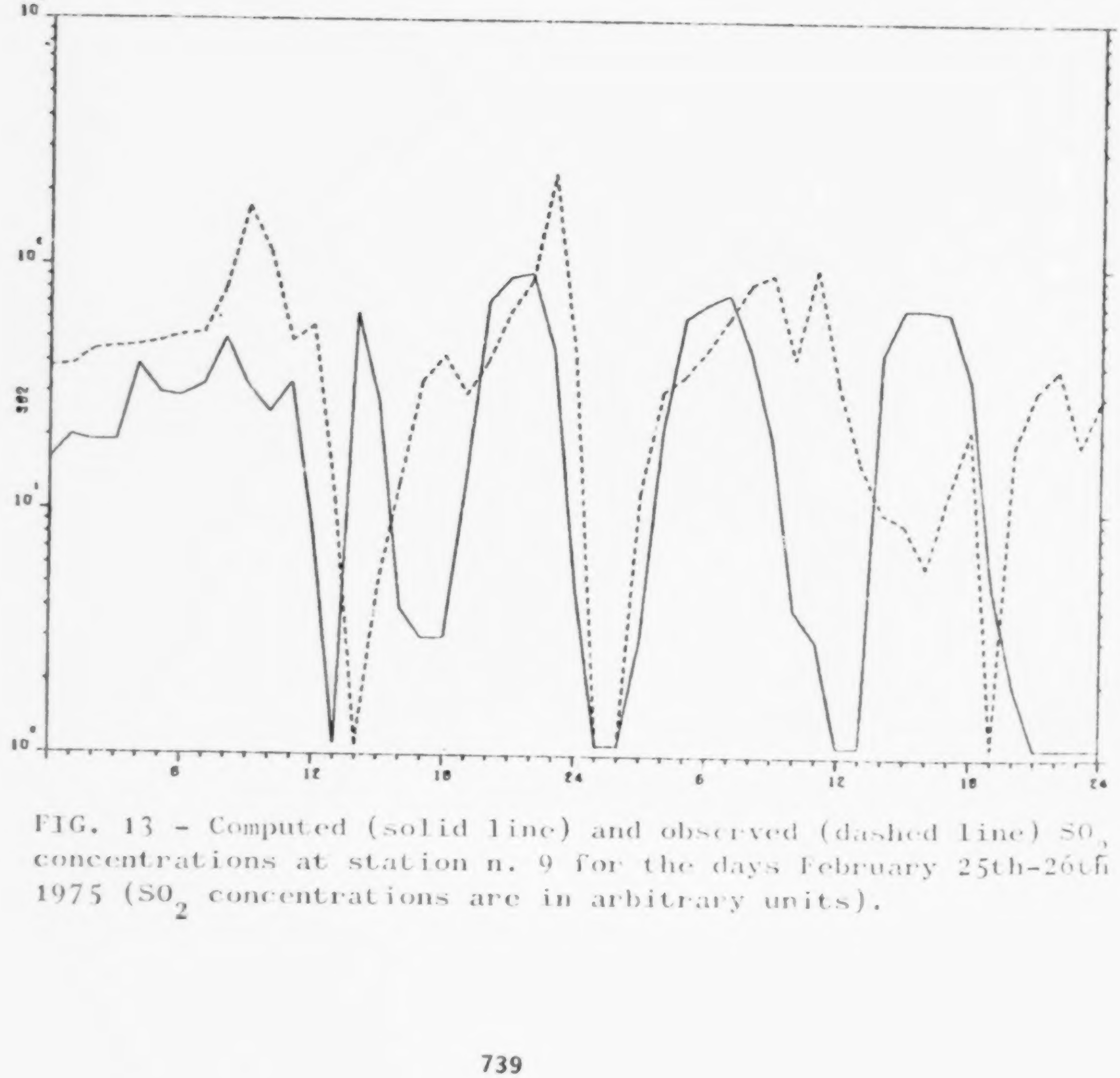

FIG. 13 - Computed (solid line) and observed (dashed line) SO_2 concentrations at station n. 9 for the days February 25th-26th 1975 (SO_2 concentrations are in arbitrary units).

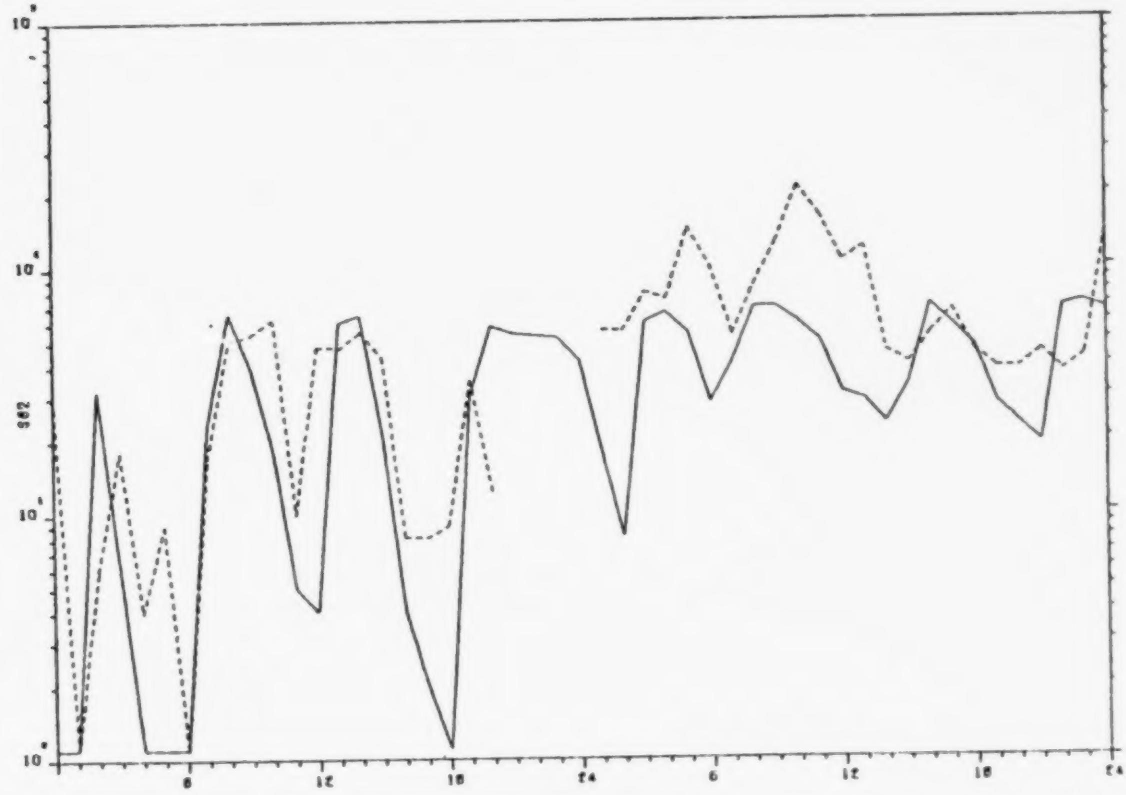

FIG. 14 - Computed (solid line) and observed (dashed line) SO_2 concentrations at station n. 9 for the days February 27th-28th 1975 (SO_2 concentrations are in arbitrary units).

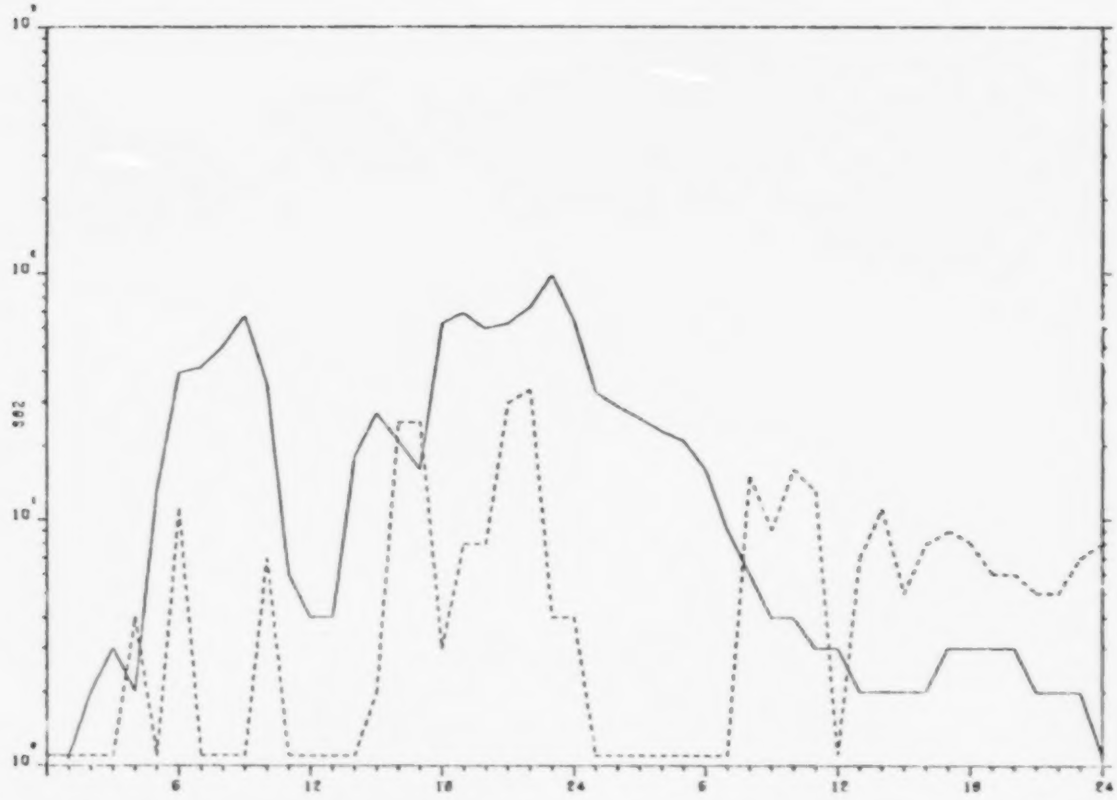

FIG. 15 - Computed (solid line) and observed (dashed line) SO_2 concentrations at station n. 19 for the days February 15th-16th 1975 (SO_2 concentrations are in arbitrary units).

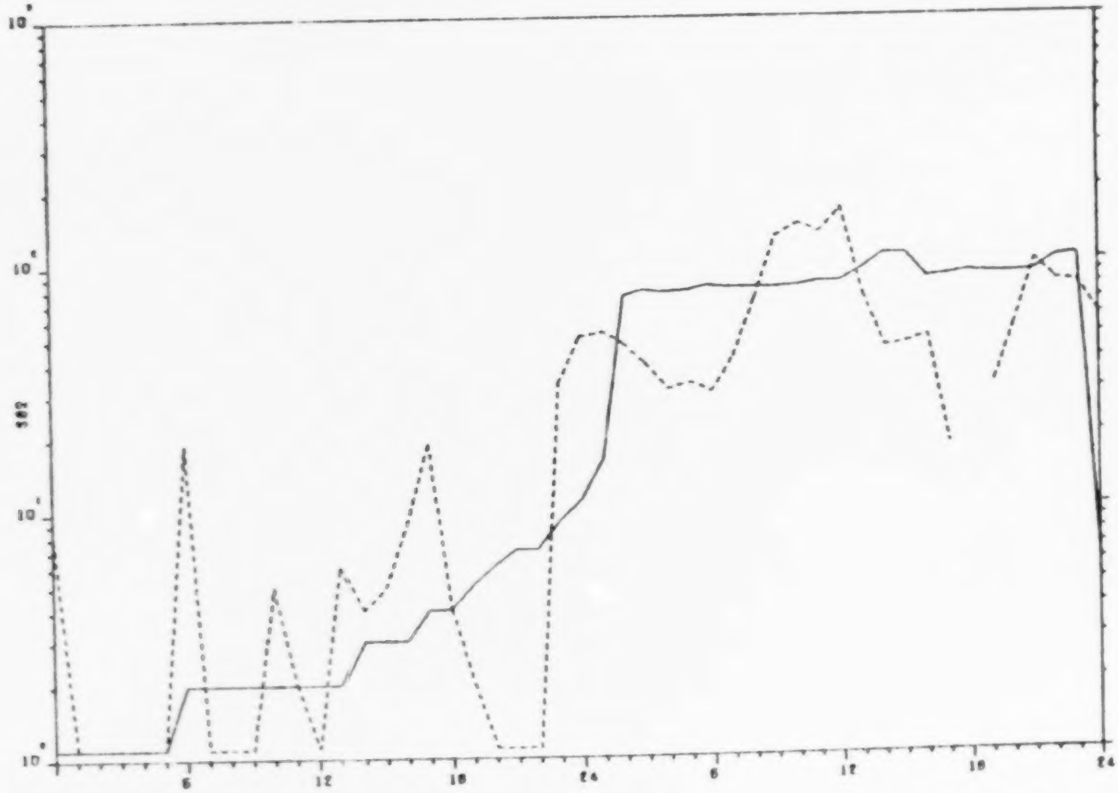

FIG. 16 - Computed (solid line) and observed (dashed line) SO_2 concentrations at station n. 19 for the days February 17th-18th 1975 (SO_2 concentrations are in arbitrary units).

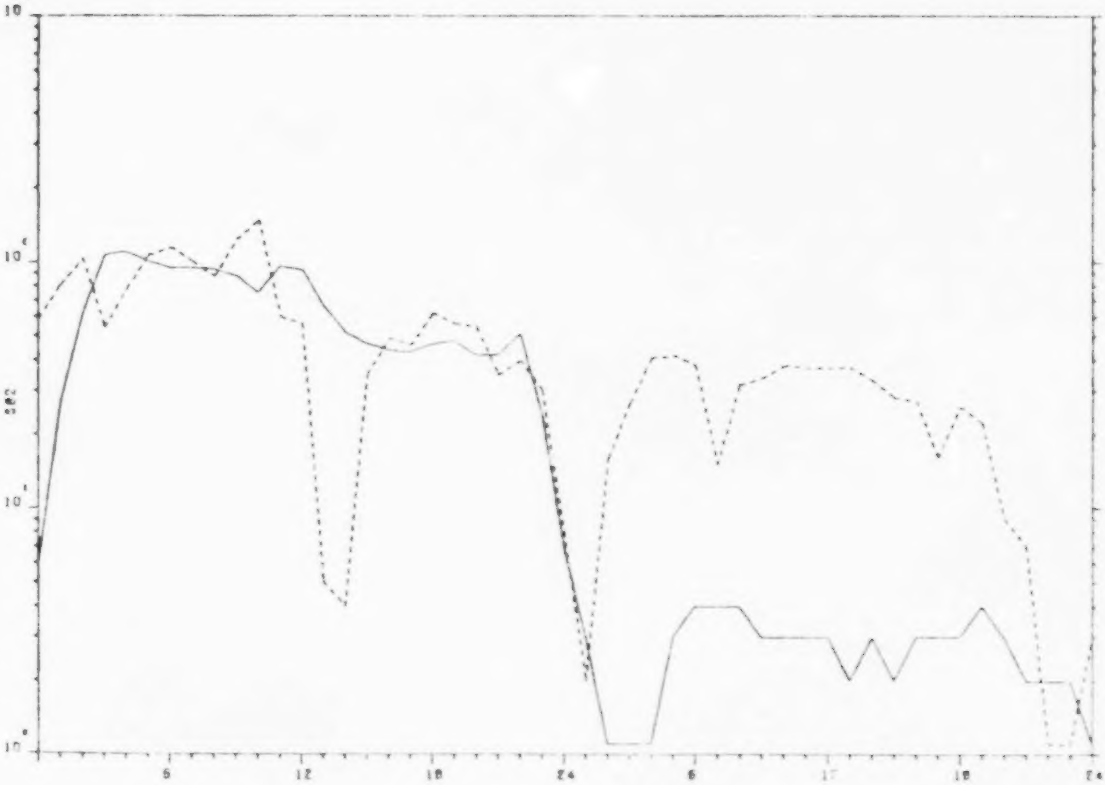

FIG. 17 - Computed (solid line) and observed (dashed line) SO concentrations at station n. 19 for the days February 19th-20th 1975 (SO_2 concentrations are in arbitrary units).

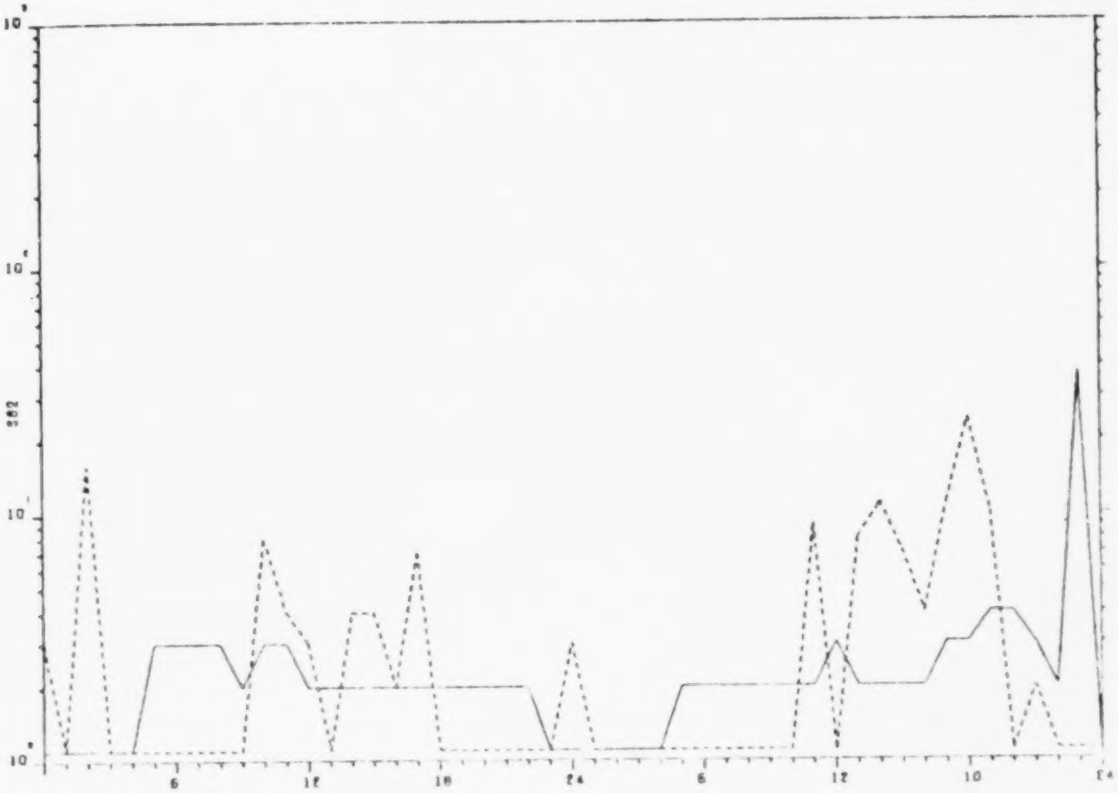

FIG. 18 - Computed (solid line) and observed (dashed line) SO_2 concentrations at station n. 19 for the days February 21st-22nd 1975 (SO_2 concentrations are in arbitrary units).

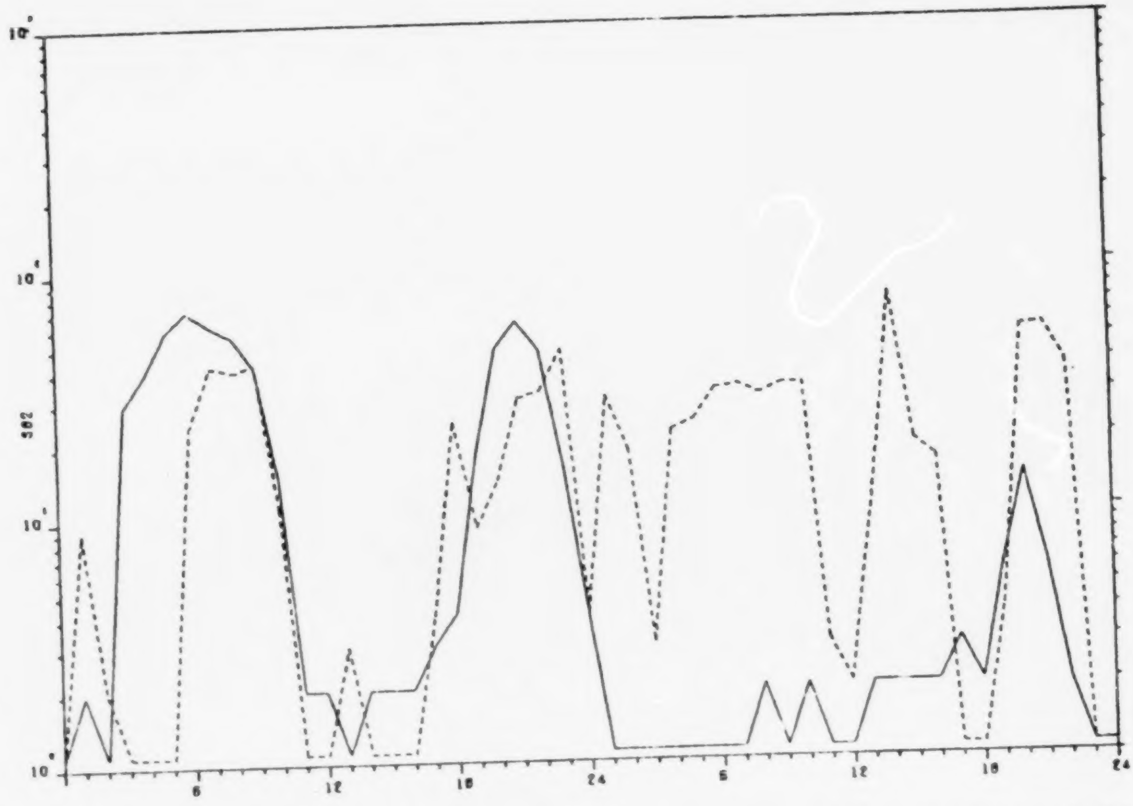

FIG. 19 - Computed (solid line) and observed (dashed line) SO_2 concentrations at station n. 19 for the days February 23rd-24th 1975 (SO_2 concentrations are in arbitrary units).

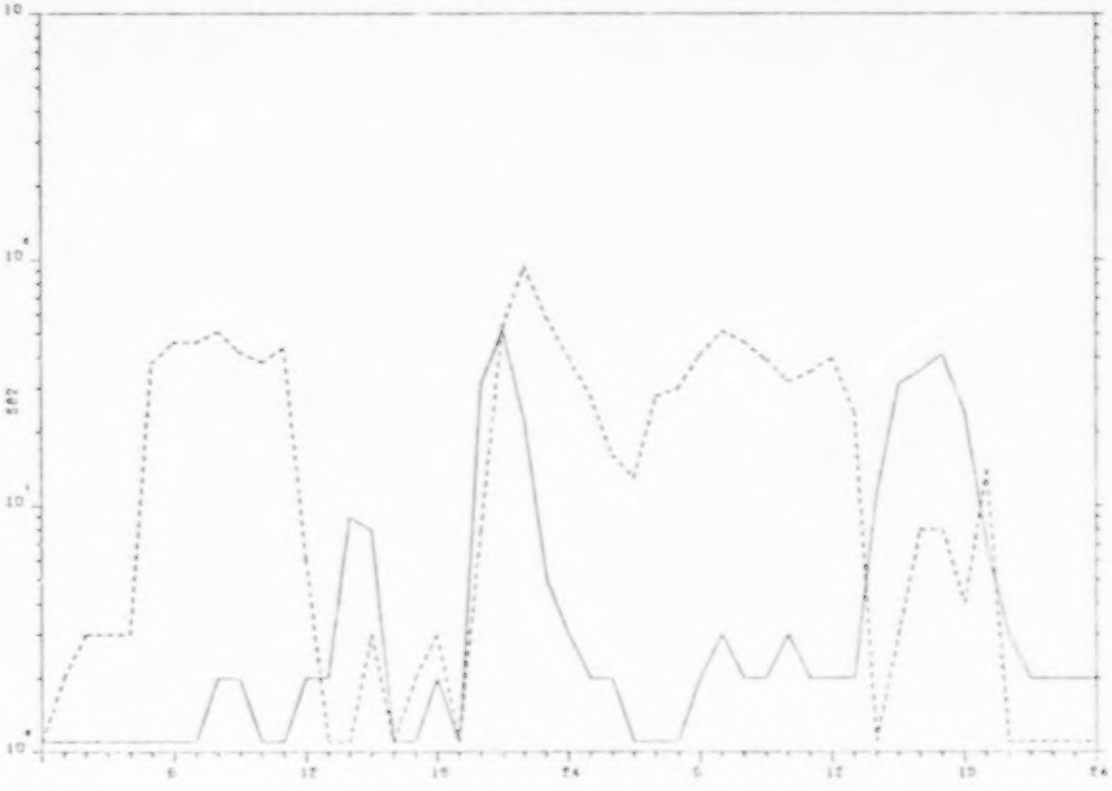

FIG. 20 – Computed (solid line) and observed (dashed line) SO_2 concentrations at station n. 19 for the days February 25th-26th 1975 (SO_2 concentrations are in arbitrary units).

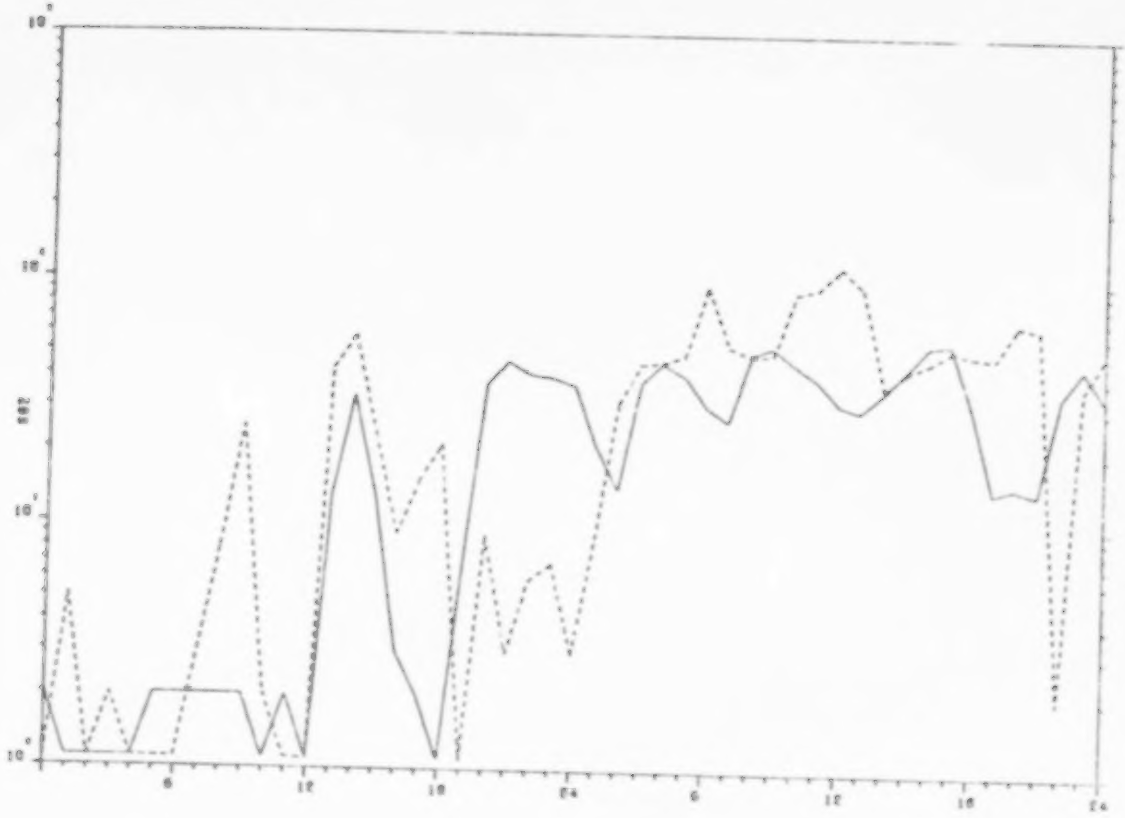

FIG. 21 - Computed (solid line) and observed (dashed line) SO_2 concentrations at station n. 19 for the days February 27th-28th 1975 (SO_2 concentrations are in arbitrary units).

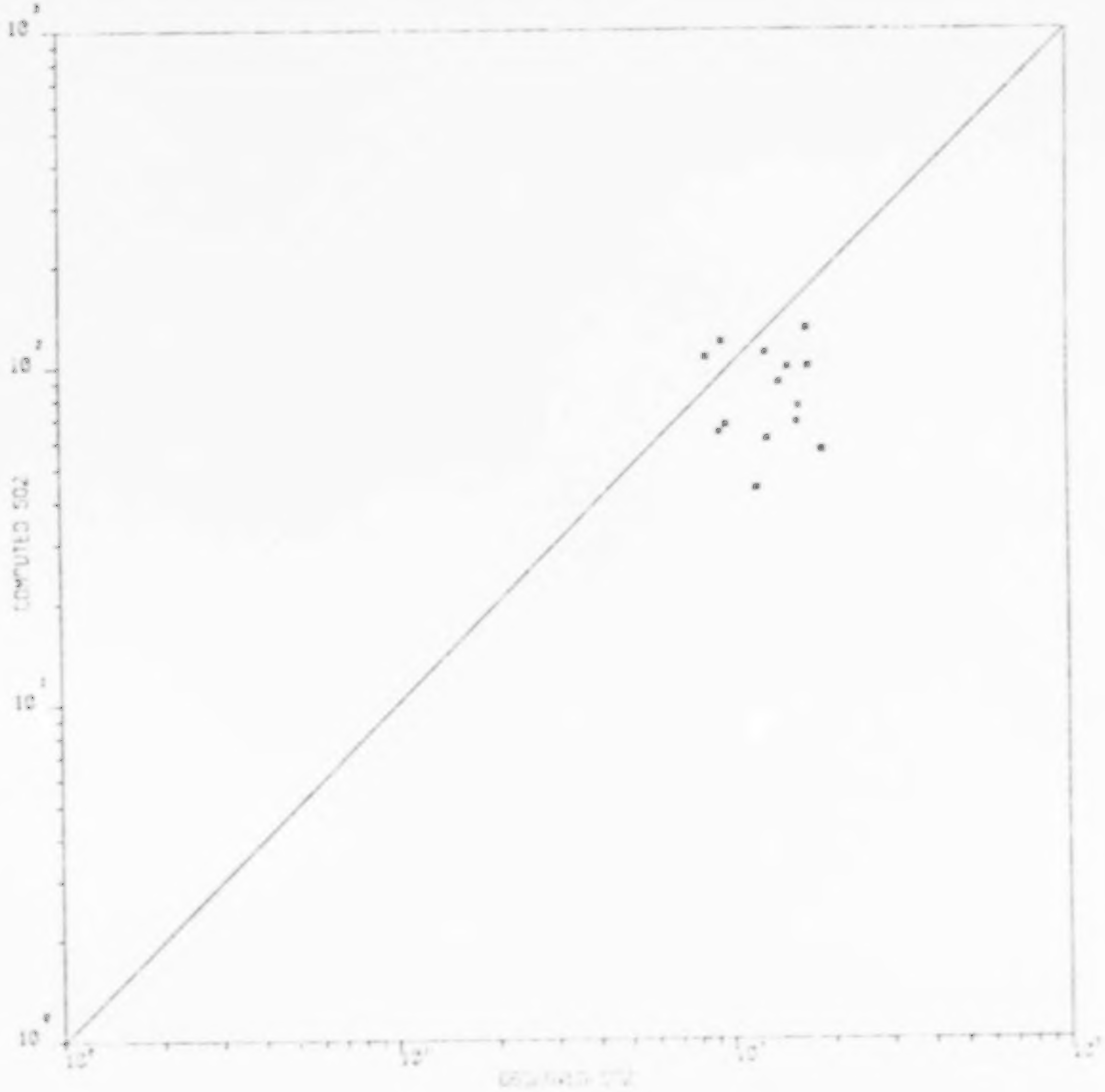

FIG. 22 - Comparison of computed and observed 24 hr averages of SO_2 concentration at station n. 4 for the period February 15th-28th 1975 (SO_2 concentrations are in arbitrary units).

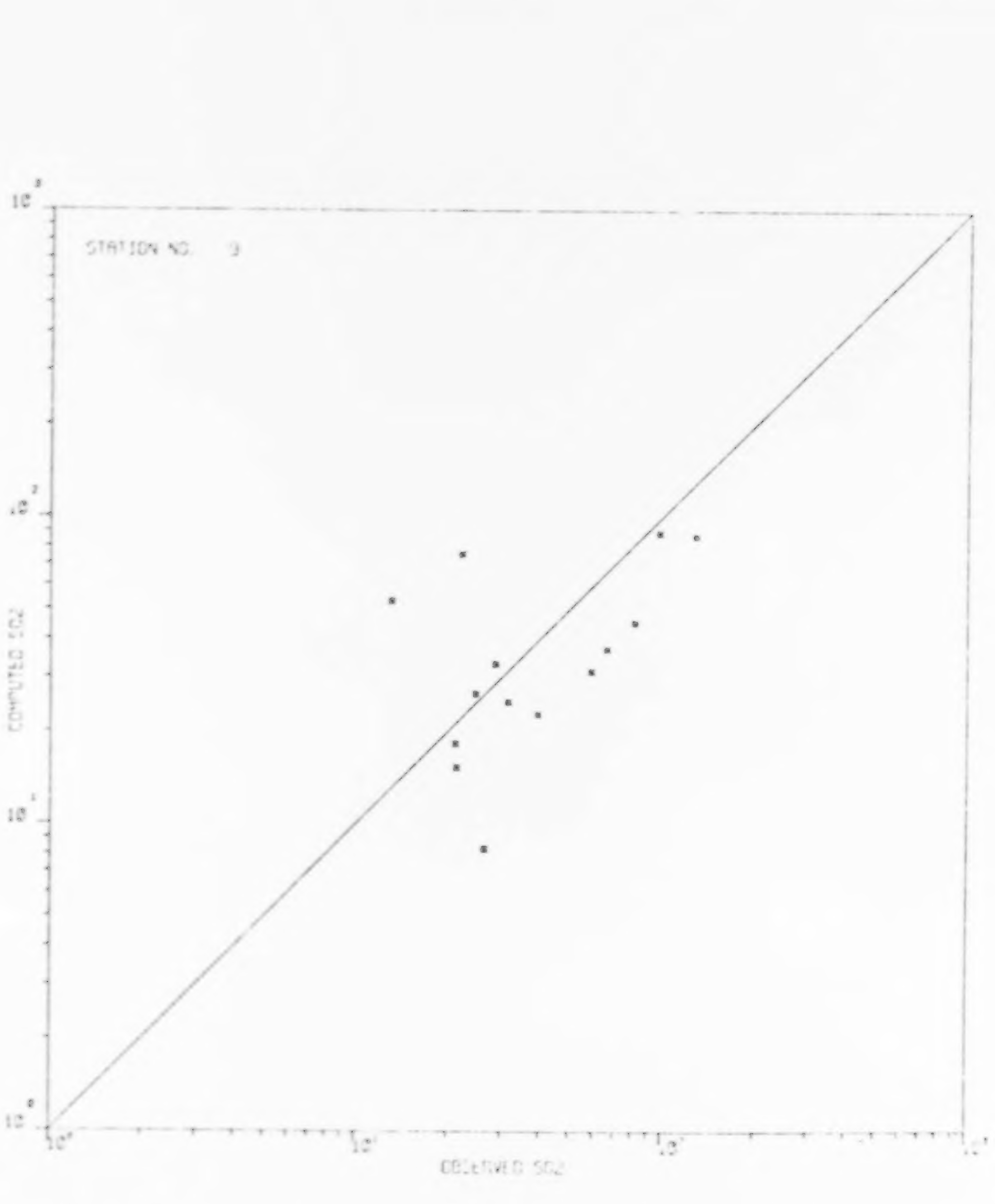

FIG. 23 - Comparison of computed and observed 24 hr averages of SO_2 concentration at station n. 9 for the period February 15th-28th 1975 (SO_2 concentrations are in arbitrary units).

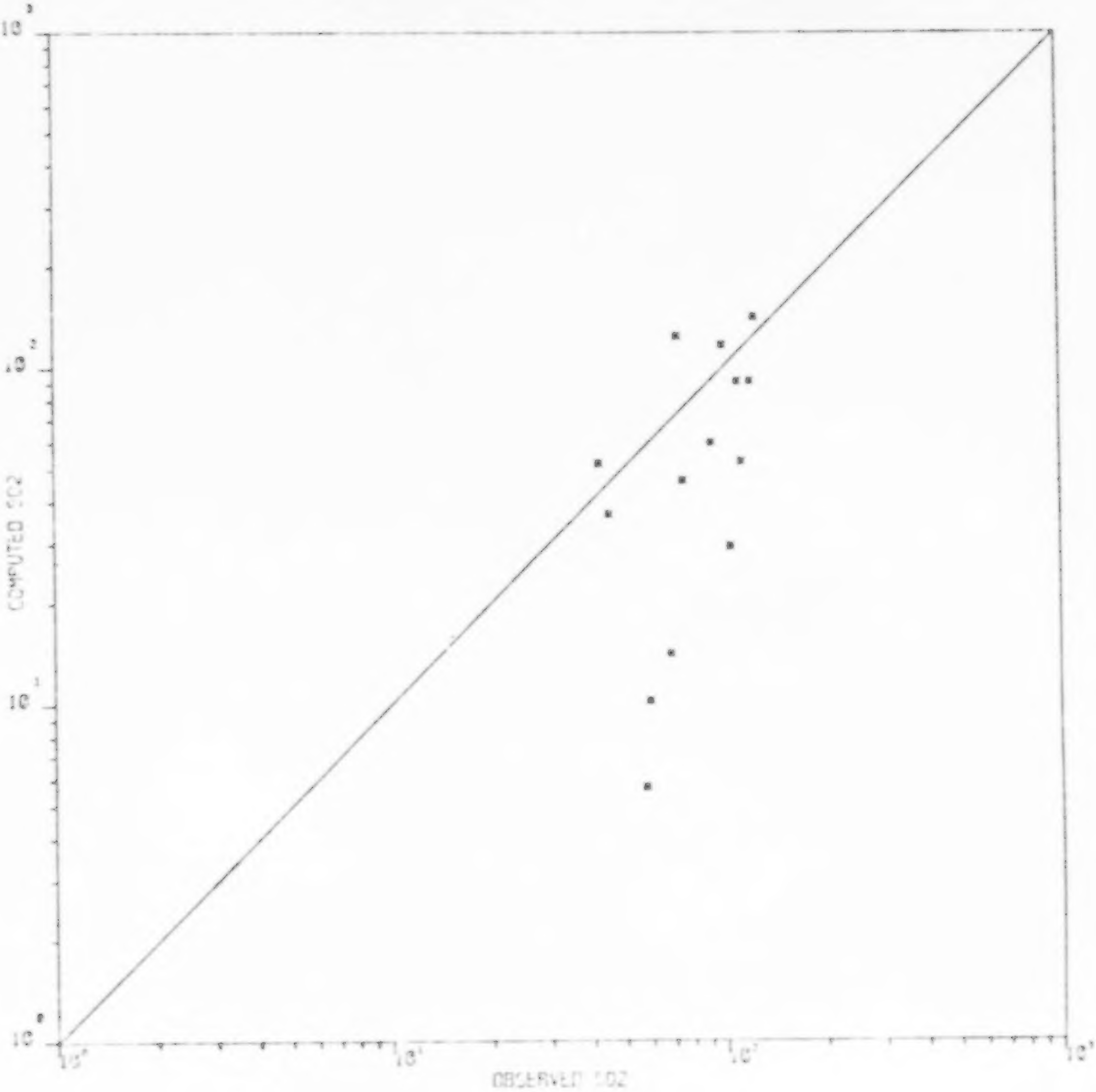

FIG. 24 - Comparison of computed and observed 24 hr averages of SO_2 concentration at station n. 13, for the period February 15th-28th 1975 (SO_2 concentrations are in arbitrary units).

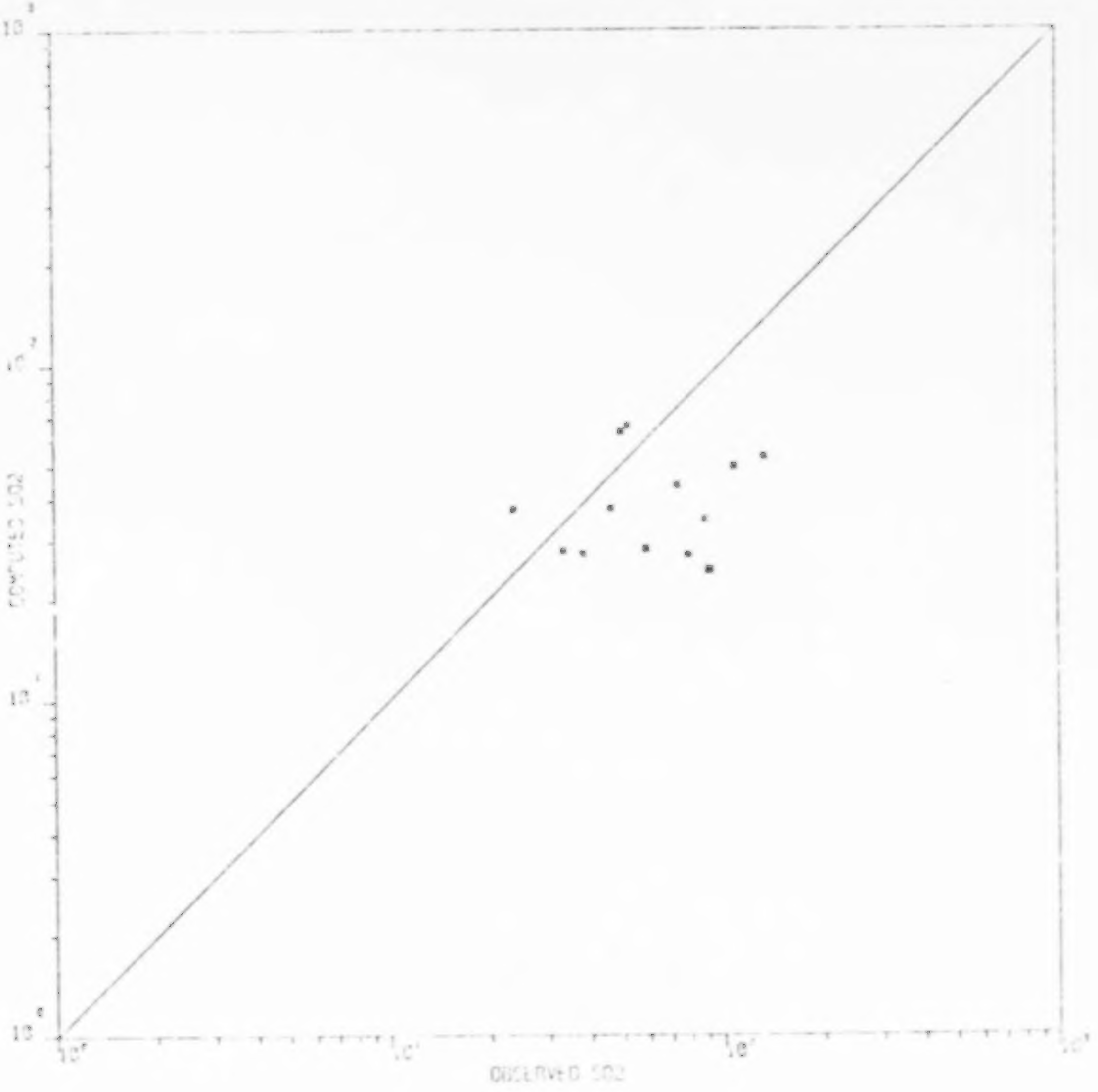

FIG. 25 - Comparison of computed and observed 24 hr averages of SO_2 concentration at station n. 17 for the period February 15th-28th 1975 (SO_2 concentrations are in arbitrary units).

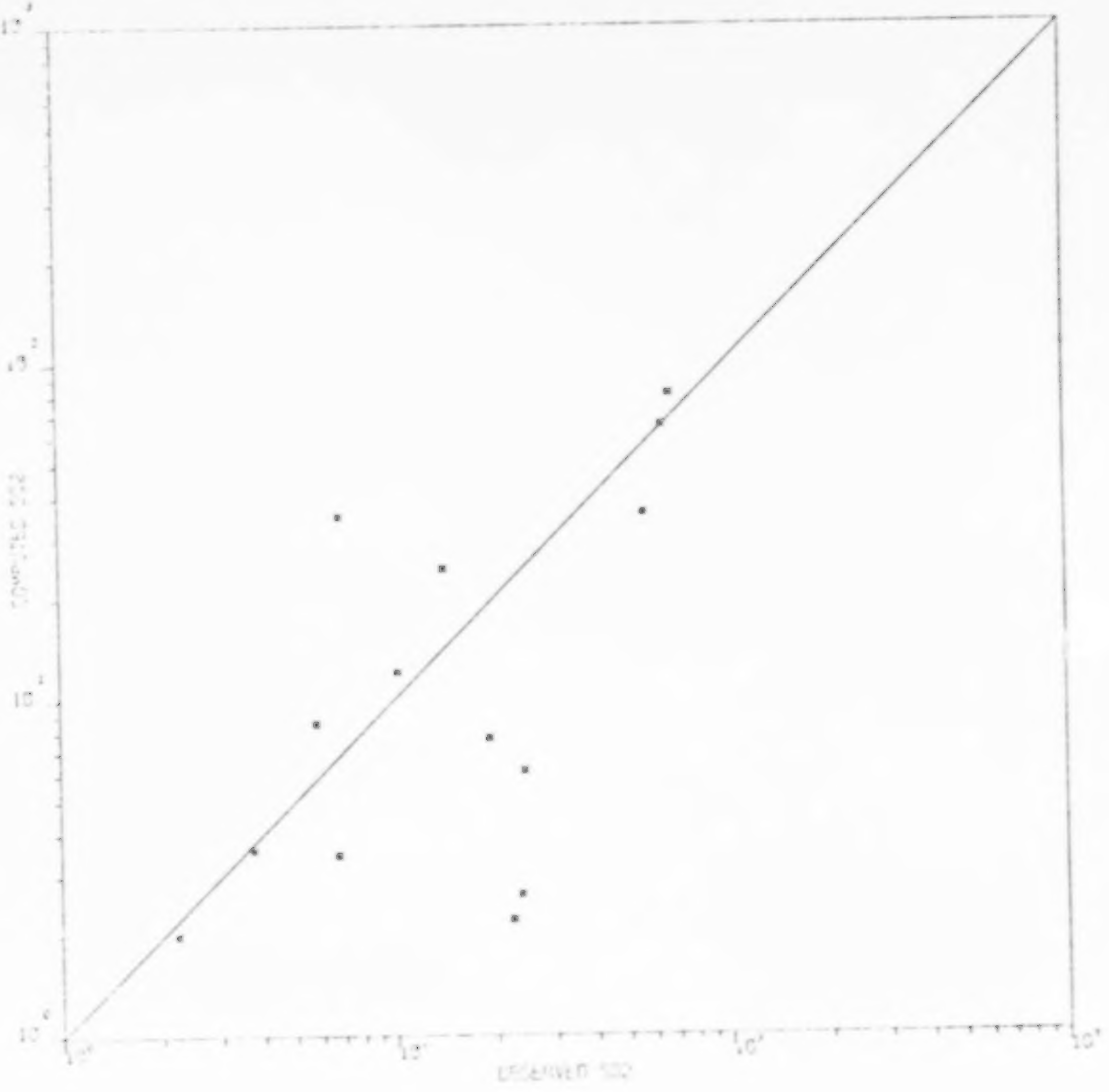

FIG. 26 - Comparison of computed and observed 24 hr averages of SO_2 concentration at station n. 19 for the period February 15th-28th 1975 (SO_2 concentrations are in arbitrary units).

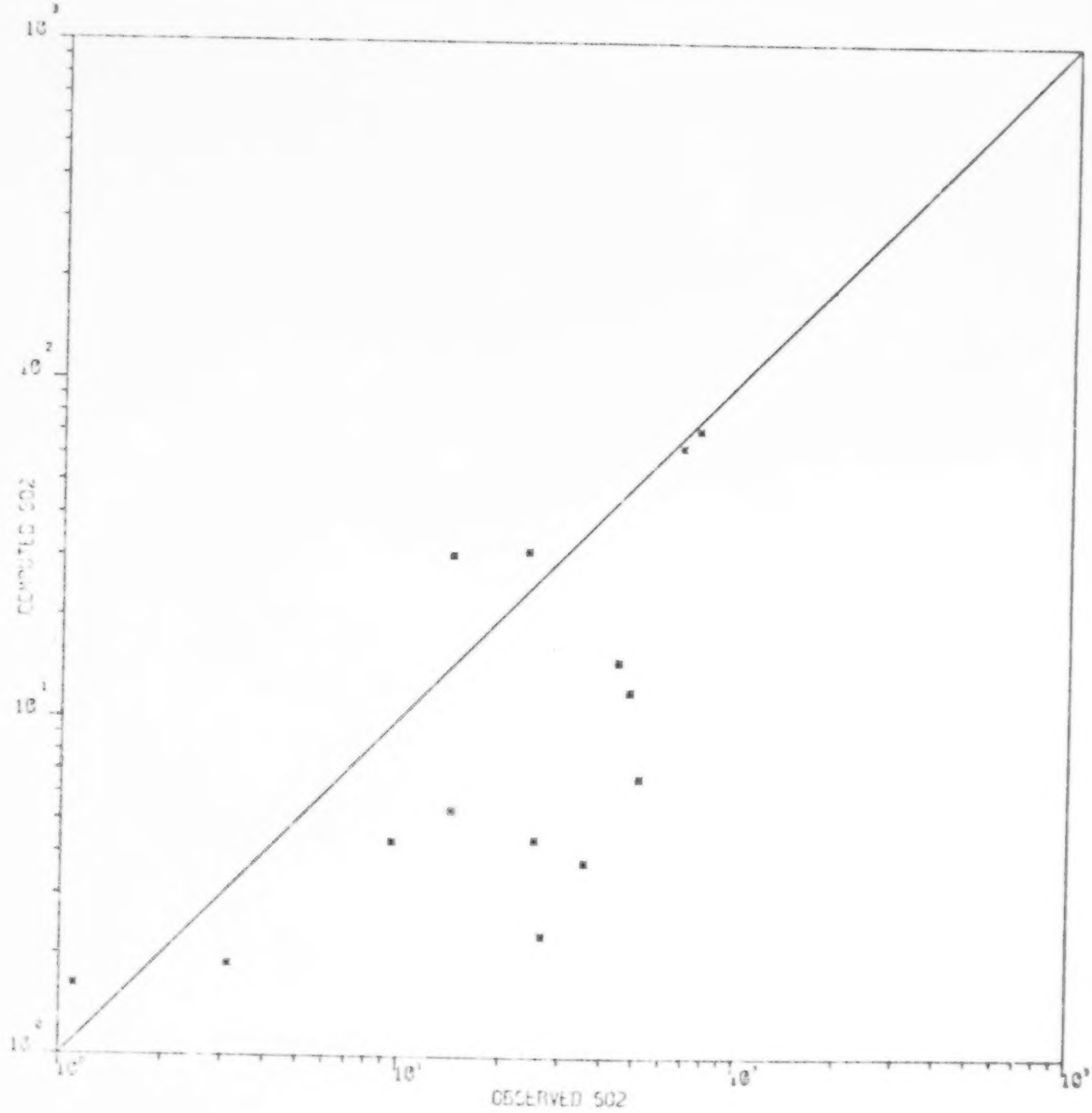

FIG. 27 - Comparison of computed and observed 24hr averages of SO_2 concentration at station n. 20 for the period February 15th-28th 1975 (SO_2 concentrations are in arbitrary units).

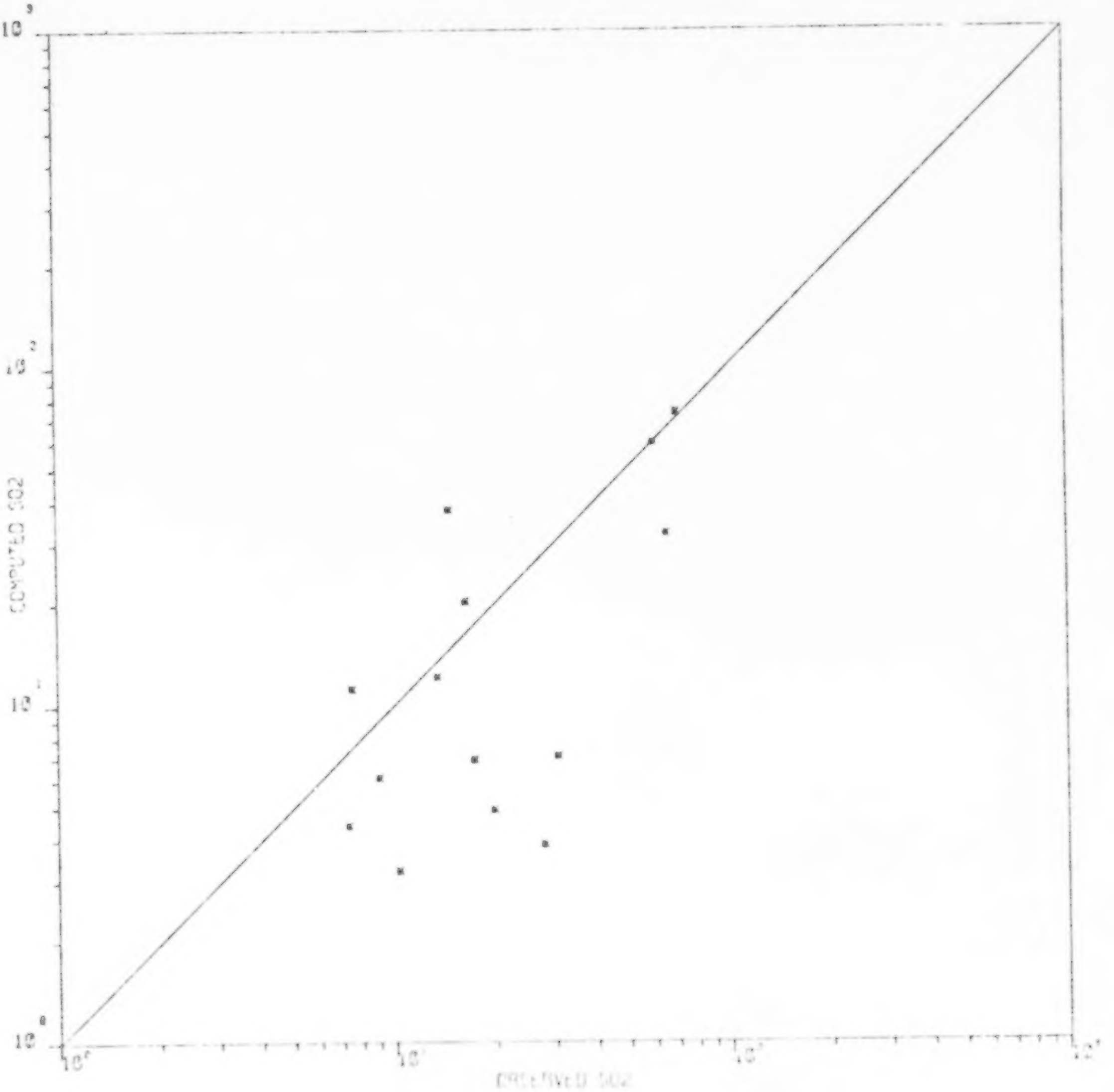

FIG. 28 - Comparison of computed and observed 24 hr averages of SO_2 concentration at station n. 21 for the period February 15th-28th 1975 (SO_2 concentrations are in arbitrary units).

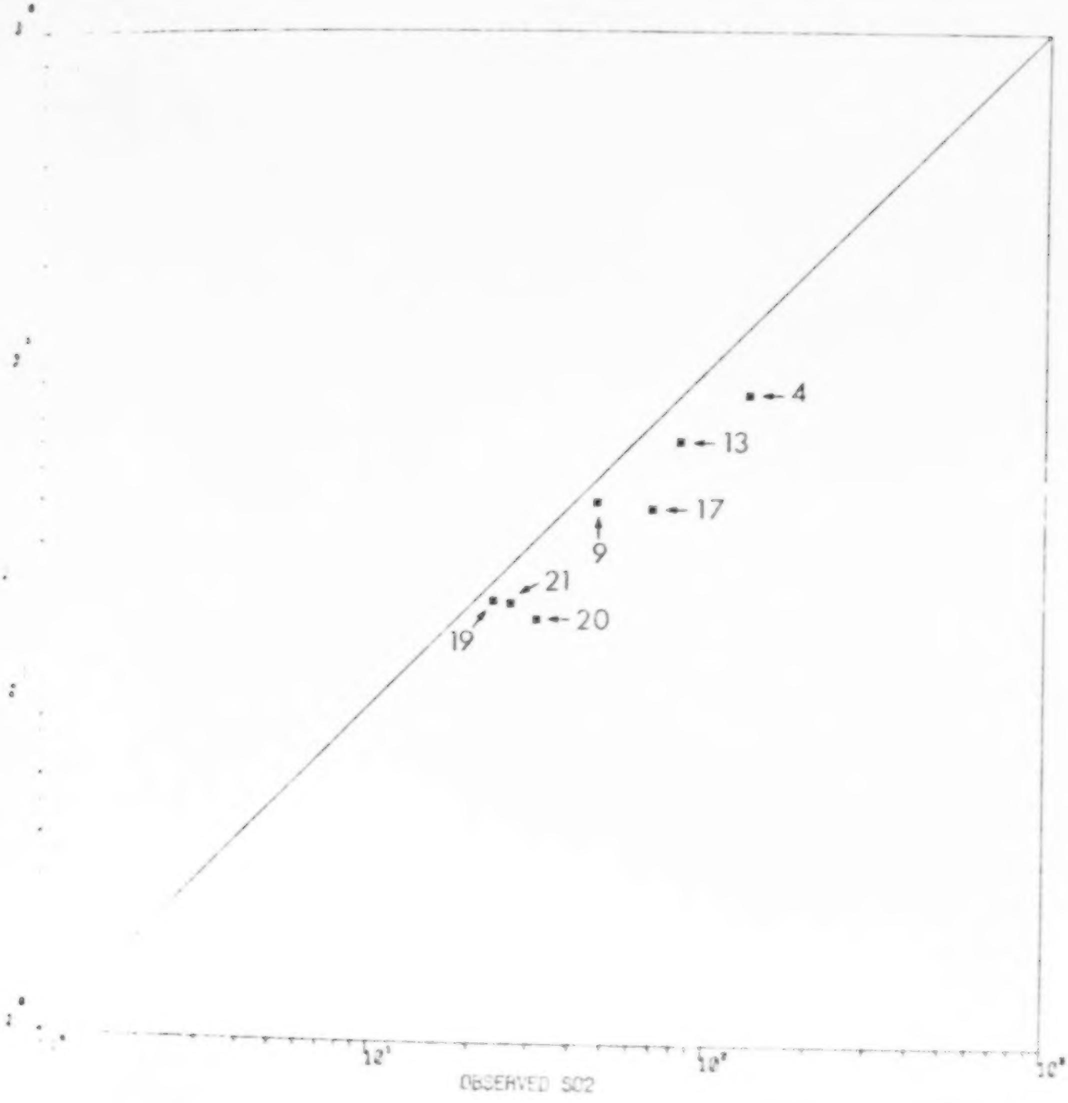

Fig. 29 - Comparison of the whole period average SO_2 concentrations computed and observed at the seven stations n. 4, 9, 13, 17, 19, 20, 21.

Reproduced from best available copy.

Reproduced from best available copy.

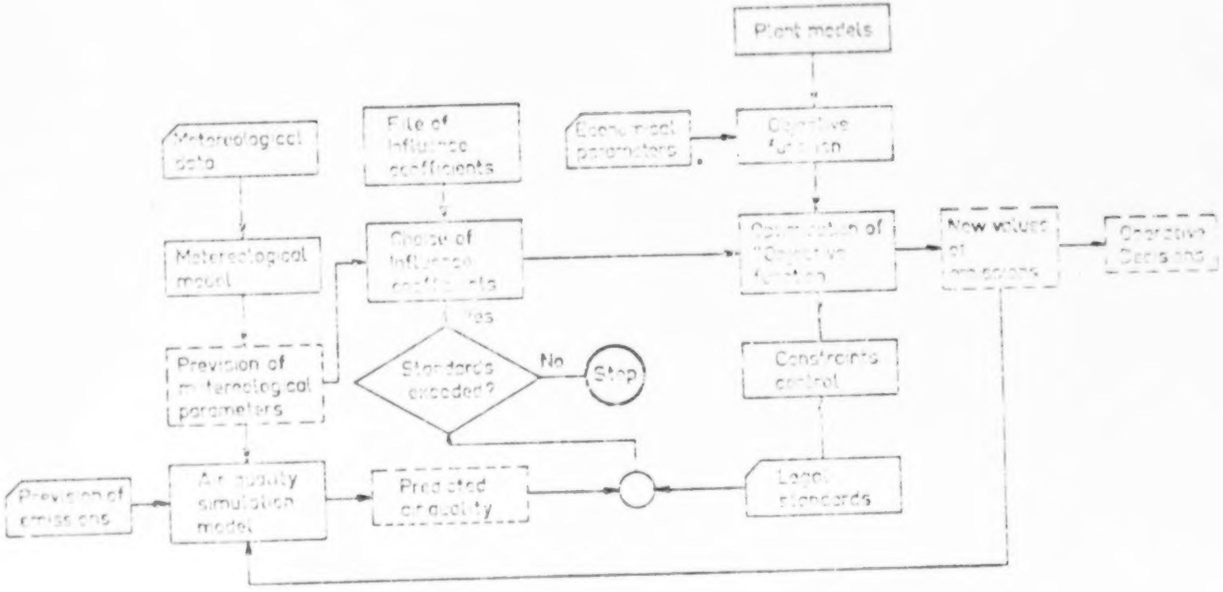

FIG. 30 - Block diagram of the control scheme.

Rapporteur's Report, Topic V, September 26, 1975
by W. B. Johnson

Chairman: B. Bringfelt

E. Runca: Simulation fo SO_2-Dispersion in the Venetian Area

Discussion:

Prahm: It would be interesting to see a test of your advection scheme only, which I understand can be significantly affected by numerical trancation errors.

Runca: I believe the result depends upon the choice of time and space scales. I expect to soon perform a multidimensional test of the advection scheme.

K. E. Grønskei: Have you calculated short-term concentrations and simulated the buildup of pollution levels?

E. Runca: No, because of the absence of input information which sufficiently detailed time resolution, the model does not perform well in the initial stages of a simulation.

K. E. Grønskei: Since one capability of the model appears to be to distinguish between the effects of ground-level and elevated sources, has this been done?

E. Runca: No, we are mainly concerned with simulating the effects of pollutants on eye irritation in the Venice area, and have not determined the sensitivity of the calculations to source height in this initial work.

A. Scholberg: Validation of a Model in Complex topographical surroundings

Discussion:

A. L. Berger: What about the effects of vertical wind shear? Are these included in your model?

A. Scholberg: No, this is not necessary because in this problem we are treating only a ground-level source.

D. Jost: At what distance from the source did the maximum concentration occur?

A. Scholberg: Because of the low stack height, the maximum occured very near the source. Other peaks downwind were associated with changes in the wind patterns.

B. Sivertsen: How did you account for the back and forth movements of the air flow, with transition periods in between?

A. Scholberg: Of course the observations covered two weeks and did not show any short term effects. The model, however considers these wind patterns separately and then averages these concentrations for comparison with observations.

B. Bringfelt: Could they be measured from your observation stations?

A. Scholberg: No, we tried this but it did not work well because of changes in the mean flow directions.

C. F. Barrett: The Role of Wind-Tunnel Modeling in
Predicting Dispersion.

Discussion:

B. Bringfelt: Have efforts been conducted to compare wind tunnel results for downwash, etc., for a given chimney configuration with results from full-scale tests?

C. F. Barrett: Yes, validations of this sort are very valuable and are going on at most wind tunnel facilities. However, this is difficult, since obtaining sufficiently detailed data in full-scale tests is an expensive matter.

7th International Technical Meeting on Air Pollution Modeling and its Application

7 - 10 September, 1976
at
Airlie House
AIRLIE, VIRGINIA
USA

Tentative Agenda

1. Examples of Model Validation
2. Sensitivity Analysis for AQSM's
3. Numerical Grid AQSM's
4. Interregional and Regional Models
5. Tall Stack Plume, including Sulphate Transformation and Removal Processes
6. Dispersion in Conditions of Low Wind Speed
7. Physical Modeling, e.g. Wind and Water Tunnels
8. Diffusion Parameters and Stability Categories
9. Innovative Modeling Techniques

Call for Papers by the Pilot Country: January 1976

Deadline for Submission of Titles: February 28, 1976

Deadline for Submission of Abstracts: July 1, 1976

to the Umweltbundesamt
1 Berlin 33
Bismarckplatz 1

Local Organization:

United States Environmental Protection Agency
Research Triangle Park
North Carolina 277711

OTHER NATO/CCMS AIR POLLUTION PUBLICATIONS

Technical Report on the Conference on Low Pollution Power Systems Development, N. 4

Proceedings of the Second Meeting of the Expert Panel on Air Pollution Modeling, N. 5

Guidelines to Assessment of Air Quality (Revised) SO_x, TSP, CO, HC, NO_x and Oxidants, N. 6 [+]

Air Quality Criteria for Sulfur Oxides, N. 7 [+]

Air Quality Criteria for Particulate Matter, N. 8 [+]

Air Quality Criteria for Carbon Monoxide, N. 10 [+]

Control Techniques for Sulfur Oxide Air Pollutants, N. 12 [+]

Control Techniques for Particulate Air Pollutants, N. 13 [+]

Proceedings of the Third Meeting of the Expert Panel on Air Pollution Modeling, N. 14

Air Quality Criteria for Nitrogen Oxides, N. 15 [+]

Control Techniques for Carbon Monoxide Emissions from Stationary Sources, N. 18 [+]

Control Techniques for Hydrocarbons and Organic Solvent Emissions from Stationary Sources, N. 19 [+]

Control Techniques for Photochemical Oxidants and Related Hydrocarbons, N. 29 [++]

Proceedings of the Fourth Meeting of the Expert Panel on Air Pollution Modeling, N. 30

Symposium on Low Pollution Power Systems Development, N. 32

Control Techniques for Nitrogen Oxide Emissions from Stationary Sources, N. 20 [+]

[+] Also available in French

[+] French version available by Fall 1974

These documents may be obtained from the NATO Committee on the Challenges of Modern Society, 1110 Bruxelles, Brussels, Belgium or from the Air Pollution Technical Information Center, Office of Air and Waste Management, Environmental Protection Agency, Research Triangle Park, North Carolina 27711, USA (English only).